"In the history of philosophy and poetry and art, we always find the interchange of two personality types, which I call *prickles* and *goo*.

The prickly people are advocates of *intellectual porcupinism*. They want rigour, they want precise statistics, and they have a certain clipped attitude in their voices—and you know this very well in academic circles! They accuse other people of being disgustingly vague and miasmic and mystical.

But the vague, miasmic and mystical people accuse the prickly people of being mere skeletons with no flesh on their bones. They say [to them] *'You just rattle! You're not really a human being. You know the words but you don't know the music.'*...

…But we know very well that this natural universe is neither prickles nor goo exclusively.

It's gooey prickles and prickly goo.**"**

-Alan Watts

"A notable feature of the Canadian Arctic marine flora is that despite the unique habitat its species composition is distinctly temperate Atlantic. One apparent reason for such an affiliation is the relatively wide-open communication between the Atlantic and Arctic waters. On the other hand, the continuous northward flow of Pacific water through the narrow Bering Strait should not be overlooked, for this intrusion occurs in a volume great enough to alter the character of the Arctic Ocean water."

-Lee R.K.S. 1973

THE BIOGEOGRAPHIC HISTORY AND CONTEMPORARY ORIGINS OF NORTH AMERICAN ARCTIC MARINE MACROALGAE

by

Trevor T. Bringloe

B.Sc., University of New Brunswick, 2012
B.A., University of New Brunswick, 2012
M.Sc., University of Guelph, 2014

A Dissertation Submitted in Partial Fulfillment
of the Requirements for the Degree of

Doctor of Philosophy

in the Graduate Academic Unit of Biology

Supervisor: Gary W. Saunders, PhD, Biology

Examining Board: Heather Sears, PhD, Assistant Dean of Graduate Studies

Les Cwynar, PhD, Biology
René Malenfant, PhD, Biology
Graham Forbes, PhD, Forestry and Environmental Management

External Examiner: Zi-Min Hu, PhD, Institute of Oceanology, Chinese Academy of Sciences

This dissertation is accepted by the
Dean of Graduate Studies

THE UNIVERSITY OF NEW BRUNSWICK

August, 2018

ABSTRACT

Arctic coastal communities are expected to change in response to warming climate trends, and yet basic information is lacking in these systems. Marine macroalgae provide an opportunity to examine historical migration pathways into the Arctic, and may serve as a model system for future changes. In this thesis, phylogeographic and population level biogeographic patterns were examined in Arctic marine macroalgae. Multiple markers were used to examine phylogeographic patterns in 14 trans-Arctic lineages of red marine macroalgae and determine what role the opening of the Bering Strait and Pleistocene glaciation had on contemporary biogeographic distributions. Results confirmed the opening of the Bering Strait resulted in a predominantly Pacific-to-Arctic/Atlantic movement of species, while Pleistocene glaciation did not appear to play a significant role in promoting trans-Arctic speciation events. The Last Glacial Maximum, however, is hypothesized to have extirpated marine coastal populations in the Northwest Atlantic, with subsequent recolonization out of the Northeast Atlantic. DNA barcode data were used to determine if trans-Atlantic populations of brown and red macroalgae were consistent with this hypothesis. Contrary to the historical consensus, isolation times in 60% of the species examined suggested populations were not recently derived from Europe. Sequence data were also used to assess recolonization pathways of marine macroalgae into the Arctic following the Last Glacial Maximum. Of the 100 species with Arctic populations examined (including brown, green, and red macroalgae), 39 had uncertain origins, 46 had origins in the North Atlantic, five had origins in the Pacific and the Atlantic, while the remaining 10 had origins in the North Pacific. Pacific contributions to Arctic recolonization, however, were inferred in 9 of the

12 best sampled species. Surprisingly, 18 genetic groups and some Arctic haplotypes in 28 species were not assignable to Atlantic or Pacific populations. The results from this thesis indicated that the Pacific Ocean has played a major role in establishing Arctic and North Atlantic lineages/populations of marine macroalgae. In addition, some marine populations may have survived glaciation in the Arctic basin, reducing the role of recolonization pathways out of the Atlantic and/or Pacific.

DEDICATION

I dedicate this thesis first and foremost to my wife, Lauren Murdock, who has been a source of continual support and understanding during graduate school. This time included multiple long trips away from home, at times with little contact, both during her pregnancy with our first child and while handling baby/toddler stages. She is an amazing wife and mother, and played an integral role in fostering this thesis. We make a point to thank collaborators in academia, but oftentimes the most important collaborator is the one closest to home.

I also dedicate this thesis to my parents, Barb and Chris Bringloe, who first introduced me to the intertidal during our family trips to New River Beach in the Bay of Fundy. They provided the freedom and opportunity to cultivate my curiosity at a young age, and have always supported my endeavours in academia, both in Biology and English Language Arts.

Finally, I dedicate this thesis to my children, Avery David Bringloe, and his sister, Nova Bringloe who will be born shortly after this thesis is defended. In a way, I have learned the most from Avery during my time as a PhD student, as he rediscovered the natural world around him.

ACKNOWLEDGEMENTS

I want to thank my supervisor, Dr. Gary Saunders, for his continual guidance during my time as a PhD student. His mentorship went beyond the normal bounds of a PhD program; he taught me to be a calm and confident diver, to seize opportunity with regards to research and publishing, and how to have a good laugh and enjoy myself along the way. Though I was continually learning, Gary did not treat me simply as a student, but rather as a research partner. It has been a blast travelling and having adventures together.

I want to thank various people in academia who helped to make my time here at UNB successful and memorable. In particular, I want to thank my committee members Drs. Adrian Reyes-Prieto and Jason Addison for their input and support over the past four years. Jason was always a source of encouragement and comic relief as I endeavoured into parenthood early in my degree. I want to especially thank Dr. René Malenfant for his extremely thorough review of my thesis. Dr. Kenneth Dunton was keen to facilitate our work at the Boulder Patch in Northern Alaska, and Dr. Kjersti Sjøtun was also very supportive during my time in Norway. The work presented here would not have been possible without their support and collaboration.

Finally, I want to thank all my labmates and friends at UNB: Cody Brooks, Dr. Meghann Bruce, Katherine Cripps, Marie Dankworth, Dr. Kyatt Dixon, Dr. Tony Einfeldt, Josh Evans, Lesleigh Kraft, Tanya Moore, Kirby Morrill, and Dr. Amanda Savoie. I will remember fondly all the intellectual and silly conversations at coffee, your support as I grew my family, and how each of you made my time here at UNB productive, but most importantly, enjoyable.

Table of Contents

List of Tables

List of Figures

Chapter 1 General Introduction

Contemporary conditions in the Arctic Ocean are young from a geological perspective. The Arctic Ocean began its evolution as an embayment of the Pacific Ocean until tectonic plate movement severed this connection by the end of the Cretaceous period (66 million years ago [Ma]; Lawver *et al.* [1990]; Marincovich *et al.* [1990]). Up until that time, the Arctic basin maintained oceanic connections with the Atlantic through the Western Interior Seaway, which flowed through the contemporary North American rocky mountain area into the Gulf of Mexico, and the Tethys Ocean through the Turgai Strait, which flowed through modern day Siberia (Marincovich *et al.* 1990). During the Paleogene (66-23 Ma), the Arctic Ocean became isolated from the earth's oceans with intermittent connections through the Turgai Strait and a seaway connecting to the North Sea Basin (modern day northwestern Europe). A reliable connection between the Arctic Ocean and the Atlantic through the Fram Strait was likely not established until 15 Ma, with deep water connection becoming subsequently established as late as 5 Ma (Lawver *et al.* 1990). The opening of the Bering Strait also re-established a Pacific connection to the Arctic basin around this time (Gladenkov *et al.* 2002), followed by the formation of the Isthmus of Panama which shifted ocean circulation patterns and caused Pacific water to flow into the Arctic (Haug & Tiedemann 1998; Marincovich 2000). Today, the Arctic Ocean features the Canadian and Eurasian basins, which are separated by the Lomonosov ridge running north of Greenland (Lawver *et al.* 1990). A large portion of the Arctic Ocean is also composed of the shallow Chukchi shelf (~50 m) extending off the coasts of Russia and Alaska.

Currents in the Arctic Ocean are primarily driven by salinity gradients. The top layer of ocean water (~80 m) is supplied by Pacific water entering through the Bering

Strait, freshwater runoff from the Canadian and Siberian coastlines, and seasonal ice-melt, creating low salinity (32.5‰) and low temperature (-1.5^{o}C) surface waters (Sverdrup *et al.* 2005a). Annual freezing of ice-sheets increase the salinity of surrounding water, creating a halocline extending to approximately 200 m. Relatively warm and salty North Atlantic waters (2^{o}C and 35‰) flow under this halocline, entering the Arctic along the Siberian coastline and upwelling along the continental shelves, with Arctic water exiting along either side of Greenland and south along the Canadian coastline, rejoining North Atlantic deep water (Fig. 1.1; Sverdrup *et al.* [2005a, 2005b]). The exchange of heat through these ocean currents entering and exiting the Arctic is crucial in the regulation of today's climate (Vellinga & Wood 2002).

The Arctic is also characterized by a dynamic paleoclimatic history. The Arctic basin has been cooling since the beginning of the Cenozoic era (66 Ma), when temperatures at northern latitudes were 30^{o}C warmer than today (Jenkyns *et al.* 2004). Large ice-sheets formed in the Arctic approximately 2.6 Ma ago (Miller *et al.* 2010a), marking the beginning of the Quaternary Ice Age (or Pleistocene Epoch; Raymo [1994]). During this time, glaciation occurred on average every 41 thousand years (ka) in accordance to the precession and obliquity of earth's axis (Imbrie & Imbrie 1979). These cycles continued until 700 ka, at which point glacial events became dominated by 100 ka cycles (Miller *et al.* 2010a). Transitions to interglacial periods were abrupt, typically lasting 10-40 ka (Lisiecki & Raymo 2005; Miller *et al.* 2010a; Berger *et al.* 2016). These cycles were occasionally punctuated by longer lasting interglacial periods during which ice-sheets were severely reduced in the Northern Hemisphere (Anderson *et al.* 2006; Stein *et al.* 2017). The Last Glacial Maximum (LGM) occurred between 30

and 15 ka ago, with global ice volumes peaking 21 ka ago (Miller *et al.* 2010a). The end of the Younger Dryas 12 ka ago marks the end of the Pleistocene Epoch and the beginning of the interglacial Holocene (Rasmussen *et al.* 2006). Pre-industrial ice volume, sea-level, and greenhouse gas levels were established by 6 ka ago, with some warmer or cooler climatic events occurring, such as the Medieval Warm Period between the years 950 and 1200 followed by the Little Ice Age, which persisted until 1850 (Miller *et al.* 2010a). Arctic perennial ice cover has since declined to record lows for the current interglacial period (Serreze *et al.* 2007, Stroeve *et al.* 2012), with the next glacial event not expected to occur within the next 50 ka due to elevated global CO_2 levels (Berger *et al.* 2016).

A history of flux in the geographic and climatic profile of the Arctic basin had a major impact on current day marine biodiversity patterns in the Northern Hemisphere. For one, the initial opening of the Bering Strait initiated interchange of marine species that had been isolated for at least 60 million years (Lawver *et al.* 1990, Marincovich *et al.* 1990). Invertebrate studies indicate this interchange began with Arctic and Atlantic species moving into the Pacific basin until ocean circulation patterns shifted due to the formation of the Isthmus of Panama (Haug & Tiedemann 1998; Marincovich 2000), at which point Pacific species flooded into the Arctic and North Atlantic (Briggs 1970; Reid 1990; Vermeij 1991). Besides biotic interchange between the Arctic, Atlantic, and Pacific basins, repeated glaciations over the past 2.6 Ma also may have played a role in speciation, a mechanism dubbed the "species pump" by Haffer in 1969. In particular, populations were pushed to the margins of ice-sheets during glaciation (or constricted to pockets of suitable habitat, such as in the tropics), resulting in various patterns of

repeated population contraction and expansion that may have initiated speciation events in some taxa (Haffer 1969; Bennett & Provan 2008). Divergence time estimates in terrestrial taxa support this hypothesis as an important mechanism leading to increased levels of biodiversity during the Pleistocene (Lovette 2005; Schoville *et al.* 2012; April *et al.* 2013). The repeated opening and closing of the Bering Strait during cycles of glaciation appears particularly tenable to the "species pump" hypothesis as it relates to marine taxa. The locations of marine refugia have also received attention in recent years. Perennial sea ice likely prevented the persistence of most marine taxa in the Arctic basin, particularly photosynthetic organisms (Bradley & England 2008; Xiao 2014). As such, Arctic populations ought to be an extension of Atlantic and/or Pacific populations following glaciation. Arctic marine populations likely sought refuge in the Bering Sea (Katsuki & Takahashi 2005), while conditions in the Northwest Atlantic were considerably harsher due to ice-sheets extending to the margins of continental shelves (Dyke & Prest 1987). It was originally thought all populations in the Northwest Atlantic were extirpated and subsequently recolonized from European refugia following the LGM (i.e. the "tabula rasa" hypothesis; see Brochmann *et al.* [2003] for a review on North Atlantic biota). This picture is complicated, however, by growing amounts of DNA sequence data that indicate some species of marine invertebrates and macroalgae survived glaciation in the Northwest Atlantic (Wares & Cunningham 2001; Maggs *et al.* 2008; Li *et al.* 2016).

Unsurprisingly, Arctic populations are responding to modern day climate change. The Arctic appears to be uniquely susceptible to shifting climatic conditions, as temperature change in the Arctic over the past 3 million years has been 3-4 times greater

than average temperature change in the entire Northern Hemisphere (Miller *et al.* 2010b). Feedback mechanisms in the forms of ice-albedo, vegetation, permafrost, isostatic adjustments, freshwater balance, and thermohaline circulation all contribute to runaway changes that quickly and drastically alter the Arctic landscape (Miller *et al.* 2010a, b). Such changes are already documented, such as in declining perennial ice cover, ocean acidification and changes to circulation patterns, and changes to sea-surface temperatures and salinity (Stroeve *et al.* [2012]; Renaud *et al.* [2015] and references therein). As a result, some marine benthic communities have undergone northward range expansions, increases or decreases in biomass, and changes to species composition (Renaud *et al.* 2015). Marine introductions and continued northward range extensions are expected as the Arctic continues to warm (Vermeij & Roopnarine 2008; Renaud *et al.* 2015; Ware *et al.* 2016; Jueterbock *et al.* 2016), and though difficult to predict, these changes are projected to have significant impacts on Arctic coastal biodiversity, ecosystem functioning, and economic development (Krause-Jensen & Duarte 2014).

Marine macroalgae are conspicuous members of Arctic benthic communities (Lee 1973; Wynne & Heine 1992; Saunders & McDevit 2013; Wilce & Dunton 2014; Mikhaylova 2017). They fall into three evolutionary lineages, viz. the red, brown, and green algae, and represent some of the oldest multi-cellular lineages of life (Yang *et al.* 2016). These various lineages perform crucial roles in coastal ecosystems throughout the world, such as primary production, providing food and habitat for marine fauna (e.g. kelp forests), consolidating and stabilizing coral reefs (e.g. coralline red algae), in addition to being of economic importance in many countries (e.g. production of

phycocolloids, fertilizers, and food; Graham & Wilcox [2000a, b]; Carss & Elston [2003]; Christie *et al.* [2009]; Mansilla *et al.* [2012]). Life history strategies amongst lineages of marine macroalgae vary greatly, and may include an alternation of isomorphic or heteromorphic generations (e.g. kelp; Fig. 1.2), a triphasic life cycle wherein fertilization is amplified through a carposporophyte stage (e.g. some red algae; Fig. 1.3), or asexual reproduction through spores or fragmentation (common in *Fucus* [Graham & Wilcox 2000a, b, c]). The potential for cryptic and physiologically tolerant life history stages, combined with the potential for asexual reproduction, make marine macroalgae particularly well adapted for becoming established in harsh or newly opened environments. Dispersal likely follows a leptokurtic pattern, wherein dispersal is clustered at the source, but with rare events sustained at larger distances (i.e. fat-tailed distribution), a pattern reported in kelp (Reed *et al.* 1988). Such a dispersal pattern is likely to establish founder populations outside of a species range, quickly expanding the total range of a species as the founder population grows into the parental one (Clark *et al.* 1998). Buoyant species of kelp are also known to raft flora and fauna over oceanic distances (Fraser *et al.* 2011; Saunders 2014; Macaya *et al.* 2016). Marine macroalgae therefore have the potential to fundamentally change Arctic coastal marine systems in response to climate change (Krause-Jensen & Duarte 2014). Indeed, distributions of marine macroalgae are highly dependent on temperature isotherms (Campana *et al.* 2009; Müller *et al.* 2009), and marine macroalgae are forecasted to shift their ranges into the Arctic basin as ocean temperature regimes change and perennial ice cover diminishes (Jueterbock *et al.* 2016). The total impact of these changes remains difficult to predict and understand. Knowledge gaps include the interactions between multiple

stressors at the species and community levels, the impact of stressors among life-history stages, potential for adaptation, and a lack of baseline data regarding species diversity and biogeographic distributions (Harley *et al.* 2012; Mineur *et al.* 2015).

DNA sequence data have the potential to revolutionize our understanding of Arctic marine macroalgal diversity, and will play a critical role in future biomonitoring of the Arctic. Currently, marine floral inventories for Arctic locations remain poorly sampled, and by extension poorly understood; our current understanding is based on a limited number of studies that suggest the Arctic flora is primarily an extension of Northwest Atlantic species (Taylor 1957; Lee 1973; Dunton 1992; Wilce & Dunton 2014). Information regarding the Arctic marine flora is further confounded by morphological identifications, which are problematic due to simple morphology, cryptic diversity, convergent evolution, and phenotypic plasticity of marine macroalgae (Saunders 2005). DNA barcoding emerged 15 years ago to address such issues regarding species identifications, and has seen applications in taxonomy, species discovery, community ecology and phylogeography, trait evolution, diet analyses, and conservation biology (Kress *et al.* 2015). Specifically, DNA barcoding involves the use of a standardized gene fragment, typically the 5' end of the cytochrome *c* oxidase subunit I gene (COI-5P), to identify unknown specimens based on previously identified genetic records (Hebert *et al.* 2003a, b). DNA barcoding has been enormously successful in resolving taxonomic relationships of marine macroalgae (Saunders 2005; Le Gall & Saunders 2010), and the abundance of available data has primed the field for population and phylogeographic analyses. Recent DNA barcoding work on marine macroalgae in the Arctic has revealed misidentified species, cryptic diversity, and

population level data consistent with recent origins in the Pacific basin (Saunders & McDevit 2013, Küpper *et al.* 2016, Bringloe *et al.* 2017), indicating we continue to lack a basic understanding of the Arctic marine flora. Expanding on the available DNA barcoding work for Arctic marine macroalgae will be critical to further establishing reliable baseline data for Arctic species; what species are in the Arctic and how are they distributed? In addition, by looking retrospectively at the various factors that led to present day biogeographic distributions in the Arctic, particularly with regards to marine recolonization and migration at the species and population levels, we may gain insight into contemporary and future changes to Arctic biodiversity; in other words, how did contemporary species and populations become established in the Arctic, and what does this tell us about migration pathways that can be monitored for future ecosystem shifts into the Arctic? Understanding these various processes will be integral to mitigating and/or adapting to further climate change and ensuring future sustainability of the Canadian North.

The main objective of this thesis was to re-evaluate the phylogeographic and contemporary origins of marine macroalgal biodiversity in the North American Arctic in light of molecular data. In particular, this thesis focused on a large number of species simultaneously to draw broad scale, community-wide conclusions regarding past processes that led to biogeographic patterns in the North American Arctic. The species examined in this thesis belong to the three lineages of macroalgae (browns, greens, and reds), and though these lineages represent three separate phyla from two different kingdoms, they serve similar ecological functions in coastal communities (e.g. primary productivity, habitat). Some of the species investigated in this thesis are featured in

multiple chapters, that is to say, there is overlap in the various amalgamated datasets. In addition, this thesis was intended to improve on previous studies by sampling critical locations for which molecular data were notably absent, such as the Northern Bering Sea and Northern Alaska. Besides shedding light on the origins of Arctic marine macroalgae, this work resulted in new genetically verified records for several Arctic locations. The importance of such baseline data cannot be overstated. Successful conservation and management of Arctic biodiversity inherently depends on an accurate understanding of current day biogeographic distributions and the processes that led to these patterns. Such basic information has unfortunately lagged behind increasing concerns regarding the progression and impacts of climate change.

In Chapter 2, I examined time-calibrated phylogenies in 14 trans-Arctic lineages of red marine macroalgae within the class Florideophyceae to investigate if repeated opening and closing of the Bering Strait during the Pleistocene drove speciation events between the Atlantic and Pacific basins (i.e. the "species pump" hypothesis). Twelve cases of Pacific-to-Atlantic speciation events were inferred, in contrast to only one Atlantic-to-Pacific speciation event. These results agreed with the previously held view that Pacific-to-Atlantic trans-Arctic migrations since the opening of the Bering Strait have contributed significantly to current day species diversity and biogeographic patterns in the North Atlantic (as compared to Atlantic-to-Pacific interchange). These results, however, did not support the "species pump" hypothesis, in that speciation events were not primarily confined to the Pleistocene. I speculated that the "species pump," as applied to trans-Arctic lineages, is inhibited by recurrent secondary contact between trans-Arctic populations during interglacial periods (as evidenced by

contemporary trans-Arctic populations) and a relatively slow rate of evolution in marine macroalgae. As such, the opening of the Bering Strait had a far greater impact on contemporary species diversity in the North American Arctic and North Atlantic flora as compared to Pleistocene glaciation.

In Chapter 3, I examined contemporary origins in 20 North Atlantic species of marine macroalgae using COI-5P data, specifically whether Northwest Atlantic flora have recent origins from the Northeast Atlantic (i.e. the "tabula rasa" hypothesis) or if these species likely survived in local glacial refugia during the LGM. Of the species examined, 60% appeared to have survived the LGM in the Northwest Atlantic. This study stands in contrast to the traditionally held and persistent view that a large portion of Northwest Atlantic marine flora was recolonized from the Northeast Atlantic following the LGM. These findings indicate that the Northwest Atlantic is a phylogenetically distinct basin, with underappreciated levels of endemism at the population and possibly species levels. This work also has implications for the recolonization of Arctic marine macroalgae following the LGM; rather than secondary migration out of the Northeast Atlantic, some portion of the Arctic flora may have recent origins in Northwest Atlantic glacial refugia.

In Chapter 4, I re-examined contemporary origins in 100 species of North American Arctic marine macroalgae by comparing Arctic haplotypes to Pacific and Atlantic conspecifics. This chapter expanded on the work of Saunders and McDevit (2013), in particular by including sampling locations in Northern Alaska and the Northern Bering Sea. Results indicated that the Pacific contribution to Arctic recolonization has been historically underestimated, as evidenced by the best-sampled

species in the study; 75% of these species appeared to have a Pacific contribution to Arctic populations. In addition, several suggestive patterns were noted; secondary contact was inferred in several species, and unique Arctic haplotypes/species were also common. In particular, 18 genetic groups and some Arctic haplotypes in 28 species were not assignable to Atlantic or Pacific populations, suggesting marine macroalgae may have survived in periglacial refugia along seasonally ice-free coastal areas of Siberia or Greenland. If true, the Arctic may represent yet another phylogenetically distinct basin, in contrast to the currently held view that the Arctic flora was largely recolonized from the Atlantic following the LGM. This work has implications for conservation and management work in marine Arctic environments, and highlights the need for more sampling in the high Arctic.

Appendix A and B include additional studies conducted during my PhD. Appendix A is an updated marine floral species list for the Boulder Patch, a site of ecological study in Northern Alaska. DNA barcode data were generated for 20 species of macroalgae, which revealed five cases of misapplied species names, and an additional four genetic groups in need of taxonomic work. These results showcased the need for DNA barcoding and taxonomic work in the Arctic to better understand marine floral biodiversity. Appendix B is a species list for DNA barcoded specimens of marine macroalgae from Nome, Alaska (Northern Bering Sea). This work indicated that most of the Nome flora has conspecifics spanning the Arctic and extending into the North Atlantic. Consequently, the genetically verified biogeographic distribution in several species was significantly expanded. Cryptic diversity and new genetic groups were also retrieved. Collectively, these two studies provided consistent and reliable baseline data

for marine floral species diversity at two sites that can be used for future biomonitoring in the Arctic. These studies also indicated considerably more sampling and DNA barcoding work is needed to understand Arctic marine biodiversity.

Statement of Publications and Intended Submissions

Chapter 2 is currently in review with *Journal of Biogeography*.

Chapter 3 was published in *Marine Ecology Progress Series* (Vol. 589; February 2018).

Chapter 4 is in preparation for *Arctic Science*.

Appendix A was published in *ARCTIC* (Vol. 70, Issue 4; December 2017).

Appendix B is currently in review with *Polar Biology*.

Statement of Contribution to Research and Writing

I developed and implemented the objectives of this research with the support and guidance of Dr. Gary Saunders.

I was involved with the collection of specimens over the course of this project (2014-2017), which was also aided by several lab members. This field work resulted in ~2000 new genetically verified records. I also used data collected and generated by previous lab members prior to the beginning of this project. Collaborators are recognized in the acknowledgements section following each chapter.

I conducted the majority of the lab work for specimens collected over the course of this project. Lab work was conducted with the assistance and guidance of Tanya Moore. Of the ~4960 specimens included in the study, representing ~4450 COI-5P records, I generated COI-5P data for ~1800, ITS for ~200, *rbc*L for ~30, *tufA* for ~50, and y*cf35* for 61 specimens.

I completed all the data analyses for this project with guidance and assistance from Dr. Gary Saunders.

I wrote all the chapters for this thesis with guidance and comments from Dr. Gary Saunders.

References

Anderson P, Bennike O, Bigelow N, *et al*. (2006) Last interglacial Arctic warmth confirms polar amplification of climate change. *Quaternary Science Reviews*, **25**, 1383–1400.

April J, Hanner RH, Dion-Côté AM, Bernatchez L (2013) Glacial cycles as an allopatric speciation pump in north-eastern American freshwater fishes. *Molecular Ecology*, **22**, 409–422.

Bennett KD, Provan J (2008) What do we mean by "refugia"? *Quaternary Science Reviews*, **27**, 2449–2455.

Berger A, Crucifix M, Hodell DA, *et al.* (2016). Interglacials of the last 800,000 years. *Reviews of Geophysics*, **54**, 162–219.

Bradley RS, England JH (2008) The Younger Dryas and the Sea of Ancient Ice. *Quaternary Research*, **70**, 1–10.

Briggs JC (1970) A faunal history of the North Atlantic Ocean. *Systematic Zoology*, **19**, 19–34.

Bringloe TT, Dunton KH, Saunders GW (2017) Updates to the marine algal flora of the Boulder Patch in the Beaufort Sea off Northern Alaska as revealed by DNA Barcoding. *ARCTIC*, **70**, 3–6.

Brochmann C, Gabrielsen TM, Nordal I, Landvik JY, Elven R (2003) Glacial survival or tabula rasa? The history of North Atlantic biota revisited. *Taxon*, **52**, 417−450.

Campana GL, Zacher K, Fricke A, Molis M, Wulff A, Quartino ML, Wiencke C (2009) Drivers of colonization and succession in polar benthic macro- and microalgal communities. *Botanica Marina*, **52**, 655–667.

Carss DN, Elston DA (2003) Patterns of association between algae, fishes and grey herons *Ardea cinerea* in the rocky littoral zone of a Scottish sea loch. *Estuarine, Coastal and Shelf Science*, **58**, 265–277.

Christie H, Norderhaug KM, Fredriksen S (2009) Macrophytes as habitat for fauna. *Marine Ecology Progress Series*, **396**, 221−233.

Clark JS, Fastie C, Hurtt G, *et al.* (1998) Reid's paradox of rapid plant migration: dispersal theory and interpretation of paleoecological records. *BioScience*, **48**, 13–24.

Dunton KH (1992) Arctic biogeography: The paradox of the marine benthic fauna and flora. *Trends in Ecology and Evolution* **7,** 183–189.

Dyke AS, Andrews JT, Clark PU, England JH, Miller GH, Shaw J, Veillette JJ (2002) The Laurentide and Innuitian ice sheets during the Last Glacial Maximum. *Quaternary Science Reviews*, **21**, 9–31.

Fraser CI, Nikula R, Waters JM (2011) Oceanic rafting by a coastal community. *Proceedings of the Royal Society B*, **278**, 649−655.

Gladenkov AY, Oleinik AE, Marincovich L Jr., Barinov KB. (2002) A refined age for the earliest opening of Bering Strait. *Palaeogeography, Palaeoclimatology, Palaeoecology*, **183**, 321–328.

Graham L, Wilcox L (2000a) Introduction to the algae: occurrence, relationships, nutrition, definition, general features. In *Algae*. Prentice Hall, Upper Saddle River, p 1–21.

Graham L, Wilcox L (2000b) Ochrophytes IV: Chrysomedidaleans, Phaeothamniophyceans, Tribophyceans, and Phaeophyceans. In *Algae*. Prentice Hall, Upper Saddle River, p 301–341.

Graham L, Wilcox L (2000c) Red Algae. In *Algae*. Prentice Hall, Upper Saddle River, p 343–396.

Haffer J (1969) Speciation in Amazonian forest birds. *Science*, **165**, 131-137.

Harley CDG, Anderson KM, Demes KW, Jorve JP, Kordas RL, Coyle TA, Graham MH (2012) Effects of climate change on global seaweed communities. *Journal of Phycology*, **48**, 1064–1078.

Haug GH, Tiedemann R (1998) Effect of the formation of the Isthmus of Panama on Atlantic Ocean thermohaline circulation. *Nature*, **393**, 673–676.

Hebert PDN, Cywinska A, Ball SL, DeWaard JR (2003) Biological identifications through DNA barcodes. *Proceedings of the Royal Society B*, **270,** 313–321.

Hebert PDN, Ratnasingham S, deWaard JR (2003) Barcoding animal life: cytochrome c oxidase subunit 1 divergences among closely related species. *Proceedings of the Royal Society B*, **270**, S96-99.

Imbrie J, Imbrie KP (1979) The astronomical theory of James Croll. In *Ice Ages, Solving the Mystery*, Enslow Publishers, New Jersey, p 77–88.

Jenkyns HC, Forster A, Schouten S, Sinninghe Damsté JS (2004) High temperatures in the Late Cretaceous Arctic Ocean. *Nature*, **432**, 888–892.

Jueterbock A, Smolina I, Coyer JA, Hoarau G (2016) The fate of the Arctic seaweed *Fucus distichus* under climate change: an ecological niche modelling approach. *Ecology and Evolution*, **6**, 1712−1724.

Katsuki K, Takahashi K (2005) Diatoms as paleoenvironmental proxies for seasonal productivity, sea-ice and surface circulation in the Bering Sea during the late Quaternary. *Deep-Sea Research Part II: Topical Studies in Oceanography*, **52**, 2110–2130.

Krause-Jensen D, Duarte CM (2014) Expansion of vegetated coastal ecosystems in the future Arctic. *Frontiers in Marine Science*, **1**, 1-10.

Kress WJ, García-Robledo C, Uriarte M, Erickson DL (2015) DNA barcodes for ecology, evolution, and conservation. *Trends in Ecology and Evolution*, **30**, 25–35.

Küpper FC, Peters AF, Shewring DM, *et al.* (2016) Arctic marine phytobenthos of northern Baffin Island. *Journal of Phycology*, **52**, 532-549.

Lawver L, Müller R, Srivastava S, Roest W (1990) The opening of the Arctic Ocean. In Bleil U, Thiede J (eds) *Geological History of the Polar Oceans: Arctic vs Antarctic.* Kluwer Academic Publishers, Netherlands, p 29–62.

Le Gall L, Saunders GW (2010) DNA barcoding is a powerful tool to uncover algal diversity: a case study of the phyllophoraceae (Gigartinales, Rhodophyta) in the Canadian flora. *Journal of Phycology*, **46**, 374–389.

Lee RKS (1973) General ecology of the Canadian Arctic benthic marine algae. *ARCTIC*, **26**, 32−43.

Li JJ, Hu ZM, Duan DL (2016) Survival in glacial refugia versus postglacial dispersal in the North Atlantic: the cases of red seaweeds. In: Hu ZM, Fraser C (eds) *Seaweed phylogeography: adaptation and evolution of seaweeds under environmental change*. Springer, Dordrecht, p 309−330.

Lippsett L (2005) Is global warming changing the Arctic? *Oceanus Magazine*, **44**, 24-25.

Lisiecki LE, Raymo ME (2005) A Pliocene-Pleistocene stack of 57 globally distributed benthic δ18O records. *Paleoceanography*, **20**, 1−17.

Lovette IJ (2005) Glacial cycles and the tempo of avian speciation. *Trends in Ecology and Evolution*, **20**, 57–59.

Macaya EC, Lopez B, Tala F, Tellier F, Thiel M (2016) Float and raft: role of buoyant seaweeds in the phylogeography and genetic structure of non-buoyant associated flora. In: Hu ZM, Fraser C (eds) *Seaweed phylogeography: adaptation and evolution of seaweeds under environmental change*. Springer, Dordrecht, p 97−130.

Maggs CA, Castilho R, Foltz D, Henzler C and others (2008) Evaluating signatures of glacial refugia for North Atlantic benthic marine taxa. *Ecology*, **89**, S108−S122.

Mansilla A, Ávila M, Yokoya NS (2012) Current knowledge on biotechnological interesting seaweeds from the Magellan Region, Chile. *Brazilian Journal of Pharmacognosy*, **22**, 760–767.

Marincovich L Jr (2000) Central American paleogeography controlled Pliocene Arctic Ocean molluscan migrations. *Geology*, **28**, 551–554.

Marincovich JL, Brouwers EM, Hopkins DM, McKenna MC (1990) Late Mesozoic and Cenozoic paleogeographic and paleoclimatic history of the Arctic Ocean Basin, based on shallow-water marine faunas and terrestrial vertebrates. In Grantz A, Johnson L, Sweeney J (eds) *The Arctic Ocean Region.* Geological Society of America, Boulder, Colorado, p 403–426.

Mikhaylova TA (2017) Checklist of Rhodophyta of the White Sea (the Arctic Ocean). *Botanica Marina*, **60**, 55–65.

Miller GH, Brigham-Grette J, Alley RB, *et al.* (2010a) Temperature and precipitation history of the Arctic. *Quaternary Sciences Reviews*, **29**, 1679−1715.

Miller GH, Alley RB, Brigham-Grette J, Fitzpatrick JJ, Polyak L, Serreze MC, White JWC (2010b) Arctic amplification: Can the past constrain the future? *Quaternary Sciences Reviews*, **29**, 1779−1790.

Mineur F, Arenas F, Assis J, *et al.* (2015) European seaweeds under pressure: consequences for communities and ecosystem functioning. *Journal of Sea Research*, **98**, 91–108.

Müller R, Laepple T, Bartsch I, Wiencke C (2009) Impact of oceanic warming on the distribution of seaweeds in polar and cold-temperate waters. *Botanica Marina*, **52**, 617–638.

Rasmussen SO, Andersen KK, Svensson AM, *et al.* (2006) A new Greenland ice core chronology for the last glacial termination. *Journal of Geophysical Research Atmospheres*, **111**, D06102.

Raymo ME (1994) The initiation of northern hemisphere glaciation. *Annual Review of Earth and Planetary Sciences*, **22**, 353–383.

Reed DC, Laur DR, Ebeling AW (1988) Variation in algal dispersal and recruitment: the importance of episodic events. *Ecological Monographs*, **58**, 321–335.

Reid DG (1990) Trans-Arctic migration and speciation induced by climatic change: the biogeography of *Littorina* (Mollusca: Gastropoda). *Bulletin of Marine Science*, **47**, 35–49.

Renaud PE, Sejr MK, Bluhm BA, Sirenko B, Ellingsen IH (2015) The future of Arctic benthos: expansion, invasion, and biodiversity. *Progress in Oceanography*, **139**, 244−257.

Saunders GW (2005) Applying DNA barcoding to red macroalgae: A preliminary appraisal holds promise for future applications. *Philosophical Transactions of the Royal Society B*, **360**, 1879−1888.

Saunders GW (2014) Long distance kelp rafting impacts seaweed biogeography in the northeast Pacific: the kelp conveyor hypothesis. *Journal of Phycology*, **50**, 968–974.

Saunders GW, McDevit DC (2013) DNA barcoding unmasks overlooked diversity improving knowledge on the composition and origins of the Churchill algal flora. *BMC Ecology*, **13**, 9.

Schoville SD, Roderick GK, Kavanaugh DH (2012) Testing the "Pleistocene species pump" in alpine habitats: lineage diversification of flightless ground beetles (Coleoptera: Carabidae: *Nebria*) in relation to altitudinal zonation. *Biological Journal of the Linnean Society*, **107**, 95–111.

Serreze MC, Holland MM, Stroeve J (2007) Perspectives on the Arctic's shrinking sea-ice cover. *Science*, **315**, 1533–1536.

Stein R, Fahl K, Gierz P, Niessen F, Lohmann G (2017) Arctic Ocean sea ice cover during the penultimate glacial and the last interglacial. *Nature Communications*, **8**, 373.

Stroeve JC, Serreze MC, Holland MM, Kay JE, Malanik J, Barrett AP (2012) The Arctic's rapidly shrinking sea ice cover: a research synthesis. *Climatic Change*, **110**, 1005–1027.

Sverdrup K, Duxbury A, Duxbury A (2005a) Circulation and Ocean Structure. In *An Introduction to the World's Oceans.* McGraw-Hill Publishers, p 208–226.

Sverdrup K, Duxbury A, Duxbury A (2005b). The Surface Currents. In *An Introduction to the World's Oceans.* McGraw-Hill Publishers, p 227–247.

Taylor W (1957) *Marine algae of the northeastern coast of North America*, 2nd edn. University of Michigan Press, Ann Arbor, MI, p 427.

Vellinga M, Wood RA (2002) Global climatic impacts of a collapse of the Atlantic thermohaline circulation. *Climatic Change*, **54**, 251–267.

Vermeij GJ (1991) Anatomy of an invasion: the trans-Arctic interchange. *Paleobiology*, **17**, 281–307.

Vermeij GJ, Roopnarine PD (2008) The coming Arctic invasion. *Science*, **321**, 780−781.

Ware C, Berge J, Jelmert A, *et al.* (2016). Biological introduction risks from shipping in a warming Arctic. *Journal of Applied Ecology*, **53**, 340–349.

Wares JP, Cunningham CW (2001) Phylogeography and historical ecology of the North Atlantic intertidal. *Evolution*, **55**, 2455−2469.

Wilce RT, Dunton KH (2014) The Boulder Patch (North Alaska, Beaufort Sea) and its benthic algal flora. *ARCTIC*, **67**, 43–56.

Wynne MJ, Heine JN (1992) Collections of marine red algae from St. Matthew and St. Lawrence Islands, the Bering Sea. *Nova Hedwigia*, **55**, 55−97.

Xiao, X (2014). Last Glacial Maximum to Holocene Arctic sea-ice variability: reconstruction from biomarkers. Thesis (PhD). University of Bremen, Germany.

Yang EC, Boo SM, Bhattacharya D, Saunders GW, Knoll AH, Fredericq S, Graf L, Yoon HS (2016) Divergence time estimates and the evolution of major lineages in the florideophyte red algae. *Scientific Reports*, **6**, 21361.

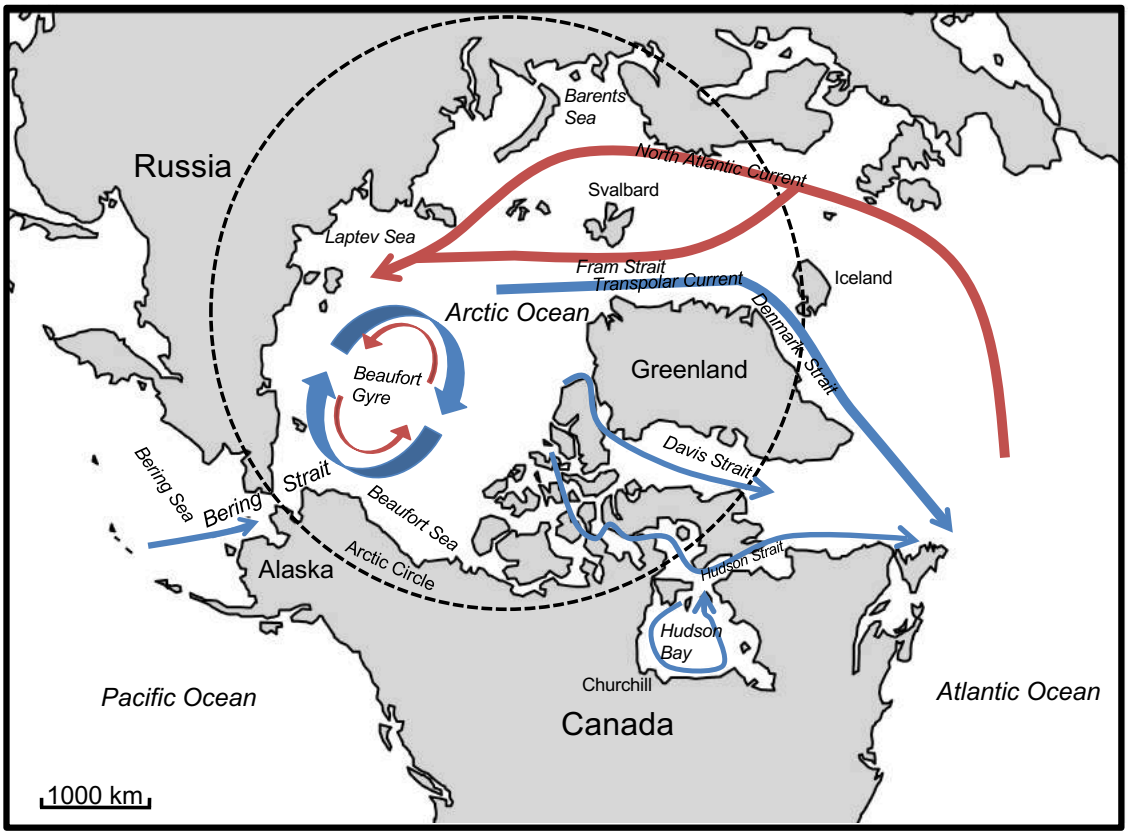

Figure 1.1 Major ocean currents entering and exiting the Arctic basin. Red arrows denote relatively warm water, blue arrows denote relatively cold water. This figure is adapted from Lipsett (2005).

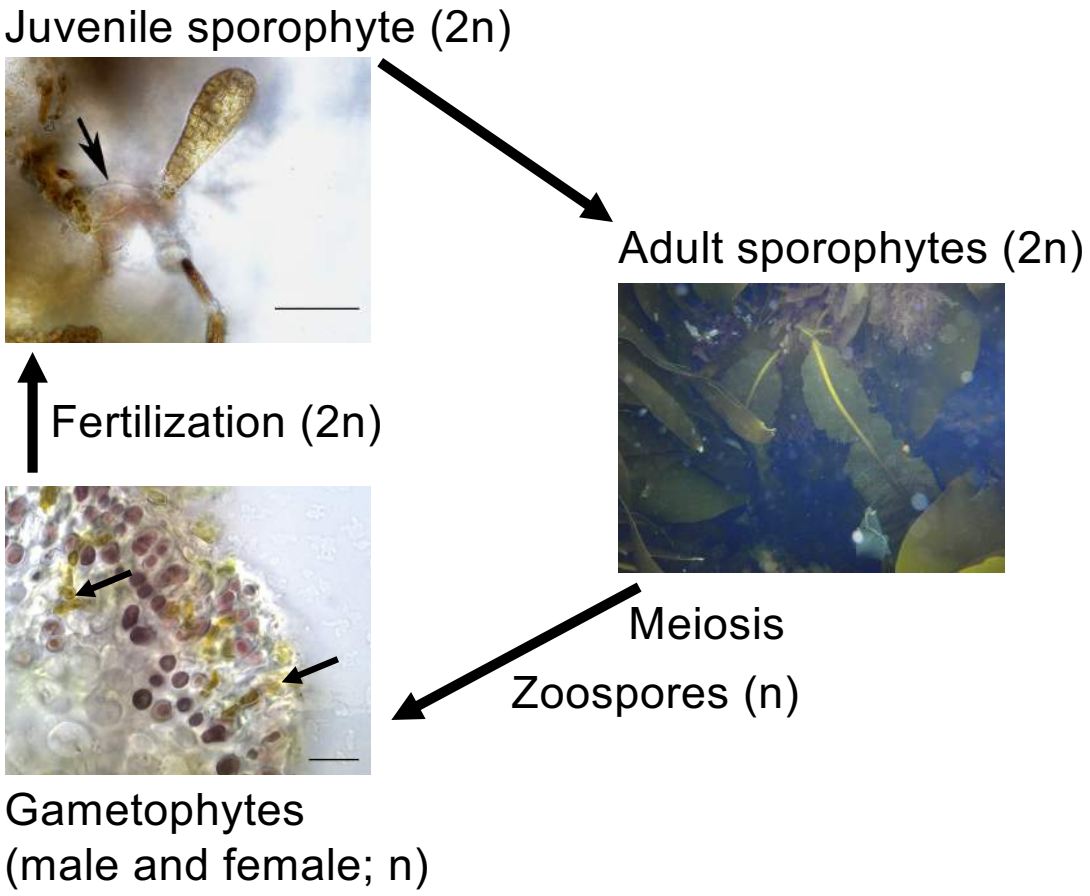

Figure 1.2 Heteromorphic alternation of generations in the brown alga *Alaria esculenta*. For the juvenile sporophyte, the arrow indicates an empty oogonium, and the scale bar=60 µm. For the gametophyte, the arrows indicate endophytic gametophytes in *Chondrus crispus*, and the scale bar=25 µm. n refers to ploidy.

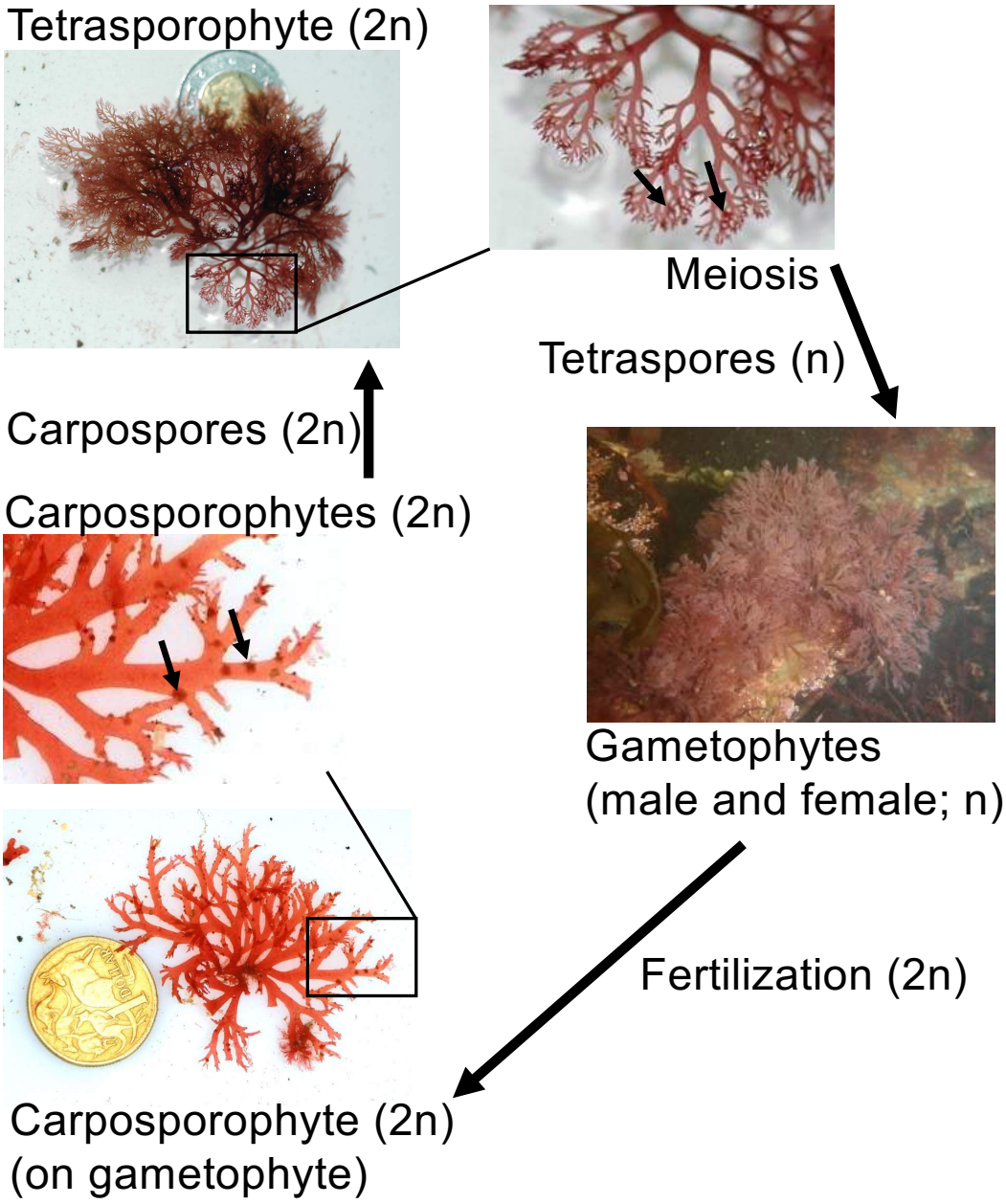

Figure 1.3 Triphasic life history of the red alga *Euthora cristata*. For the tetrasporophyte, the arrows indicate tetrasporangia within the individual. For the carposporophyte, the arrows indicate the carposporophyte growing on the gametophyte. n refers to ploidy.

Chapter 2 Trans-Arctic speciation of Florideophyceae (Rhodophyta) since the opening of the Bering Strait, with consideration of the "species pump" hypothesis

Abstract: The opening of the Bering Strait initiated significant biotic interchange that is postulated to have played a major role in phylogeographic patterns of northern marine flora and fauna. In addition, the "species pump" hypothesis asserts that glaciation events promoted speciation due to repeated isolation of populations over the past 2.6 million years. Here, trans-Arctic speciation events in red marine macroalgae (Florideophyceae) were assessed using time-calibrated phylogenies, and the applicability of the "species pump" hypothesis was considered. Species records and sequence data for trans-Arctic genera of marine macroalgae were amalgamated and supplemented with sampling from the Northwest Atlantic, Northern Alaska (Beaufort Sea), Norway, and Nome, Alaska (Bering Sea). Bayesian and maximum-likelihood phylogenies were variously built using the 5' end of the cytochrome *c* oxidase subunit I gene (COI-5P), the full length nuclear internal transcribed spacer region (ITS), and/or the ribulose-1 5-biphosphate carboxylase large subunit gene (*rbc*L), and nodes were timed using calibrated COI-5P and *rbc*L molecular clocks. The final dataset represented approximately 183 species, broadly representing 14 trans-Arctic lineages. Pacific-to-Atlantic migration and subsequent speciation was inferred in 11 cases, whereas the opposite scenario, Atlantic-to-Pacific, was inferred once; 27% of speciation events appeared to occur during the Pleistocene. Our results are in agreement with previous studies in that trans-Arctic speciation events post-dated the opening of the Bering Strait with a clear Pacific to Atlantic bias. Evidence for the "species pump" (as applied to trans-Arctic interchange) was lacking given trans-Arctic speciation events did not appear to occur primarily during the Pleistocene.

Introduction

Allopatry has historically been viewed as the main mechanism by which speciation occurs (Coyne & Orr 2004). Glaciation events during the Pleistocene are hypothesized to have driven allopatric speciation events due to repeated isolation of populations into glacial refugia, a mechanism originally forwarded by Haffer (1969) called the "species pump." This hypothesis was originally intended to explain Amazonian bird diversity, though the "species pump" hypothesis for Neotropical settings has since undergone scrutiny (Knapp & Mallet 2003). Nonetheless, investigations into the species pump *sensu* Haffer (1969) in other settings have been conducted, and have generally produced favorable evidence, including results from alpine habitats (Schoville *et al.* 2012), freshwater systems (April *et al.* 2013), and marine Antarctica (Clarke & Crame 1992; Wilson *et al.* 2009), although results for invertebrates on island systems do not appear to support this hypothesis (Papadopoulou & Knowles 2015, 2017). The "species pump" hypothesis may also apply to the repeated opening and closing of the Bering Strait, which may have promoted interchange followed by vicariance of conspecifics in the North Atlantic and North Pacific during glacial periods. Atlantic and Arctic marine invertebrate taxa are believed to have initially migrated into the Pacific basin upon the opening of the Bering Strait 4.8-7.4 million years (Ma) ago (Marincovich & Gladenkov 1999; Marincovich 2000). Changes to ocean circulation patterns, mediated by the formation of the Isthmus of Panama (Haug & Tiedemann 1998; Raymo 1994), subsequently caused Pacific species to flow into the Atlantic, a pattern again documented in invertebrate taxa (Briggs 1970; Reid 1990; Vermeij 1991). Recent genetic studies in various taxa have confirmed the

presence of sister lineages on either side of the North American Arctic, further suggesting interchange between the Pacific and Atlantic basins has driven speciation, or at the very least, divergent populations (cod: Bigg *et al.* 2008, and references therein; seagrass: *Zostera marina* Linnaeus: Olsen *et al.* 2004; *Macoma balthica* Linnaeus complex: Nikula *et al.* 2007; Echinoderms and Polychaetes: Carr *et al.* 2011; Hardy *et al.* 2011; Loeza-Quintana & Adamowicz 2018).

Marine macroalgae are an ideal group for investigating speciation patterns related to the opening of the Bering Strait. For one, buoyant species of marine macroalgae are known to disperse large oceanic distances, commonly rafting associated flora and fauna (Fraser *et al.* 2011; Saunders 2014; Macaya *et al.* 2016). Dispersal across the Arctic is also likely facilitated by asexual reproduction and heteromorphic generations that may tolerate a wide range of environmental conditions, easing the establishment of flora in new environments (Graham & Wilcox 2000). As such, the opening of the Bering Strait is expected to have left phylogenetic signatures in a variety of marine macroalgae, a signature that is possibly mirrored in the fauna utilizing macroalgae as habitat. Investigations of trans-Arctic interchange on phylogeographic patterns in marine macroalgae have demonstrated a strong Pacific-to-Atlantic migration pattern. Sister lineages of marine macroalgae in the North Pacific and North Atlantic have been recognized for some time (Lindstrom 1987), with trans-Arctic interchange and speciation inferred from patterns in phylogenies (Lindstrom 2001). Notable Atlantic species that are hypothesized to have resulted from a Pacific ancestor include *Chondrus crispus* Stackhouse, *Dilsea carnosa* (Schmidel) Kuntze, *Dumontia contorta* (S.G.Gmelin) Ruprecht, and *Phycodrys rubens* (Linnaeus) Batters (Lindstrom 2001).

Atlantic to Pacific migrants noted by Lindstrom (2001) represented conspecifics (e.g. *Coccotylus truncatus* [Pallas] M.J.Wynne & J.N.Heine and *Fucus distichus* Linnaeus). In contrast, Coyer *et al.* (2011) hypothesized *F. distichus* colonized the Atlantic from the Pacific on two occasions, however, recent analyses indicate that this species may have a uniquely Arctic origin for both Pacific and Atlantic species/sub-populations (Laughinghouse *et al.* 2015). Species of *Porphyra* in Greenland ally closely with species in the North Pacific (Mols-Mortensen *et al.* 2014), while *Laminaria* spp. are hypothesized to have migrated into the Atlantic twice since the opening of the Bering Strait (Rothman *et al.* 2017). The above speciation scenarios are further supported by thermogeographic modeling that indicate a strong Pacific-to-Atlantic connection exists in marine macroalgae, which played a critical role in the establishment of the Arctic and North Atlantic flora during the Pleistocene (Adey & Hayek 2011; Adey *et al.* 2008). Vicariant trans-Arctic populations also appear to be a common feature in the Arctic marine flora, suggesting trans-Arctic migrations continue to play a role in promoting biological diversity (Saunders & McDevit 2013).

Despite the above evidence, it remains unclear whether the "species pump" is applicable to trans-Arctic lineages of marine macroalgae. For one, the studies cited above interpret migration and speciation through the Bering Strait post factum to explain phylogeographic patterns. Indeed, the opening of the Bering Strait is used as a calibration point for the Atlantic clade (excluding *Laminaria solidungula* J.Agardh) in the Rothman *et al.* (2017) study on *Laminaria* (although time points calibrated using fossil evidence are also used). An independently calibrated molecular clock testing divergence time estimates in trans-Arctic lineages is needed to assess whether these

events occurred after the opening of the Bering Strait, and if these events took place during glaciation. In particular, the "species pump" hypothesis asserts that Pleistocene glaciation precipitated speciation events by repeatedly pushing populations into refugia. Many of the speciation events cited above may be the result of the initial opening of the Bering Strait, and not precipitated or amplified directly through glaciation events *per se*. These processes could be teased apart by examining whether or not the number of trans-Arctic speciation events (i.e. migration across the Arctic followed by vicariance) appear to increase or are more common during the Pleistocene (2.6 Ma-12 ka; Miller *et al.* 2010) as compared to the the estimated time frame between the opening of the Bering Strait and the Pleistocene (7.4-2.6 Ma; Gladenkov *et al.* 2002).

Given the above uncertainties, we sought to determine if time-calibrated phylogenetic trees are consistent with trans-Arctic interchange of red marine macroalgae and considered the applicability of the "species pump" hypothesis. Our research questions were: 1) do time calibrated phylogenies support the view that marine macroalgae have undergone trans-Arctic migration events since the opening of the Bering Strait, primarily from the Pacific to the Atlantic? And if so, 2) did these speciation events primarily occur during the Pleistocene, in support of the "species pump" hypothesis? This investigation will yield insight on recent evolutionary events in the Northern Hemisphere and add to the understanding of biotic interchange through the Bering Strait and its impacts on contemporary bieogeographic distributions in marine coastal systems. Understanding historical migration pathways in Arctic marine species is urgently needed as biotic interchange across the Arctic basin is expected to increase in the wake of climate change, and past events may provide insight on future

biogeographic changes (e.g. direction of migrations, lineages of interest for biomonitoring; Vermeij & Roopnarine 2008). Furthermore, updated phylogenies assessing trans-Arctic speciation events are timely given the surge in genetic data since the last review of this topic nearly two decades ago (Lindstrom 2001).

Materials and Methods

To assess if trans-Arctic migrations have resulted in speciation events during the Pleistocene, we amalgamated pre-existing records for three markers (5' end of the cytochrome *c* oxidase subunit I gene [COI-5P; 664 bp], the full length nuclear internal transcribed spacer region [ITS; 858-1071 bp], and the ribulose-1 5-biphosphate carboxylase large subunit gene [*rbc*L; 1358 bp]) in targeted macroalgal species from the Barcode of Life Datasystems and GenBank, and supplemented our dataset with collections from Baffin Island, through northern Labrador to Makkovik (Canada; September 2-12, 2014); the Beaufort Sea, Northern Alaska (USA; August 20-21, 2014, and July 20-25, 2015); Bergen and surrounding area (Norway; June 3-13, 2016); and Nome, Alaska, and surrounding area (Northern Bering Sea, USA; August 12-22nd, 2017). Specimens were collected from the intertidal or subtidally via scuba. Vouchers were taken as bits of material in silica or as presses and/or as electronic images. A cm^2 portion of tissue was also preserved in silica and brought back to the University of New Brunswick for DNA extraction using a QIAGEN TissueLyser II and QIAxtractor robot for high throughput protocols (Saunders & McDevit 2012a). Primers and thermocycling regimes are listed in Table 2.1. Successful PCR products were sent to Genome Quebec for forward and reverse sequencing. Sequences were edited and aligned in Geneious

v.10 (Kearse *et al.* 2012) for each species. A specimen list with GenBank accession numbers is presented in Appendix C, Table C1; specimen information and sequences are also available online (Barcode of Life Datasystems [BOLD]: DS-TASAP).

Phylogenetic trees were built for trans-Arctic lineages of red macroalgae, and nodes were dated using calibrated COI-5P and *rbc*L clocks in BEAST v.1.8.3 (Drummond *et al.* 2012). Trans-Arctic genera were included in the analyses based on previous DNA barcoding and taxonomic work (genera previously targeted for taxonomic work in the North Atlantic and North Pacific are likely to have most of their genetic groups sampled across a broad geographic range and several genetic markers sequenced, typically COI-5P and *rbc*L); less well-studied taxa, such as red crusts, were excluded from the analyses. The following genera of interest were used to build 14 phylogenetic trees: from Ahnfeltiales *Ahnfeltia*; from Palmariales *Devaleraea*, *Halosaccion*, and *Palmaria*; from Gigartinales *Coccotylus*, *Phyllophora,* and *Ozophora*; *Dilsea*, *Hyalosiphon*, and *Neodilsea*; *Mastocarpus*; *Opuntiella* and *Turnerella*; from Ceramiales *Melanothamnus*; *Membranoptera*; *Odonthalia*, *Neorhodomela*, and *Rhodomela*; *Polysiphonia*; *Phycodrys*; *Polyostea*; *Ptilota*; *Vertebrata*. We began by calibrating the COI-5P clock by analyzing trans-Atlantic sequences of *Palmaria palmata* (Linnaeus) F.Weber & D.Mohr (20 mitotypes, 661 bp) with an estimated isolation time between Northeast and Northwest Atlantic populations of 0.906 Ma, which was estimated using *cox*2-3 and plastid *rps* markers (owing to an error confusing divergence rate with mutation rate, the isolation times reported by Li *et al*. [2015] were doubled). These markers were initially calibrated using divergence estimates in *Bostrychia calliptera* (Montagne) Montagne and *Bostrychia pinnata* J.Tanaka &

Chihara, and a calibration point of the formation of the Isthmus of Panama 3-3.5 Ma (Zuccarello & West 2002; Coates & Stallard 2013). BEAST runs consisted of the following parameters: empirical base frequencies; an HKY substitution model; a strict clock; a Yule speciation tree prior; a random starting tree; priors on the root height of the tree set to a normal distribution with a mean of 0.906 and a normal distribution truncated around 1.432 and 0.696 (as per pairwise populations min and max isolation time estimates in Li *et al*. [2015]), and a standard deviation of 0.1; and otherwise uninformative (e.g. uniform) priors. Three 10 million length chains were run with sampling every 1000 steps, for a total of 30,000 geneologies saved. Results were combined and assessed after a burn-in of 1000 geneologies in Tracer v.1.6.0 (Rambaut *et al.* 2014). The combined runs resulted in an HKY COI-5P substitution rate of 0.0076 substitutions/site/Ma (with 95% Highest Posterior Density [HPD] min and max estimates of 0.0035207 and 0.01205 substitutions/site/Ma). The above parameters were used to build a first round of phylogenetic trees in each trans-Arctic lineage assessed, using a COI-5P clock rate prior of 0.0076, with a normal distribution and a standard deviation of 0.005 (approximating the min and max clock estimates of 0.0035207 and 0.01205), in addition to unlinked HKY substitution and strict clock models across markers and partitioning of three codon positions (except in the case of ITS); parameters for the analyses were otherwise the same as above for the calibration of COI-5P.

The molecular clock assumption was tested on the initial phylogenetic trees using Maximum Likelihood (ML) tests under the Tamura-Nei model in MEGA v.7.0.26 (Appendix C, Table C2; Tamura & Nei 1993; Kumar *et al.* 2016). In some cases, a subset of the initial tree for a given lineage was tested for the molecular clock

hypothesis (Table C2). Tajima's Relative Rate Test was also used to test the molecular clock hypothesis in *Ahnfeltia* and *Opuntiella*/*Turnerella* (Appendix C, Table C3; Tajima 1993; Kumar *et al.* 2016). A second round of phylogenetic analyses were then conducted wherein the molecular clock constraint was loosened based on the results from ML and Relative Rate tests (Appendix C, Table C4). This process began by loosening the molecular clock assumption for *rbc*L in lineages where a uniform rate of *rbc*L evolution was rejected, using an uncorrelated relaxed clock model (Drummond *et al.* 2006), and enforcing a strict COI-5 clock using the same priors as in the initial analyses (Table C4). We also re-analyzed a subset of taxa in some lineages wherein the molecular clock was not rejected for COI-5P and *rbc*L (Table C2), again enforcing strict clocks and the same priors as in the initial analyses. The average global *rbc*L rate from these analyses (0.00301392 substitutions/site/Ma, with average 95% HPD min and max estimates of 0.00141571 and 0.00452636; Appendix C, Table C5) was then used in lineages for which the molecular clock hypothesis was rejected for COI-5P; a strict *rbc*L clock with a normal distribution approximating the above clock range was employed in these analyses, while a random local clock was used for COI-5P (Table C4). Uncorrelated relaxed clocks for COI-5P and *rbc*L were used in *Polyostea* and *Odonthalia*, setting priors on the global COI-5P and *rbc*L clocks to the above estimated rates for each marker. Finally, Relative Rate Tests detected rate heterogeneity in *Turnerella* sp. 1BC in the analysis of *Opuntiella*/*Turnerella* (Table C3). We therefore reanalyzed this lineage without *T.* sp. 1BC, using a strict *rbc*L clock. Divergence time estimates (proxied through mean node heights) were derived from the updated analyses wherein the molecular clock constraints were loosened.

In addition to the BEAST analyses, tree topology and node support was assessed by building ML trees using the RaxML v7.2.8 plugin in Geneious v.10 (Stamatakis 2006), utilizing an HKY substitution model, and partitioning the data according to marker and codon position. Saturation was assessed for COI-5P and *rbc*L for each lineage by plotting the number of transitions and transversions against F84 genetic distances between pairs of sequences using DAMBE6 (Xia 2017). Outgroups were not included in these analyses. Saturation was visually assessed, and defined as the approximate genetic distance at which the number of transversions notably increased relative to the number of transitions (Appendix C, Figs. C1 and C2).

Trans-Arctic speciation events were inferred according the following criteria: a given species or clade had to be embedded in a clade of species from the opposite basin (e.g. an Atlantic species embedded in a clade of Pacific species would imply a trans-Arctic speciation event wherein a Pacific ancestor migrated into the Atlantic basin and subsequently speciated); node support had to be $\geq$0.95 posterior probability for a given time-calibrated node (although poorly supported nodes were used to approximate divergence times in *Polysiphonia* and an earlier event in *Dilsea*; inconsistencies between Bayesian and ML trees are discussed); and the timeframe for divergence estimates between taxa had to fall within the past 7.4 Ma, given this is the oldest date the Bering Strait is hypothesized to have opened (Gladenkov *et al.* 2002). Note that species name assignment is likely not correct for some genetic groups. Taxonomic work, where available, is referenced, while groups in need of taxonomic work are noted.

The inferences made here rest on the critical assumption that phylogenetic patterns should be interpreted in such a way that minimizes the number of trans-Arctic

speciation events. There is, however, precedence to interpret genetic patterns within a species or species complex as the result of recurrent Pacific to Atlantic migration events in both macroalgae and invertebrate taxa (Nikula *et al.* 2007; Coyer *et al.* 2011), which would appear as cascading speciation events in a phylogenetic tree (e.g. an Atlantic species/ancestor seeding multiple Pacific lineages through time). Justification for the former interpretation was thus: the primary mechanism by which speciation occurs is via allopatry (Coyne & Orr 2004), and as such, speciation within and between oceanic basins generally occurs in this manner. Indeed, recent work has demonstrated that trans-Atlantic populations of marine macroalgae commonly exhibit COI-5P divergence, implying speciation has occurred through this distribution in the past (Bringloe *et al.* 2018). If speciation within an oceanic basin typically occurs via allopatry, then this scenario should be given preference in interpreting the phylogenetic patterns presented here given 1) the impediments to dispersal presented by the Arctic (ice scour, patchy rocky habitat, and extreme seasonality) and 2) the greater number of avenues for allopatric speciation in the Atlantic and Pacific (east-west and north-south distributions) versus the Arctic (east-west distributions exclusively). As such, the occurrence of trans-Arctic speciations should be minimized when interpreting the topology of phylogenetic trees.

Results

In total, records were amalgamated from 284 specimens, 54 of which were collected during the course of this study (2014-2018; Table C1; BOLD DS-TASAP). Approximately 183 species were analyzed, broadly representing 14 trans-Arctic lineages

(Figs. 2.1 and 2.2). Overall, Pacific-to-Atlantic migration and subsequent speciation since the opening of the Bering Strait were inferred in 11 cases (not including *Odonthalia dentata*, see results below), whereas the opposite scenario, Atlantic-to-Pacific, was inferred in one; the direction of a further two cases of trans-Arctic migration and speciation remained uncertain (Fig. 2.3). Regarding the timeframe for these events, speciation during the Pleistocene was inferred in three cases, while another eight events appeared to occur after the opening of the Bering Strait but prior to the Pleistocene; a trans-Arctic speciation event in *Ahnfeltia* and *Odonthalia* may fall into either time frame (Fig. 2.3). Specific findings for each trans-Arctic lineage are summarized in the following sections.

Ahnfeltiales

***Ahnfeltia* (one event, timeframe and direction uncertain; Figs. 2.1A and C3)**

Ahnfeltia is the only genus in Ahnfeltiales, with only three genetically verified species at this time (Milstein & Saunders 2012). *Ahnfeltia borealis* D.Milstein & G.W.Saunders is trans-Arctic (Table C1; Fig. 2.1A), indicating that this species recently migrated between the Atlantic and Pacific basins. Divergence time estimates between species are also within the time frame of the opening of the Bering Strait (Fig. 2.1A). If *A. borealis* speciated in the Pacific, then it is possible that the ancestor of the three species of *Ahnfeltia* migrated across the Arctic and speciated in the Atlantic basin, giving rise to modern day *Ahnfeltia plicata* (Hudson) Fries, which corresponds to the earlier divergence time estimate in Fig. 2.3. On the other hand, if *A. borealis* is an Atlantic species, then *Ahnfeltia fastigiata* (Endlicher) Makienko may be the result of the recent common ancestor to both these species migrating into the Pacific basin (most

recent time estimate in Fig. 2.3). Population level data in *A. borealis* will be needed to infer contemporary origins in this species, and subsequently distinguish between these two scenarios.

Palmariales

***Devaleraea*, *Halosaccion*, and *Palmaria* (one pre-Pleistocene event, direction uncertain; one Pacific-to-Atlantic Pleistocene event; Figs. 2.1B and C4)**

The taxonomy of this group has recently undergone revision (Saunders *et al.* 2018). Two patterns are notable. For one, *Palmaria palmata* (Linnaeus) F.Weber & D.Mohr is rooted at the base of all the other species analysed in this group (Fig. 2.1B), a finding consistent with ITS data (Lindstrom *et al.* 1996), suggesting a possible early trans-Arctic migration/speciation event. Lindstrom *et al.* (1996) suggested that *P. palmata* and the rest of the Pacific species in this group speciated in the Pacific, and that *P. palmata* migrated into the Atlantic following the opening of the Bering Strait with regional extinction in the Pacific. This conclusion was based on an estimated divergence date of 6.9-17.3 Ma for *P. palmata*, and a later opening of the Bering Strait (3.5 Ma). Our results, however, indicated *P. palmata* may have diverged after the opening of the Bering Strait, though the direction of trans-Arctic migration in the ancestor cannot be confirmed (Figs. 2.1B & 2.3). Lindstrom *et al.* (1996) also recognized *Devaleraea ramentacea* (Linnaeus) Guiry as resulting from a Pacific to Atlantic migration event, which is consistent with the analyses here (Fig. 2.1B). The dating of divergence of *D. ramentacea* from a Pacific ancestor sits comfortably within the time frame of the Pleistocene (1.352 Ma [95% min and max HPD estimates of 0.628 and 2.158], or 1.874 Ma [0.872, 2.928] for an internal node with higher support, Fig. 2.1B).

Gigartinales

***Coccotylus*, *Erythrodermis*, *Phyllophora*, and *Ozophora* (Figs. 2.1C and C5)**

No trans-Arctic speciation events are inferred from this group. *Ozophora* is a Pacific genus, while *Coccotylus*, *Erythrodermis* and *Phyllophora* form a distinct Atlantic clade (Fig. 2.1C). It is possible the ancestor to both groups underwent a trans-Arctic migration event and subsequently radiated in the newly found basin, however, these clades are estimated to have diverged approximately 14.442 Ma (Fig. 2.1C), and COI-5P and *rbc*L saturation suggests this date is likely older (Figs. C1 and C2). It is worth noting *Coccotylus truncatus* (Pallas) M.J.Wynne & J.N.Heine is genetically verified as trans-Arctic (Table C1), and has therefore undergone a recent trans-Arctic migration; however, population level data are needed to resolve details on this event, particularly the direction of migration, though Atlantic to Pacific is most parsimonious (speciation of *C. truncatus* in the Pacific basin requires an extra trans-Arctic migration event).

***Dilsea*, *Hyalosiphon*, and *Neodilsea* (one Pacific-to-Atlantic event, timeframe uncertain; Figs. 2.1D and C6)**

Dilsea is another genus clearly dominated by Pacific species. *Dilsea carnosa* (Schmidel) Kuntze, on the other hand, is an Atlantic endemic, while *Dilsea socialis* (Postels & Ruprecht) Perestenko has been previously reported from the Northern Bering Sea and Northwest Atlantic basins (Saunders 2008). Two scenarios are plausible. The ancestor to *D. carnosa*, *D. socialis*, and *D. natashae* (S.C.Lindstrom) G.W.Saunders & S.C.Lindstrom migrated from the Pacific into the Atlantic, giving rise to *D. carnosa* and *D. socialis* in the Atlantic with subsequent recent trans-Arctic migration of *D. socialis*

from the Atlantic into the Pacific; or a more recent event occurred wherein the ancestor to *D. carnosa* and *D. socialis* migrated into the Atlantic basin where *D. carnosa* subsequently evolved, with recent Pacific-to-Atlantic trans-Arctic migration in *D. socialis*, in which case *D. socialis* evolved in the Pacific basin. Population level data suggest recent Pacific-to-Atlantic migration occurred in *D. socialis*, supporting the latter scenario; however, additional collections from the Northern Bering Sea are needed to corroborate this conclusion (Saunders & McDevit 2013). Regardless, a Pacific to Atlantic trans-Arctic speciation event is inferred in *Dilsea* (during the Pleistocene if *D. socialis* evolved in the Pacific: 1.040 Ma [95% HPD min and max estimates of 0.386 and 1.916]; a pre-Pleistocene event if *D. socialis* evolved in the Atlantic: 3.900 Ma [1.988 and 6.478], or 4.842 Ma [2.682, 7.970] for an internal node with higher bootstrap support; Figs.2.1D and 2.3).

***Mastocarpus* (one pre-Pleistocene Pacific-to-Atlantic event; Figs. 2.1E, C7, and C8)**

Mastocarpus is a speciose genus, having recently undergone taxonomic revision (Lindstrom *et al.* 2011). This group is once again dominated by Pacific species, with two Atlantic genetic groups assigned to *Mastocarpus stellatus* (Stackhouse) Guiry (Li *et al.* 2016). Bayesian analyses confidently grouped *M. stellatus* with *Mastocarpus pacificus* (Kjellmann) Perestenko (Fig. 2.1E), with an estimated divergence time of 6.656 Ma (min and max 95% HPD estimates of 3.616 and 10.988) between these two species. Interestingly, *M. pacificus* was the only species of *Mastocarpus* genetically verified in the Northern Bering Sea (Table C1), a finding consistent with an ancestor that occurred near the Bering Strait and subsequently migrated across the Arctic into the Atlantic basin, giving rise to *M. stellatus* (Fig. 2.1E). Node support for the *M.*

pacificus/*M.stellatus* clade, however, was lacking in the ML analyses, which tended to root most of the *Mastocarpus* phylogeny with *M. stellatus* (Fig. C8).

***Opuntiella* and *Turnerella* (one pre-Pleistocene Pacific-to-Atlantic event; one Pacific-to-Atlantic event, timeframe uncertain; Figs. 2.1F and C9)**

Genetic groups currently assigned to *Turnerella* form a paraphyletic clade to *Opuntiella*, although correct taxonomic assignment to the genus is clearly lacking for *Turnerella* sp. 1BC and *Turnerella* sp. 1Atl (Fig. 2.1F). Nonetheless, this group appears to be dominated by Pacific species, with two Atlantic species reported here. *Turnerella* sp. 1Atl appears to represent an early Pacific to Atlantic speciation event, however, inner node support was inconsistent between Bayesian and ML analyses. *Turnerella pennyi* (Harvey) F.Schmitz represents another Pacific to Atlantic speciation event (time estimates are distributed among pre-Pleistocene and Pleistocene timesframes), which may have been precipitated by its shared ancestor with *Turnerella mertensiana* (Postels & Ruprecht) F.Schmitz (for which there is poor bootstrap support; 2.848 Ma [min and max 95% HPD estimates of 1.428 and 4.388]), or an ancestor in common with the broader *Opuntiella* and *T. mertensiana*/*pennyi* lineage (relatively well supported in both Bayesian and ML analyses; 5.090 Ma [3.204 and 7.202]; Fig. 2.1F).

Ceramiales

***Melanothamnus* (one Pleistocene Pacific-to-Atlantic event; Figs. 2.2A and C10)**

This genus is part of the large and taxonomically challenging tribe Polysiphonieae. Species name assignments for genetic groups are therefore inaccurate in some cases, however, *Melanothamnus* as used here has been resolved at the genus level

(Savoie & Saunders 2018). This genus is widespread, with species recorded in the Southwest Pacific, Midwest Atlantic, and Indian Ocean (Fig. C10). Two events can be inferred in *Melanothamnus*. First, a well-resolved North Pacific clade is rooted with species predominantly from the Midwest Atlantic, including *Melanothamnus collabens* (C.Agardh) Díaz-Tapia & Maggs from the Northeast Atlantic. Dating of divergence indicates the North Pacific clade was established from an ancestor 12.714 Ma (min and max 95% HPD estimates of 8.766 and 17.256). Given the earlier timeframe for divergence and that the Pacific clade is predominantly rooted with species from the Midwest Atlantic, we hypothesize the Pacific clade was established from an ancestor through the Proto-Caribbean Seaway, which allowed the exchange of tropical Atlantic and Pacific species prior to the formation of the Isthmus of Panama approximately 3.5 Ma (Coates & Stallard 2013). Focusing on the well resolved northern clade, it is clear there is a North Pacific bias in the distribution of species (Fig. 2.2A). At least one species is reported as introduced to the Northwest Atlantic (*Melanothamnus japonicus* ([Harvey] Díaz-Tapia & Maggs), while another is possibly introduced (*Melanothamnus akkeshiensis*, reported as *Polysiphonia akkeshiensis* Segi; Savoie & Saunders 2015). Even if *M. akkeshiensis* is conceded as having a natural distribution in the Northwest Atlantic (i.e. not introduced), the ancestor giving rise to *Melanothamnus decumbens* (T.Segi) Díaz-Tapia & Maggs, *Melanothamnus* sp. 21GWS, *M. japonicus*, *M. akkeshiensis*, and *Melanothamnus harveyi* (Bailey) Díaz-Tapia & Maggs (the Atlantic species) is estimated to have occurred 1.998 Ma (min and max 95% HPD estimates of 1.204 and 2.862; Fig. 2.2A). If *M. akkeshiensis* is treated as an introduced species to the Northwest Atlantic, then the Pacific-to-Atlantic speciation event will have occurred

more recently (approximately 1.052 Ma; Fig. 2.2A). Either way, this group serves as another example of a Pacific dominant clade seeding an Atlantic species or lineage during the Pleistocene.

***Membranoptera* (one Pleistocene Atlantic-to-Pacific event; Figs. 2.2B and C11)**

Membranoptera stands in contrast to many of the genera studied here, in that the number of Atlantic and Pacific species in the genus is more balanced (i.e. not Pacific dominant). Species name assignment to genetic groups has also been resolved in most cases (Hughey *et al.* 2017; Wynne & Saunders 2012). Well resolved Pacific and Atlantic clades suggest a pre-Pleistocene Pacific-to-Atlantic migration event (Fig. 2.2B), however, divergence time estimates predate the opening of the Bering Strait (11.106 Ma; min and max 95% HPD estimates of 7.472 and 15.146). The Pacific genetic group *Membranoptera* sp. (AF257383), however, is nested in the Atlantic clade, suggesting at a notably rare Atlantic-to-Pacific speciation event 1.188 Ma (min and max 95% HPD estimates of 0.448 and 2.030), though Wynne & Saunders (2012) note that further work is needed to confirm its status as a species distinct from Atlantic *Membranotera fabriciana* (Lyngbye) M.J.Wynne & G.W.Saunders.

***Odonthalia*, *Neorhodomela*, and *Rhodomela* (one pre-Pleistocene Pacific-to-Atlantic event; Figs. 2.2C, C12, and C13)**

The closely related genera *Odonthalia* and *Rhodomela* both have conspecifics and/or congeners in the North Atlantic and North Pacific. *Odonthalia* is dominated by Pacific species, with the trans-Arctic *Odonthalia dentata* (Linnaeus) Lyngbye occurring on both sides of the North Atlantic. Indeed, trans-Atlantic populations are divergent by

seven substitutions in COI-5P (Bringloe & Saunders 2018), while Northwest Atlantic populations ally most closely with trans-Arctic populations (including populations in the Northern Bering Sea; Fig. C12). Two scenarios are thus possible. For one, a Pacific ancestor to the *O. dentata*, *Odonthalia lyallii* (Harvey) J.G.Agardh, and *Odonthalia kamtschatica* (Ruprecht) J.Agardh clade may have migrated across the Arctic and speciated into *O. dentata*, establishing divergent populations on both sides of the Atlantic, with Northwest Atlantic populations subsequently migrating back to the Pacific. Alternatively, a Pacific ancestor to *O. dentata* may have crossed the Arctic and established the Northeast Atlantic population, with a subsequent more recent migration event out of the North Pacific establishing the Northwest Atlantic population, similar to the cascading events reported in *Macoma* and *Fucus* (Nikula *et al.* 2007; Coyer *et al.* 2011). Both scenarios require two trans-Arctic migration events. Population level data will be needed to infer the direction of recent trans-Arctic migration and resolve which of the above two scenarios are most plausible. In addition, it is not clear that the latter scenario (wherein the ancestor to trans-Atlantic *O. dentata* evolved in the Pacific) represents a speciation event, given how closely related Northeast Atlantic populations are to Northwest Atlantic counterparts (Bringloe & Saunders 2018).

Inferences regarding trans-Arctic speciation in *Rhodomela* is similarly complicated by trans-Arctic populations in several species (Fig. 2.2C). The timing of divergence in the most ancestral node (6.446 Ma [min and max 95% HPD estimates of 3.378 and 10.748]) suggests at a pre-Pleistocene Pacific to Atlantic migration event that yielded the Atlantic *Rhodomela confervoides* (Hudson) P.C.Silva and *Rhodomela lycopodioides* (Linnaeus) C.Agardh clade. This scenario assumes that *Rhodomela*

sibirica A.D.Zinova & Vinogradova and the clade including *Rhodomela virgata* Kjellman and *Rhodomela* sp. 1virgata are Pacific lineages, which we infer based on two lines of evidence: 1) the closely related *Neorhodomela* is a distinctly Pacific genus, and 2) the putative Pacific *Rhodomela* genetic groups are present in the Bering Sea but are all rare in the Northwest Atlantic (or absent in the case of *R. sibirica*, through it is recorded in the Eastern Canadian Arctic, Table C1), suggesting these species recently migrated into the Atlantic. Population level data are needed to confirm this.

Polysiphonia **(one pre-Pleistocene Pacific-to-Atlantic event; Figs. 2.2D, C14, and C15)**

Though taxonomic confusion has persisted in *Polysiphonia*, the species presented here are members of *Polysiphonia sensu stricto* (Savoie & Saunders 2018). Trans-Arctic patterns are less clear in this genus. Several Atlantic species at the base of the phylogenetic tree suggest at a long history in this basin, though Pacific species are also abundant (Fig. 2.2D). The clade including *Polysiphonia atlantica* Kapraun & J.N.Norris, *Polysiphonia dokdoensis* D.E.Bustamante, B.Y.Won & T.O.Cho, *Polysiphonia macrocarpa* (C.Agardh) Sprengel, and *Polysiphonia koreana* D.Bustamanta B.Y.Won & T.O.Cho could represent a trans-Arctic speciation event, except that node support is weak in this clade (indeed this clade was not resolved in the ML analyses; Fig. C15). In addition, *P. macrocarpa* is recorded from the Midwest Atlantic (Panama), meaning speciation could have been mediated by migration into the Pacific prior to the formation of the Isthmus of Panama. Compelling evidence for a trans-Arctic speciation event, however, occurs in the remaining *Polysiphonia* species, most of which appear to be Pacific in origin. *Polysiphonia marrowii* Harvey is widely

distributed, but hypothesized to be introduced to the North and South Atlantic basins, though it may also represent a cryptogenic species (Geoffroy *et al.* 2016; Kim *et al.* 2004). *Polysiphonia* sp. 1stricta has a trans-Arctic distribution, so population level data are needed to ascertain its recent history. The most parsimonious hypothesis would suggest that *P.* sp. 1stricta is a Pacific species with recent migration, and that the ancestor to *Polysiphonia* sp. (AY958168 and AY958169) and the *Polysiphonia stricta* (Mertens ex Dillwyn) Greville genetic groups (sp.1, sp.2, sp.3) seeded the Atlantic *P. stricta* genetic groups 4.132 Ma (min and max 95% HPD estimates of 2.208 and 6.778; Fig. 2.2D). We note that node support was lacking for this clade, meaning the above scenario should be interpreted with caution.

Phycodrys **(one pre-Pleistocene Pacific-to-Atlantic event; Figs. 2.2E, C16, and C17)**

Though *Phycodrys* is apparently widespread, it also suffers from polyphyly, indicating that taxonomic study is needed (Fig. 2.2E, Fig. C17). Regardless, a clear North Pacific/Atlantic clade occurs in this genus, distinct from lineages reported in the southern hemisphere (Fig. C17). The most parsimonious scenario for this group requires the ancestor to *Phycodrys rubens* (Linnaeus) Batters, *Phycodrys* sp. 1NB, *Phycodrys fimbriata* (Kuntze) Kylin, and *Phycodrys riggii* N.L.Gardner to have migrated from the Pacific to the Atlantic basin (which subsequently yielded *P. rubens* and *P.* sp. 1NB), followed by a secondary migration event of Pacific *P. fimbriata* into the Northwest Atlantic. Indeed, a similar scenario is hypothesized by van Oppen *et al.* (1995), though, lacking records of *P. fimbriata* from the North Pacific, they interpreted *P. fimbriata* as a secondary post-glacial migration event into the Northwest Atlantic (the unique Eastern Arctic/Northwest Atlantic *P. fimbriata* sequences presented here suggest *P. fimbriata*

survived glaciation in the Northwest Atlantic; Fig. C16). Alternatively, it is also possible the ancestor to *P. fimbriata* and *P. riggii* migrated into the Atlantic, with subsequent backflow of *P. fimbriata* into the Pacific basin, which would represent another trans-Arctic speciation event, though this scenario requires an additional trans-Arctic event in *Phycodrys*. As such, we tentatively forward the first scenario; population level data in trans-Arctic *P. fimbriata* are needed to further clarify the above details.

***Polyostea* (one pre-Pleistocene Pacific-to-Atlantic event; Figs. 2.2F and C18)**

Polyostea represents another genus dominated by Pacific species (Savoie & Saunders 2018). The single Atlantic species *Polyostea arctica* (J.Agardh) Savoie & G.W.Saunders appears to have diverged from a Pacific lineage including *Polyostea bipinnata* (Postels & Ruprecht) Ruprecht, *Polyostea* sp. 1Nome, and *Polyostea hamata* (E.S.Sinova) Savoie & G.W.Saunders approximately 6.396 Ma (min and max 95% HPD estimates of 4.026, 9.162), suggesting this event occurred prior to the Pleistocene.

***Ptilota* (one pre-Pleistocene Pacific-to-Atlantic event; Figs. 2G, S19, and S20)**

Ptilota is another genus predominantly composed of Pacific species, with only two genetically verified in the North Atlantic (*Ptilota gunneri* P.C.Silva, Maggs, & L.M.Irvine and trans-Arctic *Ptilota serrata* Kützing; Bruce & Saunders, 2016). The topology of the tree suggests at an Arctic crossing approximately 5.648 Ma (min and max 95% HPD estimates of 3.754 and 7.790), yielding *P. gunneri*, which appears to be restricted to Atlantic and Arctic waters (Saunders & McDevit 2013). This interpretation assumes recent migration of *P. serrata* from the Pacific into the Atlantic. Alternatively, and similar to *Phycodyrs*, *Ptilota sloanii* Bruce & G.W.Saunders could be interpreted as

backflow from the Atlantic, if *P. serrata* is derived from an Atlantic ancestor, however, this scenario proposes an additional trans-Arctic migration event as compared to the first scenario forwarded. We also note that the ML analysis failed to resolve the topology presented in Fig. 2G.

***Vertebrata* (Figs. 2.2H, C21, and C22)**

Another member of the tribe Polysiphonieae, species of *Vertebrata* occur throughout the Northern and Southern hemispheres, with few species in the North Pacific (Savoie & Saunders 2018). Most of the Atlantic species group together in this genus, suggesting at a long history in the North Atlantic (Fig. 2.2H). The grouping of *Vertebrata lanosa* (Linnaeus) T.A.Christensen with North Pacific species is weakly supported by the Bayesian analysis, but the ML analysis does not support this topology (Fig. C22). In short, *Vertebrata* does not currently show evidence of trans-Arctic speciation events.

Discussion

Trans-Arctic interchange of species since the opening of the Bering Strait is believed to have played a major role in the establishment of current day northern marine flora and fauna. In addition, the "species pump" hypothesis asserts that Pleistocene glaciation promoted speciation by repeatedly isolating populations over the past 2.6 Ma. Here, we have attempted to confirm the timing of putative trans-Arctic speciation events in marine red macroalgae to assess whether these events post-date the opening of the

Bering Strait, and if these events are notably greater in frequency during the Pleistocene in support of the "species pump" hypothesis.

Before continuing, inherent uncertainty in the estimation of divergence times must be addressed. Uncertainty in divergence time estimates in the analyses presented here manifested as inconsistency between Bayesian and ML analyses (e.g. tree topology differed), poor node support in some cases, and broad ranges in the divergence time estimates themselves. Indeed, the broad divergence time estimates largely preclude confident assessment of the relative frequency of speciation events that occurred during the Pleistocene, as compared to speciation events prior to glaciation but following the opening of the Bering Strait (Fig. 2.3). Uncertainty in the relative frequency of speciation events is somewhat mediated here by "sampling" multiple trans-Arctic lineages, but nonetheless, the results presented here remain suggestive. Furthermore, the range in molecular clocks applied here across a broad range of taxa (i.e. Florideophyceae) will undoubtedly be inaccurate in some cases (saturation estimates suggested the rate of COI-5P evolution in Ceramiales was considerably higher than in the Gigartinales, from which the clock was derived; Fig. C1), though we attempted to address molecular clock assumptions by relaxing this constraint where rate heterogeneity was detected. On a positive note, our timed phylogenies appeared to accommodate independent geological time events (possible movement of an ancestor through the Proto-Caribbean Seaway in *Melanothamnus*; Fig. 2.3), and were consistent with previously hypothesized scenarios of dispersal through the Bering Strait (see discussion below), meaning the molecular clocks forwarded here are likely within the actual range. Nonetheless, it is important to emphasize that all the scenarios presented

here are strictly hypotheses, though it seems reasonable to forward some as more likely than others (in cases where node support is consistent between Bayesian and ML analyses, and/or cases where the range of divergence time estimates for a given species fall predominantly into the Pliocene or Pleistocene). Such is the nature of inferring past processes that cannot be directly tested. Improvements to the results presented here, such as the calibration of alternate markers or improved data resolution through genomic level datasets (e.g. Jackson *et al.* 2017), are therefore inevitable and eagerly anticipated. Some general conclusions, however, can be drawn from the phylogenies presented here.

Time-calibrated phylogenies are in agreement with previous studies that suggest dispersal through the Bering Strait has played an important role for speciation in several trans-Arctic lineages of marine macroalgae. For instance, the ancestor to *Palmaria palmata* is hypothesized to have crossed the North American Arctic following the opening of the Bering Strait (Lindstrom *et al.* 1996), which is in close agreement with our time calibrated phylogeny for Palmariales (Fig. 1B). Similar hypotheses have been forwarded to explain the presence of *Dilsea* and *Phocodrys* in the North Atlantic (Lindstrom 2001; van Oppen *et al.* 1995), which are also in agreement with the time calibrated phylogenies presented here (Figs. 2.1D and 2.2E). Lindstrom (1987) emphasized the importance of biogeographic tracks (e.g. consistent results between lineages) to asserting whether or not dispersal through the Bering Strait played a critical role in establishing Arctic and temperate North Atlantic flora. Thirty years later, these tracks have been sufficiently laid to confidently assert the opening of the Bering Strait represented a major biogeographic event in the establishment of contemporary Arctic and Northwest Atlantic marine macroalgae (Fig. 2.3). A similar history of biotic

interchange between the Atlantic and Pacific through the Bering Strait is expected to have played a significant role structuring biogeographic distributions in other marine taxa. Indeed, similar results have already emerged in other marine flora (Olsen *et al.* 2004) and fauna (Bigg *et al.* 2008; Carr *et al.* 2011, Hardy *et al.* 2011). The opening of the Bering Strait therefore appears to have played a significant role structuring contemporary boreal and temperate marine coastal communities.

These results further support the view that Pacific-to-Atlantic speciation events were far more common than Atlantic-to-Pacific events. The results presented here indicated that Pacific-to-Atlantic speciations following the opening of the Bering Strait occurred at a rate of 11:1 compared to Atlantic-to-Pacific speciations (Fig. 2.3). This Pacific-to-Atlantic bias has remained practically unchanged since the beginning of investigations on the Bering Strait and its impact on the phylogeographic history of northern flora and fauna (Briggs 1970; Vermeij 1978; Lindstrom 1987, 2001; Reid 1990; Coyer *et al.* 2011, and references therein). Several explanations have been forwarded to explain this bias. For one, the Pacific basin is much older compared to the Arctic and Atlantic basins (Lawver *et al.* 1990), and as such, more evolutionary lineages have become established in the Pacific. Holding enriched species diversity, the Pacific is more likely to serve as the origin center for new lineages crossing the Arctic. In addition, the predominant motion of water has been West to East through the Arctic for approximately the past 4.6 Ma (Haug & Tiedemann 1998), which may have enhanced asymmetric dispersal pathways in marine macroalgae through the Arctic. Vermeij (1991) favoured an ecological opportunity hypothesis to explain marine mollusk distributions that similarly displayed a Pacific bias in Northwest Atlantic fauna. This

hypothesis asserts that invaders are proportional to extinction rates in a region; if true, it may be that ecological niches were regularly left vacant in the Northwest Atlantic due to relatively harsher glaciation conditions, facilitating the establishment of Pacific flora and fauna, though this hypothesis is discordant with the timeframes for speciation events forwarded here (Fig. 2.3). More recently, thermogeographic modelling has indicated that Arctic and Atlantic sub-Arctic species have continually been derived from the North Pacific due to Pleistocene climate and geography (Adey *et al.* 2008; Adey & Hayek 2011). A combination of factors likely played a role in the establishment of Pacific lineages in the Atlantic since the opening of the Bering Strait, and phylogeographers will undoubtedly continue to unravel these processes.

Dispersal through the Bering Strait may have played an important role in diversification of Arctic and North Atlantic flora, but the "species pump" *sensu* Haffer (1969) did not find support in our analyses. Speciation events did occur during the Pleistocene, however, there was no obvious bias for trans-Arctic speciation events to have occurred during this time (Fig. 2.3). In other words, speciation through the Bering Strait in the absence of glaciation appears to be just as common as speciation during the Pleistocene (if the number of events is standardized by the length of the timeframes). This implies that speciation facilitated by an opened Bering Strait is a sufficient explanation for the phylogeographic patterns reported here, with the "species pump" offering little additional explanatory power. In particular, multiple trans-Arctic speciation events within a genus are notably absent during the Pleistocene. Though this is not a criterion for the "species pump" (as this hypothesis applies to the potential for all species diversity to further diversify), the lack of an amplifying effect to speciation

during the Pleistocene suggests populations were not regularly isolated on either side of the Bering Strait, or were not isolated for long enough periods of time to develop reproductive isolation. We suggest that secondary contact between trans-Arctic refugial populations inhibited the speciation process. This is suggested by the large portion of lineages analysed here with trans-Arctic species (n=7/14, not including potential introductions; Figs. 2.1 and 2.2), indicating dispersal across the North American Arctic is common (at least in contemporary populations). In addition, secondary contact in the Canadian Arctic by vicariant populations is evident in *Saccharina latissima* (Linnaeus) C.E.Lane, C.Mayes, Druehl & G.W.Saunders (McDevit & Saunders 2010; Neiva *et al.* 2017) and in *Scagelia pylaisaei* (Montagne) M.J.Wynne (Bruce unpublished). In another study assessing the applicability of the "species pump," increased gene flow during glaciation in island systems (due to land bridges) was forwarded as a mechanism preventing vicariant speciation in a species of cricket (Papadopoulou & Knowles 2015). The dilution of divergence through secondary contact is likely facilitated by the slow rate of mutation estimated for marine macroalgae (approximately 0.75%/Ma for COI-5P, see methods), meaning divergent populations are likely not reproductively isolated if/when they come into contact. This could be particularly true for brown macroalgae, as they appear to evolve slower compared to red lineages (Bringloe & Saunders 2018; Smith 2015). On a final note, glacial cycles occurred every 41 ka for most of the Pleistocene, but increased in duration during the last 700 ka (100 ka cycles; Lisiecki & Raymo 2005; Miller *et al.* 2010). This raises the possibility that trans-Arctic populations did not have the potential to develop reproductive isolation until the late Pleistocene, in which case, it is possible a "species pump" indeed emerged but insufficient time has

passed for species diversity to notably increase as a result. If true, the more recent speciation events reported here could be interpreted as priming the "species pump" (e.g. *Dilsea*, *Devaleraea*, *Melanothamnus*, *Odonthalia*, and possibly *Phycodrys*), and contemporary trans-Arctic populations may be the seed for future speciation events. In sum, the "species pump" is perhaps more like a "species pulse" as applied to trans-Arctic lineages of marine macroalgae. Unoccupied niches in the North Atlantic were possibly filled by Pacific lineages following the opening of the Bering Strait and various glacial retreats, leading to long term establishment and speciation. Subsequent population divergence due to glaciation events were likely ephemeral as evolution was slow and secondary contact was apparently common during interglacial periods. If a trans-Arctic "species pump" is invoked, it may apply to speciation events during the late Pleistocene but has contributed little to contemporary species diversity. Population level datasets in trans-Arctic species of marine macroalgae are needed to confirm if admixture is common in the Canadian Arctic, and will additionally help resolve some of the speciation scenarios outline above (e.g. *Ahnfeltia*, *Coccotylus*, *Dilsea*, *Odonthalia*, *Phycodrys*, *Ptilota*, *Rhodomela*).

Conclusions

A few more limitations warrant mentioning. The interpretations of phylogenies presented here were drawn under the principle of parsimony. More complex scenarios (involving more than one migration event across the Arctic, or sympatric speciation followed by migration and extinction of a given species in the parental basin) could have occurred (e.g. *Phycodrys*). Indeed, the scenarios presented here are certainly incomplete, as now-extinct species may have played an important role. Given extinct species are

more likely to have emerged during the Pliocene (since this is an earlier timeframe, and as such, more time has passed wherein extinction might occur), the number of Pliocene speciation events may be underestimated here. As such, conclusions regarding the species pump, if anything, are bolstered by this shortcoming. Unsampled extant species, similarly, have the potential to change interpretations of the phylogenies. Despite these inherent limitations, the role of the Bering Strait and biotic interchange between the Pacific and the Atlantic has captured the attention of biologists for nearly half a century (Briggs 1970; Lindstrom 1987, 2001), and our understanding of this phenomenon has certainly improved during this time. Here, time-calibrated phylogenies confirmed that Pacific to Atlantic speciation events post-dating the opening of the Bering Strait were common in trans-Arctic lineages of marine macroalgae. Despite this, the "species pump" hypothesis does not appear to be applicable during the Pleistocene given the lack of amplification in species diversity. The putative slow rate of evolution in marine macroalgae and hypothesized regularity of secondary contact between divergent trans-Arctic lineages likely inhibit the speciation process. While Pleistocene glaciation clearly has played a major role in structuring contemporary populations of marine macroalgae, its role has likely been limited in the emergence of these species.

Acknowledgements

We thank the many people who facilitated the collection of specimens, particularly Dr. Meghann Bruce and Dr. Kyatt Dixon; Dr. Ken Dunton at the University of Texas for facilitating our sampling in the Beaufort (Northern Alaska); Dr. Kjersti Sjøtun at the University of Bergen for facilitating our sampling in Norway; Don Stiles and James Horner for facilitating the collection of samples in Nome, Alaska. We also

thank everyone who helped generate data, particularly Tanya Moore. Collections of marine plants in Nome, Alaska, were approved through the State of Alaska Department of Fish and Game (Permit No. CF-17-004). This project was funded by the Northern Scientific Training Program, the Natural Sciences & Engineering Research Council of Canada through an NSERC Post-Graduate Scholarship to T.T. Bringloe and a Discovery Grant (170151-2013) to G.W. Saunders, and the New Brunswick Innovation Foundation.

References

Adey WH, Hayek LAC (2011) Elucidating marine biogeography with macrophytes: quantitative analysis of the North Atlantic supports the Thermogeographic Model and demonstrates a distinct subarctic region in the Northwestern Atlantic. *Northeastern Naturalist*, **18**, 1–128.

Adey WH, Lindstrom SC, Hommersand MH, Müller KM (2008) The biogeographic origin of Arctic endemic seaweeds: a thermogeographic view. *Journal of Phycology*, **44**, 1384–1394.

April J, Hanner RH, Dion-Côté AM, Bernatchez L (2013) Glacial cycles as an allopatric speciation pump in north-eastern American freshwater fishes. *Molecular Ecology*, **22**, 409–422.

Bigg GR, Cunningham CW, Ottersen G, Pogson GH, Wadley MR, Williamson P (2008) Ice-age survival of Atlantic cod: agreement between paleoecology models and genetics. *Proceedings of the Royal Society B*, **275**, 163-172.

Briggs JC (1970) A faunal history of the North Atlantic Ocean. *Systematic Zoology*, **19**, 19–34.

Bringloe TT, Saunders GW (2018) Mitochondrial DNA sequence data reveal the origins of postglacial marine macroalgal flora in the Northwest Atlantic. *Marine Ecology Progress Series*, **589**, 45–58.

Bruce M, Saunders GW (2016) A molecular-assisted investigation of diversity, biogeography and phylogenetic relationships for species of *Neoptilota* and *Ptilota* (Wrangeliaceae, Rhodophyta) reported along Canadian coasts. *Phycologia*, **56**, 36–53.

Carr CM, Hardy SM, Brown TM, Macdonald TA, Hebert PDN (2011) A Tri-oceanic perspective: DNA barcoding reveals geographic structure and cryptic diversity in Canadian Polychaetes. *PLoS ONE*, **6,** e22232.

Clarke A, Crame JA (1992) The Southern Ocean benthic fauna and climate change: a historical perspective. *Philosophical Transactions of the Royal Society B: Biological Sciences*, **338**, 299–309.

Coates AG, Stallard RF (2013) How old is the Isthmus of Panama? *Bulletin of Marine Science*, **89**, 801–813.

Coyer JA, Hoarau G, Schaik JV, Luijckx P, Olsen JL (2011) Trans-Pacific and trans-Arctic pathways of the intertidal macroalga *Fucus distichus* L. reveal multiple glacial refugia and colonizations from the North Pacific to the North Atlantic. *Journal of Biogeography*, **38**, 756-771.

Coyne J, Orr HA (2004) Allopatric and Parapatric Speciation. In: *Speciation*, pp. 83–124.

Drummond AJ, Ho SYW, Phillips MJ, Rambaut A (2006) Relaxed phylogenetics and dating with confidence. *PLoS Biology*, **4**, e88

Drummond AJ, Suchard MA, Xie D, Rambaut A (2012) Bayesian phylogenetics with BEAUti and the BEAST 1.7. *Molecular Biology and Evolution*, **29**, 1969–1973.

Fraser CI, Nikula R, Waters JM (2011) Oceanic rafting by a coastal community. *Proceedings of the Royal Society B*, **278**, 649−655.

Freshwater DW, Rueness J (1994) Phylogenetic relationships of some European *Gelidium* (Gelidiales, Rhodophyta) species, based on *rbc*L nucleotide sequence analysis. *Phycologia* **33**, 187–194.

Geoffroy A, Destombe C, Kim B, Mauger S, Raffo MP, Kim MS, Le Gall L (2016). Patterns of genetic diversity of the cryptogenic red alga *Polysiphonia morrowii* (Ceramiales, Rhodophyta) suggest multiple origins of the Atlantic populations. *Ecology and Evolution*, **6**, 5635–5647.

Gladenkov AY, Oleinik AE, Marincovich L Jr., Barinov KB. (2002) A refined age for the earliest opening of Bering Strait. *Palaeogeography, Palaeoclimatology, Palaeoecology*, **183**, 321–328.

Graham L, Wilcox L (2000b) Ochrophytes IV: Chrysomedidaleans, Phaeothamniophyceans, Tribophyceans, and Phaeophyceans. In *Algae*. Prentice Hall, Upper Saddle River, p 301–341.

Haffer J (1969) Speciation in Amazonian forest birds. *Science*, **165**, 131-137.

Hardy SM, Carr CM, Hardman M, Steinke D, Corstorphine E, Mah C (2011) Biodiversity and phylogeography of Arctic marine fauna: insights from molecular tools. *Marine Biodiversity*, **41**, 195–210.

Haug GH, Tiedemann R (1998) Effect of the formation of the Isthmus of Panama on Atlantic Ocean thermohaline circulation. *Nature*, **393**, 673–676.

Hughey JR, Hommersand MH, Gabrielson PW, Miller KA, Fuller T (2017) Analysis of the complete plastomes of three species of *Membranoptera* (Ceramiales, Rhodophyta) from Pacific North America. *Journal of Phycology*, **53**, 32–43.

Jackson C, Salomaki ED, Lane CE, Saunders GW (2017) Kelp transcriptomes provide robust support for interfamilial relationships and revision of the little known Arthrothamnaceae (Laminariales). *Journal of Phycology*, **53**, 1–6.

Kearse M, Moir R, Wilson A, *et al.* (2012). Geneious Basic: An integrated and extendable desktop software platform for the organization and analysis of sequence data. *Bioinformatics*, **28**, 1647–1649.

Kim MS, Yang EC, Mansilla A, Boo SM (2004) Recent introduction of *Polysiphonia marrowii* (Ceramiales, Rhodophyta) to Punta Arenas, Chile. *Botanica Marina*, **47**, 389–394.

Knapp, S, Mallet J (2003) Refuting refugia? *Science*, **300**, 71–72.

Kumar S, Stecher G, Tamura K (2016) MEGA7: Molecular Evolutionary Genetics Analysis version 7.0 for bigger datasets. *Molecular Biology and Evolution*, **33**, 1870–1874.

Laughinghouse HD, Müller KM, Adey WH, Lara Y, Young R, Johnson G (2015) Evolution of the northern rockweed, *Fucus distichus*, in a regime of glacial cycling: implications for benthic algal phylogenetics. *PloS One*, **10**, e0143795.

Lawver L, Müller R, Srivastava S, Roest W (1990) The opening of the Arctic Ocean. In Bleil U, Thiede J (eds) *Geological History of the Polar Oceans: Arctic vs Antarctic.* Kluwer Academic Publishers, Netherlands, p 29–62.

Le Gall L, Saunders GW (2010) DNA barcoding is a powerful tool to uncover algal diversity: a case study of the phyllophoraceae (Gigartinales, Rhodophyta) in the Canadian flora. *Journal of Phycology*, **46**, 374–389.

Li JJ, Hu ZM, Duan DL (2015) Genetic data from the red alga *Palmaria palmata* reveal a mid-Pleistocene deep genetic split in the North Atlantic. *Journal of Biogeography*, **42**, 902–913.

Li JJ, Hu ZM, Liu RY, Zhang J, Liu SL, Duan DL (2016) Phylogeographic surveys and apomictic genetic connectivity in the North Atlantic red seaweed *Mastocarpus stellatus*. *Molecular Phylogenetics and Evolution*, **94**, 463–472.

Lindstrom SC (1987) Possible sister groups and phylogenetic relationships among selected North Pacific and North Atlantic Rhodophyta. *Helgoländer Meeresunters*, **41**, 245–260.

Lindstrom SC (2001) The Bering Strait connection: dispersal and speciation in boreal macroalgae. *Journal of Biogeography*, **28**, 243–251.

Lindstrom SC, Hughey JR, Martone PT (2011) New, resurrected and redefined species of *Mastocarpus* (Phyllophoraceae, Rhodophyta) from the northeast Pacific. *Phycologia*, **50**, 661–683.

Lindstrom SC, Olsen JL, Stam WT (1996) Recent radiation of the Palmariaceae (Rhodophyta). *Journal of Phycology*, **32**, 457–468.

Lisiecki LE, Raymo ME (2005) A Pliocene-Pleistocene stack of 57 globally distributed benthic $\delta^{18}O$ records. *Paleoceanography and Paleoclimatology*, **20**, 1–17.

Loeza-Quintana T, Adamowicz SJ (2018) Iterative calibration: a novel approach for calibrating the molecular clock using complex geological events. *Journal of Molecular Evolution*, **86**, 118–137.

Macaya EC, Lopez B, Tala F, Tellier F, Thiel M (2016) Float and raft: role of buoyant seaweeds in the phylogeography and genetic structure of non-buoyant associated flora. In: Hu ZM, Fraser C (eds) *Seaweed phylogeography: adaptation and evolution of seaweeds under environmental change*. Springer, Dordrecht, p 97−130.

Marincovich L Jr (2000) Central American paleogeography controlled Pliocene Arctic Ocean molluscan migrations. *Geology*, **28**, 551–554.

Marincovich L Jr, Gladenkov AY (1999) Evidence for an early opening of the Bering Strait. *Nature*, **397**, 149–151.

McDevit DC, Saunders GW (2010) A DNA barcode examination of the Laminariaceae (Phaeophyceae) in Canada reveals novel biogeographical and evolutionary insights. *Phycologia*, **49**, 235–248.

Miller GH, Brigham-Grette J, Alley RB, *et al.* (2010) Temperature and precipitation history of the Arctic. *Quaternary Science Reviews*, **29**, 1679–1715.

Milstein D, Saunders GW (2012) DNA barcoding of Canadian Ahnfeltiales (Rhodophyta) reveals a new species – *Ahnfeltia borealis* sp. nov. *Phycologia*, **51**, 247–259.

Mols-Mortensen A, Neefus CD, Pedersen PM, Brodie J (2014) Diversity and distribution of foliose Bangiales (Rhodophyta) in West Greenland: a link between the North Atlantic and North Pacific. *European Journal of Phycology*, **49**, 1–10.

Neiva J, Paulino C, Nielsen MM, *et al.* (2017) Glacial vicariance drives phylogeographic diversification in the amphi-boreal kelp *Saccharina latissima*. *Scientific Reports*, **8**, 1112.

Nikula R, Strelkov P, Väinölä R (2007) Diversity and trans-arctic invasion history of mitochondrial lineages in the North Atlantic *Macoma balthica* complex (Bivalvia: Tellinidae). *Evolution*, **61**, 928–941.

Olsen JL, Stam WT, Coyer JA (2004) North Atlantic phylogeography and large-scale population differentiation of the seagrass *Zostera marina* L. *Molecular Ecology*, **13**, 1923-1941.

van Oppen MJH, Draisma SGA, Olsen JL, Stam WT (1995) Multiple trans-Arctic passages in the red alga *Phycodrys rubens*: evidence from nuclear rDNA ITS sequences. *Marine Biology*, **123**, 179–188.

Papadopoulou A, Knowles LL (2015) Genomic tests of the species-pump hypothesis: Recent island connectivity cycles drive population divergence but not speciation in Caribbean crickets across the Virgin Islands. *Evolution*, **69**, 1501–1517.

Papadopoulou A, Knowles LL (2017) Linking micro- and macroevolutionary perspectives to evaluate the role of Quaternary sea-level oscillations in island diversification. *Evolution*, **71**, 2901–2917.

Rambaut A, Suchard MA, Xie D, Drummond AJ (2014) Tracer v1.6. http: //tree.bio.ed.ac.uk/software/tracer/.

Raymo ME (1994) The initiation of northern hemisphere glaciation. *Annual Review of Earth and Planetary Sciences*, **22**, 353–383.

Reid DG (1990) Trans-Arctic migration and speciation induced by climatic change: the biogeography of *Littorina* (Mollusca: Gastropoda). *Bulletin of Marine Science*, **47**, 35–49.

Rothman MD, Mattio L, Anderson RJ, Bolton JJ (2017) A phylogeographic investigation of the kelp genus *Laminaria* (Laminariales, Phaeophyceae), with emphasis on the south Atlantic Ocean. *Journal of Phycology*, **53**, 778–789.

Saunders GW (2008) A DNA barcode examination of the red algal family Dumontiaceae in Canadian waters reveals substantial cryptic species diversity. 1. The foliose *Dilsea – Neodilsea* complex and *Weeksia*. *Botany*, **86**, 773–789.

Saunders GW, McDevit DC (2012a). Methods for DNA barcoding photosynthetic protists emphasizing the macroalgae and diatoms. *Methods in Molecular Biology*, **858**, 207–222.

Saunders GW, McDevit DC (2012b) Acquiring DNA sequence data from dried archival red algae (Florideophyceae) for the purpose of applying available names to contemporary genetic species: a critical assessment. *Botany*, **90**, 191–203.

Saunders GW (2014) Long distance kelp rafting impacts seaweed biogeography in the northeast Pacific: the kelp conveyor hypothesis. *Journal of Phycology*, **50**, 968–974.

Saunders GW, Jackson C, Salomaki ED (2018) Phylogenetic analyses of transcriptome data resolve familial assignments for genera of the red-algal Acrochaetiales-Palmariales Complex (Nemaliophycidae). *Molecular Phylogenetics and Evolution*, **119**, 151–159.

Saunders GW, McDevit DC (2013) DNA barcoding unmasks overlooked diversity improving knowledge on the composition and origins of the Churchill algal flora. *BMC Ecology*, **13**, 1–23.

Saunders GW, Moore TE (2013) Refinements for the amplification and sequencing of red algal DNA barcode and RedToL phylogenetic markers: a summary of current primers, profiles and strategies. *Algae*, **28**, 31–43.

Savoie AM, Saunders GW (2015) Evidence for the introduction of the Asian red alga *Neosiphonia japonica* and its introgression with *Neosiphonia harveyi* (Ceramiales, Rhodophyta) in the Northwest Atlantic. *Molecular Ecology*, **24**, 5927–5937.

Savoie AM, Saunders GW (2018) A molecular assessment of species diversity and generic boundaries in the red algal tribes Polysiphonieae and Streblocladieae (Rhodomelaceae, Rhodophyta) in Canada. *European Journal of Phycology*.

Schoville SD, Roderick GK, Kavanaugh DH (2012) Testing the "Pleistocene species pump" in alpine habitats: lineage diversification of flightless ground beetles (Coleoptera: Carabidae: *Nebria*) in relation to altitudinal zonation. *Biological Journal of the Linnean Society*, **107**, 95–111.

Smith DR (2015) Mutation rates in plastid genomes: they are lower than you might think. *Genome Biology and Evolution*, **7**, 1227–1234.

Stamatakis A (2006) RAxML-VI-HPC: maximum likelihood-based phylogenetic analyses with thousands of taxa and mixed models. *Bioinformatics*, **22**, 2688-2690.

Tajima F (1993) Simple methods for testing the molecular evolutionary clock hypothesis. *Genetics*, **135**, 599–607.

Tamura K, Nei M (1993) Estimation of the number of nucleotide substitutions in the control region of mitochondrial DNA in humans and chimpanzees. *Molecular Biology and Evolution*, **10**, 512–526.

Vermeij GJ (1978) Patterns of biotic history. In *Biogeography and adaptation: patterns of marine life*, pp. 207–241.

Vermeij GJ (1991) Anatomy of an invasion: the trans-Arctic interchange. *Paleobiology*, **17**, 281–307.

Vermeij GJ, Roopnarine PD (2008) The coming Arctic invasion. *Science*, **321**, 780–781.

Wilson NG, Schrödl M, Halanych KM (2009) Ocean barriers and glaciation: evidence for explosive radiation of mitochondrial lineages in the Antarctic sea slug *Doris kerguelenensis* (Mollusca, Nudibranchia). *Molecular Ecology*, **18**, 965–984.

Wynne MJ, Saunders GW (2012) Taxonomic assessment of North American species of the genera *Cumathamnion*, *Delesseria*, *Membranoptera* and *Pantoneura* (Delesseriaceae, Rhodophyta) using molecular data. *Algae*, **27**, 155–173.

Xia X (2017) DAMBE6: new tools for microbial genomics, phylogenetics, and molecular evolution. *Journal of Heredity*, **108**, 431–437.

Zuccarello GC, West JA (2002) Phylogeography of the *Bostrychia calliptera-B. pinnata* complex (Rhodomelaceae, Rhodophyta) and divergence rates based on nuclear, mitochondrial and plastid DNA markers. *Phycologia*, **41**, 49–60.

Table 2.1. Primers used for amplification and sequencing of various genes in marine macroalgae. Primer sequence portions underlined and in bold for M13LF3 and M13Rx forward and reverse primers, respectively, refer to sequencing primers (M13F and M13R).

Locus	Taxa	Primers	Primer sequence (5'-3')	Reference/thermocycling regime
COI-5P	Red algae	M13LF3	**TGTAAAACGACGGCCAGT**ACHAAYCAYAARGATATHGG	Saunders and Moore (2013)
		M13Rx	**CAGGAAACAGCTATGAC**ACTTCTGGRTGICCRAARAAYCA	
	Coccotylus	GWSFn	TCAACAAAYCAYAAAGATATYGG3	Le Gall and Saunders (2010)
		GWSRx	ACTTCTGGRTGICCRAARAAYCA	Saunders and McDevit (2012b)
	Devaleraea	DevF1	CAGGAGTTATTGGAGGYTGT	Newly developed. Thermocycling regime followed Saunders and Moore (2013)
		M13Rx	**CAGGAAACAGCTATGAC**ACTTCTGGRTGICCRAARAAYCA	
*rbc*L-3P	Red algae	F57	GTAATTCCATATGCTAAAATGGG	Freshwater and Rueness (1994) Saunders and Moore (2013)
		rbcLrevNEW	ACATTTGCTGTTGGAGTYTC	
ITS	*Ahnfeltia*	P1	GGAAGGAGAAGTCGTAACAAGG	Saunders and Moore (2013)
		G4	CTTTTCCTCCGCTTATTGATATG	
	Odonthalia	P1	GGAAGGAGAAGTCGTAACAAGG	Newly developed. Thermocycling regime followed Saunders and Moore (2013)
		OdenG4	CTTTTCCTCCGCTTAATTATATG	
	Phycodrys	P1	GGAAGGAGAAGTCGTAACAAGG	Newly developed. Thermocycling regime followed Saunders and Moore (2013)
		PhyG4	CTTTTCCTGCGCTTAATAATATG	
	Rhodomela	RLycF1	TAGGGGTACAGTGGTCTCAC	Newly developed. Thermocycling regime followed Saunders and Moore (2013)
		RLycR1	GAATCATTCGTCCTAAACGTC	

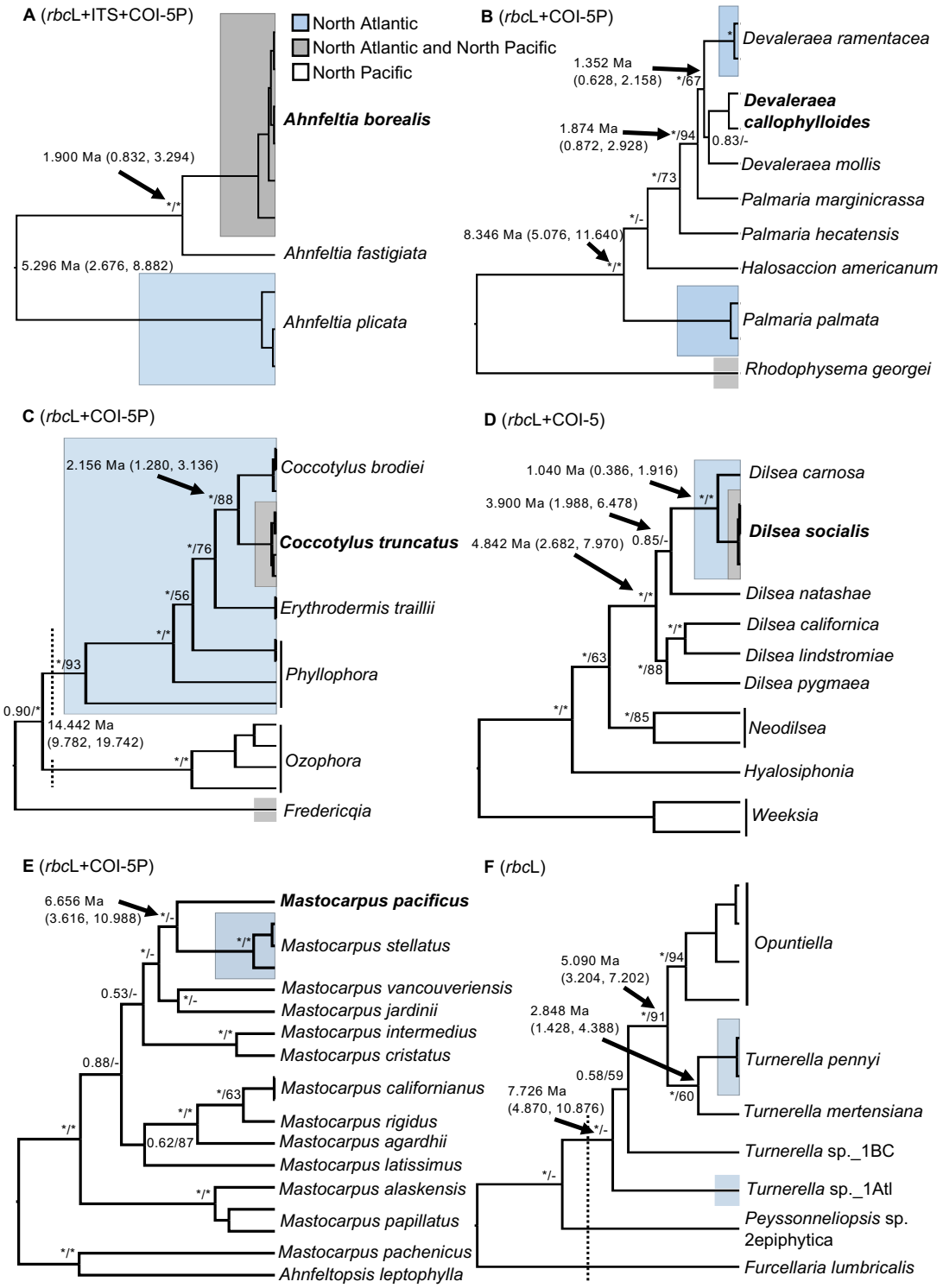

Figure 2.1 Trans-Arctic genera of the orders Ahnfeltiales, Palmariales, and Gigartinales (Florideophyceae). Bayesian phylogenetic trees are presented for: A) *Ahnfeltia*; B) *Devaleraea*, *Halosaccion,* and *Palmaria*; C) *Coccotylus*, *Erythrodermis*,

***Phyllophora*, and *Ozophora*; D) *Dilsea*, *Hyalosiphon*, and *Neodilsea*; E) *Mastocarpus*; and F) *Opuntiella* and *Turnerella.* Support values are presented at each node for posterior probabilities and Maximum-Likelihood bootstrap support, respectively. Nodes with greater than 0.95 posterior probability and/or 95% Maximum-Likelihood bootstrap support are indicated by an asterisk; nodes with less than 0.5 posterior probability and/or 50% bootstrap support are indicated with a negative symbol. *Rbc*L saturation is indicated with a dashed line. Species genetically verified from the Northern Bering Sea are indicated with bold type.**

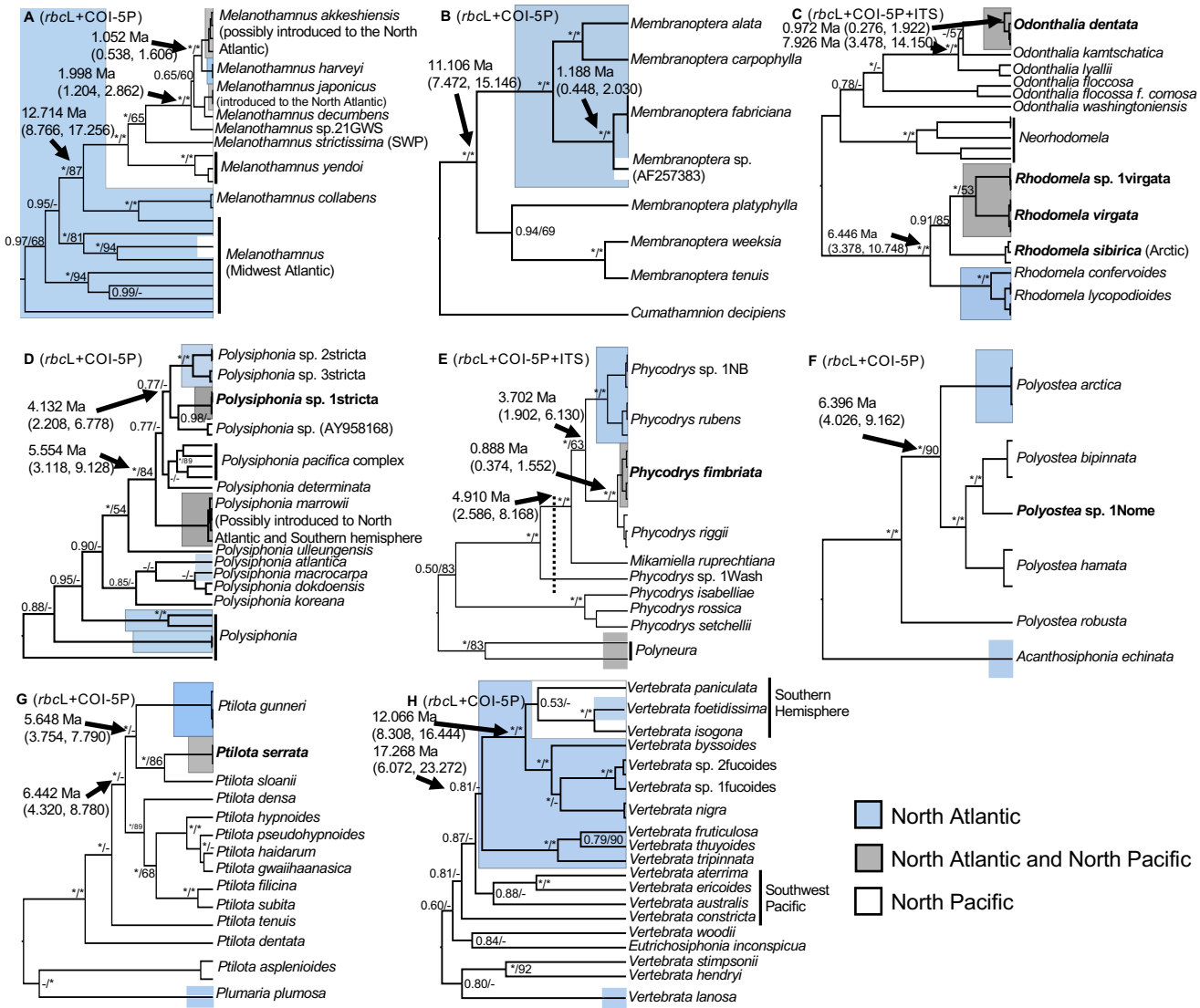
A (rbcL+COI-5P)
1.052 Ma (0.538, 1.606)
1.998 Ma (1.204, 2.862)
12.714 Ma (8.766, 17.256)
Melanothamnus akkeshiensis (possibly introduced to the North Atlantic)
Melanothamnus harveyi
Melanothamnus japonicus (introduced to the North Atlantic)
Melanothamnus decumbens
Melanothamnus sp.21GWS
Melanothamnus strictissima (SWP)
Melanothamnus yendoi
Melanothamnus collabens
Melanothamnus (Midwest Atlantic)
B (rbcL+COI-5P)
11.106 Ma (7.472, 15.146)
1.188 Ma (0.448, 2.030)
Membranoptera alata
Membranoptera carpophylla
Membranoptera fabriciana
Membranoptera sp. (AF257383)
Membranoptera platyphylla
Membranoptera weeksia
Membranoptera tenuis
Cumathamnion decipiens
C (rbcL+COI-5P+ITS)
0.972 Ma (0.276, 1.922)
7.926 Ma (3.478, 14.150)
6.446 Ma (3.378, 10.748)
Odonthalia dentata
Odonthalia kamtschatica
Odonthalia lyallii
Odonthalia floccosa
Odonthalia flocossa f. comosa
Odonthalia washingtoniensis
Neorhodomela
Rhodomela sp. 1virgata
Rhodomela virgata
Rhodomela sibirica (Arctic)
Rhodomela confervoides
Rhodomela lycopodioides
D (rbcL+COI-5P)
4.132 Ma (2.208, 6.778)
5.554 Ma (3.118, 9.128)
Polysiphonia sp. 2stricta
Polysiphonia sp. 3stricta
Polysiphonia sp. 1stricta
Polysiphonia sp. (AY958168)
Polysiphonia pacifica complex
Polysiphonia determinata
Polysiphonia marrowii
(Possibly introduced to North Atlantic and Southern hemisphere
Polysiphonia ulleungensis
Polysiphonia atlantica
Polysiphonia macrocarpa
Polysiphonia dokdoensis
Polysiphonia koreana
Polysiphonia
E (rbcL+COI-5P+ITS)
3.702 Ma (1.902, 6.130)
0.888 Ma (0.374, 1.552)
4.910 Ma (2.586, 8.168)
Phycodrys sp. 1NB
Phycodrys rubens
Phycodrys fimbriata
Phycodrys riggii
Mikamiella ruprechtiana
Phycodrys sp. 1Wash
Phycodrys isabelliae
Phycodrys rossica
Phycodrys setchellii
Polyneura
F (rbcL+COI-5P)
6.396 Ma (4.026, 9.162)
Polyostea arctica
Polyostea bipinnata
Polyostea sp. 1Nome
Polyostea hamata
Polyostea robusta
Acanthosiphonia echinata
G (rbcL+COI-5P)
5.648 Ma (3.754, 7.790)
6.442 Ma (4.320, 8.780)
Ptilota gunneri
Ptilota serrata
Ptilota sloanii
Ptilota densa
Ptilota hypnoides
Ptilota pseudohypnoides
Ptilota haidarum
Ptilota gwaiihaanasica
Ptilota filicina
Ptilota subita
Ptilota tenuis
Ptilota dentata
Ptilota asplenioides
Plumaria plumosa
H (rbcL+COI-5P)
12.066 Ma (8.308, 16.444)
17.268 Ma (6.072, 23.272)
Vertebrata paniculata
Vertebrata foetidissima
Vertebrata isogona
Vertebrata byssoides
Vertebrata sp. 2fucoides
Vertebrata sp. 1fucoides
Vertebrata nigra
Vertebrata fruticulosa
Vertebrata thuyoides
Vertebrata tripinnata
Vertebrata aterrima
Vertebrata ericoides
Vertebrata australis
Vertebrata constricta
Vertebrata woodii
Eutrichosiphonia inconspicua
Vertebrata stimpsonii
Vertebrata hendryi
Vertebrata lanosa
Southern Hemisphere
Southwest Pacific
North Atlantic
North Atlantic and North Pacific
North Pacific

Figure 2.2 Trans-Arctic genera of the order Ceramiales. Phylogenetic trees are presented for: A) *Melanothamnus*; B) *Membranoptera*; C) *Odonthalia, Neorhodomela, and Rhodomela*; D) *Polysiphonia*; E) *Phycodrys*; F) *Polyostea*; G) *Ptilota*; and H) *Vertebrata*. Support values are presented at each node for posterior probabilities and Maximum-Likelihood bootstrap support, respectively. Nodes with greater than 0.95 posterior probability and/or 95% bootstrap support are indicated by an asterisk; nodes with less than 0.5 posterior probability and/or 50% bootstrap support are indicated with a negative symbol. Species genetically verified from the Northern Bering Sea are indicated with bold type.

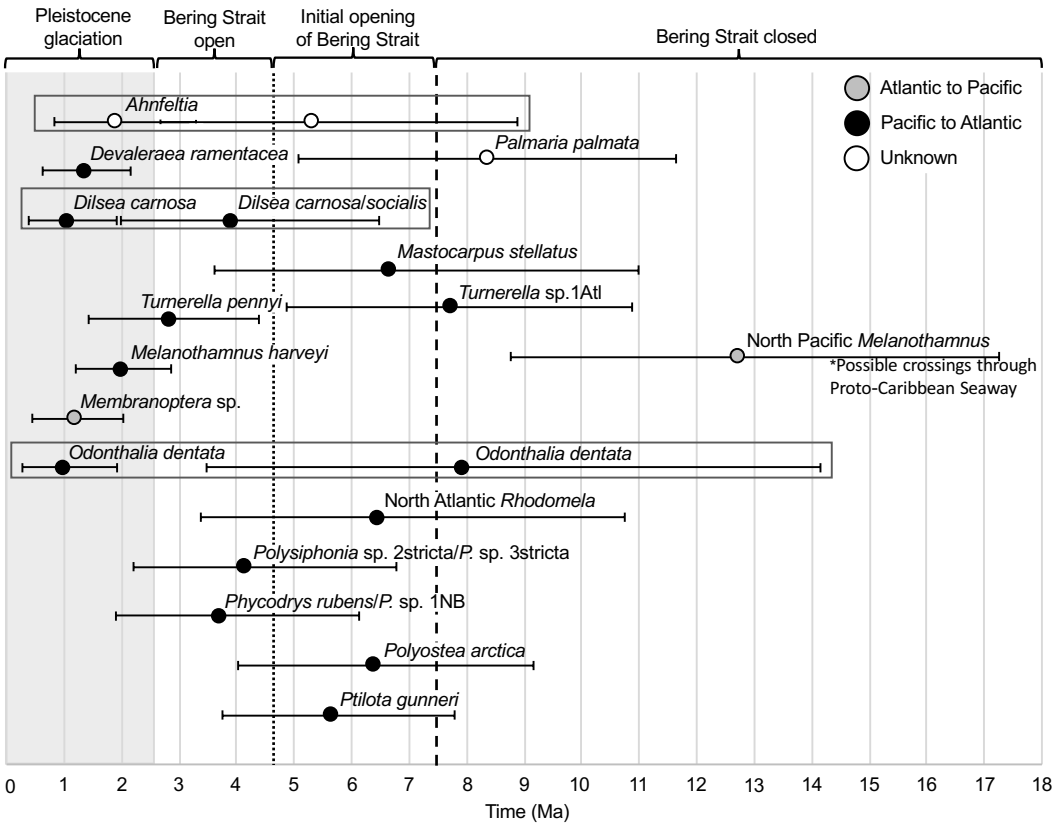

Figure 2.3 Divergence time estimates in species of Florideophyceae (Rhodophyta) that are hypothesized to have undergone trans-Arctic migration and subsequent speciation. The shaded area indicates the time frame for the Pleistocene (e.g. glaciation cycles present). The square dot line indicates the latest hypothesized opening of the Bering Strait; the dashed line indicates the earliest hypothesized opening of the Bering Strait (Gladenkov *et al.* 2002). Error bars represent 95% minimum and maximum highest posterior density estimates. Species names refer to the lineage established from a trans-Arctic speciation event. Events in grey boxes should be interpreted as a single event (either the event occurred earlier or later in time).

Chapter 3 Mitochondrial DNA sequence data reveal the origins of postglacial marine macroalgal flora in the Northwest Atlantic

Citation for published manuscript: Bringloe TT, Saunders GW (2018) Mitochondrial DNA sequence data reveal the origins of postglacial marine macroalgal flora in the Northwest Atlantic. *Marine Ecology Progress Series*, **589**, 45-58.

Abstract: Following the Last Glacial Maximum, marine macroalgal flora in the Northwest (NW) Atlantic reportedly recolonized from Northeast (NE) Atlantic refugia. Genetic evidence for the few species tested, however, has indicated that some species survived glaciation in the NW Atlantic. Owing to the substantial amount of data currently available, we sought to determine if COI-5P (5' end of the cytochrome *c* oxidase subunit I gene) could distinguish between populations surviving glaciation on both sides of the Atlantic versus postglacial recolonization. COI-5P results were consistent with published findings using other markers in *Chondrus crispus*, *Mastocarpus stellatus*, *Palmaria palmata*, and *Saccharina latissima*. Having success, we then analyzed molecular data for several species of red and brown macroalgae to date isolation times between NE and NW Atlantic populations and determine what percentage of species survived in NW Atlantic refugia. We generated and gathered genetic data from COI-5P in 1560 specimens representing 20 amphi-Atlantic species, and estimated isolation times between NE and NW populations using calibrated red and brown COI-5P clocks in IMa2. Of the species surveyed, 60% had isolation time estimates between NE and NW Atlantic populations predating the Last Glacial Maximum. Recent shared ancestry was inferred in the remaining cases. Our results indicate that local refugia and/or trans-Arctic migration from the Pacific are the source populations for the majority of the NW Atlantic macroalgal flora. By shedding light on the phylogeographic history of the North Atlantic, we can better understand the nature of postglacial recolonization and forecast future changes to the NW Atlantic and Canadian Arctic.

Introduction

Glaciation events undoubtedly had a major influence on present-day biota and biogeographic distributions. In the North Atlantic, glaciation events resulted in ice sheets covering most of the northern coastlines, displacing or extirpating local populations repeatedly over the past ~2.6 million years (Myr) (Miller *et al.* 2010a). Recent climate change, however, is accelerating warming in the Arctic and potentially allowing southerly biota to move northward, particularly marine species (Vermeij & Roopnarine 2008; Miller *et al.* 2010b; IPCC 2014; Renaud *et al.* 2015). Macroalgae act as ecosystem engineers, providing food and habitat for other species (Christie *et al.* 2009) and are known to raft invertebrate taxa across large oceanic distances (Fraser *et al.* 2011; Macaya *et al.* 2016). As such, macroalgae can be used to predict future changes in marine species distributions along boreal and Arctic shorelines in light of diminishing perennial ice cover (Jueterbock *et al.* 2016). By understanding the origins of Arctic macroalgae, we may be able to better predict northward movement of larger-scale communities of marine species.

Understanding the origins of marine algae in the Canadian Arctic begins with understanding the origins of the Northwest (NW) Atlantic flora. Arctic species of algae are traditionally believed to be a northward range extension of cold-adapted species on the east coast of Canada (Taylor 1957; Lee 1973). Meanwhile, the prevalent understanding of the NW Atlantic marine flora was that it was extirpated during the Last Glacial Maximum (LGM), and subsequently repopulated from Northeast (NE) Atlantic populations (Vermeij 1978; Ingolfsson 1992). If true, then Arctic marine algae would have recent origins stemming from European populations. Extirpation of the NW

Atlantic flora during glaciation was predicated on several factors, namely, (1) the paleoclimatic history of the NW Atlantic was much harsher as compared to the NE Atlantic (Knott & Hoskins 1968; Pflaumann *et al.* 2003), (2) constricted isotherms and a lack of suitable substrate south of the Laurentide Ice Sheet (Vermeij 1978, Ingolfsson 1992; Maggs *et al.* 2008), and (3) species lists indicated that the NW Atlantic flora appeared to be a subset of NE species, with few endemics to the NW Atlantic (Taylor 1957; South 1983; Ingolfsson 1992). The 'tabula rasa' hypothesis, the notion that all NW Atlantic flora and fauna are the result of postglacial recolonizations, has since undergone substantial scrutiny with the advent of molecular data (Brochmann *et al.* 2003).

A surge in genetic data and mathematical modeling is shedding new light on the phylogeographic origins of algal communities (e.g. Hu *et al.* 2016). This surge in data has been partly propelled by the DNA barcoding movement, which utilizes a 664 bp fragment of the 5' end of the cytochrome *c* oxidase subunit I (COI-5P) gene to assign specimens to previously sequenced and identified species (Saunders 2005; Le Gall & Saunders 2010). The accumulating data can be used to make inferences regarding the phylogeographic history of the North Atlantic, such as examining allelic diversity to test the 'tabula rasa' hypothesis or determining if certain populations survived in refugia. These contrasting scenarios are expected to have left distinct signatures in the genetics of amphi-Atlantic populations of marine macroalgal species. If the NE or NW Atlantic flora was reestablished by its neighboring basin within the past 10 thousand years (ka), there should be little to no genetic divergence between amphi-Atlantic populations (Li *et al.* 2016a, their Fig. 12.1); directionality of recolonization may be inferred depending on

the resolution of the data. In particular, recently established populations should represent a subset of the allelic diversity found in parental populations (Maggs *et al.* 2008). If macroalgal flora survived in refugia on both sides of the Atlantic, this should appear as divergent lineages between NE and NW Atlantic populations (Li *et al.* 2016a, their Fig. 12.1).

Genetic studies into the phylogeographic history of amphi-Atlantic marine flora and fauna suggest that both scenarios commonly occurred. Wares & Cunningham (2001) used COI data to conclude that four species of intertidal invertebrates in the NW Atlantic recolonized from Europe since the LGM, while two species appeared to have survived the most recent glaciation event. In addition, the authors pointed out several species of intertidal invertebrates endemic to the NW Atlantic with sister species in European waters, further suggesting that these species survived repeated glaciation in the NW Atlantic (Wares & Cunningham 2001). Genetic studies on amphi-Atlantic species of macroalgae are revealing a similarly mixed picture. Macroalgal species for which genetic data are consistent with recent recolonization of the NW Atlantic from the NE include *Mastocarpus stellatus* (Stackhouse) Guiry (*cox2-3*, ITS, and RLS data; Li *et al.* 2016b), *Porphyra umbilicalis* Kützing (ITS, 18S; Teasdale & Klein 2010), *Fucus spiralis* Linnaeus, and *F. vesiculosis* Linnaeus (microsatellite data and mtIGS, Coyer *et al.* 2011a). Interpretations of phylogeographic patterns in *Chondrus crispus* Stackhouse vary; Hu *et al.* (2010) concluded that this species recolonized the NW Atlantic postglacially, whereas Hu *et al.* (2011) and Provan & Maggs (2012) concluded that this species survived in NW Atlantic refugia. Recent findings in other species indicate that populations survived on both sides of the Atlantic during the LGM, including

Ascophyllum nodosum (Linnaeus) Le Jolis (two microsatellites and mtIGS and *trn*W; Olsen *et al.* 2010), *F. distichus* Linnaeus (mtIGS and COI-5P; Coyer *et al.* 2011b), *Palmaria palmata* (Linnaeus) F.Weber & D.Mohr (*cox2-3* and plastid *rpl-rps* data; Li *et al.* 2015), and *Saccharina latissima* (Linnaeus) C.E.Lane, C.Mayes, Druehl & G.W.Saunders (COI-5P and microsatellites; Neiva *et al.* 2018). In a survey of the Arctic flora in Churchill (Canada), Saunders & McDevit (2013) found that of six species for which limited amphi-Atlantic COI-5P data were available, four showed distinct haplotypes between the NW and NE Atlantic.

In light of these recent studies, the 'tabula rasa' hypothesis regarding NW Atlantic marine macroalgae can clearly be rejected in favor of a more nuanced picture, wherein some species survived glaciation in the NW Atlantic while others did indeed migrate recently out of the NE Atlantic. To our knowledge, no macroalgal species are recorded recolonizing the NE Atlantic from the NW. Given the vast amount of DNA barcode data that has accumulated over the past decade (Saunders 2005), we decided to (1) determine if COI-5P was a suitable proxy for inferring whether or not a given species may have recolonized the NW Atlantic since the LGM or if the species survived in refugia, and (2) screen COI-5P data in 20 amphi-Atlantic species of macroalgae to quantify the percentage of species that appear to have survived glaciation in the NW Atlantic (as evidenced by divergent NE and NW Atlantic populations) versus the percentage of species that may have recent origins in the NE Atlantic (as evidenced by low divergence times estimates between NE and NW Atlantic populations). While we do not make inferences about population history beyond isolation times (e.g. estimating migration vectors and effective population sizes), we hope that our broad approach to

inferring the origins of NW Atlantic flora will lead to more detailed analyses that will enhance our understanding of phylogeographic patterns in specific species, particularly in cases where NW and NE populations are closely related and the directionality of putative postglacial recolonization remains uncertain.

Methods

Sampling and sequencing of macroalgae

In order to infer whether or not NW Atlantic populations of marine algae are the result of survival in glacial refugia, and identify cases where ancestry is recent between NE and NW Atlantic populations, macroalgae were sampled from Europe and 487–664 bp of COI-5P data were compared from European populations to existing and newly generated COI-5P records from the NW Atlantic. We specifically sampled the area surrounding Bergen, Norway (3–14 June 2016), and various locations in the NW Atlantic (2014–2016; specimen information available online, doi: dx.doi.org/10.5883/DS-PGCSW). Specimens were collected from the intertidal and subtidally via scuba, and occasionally via dredge in Norway. Specimens were stored in plastic bags and returned to the lab for processing, which consisted of assigning a specimen ID and storing a cm^2 portion of tissue in silica for DNA extraction with pressed material prepared as representative vouchers (Saunders & McDevit 2012a). Collections were supplemented with available records from the Barcode of Life Datasystem and from publicly available data available on GenBank (Appendix D, Table D1; doi: dx.doi.org/10.5883/DS-PGCSW).

DNA extraction and amplification procedures were followed as per Saunders & McDevit (2012b), using a Qiagen TissueLyser II and QIAxtractor robot for high-throughput protocols for COI-5P amplification. The red algal primers M13LF3 (5'-TGTAAAACGACGGCCAGTACHAAYCAYAARGATATHGG-3') and M13Rx (5'-CAGGAAACAGCTATGACACTTCTGGRTGICCRAARAAYCA -3'; Saunders & Moore 2013) and the brown algal primers GazF2 (5'-CCAACCAYAAAGATATWGGTAC-3') and GazR2 (5'-GGATGACCAAARAACCAAAA-3') were used (Lane *et al.* 2007). The primers GWSFn (5'-TCAACAAAYCAYAAAGATATYGG-3'; Le Gall & Saunders 2010) and GWSRx (5'-ACTTCTGGRTGICCRAARAAYCA-3'; Saunders & McDevit 2012a) were used for some specimens of the red algal genus *Coccotylus*. Our thermocycling regime consisted of an initial temperature of 94°C for 2 min; 5 cycles of 94°C for 30 s, 45°C for 30 s, and 72°C for 1 min; 35 cycles of 94°C for 30 s, 46.5°C for 30 s, and 72°C for 1 min; and a final elongation step of 72°C for 5 min (Saunders & Moore 2013). PCR products were visualized using gel electrophoresis on an 0.8% agarose gel. Successful PCR products were sent to Genome Quebec for forward and reverse sequencing using the sequencing primers M13F (5'-TGTAAAACGACGGCCAGT-3') and M13R (5'-CAGGAAACAGCTATGAC-3'; Saunders & Moore 2013) for red algae (with the exception of *Coccotylus* specimens, which were sequenced using GWSFn and GWSRx primers) and GazF2 and GazR2 for brown algae. All genetic data were edited in Geneious version 8.0 (www.geneious.com; Kearse *et al.* 2012).

Haplotype networks and maps

The population structure of North Atlantic populations was visualized using COI-5P haplotype maps and networks. Species were included in the analyses if they were not listed as being introduced (e.g. moved between NE and NW Atlantic basins by human activity) and we had at least five sequences for a given species from both sides of the Atlantic; see Appendix D, Table D2 for amphi-Atlantic species not meeting these criteria and subsequently removed from the dataset). The cut-off for pooling divergent populations was a maximum pairwise distance of 2% between haplotypes except in the case of *Ceramium virgatum* Roth given the exceptionally wide and continuous range of haplotypes sampled. We also ignored alpha taxonomy, in particular pooling data for *Dilsea carnosa* (Schmidel) Kuntze and *D. socialis* (Postels & Ruprecht) Perestenko given that they were within the 2% threshold for genetic relatedness. Haplotype networks were visualized using TCS v1.21 (Clement *et al.* 2000), and haplotype maps and networks were created in PowerPoint. TCS was also used to assign a putative ancestral haplotype for each species (Castelloe & Templeton 1994). The majority of the COI-5P haplotype maps and networks can be found in Appendix D, Figs. D1–D18.

Assessment of COI-5P as a proxy for glacial survival or postglacial recolonization

In order to determine if COI-5P was a reliable proxy for recent population history in the North Atlantic, we compared our results to detailed findings in *Chondrus crispus* (Hu *et al.* 2010, 2011, Provan & Maggs 2012), *Mastocarpus stellatus* (Li *et al.* 2016b), *Palmaria palmata* (Li *et al.* 2015), and *Saccharina latissima* (Neiva *et al.* 2018).

Dating divergence times

Isolation times were estimated in amphi-Atlantic species of red and brown algae that met our selection criteria. We began this process by calibrating separate red and brown algal COI-5P clocks, and calculating minimum, medium, and maximum rate estimates for each clock. The red algal COI-5P mutation rate was estimated using the pooled NE and NW Atlantic divergence time of 0.906 Myr in *P. palmata* (owing to an error confusing divergence rate with mutation rate, the isolation times reported by Li. *et al*. [2015] were doubled), which was estimated using mitochondrial *cox2-3* and plastid *rpl-rps* markers (Li *et al.* 2015). This clock was initially calibrated using divergence estimates in *Bostrychia calliptera* (Montagne) Montagne and *B. pinnata* J.Tanaka & Chihara, and a calibration point of the closing of the Isthmus of Panama 3–3.5 Myr ago (Zuccarello & West 2002). In order to estimate the COI-5P mutation rate, 20 COI-5P haplotypes (661 bp) from *P. palmata* were analyzed in BEAST 1.8.3 (Drummond *et al.* 2012) using the following parameters: an HKY substitution model (given this model would be used in IMa2 analyses); a strict clock; a coalescent Bayesian skyline tree prior (Drummond *et al.* 2005); an UPGMA starting tree; a prior for the root height of the tree set to a mean of 906 ka with a normal distribution truncated around 696 and 1432 ka (as per pairwise population minimum and maximum isolation time estimates of Li *et al.* 2015), and a standard deviation of 100; and uninformative (e.g. uniform) priors for base frequencies, kappa, and population size parameters. A 10 million length chain was run with sampling every 1000 steps. The analysis was completed five times, and combined results were viewed in Tracer v1.6.0 (Rambaut *et al.* 2014) with a burn-in of 1 million steps for each analysis. The combined results provided a final HKY clock rate of 0.007

substitutions site^{-1} Myr^{-1} (95% highest posterior density estimates of 0.00298 and 0.01169, which acted as minimum and maximum rate estimates in our IMa2 analyses, see below). The brown algal COI-5P mutation rate was estimated based on a 10–16 Myr divergence time in *Fucus vesiculosis* and *Ascophyllum nodosum*. This divergence time had been previously estimated using two independent approaches: (1) indirectly based on a *psbA* clock calibration in diatoms (Hoarau *et al.* 2007), and (2) calibration using fossil record evidence (Silberfeld *et al.* 2010; Cánovas *et al.* 2011). Due to a lack of known haplotypes in these species, F84 genetic distance was calculated between a single COI-5P sequence from each species using the dnadist program in PHYLIP v.3.695 (Felsenstein 1989). The resulting F84 distance (0.063582) was divided by two (0.031791), and then by 10, 13, and 16 for fast, medium, and slow HKY clock rate estimates of 0.0031791, 0.002446, and 0.001987 substitutions site^{-1} Myr^{-1}. These clocks were subsequently converted to locus-wide substitution rates yr^{-1} for IMa2 analyses, which consisted of multiplying the HKY clock rate by the species-specific COI-5P bp length and dividing by 1 million.

Isolation times between NE and NW Atlantic populations were calculated in IMa2, a program that uses a Bayesian search strategy and coalescent theory to estimate population parameters (Hey 2010). With regards to our prediction, we were only interested in isolation times between populations, and ran strictly isolation models. Once the run parameters (priors, heating terms) were optimized, three independent 1 million length chains were run for each species using an HKY substitution model, and geometric heating (10 chains), with sampling every 100 steps, for a total of 10 000 genealogies saved per run. The results from the three species-specific runs were

combined using L mode, and the highest value of the posterior distribution after smoothing was used as the isolation time estimate between NE and NW basins. Convergence on estimates was assessed based on consistency between first and second halves of runs, the consistency of values across the three independent runs, and visual inspection of the posterior probability distributions for isolation time estimates (Appendix D, Fig. D19). The above analysis was run for each clock estimate (minimum, medium, and maximum rates; Appendix D, Table D3).

A given species was considered to have divergent NE and NW Atlantic lineages if the lower 95% highest posterior density estimate for isolation times predated the LGM (20 ka). The population history of a given species was otherwise considered recent between NE and NW basins if estimates of isolation times postdated the LGM. Evident migrant and/or Arctic populations occurred in some species, and so isolation times between NE and NW Atlantic populations were timed with and without these populations, and the estimates without putative migrant populations were used in our final estimates as described above. Canadian Arctic populations were considered as specimens from sub-Arctic Labrador (Makkovik) and northwards. We elaborate briefly on haplotype distributions in Table 3.1.

Results

We accumulated COI-5P records for 1560 specimens, 550 of which were generated during this study (2014–2016). These specimens represented five species of brown algae and 15 species of red algae, several of which represent multiple genetic groups (numbers in species names are used to indicate this; Table 3.1). The most COI-

5P haplotypes sampled for a given species was 51 (in the case of *Ceramium virgatum*, Fig. D2), while the fewest haplotypes sampled for a given species was two (*Polysiphonia* sp. 2stricta, Fig. D12). On average, the number of haplotypes sampled for a given species was 10, of which six tended to be singletons (e.g. sampled only once).

Our results for COI-5P were in agreement with previous population studies in *Chondrus crispus* (Hu *et al.* 2010, 2011; Provan & Maggs 2012), *Mastocarpus stellatus* (Li *et al.* 2016b), *Palmaria palmata* (Li *et al.* 2015), and *Saccharina latissima* (Neiva *et al.* 2018). *Chondrus crispus* generally shares haplotypes with European populations, although endemic haplotypes have been detected in the NW Atlantic (ITS and COI-5P: Hu *et al.* 2010; *trn*I, two single copy nuclear genes, eight microsatellites: Provan & Maggs 2012). We similarly recovered two unique haplotypes in the NW Atlantic (Fig. D3), but estimated the divergence time between the NE and NW population to be approximately 10 ka (Table 3.1). It is worth noting that Hu *et al.* (2011) also estimated divergence times between the NE and NW Atlantic based solely on COI-5P data using a slower clock rate of 0.0034 substitutions site^{-1} Myr^{-1}; they estimated the time of divergence between the NW Atlantic and Ireland to be 43 ka, and the divergence time between the NW Atlantic and Portugal (not sampled in our study) to be 193 ka. We reanalyzed our COI-5P data in *C. crispus* using the same clock rate as Hu *et al.* (2011) and received a divergence time estimate of 46 ka. *Mastocarpus stellatus* is considered to have recolonized the NW Atlantic following the LGM based on ITS, *cox2-3*, and plastid RuBisCo spacer (RLS) markers; our IMa2 analyses were consistent with these findings, with an estimated divergence time of 11 ka (Table 3.1). *Palmaria palmata* reportedly survived multiple glaciations in the NW Atlantic, a conclusion based on *cox2-3* and

plastid *rpl-rps* data (Li *et al.* 2015); our COI-5P data similarly indicated a genetic break between NE and NW populations, with IMa2 analyses indicating a divergence time estimate between NE and NW Atlantic populations of 1040 ka (Table 3.1). Finally, Neiva *et al.* (2018) identified several divergent lineages in *S. latissima* in the Pacific, NE and NW Atlantic, a result congruent between COI-5P and 12 microsatellite markers; our analysis of just COI-5P data yielded a divergence time estimate between NE and NW Atlantic populations of 1416 ka. ITS data also suggest there is contemporary migration of Pacific and European phylogroups into the NW Atlantic (McDevit & Saunders 2010).

Regarding the 20 species we surveyed, 12 species (60%) exhibited trans-Atlantic isolation time estimates predating the LGM (Table 3.1). This result was consistent between slow-, medium-, and fast-evolving COI-5P clocks, with the exception of *Euthora cristata* (C.Agardh) J.Agardh, which had a lower 95% HPD estimate of 6 ka in the fast-evolving analysis (Table D3). *Odonthalia dentata* (Linnaeus) Lyngbye is presented as an example species for the 12 cases where NE and NW Atlantic populations exhibited divergent lineages. In the case of *O. dentata*, NW and NE populations are reciprocally monophyletic, with six hypothesized haplotypes occurring between NE and NW clades (Fig. 3.1A), and an isolation time of 662 ka between basins. Isolation time estimates in species with divergent NE and NW Atlantic populations generally occurred within the past 800 ka, but extended as far back as 1416 ka (in the case of *S. latissima*; Table 3.1, Fig 3.2).

Forty percent of the species surveyed had estimated isolation times postdating the LGM (Fig. 3.2). Of these species, one is previously confirmed as having recolonized the NW Atlantic out of the NE (*M. stellatus*; Li *et al.* 2016b). *Coccotylus brodiei*

(Turner) Kützing is used as our representative species for this scenario (Fig. 3.1B). *Coccotylus brodiei* has a putative ancestral allele that is common in Norway, while NW Atlantic populations are a subset of NE Atlantic haplotypes and are dominated by a sister haplotype to the putative ancestral allele (Fig. 3.1B). Three species wherein isolation estimates were recent (e.g. postglacial) had extremely low haplotype diversity (a single haplotype dominating both sides of the Atlantic; *Laminaria digitata* [Hudson] J.V.Lamouroux [Fig. D16], *Polyides rotundus* [Hudson] Gaillon [Fig. D11], and *Polysiphonia* sp. 2stricta [Fig. D12]).

Four species appeared to have migrant populations from Europe into the NW Atlantic or Canadian Arctic (*Alaria esculenta* [Linnaeus] Greville [Fig. D14], *Ceramium virgatum* [Fig. D2], *Rhodomela lycopodioides* (Linnaeus) C.Agardh [Fig. D13]), and/or had distinct Arctic populations not matching NW or NE Atlantic populations (*A. esculenta* [Fig. D14], *S. latissima* [Fig. D18]). Isolation times in these species were timed with and without these putative migrant/Arctic populations. Results were generally the same, except in the case of *R. lycopodioides*, wherein the isolation time was much greater when an Arctic sequence was removed from the NW Atlantic population (24 ka with putative migrant population, 464 ka without, though 95% HPD intervals overlapped).

Discussion

The hypothesis that the NW Atlantic marine flora was mostly recolonized from the NE Atlantic following the LGM (Vermeij 1978; Ingolfsson 1992) is no longer tenable in light of repeated DNA-based studies, including the trans-Atlantic survey

presented herein. Given that a variety of population scenarios likely occurred, we sought to quantify the number of species with genetic patterns consistent with survival in refugia in the NW Atlantic (namely divergence between NE and NW Atlantic populations) using COI-5P data; species with low divergence times between populations (e.g. <20 ka) would likely indicate recent shared ancestry between basins, although details such as the directionality of recolonization will require more in-depth population genetic analyses. By studying 20 species in tandem, we hope to comment on broad-scale patterns across species and improve on current understanding of postglacial recolonization in the North Atlantic and its impact on biodiversity distributions.

COI-5P as a proxy for glacial survival or postglacial recolonization

We began by examining whether or not COI-5P was a suitable proxy for distinguishing between the two contrasting population histories under question (i.e. postglacial shared ancestry between NE and NW Atlantic populations, and survival on both sides of the Atlantic in glacial refugia). COI-5P patterns were consistent with other genetic markers used in more detailed population genetic studies in four of our target species (*Chondrus crispus, Mastocarpus stellatus, Palmaria palmata,* and *Saccharina latissima*). Indeed, the consistent genetic break between NE and NW Atlantic populations in *P. palmata* detected in *cox2-3*, *rpl-rps* (Li *et al.* 2015), and our own COI-5P data were the basis for the calibration of our red algal molecular clock. COI-5P was also able to assign the correct population scenario of recent shared ancestry between NE and NW Atlantic populations in *M. stellatus* (Li *et al.* 2016b). Interestingly, molecular data show consistent patterns across genomes in *C. crispus* (Hu *et al.* 2010, 2011; Provan & Maggs 2012), but conclusions as to whether or not this species recolonized

the NW Atlantic following the LGM varied across studies. Our analysis indicated that ancestry is recent between NE and NW Atlantic basins, despite a small number of rare endemic haplotypes to the NW Atlantic that may point to NW refugial populations (Hu *et al.* 2011; Provan & Maggs 2012). Li *et al.* (2016a) estimated migration vectors in *C. crispus* and found that trans-Atlantic dispersal likely occurred between Ireland and the NW Atlantic. It therefore seems reasonable to expect that both scenarios contributed to postglacial NW Atlantic populations of *C. crispus* (Table 3.1). Genomic-level datasets may be needed to confidently resolve whether or not *C. crispus* survived in glacial refugia in the NW Atlantic and where these refugia occurred. It is worth reemphasizing that the COI-5P data were consistent overall with the results from microsatellite data, and nuclear (ITS, single copy nuclear regions), plastid (RLS, *rpl-rps*), and other mitochondrial genes (*cox2-3, trn*I) for these four species in all studies published to date.

We also note the critical importance of a reliably calibrated molecular clock for estimations of population divergence times. This is evidenced by the discrepancy in isolation time estimates between our present study and that of Hu *et al.* (2011) for *C. crispus*. Hu *et al.* (2011) calibrated their COI-5P clock using an isolation time between *C. crispus* and congeners in the North Pacific, and a calibration time of 3.5 Myr. The resulting clock rate (0.34% Myr^{-1}, 2× slower than our clock estimate of 0.7% Myr^{-1}), yielded an estimated divergence time between Irish and NW Atlantic populations of 43 ka (Hu *et al.* 2011), a result we replicated in our IMa2 analyses using the same clock rate. Differing clock rates were therefore the crux between determining if NW Atlantic populations survived the LGM or otherwise had very recent shared ancestry with European populations. We believe our red algal COI-5P clock rates are more accurate

for several reasons. For one, our red algal clock was indirectly calibrated from markers calibrated using the closing of the Isthmus of Panama (Zuccarello & West 2002); the estimated closing time of the Isthmus is likely more accurate than estimations of the opening time of the Bering Strait (Gladenkov *et al.* 2002; Coates & Stallard 2013), and the cessation of gene flow likely coincides closer to the closing of the Isthmus of Panama than the congruency between the opening of the Bering Strait and the initiation of gene flow (e.g. species may not have speciated out of the Pacific into the Atlantic immediately after the Bering Strait opened). In addition, the rate of mitochondrial evolution in red algae appears to be greater than the rate in Ochrophyta (the Phylum containing brown algae; Smith 2015), a finding in agreement with our rate estimations.

We also tested a range of clock rates in both red and brown algal lineages, all of which yielded consistent results (Table D3). The notable exception was *Euthora cristata*, which had a shallow phylogenetic break between NE and NW Atlantic populations (Table 3.1, Fig. 3.2). While the break suggests that these populations are indeed isolated, a fast clock scenario (>1% change Myr^{-1}) could not exclude more recent divergence dates between populations (<20 ka). Given the uncertainty surrounding the rate estimates for COI-5P evolution, a transition period is expected wherein the range of divergence time estimates cannot definitively exclude one scenario over another (recent shared ancestry between the NW and NE Atlantic, or glacial survival in the NW Atlantic). While our estimates of divergence dates certainly side with glacial survival of *E. cristata* in the NW Atlantic, additional markers will be needed to further resolve its population history.

Glacial survival in the NW Atlantic: the rule, not the exception

Having established COI-5P as a reasonable proxy for our two population scenarios, we went on to consider broad-scale patterns regarding the phylogeographic history of the North Atlantic by amalgamating general patterns in 20 trans-Atlantic species. While it is generally accepted that some species of macroalgae survived glaciation in the NW Atlantic while others likely recolonized from the NE Atlantic, it is not clear if one scenario is more common than the other. Premolecular hypotheses favored a postglacial migration hypothesis (Vermeij 1978; Ingolfsson 1992); however, emerging molecular studies have challenged this paradigm (Li *et al.* 2016a). Our results indicate that possibly 60% of the NW Atlantic marine flora survived the LGM, as evidenced by isolation times between NE and NW Atlantic populations predating 20 ka (Fig. 3.1, Table 3.1). Such a scenario was exemplified in *Odonthalia dentata* (Fig. 3.1A). In this case, a putative ancestor likely migrated into the Atlantic from the North Pacific, where several species of *Odonthalia* occur, sometime since the Bering Strait opened (Lindstrom 1987, 2001; Wynne & Heine 1992). This ancestor subsequently became established along NE and NW Atlantic coasts and has possibly undergone incipient speciation, as evidenced by the deep COI-5P divergence among NE and NW Atlantic populations (Figs. 3.1A & 3.2). Phylogeographic analyses are needed to fully resolve the origins of this species and its current taxonomic status in the North Atlantic, but prior to this study, there was no reason to question the assumption that this species represented a single population/species in the North Atlantic.

The deep lineage splits in several of the species studied here, particularly in *O. dentata* (Fig. 3.1A), *P. palmata* (Fig. D8), *Phycodrys rubens* (Linnaeus) Batters (Fig.

D10), *Pylaiella* sp. 2littoralis (Fig. D17), *Rhodomela lycopodioides* (Fig. D13), and *S. latissima* (Fig. D18), warrant taxonomic investigation. Presumably the NE and NW Atlantic populations are on their way to speciation. Most of these species have isolation times greater than *Dilsea carnosa* and *D. socialis*, which have haplotype variation similar to the abovementioned species, and yet they are recognized as two separate species (Saunders 2008; Fig. 3.2). Note, however, that COI-5P divergence alone does not indicate that populations of the above species have reached reproductive isolation on either side of the Atlantic. Additional markers and detailed molecular analyses are needed to determine if these populations are separate species, or if previously recognized amphi-Atlantic sister species are simply divergent populations (e.g. *D. socialis/carnosa*). Either way, this discussion further highlights that endemism, either at the population or species level, is far greater in the NW Atlantic than previously realized (Fig. 3.2).

Our results highlight important questions regarding the origins of NW Atlantic macroalgal species. Firstly, our results suggest that marine refugia were more readily available in the NW Atlantic than previously thought. Reconstructions of past sea-surface conditions suggest that the Grand Banks off Newfoundland remained unglaciated (Pflaumann *et al.* 2003; Maggs *et al.* 2008), while genetic evidence in several marine and terrestrial species indicates the presence of a refugium near Nova Scotia (Coyer *et al.* 2011b and references therein; Einfeldt *et al.* 2017). Indeed, COI-5P variation in *Ceramium virgatum* indicates that refugia likely existed in these locations (Fig. D2). Given the lack of suitable substrate and constricted isotherms south of the Laurentide Ice Sheet (Vermeij 1978; Ingolfsson 1992; Maggs *et al.* 2008), it is likely

that the species studied here survived in the above locations, or in yet unidentified refugia. Genomic-level analyses could be carried out in the species identified here as having survived the LGM in the NW Atlantic to identify refugial locations. Secondly, it is worth considering whether some of these 'survivor' species are the result of recent trans-Arctic migrations from the North Pacific. Some North Pacific species of algae have colonized the Canadian Arctic and subsequently extended into the NW Atlantic (Saunders & McDevit 2013). Indeed, some of the species analyzed here have unique Arctic haplotypes that appear to have migrated from the Pacific, in addition to having migrants out of the NE Atlantic (*Alaria esculenta,* Fig. D14) or NW Atlantic populations (*S. latissima*, Fig. D18; also see McDevit & Saunders 2010), while other species (e.g. *E. cristata* and *O. dentata*) are also reported as having conspecifics in the North Pacific (Wynne & Heine 1992). An analysis of population genetic structure in trans-Arctic species would help resolve this question.

Uncertain origins

Low isolation time estimates postdating the LGM occurred in 8 out of 20 of the species surveyed. Of these species, *M. stellatus* was identified as having postglacial origins stemming out of the NE Atlantic, as was reported in a more detailed study (Li *et al.* 2016a,b); *C. crispus* possibly survived in NW Atlantic refugia, but European migrants also likely contributed to the present-day population (Table 3.1, Fig. 3.2; Hu *et al.* 2010, 2011; Provan & Maggs 2012; Li *et al.* 2016a). The remaining six species require more extensive population-level work to resolve details about their recent history, particularly whether or not they originated out of the NE Atlantic. Shared haplotypes between NW and NE Atlantic basins in these species suggest a recent shared

ancestry and possible contemporary migration pathways across the Atlantic. *Coccotylus brodiei*, in particular, appeared to have haplotype distributions suggesting that a recent recolonization event occurred in the NW Atlantic from European populations (Fig. 3.1B), namely a single widespread haplotype in the NW Atlantic that occurs in the NE, and seemingly greater haplotype diversity in the NE Atlantic (Wares & Cunningham 2001). Again, while the patterns here are suggestive, more detailed population work is needed. Indeed, we may find that some of these species survived very recent glaciation events in the NW Atlantic, further bolstering the 60% figure reported here.

The generally low haplotype diversity in nearly all of the species studied indicates that genetic drift is playing an important role in North Atlantic populations of marine algae. Given that these populations are undergoing repeated bottlenecking due to glaciation events, the low amounts of genetic variation within species are not surprising. Genetic drift may lead to spurious results by masking genetic patterns, causing populations to randomly appear more or less related and impacting isolation time estimates. In our case, all but one of the species with isolation times predating the LGM had unique NE and NW Atlantic lineages, often separated by several mutational steps (e.g. *Ectocarpus fasciculatus* Harvey shared haplotypes between basins but had an estimated isolation time of 328 ka; Table 3.1). As such, genetic drift is generally a concern with interpreting patterns in the species for which NW Atlantic populations appear to have a recent shared history with European populations. Detailed population-level or genomic datasets (e.g. *C. crispus*) will be needed to confirm the nature of recent ancestry between the NE and NW Atlantic in these species (Table 3.1).

Conclusions

We attempted to address assumptions regarding molecular clocks and single-marker use in our study, but some additional limitations must be addressed regarding sampling effort. Our data may be biased where we have not sampled the full biogeographic range in some species, and where sample sizes are small in several populations. Southern Europe ought to be better sampled considering this is where many refugia are hypothesized to have occurred (Maggs *et al.* 2008). Because we may have missed the southern European distribution in some species, it is entirely possible the putative scenarios presented here will change in light of more data; however, we note that several of the sampled species likely have their southern limit close to the sampling locations in Norway (e.g. *R. lycopodioides*, *Phycodrys* spp., *O. dentata*, *E. cristata*, *C. brodiei*). Sampling sufficient numbers of specimens for species with ambiguous field identifications also proved difficult. For instance, *Phycodrys* occurs as three species in the North Atlantic: the abundant *P. fimbriata* (Kuntze) Kylin is found at high densities only on the western coast of the North Atlantic, and *P. rubens* and *Phycodrys* sp. 1NB occur concurrently with *P. fimbriata* in very specific and patchy locations, or at low densities across a much wider area in the NW, but dominating in the NE Atlantic. Until methods to discriminate these species in the field are developed, detailed population studies will be challenging because it will be difficult to obtain sufficient specimen numbers for the rare cryptic species. Lastly, many amphi-Atlantic species were not included in our analysis due to insufficient sampling numbers, but could be targeted in the future (Table D2). Sampling more species will yield a more complete picture of the phylogeographic history of the North Atlantic.

To conclude, we have shown that COI-5P is in agreement with other markers used in more detailed studies to resolve the population history of several species in the North Atlantic. Surveying COI-5P data in 20 species also revealed that 60% of the NW Atlantic marine flora appears to have survived the LGM. This finding was consistent across the two phyla studied here (Rhodophyta and Ochrophyta), suggesting that our results may be broadly applicable to marine coastal species. In addition, it would be worth investigating what physiological or life history differences, if any, may have allowed these species to survive glaciation in the NW Atlantic as compared to species that were extirpated during the last glaciation. Macroalgal species with recent shared ancestry between NE and NW Atlantic populations can be further investigated using other markers or genomic datasets to resolve details like migration rates and location(s) of origin. The proportion of NW Atlantic refugial species is likely to increase as we resolve recent population histories in several of the species studied here (e.g. *Ahnfeltia plicata*, *C. crispus*; Table 3.1) and include known NW Atlantic endemic species. On a final note, detailed floristic comparisons between the NW Atlantic and North Pacific will be the next step to further elucidating past and contemporary origins of marine flora in the North Atlantic and Canadian Arctic.

Acknowledgements

We thank the many researchers who participated in the large number of collecting episodes associated with our dataset. In particular, we thank Dr. Kjersti Sjøtun at the University of Bergen for facilitating our sampling in Norway. We also thank everyone who generated the COI-5P data, particularly Tanya Moore, and the following researchers for providing sequence data and trace files: Alex Geoffroy, Line

Le Gall, Akira F. Peters, and Hu Zi-Min. We also thank Jason Addison for helpful comments on the manuscript. This project was funded by the Natural Sciences & Engineering Research Council of Canada through an NSERC Post-Graduate Scholarship to T.T. Bringloe and a Discovery Grant (170151-2013) to G.W. Saunders, the New Brunswick Innovation Foundation, and the Northern Scientific Training Program.

References

Brochmann C, Gabrielsen TM, Nordal I, Landvik JY, Elven R (2003) Glacial survival or tabula rasa? The history of North Atlantic biota revisited. *Taxon*, **52**, 417−450.

Cánovas FG, Mota CF, Serrão EA, Pearson GA (2011) Driving south: a multi-gene phylogeny of the brown algal family Fucaceae reveals relationships and recent drivers of a marine radiation. *BMC Evolutionary Biology*, **11**, 371.

Castelloe J, Templeton AR (1994) Root probabilities for intraspecific gene trees under neutral coalescent theory. *Molecular Phylogenetics and Evolution*, **3**, 102−113.

Christie H, Norderhaug KM, Fredriksen S (2009) Macrophytes as habitat for fauna. *Marine Ecology Progress Series*, **396**, 221−233.

Clement M, Posada D, Crandall KA (2000) TCS: a computer program to estimate gene genealogies. *Molecular Ecology*, **9**, 1657−1659.

Coates AG, Stallard RF (2013) How old is the Isthmus of Panama? *Bulletin of Marine Science*, **89**, 801−813.

Coyer JA, Hoarau G, Costa JF, Hogerdijk B and others (2011a) Evolution and diversification within the intertidal brown macroalgae *Fucus spiralis*/*F. vesiculosus* species complex in the North Atlantic. *Molecular Phylogenetics and Evolution*, **58**, 283−296.

Coyer JA, Hoarau G, van Schaik J, Luijckx P, Olsen JL (2011b) Trans-Pacific and trans-Arctic pathways of the intertidal macroalga *Fucus distichus* L. reveal multiple glacial refugia and colonizations from the North Pacific to the North Atlantic. *Journal of Biogeography*, **38**, 756−771.

Drummond AJ, Rambaut A, Shapiro B, Pybus OG (2005) Bayesian coalescent inference of past population dynamics from molecular sequences. *Molecular Biology and Evolution*, **22**, 1185−1192.

Drummond AJ, Suchard MA, Xie D, Rambaut A (2012) Bayesian phylogenetics with BEAUti and the BEAST 1.7. *Molecular Biology and Evolution*, **29**, 1969−1973.

Einfeldt AL, Zhou F, Addison JA (2017) Genetic discontinuity in two high dispersal marine invertebrates in the northwest Atlantic. *Facets,* **2**, 160−177.

Felsenstein J (1989) PHYLIP: phylogeny inference package (version 3.2). *Cladistics*, **5**, 164−166.

Fraser CI, Nikula R, Waters JM (2011) Oceanic rafting by a coastal community. *Proceedings of the Royal Society B*, **278**, 649−655.

Geoffroy A, Mauger S, De Jode A, Le Gall L, Destombe C (2015) Molecular evidence for the coexistence of two sibling species in *Pylaiella littoralis* (Ectocarpales, Phaeophyceae) along the Brittany coast. *Journal of Phycology*, **51**, 480−489.

Gladenkov AY, Oleinik AE, Marincovich L, Barinov KB (2002) A refined age for the earliest opening of Bering Strait. *Palaeogeography, Palaeoclimatology, Palaeoecology*, **183**, 321−328.

Hey J (2010) Isolation with migration models for more than two populations. *Molecular Biology and Evolution*, **27**, 905−920.

Hoarau G, Coyer JA, Veldsink JH, Stam WT, Olsen JL (2007) Glacial refugia and recolonization pathways in the brown seaweed *Fucus serratus*. *Molecular Ecology*, **16**, 3606−3616.

Hu ZM, Guiry MD, Critchley AT, Duan DL (2010) Phylogeographic patterns indicate transatlantic migration from Europe to North America in the red seaweed *Chondrus crispus* (Gigartinales, Rhodophyta). *Journal of Phycology*, **46**, 889−900.

Hu ZM, Li W, Li JJ, Duan DL (2011) Post-Pleistocene demographic history of the North Atlantic endemic Irish moss *Chondrus crispus*: glacial survival, spatial expansion and gene flow. *Journal of Evolutionary Biology*, **24**, 505−517.

Hu ZM, Duan DL, Lopez-Bautista J (2016) Seaweed phylogeography from 1994–2014: an overview. In: Hu ZM, Fraser C (eds) *Seaweed phylogeography: adaptation and evolution of seaweeds under environmental change*. Springer, Dordrecht, p 3−22.

Ingolfsson A (1992) The origin of the rocky shore fauna of Iceland and the Canadian Maritimes. *Journal of Biogeography*, **19**, 705−712.

IPCC (Intergovernmental Panel on Climate Change) (2014) Climate Change 2014 Synthesis Report. IPCC, Geneva.

Jueterbock A, Smolina I, Coyer JA, Hoarau G (2016) The fate of the Arctic seaweed *Fucus distichus* under climate change: an ecological niche modelling approach. *Ecology and Evolution*, **6**, 1712−1724.

Kearse M, Moir R, Wilson A, Stones-Havas S and others (2012) Geneious Basic: an integrated and extendable desktop software platform for the organization and analysis of sequence data. *Bioinformatics*, **28**, 1647−1649.

Knott S, Hoskins H (1968) Evidence of Pleistocene events in the structure of the continental shelf off the northeastern United States. *Marine Geology*, **6**, 5−43.

Lane CE, Lindstrom SC, Saunders GW (2007) A molecular assessment of northeast Pacific Alaria species (Laminari- ales, Phaeophyceae) with reference to the utility of DNA barcoding. *Molecular Phylogenetics and Evolution*, **44**, 634−648.

Le Gall L, Saunders GW (2010) DNA barcoding is a powerful tool to uncover algal diversity: a case study of the Phyllophoraceae (Gigartinales, Rhodophyta) in the Canadian flora. *Journal of Phycology*, **46**, 374−389.

Lee RKS (1973) General ecology of the Canadian Arctic benthic marine algae. *ARCTIC*, **26**, 32−43.

Li JJ, Hu ZM, Duan DL (2015) Genetic data from the red alga Palmaria palmata reveal a mid-Pleistocene deep genetic split in the North Atlantic. *Journal of Biogeography*, **42**, 902−913.

Li JJ, Hu ZM, Duan DL (2016a) Survival in glacial refugia versus postglacial dispersal in the North Atlantic: the cases of red seaweeds. In: Hu ZM, Fraser C (eds) *Seaweed phylogeography: adaptation and evolution of seaweeds under environmental change*. Springer, Dordrecht, p 309−330.

Li JJ, Hu ZM, Liu RY, Zhang J, Liu SL, Duan DL (2016b) Phylogeographic surveys and apomictic genetic connec- tivity in the North Atlantic red seaweed *Mastocarpus stellatus*. *Molecular Phylogenetics and Evolution*, **94**, 463−472.

Lindstrom SC (1987) Possible sister groups and phylogenetic relationships among selected North Pacific and North Atlantic Rhodophyta. *Helgolander Meeresunters*, **41**, 245−260.

Lindstrom SC (2001) The Bering Strait connection: dispersal and speciation in boreal macroalgae. *Journal of Biogeography*, **28**, 243−251.

Lisiecki LE, Raymo ME (2005) A Pliocene-Pleistocene stack of 57 globally distributed benthic δ18O records. *Paleoceanography*, **20**, 1−17.

Macaya EC, Lopez B, Tala F, Tellier F, Thiel M (2016) Float and raft: role of buoyant seaweeds in the phylogeography and genetic structure of non-buoyant associated flora. In: Hu ZM, Fraser C (eds) *Seaweed phylogeography: adaptation and evolution of seaweeds under environmental change*. Springer, Dordrecht, p 97−130.

Maggs CA, Castilho R, Foltz D, Henzler C and others (2008) Evaluating signatures of glacial refugia for North Atlantic benthic marine taxa. *Ecology*, **89**, S108−S122.

McDevit DC, Saunders GW (2010) A DNA barcode examination of the Laminariaceae (Phaeophyceae) in Canada reveals novel biogeographical and evolutionary insights. *Phycologia*, **49**, 235−248.

Miller GH, Brigham-Grette J, Alley RB, *et al.* (2010a) Temperature and precipitation history of the Arctic. *Quaternary Sciences Reviews*, **29**, 1679−1715.

Miller GH, Alley RB, Brigham-Grette J, Fitzpatrick JJ, Polyak L, Serreze MC, White JWC (2010b) Arctic amplification: Can the past constrain the future? *Quaternary Sciences Reviews*, **29**, 1779−1790.

Neiva J, Paulino C, Nielsen MM, *et al.* (2018) Glacial vicariance drives phylogeographic diversification in the amphi-boreal kelp *Saccharina latissima*. *Scientific Reports*, **8**, 1112.

Olsen JL, Zechman FW, Hoarau G, Coyer JA, Stam WT, Valero M, Åberg P (2010) The phylogeographic architecture of the fucoid seaweed *Ascophyllum nodosum*: an intertidal 'marine tree' and survivor of more than one glacial-interglacial cycle. *Journal of Biogeography*, **37**, 842−856.

Pflaumann U, Sarnthein M, Chapman M, *et al.* (2003) Glacial North Atlantic: sea-surface conditions reconstructed by GLAMAP 2000. Paleoceanography, **18**, 1065.

Provan J, Maggs CA (2012) Unique genetic variation at a species' rear edge is under threat from global climate change. *Proceedings of the Royal Society B*, **279**, 39−47.

Rambaut A, Suchard M, Xie D, Drummond A (2014) Tracer v1.6. http: //tree.bio.ed.ac.uk/software/tracer/.

Renaud PE, Sejr MK, Bluhm BA, Sirenko B, Ellingsen IH (2015) The future of Arctic benthos: expansion, invasion, and biodiversity. *Progress in Oceanography*, **139**, 244−257.

Saunders GW (2005) Applying DNA barcoding to red macroalgae: A preliminary appraisal holds promise for future applications. *Philosophical Transactions of the Royal Society B*, **360**, 1879−1888.

Saunders GW (2008) A DNA barcode examination of the red algal family Dumontiaceae in Canadian waters reveals substantial cryptic species diversity. 1. The foliose *Dilsea− Neodilsea* complex and *Weeksia*. *Botany*, **86**, 773−789.

Saunders GW, McDevit DC (2012) Methods for DNA barcoding photosynthetic protists emphasizing the macroalgae and diatoms. *Methods in Molecular Biology*, **858**, 207−222.

Saunders GW, McDevit DC (2013) DNA barcoding unmasks overlooked diversity improving knowledge on the composition and origins of the Churchill algal flora. *BMC Ecology*, **13**, 9.

Saunders GW, Moore TE (2013) Refinements for the amplification and sequencing of red algal DNA barcode and RedToL phylogenetic markers: a summary of current primers, profiles and strategies. *Algae*, **28**, 31−43.

Silberfeld T, Leigh JW, Verbruggen H, Cruaud C, de Reviers B, Rousseau F (2010) A multi-locus time-calibrated phylogeny of the brown algae (Heterokonta, Ochrophyta, Phaeophyceae): investigating the evolutionary nature of the 'brown algal crown radiation.' *Molecular Phylogenetics and Evolution*, **56**, 659−674.

Smith DR (2015) Mutation rates in plastid genomes: They are lower than you might think. *Genome Biology and Evolution*, **7**, 1227−1234.

South GR (1983) *Biogeography and ecology of the island of Newfoundland*. Springer Science & Business Media, Berlin.

Taylor W (1957) *Marine algae of the northeastern coast of North America*, 2nd edn. University of Michigan Press, Ann Arbor, MI, p 427.

Teasdale BW, Klein AS (2010) Genetic variation and biogeographical boundaries within the red alga *Porphyra umbilicalis* (Bangiales, Rhodophyta). *Botanica Marina*, **53**, 417−431.

Vermeij GJ (1978) *Biogeography and adaptation: patterns of marine life*. Harvard University Press, Cambridge, MA.

Vermeij GJ, Roopnarine PD (2008) The coming Arctic invasion. *Science*, **321**, 780−781.

Wares JP, Cunningham CW (2001) Phylogeography and historical ecology of the North Atlantic intertidal. *Evolution*, **55**, 2455−2469.

Wynne MJ, Heine JN (1992) Collections of marine red algae from St. Matthew and St. Lawrence Islands, the Bering Sea. *Nova Hedwigia*, **55**, 55−97.

Zuccarello G, West JA (2002) Phylogeography of the *Bostrychia calliptera-B. pinnata* complex (Rhodomelaceae, Rhodophyta) and divergence rates based on nuclear, mitochondrial and plastid DNA markers. *Phycologia*, **41**, 49−60.

Table 3.1 Isolation times of trans-Atlantic species of macroalgae based on COI-5P data, and a medium COI-5P clock rate (red algae: 0.007 substitutions site−1 Myr−1; brown algae: 0.00245 substitutions site−1 Myr−1). Species with isolation time estimates predating the Last Glacial Maximum (LGM; 20 ka) are in bold; n (sample size) and No. of haplotypes read as western/eastern North Atlantic. Divergence times (in ka) are given with 95% highest posterior density (HPD) intervals. See Figs. D1−D18 for detailed biogeographic maps and haplotype networks. Divergence times in some species are tested twice, with and without certain populations (see Methods and Discussion).

Species	***n***	**# of haplotypes**	**Isolation time ka (95% HPD)**	**Comments**
Rhodophyta				
Ahnfeltia plicata (Fig. D1)	120/21	6/4	24.432 (3.676, 80.216)	Shared haplotypes indicate population level data are needed to resolve recent history. NW Atlantic endemic haplotypes indicate this species may have survived in NW refugia. Trans-Atlantic dispersal from the NE to the NW may also account for some of the patterns seen in *A. plicata* (see *C. crispus*).
***Ceramium virgatum* (Fig. D2)**	**165/5**	**50/2**	**100.540 (50.810, 154.594)**	A long history in the NW Atlantic is implied by an extensive haplotype network. Rhode Island populations could be interpreted as recent introductions from Europe.
***Ceramium virgatum* (without Rhode Island population)**	**146/5**	**49/2**	**117.838 (55.136, 243.244)**	
Chondrus crispus (Fig. D3)	53/48	6/9	21.120 (2.136, 53.868)	Shared haplotypes indicate recent shared ancestry exists between NE and NW Atlantic

				basins, though some haplotypes are endemic to the NW Atlantic, suggesting refugial populations existed in the NW Atlantic (see also Hu *et al.* 2011, Provan & Maggs 2012). Trans-Atlantic dispersal from Europe to the NW Atlantic has been inferred (Li *et al.* 2016a).
Coccotylus brodiei (Fig. 3.1B)	71/31	2/3	10.594 (0.648, 87.568)	Shared haplotypes indicate population level data are needed to resolve recent history. The distribution of haplotypes (NW is subset of NE) suggests this species was reestablished in the NW Atlantic postglacially.
***Cystoclonium purpureum* (Fig. D4)**	**39/14**	**4/2**	**288.648 (74.594, 913.514)**	A phylogenetic break indicates a long period of isolation between NE and NW populations.
***Dilsea socialis/carnosa* (Fig. D5)**	**60/18**	**1/2**	**515.676 (83.244, 1322.162)**	A phylogenetic break indicates a long period of isolation between NE and NW populations. NW populations were recognized as *D. socialis*, NE populations were recognized as *D. carnosa* (Saunders 2008), but this taxonomic conclusion has not been robustly tested.
***Euthora cristata* (Fig. D6)**	**67/29**	**5/1**	**282.162 (44.324, 742.702)**	A shallow phylogenetic break indicates relatively recent isolation between NE and NW Atlantic populations.
Mastocarpus stellatus (Fig. D7)	19/26	2/3	22.00 (1.466, 168.672)	This species is listed as having recolonized the NW Atlantic from Europe postglacially (Li *et al.* 2016b), which is consistent with the data presented here.
***Odonthalia dentata* (Fig. 3.1A)**	**53/26**	**6/1**	**662.918 (125.838, 1443.892)**	A phylogenetic break indicates a long period of isolation between NE and NW populations.

***Palmaria palmata* (Fig. D8)**	**58/19**	**11/9**	**1039.488 (259.002, 1736.354)**	A phylogenetic break indicates a long period of isolation between NE and NW populations, a result consistent with other markers *(Li et al.* 2015).
Phycodrys sp. 1NB (Fig. D9)	17/22	2/4	44.432 (4.864, 305.838)	Shared haplotypes indicate population level data are needed to resolve recent history. This is a rare member of the NW Atlantic flora.
***Phycodrys rubens* (Fig. D10)**	**9/45**	**2/5**	**583.870 (121.506, 1284.946)**	A phylogenetic break indicates a long period of isolation between NE and NW populations. This is a rare member of the NW Atlantic flora.
Polyides rotundus (Fig. D11)	29/10	4/3	25.964 (6.244, 76.578)	Low genetic diversity and a single widespread haplotype indicate population level data are needed to resolve recent history.
Polysiphonia sp. 2stricta (Fig. D12)	23/10	1/2	6.966 (0, 165.880)	Low genetic diversity and a single widespread haplotype indicate population level data are needed to resolve recent history.
Rhodomela lycopodioides (Fig. D13)	97/12	11/1	24.204 (4.840, 346.924)	A putative migrant population from Europe occurs in the Canadian Arctic. NE and NW populations otherwise exhibit a phylogenetic break.
***Rhodomela lycopodioides* (without Arctic sequence)**	**96/12**	**10/1**	**463.640 (143.072, 1393.072)**	
Phaeophyceae				
Alaria esculenta (Fig. D14)	33/21	4/2	164.698 (15.538, 1190.180)	A putative migrant population from Europe occurs in sub-Arctic Northern Newfoundland. Otherwise the NE, NW and Arctic basins all appear to be evolving independently. Possible Pacific origins in Arctic collections.
***Alaria esculenta* (without Arctic populations)**	**23/21**	**2/2**	**706.650 (62.461, 2183.344)**	

***Ectocarpus fasciculatus* (Fig. D15)**	**16/35**	**4/14**	**328.776 (92.604, 634.566)**	High haplotype diversity in southern Europe suggests this species has origins in the NE Atlantic, having moved into the NW Atlantic sometime before the LGM.
Laminaria digitata (Fig. D16)	52/13	3/1	19.266 (0, 113.736)	Low genetic diversity and a single widespread haplotype indicates population level data are needed to resolve recent history.
***Pylaiella* sp. 2littoralis (Fig. D17)**	**8/14**	**13/6**	**654.688 (248.438, 1257.812)**	A phylogenetic break indicates a long period of isolation between NE and NW populations. Possible incomplete lineage sorting or trans-Atlantic introductions combined with sampling artifacts may explain haplotypes from each lineage occurring on either side of the Atlantic. This amphi-Atlantic genetic group corresponds to MtA in Geoffroy *et al.* (2015).
***Saccharina latissima* (Fig. D18)**	**132/21**	**11/2**	**1575.092 (442.890, 3486.514)**	A phylogenetic break indicates a long period of isolation between NE and NW Atlantic, and Arctic/Pacific populations (McDevit & Saunders 2010).
***Saccharina latissima* (without Arctic populations)**	**97/21**	**8/2**	**1415.252 (449.550, 3439.894)**	

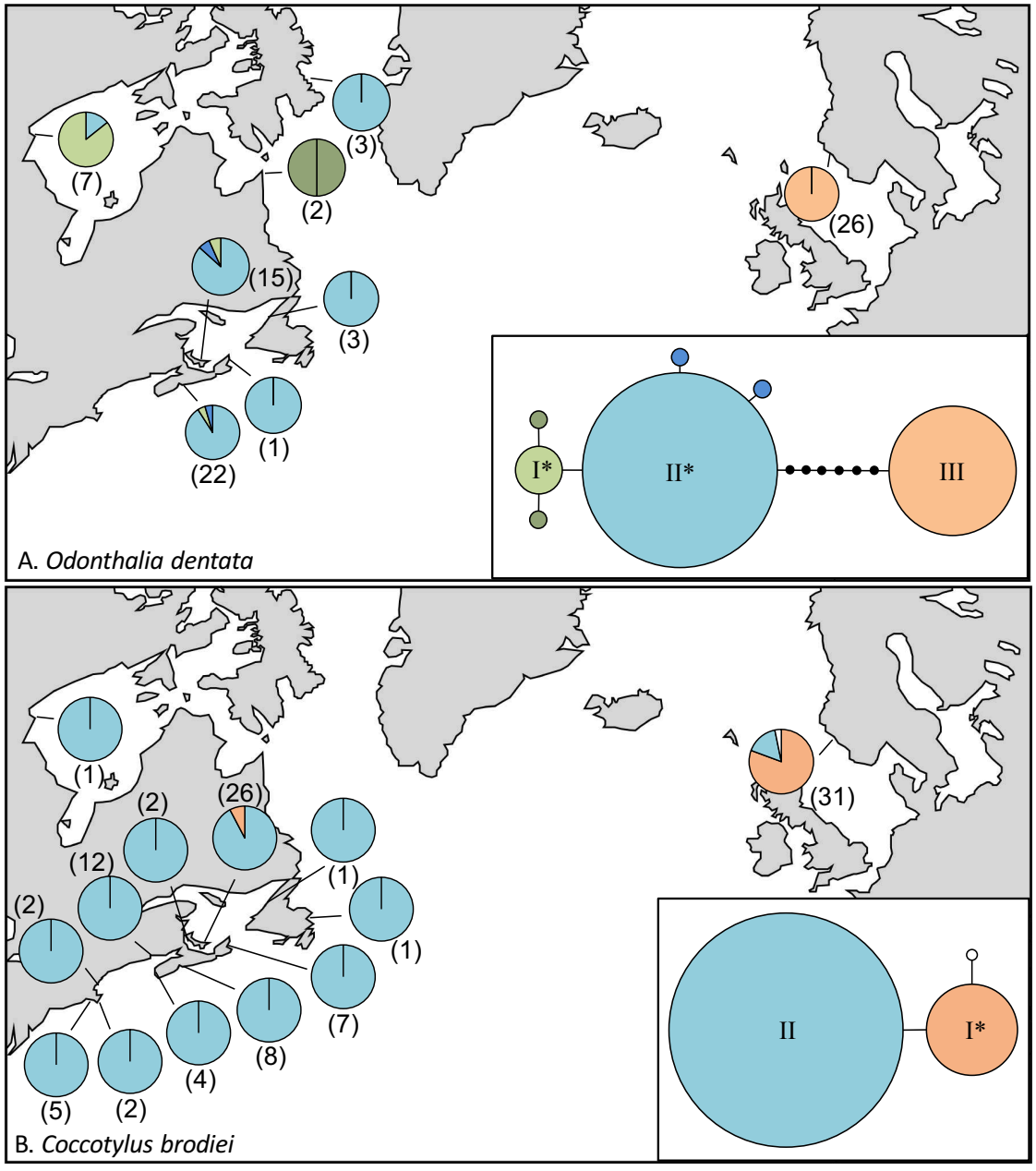

Figure 3.1 Haplotype networks and maps based on COI-5P data for two trans-Atlantic species. In the maps, numbers in parentheses refer to sample sizes from given locales. In the haplotype network, roman numerals refer to repeatedly sampled haplotypes. An asterisk indicates putative ancestral haplotypes based on TCS analyses. Black circles indicate hypothesized haplotypes between clades. The

size of each circle is proportional to sampling frequency. A) Depiction of haplotype distributions for *Odonthalia dentata*, an example consistent with allopatric fragmentation (e.g. NW Atlantic populations are not derived from the NE Atlantic). B) Depiction of haplotype distributions for *Coccotylus brodiei*, an example wherein recent population history cannot be resolved with COI-5P data, but shared haplotypes suggest recent connectivity between populations.

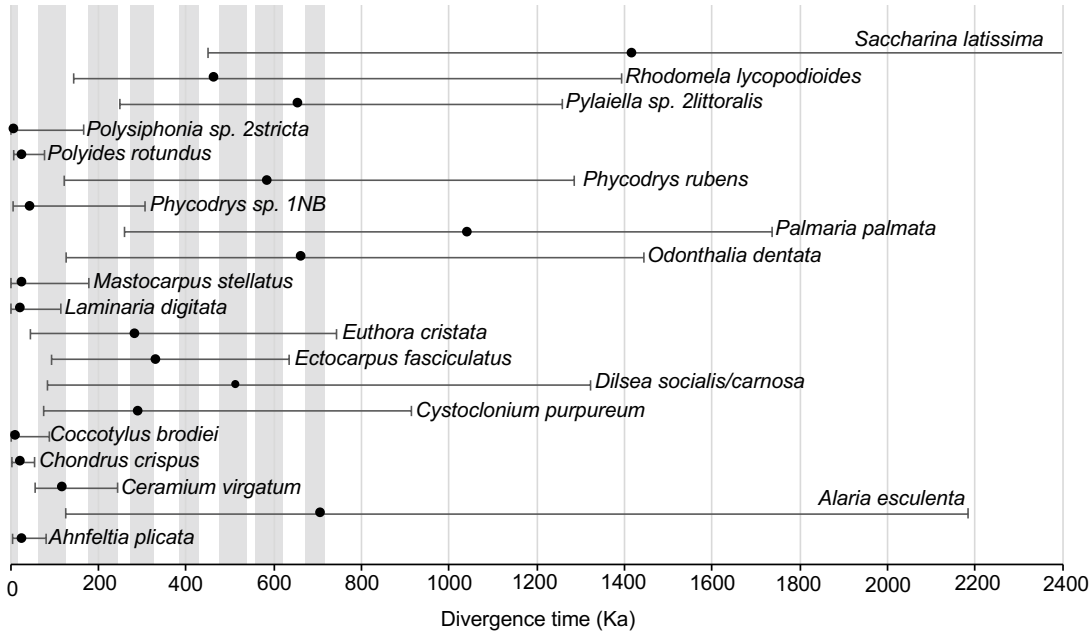

Figure 3.2 Divergence times in trans-Atlantic red and brown macroalgae in conjunction with glaciation events over the past 800 ka (as proxied from globally distributed $\delta^{18}O$ records [Lisiecki & Raymo 2005]). Non-shaded intervals approximate glacial maxima. The error bars are 95% highest posterior density intervals; note, sampling densities across the range of divergence times is normally distributed around the means; note the upper bound of the highest posterior density for *Saccharina latissima* is 3438 ka.

Chapter 4 On the origins of North American Arctic marine macroalgae since the Last Glacial Maximum and evidence for Arctic periglacial refugia

Abstract: Marine macroalgae are expected to move northwards into the Arctic as isotherms retreat and perennial ice-cover diminishes. Understanding the nature of Arctic recolonization since the Last Glacial Maximum may aid in biomonitoring efforts by identifying key pathways for marine flora entering the North. We sought to improve understanding of Arctic recolonization in marine macroalgae by supplementing existing DNA barcode records with sampling from Baffin Island, through Northern Labrador (Canada), the Beaufort Sea and Nome (Alaska, USA), and Bergen (Norway). The origins of North American Arctic populations were inferred based on haplotype patterns. We accumulated sequence data for 4233 specimens, which included 3813 COI-5P, 375 *tufA*, 32 *rbc*L-3P, 163 ITS, and 61 *ycf35* sequences. This dataset represented 42 species of red, 46 brown, and 12 green algae, for a total of 100 Arctic species for which populations were variously recorded from the North Pacific and/or Northern Bering Sea, through the Arctic and into the North Atlantic. Of these species, 39 had uncertain origins, 46 had origins in the North Atlantic, five had origins in the Pacific and the Atlantic, while the remaining 10 had origins in the North Pacific. Pacific contributions to Arctic recolonization, however, were inferred in 9/12 of the best sampled species (e.g. broad coverage across all three basins and >20 Arctic records). Our results indicated that the Pacific contribution to Arctic recolonization has been historically underestimated. Surprisingly, 18 genetic groups and some Arctic haplotypes in 28 species were not assignable to Atlantic or Pacific populations, suggesting marine macroalgae may have survived in periglacial refugia along seasonally ice-free coastal areas of Siberia or Greenland. The Arctic may therefore represent an independent evolutionary basin, with

input from both the Atlantic and the Pacific following glaciation events, as well as Arctic refugia.

Introduction

The North American Arctic is a uniquely dynamic ecosystem, having undergone repeated glaciations over the past 2.6 Ma (Miller *et al.* 2010a). These glacial events undoubtedly had a lasting impact on northern flora and fauna, as populations repeatedly contracted and expanded with the formation and retreat of ice-sheets. Contemporary populations in the North American Arctic are especially young from a geological perspective, and were likely established within the past 12 ka following the decline of ice-sheets (Briner *et al.* 2009; Dyke *et al.* 2002; Kaufman *et al.* 2004; Polyak *et al.* 2010). Insight into how Arctic populations historically reacted to changing temperature regimes is urgently needed; warming in the Arctic is significantly exceeding the Northern Hemisphere average (Huang *et al.* 2017; Miller *et al.* 2010a, b), and boreal and temperate regimes are expected to shift northwards as a result (Krause-Jensen & Duarte 2014; Renaud *et al.* 2015). The impact of ecosystem shifts could be especially pronounced in marine taxa. For example, using an ecological niche modelling approach, Jueterbock *et al.* (2016) estimated the amount of suitable Arctic shoreline for the macroalga *Fucus distichus* Linnaeus may triple within the next 100 years. It is imperative baseline data are established in the North before such changes occur.

Marine macroalgae are promising taxa for predicting and monitoring changes to the North American Arctic. Jueterbock *et al.* (2016) reasoned that marine macroalgae can be used to forecast impacts to rocky shore systems given 1) macroalgal biogeographic distributions are highly dependent on temperature isotherms (Campana *et al.* 2009; Müller *et al.* 2009), and 2) macroalgae are foundational species, providing habitat for marine fauna (Christie *et al.* 2009). In addition, recent work has demonstrated

that macroalgae can raft marine flora and fauna over large oceanic distances (e.g. Fraser *et al.* 2011; Saunders 2014; Macaya *et al.* 2016). The expansion of macroalgal ranges northwards may therefore serve as an early indication of community-wide ecosystem shifts into the Arctic Ocean. Understanding past migration events into the Arctic can be a first step towards providing insight on the anticipated movement of species northwards (Vermeij & Roopnarine 2008), and ultimately between the North Atlantic and Pacific Oceans. In addition to establishing baseline data, investigating source basins and migration routes for contemporary Arctic populations will highlight key locations that can be monitored for ecosystem shifts.

DNA based methods for species identification have recently enhanced our understanding of Arctic diversity and recolonization. The marine flora in the Arctic has historically been considered an extension of the North Atlantic, with few Pacific and endemic species (Taylor 1957; Lee 1973; Dunton 1992). These conclusions were certainly imprecise in some cases given that they were predicated on morphological identifications of species. Such morphological identifications in marine macroalgae are problematic due to simple morphology, cryptic diversity, convergent evolution, and phenotypic plasticity (Saunders 2005). Indeed, recent work on the Beaufort flora (Northern Alaska) indicated that taxonomic confusion likely persists in 45% of its recorded species (Bringloe *et al.* 2017). DNA based species identifications (e.g. DNA barcoding; Saunders 2005) in the Canadian Arctic have subsequently led to novel insight regarding the origins of Arctic flora. In particular, Saunders and McDevit (2013) demonstrated that cryptic macroalgal species diversity exists in the Canadian Arctic, and that some species clearly have intra-specific genetic variation consistent with recent

origins from the Pacific Ocean. Such findings were consistent with phylogeographic studies (Lindstrom 1987, 2006; Lindstrom *et al.* 1996) and thermogeographic modelling (Adey *et al.* 2008), which indicated that a persistent and ongoing Pacific to Atlantic connection occurs in marine macroalgae. These studies suggest at an underappreciated Pacific component to the Arctic flora; if true, biomonitoring ought to be concerned about Pacific populations migrating into a warming Arctic.

Unfortunately, uncertainty regarding the origins of Arctic macroalgal flora persist due to a lack of collections from several critical Arctic and sub-Arctic locations. This is particularly true of the Northern Bering Sea, where Pacific populations are possibly moving into the Arctic through the Bering Strait. Our objective was to improve understanding of the origins of contemporary Arctic marine macroalgal flora by building on the DNA barcoding dataset of Saunders and McDevit (2013), and sampling critical locations notably absent from their study (e.g. Northern Bering Sea and the Western Arctic). By utilizing a conceptually simplified approach (inferring origins of Arctic populations based on haplotype patterns), we investigated patterns in multiple species concurrently to obtain a comprehensive understanding of the recent recolonization history of Arctic marine macroalgal flora.

Methods

In order to infer the origins of marine macroalgae in the North American Arctic, previously existing DNA barcode records were supplemented with sampling in several key locations over the course of four years (see Appendix E, Table E1 for data mined from GenBank; specimen information is otherwise available online; Barcode of Life

Datasystems [BOLD], DS-TAMMA). These locations included Baffin Island, through Northern Labrador to Makkovik (September 2-12, 2014); Haida Gwaii, British Columbia, Canada (July 10-16, 2015); the Beaufort Sea, Northern Alaska (August 20-21, 2014, and July 20-25, 2015); Bergen and surrounding area, Norway (June 3-13, 2016); and Nome, Alaska, and surrounding area (Northern Bering Sea; August 12-22, 2017). We additionally received collections from Norway (collected 14-20 April, 2016) and Japan (collected 25-26 April, 2016). Marine macroalgae were generally collected from the intertidal and via scuba, but occasionally via dredge. A portion of each specimen (approx. 1 cm^2) was preserved in silica gel for DNA extraction, while several representatives of putative species were preserved as pressed material. Specimens were brought back to the University of New Brunswick (where specimens are stored) for DNA extraction (Saunders & McDevit 2012a). Several genes were amplified, including the 5' end of the cytochrome *c* oxidase subunit I gene (COI-5P) in red and brown algae, *tufA* in green algae, and partial reads of the ribulose-1, 5-biphosphate carboxylase large subunit (*rbc*L-3P). Secondary markers were acquired in some species, including the full length nuclear internal transcribed spacer region (ITS) and plastid *ycf35*, in order to further clarify or support COI-5P patterns. See Table 4.1 for primer information. Successful PCR products were sent to Genome Quebec for forward and reverse sequencing. All genetic data were edited in Geneious v.8.0 (http://www.geneious.com; Kearse *et al.* 2012).

Haplotype networks and maps were used to make inferences regarding the origins of Arctic marine algae. Inclusion in the Arctic flora was based on the 10^{o}C air temperature isotherm for July, as per D'Odorico *et al.* (2013), with the exception of

Nome, Alaska, which was considered a conduit for Pacific populations migrating into the Arctic. Inferences were based on the prediction that recolonized Arctic populations will represent a subset of haplotype variation from the parental basin (i.e. coalescent theory; Castelloe & Templeton 1994; Maggs *et al.* 2008). The origin of Arctic populations was therefore considered Atlantic and/or Pacific if haplotypes matched a given oceanic basin. If all Arctic haplotypes for a given species occurred in both the Atlantic and Pacific Ocean, then the origin of Arctic populations was considered uncertain, unless haplotype diversity was greater in the Atlantic or Pacific, and a subset of this variation was observed in the other two basins (implying recent migration from the basin with the greatest haplotype diversity). The origin of Arctic species was also considered uncertain in species lacking comparable records from either the Atlantic or Pacific, and in cases where Arctic haplotype(s) did not match either basin. In order to consider known species ranges in the interpretation of haplotype networks/maps, locations for genetically verified records based on markers other than the one(s) used in our haplotype networks were also noted in each species. This was typically done by blasting through GenBank's nucleotide database (Altschul *et al.* 1990) *rbc*L data linked to the COI-5P genetic groups investigated in the haplotype maps/networks. The locations of specimens that differed by three or fewer base pairs (a threshold generally corresponding to interspecific divergence in *rbc*L) were noted on the haplotype maps.

Besides interpreting the origins of Arctic populations with regards to the Atlantic and/or Pacific basins, two additional scenarios were considered. Given the large amount of unique haplotype and species level genetic variation detected in the Arctic, these populations were interpreted with potential origins in all three oceanic basins, meaning

that, Arctic periglacial refugial populations were invoked to explain unique Arctic genetic groups and haplotypes. In addition, given the limited amount of sampling in most species, both in terms of geographical coverage and number of specimens collected, the origin of Arctic populations was considered in a subset of "well-sampled" species with at least 50 total records, and at least 20 Arctic records, once again with potential origins in all three basins. Note that the term "Arctic periglacial refugia" is used to distinguish sources of Arctic recolonization other than known or hypothesized sources in the Atlantic and Pacific basins, and geographically refers to potential refugia at the margins of ice sheets within the Arctic basin, as delineated above. In addition, regions within an oceanic basin are referenced where possible, but references to the North Pacific and the North Atlantic otherwise indicate the entire oceanic basin in the Northern Hemisphere (Pacific regions: Northwest [Japan and Russia], Northern Bering Sea [St. Lawrence Island and Nome, Alaska], and Northeast Pacific [British Columbia, Canada, and Washington state, USA]; Atlantic regions: Northwest [Canadian Atlantic provinces and New England States] and Northeast Atlantic [Europe]). Finally, the terms "species" and "genetic group" are used interchangeably, but considerable taxonomic work remains to be done on many of the genetic groups presented here, especially in cases where new groups were sampled in the Arctic. Specimen information and GenBank accession numbers can be found online (BOLD, DS-TAMMA). The interpretation of haplotype patterns can be found in Appendix E, Table E2.

Results

In total, we amalgamated records for 4233 specimens, 1814 of which were collected during this study (2014-2017). Our dataset consisted of 3813 sequences for COI-5P, 375 for *tufA*, 32 for *rbc*L-3P, 163 for ITS, and 61 for *ycf35*. Our dataset represented 42 species of red algae, 46 brown algae, and 12 green algae, for a total of 100 Arctic species. Geographically, these records represented 65 from the Northwest Pacific, 499 from the Northern Bering Sea, 387 from the Northeast Pacific, 205 from the Western Arctic (e.g. Beaufort Sea), 625 from the East Arctic (Churchill and Northern Baffin Island through to Nain, Labrador), 2171 from the Northwest Atlantic, and 281 from the Northeast Atlantic.

Haplotype maps and networks revealed several scenarios for Arctic recolonization. Some species were consistent with recolonization of the North American Arctic from the North Pacific (e.g. *Rhodomela sibirica* A.D.Zinova & Vinogradova, Fig. 4.1A). In other cases, species appeared to recolonize the Arctic from both the North Pacific and the North Atlantic (e.g. *Saccharina latissima* (Linnaues) C.E.Lane, C.Mayes, Druehl & G.W.Saunders, Fig. 4.1B). Many species appeared to have recolonized solely from the North Atlantic; these were typically cases with low numbers of records from Churchill (Hudson Bay; e.g. *Dictyosiphon foeniculaceus* [Hudson] Greville; Fig. 4.1C). Finally, the origin of Arctic populations in many species remained uncertain due to low sample size or a lack of haplotype variation from the North Pacific through to populations in the North Atlantic (e.g. *Chordaria chordaeformis* [Kjellman] H.Kawai & S.-H.Kim, Fig. 4.1D). Of the 100 species included in our analysis, we concluded that 39 had uncertain origins, 46 had origins in the Atlantic basin, five had

origins in the Atlantic and the Pacific, and the remaining 10 had origins in the Pacific (Fig. 4.2A). Surprisingly, 18 genetic groups were unique to the Arctic basin, and private Arctic haplotype(s) occurred in a further 28 species, which were interpreted as populations surviving in Arctic periglacial refugia in Fig. 4.2B. This result was consistent with the analysis of well sampled species. When considering the twelve species with at least 20 Arctic records, and at least 50 records overall, one (8%) had uncertain origins, two (17%) had origins in the Arctic and the Atlantic, four (33%) had origins in all three basins, two (17%) had origins in the Arctic and the Pacific, while the remaining three (25%) had origins in the Pacific (Fig. 4.2C). Eight out of the 12 species had Arctic haplotype variation not assignable to the Atlantic or Pacific basins.

Other interesting patterns are notable. Some species showed signs of admixture between North Pacific and North Atlantic populations, particularly in Churchill (Hudson Bay) and Northern Labrador (Northwest Atlantic; Fig. 4.3); these species included *Chaetopteris plumosa* (Lyngbye) Kützing (Fig. E45), *Coccotylus truncatus* (Pallas) M.J.Wynne & J.N.Heine (Fig. E10), *Eudesme virescens* (Carmichael ex Berkeley) J.Agardh (Fig. E52), *Saccharina latissima* (Fig. 1B), *Scagelia pylaisaei* (Montagne) M.J.Wynne (Fig. E36), and possibly *Phycodrys fimbriata* (Kuntze) Kylin (Fig. E23). Several North Atlantic species sampled in Churchill were notably not detected along the coast of Labrador, including *Ahnfeltia plicata* (Hudson) Fries (Fig. E3), *Coccotylus brodiei* Turner Kützing (Fig. E8), *Laminaria digitata* (Hudson) J.V.Lamouroux (Fig. E57), *Ptilota gunneri* P.C.Silva, Maggs & L.M.Irvine (Fig. E28), and *Pylaiella* sp. 1littoralis (Fig. E66). The population structure of several species in the Western Arctic (Northern Alaska) was markedly different from conspecifics in the Northern Bering Sea,

and sometimes included private haplotypes. These species included *Coccotylus truncatus* (Fig. E9 and E10), *Odonthalia dentata* (Linnaeus) Lyngbye (Fig. E20), *Phycodrys fimbriata* (Fig. E23), and *Rhodomela sibirica* (Figs. 4.1A and E33). Some species featured private Arctic haplotypes, despite having records from the North Pacific and/or North Atlantic; in addition to the previously mentioned species, noteworthy examples included *Alaria esculenta* (Linnaeus) Greville (Fig. E41), *Chaetopteris plumosa* (Fig. E45), *Chordaria flagelliformis* (O.F.Müller) C.Agardh (Fig. E48), *Devaleraea ramentacea* (Linnaeus) Guiry (Fig. E11), *Dictyosiphon foeniculaceus* (Fig. 1C), *Euthora cristata* (C.Agardh) J.Agardh (Fig. E13), *Laminaria solidungula* J.Agardh (Fig. E58), *Petalonia filiformis* Batters Kuntze (Fig. E61), *Polysiphonia* sp. 3stricta (Fig. E27), *Rhodomela* sp. 1virgata (Fig. E34), *Pylaiella washingtoniensis* C.C.Jao (Fig. E67), *Saccharina latissima* (Fig. E68), *Scagelia pylaisaei* (Fig. E36), *Ulva prolifera* O.F.Müller (Fig. E85), and *Ulvaria obscura* (Kützing) Gayral ex Bliding (Fig E86).

Discussion

Marine species diversity in the Arctic is expected to change in response to shifting isotherms and the decline of perennial ice-cover (Campana *et al.* 2009; Jueterbock *et al.* 2016; Müller *et al.* 2009; Vermeij & Roopnarine 2008; Krause-Jensen & Duarte 2014). Understanding the origins of marine Arctic macroalgae since the Last Glacial Maximum (LGM) can help forecast these changes by providing baseline data and identifying critical migration routes into the Arctic for biomonitoring. The work presented here represents a significant addition to marine Arctic records, with DNA

barcode data from the Northern Bering Sea, the Western Arctic (Alaska), and the Eastern Arctic (Baffin Island, through to Northern Labrador; Fig. 4.1).

Underappreciated Pacific origins

Our dataset, updated from the work of Saunders and McDevit (2013), confirmed that a significant Pacific component exists in Arctic marine macroalgal flora (Figs. 4.1 and 4.2). Saunders and McDevit (2013) estimated that, minimally, seven species from Churchill (Hudson Bay) had recent origins in the Pacific basin, whereas our work indicated 15 Arctic macroalgal species have some Pacific component to their origins, representing nearly the same proportion of species in both analyses (Fig. 4.2A); if species of uncertain origin are removed from the above calculations, we find that Saunders and McDevit (2013) report 75% of species have Atlantic origins, 4% have Atlantic and Pacific origins, while 21% have Pacific origins, similar to 76%, 8%, and 16%, respectively, in our study. The breakdown in origins of Churchill species hypothesized by Saunders and McDevit (2013) effectively scaled up when considering Arctic species on a broader geographic scale and when considering population-level data (their analysis was predominantly at the species level, and was restricted to Churchill). These breakdowns, however, are likely to be inaccurate given the low number of genetic records in many species, particularly from Arctic locations, sampling bias in the Northwest Atlantic (where the majority of records were collected), and a lack of sampling coverage across the entire range in some species. In fact, an increase in the Pacific influence on Arctic recolonization becomes evident when considering species that are relatively well sampled in the North American Arctic (e.g. at least 50 total records, and 20 Arctic records). Nine out of the 12 well sampled species (75%) appeared

to have a Pacific component to Arctic recolonization, three (25%) of which appeared to have origins exclusively from the Pacific (Fig. 4.2C). The shift in proportions is undoubtedly driven by the enhanced sampling cover in the Western Arctic and Northern Bering Sea in these species, and highlights the need for additional sampling from these areas, particularly in less well sampled species (Table E2). Results from the well sampled species indicate that marine macroalgal flora has recently recolonized the Arctic from both the Atlantic and Pacific, as opposed to being predominantly recolonized from the North Atlantic as was historically thought (Taylor 1957; Lee 1973; Dunton 1992). It is worth noting that these results are consistent with the phylogeographic analyses in Chapter 2 and thermogeographic modelling (Adey *et al.* 2008), which highlight a persistent Pacific to Atlantic connection in marine macroalgae. Multiple lines of evidence are therefore converging on an updated understanding of Arctic recolonization in marine Arctic flora.

Additional sampling in the Northwest Pacific will be critical to further resolve origins in some Arctic populations. Several species with uncertain origins had a single haplotype extending from the Northeast Pacific and/or Northern Bering Sea into the Atlantic (n=7), suggesting at recent dispersal across these areas (Fig. 4.1D). It is possible these species have evolutionary origins in the Northwest Pacific, particularly along the non-sampled Russian coastline where refugia are likely to have occurred (Katsuki & Takahashi 2005; Caissie *et al.* 2010; Fig. 4.3). Indeed, some of the species with monotypic haplotype populations across the Arctic and North Atlantic are reported from the Northwest Pacific, such as *Chordaria chordaeformis* (Kjellmann) H.Kawai & S.H.Kim (Fig. 4.1D; Kim & Kawai 2002; Lindstrom 2006; Guiry & Guiry 2018); if

Chordaria chordaeformis is designated as having recent Pacific origins, then our estimate of Pacific origins in well-sampled Arctic populations increases to 83% (Fig. 4.2). Several species with inferred Pacific origins from this study displayed similarly low haplotype variation across the Arctic, including *Ahnfeltia borealis* D.Milstein & G.W.Saunders (Figs. E1 and E2), *Agarum clathratum* Dumortier (Fig. E40), *Dilsea socialis* (Fig. E12), *Rhodomela sibirica* (Hudson Bay and eastwards; Fig. 4.1A and E33), and *Rhodomela virgata* Kjellman (Fig. E35). These patterns indicate that the Pacific contribution to the Arctic flora likely remains underestimated in the analysis of the 100 species, despite the expanded dataset. In addition, the above patterns further suggest several of the Arctic genetic groups may be assignable to species from the Northwest Pacific. DNA barcoding work in this area will be imperative to resolving recent Arctic origins and species name assignment in some of the genetic groups reported here (Table E2).

Synopsis of Arctic marine recolonization

The haplotype patterns observed in our study are consistent with the progression of retreating ice sheets following the LGM. Peak Holocene warming occurred in the Western Arctic (e.g. Beringia) approximately 13 ka, 4 ka prior to peak warming in the Eastern Arctic, a delay due in part to the residual Laurentide Ice Sheet in Quebec and Labrador (Dyke & Prest 1987; Kaufman *et al.* 2004; Miller *et al.* 2010a). The flooding of the Bering Strait initiated an influx of Pacific water into the Arctic ocean that began around 12 ka, and peaked somewhere between 9 and 5 ka (Miller *et al.* 2010a). Given this timeline, species in the North Pacific, particularly in the Northern Bering Sea, had an earlier chance to colonize the Arctic compared to Atlantic species, as the retreat of

ice sheets progressed from West to East (Dyke & Prest 1987; Fig. 4.3). This would explain why Pacific haplotypes dominated the Arctic flora in some species (Fig. 4.1A). The timeline for the progression of ice retreat is also consistent with the high number of Atlantic species sampled in the Hudson Bay, as the Tyrell Sea (modern day Hudson Bay) became accessible to the Atlantic basin through the Hudson Strait approximately 8 ka (Dyke & Prest 1987; Fig. 4.3). As the Arctic opened up completely, particularly 7 ka in the Northern Tyrrell Sea (Dyke & Prest 1987), Pacific and Atlantic populations will have come into secondary contact (Fig. 4.3). Admixture of populations is evident in several species reported here, either in the Hudson Bay or Northern Labrador, including *Chaetopteris plumosa* (Fig. E45, Chan 2018) *Coccotylus truncatus* (Fig. E10), *Eudesme virescens* (Fig. E52), *Saccharina latissima* (Fig. 4.1B; McDevit & Saunders 2010; Neiva *et al.* 2017), *Scagelia pylaisaei* (Fig. E36), and possibly *Phycodrys fimbriata* (Fig. E23). In summary, the haplotype patterns here, combined with the known progression of ice retreat in the North American Arctic, indicate Pacific marine populations entered the Arctic 12 ka, much earlier than Atlantic populations that flowed into the modern-day Hudson Bay 8 ka; the further melting of ice sheets allowed Pacific populations to continue migrating east, admixing with Atlantic populations 7 ka.

Another curiosity in our dataset is the number of North Atlantic macroalgal species sampled in Churchill (Hudson Bay) but not sampled along the coast of Labrador where these species presumably occurred at some point as they migrated into the Arctic. These species included *Ahnfeltia plicata* (Fig. E3), *Coccotylus brodiei* (Fig. E8), *Laminaria digitata* (Fig. E57), *Ptilota gunneri* (Fig. E28), and *Pylaiella* sp. 1littoralis (Fig. E66). Although *Ahnfeltia plicata* and *Laminaria digitata* are reported from the

coast of Northern Labrador (South & Tittley 1986), these reports may correspond to the genetic groups sampled here (*Ahnfeltia borealis* and *Laminaria solidungula*). A period of cooling also occurred in the Arctic 3 to 6 ka ago, an event dubbed Neoglaciation during which glaciers grew or reformed in some areas, causing some warm-adapted flora and fauna to adjust their ranges southwards (Miller *et al.* 2010a). It is possible previously established species were eliminated along the coast of Northern Labrador during this time, allowing congeners to move in, including *Ahnfeltia borealis*, *Coccotylus truncatus*, *Ptilota serrata* Kützing, and *Laminaria solidungula*. Indeed, *Ahnfeltia borealis* and *Laminaria solidungula* appear to be cold-adapted species, with collections of both species largely restricted to Arctic and sub-Arctic waters (Fig. E1 and E58), the latter considered an "Arctic-type" species (Lee 1973).

Potential for Arctic origins in Arctic marine flora

The possibility of marine macroalgal populations surviving glaciations in the Arctic basin has received little to no attention, largely because multi-year sea ice in the Arctic is assumed to preclude the persistence of marine flora during peak glaciation. This assumption, however, must be reconciled with the population level data presented here that revealed the presence of unique genetic groups and haplotypes in the Arctic not attributable to North Atlantic or North Pacific collections, a pattern upheld in 8/12 of the well sampled species (Fig. 4.2C). The differentiated population structure of some species sampled in the Northern Bering Sea and Northern Alaska is particularly striking given the proximity of the two populations, though shared haplotypes were frequent (viz. *Coccotylus truncatus* [Fig. E9 and E10], *Odonthalia dentata* [Fig. E20], *Phycodrys fimbriata* [Fig. E23], and *Rhodomela sibirica* [Figs. 4.1A and E33]). Other species were

notable for having private Arctic haplotypes in Northern Alaska (viz. *Alaria esculenta* [Fig. E41], *Chaetopteris plumosa* [Fig. E45], *Laminaria solidungula* [Fig. E58], and *Ulva prolifera* [Fig. E86], in addition to the above species). This suggests that some elements of the Arctic flora may have persisted in glacial refugia in the North Pacific and in the Arctic basin, with recent migration between populations in some species. During the LGM, coastal margins of the Bering Land Bridge extended into the Bering Sea, with seasonal ice cover occurring in the southwestern Bering Sea, making this a likely refugial location from some of the Pacific species hypothesized to have recolonized the Arctic (Katsuki & Takahashi 2005; Caissie *et al.* 2010). Though the Western Arctic was locked in multi-year sea ice, portions of the Siberian coastline as far East as the Laptev Sea appear to have remained seasonally ice-free at least as early as 16 ka due to warm Atlantic water entering the Arctic through the Fram Strait (Svendsen *et al.* 2004; Bradley & England 2008; Taldenkova *et al.* 2008; Xiao 2014), which may have provided Arctic refuge for some species of macroalgae. The role of katabatic winds and the formation of polynyas, recurrent areas of ice-free water, also may have played a role maintaining a seasonally ice-free shoreline (Bradley & England 2008); the modern day Arctic features numerous polynyas, particularly along the margins of the Arctic basin, enhancing early spring productivity and creating biodiversity hotspots (Christine 2013).

Private Arctic haplotypes and unique genetic groups sampled in Churchill (Hudson Bay) also suggest the existence of Arctic periglacial refugia in the Eastern Arctic (see Results). Recent work in *Fucus distichus* suggested Arctic populations may be seeding Atlantic and Pacific populations (Laughinghouse *et al.* 2015), though the

proposed refugial locations in the Canadian Arctic Archipelago were almost certainly locked in multi-year sea ice during the LGM (Xiao 2014). Reconstructions of peak glacial sea-surface temperatures indicate that the coastlines of Svalbard and Greenland likely experienced seasonal ice-cover (Pflaumann *et al.* 2003), meaning refugial populations of marine flora could have survived in these Arctic areas providing suitable coastal habitat was available despite terrestrial ice-sheets. The Barents Sea also should not be overlooked (Bradley & England 2008; Taldenkova *et al.* 2008; Xiao 2014). Given coastal habitat in the Northwest Atlantic appears to have been more available during the LGM than previously assumed (see Chapter 3), the above scenarios do not seem unreasonable. The notion that a significant portion (up to 46%; Fig. 4.2B) of species with contemporary Arctic populations survived glaciation, at least in part for some, in the Arctic basin is a radical shift from the current consensus (Lee 1973; Dunton 1992). If true, it means the Arctic basin may be evolutionarily independent as compared to the Atlantic and Pacific basins, having harbored unique species and population level biodiversity at the fringes of ice sheets during peak glaciation. More sampling in the North (e.g. Greenland, Siberia) will be necessary to further explore the possibility of Arctic periglacial refugia.

Conclusions

The haplotype patterns presented here indicated that the Arctic marine macroalgal flora was recolonized from both the Atlantic and Pacific basins following the LGM, and that the Pacific contribution to Arctic recolonization is greater than previously recognized, confirming the work of Adey *et al.* (2008) and Saunders and McDevit (2013). The haplotype patterns presented here were consistent with the

paleogeography of the North American Arctic, in that species moved into the Western Arctic from the Pacific while Atlantic species migrated into the Hudson Bay, shortly followed by secondary contact of Pacific and Atlantic populations. Future monitoring of the Arctic for ecosystem shifts northward should therefore recognize the fluidity of both the North Atlantic and the North Pacific with the Arctic basin. It should be noted that the scenarios presented here for individual species are hypotheses; increased sampling, genomic level datasets, and coalescent based population genetic analyses will be needed to elucidate the specific details regarding the history in individual species. The conclusions drawn here will no doubt become updated with time, just as the conclusions of authors such as Taylor (1957) and Lee (1973) were revised in light of the data presented here. Taxonomic work also remains to be done in much of the marine Arctic flora; Russian species need to be considered as names become assigned to the genetic groups used here. Haplotype variation was also indicative of periglacial Arctic refugia, possibly along the coastlines of Siberia and Greenland. This raises new questions and possibilities regarding the phylogeographic history of marine Arctic biodiversity. Continued sampling in the North Pacific and Arctic will be critical to further unraveling the nature of marine Arctic recolonization.

Acknowledgements

We thank the many people who facilitated the collection of specimens: Dr. Meghann Bruce, Dr. Kyatt Dixon, Kirby Morrill, Dr. Amanda Savoie; Dr. Kenneth Dunton at the University of Texas for facilitating our sampling in the Beaufort (Northern Alaska); Dr. Yotsukura Norishige at Hokkaido University for providing collections from Hokkaido; Dr. Kjersti Sjøtun at the University of Bergen for facilitating

our sampling in Norway; Don Stiles and James Horner for facilitating the collection of samples in Nome, Alaska. We also thank everyone who helped generate COI-5P data, particularly Tanya Moore, and Alex Geoffroy and Line Le Gall for providing trace files. This project was funded by the Northern Scientific Training Program, the Natural Sciences & Engineering Research Council of Canada through an NSERC Post-Graduate Scholarship to T.T. Bringloe and a Discovery Grant to G.W. Saunders, and the New Brunswick Innovation Foundation.

References

Adey WH, Lindstrom SC, Hommersand MH, Müller KM (2008) The biogeographic origin of Arctic endemic seaweeds: a thermogeographic view. *Journal of Phycology*, **44**, 1384–1394.

Altschul SF, Gish W, Miller W, Myers EW, Lipman DJ (1990) Basic local alignment search tool. *Journal of Molecular Biology*, **215**, 403-410

Bradley RS, England JH (2008) The Younger Dryas and the Sea of Ancient Ice. *Quaternary Research*, **70**, 1–10.

Briner JP, Davis PT, Miller GH (2009) Latest Pleistocene and Holocene glaciation of Baffin Island, Arctic Canada: key patterns and chronologies. *Quaternary Science Reviews*, **28**, 2075–2087.

Bringloe TT, Dunton KH, Saunders GW (2017) Updates to the marine algal flora of the Boulder Patch in the Beaufort Sea off Northern Alaska as revealed by DNA Barcoding. *ARCTIC*, **70**, 3–6.

Caissie BE, Brigham-Grette J, Lawrence KT, Herbert TD, Cook MS (2010) Last Glacial Maximum to Holocene sea surface conditions at Umnak Plateau, Bering Sea, as inferred from diatom, alkenone, and stable isotope records. *Paleoceanography*, **25**, 1–16.

Campana GL, Zacher K, Fricke A, Molis M, Wulff A, Quartino ML, Wiencke C (2009) Drivers of colonization and succession in polar benthic macro- and microalgal communities. *Botanica Marina*, **52**, 655–667.

Castelloe J, Templeton AR (1994) Root probabilities for intraspecific gene trees under neutral coalescent theory. *Molecular Phylogenetics and Evolution*, **3**, 102−113.

Chan A (2018). DNA barcode and phylogenetic analyses of sphacelariales (Phaeophyceae) emphasizing Canada and contiguous coastal areas. Thesis (Honours). University of New Brunswick, Canada.

Christie H, Norderhaug KM, Fredriksen S (2009) Macrophytes as habitat for fauna. *Marine Ecology Progress Series*, **396**, 221−233.

Christine M (2013) Marine Ecosystems. In *Arctic Biodiversity Assessment: Status and Trends in Arctic Biodiversity*, Narayana Press, Denmark, p 487–527.

D'Odorico P, He Y, Collins S, De Wekker SFJ, Engel V, Fuentes JD (2013) Vegetation-microclimate feedbacks in woodland-grassland ecotones. *Global Ecology and Biogeography*, **22**, 364–379.

Dunton KH (1992) Arctic biogeography: The paradox of the marine benthic fauna and flora. *Trends in Ecology and Evolution* **7,** 183–189.

Dyke AS, Andrews JT, Clark PU, England JH, Miller GH, Shaw J, Veillette JJ (2002) The Laurentide and Innuitian ice sheets during the Last Glacial Maximum. *Quaternary Science Reviews*, **21**, 9–31.

Dyke AS, Prest VK (1987) Paleogeography of northern North America, 18000-5000 years ago. Geological Survey of Canada, 1-3.

Fraser CI, Nikula R, Waters JM (2011) Oceanic rafting by a coastal community. *Proceedings of the Royal Society B*, **278**, 649−655.

Freshwater DW, Rueness J (1994) Phylogenetic relationships of some European *Gelidium* (Gelidiales, Rhodophyta) species, based on *rbc*L nucleotide sequence analysis. *Phycologia* **33**, 187–194.

Guiry M, Guiry G (2018) AlgaeBase. http://www.algaebase.org.

Huang J, Zhang X, Zhang Q, *et al.* (2017) Recently amplified arctic warming has contributed to a continual global warming trend. *Nature Climate Change*, **7**, 875–879.

Jueterbock A, Smolina I, Coyer JA, Hoarau G (2016) The fate of the Arctic seaweed *Fucus distichus* under climate change: an ecological niche modelling approach. *Ecology and Evolution*, **6**, 1712−1724.

Katsuki K., Takahashi K (2005) Diatoms as paleoenvironmental proxies for seasonal productivity, sea-ice and surface circulation in the Bering Sea during the late

Quaternary. *Deep-Sea Research Part II: Topical Studies in Oceanography*, **52**, 2110–2130.

Kaufman DS, Ager TA, Anderson NJ, *et al.* (2004) Holocene thermal maximum in the western Arctic (0-180°W). *Quaternary Science Reviews*, **23,** 529–560.

Kearse M, Moir R, Wilson A, *et al.* (2012). Geneious Basic: An integrated and extendable desktop software platform for the organization and analysis of sequence data. *Bioinformatics*, **28**, 1647–1649.

Kim SH, Kawai H (2002) Taxonomic revision of *Chordaria flagelliformis* (Chordariales, Phaeophyceae) including novel use of the intragenic spacer region of rDNA for phylogenetic analysis. *Phycologia*, **41**, 328–339.

Krause-Jensen D, Duarte CM (2014) Expansion of vegetated coastal ecosystems in the future Arctic. *Frontiers in Marine Science*, **1**, 1-10.

Lane CE, Lindstrom SC, Saunders GW (2007) A molecular assessment of northeast Pacific *Alaria* species (Laminariales, Phaeophyceae) with reference to the utility of DNA barcoding. *Molecular Phylogenetics and Evolution*, **44**, 634–648.

Laughinghouse HD, Müller KM, Adey WH, Lara Y, Young R, Johnson G (2015) Evolution of the Northern Rockweed, *Fucus distichus*, in a regime of glacial cycling: implications for benthic algal phylogenetics. *PloS ONE*, **10**, e0143795.

Le Gall L, Saunders GW (2010) DNA barcoding is a powerful tool to uncover algal diversity: A case study of the phyllophoraceae (Gigartinales, Rhodophyta) in the Canadian flora. *Journal of Phycology*, **46**, 374–389.

Lee RKS (1973) General ecology of the Canadian Arctic benthic marine algae. *ARCTIC*, **26**, 32−43.

Lindstrom SC (1987) Possible sister groups and phylogenetic relationships among selected North Pacific and North Atlantic Rhodophyta. *Helgolander Meeresunters*, **41**, 245−260.

Lindstrom SC (2006) Biogeography of Alaskan seaweeds. *Journal of Applied Phycology*, **18**, 637–641.

Lindstrom SC, Olsen JL, Stam WT (1996) Recent radiation of the Palmariaceae (Rhodophyta). *Journal of Phycology*, **32**, 457–468.

Macaya EC, Lopez B, Tala F, Tellier F, Thiel M (2016) Float and raft: role of buoyant seaweeds in the phylogeography and genetic structure of non-buoyant associated flora. In: Hu ZM, Fraser C (eds) *Seaweed phylogeography: adaptation and*

evolution of seaweeds under environmental change. Springer, Dordrecht, p 97−130.

Maggs CA, Castilho R, Foltz D, *et al.* (2008) Evaluating signatures of glacial refugia for North Atlantic benthic marine taxa. *Ecology*, **89**, S108–S122.

Manhart JR (1994) Phylogenetic analysis of green plant *rbc*L sequences. *Molecular Phylogenetics and Evolution*, **3**, 114–127.

McDevit DC, Saunders GW (2010) A DNA barcode examination of the Laminariaceae (Phaeophyceae) in Canada reveals novel biogeographical and evolutionary insights. *Phycologia*, **49**, 235–248.

Miller GH, Brigham-Grette J, Alley RB, *et al.* (2010a) Temperature and precipitation history of the Arctic. *Quaternary Sciences Reviews*, **29**, 1679−1715.

Miller GH, Alley RB, Brigham-Grette J, Fitzpatrick JJ, Polyak L, Serreze MC, White JWC (2010b) Arctic amplification: Can the past constrain the future? *Quaternary Sciences Reviews*, **29**, 1779−1790.

Müller R, Laepple T, Bartsch I, Wiencke C (2009) Impact of oceanic warming on the distribution of seaweeds in polar and cold-temperate waters. *Botanica Marina*, **52**, 617–638.

Neiva J, Paulino C, Nielsen MM, *et al.* (2017) Glacial vicariance drives phylogeographic diversification in the amphi-boreal kelp *Saccharina latissima*. *Scientific Reports*, **8**, 1112.

O'Reilly P, Reimchen TE, Beech R, Strobeck C (1993) Mitochondrial DNA in Gasterosteus and Pleistocene glacial refugium on the Queen Charlotte Islands, British Columbia. *Evolution*. **47**, 678-684.

Pflaumann U, Sarnthein M, Chapman M, *et al.* (2003). Glacial North Atlantic: sea-surface conditions reconstructed by GLAMAP 2000. *Paleoceanography*, **18,** 1–21.

Polyak L, Alley RB, Andrews JT, *et al.* (2010). History of sea ice in the Arctic. *Quaternary Science Reviews*, **29**, 1757–1778.

Renaud PE, Sejr MK, Bluhm BA, Sirenko B, Ellingsen IH (2015) The future of Arctic benthos: expansion, invasion, and biodiversity. *Progress in Oceanography*, **139**, 244−257.

Saunders GW (2005) Applying DNA barcoding to red macroalgae: A preliminary appraisal holds promise for future applications. *Philosophical Transactions of the Royal Society B*, **360**, 1879−1888.

Saunders GW (2014) Long distance kelp rafting impacts seaweed biogeography in the northeast Pacific: the kelp conveyor hypothesis. *Journal of Phycology*, **50**, 968–974.

Saunders GW, Kucera H (2010) An evaluation of *rbc*l, *tufA*, UPA, LSU and ITS as DNA barcode markers for the marine green macroalgae. *Cryptogamie Algologie*, **31**, 487–528.

Saunders GW, McDevit DC (2012a). Methods for DNA barcoding photosynthetic protists emphasizing the macroalgae and diatoms. *Methods in Molecular Biology*, **858**, 207–222.

Saunders GW, McDevit DC (2012b) Acquiring DNA sequence data from dried archival red algae (Florideophyceae) for the purpose of applying available names to contemporary genetic species: a critical assessment. *Botany*, **90**, 191–203.

Saunders GW, McDevit DC (2013) DNA barcoding unmasks overlooked diversity improving knowledge on the composition and origins of the Churchill algal flora. *BMC Ecology*, **13**, 9.

Saunders GW, Moore TE (2013) Refinements for the amplification and sequencing of red algal DNA barcode and RedToL phylogenetic markers: a summary of current primers, profiles and strategies. *Algae*, **28**, 31−43.

South GR, Tittley I (1986) A checklist and distributional index of the benthic marine algae of the North Atlantic Ocean. Huntsman Marine Laboratory and British Museum (Natural History), St. Andrews and London, p 76.

Stroeven AP, Hättestrand C, Kleman J, *et al.* (2016) Deglaciation of Fennoscandia. *Quaternary Science Reviews*, **147**, 91–121.

Svendsen JI, Alexanderson H, Astakhov VI, *et al.* (2004). Late Quaternary ice sheet history of northern Eurasia. *Quaternary Science Reviews*, **23**, 1229–1271.

Taldenkova E, Bauch HA, Stepanova A, Strezh A, Dem'yankov S, Ovsepyan Y (2008) Postglacial to Holocene history of the Laptev Sea continental margin: palaeoenvironmental implications of benthic assemblages. *Quaternary International*, **183**, 40–60.

Taylor W (1957) Marine algae of the northeastern coast of North America, 2nd edn. University of Michigan Press, Ann Arbor, MI, p 427.

Vermeij GJ, Roopnarine PD (2008) The coming Arctic invasion. *Science*, **321**, 780−781.

Xiao, X (2014). Last Glacial Maximum to Holocene Arctic sea-ice variability: reconstruction from biomarkers. Thesis (PhD). University of Bremen, Germany.

Table 4.1. Primers used for amplification of various genes in marine macroalgae. Primer sequence portions underlined and in bold type for M13LF3 and M13Rx forward and reverse primers, respectively, refer to sequencing primers (M13F and M13R).

Locus	Taxa	Primers	Primer sequence (5'-3')	Reference/thermocycling regime
COI-5P	Red algae	M13LF3	**TGTAAAACGACGGCCAGT**ACHAAYCAYAARGATATHGG	Saunders and Moore (2013).
		M13Rx	**CAGGAAACAGCTATGAC**ACTTCTGGRTGICCRAARAAYCA	
COI-5P	Brown algae	GazF2	CCAACCAYAAAGATATWGGTAC3	Lane *et al.* (2007).
		GazR2	GGATGACCAAARAACCAAAA	
COI-5P	*Coccotylus*	GWSFn	TCAACAAAYCAYAAAGATATYGG3	Le Gall and Saunders (2010).
		GWSRx	ACTTCTGGRTGICCRAARAAYCA	Saunders and McDevit (2012b).
tufA	Green algae	TufGF4	GGNGCNGCNCAAATGGAYGG	Saunders and Kucera (2010).
		TufAR	CCTTCNCGAATMGCRAAWCGC	
*rbc*L-3P	*Rhodochorton*	F57	GTAATTCCATATGCTAAAATGGG	Freshwater and Rueness (1994).
		rbcLrevNEW	ACATTTGCTGTTGGAGTYTC	
*rbc*L-3p	*Battersia*, *Lithoderma*	L2	AAAAGTGACCGTTATGAATC	Thermocycling regime followed Saunders and Moore (2013).
		L8	CCAATAGTACCACCACCAAAT	
*rbc*L-3P	*Ulothrix*	GrbcLFi	TCTCARCCWTTYATGCGTTGG	Saunders and Kucera (2010).
		1385R	AATTCAAATTTAATTTCTTTCC	Manhart (1994).
ITS	*Coccotylus truncatus*	P1	GGAAGGAGAAGTCGTAACAAGG	Saunders and Moore (2013).
		G4	CTTTTCCTCCGCTTATTGATATG	

ITS	*Rhodomela sibirica*	RLycF1 RLycR1	TAGGGGTACAGTGGTCTCAC GAATCATTCGTCCTAAACGTC	Newly developed. Thermocycling regime followed Saunders and Moore (2013).
ycf35	*Ahnfeltia borealis*	ycf35F1 ycf35R1	CTTGCGCTTTCGCGTCTTTCT CGCTAGATTTAGGTTCTAGTG	Newly developed. Thermocycling regime: 95^{o}C for 2 mins; 35 cycles of 93^{o}C for 1 min, 55^{o}C for 1 min, and 72^{o}C for 2 mins; 72^{o}C for 2 mins.

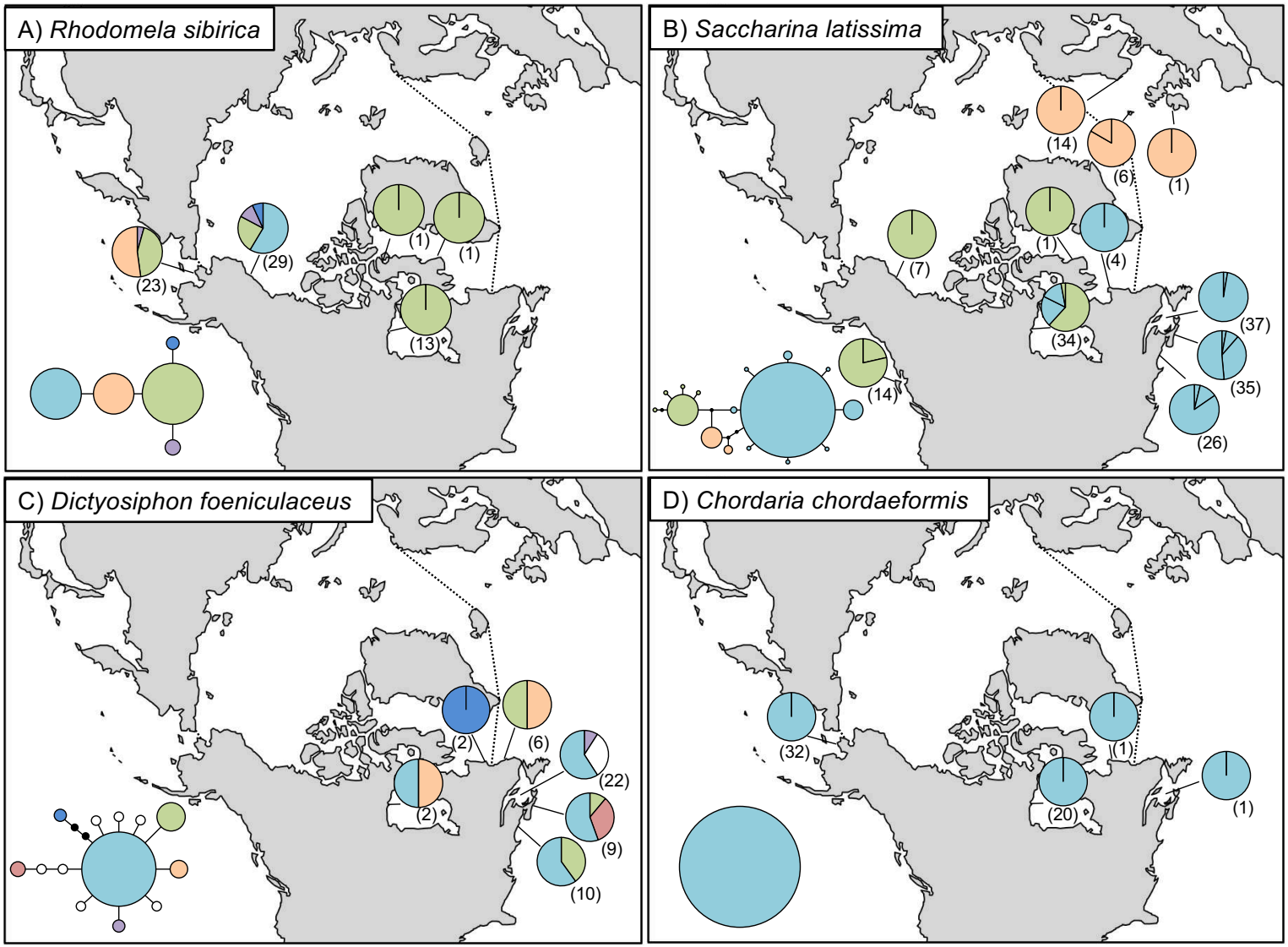
A) Rhodomela sibirica
(23)
(29)
(1)
(1)
(13)
B) Saccharina latissima
(14)
(6)
(1)
(7)
(1)
(4)
(34)
(37)
(35)
(14)
(26)
C) Dictyosiphon foeniculaceus
(2)
(6)
(22)
(2)
(9)
(10)
D) Chordaria chordaeformis
(32)
(1)
(20)
(1)

Figure 4.1 Haplotype maps and networks based on COI-5P data for four species of marine macroalgae, depicting various scenarios for recolonization of the North American Arctic. In the maps, numbers in parentheses represent sample size at a given locale, while the dotted lined delineates the Arctic basin. In the accompanying haplotype networks, circle size is proportional to sampling frequency for a given haplotype, and black circles indicate hypothesized substitutions between haplotypes. A) Biogeographic distribution of *Rhodomela sibirica*, depicting a case wherein Arctic populations were recently recolonized from the North Pacific. B) Biogeographic distribution of *Saccharina latissima*, depicting a case wherein Arctic populations were recently recolonized from both the North Pacific and the Northwest Atlantic. C) Biogeographic distribution of *Dictyosiphon foeniculaceus*, depicting a case wherein Arctic populations were recently recolonized from the Northwest Atlantic. D) Biogeographic distribution of *Chordaria chordaeformis*, depicting a case wherein the origin of Arctic populations remains uncertain given haplotype populations are monotypic from the North Pacific through to the Northwest Atlantic.

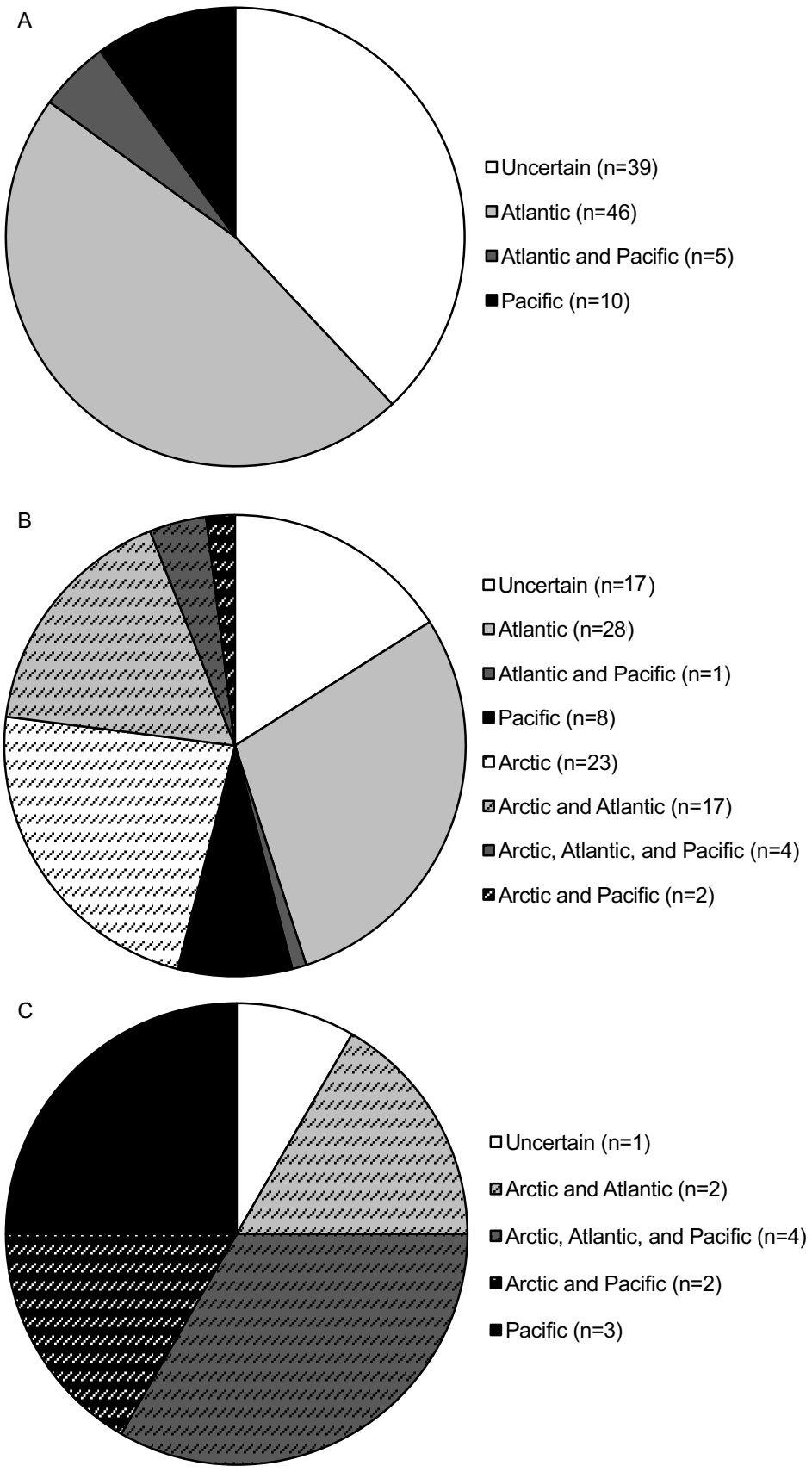
A
Uncertain (n=39)
Atlantic (n=46)
Atlantic and Pacific (n=5)
Pacific (n=10)
B
Uncertain (n=17)
Atlantic (n=28)
Atlantic and Pacific (n=1)
Pacific (n=8)
Arctic (n=23)
Arctic and Atlantic (n=17)
Arctic, Atlantic, and Pacific (n=4)
Arctic and Pacific (n=2)
C
Uncertain (n=1)
Arctic and Atlantic (n=2)
Arctic, Atlantic, and Pacific (n=4)
Arctic and Pacific (n=2)
Pacific (n=3)

Figure 4.2 The origins of Arctic species of marine macroalgae, based largely on COI-5P data. A) Breakdown in the origins of 100 species of Arctic marine macroalgae, allowing only for Pacific and Atlantic refugia. B) Breakdown in the origins of 100 species of Arctic marine macroalgae when Arctic periglacial refugia are considered as a potential origin for Arctic populations. C) Breakdown in the origins of 12 well sampled Arctic marine macroalgae (e.g. species with at least 20 Arctic records and 50 total records), allowing for Arctic refugia, as in B.

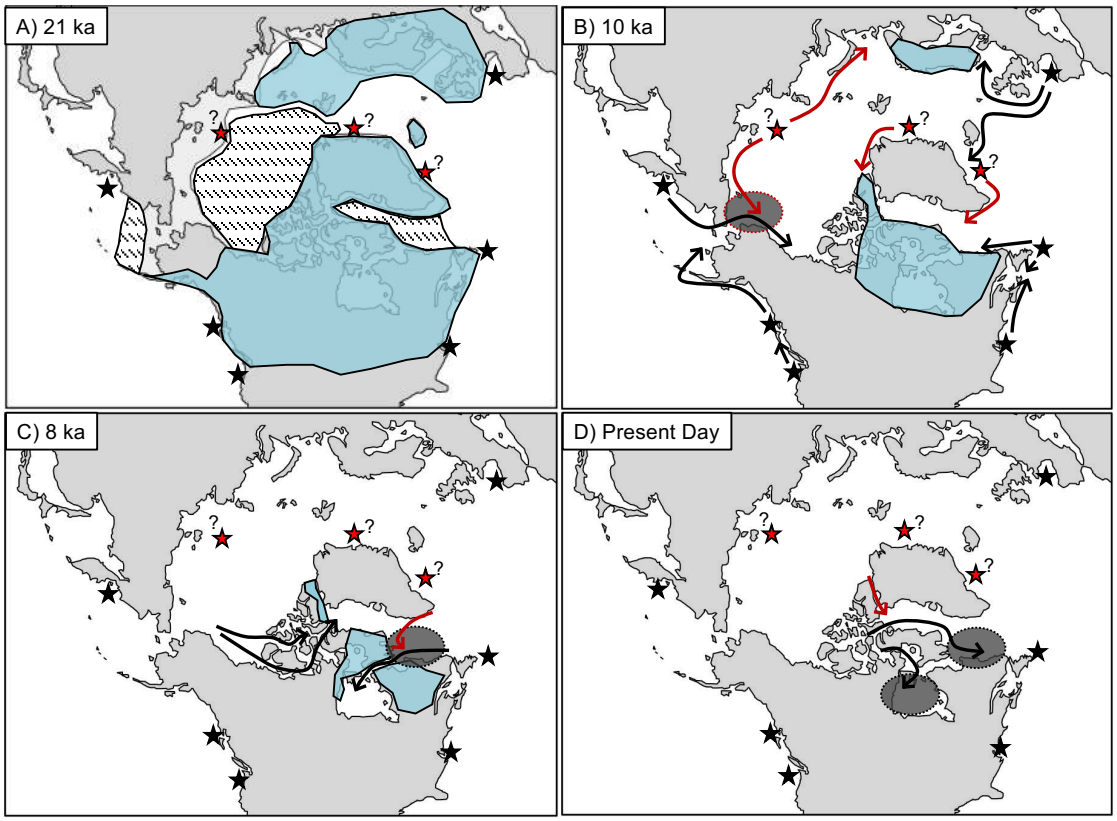

Figure 4.3 Hypothetical recolonization scenario following the Last Glacial Maximum for Arctic marine macroalgae. Stars denote refugial locations, with uncertain periglacial refugia denoted as red. A) Hypothesized refugial locations for marine macroalgae during the Last Glacial Maximum. Exposed continental shelf is depicted in lightest grey, continental ice-sheets are depicted in blue, while the hatched areas represent perennial ice cover. B) Population expansion from refugial locations upon the retreat of ice-sheets; red arrows represent movement from hypothesized periglacial refugia. The dark grey dashed oval represents a hypothesized zone of secondary contact. C) Expansion of Atlantic populations into modern day Hudson Bay; secondary contact occurred between Northeast and Northwest Atlantic populations. D) The final retreat of continental ice-sheets, allowing Pacific and Atlantic refugial populations to come into secondary contact

in the Hudson Bay and along the coast of Northern Labrador. This figure is adapted from the works of Dyke and Prest (1987), O'Reilly *et al.* (1993), Pflaumann *et al.* (2003), Bradley and England (2008), Taldenkova *et al.* (2008), Stroeven *et al.* (2016).

Chapter 5 General Conclusions

The Arctic faces many uncertainties in the future. During previous interglacial periods, Arctic warming rates significantly exceeded the global average (Anderson *et al.* 2006; Miller *et al.* 2010), a trend that appears to be continuing today (Huang *et al.* 2017). Predicting the response of marine organisms to contemporary warming is a daunting task. For instance, warmer waters are likely to promote the proliferation of calcified herbivores, in turn negatively impacting canopy-forming kelps due to herbivory, yet ocean acidification will also negatively impact the same herbivores and promote growth of macroalgae (Harley *et al.* 2012). Crustose red algae, conspicuous members of the Arctic flora, are likely to decline; increased storm severity may alter benthic communities; and boreal and temperate species could replace native cold-adapted species as they retreat further north in the Arctic (Brodie *et al.* 2014), with species specific responses to changing isotherms (Müller *et al.* 2009). Indeed, time-series studies have already recorded changes to Arctic benthic communities, with some studies reporting increased biomass, northward range expansions, and changes to species composition (Krause-Jensen & Duarte 2014; Renaud *et al.* 2015). Despite the efforts to model changes to a warming Arctic (e.g. IPCC 2014), the projected impact of these changes remains poorly understood. Ultimately, the following questions must be addressed: 1) will the net change to the Arctic be positive or negative; 2) what are the parameters by which we define this change as positive or negative; and 3) given humans are the cause of recent climate change, are we obligated to correct or reverse the current warming trend? Though these questions are beyond the scope of this thesis, the work presented here offers insight worth considering as part of the ongoing discussion about climate change.

This thesis has helped resolve the phylogeographic and recent history (since the Last Glacial Maximum [LGM]) of marine macroalgal species, improving our understanding of how current day Arctic biodiversity came to exist. Previous to this thesis, the opening of the Bering Strait was hypothesized to have initiated significant Pacific to Atlantic biotic interchange that precipitated numerous contemporary North Atlantic lineages (Reid 1990; Vermeij 1991; Lindstrom 2001). Glaciation was also believed to have had a significant impact on northern coastal communities. Marine flora in the Northwest Atlantic were largely assumed to have recolonized recently from the Northeast Atlantic (Taylor 1957; Vermeij 1978; Ingolfsson 1992), and Arctic populations were thought to be an extension of newly founded populations in the Northwest Atlantic (Taylor 1957; Lee 1973; Dunton 1992). This view painted a picture of Arctic flora as an impoverished extension of biodiversity in the Northeastern Atlantic. Genetic studies, however, began to tell a different story, suggesting some species survived glaciation in the Northwest Atlantic (Wares & Cunningham 2001; Li *et al.* 2016), while DNA barcording of marine flora in the Canadian Arctic revealed the presence of cryptic species diversity and population-level data suggesting some species recolonized the Arctic from the Pacific (Saunders & McDevit 2013). These studies indicated the consensus regarding current sources of Arctic biodiversity and the impacts of glaciation on contemporary populations was inaccurate and possibly misleading. Conservation and management, community ecology, and biomonitoring all depend on fundamental information such as what exists (i.e. biodiversity at the species and population levels), where it exists, and how it came to be (i.e. mechanisms promoting biological diversity). The conclusions from this thesis, drawn from a wide range of taxa,

have contributed to this basic understanding of Arctic marine coastal biodiversity. In addition, these findings highlight the Arctic as an ideal marine system for investigating questions related to evolutionary biology, particularly the counteracting forces of population divergence and secondary contact, and the development of reproductive isolation. Several species investigated in this thesis are candidates for further exploring contemporary interplay between these processes.

In Chapter 2, I investigated the phylogeographic history of 14 trans-Arctic lineages of red marine macroalgae. Time-calibrated phylogenies indicated the opening of the Bering Strait represented a significant geological event that promoted trans-Arctic speciation events, primarily from the Pacific to the Atlantic. These results were consistent with invertebrate studies (Briggs 1970; Reid 1990; Vermeij 1991), indicating Pacific-to-Atlantic invasion upon the opening of the Bering Strait was a community-wide phenomenon. A naturally occurring "Pacification" of the North Atlantic has therefore been ongoing for the past 4.8-7.4 Ma, promoting biological diversity by establishing new evolutionary lineages along Atlantic coastlines. The role of glaciation (i.e. the "species pump" hypothesis) in promoting trans-Arctic marine macroalgal species diversity, however, appears to have been minimal given the number of speciation events inferred during the Pleistocene was comparable to the number inferred during the Pliocene (the approximate timeframe between the opening of the Bering Strait and glaciation). This may be due to a slow rate of evolution and high likelihood of secondary contact between trans-Arctic lineages of marine macroalgae during interglacial periods. If true, then genetic differentiation between refugial populations in marine macroalgae is largely ephemeral during cycles of glaciation.

In Chapter 3, I investigated the recent population history of 20 species of trans-Atlantic marine macroalgae to determine if Northwest Atlantic populations were largely recolonized from Northeast Atlantic refugia following the LGM (20 ka). I uncovered population differentiation predating the LGM in 60% of the species examined, indicating the majority of the Northwest Atlantic flora was not recently (since the LGM) established from the Northeast Atlantic, in opposition to the historical consensus. The results presented in Chapter 3 suggest that the Northwest Atlantic marine flora survived glaciation, or, alternatively, may have been recently established from Pacific populations. A combination of all the previous recolonization scenarios certainly occurred. More importantly, these results shift the focus away from European populations and their role in establishing the contemporary Northwest Atlantic flora, and recast the Northwest Atlantic flora as having varied origins, including an evolutionary history in the Northwest Atlantic itself that generated units of biodiversity worth considering for conservation and management. In addition, these results have implications for understanding the nature of recolonization in the Arctic following the LGM, in that the Northwest Atlantic is likely an independent source of diversity that contributed to the establishment of contemporary Arctic marine flora.

In Chapter 4, I investigated recent origins in 100 Arctic species of marine macroalgae, building off the work of Saunders and McDevit (2013). This work revealed that, while species certainly recolonized the Arctic following the LGM from the Atlantic and the Pacific, the contribution of Pacific populations has been historically underestimated. Estimates from the best sampled species in the study indicated that the majority of Arctic populations had a Pacific contribution (75%, n=9/12). These results

were consistent with Chapter 2 and thermogeographic modelling (Adey *et al.* 2008; Adey & Hayek 2011) that indicated a Pacific connection with the Arctic and Atlantic basins has been ongoing since the opening of the Bering Strait. In addition, zones of secondary contact were identified in several species, particularly in Churchill (Hudson Bay, Manitoba) and along the northern coast of Labrador. Collectively, these results indicated that marine macroalgae may traverse the Arctic with relative ease (albeit, over geological time scales), suggesting a warming Arctic may be particularly amendable to the movement of species northwards, from both the Atlantic and Pacific Oceans. Perhaps the most surprising discovery from Chapter 4 was the large amount of species and population-level diversity not assignable to the Atlantic or Pacific basin, indicating upwards of 46% of contemporary Arctic populations may have origins in periglacial Arctic refugia. This finding has implications for future biomonitoring in the Arctic; it suggests the Arctic itself may harbour unique evolutionary lineages, once again shifting the focus away from recolonization processes, to considering Arctic marine coastal systems as phylogenetically distinct from the Atlantic and the Pacific. Besides revealing the origins of the contemporary Arctic marine macroalgal populations, this chapter contributed significantly to baseline species distribution data from several Arctic locations. The records generated for Nome, Alaska, given its proximity to the Bering Strait, will be particularly insightful as species are monitored for northward range extensions into the Arctic.

Overall, this thesis indicated that the world of Arctic marine macroalgae is an extraordinarily chimeric system, with input from both sides of the Atlantic and the North Pacific basins, and raises the possibility of its own evolutionary history contributing to

contemporary populations. The Arctic is generally viewed as harsh and punishing, with coastal marine species clinging to habitat barely left available by ice scour, and yet the genetic data presented here suggest Arctic lineages survive and thrive through cycles of glaciation. The need to document Arctic biodiversity has therefore never been so exigent, as climate change continues to reshape its seascape.

Future research

This thesis identified several avenues for further research. Perhaps the most consistent issue among the chapters presented here is the need for taxonomic work. Genetic groups lacking proper species names were common. While this generally did not present a problem for the analyses conducted, assigning species names will be critical to establishing a unified framework for labeling Arctic specimens in the future. An integrative approach to taxonomy, considering morphological traits in addition to DNA sequence data, would help to define species units (some of which were not clear in the above chapters). Consideration of the Northwest Pacific flora will be paramount when assigning species names to genetic units sampled in the Arctic. *Rhodomela sibirica* A.D.Zinova & Vinogradova serves as a telling example of the bias imparted by the historical view of Arctic flora as an extension of Northwest Atlantic species. This species was previously identified as the Atlantic *Rhodomela lycopodioides* f. *flagellaris* Kjellman (Saunders & McDevit 2013; Bringloe *et al.* 2017) and *Rhodomela lycopodioides* (Wilce & Dunton 2014), but recent work suggested this was the Russian species *R. sibirica* (Cripps 2018). DNA barcoding the Russian flora will likely lead to novel insights regarding the taxonomy and recent origins in many of the species presented in Chapter 4. Despite the need for taxonomic work, biodiversity research

currently faces a discordance between increasing sequencing power and diminishing taxonomic expertise; as such, alternative frameworks will likely be needed for recording species distributions in the Arctic.

More sampling is needed in the Arctic basin. The patterns presented in Chapter 4 suggested that many species survived in periglacial refugia, possibly along the coastlines of Siberia or Greenland. Sampling is also generally needed along the North American Arctic coastline in order to boost the number of Arctic collections in many of the species investigated. Adding these locations to the data presented in this thesis will further clarify the biogeography and recent origins of the Arctic flora. A major impediment to this work, however, is the logistical complications associated with sampling marine flora and fauna in the Arctic. Most locations are inaccessible and/or lack the proper equipment needed for scuba diving. There is also the added caveat that rocky habitat is likely patchy along Arctic coastlines (e.g. the Boulder Patch in Northern Alaska; Wilce & Dunton 2014), meaning flora may be absent in locations that otherwise facilitate collections. A survey of benthic substrate composition along Arctic coastlines would be enlightening. Dedicated coastal sampling via a research vessel will likely be the most promising method of guaranteeing successful collection of specimens. Sampling of invertebrates should also be conducted to maximize the gains from such endeavors, and would add another layer of depth to inferring community-wide patterns.

The Northwest Atlantic would also benefit from additional sampling in order to identify refugial locations, which were implied in Chapter 3. This sampling will require careful consideration. The datasets amalgamated in this thesis were coarse, in that broad scale patterns were inferred from limited collections, typically using a single genetic

marker. Investigating refugial patterns will require a high degree of resolution in terms of the spatial locations sampled and the genetic data generated. High-throughput sequencing will likely be needed, leading to novel insights regarding recolonization pathways following the LGM and subsequent evolution in local populations (e.g. Einfeldt 2018). It would be interesting to see how the patterns reported in this thesis compare to inferences from higher resolution datasets.

There is some opportunity to examine divergent trans-Arctic populations as they relate to the "species pump" hypothesis. These species are in the "grey" zone for speciation, and so were not included in the analyses in Chapter 2 (which attempted to focus on species-level diversity). Examples included *Ahnfeltia borealis* D.Milstein & G.W.Saunders, *Chaetopteris plumosa* (Lyngbye) Kützing, *Dictyosiphon* sp. 1GWS, *Eudesme virescens* (Carmichael ex Berkeley) J.Agardh, *Euthora cristata* (C.Agardh) J.Agardh, *Ralfsia fungiformis* (Gunnerus) Setchell & N.L.Gardner, and *Scagelia pylaisaei* (Montagne) M.J.Wynne. Divergence between trans-Arctic populations in these species certainly occurred much later in time compared to the speciation events presented in Chapter 2, which would boost divergence events during the Pleistocene. A reinterpretation of the "species pump" hypothesis may therefore be warranted in light of the expanded dataset, though it remains unclear whether the above species will indeed eventually speciate. The "species pump" could also be investigated as it applies to lineages within a given oceanic basin. Pleistocene glaciation may have promoted divergence in the Atlantic, for instance, if populations were regularly pushed into trans-Atlantic refugia (which appeared to be the case, see Chapter 3). On a final note, brown and green algal lineages could also be investigated.

The reliance on molecular clocks in Chapters 2 and 3 is a shortcoming that requires revisiting in future work. Molecular clocks are crucial for linking phylogenetic events to environmental conditions and/or changes. Molecular clocks are typically calibrated using fossil data, but geological records are limited in marine macroalgae; calibration points have been inferred from early Cretaceous fossil remains of *Padina* from the Gangapur formation, Miocene deposits from the Monterey formation with green, red, and brown algal remains (Parker & Dawson 1965; Silberfeld *et al.* 2010), and Cretaceous remains of coralline algae (Aguirre *et al.* 2010). Recent work has also proposed methods to link rates of molecular evolution with geological events, such as the opening of the Bering Strait (i.e. the geological event is the point of calibration; Loeza-Quintana & Adamowicz 2018). The calibration point for the molecular clocks presented in this thesis was the closing of the Isthmus of Panama. Weaknesses in the calibration method outlined in Chapters 2 and 3 included indirectly calibrating the clocks (COI-5P was calibrated from data presented in *Palmaria palmata* [Linnaeus] F.Weber & D.Mohr, which was calibrated using *cox*2-3 and *rpl*-*rps* data; Li *et al.* 2015) and applying the calibrated COI-5P and *rbc*L clocks across a wide range of taxa. An investigation into rate heterogeneity in COI-5P and *rbc*L among algal lineages would be of use, particularly as it relates to generation time, metabolic rates, DNA repair mechanisms, population sizes, and selective pressures. Because the inferences in Chapters 2 and 3 depend entirely on the range of clocks applied in the analyses, inaccuracies during the calibration process have the potential to significantly impact results, and in turn the interpretation of patterns observed (Ho *et al.* 2008). I attempted to compensate for this by applying a broad range of molecular clocks, and by

interpreting results within the range of divergence times estimated. The ranges of evolutionary rates applied in the analyses were reasonably large (0.3-1.2%/Ma in COI-5P, 0.14-0.45%/Ma in *rbc*L), yet they remained slower than the lower Kimura 2-parameter rate ranges invoked for COI-5P in marine invertebrates; reported ranges are 1.4%/Ma in the shrimp genus *Alpheus* (Knowlton & Weigt 1998), to 5.1%/Ma in tropical molluscs (Marko & Moran 2002), with recent work forwarding a rate of 2.8% in northern echinoderms (Loeza-Quintana & Adamowicz 2018). If the rate of COI-5P evolution is slower in marine plants as compared to marine invertebrates, it would be interesting to investigate why this is the case; metabolic rates, life history traits, and generation times are obvious starting points. Rate heterogeneity in *rbc*L for land plants has also been reported, varying by an order of magnitude; unfortunately, these rates were either for non-synonymous substitutions (Bousquet *et al.* 1992) or did not appear to account for saturation in synonymous substitutions (Frascaria *et al.* 1993), complicating comparison of these rates to those presented in this thesis. Zurawski *et al.* (1984) forwarded a chloroplast rate of evolution of 0.11%/Ma (based on *rbc*L and *atpB*), a rate three times slower than the average *rbc*L rate presented in this thesis. More work is needed to compare the rate of *rbc*L evolution in marine algae and other photosynthetic lineages, and to determine the drivers of rate heterogeneity. In the end, some level of uncertainty will remain regarding the molecular clocks used in Chapter 2 and 3, and the reader will have to decide if a broad enough range of rates was applied.

Many hypotheses have been advanced in this thesis, but their validity remains to be tested through further studies. Some of the hypotheses forwarded in Chapter 2 predicted certain population level patterns in specific species (e.g. if the trans-Arctic

divergence event inferred in *Rhodomela* is true, then *R. sibirica* and the *Rhodomela virgata* Kjellman genetic groups ought to have population level patterns consistent with recent Pacific to Atlantic trans-Arctic migration events). In Chapter 3, several trans-Atlantic species exhibited little to no COI-5P variation, implying recent trans-Atlantic migration, however, additional sampling and a more variable marker or high-throughput sequencing is needed to confirm this hypothesis and infer the direction of migration. In Chapter 4, periglacial Arctic refugia were inferred, but additional sampling is required from key locations to assess this proposal. For instance, if periglacial refugia were common along the eastern coast of Greenland, additional sampling could detect private haplotypes along this shoreline. It is worth reemphasizing that the conclusions reported in this thesis were inferred based on multi-species datasets, meaning incorrect scenarios for individual species were likely presented in some cases. Such is the trade-off for the opportunity to draw community wide conclusions. If drawn conservatively, community-wide inferences have the potential to be more broadly applicable than single species studies, however, single species studies will invariably have greater data resolution and thus present a more accurate picture for the actual species under study. At the same time, extrapolating community-wide conclusions from single species studies can be misleading, and yet the majority of phylogeographic studies of macroalgae focus on a single taxon (Hu *et al.* 2016). With the ongoing developments in bioinformatics, it seems inevitable that the divided research effort between the number of species studied and the resolution of the data for each species will eventually fade. Additional work improving on the population datasets presented in this thesis will undoubtedly shed new light on the history of many Arctic species. In addition, improved understanding of the

physiology, life history, and ecological role of marine coastal flora will add further depth to the conversation of how Arctic biodiversity came to exist. Indeed, biomonitoring of Arctic coastal communities will depend on such integrative studies, both at the species and community levels.

References

Anderson P, Bennike O, Bigelow N, *et al*. (2006) Last interglacial Arctic warmth confirms polar amplification of climate change. *Quaternary Science Reviews*, **25**, 1383–1400.

Adey WH, Hayek LAC (2011) Elucidating marine biogeography with macrophytes: quantitative analysis of the North Atlantic supports the Thermogeographic Model and demonstrates a distinct subarctic region in the Northwestern Atlantic. *Northeastern Naturalist*, **18**, 1–128.

Adey WH, Lindstrom SC, Hommersand MH, Müller KM (2008) The biogeographic origin of Arctic endemic seaweeds: a thermogeographic view. *Journal of Phycology*, **44**, 1384–1394.

Aguirre J, Perfectti F, Braga JC (2010) Integrating phylogeny, molecular clocks, and the fossil record in the evolution of coralline algae (Corallinales and Sporolithales, Rhodophyta). *Paleobiology*, **36**, 519–533.

Bousquet J, Strauss SH, Doerksen AH, Price RA (1992) Extensive variation in evolutionary rate of *rbc*L gene sequences among seed plants. *Proceedings of the National Academy of Sciences USA*, **89**, 7844–7848.

Briggs JC (1970) A faunal history of the North Atlantic Ocean. *Systematic Zoology*, **19**, 19–34.

Bringloe TT, Dunton KH, Saunders GW (2017) Updates to the marine algal flora of the Boulder Patch in the Beaufort Sea off Northern Alaska as revealed by DNA Barcoding. *ARCTIC*, **70**, 3–6.

Brodie J, Williamson CJ, Smale DA, *et al.* (2014). The future of the northeast Atlantic benthic flora in a high CO_2 world. *Ecology and Evolution*, **4**, 2787–2798.

Cripps KSA (2018) Unravelling *Rhodomela* spp. in Eastern Canadian waters: revisions in a cryptic red algal genus of the Ceramiales (Florideophyceae). Thesis (honours), University of New Brunswick.

Dunton KH (1992) Arctic biogeography: The paradox of the marine benthic fauna and flora. *Trends in Ecology and Evolution* **7,** 183–189.

Einfeldt AL (2018) Evolution in the North Atlantic: processes shaping spatial patterns of genetic diversity in introduced intertidal invertebrates. Thesis (PhD), University of New Brunwick.

Frascaria N, Maggia L, Michaud M, Bousquet J (1993) The *rbc*L gene sequence from chestnut indicates a slow rate of evolution in the Fagaceae. *Genome*, **36**, 668–671.

Harley CDG, Anderson KM, Demes KW, Jorve JP, Kordas RL, Coyle TA, Graham MH (2012) Effects of climate change on global seaweed communities. *Journal of Phycology*, **48**, 1064–1078.

Ho SYW, Saarma U, Barnett R, Haile J, Shapiro B (2008) The effect of inappropriate calibration: three case studies in molecular ecology. *PLoS ONE*, **3**, e1615.

Hu ZM, Duan DL, Lopez-Bautista J (2016) Seaweed phylogeography from 1994–2014: an overview. In: Hu ZM, Fraser C (eds) *Seaweed phylogeography: adaptation and evolution of seaweeds under environmental change*. Springer, Dordrecht, p 3−22.

Huang J, Zhang X, Zhang Q, *et al.* (2017) Recently amplified arctic warming has contributed to a continual global warming trend. *Nature Climate Change*, **7**, 875–879.

Ingolfsson A (1992) The origin of the rocky shore fauna of Iceland and the Canadian Maritimes. *Journal of Biogeography*, **19**, 705−712.

IPCC (Intergovernmental Panel on Climate Change) (2014) Climate Change 2014 Synthesis Report. IPCC, Geneva.

Knowlton N, Weigt LA (1998) New dates and new rates for divergence across the Isthmus of Panama. *Proceedings of the Royal Society of London B*, **265**, 2257–2263.

Krause-Jensen D, Duarte CM (2014) Expansion of vegetated coastal ecosystems in the future Arctic. *Frontiers in Marine Science*, **1**, 1-10.

Lee RKS (1973) General ecology of the Canadian Arctic benthic marine algae. *ARCTIC*, **26**, 32−43.

Li JJ, Hu ZM, Duan DL (2015) Genetic data from the red alga Palmaria palmata reveal a mid-Pleistocene deep genetic split in the North Atlantic. *Journal of Biogeography*, **42**, 902−913.

Li JJ, Hu ZM, Duan DL (2016) Survival in glacial refugia versus postglacial dispersal in the North Atlantic: the cases of red seaweeds. In: Hu ZM, Fraser C (eds) *Seaweed phylogeography: adaptation and evolution of seaweeds under environmental change*. Springer, Dordrecht, p 309−330.

Lindstrom SC (2001) The Bering Strait connection: dispersal and speciation in boreal macroalgae. *Journal of Biogeography*, **28**, 243−251.

Loeza-Quintana T, Adamowicz SJ (2018) Iterative calibration: a novel approach for calibrating the molecular clock using complex geological events. *Journal of Molecular Evolution*, **86**, 118–137.

Marko PB, Moran AL (2002) Correlated evolutionary divergence of egg size and a mitrochondrial protein across the Isthmus of Panama. *Evolution*, **56**, 1303–1309.

Miller GH, Alley RB, Brigham-Grette J, Fitzpatrick JJ, Polyak L, Serreze MC, White JWC (2010b) Arctic amplification: Can the past constrain the future? *Quaternary Sciences Reviews*, **29**, 1779−1790.

Müller R, Laepple T, Bartsch I, Wiencke C (2009) Impact of oceanic warming on the distribution of seaweeds in polar and cold-temperate waters. *Botanica Marina*, **52**, 617–638.

Parker BC, Dawson EY (1965) Non calcareous marine algae from California Miocene deposits. *Nova Hedwigia*, **10**, 273-295.

Reid DG (1990) Trans-Arctic migration and speciation induced by climatic change: the biogeography of *Littorina* (Mollusca: Gastropoda). *Bulletin of Marine Science*, **47**, 35–49.

Renaud PE, Sejr MK, Bluhm BA, Sirenko B, Ellingsen IH (2015) The future of Arctic benthos: expansion, invasion, and biodiversity. *Progress in Oceanography*, **139**, 244−257.

Saunders GW, McDevit DC (2013) DNA barcoding unmasks overlooked diversity improving knowledge on the composition and origins of the Churchill algal flora. *BMC Ecology*, **13**, 9.

Silberfeld T, Leigh JW, Verbruggen H, Cruaud C, de Reviers B, Rousseau F (2010) A multi-locus time-calibrated phylogeny of the brown algae (Heterokonta, Ochrophyta, Phaeophyceae): investigating the evolutionary nature of the 'brown algal crown radiation.' *Molecular Phylogenetics and Evolution*, **56**, 659−674.

Taylor W (1957) *Marine algae of the northeastern coast of North America*, 2nd edn. University of Michigan Press, Ann Arbor, MI, p 427.

Vermeij GJ (1978) *Biogeography and adaptation: patterns of marine life*. Harvard University Press, Cambridge, MA.

Vermeij GJ (1991) Anatomy of an invasion: the trans-Arctic interchange. *Paleobiology*, **17**, 281–307.

Wares JP, Cunningham CW (2001) Phylogeography and historical ecology of the North Atlantic intertidal. *Evolution*, **55**, 2455−2469.

Wilce RT, Dunton KH (2014) The Boulder Patch (North Alaska, Beaufort Sea) and its benthic algal flora. *ARCTIC*, **67**, 43–56.

Zurawski G, Clegg MT, Brown AHD (1984) The nature of nucleotide sequence divergence between barley and maize chloroplast DNA. *Genetics*, **106**, 735–749.

Appendix A Updates to the marine algal flora of the Boulder Patch in the Beaufort Sea off Northern Alaska as revealed by DNA barcoding

Citation for published manuscript: Bringloe TT, Dunton KH, Saunders GW (2017) Updates to the marine algal flora of the Boulder Patch in the Beaufort Sea off Northern Alaska as revealed by DNA Barcoding. *ARCTIC*, **70**, 3–6.

Abstract: Since its discovery four decades ago, the Boulder Patch kelp bed community in the Beaufort Sea has been an important site for long-term ecological studies in northern Arctic Alaska. Given the difficulties associated with identifying species of marine algae on the basis of morphology, we sought to DNA barcode a portion of the flora from the area and update a recently published species list. Genetic data were generated for 20 species in the area. Fifty-five percent of the barcoded flora confirmed the morphological species identifications. Five barcoded species revealed what are likely misapplied names to the Boulder Patch flora; the updated names include *Ahnfeltia borealis*, *Phycodrys fimbriata*, *Pylaiella washingtoniensis*, *Rhodomela lycopodioides* f. *flagellaris*, and *Ulva prolifera*. The remaining four species require taxonomic work and possibly represent new records for the Boulder Patch. Our observations indicate that we need considerably more research to understand marine macroalgal biodiversity in the Arctic. Supplementing Arctic species lists using genetic data will be essential in establishing an accurate and reliable baseline for monitoring changes in ecosystem biodiversity driven by long-term changes in regional climate.

Introduction

The Boulder Patch kelp bed community of the Beaufort Sea lies in Stefansson Sound off the northern coast of Alaska. The boulders and cobbles are part of a Quaternary deposit that is unique to the Beaufort Sea inner shelf, which is otherwise composed of silty clays and mud in relatively shallow water (4 – 7 m) that is estuarine in character (Dunton *et al.* 1982). The surprising faunal and floral diversity of the Boulder Patch, in concert with its relative isolation, has attracted scientific interest since its discovery by geologists in the mid 1970s (Reimnitz & Ross 1979). Subsequent ecological studies have focused on gaining an understanding of the community and the abiotic factors that influence productivity, kelp growth, community assemblages, and trophic structure (Dunton *et al.* 1982; Martin & Gallaway 1994; Aumack *et al.* 2007).

Long-term and nearly continuous studies in the Boulder Patch have provided a valuable baseline dataset for documenting biological responses to regional climatic change. Assessments of benthic diversity based on years of intensive sampling have also provided species inventories for infaunal and epilithic fauna (Dunton & Schonberg 2000) and for benthic algae (Wilce & Dunton 2014). These databases hold great promise for monitoring future changes in the Western Arctic since species from southern marine communities are expected to invade northward areas as perennial ice cover diminishes and isotherms retreat (Müller *et al*. 2009; Jueterbock *et al.* 2016). Accurate species inventories from multiple Arctic locations are critical to monitoring these changes as they relate to local flora and fauna. However, correct species identifications are critical to the accuracy and reliability of such baseline data. Marine algae can be extremely difficult to identify from morphology alone because of phenotypic plasticity, convergent

evolution, and cryptic species diversity (Saunders 2005). It is therefore important to corroborate morphological species identifications of marine algae with genetic data. Given the ecological importance of the Boulder Patch and its value for assessing shifts in benthic species composition and distribution, we sought to DNA barcode some of the flora reported by Wilce and Dunton (2014; DNA barcoding: Hebert *et al.* 2003; Saunders 2005). This note represents updates to the Boulder Patch flora in light of DNA barcoding efforts. We feel these updates are important considering the ongoing ecological work at the Boulder Patch, the overall difficulty of obtaining specimens from Arctic locations, and the limited number of genetically verified species records for Arctic algae.

Methods

We used scuba equipment to collect marine algae from several sites in the Boulder Patch area (Fig. A1) during two summer seasons (20-21 August 2014 and 20-25 July 2015). A portion of each specimen (approx. 1 cm^2) was preserved in silica gel (not as pressed material) and brought back to the University of New Brunswick for DNA extraction (Saunders & McDevit 2012) and amplification of the 5' end of the cytochrome c oxidase subunit I gene (COI-5P) in red algae (Saunders & Moore 2013) and brown algae (Saunders & McDevit 2012), and *tufA* in green algae (Saunders & Kucera 2010). These specimens are currently stored at the University of New Brunswick. Partial ribulose-1, 5-biphosphate carboxylase large subunit (rbcL-3P) or full-length reads of *rbc*L were amplified and sequenced for some specimens of brown algae for which COI-5P either did not amplify or was contaminated, and in specimens

for which additional markers were needed to resolve taxonomy (Saunders & McDevit 2012). Successful PCR products were sent to Genome Quebec for forward and reverse sequencing. All genetic data were edited in Geneious version 8.0 (http://www.geneious.com; Kearse *et al*. 2012).

Results and Discussion

We generated genetic data for two species of Chlorophyta, nine species of Ochrophyta, and nine species of Rhodophyta (Table A1; doi: dx.doi.org/10.5883/DS-UBPMF). For 11 (55%) of the species barcoded, genetic data were consistent with their name assignment based on morphology, though two of these remain only tentatively confirmed. The remaining 45% represented five species requiring name updates, two species of uncertain genetic assignment, and two species representing new records for the Boulder Patch (Table A1). We elaborate briefly on the updated species names below; however, we emphasize that these records may represent names misapplied by Wilce and Dunton (2014) or otherwise represent new records for the Boulder Patch (if both species identified occur in the area). In cases where sample sizes are large (e.g., >20 specimens barcoded in *Ahnfeltia borealis* D.Milstein & G.W.Saunders, *Phycodrys fimbriata* [Kuntze] Kylin, and *Rhodomela lycopodioides* f. *flagellaris* Kjellman), if the congener identified by Wilce and Dunton (2014) does occur in the Boulder Patch, it is likely a rare member of the flora.

Ulva prolifera O.F.Müller (previously identified as *Ulva flexuosa* Wulfen by Wilce and Dunton [2014]) is a species with genetically verified collections in Pacific, Arctic, and Atlantic basins but has only recently been DNA barcoded from Canadian Arctic waters (Hudson Bay; Saunders & McDevit 2013). *Pylaiella washingtoniensis*

C.C.Jao (previously identified as *Pylaiella littoralis* [Linnaeus] Kjellman) is similarly reported in all three oceans and has again only recently been DNA barcoded in the Arctic (Hudson Bay and Baffin Island; Saunders & McDevit 2013; Küpper *et al.* 2016). *Pylaiella littoralis* is also reported from the Arctic, but occurs as three genetic groups, one in the Pacific and two in the Atlantic (one of the Atlantic groups is confirmed in the Arctic; Saunders & McDevit 2013; Küpper *et al.* 2016). Substantial taxonomic work remains for species of *Pylaiella*.

In the red algae, *Ahnfeltia borealis* (previously identified as *Ahnfeltia plicata* [Hudson] Fries) is a recently described species occurring in Hudson Bay Arctic waters (Milstein & Saunders 2012), and although *A. plicata* is reported from the Arctic, it is a rare member of sub-Arctic flora (only two genetically verified collections from Churchill, Manitoba; Saunders & McDevit 2013) as compared to *A. borealis*. *Phycodrys rubens* (Linnaeus) Batters (updated to *Phycodrys fimbriata*) had been previously reported from the Arctic, but subsequent studies revealed that these specimens were assignable to *P. fimbriata* (Lindeberg & Lindstrom 2010; Saunders & McDevit 2013). Other genetically verified records of *Phycodrys* from Alaska include an *rbc*L sequence from St. Lawrence Island that matches *P. fimbriata* (published as *Phycodrys riggii* N.L. Gardner; Lin *et al.* 2001), and *P. riggii* from Southeast Alaska (van Oppen *et al.* 1995). Bona fide *Phycodrys rubens* is also rare in the Atlantic provinces of Canada and the New England states (only nine genetically verified records, with all records of *Phycodrys* from the Canadian Arctic assignable to *P. fimbriata*; Saunders & McDevit 2013). In short, *Phycodrys rubens* is relatively rare compared to *P. fimbriata* on Northwest Atlantic coasts, but it is common in the Northeast Atlantic, where *P.*

fimbriata does not appear to occur. *Rhodomela lycopodioides* f. *f lagellaris* (previously identified as *Rhodomela lycopodioides* [Linnaeus] C.Agardh) was previously reported only from the Arctic (Hudson Bay) along with several other genetic groups, including one that reportedly matches the features of *Rhodomela lycopodioides* sensu stricto (Saunders & McDevit 2013). We did not, however, verify *Rhodomela lycopodioides* sensu stricto in our Boulder Patch collections. We did recover a second species of *Rhodomela*, *Rhodomela* cf. *virgata* Kjellman, that also occurs in Churchill (Saunders & McDevit 2013) and has since been collected in the Northwest Atlantic (Saunders & Bringloe, unpublished data). Considerable taxonomic work is needed in *Rhodomela*.

Substantial DNA barcoding work remains to be done in the Boulder Patch. If the same proportion of mismatches between morphological and DNA species identifications found in our sampling holds true for all other species on the list from Wilce and Dunton (2014), then nearly half of the remaining identifications may also be uncertain. A concerted effort to continue DNA barcoding in both freshly collected benthic algae and archived algal specimens from the Boulder Patch is a high priority. The long history of ecological study in the area (Dunton *et al.* 1982; Wilce & Dunton 2014) has provided baseline information that will permit us to monitor impending ecological and species shifts due to climate change that may subsequently affect biodiversity. However, such monitoring requires accurate species lists, which highlights the urgent need to corroborate morphological identifications of marine algae with genetic data before such changes occur.

Acknowledgements

We thank the crew of the RV Proteus for their support of our diving efforts in Stefansson Sound and M. Bruce for her diving assistance in the collecting effort. We are grateful to A. Chan and T. Moore for their help with the generation of the molecular data. This project was funded by the Natural Sciences and Engineering Research Council of Canada, through a Post-Graduate Scholarship to T.T. Bringloe and a Discovery Grant to G.W. Saunders, and by the New Brunswick Innovation Foundation.

References

Aumack CF, Dunton KH, Burd AB, Funk DW, Maffione RA (2007) Linking light attenuation and suspended sediment loading to benthic productivity within an Arctic kelp-bed community. *Journal of Phycology*, **43**, 853–863.

Coastal Frontiers Corporation and LGL Ecological Research Associates, Inc. (1998) Liberty Development 1997-98 Boulder Patch survey. Final Report. Prepared for BP Exploration (Alaska) Inc. Anchorage.

Dunton KH, Schonberg SV (2000) The benthic faunal assemblage of the Boulder Patch kelp community. In: Truett, J.C., and Johnson, S.R. eds. *The Natural History of an Arctic Oil Field*, Elsevier Inc, 371–397.

Dunton KH, Reimnitz E, Schonberg SV (1982) An Arctic kelp community in the Alaskan Beaufort Sea. *ARCTIC*, **35**, 465–484.

Guiry M, Guiry G (2017) AlgaeBase. http://www.algaebase.org.

Hebert PDN, Cywinska A, Ball SL, DeWaard JR (2003) Biological identifications through DNA barcodes. *Proceedings of the Royal Society B*, **270,** 313–321.

Jueterbock A, Smolina I, Coyer JA, Hoarau G (2016) The fate of the Arctic seaweed *Fucus distichus* under climate change: an ecological niche modelling approach. *Ecology and Evolution*, **6**, 1712−1724.

Kearse M, Moir R, Wilson A, *et al.* (2012). Geneious Basic: An integrated and extendable desktop software platform for the organization and analysis of sequence data. *Bioinformatics*, **28**, 1647–1649.

Küpper FC, Peters AF, Shewring DM, *et al.* (2016) Arctic marine phytobenthos of northern Baffin Island. *Journal of Phycology*, **52**, 532-549.

Lin SM, Fredericq S, Hommersand MH (2001) Systematics of the Delesseriaceae (Ceramiales, Rhodophyta) based on large subunit rDNA and *rbc*L sequences, including the Phycodryoideae, subfam. nov. *Journal of Phycology*, **37**, 881-899.

Lindeberg MR, Lindstrom SC (2010) *Field guide to Seaweeds of Alaska*. University of Alaska Fairbanks: Alaska Sea Grant College Program.

Martin LR, Gallaway BJ (1994) The effects of the Endicott Development Project on the Boulder Patch, an Arctic kelp community in Stefansson Sound, Alaska. *ARCTIC*, **47**, 54–64.

Milstein D, Saunders GW (2012) DNA barcoding of Canadian Ahnfeltiales (Rhodophyta) reveals a new species – *Ahnfeltia borealis* sp. nov. *Phycologia*, **51**, 247–259.

Müller R, Laepple T, Bartsch I, and Wiencke C (2009) Impact of oceanic warming on the distribution of seaweeds in polar and cold-temperate waters. *Botanica Marina*, **52**, 617–638.

Reimnitz E, Ross CR (1979) Lag deposits of boulders in Stefansson Sound, Beaufort Sea, Alaska. U.S. Geological Survey Open File Report, 79-1205, p. 26.

Saunders GW (2005) Applying DNA barcoding to red macroalgae: A preliminary appraisal holds promise for future applications. *Philosophical Transactions of the Royal Society B*, **360**, 1879−1888.

Saunders GW, Kucera H (2010) An evaluation of *rbc*l, *tufA*, UPA, LSU and ITS as DNA barcode markers for the marine green macroalgae. *Cryptogamie Algologie*, **31**, 487–528.

Saunders GW, McDevit DC (2012) Acquiring DNA sequence data from dried archival red algae (Florideophyceae) for the purpose of applying available names to contemporary genetic species: a critical assessment. *Botany*, **90**, 191–203.

Saunders GW, McDevit DC (2013) DNA barcoding unmasks overlooked diversity improving knowledge on the composition and origins of the Churchill algal flora. *BMC Ecology*, **13**, 9.

Saunders GW, Moore TE (2013) Refinements for the amplification and sequencing of red algal DNA barcode and RedToL phylogenetic markers: a summary of current primers, profiles and strategies. *Algae*, **28**, 31−43.

Toimil LJ, England JM (1980) Investigation of rock habitats and sub-seabed conditions, Beaufort Sea, Alaska. Anchorage: Harding Lawson Associates.

van Oppen MJH, Draisma SGA, Olsen JL, Stam WT (1995) Multiple trans-Arctic passages in the red alga *Phycodrys rubens*: evidence from nuclear rDNA ITS sequences. *Marine Biology*, **123**, 179-188.

van Oppen MJH, Draisma SGA, Olsen JL, Stam WT (1995) Multiple trans-Arctic passages in the red alga *Phycodrys rubens*: evidence from nuclear rDNA ITS sequences. *Marine Biology*, **123**, 179-188.

Wilce RT, Dunton KH (2014) The Boulder Patch (North Alaska, Beaufort Sea) and its benthic algal flora. *ARCTIC*, **67**, 43–56.

Table A1. Summary of results from a DNA barcode survey of the Boulder Patch (Beaufort, North Alaska) marine flora. See Fig. A1 for site locations.

Morphological listing	Site(s) collected	Molecular Listing
Chlorophyta		
Blidingia spp.	Narwhal Is.	Confirmed (tentative): taxonomy of group needs study. Two species listed in Wilce & Dunton (2014) with a single genetic group confirmed (*Blidingia* sp._5GWS, n = 1).
Ulva flexuosa Wulfen	Endicott Is.	Updated: *Ulva prolifera* O.F.Müller (n = 2).
Ochrophyta		
Alaria esculenta (Linnaeus) Greville	DS11	Confirmed (n = 3).
Battersia arctica (Harvey) Draisma, Prud'homme & H.Kawai	E2	Confirmed (n = 2).
Chaetopteris plumosa (Lyngbye) Kützing	E3	Uncertain: cryptic complex (n = 2); material needed from type locality, but may represent a new species (recorded in Table A1 as *Chaetopteris* sp. _2plumosa).
Laminaria solidungula J.Agardh	DS11, E3, W3	Confirmed (n = 7).
Lithoderma fatiscens Areschoug	E3	Confirmed (tentative; recorded in Table A1 as *Lithoderma* sp. _2GWS): taxonomy of group needs study (n = 1).
Pylaiella littoralis (Linnaeus) Kjellman	Endicott Is.	Updated: *Pylaiella washingtoniensis* C.C.Jao (n = 2).
Saccharina latissima (Linnaeus) C.E.Lane, C.Mayes, Dreuhl, & G.W.Saunders	DS11, E3	Confirmed (n = 7).
Sorapion kjellmanii (Wille) Rosenvinge	DS11, E3, W3	Uncertain and new: two closely allied tilopteridalean crusts (Tilopteridalean sp._2GWS, n = 4;

		Tilopteridalean sp._3GWS, n = 2), which may account for records of this species. Taxonomic work is needed.
Rhodophyta		
Ahnfeltia plicata (Hudson) Fries	DS11, E2, E3, W3	Updated: *Ahnfeltia borealis* D.Milstein & G.W.Saunders (n = 23).
Coccotylus truncatus (Pallas) M.J.Wynne & J.N.Heine	DS11, E2, E3, L1, W3	Confirmed (n = 31).
Dilsea socialis (Postels & Ruprecht) Perestenko	DS11, E3, W3	Confirmed (n = 28).
Odonthalia dentata (Linnaeus) Lyngbye	DS11, E3, W2, W3	Confirmed (n = 24).
Phycodrys rubens (Linnaeus) Batters	DS11, E3, L1, W3	Updated: *Phycodrys fimbriata* (Kuntze) Kylin (n = 33).
Phymatolithon foecundum (Kjellman) Düwel & Wegeberg	DS11, E3	Confirmed (n = 2). Current name *Leptophytum foecundum* (Kjellmann) Adey.
Phymatolithon tenue (Rosenvinge) Düwel & Wegeberg	W3	Confirmed (n = 1). Considerable nomenclatural confusion surrounds the correct name for this genetic group (Guiry and Guiry 2017).
Rhodomela lycopodioides (Linnaeus) C.Agardh	DS11, E2, E3, W3	Updated & new: two species uncovered, neither is *Rhodomela lycopodioides sensu stricto*; *Rhodomela lycopodioides* f. *flagellaris* Kjellman (n = 29) and *R.* cf. *virgata* Kjellman (n = 1).

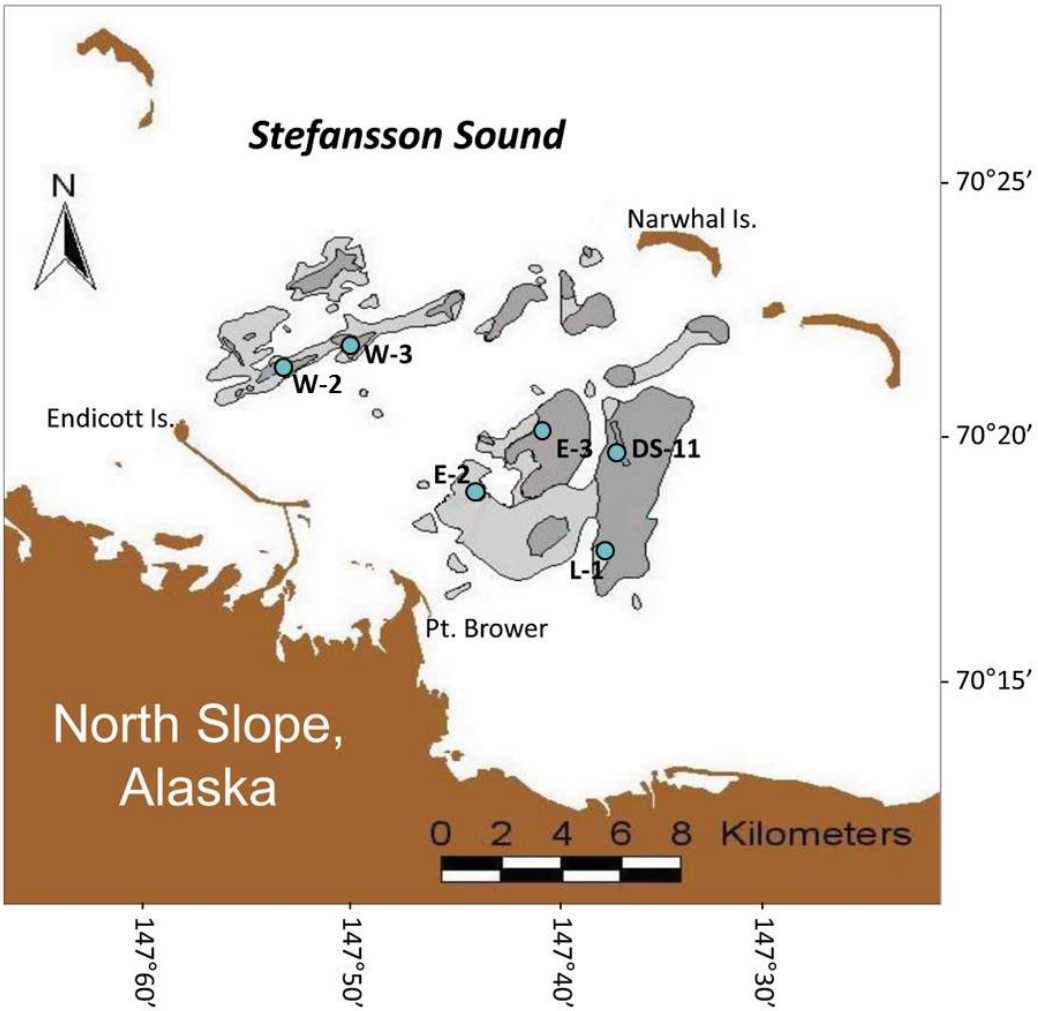

Fig A1: Long-term monitoring stations in the Boulder Patch in Stefansson Sound. Grey shaded areas represent Boulder Patch extent based on geological surveys conducted in 1980 and 1997 (Toimil & England, 1980; Coastal Frontiers and LGL, 1998). Light grey areas represent boulder cover between 10% and 25%, dark grey represents boulder cover greater than 25%.

Appendix B DNA barcoding of the marine macroalgae from Nome, Alaska (Northern Bering Sea) reveals many trans-Arctic species

Abstract: Marine macroalgal species are expected to shift northward with temperature regimes in the wake of climate change. Monitoring ecosystem shifts in the Arctic will depend on accurate and consistent species level datasets from a number of key locations. The Northern Bering Sea will be critical to monitoring the potential movement of Pacific species into the Arctic, yet currently has limited sampling. We therefore sampled the marine flora of Nome, Alaska, and surrounding area, August 12-22 (2017). Specimens were pressed and/or preserved in silica gel for DNA barcoding procedures. Several genetic markers were sequenced including the 5' end of the cytochrome *c* oxidase subunit I gene (COI-5P; n=551), elongation factor Tu (*tufA*; n=41), full length reads of the internal transcribed spacer of the ribosomal cistron (ITS; n=56), and full or partial reads of the ribulose-1, 5-biphosphate carboxylase large subunit (*rbc*L or *rbc*L-3P, respectively; n=24). These collections represented eight species of green algae, 20 species of brown algae, and 24 species of red algae. Most of the species sampled (67%, n=35) represented trans-Arctic species, 19% (n=10) represented species with distributions restricted to the Pacific, 8% (n=4) represented species restricted to the Arctic, and the remaining 6% (n=3) represented new genetic groups. Our survey revealed that the marine flora of the Nome, Alaska, is largely contiguous with the Northwest Atlantic. Repeated sampling from Nome and other key locations in the Northern Bering Sea (e.g. St. Lawrence Island) will be critical to further establishing baseline data for monitoring ecosystem shifts in an era of climate change.

Introduction

The Arctic marine biome is expected to undergo significant ecosystem shifts due to climate change, with some changes already underway (Canada Fisheries and Oceans 2012; IPCC 2014; Renaud *et al.* 2015). Marine macroalgae, in particular, are expected to undergo ecosystem changes as ocean temperature regimes shift and perennial ice cover diminishes in the Arctic (Campana *et al.* 2009; Müller *et al.* 2009; Krause-Jensen & Duarte 2014). The total impact of these changes remains difficult to predict and understand; knowledge gaps include the interactions between multiple stressors at the species and community levels, the impact of stressors on various life-history stages, potential for adaptation, and lack of baseline data regarding species diversity and biogeographic distributions (Harley *et al.* 2012; Mineur *et al.* 2015). Nonetheless, predicting the nature of ecosystem shifts due to climate change will be imperative to mitigating or adapting to ongoing changes to the Arctic (Krause-Jensen & Duarte 2014).

Such modelling inherently depends on an accurate understanding of Arctic macroalgal diversity. Unfortunately, marine floral inventories for Arctic locations remain poorly sampled, and by extension poorly understood. For example, Bringloe *et al.* (2017) estimated that taxonomic confusion likely exists in 45% of the marine macroalgal flora listed from the Beaufort Sea (Northern Alaska) by Wilce and Dunton (2014). This is partly exacerbated by difficulties associated with species identification of marine macroalgae due to cryptic diversity, simple morphology, phenotypic plasticity, and convergent evolution (Saunders 2005). DNA based species identification (i.e. DNA barcoding) circumvents the above problems associated with morphological identifications of species, and is leading to novel insights into Arctic marine flora (e.g.

Saunders & McDevit 2013). The few recently conducted DNA barcoding studies of Arctic marine macroalgae represent critical steps towards building accurate and consistent baseline data regarding species distributions in the Arctic (Saunders & McDevit 2013; Küpper *et al.* 2016; Bringloe *et al.* 2017). Additional marine Arctic locations need to be sampled in order to facilitate future forecasting of climate-driven ecosystem shifts.

One location in need of sampling is the Northern Bering Sea. This is an area that can be strategically monitored given the Bering Strait represents the junction between Pacific and Arctic basins; any flora or fauna shifting their ranges northwards into the Arctic will pass through this area. Sampling of marine macroalgae in the Bering Sea began in the 1700s (Wynne 2009), but sampling in the northernmost waters appears largely restricted to two expeditions that occurred more than a century ago (Kjellman 1889; Setchell & Gardner 1903), with more recent sampling on St. Lawrence and St. Matthew Islands (Wynne & Heine 1992). These studies suggest the flora of the Northern Bering Sea is largely Pacific in character, but with several species with distributions in the Arctic and Atlantic basins (e.g. *Coccotylus truncatus* [Pallas] M.J.Wynne & J.N.Heine, *Odonthalia dentata* [Linnaeus] Lyngbye, and *Phycodrys fimbriata* [Kuntze] Kylin, previously reported as *Phycodrys rubens* [Linnaeus] Batters [Wynne & Heine 1992, Wilce & Dunton 2014, Bringloe *et al.* 2017]). Indeed, several studies indicate that the flora of the North Pacific Ocean has close ties to the North Atlantic (Lindstrom 1987, 2001, 2006), and thermogeographic modelling supports the idea of a critical Pacific to Atlantic connection (Adey *et al.* 2008). The flora of the Northern Bering Sea

may therefore represent a crossroad between phylogenetically distinct basins, with flora associated with the Pacific, Arctic and Atlantic Oceans.

The objective of the current study was to compile the first genetically verified list of marine macroalgal species in the area surrounding Nome, Alaska (Northern Bering Sea). Furthermore, we sought to investigate the biogeographic composition of Nome species (e.g. is the Nome flora predominantly an extension of Pacific species, Atlantic species, or unique Bering Sea/Arctic flora?). By surveying the Nome flora, we hope to contribute to baseline knowledge regarding marine species diversity and composition in an area that will be critical for monitoring ecosystem shifts into the Arctic.

Methods

Marine macroalgae were collected over a two-week period (August 12-22nd, 2017) in the intertidal and via scuba in Nome (Alaska; Bering Sea, Pacific Ocean) and surrounding area, including Cape Nome, offshore of Cripple River, and various sites at Sledge Island (Fig. B1). A portion of each specimen (approx. 1 cm^2) was preserved in silica gel for DNA extraction, while several representatives of putative species were pressed to serve as vouchers (Saunders & McDevit 2012a). Specimens were brought back to the University of New Brunswick (where specimens are housed) for DNA extraction (Saunders & McDevit, 2012a). Several genes were amplified, including the 5' end of the cytochrome *c* oxidase subunit I gene (COI-5P) in red and brown algae, elongation factor Tu (*tufA*) in green algae, and full length reads of the internal transcribed spacer of the ribosomal cistron (ITS) and/or full or partial reads of the

ribulose-1, 5-biphosphate carboxylase large subunit (*rbc*L-3P or *rbc*L, respectively) for specimens for which COI-5P either did not amplify or was contaminated, and in specimens for which additional markers were needed for identification. The following primer combinations (forward/reverse) were used: for COI-5P, M13LF3/M13Rx in red algae (Saunders & Moore 2013), GazF2/GazR2 in brown algae (Lane *et al.* 2007), SphCOIF1 (5'-ATTTTTGGYGGTATYGCYGG-3')/SphCOIR1 (5'-TGCTGRTAAAGMACAGGATC-3') in *Battersia*, GWSFn/GWSRx in *Coccotylus* (Le Gall & Saunders 2010; Saunders & McDevit 2012b), GazF2/AlaR2 (5'-TGCTGATATAAYACTGGATC-3') in *Alaria*, and DevF1 (5'-CAGGAGTTATTGGAGGYTGT-3')/M13Rx in *Devaleraea*; for *tufA*, TufGF4/TufAR (Saunders & Kucera 2010); for *rbc*L, F57/rbcLrevNEW in *Boreophyllum*, *Devaleraea*, *Polyostea*, and *Mastocarpus* (Saunders & Moore 2013), and ND*rbc*L2/ND*rbc*L8 in *Alaria* and *Heterosaundersella* (Daugbjerg & Andersen 1997); for ITS, P1/G4 in *Alaria*, *Devaleraea* and *Heterosaundersella* (Saunders & Moore 2013), and P1/MasR1 in *Mastocarpus* (Bringloe *et al.* in review). All PCR thermocycling regimes for respective markers followed Saunders and Moore (2013), except *tufA* (Saunders & Kucera 2010). Successful PCR products were sent to Genome Quebec for forward and reverse sequencing using the same primers as above, with the exception of M13F/M13R forward and reverse sequencing primers used in red algae amplified with M13LF3/M13Rx (Saunders & Moore 2013). All genetic data were edited in Geneious version 8.0 (http://www.geneious.com; Kearse *et al.* 2012). Specimen information and GenBank accession numbers can be found online through the Barcode of Life Datasystems (BOLD; DS-NOME, Algal flora of Nome Alaska). Species delimitations

for COI-5P are based on a 2% divergence threshold, except in cases where taxonomic work supports the occurrence of two closely related but distinct species (i.e. *Corallina, Dilsea,* and *Phycodrys*). Biogeographic distributions detailed below are based on genetically verified records.

Results

In total, we sequenced COI-5P for 551 specimens, *tufA* for 41, ITS for 56, *rbc*L for 10, and *rbc*L-3P for 14, with a total of 602 specimens examined. These sequences revealed eight species of green algae, 20 species of brown algae, and 24 species of red algae. Most of the species sampled (67%, n=35) have broad distributional ranges extending from the Pacific to the Atlantic basins (e.g. trans-Arctic); of these species, 23 had genetically verified records from the Arctic (Fig. B2). Of the 52 species sampled, only 10 were previously reported strictly from the Pacific Ocean, while an additional three species represented new genetic groups (Fig. B2). Species specific results are discussed below. Parentheses following each species name indicates, in order, the number of genetically verified records from the Nome area, where specimens were sampled, and regions with genetically verified records (Pacific regions: Northwest [Japan and Russia], and Northeast Pacific [Aleutian Islands, Southwest Alaska, British Columbia, Canada, and Washington state, USA]; Arctic: Northern Bering Sea (St. Lawrence Is.), North Alaska [USA] through to Northern Labrador [Canada]; Atlantic regions: Northwest [Canadian Atlantic provinces and New England States] and Northeast Atlantic [Europe]).

CHOROPHYTA

Prasiolales, Prasiolaceae

***Prasiola calophylla* (Carmichael ex Greville) Kützing (n=1; Nome breakwater; NW Pacific, NE Atlantic):** *TufA* sequence data from the single Nome collection differs from a previously published sequence from Hokkaido, Japan, at a single site (Sutherland *et al.* 2016). *Rbc*L and *tufA* data from the Japan specimen closely allied with *P. calophylla* sequences from Ireland.

***Prasiola borealis* M.Reed (n=1, Nome breakwater; NE Pacific, NE Atlantic):** *TufA* data were an exact match to specimens attributed to *P. borealis* collected in Southeast Alaska and Chile (Garrido-Benavent *et al.* 2017), indicating this species has an amphitropical distribution. Specimens of *P. borealis* were also genetically verified from British Columbia (Canada) and Australia (one base pair different from our Nome collections in each case), however, this genetic group was also reported as European *Prasiola furfuracea* (Mertens ex Hornemann) Trevisan (also one base pair different from our Nome collections; Moniz *et al.* 2014). As noted by Garrido-Benavent *et al.* (2017), if these two species are found to be conspecifics, then *P. furfuracea* will be given nomenclatural priority, and *P. borealis* will be synonymized with the former.

Ulotrichales, Ulotrichaceae

***Acrosiphonia sonderi* (Kützing) Kornmann (n=1; SW Sledge Island; NW Pacific, NW Atlantic; taxonomic work needed):** This genetic group is verified from Russia and the Northwest Atlantic (BOLD DS-NOME, Algal flora of Nome Alaska), with *rbc*L linking this group to *A. sonderi* (Saunders & Kucera 2010), though the name assignment for this genetic group remains uncertain.

***Urospora* sp. 1NomePseudo (n=1; Nome breakwater; new genetic record; taxonomic work needed):** This genetic group does not match any published sequences for *Urospora* spp. Taxonomic work is needed to assign a species name.

***Urospora* sp. 1penicilliformis (n=1; Nome breakwater; NW Atlantic; taxonomic work needed):** This genetic group differs by three base pairs from a Northwest Atlantic genetic group published as *Urospora* sp. 1penicilliformis (Saunders & Kucera 2010). Taxonomic work is needed.

***Urospora* sp. 2Nome (n=1; Nome breakwater; new genetic group; taxonomic work needed):** As with *U.* sp.1NomePseudo, this is a new genetic group, matching most closely (97%) to *Urospora wormskioldii* (Mertens) Rosenvinge, which is reported from the North Pacific (Saunders & Kucera 2010) and North Atlantic (unpublished data). Taxonomic work is needed to assign a species name.

Ulvales, Ulvaceae

***Ulva lactuca* Linnaeus (n=22, Nome breakwater; NW & NE Pacific, Arctic, NW & NE Atlantic; taxonomic work needed):** Though widely reported, this genetic group is verified (based on *tufA* data) from the North Atlantic, Arctic, and Northeast Pacific basins (Saunders & McDevit 2013), and from Japan based on *rbc*L (AB097622).

***Ulva* sp. 3linza (n=13, Nome breakwater, Nome estuary; NE Atlantic; taxonomic work needed):** This genetic group matches unpublished sequences from Germany identified as *Ulva linza* Linnaeus (KT207446, KT290277, KT290278) and an Australian sequence that was a closest match to specimens identified as *Ulva procera* (K.Ahlner) Hayden, Blomster, Maggs, P.C.Silva, M.J.Stanhope & J.R.Waaland (six base pairs different; Kirkendale *et al.* 2013). The Australian genetic group was hypothesized to

have resulted from introduction events, and, as noted by the authors, taxonomic work is needed to assign a correct species name (Kirkendale *et al.* 2013).

OCHROPHYTA

Phaeophyceae

Desmarestiales, Desmarestiaceae

***Desmarestia aculeata* (Linnaeus) J.V.Lamouroux (n=1; SW Sledge Island; NE Pacific, Arctic, NW Atlantic; taxonomic work needed):** This species occurs as two genetic groups, one of which has been sampled in the Northeast Pacific and the Northwest Atlantic, while the second appears to be restricted to the Arctic and Northwest Atlantic (Saunders & McDevit 2013). The single Nome specimen matches the first mentioned genetic group, with sequences matching specimens from the Northwest Atlantic. Taxonomic work is needed to determine if the above genetic groups represent a single species.

***Desmarestia viridis* (O.F.Müller) J.V.Lamouroux (n=2; Nome breakwater; NW & NE Pacific, NW & NE Atlantic):** This species is widely distributed, with Pacific Northwest (KY047186-KY047190) and Pacific Northeast sequences quite divergent (up to 9 base pairs) from Northwest and Northeast Atlantic sequences (Oudot-Le Secq *et al.* 2006; Yang *et al.* 2014). The Nome sequences are most closely related to the Pacific lineage.

Ectocarpales, Acinetosporaceae

***Pylaiella washingtoniensis* Jao (n=17; East and North Sledge Island, Nome breakwater; NE Pacific, Arctic, NW Atlantic):** This species is genetically verified in the Northeast Pacific through to the Northwest Atlantic (Saunders & McDevit 2013;

Küpper *et al.* 2016), including Northern Alaska (Bringloe *et al.* 2017). This species also appears to have been introduced into the Southern hemisphere (Mystikou *et al.* 2016).

Ectocarpales, Chordariaceae

***Chordaria chordaeformis* (Kjellman) Kawai & S.H.Kim (n=34; Nome breakwater, Cape Nome; NW & NE Pacific, Arctic, NW& NE Atlantic):** This species has a broad distribution, with genetically verified records in the Arctic, both sides of the Atlantic, and both sides of the Pacific (Kim & Kawai 2002; Saunders & McDevit 2013). Interestingly, we recovered a second possible genetic group in this species, differing by 13 base pairs (just under 2% divergent). This COI-5P genetic group may correspond to the ITS Pacific group 1 sampled by Kim and Kawai (2002), which was reported from Kamchatka, Russia.

***Chordaria* sp. 1flagelliformis (n=10; Nome breakwater, East Sledge Island; NW& NE Pacific; taxonomic work needed):** This genetic group has been sampled previously in the Northwest and Northeast Pacific, and is closely related to an Arctic/Atlantic genetic group assigned to *Chordaria flagelliformis* (O.F. Müller) C.Agardh (Saunders & McDevit 2013). Kim and Kawai (2002) similarly recovered Atlantic and Pacific lineages in this species based on ITS data; this group likely corresponds to their Northwest Pacific genetic group 3, which was also sampled on St. Lawrence Island (North Pacific). Indeed, *rbc*L data for this genetic group match records from Kamchatka (Russia; Cho *et al.* 2003). Clearly, taxonomic work is needed to assign a species name to this genetic group, if indeed it is a species distinct from its Arctic/Atlantic counterpart.

***Eudesme virescens* (Carmichael ex Berkeley) J.Agardh (n=11; East and North Sledge Island; NW & NE Pacific, NW & NE Atlantic):** Though widely reported

(Guiry & Guiry 2018), previously genetically verified records exist only for the Pacific and Atlantic basins. COI-5P data indicate that this species occurs in the Northeast Pacific and Northwest Atlantic, while *rbc*L data indicate that it also occurs in the Northeast Atlantic and the Northwest Pacific (Ajisaka *et al.* 2007; Kawai *et al.* 2016). Interestingly, *rbc*L data for *E. virescens* from the Northwest Atlantic (GWS007044; BOLD; DS-NOME, Algal flora of Nome Alaska) is a match to *rbc*L data from the Northwest Pacific (AB199640), while the *rbc*L sequence for European *E. virescens* (LC108035) differs by six base pairs, indicating it may be a separate species.

***Microspongium alariae* (P.M.Pedersen) A.F.Peters (n=1; Southwest Sledge Island; NW Atlantic):** This genetic group matches most closely to Northwest Atlantic *Microspongium alariae* (P.M.Pedersen) A.F.Peters (Peters *et al.* 2015), but COI-5P differs at nine sites.

***Heterosaundersella* sp. 1Nome (n=1; North Sledge Island; NW Pacific; taxonomic work needed):** COI-5P and *rbc*L data for this specimen are an exact match to sequences published for *Saundersella simplex* (De A.Saunders) Kylin collected in Japan (disregarding likely sequence errors at the ends of the COI-5P fragment currently in GenBank; LC107841; Kawai *et al.* 2016). Our samples from the BC coastline, close to its type locality in Southeast Alaska, however, indicate *S. simplex* is assignable to a different genetic group (Guiry & Guiry 2018; BOLD; DS-NOME, Algal flora of Nome Alaska). Indeed, the Japan sequences group with *Heterosaundersella hattoriana* Tokida (*rbc*L: LC108036, AB199641), and another *Heterosaundersella* genetic group (*Heterosaundersella* sp. 1NFLD) recovered in Northern Labrador (Canada; BOLD; DS-

NOME, Algal flora of Nome Alaska), suggesting our Nome specimen is a member of this genus and that taxonomic work is needed to assign a species name.

Ectocarpales, Dictyosiphonaceae

***Dictyosiphon* sp. 1GWS (n=24; Nome breakwater, Cape Nome, East and North Sledge Island; NE Pacific, Arctic, NW Atlantic; taxonomic work needed):** This genetic group is verified in the Northeast Pacific, the Arctic, and the Northwest Atlantic (Saunders & McDevit 2013; Küpper *et al.* 2016). The two Atlantic records are somewhat divergent from Pacific specimens (up to five substitutions for COI-5P; LT546286), with Nome specimens matching Pacific and Arctic records. Taxonomic work is needed in this genus, as several other trans-Atlantic genetic groups lack species names (Saunders & McDevit 2013).

Ectocarpales, Scytosiphonaceae

***Petalonia fascia* (O.F.Müller) Kuntze (n=22; Nome breakwater, Cape Nome; NW & NE Pacific, Arctic, NW & NE Atlantic):** This species is genetically verified in the Pacific, Arctic, and Atlantic basins (Saunders & McDevit 2013; NW Pacific [based on ITS and *rbc*L]: AY154725 and AB578997; NE Atlantic [based on PSA and *rbc*L]; AY372953, AB860190, AB860189), and appears to have been introduced to Antarctica (MF419250). Two distinct genetic groups differing by 8 base pairs in COI-5P occur in this species, both of which occur in Nome, and both of which are trans-Arctic, suggesting at repeated trans-Arctic migrations in this complex.

***Planosiphon zosterifolius* (Reinke) McDevit & G.W.Saunders (n=9; Nome breakwater, Nome East beach; NW & NE Atlantic):** *Planosiphon* is a newly described genus, with members of *P. zosterifolius* previously genetically confirmed in

the Northwest (McDevit & Saunders 2017) and Northeast Atlantic (BOLD; DS-NOME, Algal flora of Nome Alaska).

Fucales, Fucaceae

***Fucus distichus* Linnaeus (n=20; East and North Sledge Island, Nome breakwater; NW & NE Pacific, Arctic, NW & NE Atlantic):** This species is widely distributed, with records confirmed in the both sides of the Pacific and Atlantic oceans, and in the Arctic (Saunders & McDevit 2013; BOLD; DS-NOME, Algal flora of Nome Alaska).

Laminariales, Chordaceae

***Chorda* sp. 1filum (n=23; East Sledge Island, Nome breakwater; Arctic, NW Atlantic; taxonomic work needed):** This genetic group is distinct from Atlantic *Chorda filum* (Linnaeus) Stackhouse (Saunders & McDevit 2013). This genetic group extends through the Canadian Arctic to the coast of Labrador (Saunders & McDevit 2013; BOLD; DS-NOME, Algal flora of Nome Alaska). Taxonomic work is needed to assign a species name.

Laminariales, Alariaceae

***Alaria esculenta* (Linnaeus) Greville sensu lato (n=19; Southwest Sledge Island; taxonomic work needed):** Specimens assigned to *A. esculenta* from Nome exhibited marker inconsistencies. COI-5P was a clear match to *Alaria crispa* Kjellman reported from nearby St. Lawrence Island (Lane *et al.* 2007) and Russia (reported as *A. esculenta*; Klochkova *et al.* 2018), while *rbc*L was a close match to *Alaria crassifolia* Kjellman (four base pairs different across 1122 base pairs; Kawai *et al.* 2013) and a unique *rbc*L-3P group sampled in Churchill, Manitoba (two base pairs different across 781 base pairs; BOLD; DS-NOME, Algal flora of Nome Alaska). Unfortunately, *rbc*L

data from the same gene region do not appear to be available for *A. crispa*. Further complicating matters, COI-5P data in the unique Churchill specimen was a 100% match to an *A. esculenta* Arctic haplotype, and ITS data indicated that Nome specimens share signatures with *A. crispa* and Arctic *A. esculenta*, a situation repeated in Russian specimens (Klochkova *et al.* 2018). ITS data poorly differentiate species of *Alaria* (Lane *et al.* 2007), indicating reproductive isolation may be incomplete between recognized species. The data for Nome specimens certainly suggest introgression, interbreeding, or incomplete lineage sorting between *A. crispa* and *A. esculenta* from the Arctic. This group is therefore tentatively assigned to *A. esculenta* sensu lato, pending further taxonomic work.

Laminariales, Laminariaceae

***Agarum clathratum* Dumortier (n=33; North and Southwest Sledge Island [drift]; NW & NE Pacific, Arctic, NW Atlantic):** This species of kelp has a wide distribution, extending from the Northwest and Northeast Pacific, through to the Northwest Atlantic, with records also genetically verified from the Arctic (Boo *et al.* 2011; Saunders & McDevit 2013).

Sphacelariales, Sphacelariaceae

***Battersia arctica* (Harvey) Draisma, Prud'homme & H.Kawai (n=1; North Sledge Island; Arctic, NW & NE Atlantic):** *Rbc*L-3P data are a match to *B. arctica* from Sweden reported by Draisma *et al.* (2010). This species is also genetically verified from the Arctic and the Northwest Atlantic (BOLD; DS-NOME, Algal flora of Nome Alaska).

Stschapoviales, Platysiphonaceae

***Platysiphon glacialis* (Rosenvinge) H.Kawai & T.Hanuda (n=16; East and North Sledge Island, Cripple River, Nome breakwater; Arctic):** This species was previously reported as an Arctic endemic described from Greenland and genetically verified only from Northern Baffin Island (Kawai *et al.* 2015a). Our Nome collections indicate that this species may not be an Arctic endemic; population level data are needed to infer whether Greenland populations were recently colonized from the North Pacific.

Tilopteridales, Halosiphonaceae

***Halosiphon* sp. 2tomentosus (n=2; Nome breakwater; Arctic; taxonomic work needed):** This is another species with cryptic Atlantic and Pacific genetic groups (Kawai & Sasaki 2000). The specimens from Nome match the Northern Bering Sea genetic group, which is also reported from the Canadian Arctic, but does not appear to extend into the Atlantic basin (Saunders & McDevit 2013). Taxonomic work is needed to assign a species name to this group.

Tilopteridales, Tilopteridaceae

***Haplospora globosa* Kjellman (n=1; East Sledge Island; Arctic, NW & NE Atlantic; taxonomic work needed):** This record represents the first report of *H. globosa* from the Pacific (Guiry & Guiry 2018), having previously been genetically verified from the Arctic and both sides of the Atlantic (Saunders & McDevit 2013; BOLD; DS-NOME, Algal flora of Nome Alaska). Taxonomic work is needed to verify the species name assignment.

Tilopteridalean sp. 3GWS (n=1; North Sledge Island; Arctic; taxonomic work needed): This genetic group has been previously sampled in Northern Alaska, where another tilopteridalean genetic group has also been recovered (Tilopteridalean sp.

2GWS; Bringloe *et al.* 2017). Taxonomic work is needed to assign species names to these groups.

RHODOPHYTA

Bangiophyceae

Bangiophycidae, Bangiales, Bangiaceae

***Boreophyllum aestivale* (S.C.Lindstrom & Frederiq) S.C.Lindstrom (n=5; Nome breakwater; NE Pacific):** *Rbc*L data indicate that this species occurs in Southeastern Alaska and the Aleutian Islands, through to Northern British Columbia (Kucera & Saunders 2012; Lindstrom *et al.* 2015).

Florideophyceae

Ahnfeltiophycidae, Ahnfeltiales, Ahnfeltiaceae

***Ahnfeltia borealis* D.Milstein & G.W.Saunders (n=24; East, North and Southwest Sledge Island and Nome Breakwater; NE Pacific, Arctic, NW Atlantic):** This recently described species is largely restricted to Arctic waters, though its sporophyte stage has been reported from more southerly regions of the Northwest Atlantic and Northeast Pacific (Milstein & Saunders 2012; BOLD; DS-NOME, Algal flora of Nome Alaska). Recent work has also confirmed the presence of this species in Northern Alaska (Bringloe *et al.* 2017).

Corallinophycidae, Corallinales, Corallinaceae

***Corallina officinalis* var. *chilensis* (Decaisne) Kützing (n=4; East, North, and Southwest Sledge Island; NW & NE Pacific):** *Corallina officinalis* is broadly distributed, with several genetic groups on both sides of the North Atlantic and North Pacific. A genetic break occurs between Atlantic and Pacific lineages, with Pacific *C.*

officinalis currently recognized as *C. officinalis var. chilensis* (Hind & Saunders 2013). Nome specimens match Northeast Pacific sequences.

***Corallina* sp. 3frondescens (n=1; Southwest Sledge Island; NW & NE Pacific; taxonomic work needed):** This genetic group spans both sides of the North Pacific (Hind & Saunders 2013). Taxonomic work is needed in this genus to assign species names to several Pacific genetic groups.

Corallinophycidae, Corallinales, Lithothamniaceae

***Lithothamnion glaciale* Kjellman (n=4; East Sledge Island; Arctic, NW & NE Atlantic):** *Lithothamnion glaciale* has been genetically verified from the Arctic, Northwest Atlantic, and the Northeast Atlantic (Saunders & McDevit 2013; Pardo *et al.* 2014). Though previously reported from the Pacific (Guiry & Guiry 2018), our Nome collections represent the first genetically verified records from this basin.

***Lithothamnion lemoineae* Adey (n=1; Cripple River; NW Atlantic):** This genetic group is verified from the Northwest Atlantic (Melbourne *et al.* 2017); though previously reported from the Northwest Pacific (Guiry & Guiry 2018), our Nome collections represent the first genetically verified records from the Pacific.

Corallinophycidae, Corallinales, Mesophyllaceae

***Clathromorphum* sp. 9GWS (n=2; East Sledge Island, Cripple River; Arctic, NW Atlantic; taxonomic work needed):** This genetic group is confirmed from the Arctic and the Northwest Atlantic, however, taxonomic work is needed to assign a species name (Saunders & McDevit 2013).

Nemaliophycidae, Acrochaetiales, Acrochaetiaceae

***Grania efflorescens* (J.Agardh) Kylin (n=2; Cripple River; NE Atlantic):** Though this species is reportedly widely distributed (Guiry & Guiry 2018), our Nome collections for *G. efflorescens* represent the first genetically verified records for the Pacific. This species is also genetically verified from Europe (Clayden & Saunders 2008).

Nemaliophycidae, Palmariales, Palmariaceae

***Devaleraea callophylloides* (M.W.Hawkes & Scagel) G.W.Saunders, Jackson & Salomaki (n=20; Southwest Sledge Island; NE Pacific; taxonomic work needed):** Nome specimens of *D. callophylloides* are divergent from southerly populations (e.g. Aleutian Islands southwards); COI-5P differs at ten sites across a 615 base pair fragment, while *rbc*L differs at two sites across 1300 base pairs. This level of divergence suggests incipient speciation, however, ITS1 data differed by only one basepair between some Nome specimens and data for Southwest Alaskan *D. callophylloides* reported by Lindstrom *et al.* (1996), while ITS2 differed by at least five sites (not including indels and ambiguities). It is worth noting that full length reads of ITS differed between some Nome specimens of *D. callophylloides* at up to ten sites. These specimens may account for reports of *Devaleraea ramentacea* (Linnaeus) Guiry from the Pacific, a closely related congener genetically verified in the Arctic and Atlantic (Saunders & McDevit 2013; Guiry & Guiry 2018; Saunders *et al.* 2018).

Rhodymeniophycidae, Ceramiales, Ceramiaceae

***Ceramium kondoi* Yendo (n= 6; East and North Sledge Island; NW Pacific; taxonomic work needed):** This species is tentatively assigned to *C. kondoi*, matching specimens from Hokkaido, Japan.

***Scagelia pylaisaiei* (Montagne) M.J. Wynne (n=36; North Sledge Island, Cripple River, Nome breakwater; NE Pacific, Arctic, NW Atlantic; taxonomic work needed):** This genetic group is tentatively assigned to *S. pylaisaiei*. COI-5P data in this species indicate the presence of distinct Northeast Pacific and Northwest Atlantic lineages, with the Pacific lineage extending through the Canadian Arctic as far East at Northern Labrador (Saunders & McDevit 2013; BOLD; DS-NOME, Algal flora of Nome Alaska). Nome specimens match the Pacific lineage.

Rhodymeniophycidae, Ceramiales, Delesseriaceae

***Phycodrys fimbriata* (Kuntze) Kylin (n=18; North, Northwest, and Southwest Sledge Island, and Nome breakwater; Arctic, NW Atlantic; taxonomic work needed):** Taxonomic confusion persists in this genus. Though several genetic groups occur in both the Atlantic and the Pacific, *P. fimbriata* appears to be the only truly trans-Arctic species of *Phycodrys* (van Oppen *et al.* 1995; Saunders & McDevit 2013; Bringloe *et al.* 2017). *Phycodrys riggii* N.L Gardner is closely related to *P. fimbriata*, differing in *rbc*L by a single base pair (BOLD; DS-NOME, Algal flora of Nome Alaska). A previously published record for *P. riggii* from St. Lawrence Island matches *P. fimbriata* (Lin & Nelson 2010; BOLD; DS-NOME, Algal flora of Nome Alaska), however, *P. riggii* is genetically verified from the Northeast and Northwest Pacific, indicating that the ranges from these two species likely overlap. *Rbc*L data from the Northwest Pacific have also been attributed to *P. fimbriata* (Lin & Nelson 2010), but differ from the *rbc*L data presented here by six base pairs (BOLD; DS-NOME, Algal flora of Nome Alaska), indicating this Northwest Pacific genetic group may be distinct

from the *P. fimbriata*/*riggii* complex. For now, Nome records are attributed to trans-Arctic populations of *P. fimbriata*, pending further taxonomic work in this genus.

Rhodymeniophycidae, Ceramiales, Rhodomelaceae

***Neorhodomela aculeata* (Perestenko) Masuda (n=2; East and North Sledge Island; NE Pacific):** This species is genetically verified from the Northeast Pacific (Savoie & Saunders 2016).

***Odonthalia dentata* (Linnaeus) Lyngbye (n=21; Southwest Sledge Island, Nome breakwater; Arctic, NW & NE Atlantic):** This species is genetically verified in the Arctic and on both sides of the Atlantic, with trans-Atlantic populations divergent by seven base pairs in COI-5P (Saunders & McDevit 2013; Bringloe *et al.* 2017; Bringloe & Saunders 2018). Nome specimens cluster with populations in the Northwest Atlantic, suggesting at a more recent population history between trans-Arctic populations compared to trans-Atlantic conspecifics.

***Polysiphonia* sp. 1stricta (n=26; East and North Sledge Island, Cape Nome, Cripple River, Nome breakwater; taxonomic work needed; NE Pacific, Arctic, NW Atlantic):** This genetic group is verified in the Northeast Pacific, the Arctic, and the Northwest Atlantic (Saunders & McDevit 2013; BOLD; DS-NOME, Algal flora of Nome Alaska). Taxonomic work is needed to assign a species names to this group.

***Polyostea* sp. 1Nome (n=12; Cripple River, Nome breakwater; new genetic group; taxonomic work needed):** These specimens represented a newly encountered genetic group that was approximately 5% divergent from Pacific *Polyostea bipinnata* (Postels & Ruprecht) Ruprecht in COI-5P, and one percent divergent in *rbc*L. Taxonomic work is needed to assign a name to this genetic group.

***Rhodomela sibirica* A.D.Zinova & Vinogradova (n=23; Southwest Sledge Island, Cape Nome, Nome breakwater; Arctic; taxonomic work needed):** Previous to our sampling in Nome, this species was genetically verified only from the Arctic (Saunders & McDevit 2013; Bringloe *et al.* 2017). The name for this genetic group has been updated from previous studies (having been previously reported as *Rhodomela lycopodioides f. flagellaris* Kjellman; Saunders & McDevit 2013; Bringloe *et al.* 2017); taxonomic work is needed to verify the species name assignment, and to evaluate the possible synonymy of *R. lycopodioides f. flagellaris* with *R. sibirica*.

***Rhodomela virgata* Kjellman (n= 38; East, North, and Northwest Sledge Island, Cape Nome, Cripple River, Nome Breakwater; Arctic, NW Atlantic; taxonomic work needed):** The name *Rhodomela virgata* was tentatively assigned to this genetic group by Saunders and McDevit (2013). This genetic group is verified from the Arctic (Saunders & McDevit 2013; Bringloe *et al.* 2017) and from the Northwest Atlantic (BOLD; DS-NOME, Algal flora of Nome Alaska).

***Rhodomela* sp. 1virgata (n=15; East Sledge Island, Cape Nome, Nome breakwater; Arctic, NW Atlantic, taxonomic work needed):** This is another genetic group from the Arctic and Northwest Atlantic originally reported by Saunders and McDevit (2013) as *Rhodomela lycopodioides* (Linnaeus) C.Agardh sensu stricto. Further taxonomic work is needed to resolve species name assignments in *Rhodomela*.

Rhodymeniophycidae, Gigartinales, Dumontiaceae

***Dilsea socialis* (Postels & Ruprecht) Perestenko (n=37; Southwest Sledge Island, Nome breakwater; Arctic, NW Atlantic):** This species has been previously reported from the Beaufort and Bering Seas, and was found to be synonymous with

Arctic/Northwest Atlantic *Dilsea integra* (Kjellman) Rosenvinge (Saunders 2008). As such, this species has a trans-Arctic distribution, with the closely related congener *Dilsea carnosa* occupying the Northeast Atlantic (Saunders 2008).

Rhodymeniophycidae, Gigartinales, Gigartinaceae

***Mazzaella macrocarpa* G.W.Saunders & K.R.Millar (n=1; East Sledge Island; NE Pacific):** This species was recently described, with genetically verified records from the Northeast Pacific (Saunders & Millar 2014).

Rhodymeniophycidae, Gigartinales, Phyllophoraceae

***Coccotylus truncatus* (Pallas) Wynne & Heine (n=11; Southwest Sledge Island, Nome breakwater; Arctic, NW & NE Atlantic):** This species is genetically verified from the Arctic and both sides of the Atlantic (Saunders & McDevit 2013; Bringloe *et al.* 2017; BOLD; DS-NOME, Algal flora of Nome Alaska).

***Mastocarpus pacificus* (Kjellman) Perestenko (n=2; Nome breakwater; NW & NE Pacific):** This species is genetically verified in the Northwest Pacific (Japan) and the Northeast Pacific (Southwest Alaska; Lindstrom *et al.* 2011). COI-5P, *rbc*L-3P, and ITS data are all consistent with this name assignment to Nome specimens of *Mastocarpus*.

Rhodymeniophycidae, Peyssonneliales, Peyssonneliaceae

***Peyssonnelia rosenvingei* F.Schmitz (n=1; Cripple River; NW Atlantic):** This Nome specimen was an exact match to Northwest Atlantic specimens identified at *P. rosenvingei* (BOLD; DS-NOME, Algal flora of Nome Alaska). Though reported world-wide, including the Arctic and the North Pacific (Guiry & Guiry 2018), this collection represents the first genetically verified record from the Pacific.

Discussion

Our objective was to sample and describe the marine macroalgal flora of Nome, Alaska (Northern Bering Sea). The most striking feature of the Nome flora is that it is primarily composed of species with trans-Arctic distributions. Thirty-five of the recorded species (67%, Fig. 2) have distributions extending into the North Atlantic, 23 of which are additionally verified from the Arctic. This has implications for monitoring species assemblages in the Northern Bering Sea. Given most of the flora is already recorded in the Arctic and Atlantic, relatively few species from Nome are contenders for extending their ranges northward due to climate change. The few species with distributions restricted to the Pacific, however, could be monitored; these species could be the first to migrate into the Arctic basin as warming trends continue. It is worth noting the contrast between the Nome flora and species from nearby St. Lawrence and St. Matthew Islands (Wynne & Heine 1992), which are largely Pacific in character and apparently share few conspecifics with the Nome flora. It is possible the flora has changed substantially during the 25 years since the report of Wynne and Heine (1992). Contemporary sampling from St. Lawrence and St. Matthew Islands, in addition to returning to Nome, is needed to further establish baseline data and better understand marine macroalgal diversity in the Northern Bering Sea.

These results have implications for understanding the origins of Arctic flora. Previous work in the Arctic has emphasized the largely "Atlantic" nature of the Arctic flora (Lee 1973; Wilce & Dunton 2014). Dunton (1992) dubbed this characterization a paradox given that invertebrate taxa in the Western Arctic are largely Pacific in origin. It seems likely that the Pacific contribution to Arctic recolonization since the Last Glacial

Maximum (approx. 21 ka; Miller *et al.* 2010) has remained underestimated simply because several Arctic/North Atlantic species had not yet been verified from the North Pacific (i.e. 37% of the species reported here; Fig. 2). Population level analyses could be conducted for several of the trans-Arctic species reported here in order to elucidate the origins of contemporary Arctic populations. Indeed, Saunders and McDevit (2013) speculated that a number of macroalgal species from sub-Arctic Churchill (Hudson Bay) could be of Northwest Pacific origin (e.g. *Dilsea socialis* [Postels & Ruprecht] Perestenko, several species of *Rhodomela*), but excluded these species from their analysis or listed their origins as uncertain due to a lack of North Pacific collections. Work by Lindstrom (1987, 2001, 2006) and Adey *et al.* (2008) also support the notion that the Pacific has played a significant role in establishing Arctic marine flora during the Pleistocene.

Several interesting biogeographic distributions and taxonomic findings can be highlighted from our sampling in Nome. *Platysiphon glacialis* (Rosenvinge) H.Kawai & T.Hanyuda was considered an Arctic endemic, with its type locality in Greenland (Kawai *et al.* 2015). Our Nome collections indicate that this species is not an Arctic endemic, and that this species has potentially migrated recently through the Arctic. Population level analyses will be needed to infer a refugial location. The genetically confirmed species range in several other species was also expanded; species previously reported from the Pacific but confirmed genetically for the first time through our collections included *Grania efflorescens, Lithothamnion lemoineae*, *Peyssonnelia rosenvingei, and Planosiphon zosterifolius* (Guiry & Guiry 2018). Regarding taxonomic findings, COI-5P data indicated we collected *Alaria crispa* Kjellman from Nome rather

than *Alaria esculenta* (Linnaeus) Greville, the latter of which is reported from the Arctic and is genetically verified in the Beaufort (Northern Alaska; Bringloe *et al.* 2017). ITS data, however, indicated Nome *Alaria* shares signatures with both *A. crispa* from St. Lawrence Island (EF218904), and *A. esculenta* from Russia (Klochkova *et al.* 2018) and the North American Arctic (EF218906). Due to persistent ITS conflicts between recognized species of *Alaria*, we tentatively assigned our Nome specimens to *A. esculenta* sensu lato (Lane *et al.* 2007), however, further taxonomic work is needed to robustly test species delineations in this genus. It could be the genetic patterns observed here are the result of incomplete lineage sorting, or hybridization/introgression between populations of *Alaria*. *Devaleraea callophylloides* (M.W.Hawkes & Scagel) G.W.Saunders, Jackson & Salomaki was also unexpectedly sampled in Nome; *Devaleraea ramentacea* (Linnaeus) Guiry is reported from the North Pacific (Guiry & Guiry 2018), but not genetically verified. Our results therefore suggest reports of *D. ramentacea* in the North Pacific are attributable to *D. callophylloides*. Further complicating matters, however, are two unique ITS types within the *Devaleraea* sampled in Nome, one of which matched southern British Columbia populations. The ITS data stands in contrast to the single COI-5P and *rbc*L types recovered. The combined COI-5P, *rbc*L, and ITS data therefore indicate *Devaleraea* sampled in Nome may represent previous incipient speciation, with recent introgression/hybridization between the putative sibling species. Additional taxonomic work is needed to clarify the status of *D. callophylloides* in the North Pacific. We also note the genetic group assigned to *Rhodomela sibirica* A.D.Zinova & Vinogradova has been updated from *Rhodomela lycopodioides f. flagellaris* Kjellmann (Saunders & McDevit 2013; Bringloe

et al. 2017); taxonomic work is needed to evaluate if these species names are synonymous. The previous name assignment further highlights the hesitation to assign Russian names to Arctic specimens historically viewed with an Atlantic bias (Lee 1973; Wilce & Dunton 2014). It seems likely some of the names assigned to genetic groups here, particularly in cases where a given species represents multiple genetic groups, may eventually be assigned to Russian species. DNA barcoding the Russian flora will be critical to this endeavor.

Conclusions

Several weaknesses must be addressed regarding the inferences gathered here. These results represent a single collection event from Nome, with limited sampling opportunities to Sledge Island. Repeated sampling from several locations (e.g. Nome and surrounding area, St. Lawrence Island) will be essential to further establishing baseline species distribution data in the Northern Bering Sea. An effort should also be made to sample faunal taxa (e.g. invertebrates) in tandem with the marine flora. In addition, the biogeographic distributions listed in the results are likely to contain some inaccuracies given the lack of sequence data from some locations (notably Russia). As such, the biogeographic distributions reported here must be interpreted with the above limitation in mind. On a final note, and as noted above, taxonomic work remains for several species reported here; 14 of the recorded species lacked formal names, and some assigned names are likely to be updated in light of additional sampling. In conclusion, our results indicate that the Nome flora is largely member to a trans-Arctic community of species. Given marine macroalgal assemblages are expected to shift northwards as climate change progresses (Campana *et al.* 2009; Müller *et al.* 2009; Jueterbock *et al.*

2016), the genetic data provided here will serve as critical baseline data for monitoring future changes to the Arctic biome.

Acknowledgements

We thank Don Stiles and James Horner for facilitating the collection of samples. This project was funded by the Northern Scientific Training Program, the Natural Sciences & Engineering Research Council of Canada through an NSERC Post-Graduate Scholarship to T.T. Bringloe and a Discovery Grant to G.W. Saunders, and the New Brunswick Innovation Foundation.

References

Adey WH, Lindstrom SC, Hommersand MH, Müller KM (2008) The biogeographic origin of Arctic endemic seaweeds: a thermogeographic view. *Journal of Phycology*, **44**, 1384–1394.

Ajisaka T, Kim SH, Uwai S, Kawai H (2007) *Cladosiphon umezakii* sp. nov. (Ectocarpales, Phaeophyceae) from Japan. *Phycological Research*, **55**, 193–202.

Cho TO, Cho GY, Yoon HS, Boo SM, Lee WJ (2003) New records of *Myelophycus cavus* (Scytosiphonaceae, Phaeophyceae) in Korea and the taxonomic position of the genus on the basis of a plastid DNA phylogeny. *Nova Hedwigia*, **76**, 381–397.

Boo GH, Lindstrom SC, Klochkova NG, *et al.* (2011) Taxonomy and biogeography of *Agarum* and *Thalassiophyllum* (Laminariales, Phaeophyceae) based on sequences of nuclear, mitochondrial, and plastid markers. *Taxon*, **60**, 831–840.

Bringloe TT, Saunders GW (in review) The phylogeographic history of amphitropical *Callophyllis variegata* and *Mastocarpus latissimus* (Florideophyceae, Rhodophyta) in the Pacific Ocean.

Bringloe TT, Dunton KH, Saunders GW (2017) Updates to the marine algal flora of the Boulder Patch in the Beaufort Sea off Northern Alaska as revealed by DNA Barcoding. *ARCTIC*, **70**, 3–6.

Bringloe TT, Saunders GW (2018) Mitochondrial DNA sequence data reveal the origins of postglacial marine macroalgal flora in the Northwest Atlantic. *Marine Ecology Progress Series*, **589**, 45-58.

Campana GL, Zacher K, Fricke A, Molis M, Wulff A, Quartino ML, Wiencke C (2009) Drivers of colonization and succession in polar benthic macro- and microalgal communities. *Botanica Marina*, **52**, 655–667.

Clayden SL, Saunders GW (2008) Resurrecting the red algal genus Grania within the order Acrochaetiales (Florideophyceae, Rhodophyta). *European Journal of Phycology*, **43**, 151-160.

Daugbjerg N, Andersen RA (1997) A molecular phylogeny of the Heterokont algae based on analyses of chloroplast-encoded rbcL sequence data. *Journal of Phycology*, **33**, 1031–1041.

Draisma SGA, Prud'homme VRWF, Kawai H (2010) A revised classification of the sphacelariales (phaeophyceae) inferred from a *psb*C and *rbc*L based phylogeny. European *Journal of Phycology*, **45**, 308–326.

Dunton KH (1992) Arctic biogeography: The paradox of the marine benthic fauna and flora. *Trends in Ecology and Evolution* **7,** 183–189.

Fisheries and Oceans Canada (2012) Canada's State of the Oceans Report.

Garrido-Benavent I, Pérez-Ortega S, de los Ríos A (2017) From Alaska to Antarctica: Species boundaries and genetic diversity of *Prasiola* (Trebouxiophyceae), a foliose chlorophyte associated with the bipolar lichen-forming fungus *Mastodia tessellata*. *Molecular Phylogenetics and Evolution,* **107**, 117–131.

Guiry M, Guiry G (2018) AlgaeBase. http://www.algaebase.org.

Harley CDG, Anderson KM, Demes KW, Jorve JP, Kordas RL, Coyle TA, Graham MH (2012) Effects of climate change on global seaweed communities. *Journal of Phycology*, **48**, 1064–1078.

Hind KR, Saunders GW (2013) A molecular phylogenetic study of the tribe Corallineae (Corallinales, Rhodophyta) with an assessment of genus-level taxonomic features and descriptions of novel genera. *Journal of Phycology*, **49**, 103–114.

IPCC (Intergovernmental Panel on Climate Change) (2014) Climate Change 2014 Synthesis Report. IPCC, Geneva.

Jueterbock A, Smolina I, Coyer JA, Hoarau G (2016) The fate of the Arctic seaweed *Fucus distichus* under climate change: an ecological niche modelling approach. *Ecology and Evolution*, **6**, 1712−1724.

Kawai H, Sasaki H (2000) Molecular phylogeny of the brown algal genera *Akkesiphycus* and *Halosiphon* (Laminariales), resulting in the circumsription of the new families Akkesiphycaceae and Halosiphonaceae. *Phycologia*, **39**, 416–428.

Kawai H, Hanyuda T, Ridgway LM, Holser K (2013) Ancestral reproductive structure in basal kelp *Aureophycus aleuticus*. *Scientific Reports*, **3**, 2491.

Kawai H, Hanyuda T, Yamagishi T, *et al.* (2015) Reproductive morphology and DNA sequences of the brown alga *Platysiphon verticillatus* support the new combination *Platysiphon glacialis*. *Journal of Phycology*, **51**, 910–917.

Kawai H, Hanyuda T, Kim SH, Ichikawa Y, Uwai S, Peter AF (2016) *Cladosiphon takenoensis* sp. nov. (Ectocarpales *s.l.*, Phaeophyceae) from Japan. *Phycological Research*, **64**, 212–218.

Kearse M, Moir R, Wilson A, *et al.* (2012). Geneious Basic: An integrated and extendable desktop software platform for the organization and analysis of sequence data. *Bioinformatics*, **28**, 1647–1649.

Kim SH, Kawai H (2002) Taxonomic revision of *Chordaria flagelliformis* (Chordariales, Phaeophyceae) including novel use of the intragenic spacer region of rDNA for phylogenetic analysis. *Phycologia*, **41**, 328–339.

Kirkendale L, Saunders GW, Winberg P (2013) A molecular survey of *Ulva* (Chlorophyta) in temperate Australia reveals enhanced levels of cosmopolitanism. *Journal of Phycology*, **49**, 69–81.

Kjellman F (1889) Om Beringhafvets Algflora. Stockholm.

Klochkova TA, Klimova AV, Klochkova NG (2018) Infraspecies forms of *Alaria esculenta* (Laminariales, Ochrophyta) in the marine flora of Eastern Kamchatka: first revision. *Bulletin of Kamchatka State Technical University*, **43**, 74-86.

Krause-Jensen D, Duarte CM (2014) Expansion of vegetated coastal ecosystems in the future Arctic. *Frontiers in Marine Science*, **1**, 1-10.

Kucera H, Saunders GW (2012) A survey of bangiales (rhodophyta) based on multiple molecular markers reveals cryptic diversity. *Journal of Phycology*, **48**, 869–882.

Küpper FC, Peters AF, Shewring DM, *et al.* (2016) Arctic marine phytobenthos of northern Baffin Island. *Journal of Phycology*, **52**, 532-549.

Lane CE, Lindstrom SC, Saunders GW (2007) A molecular assessment of northeast Pacific *Alaria* species (Laminariales, Phaeophyceae) with reference to the utility of DNA barcoding. *Molecular Phylogenetics and Evolution*, **44**, 634–648.

Le Gall L, Saunders GW (2010) DNA barcoding is a powerful tool to uncover algal diversity: A case study of the phyllophoraceae (Gigartinales, Rhodophyta) in the Canadian flora. *Journal of Phycology*, **46**, 374–389.

Lee RKS (1973) General ecology of the Canadian Arctic benthic marine algae. *ARCTIC*, **26**, 32−43.

Lin SM, Nelson WA (2010) Systematic revision of the genus *Phycodrys* (Delesseriaceae, Rhodophyta) from New Zealand, with the descriptions of three new species, *P. novae-zelandiae* sp. nov., *P. franiae* sp. nov. and *P. adamsiae* sp. nov. *European Journal of Phycology*, **45**, 200–214.

Lindstrom SC, Olsen JL, Stam WT (1996) Recent radiation of the Palmariaceae (Rhodophyta). *Journal of Phycology*, **32**, 457–468.

Lindstrom SC (1987) Possible sister groups and phylogenetic relationships among selected North Pacific and North Atlantic Rhodophyta. *Helgolander Meeresunters*, **41**, 245−260.

Lindstrom SC (2001) The Bering Strait connection: dispersal and speciation in boreal macroalgae. *Journal of Biogeography*, **28**, 243–251.

Lindstrom SC (2006) Biogeography of Alaskan seaweeds. *Journal of Applied Phycology*, **18**, 637–641.

Lindstrom SC, Hughey JR, Martone PT (2011) New, resurrected and redefined species of *Mastocarpus* (Phyllophoraceae, Rhodophyta) from the northeast Pacific. *Phycologia*, **50**, 661–683.

Lindstrom SC, Lindeberg MR, Guthrie DA (2015) Marine macroalgae of the Aleutian Islands: I. Bangiales. *Algae*, **30**, 247–263.

Mcdevit DC, Saunders GW (2017) A molecular investigation of Canadian Scytosiphonaceae (Phaeophyceae) including descriptions of *Planosiphon* gen. nov. and *Scytosiphon promiscuus* sp. nov. *Botany*, **95**, 653–671.

Melbourne LA, Hernández-Kantún JJ, Russell S, Brodie J (2017) There is more to maerl than meets the eye: DNA barcoding reveals a new species in Britain, *Lithothamnion erinaceum* sp. nov. (Hapalidiales, Rhodophyta). *European Journal of Phycology*, **52**, 166–178.

Miller GH, Brigham-Grette J, Alley RB, *et al.* (2010a) Temperature and precipitation history of the Arctic. *Quaternary Sciences Reviews*, **29**, 1679−1715.

Milstein D, Saunders GW (2012) DNA barcoding of Canadian Ahnfeltiales (Rhodophyta) reveals a new species – *Ahnfeltia borealis* sp. nov. *Phycologia*, **51**, 247–259.

Mineur F, Arenas F, Assis J, *et al.* (2015) European seaweeds under pressure: consequences for communities and ecosystem functioning. *Journal of Sea Research*, **98**, 91–108.

Moniz MBJ, Guiry MD, Rindi F (2014) *tuf*A phylogeny and species boundaries in the green algal order Prasiolales (Trebouxiophyceae, Chlorophyta). *Phycologia*, **53**, 396–406.

Müller R, Laepple T, Bartsch I, Wiencke C (2009) Impact of oceanic warming on the distribution of seaweeds in polar and cold-temperate waters. *Botanica Marina*, **52**, 617–638.

Mystikou A, Asensi AO, DeClerck O, *et al.* (2016) New records and observations of macroalgae and associated pathogens from the Falkland Islands, Patagonia and Tierra del Fuego. *Botanica Marina*, **59**, 105–121.

Oudot-Le Secq MP, Loiseaux-de Goër S, Stam WT, Olsen JL (2006) Complete mitochondrial genomes of the three brown algae (Heterokonta: Phaeophyceae) *Dictyota dichotoma*, *Fucus vesiculosus* and *Desmarestia viridis*. *Current Genetics*, **49**, 47–58.

Pardo C, Lopez L, Peña V, Hernández-Kantún J, Le Gall L, Bárbara I, Barreiro R (2014) A multilocus species delimitation reveals a striking number of species of coralline algae forming maerl in the OSPAR maritime area. *PLoS ONE*, **9**, e104073.

Peters AF, Couceiro L, Tsiamis K, Küpper FC, Valero M (2015) Barcoding of cryptic stages of marine brown algae isolated from incubated substratum reveals high diversity in Acinetosporaceae (Ectocarpales, Phaeophyceae). *Cryptogamie Algologie*, **36**, 3–29.

Renaud PE, Sejr MK, Bluhm BA, Sirenko B, Ellingsen IH (2015) The future of Arctic benthos: expansion, invasion, and biodiversity. *Progress in Oceanography*, **139**, 244−257.

Saunders GW (2005) Applying DNA barcoding to red macroalgae: A preliminary appraisal holds promise for future applications. *Philosophical Transactions of the Royal Society B*, **360**, 1879−1888.

Saunders GW (2008) A DNA barcode examination of the red algal family Dumontiaceae in Canadian waters reveals substantial cryptic species diversity. 1. The foliose *Dilsea – Neodilsea* complex and *Weeksia*. *Botany*, **86**, 773–789.

Saunders GW, McDevit DC (2012a) Methods for DNA barcoding photosynthetic protists emphasizing the macroalgae and diatoms. *Methods in Molecular Biology*, **858**, 207−222.

Saunders GW, McDevit DC (2012b) Acquiring DNA sequence data from dried archival red algae (Florideophyceae) for the purpose of applying available names to contemporary genetic species: a critical assessment. *Botany*, **90**, 191–203.

Saunders GW, Jackson C, Salomaki ED (2018) Phylogenetic analyses of transcriptome data resolve familial assignments for genera of the red-algal Acrochaetiales-Palmariales Complex (Nemaliophycidae). *Molecular Phylogenetics and Evolution*, **119**, 151–159.

Saunders GW, Kucera H (2010) An evaluation of *rbc*l, *tufA*, UPA, LSU and ITS as DNA barcode markers for the marine green macroalgae. *Cryptogamie Algologie*, **31**, 487–528.

Saunders GW, McDevit DC (2013) DNA barcoding unmasks overlooked diversity improving knowledge on the composition and origins of the Churchill algal flora. *BMC Ecology*, **13**, 9.

Saunders GW, Moore TE (2013) Refinements for the amplification and sequencing of red algal DNA barcode and RedToL phylogenetic markers: a summary of current primers, profiles and strategies. *Algae*, **28**, 31−43.

Saunders GW, Millar KR (2014) A DNA barcode survey of the red algal genus *Mazzaella* in British Columbia reveals overlooked diversity and new distributional records: descriptions of *M. dewreedei* sp. nov. and *M. macrocarpa* sp. nov. *Botany*, **92**, 223–231.

Savoie AM, Saunders GW (2016) A molecular phylogenetic and DNA barcode assessment of the tribe Pterosiphonieae (Ceramiales, Rhodophyta) emphasizing the Northeast Pacific. *Botany*, **94**, 917–939.

Setchell W, Garner N (1903) Algae of Northwestern America. In: *Algae of Northwestern America*. University of California publications, p 418.

Sutherland JE, Miyata M, Ishikawa M, Nelson WA (2016) *Prasiola* (Prasiolales, Trebouxiophyceae) in Japan: a survey of freshwater populations and new records of marine taxa. *Phycological Research*, **64**, 110–117.

van Oppen MJH, Draisma SGA, Olsen JL, Stam WT (1995) Multiple trans-Arctic passages in the red alga *Phycodrys rubens*: evidence from nuclear rDNA ITS sequences. *Marine Biology*, **123**, 179-188.

Wilce RT, Dunton KH (2014) The Boulder Patch (North Alaska, Beaufort Sea) and its benthic algal flora. *ARCTIC*, **67**, 43–56.

Wynne MJ, Heine JN (1992) Collections of marine red algae from St. Matthew and St. Lawrence Islands, the Bering Sea. *Nova Hedwigia*, **55**, 55−97.

Wynne MJ (2009) Marine algae and early explorations in the upper North Pacific and Bering Sea. *Algae*, **24**, 1-29.

Yang EC, Peters AF, Kawai H, *et al.* (2014) Ligulate *Desmarestia* (Desmarestiales, Phaeophyceae) revisited: *D. japonica* sp. nov. and *D. dudresnayi* differ from *D. ligulata*. *Journal of Phycology*, **50**, 149–166.

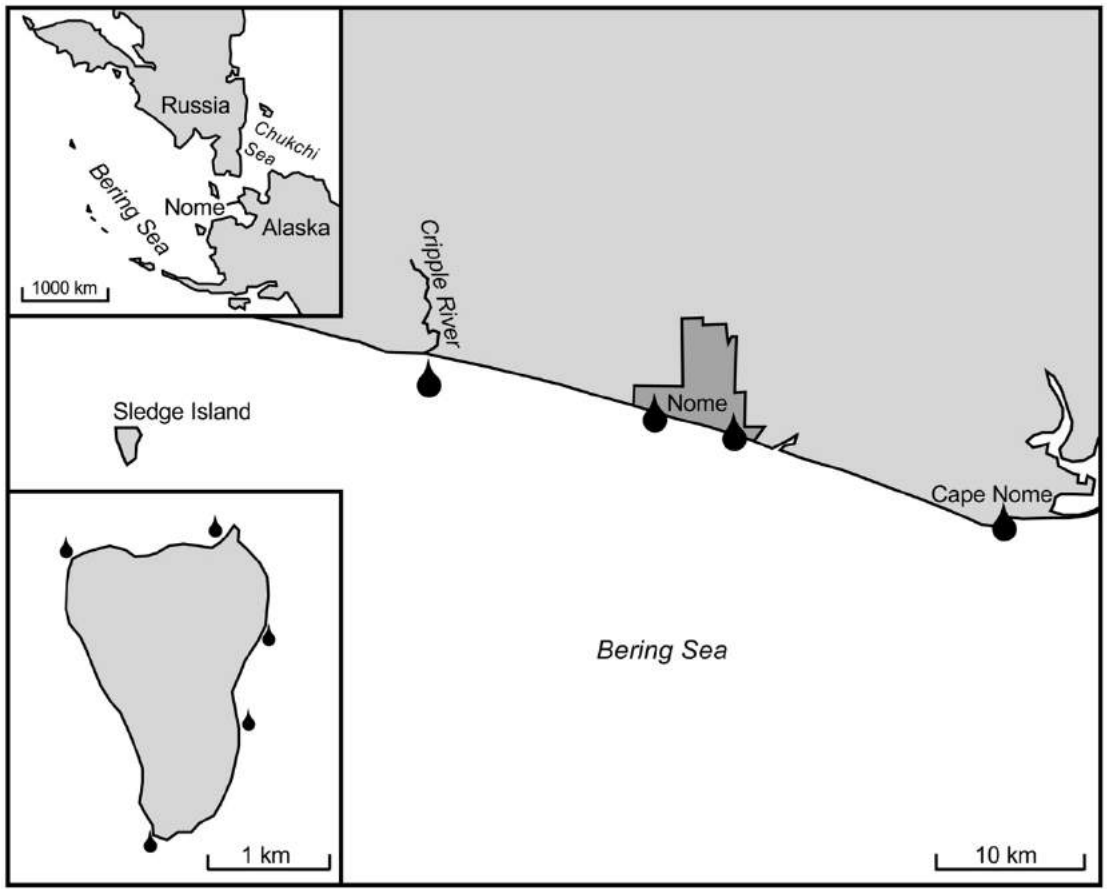

Figure B1. Locations sampled for marine macroalgae in Nome, Alaska, August 12-22, 2017. The top-left insert indicates the location of Nome within the Bering Sea. The bottom left insert indicates sampling locations around Sledge Island.

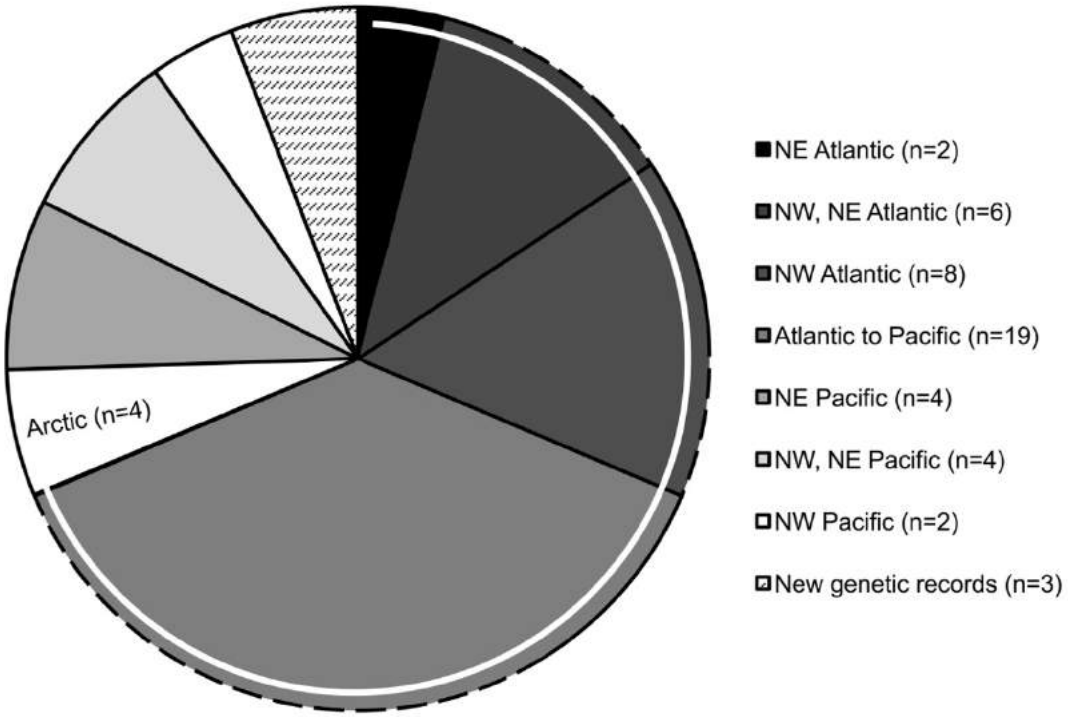

Figure B2. Reported biogeographic distributions of marine macroalgal species (n=51) sampled in Nome, Alaska, August 12-22, 2017. In the legend NE=Northeast, NW=Northwest. Outer dashed lines indicate portions of species in each category with genetically verified Arctic records. The white inner circle indicates trans-Arctic species.

Appendix C Supplementary Material for Chapter 2

Table C1. Specimen list for trans-Arctic lineages of marine red macroalgae (Florideophyceae). Specimens are listed in the order of phylogenies presented (Figs. C3-C22).

Taxa	Sample ID	Date	Country	Site	Latitude	Longitude	COI-5P	*rbc*L	ITS
Ahnfeltiales									
Ahnfeltia borealis	GWS038803	24-Jul-2015	United States	E3, off Endicott, Prudhoe Bay	70.194	-147.389	KY683396		
Ahnfeltia borealis	GWS005479	09-Jul-2007	Canada	East of Fort of Prince of Wales	58.798	-94.207	JN113241		JN113152
Ahnfeltia borealis	GWS042028	16-Aug-2017	United States	Nome, West Breakwater (west side)	64.4927	-165.441	MH143561		
Ahnfeltia borealis	GWS008782	19-Aug-2007	Canada	Cable Head	46.4628	-62.6074	JN113242		JN113153
Ahnfeltia borealis	GWS028517	10-Jul-2011	Canada	Ramsey Island (N Bay w anchorage), Gwaii Haanas	52.573	-131.399	MH143529		MH143892
Ahnfeltia borealis	GWS039320	08-Sep-2014	Canada	Hogg Island, Torngat, Labrador	59.429	-63.715	MH143555	MH277308	
Ahnfeltia borealis	GWS031010	14-Jun-2012	Canada	Tanu, Tanu Island, Gwaii Haanas	52.765	-131.611		MH277320	
Ahnfeltia fastigiata	GWS003223	17-Sep-2005	Canada	Bamfield, Bradys Beach	48.824	-125.159	GQ497301		JN113136
Ahnfeltia plicata	GWS003649	25-Apr-2006	United States	End of public road, Starboard	44.6091	-67.3966	JN113209		JN113142
Ahnfeltia plicata	GWS040784	10-Jun-2016	Norway	Hakonsund	60.1762	5.11132	KY572430		
Ahnfeltia plicata	GWS001287	29-Jan-2002	Canada	Peggys Cove, Halifax Co.	44.49	-63.917	JN113201	JX969802	
Palmariales									

Devaleraea callophylloides	GWS008352	08-Jun-2007	Canada	Ridley Island (south of coal terrminal), Prince Rupert	54.221	-130.329	HM917013	MF543841	
Devaleraea sp. _1callophylloides	GWS042452	20-Aug-2017	United States	Sledge Island, southwest corner	64.4724	-166.212	MH143567	MH277324	MH143916
Devaleraea marginicrassa	AB275867	02-Jul-1996	Japan	Hokkaido, Akkeshi				AB275867	
Devaleraea mollis	GWS035931	20-Aug-2013	Canada	Woodruff Bay (NE beach), Gwaii Haanas	51.974	-131.032	KY205175	KY250830	
Devaleraea mollis	GWS036865	14-Jul-2015	Canada	Iphigenia Pt., Langara, Haida Gwaii	54.1926	-133.017	MF543950		
Devaleraea ramentacea	GWS005484	09-Jul-2007	Canada	East of Fort of Prince of Wales	58.798	-94.207	JX572120	MH277312	MH143911
Devaleraea ramentacea	GWS009335	22-Apr-2008	Canada	Escoumins (east of town across from Rue aux Bouchets)	48.4	-69.339	HM918913	KT886264	
Devaleraea hecatensis	GWS035930	20-Aug-2013	Canada	Woodruff Bay (NE beach), Gwaii Haanas	51.974	-131.032	KY205177	KY250833	
Halosaccion americanum	GWS008214	04-Jun-2007	Canada	Bamfield, Blowhole at Bradys Beach	48.824	-125.162	GU224101	KT886265	
Palmaria palmata	RMAR2410	23-Mar-2011	France	Le Loup	48.7306	-4.00366	KJ960902		
Palmaria palmata	GWS003845	29-May-2006	Canada	Lepreau exposed biodiversity site, Bay of Fundy	45.072	-66.469	HM918608	KT886266	
Rhodophysema georgei	GWSCRG001	8-May-1986	Canada	Pomquet Harbour, Nova Scotia			KT886176	KC134338	
Rhodophysema georgei	GWS020463	15-Jun-2010	Canada	British Columbia	52.578	-131.438	HQ544927		
Gigartinales									
Coccotylus*/*Erythrodermis*/*Phyllophora*/*Ozophora									
Coccotylus brodiei	GWS040966	13-Jun-2016	Norway	Soloyna	60.159	5.23564	KY572750		

Coccotylus brodiei	GWS003640	25-Apr-2006	United States	End of public road, Starboard	44.609	-67.397	GQ380037	GQ338135	
Coccotylus brodiei	GWS005240	19-Aug-2006	Canada	Out the river & right, Churchill	58.779	-94.158	GQ380038		
Coccotylus truncatus	GWS042078	17-Aug-2017	United States	Nome, West Breakwater (west side)	64.4927	-165.441	MH143543		MH143904
Coccotylus truncatus	GWS041452	11-Aug-2016	Canada	Naufrage (deep)	46.4744	-62.5477	MH143557		
Coccotylus truncatus	GWS040983	13-Jun-2016	Norway	Soloyna	60.159	5.23564	MH143551		
Coccotylus truncatus	GWS040102	20-Jul-2015	United States	L1, off Endicott, Prudhoe Bay	70.173	-147.366	KY683361		KY683453
Coccotylus truncatus	GWS005213	19-Aug-2006	Canada	Out the river & right, Churchill	58.779	-94.158	GQ380071	GQ338134	MH143898
Erythrodermis traillii	GWS005655	03-Dec-2006	Canada	Meadow Cove exposed biodiversity site, Bay of Fundy	45.038	-66.891	GQ380105	GQ338133	
Erythrodermis traillii	GWS040635	09-Jun-2016	Norway	Kleppesjoen	60.1847	5.14938	MH143564		
Fredericqia deveauniensis	GWS005620	03-Nov-2006	United States	Cape Neddick, southern ME	43.166	-70.592	GQ380113	GQ338151	
Fredericqia deveauniensis	GWS008653	15-Jun-2007	Canada	British Columbia	49.69	-124.87	GQ380116		
Phyllophora crispa	GWS001813	28-Jul-2003	Ireland	Mullaghmore Head	54.45	-8.467	GQ380357	GQ338131	
Phyllophora herediae	J. Cabioch 27.02.1994	27-Feb-1994	France	Le Trez Hir				AY135165	
Phyllophora pseudoceranoides	GWS003648	25-Apr-2006	United States	End of public road, Starboard	44.609	-67.397	GQ380367	GQ338132	
Phyllophora pseudoceranoides	GWS040649	09-Jun-2016	Norway	Kleppesjoen	60.1847	5.14938	MH143569		
Ozophora clevelandii	GWS022005	19-May-2010	United States	Santa Cruz (Four Mile)	36.966	-122.123	KF641915	KF641917	

Ozophora lanceolata	GWS004011	15-Jun-2006	Canada	Bamfield, Sparlingia Pt.`, Bradys Beach	48.824	-125.159	GQ380341	GQ338128	
Ozophora norrisii	GWS008455	13-Jun-2007	Canada	Tuwanek, near Sechelt	49.547	-123.766	GQ380349	GQ338129	
Ozophora sp. 1crust	GWS019527	01-Jun-2010	Canada	Bamfield, off Wizard	48.86	-125.16	HQ544461	MH277293	
Dilsea*/*Neodilsea*/*Hyalosiphon									
Dilsea californica	GWS002252	19-Jun-2004	Canada	Palmerston Recreation Reserve near Raft Cove, Vancouver Island	50.593	-128.258	AY970637	KU381816	
Dilsea carnosa	GWS000746	07-Nov-1999	Ireland	Doaghbeg, Fanad Head	55.276	-7.634	AY971151	KT310705	
Dilsea lindstromiae	GWS005027	11-Jul-2006	Canada	Ridley Island (south of coal terrminal), Prince Rupert	54.221	-130.329	EU189286	JN403066	
Dilsea natashae	G0224	25-Apr-1994	United States	Shaman I., north end of Douglas I.	58.306	-134.684	AY970624	KX783046	
Dilsea pygmaea	GWS004685	03-Jul-2006	Canada	Palmerston Recreation Reserve near Raft Cove, Vancouver Island	50.593	-128.258	EU189299	JN403068	
Dilsea socialis	GWS042367	20-Aug-2017	United States	Sledge Island, southwest corner	64.4724	-166.212	MH143549		
Dilsea socialis	GWS002334	01-Sep-2004	Canada	Off Lingan Power plant, Cape Breton	46.25	-60.014	AY970634	JN403069	KY572848
Dilsea socialis	GWS040140	20-Jul-2015	United States	DS11, off Endicott, Prudhoe Bay	70.322	-147.579	KY683311		
Dilsea socialis	GWS039222	02-Sep-2014	Canada	Graveyard Pt., W of Qik	67.568	-64.067	KY572667		
Hyalosiphonia caespitosa	GWS001891	07-Apr-1998	Japan	Oshoro, Otaru, Hokkaido	42.772	140.306	HM915225	KT310684	
Neodilsea borealis	GWS005130	12-Jul-2006	Canada	Butze Rapids, Prince Rupert	54.301	-130.251	EU189309	JN403071	
Neodilsea yendoana	GWS003552	07-Aug-2005	Japan	Higashi-shizunai, Hokkaido	42.3	142.45	EU189314	KT310694	

Weeksia coccinea	GWS035698	16-Aug-2013	Canada	Burnaby Narrows (S opening, in Macrocystic bed), Gwaii Haanas	52.334	-131.337	KT307604	KT310704
Weeksia reticulata	GWS035734	16-Aug-2013	Canada	Bolkus Islands (Kelp bed to NE), Gwaii Haanas	52.332	-131.255	KT307589	KT310690
Mastocarpus								
Ahnfeltiopsis leptophylla	GWS004217	21-Jun-2006	Canada	Whiffen Spit, Sooke Harbour, Vancouver Island	48.352	-123.728	GQ380027	GQ338147
Mastocarpus agardhii	GWS021576	16-May-2010	United States	Sea Lion Point North (frontside), Point Lobos State Reserve	36.519	-121.953	KM254643	
Mastocarpus agardhii	M436	07-Jan-2008	USA	Hopkins Marine Station, Pacific Grove, CA			HQ437739	HQ437899
Mastocarpus alaskensis	GWS004391	26-Jun-2006	Canada	Botanical Beach, Port Renfrew, Vancouver I.	48.53	-124.454	GQ380241	GQ338138
Mastocarpus californianus	MasDes021	19-May-2015	Chile	Desembocadura			MG700406	
Mastocarpus californianus	GWS000073	22-Jul-1996	United States	Piedras Blancas	35.67	-121.291	GQ380171	KT310710
Mastocarpus cristatus	GWS021454	16-May-2010	United States	Sea Lion Point North (backside), Point Lobos State Reserve	36.519	-121.953	KM254822	
Mastocarpus cristatus	M406	07-Jan-2008	USA	Hopkins Marine Station, Pacific Grove, CA			HQ437728	HQ437889
Mastocarpus intermedius	GWS003481	13-Jun-2006	Canada	Bamfield, Dixon I.	48.852	-125.122	GQ380298	GQ338140
Mastocarpus jardinii	GWS000070	22-Jul-1996	United States	Piedras Blancas	35.6704	-121.291	GQ380331	GQ338142
Mastocarpus latissimus	GWS010642	04-Jun-2008	Canada	Bamfield, Dixon I.	48.8524	-125.122	GQ380225	GQ338137

Mastocarpus pachenicus	GWS001331	28-Apr-2002	Canada	Bamfield, Bradys Beach	48.824	-125.162	GQ380174	GQ338145	
Mastocarpus pacificus	GWS042001	16-Aug-2017	United States	Nome, West Breakwater (west side)	64.4927	-165.441	MH143559	MH277313	MH143912
Mastocarpus pacificus	GWS011939	01-Dec-2008	Japan	Hokkaido University Marine Station, Oshoro Bay	43.239	140.85	HM916083		
Mastocarpus papillatus	GWS003229	17-Sep-2005	Canada	Bamfield, Bradys Beach	48.824	-125.159	GQ380269	GQ338139	
Mastocarpus rigidus	GWS030398	06-Jun-2012	Canada	Raspberry Cove, Gwaii Haanas	52.167	-131.084	KM254381		
Mastocarpus rigidus	M73	17-May-2003	Canada	Cape Palmerston, BC			HQ437736	HQ437896	
Mastocarpus sp. clade9papillatus	GWS021919	19-May-2010	United States	Santa Cruz (Four Mile)	36.966	-122.123	KM254397		
Mastocarpus stellatus	GWS040905	12-Jun-2016	Norway	Oksneset, Askoy	60.5308	4.98519	MH143530		
Mastocarpus stellatus	GWS003669	25-Apr-2006	United States	End of public road, Starboard	44.609	-67.397	GQ380335	GQ338143	
Mastocarpus stellatus	GWS014672	25-Aug-2010	Ireland	Fountainstown			KY572588		
Mastocarpus vancouveriensis	GWS004004	15-Jun-2006	Canada	Bamfield, Bradys Beach	48.826	-125.155	GQ380319	GQ338141	
Opuntiella/Turnerella									
Furcellaria lumbricalis	GWS003509	11-Nov-2005	Canada	Pomquet Harbour, Antigonish	45.662	-61.833		KC130215	
Opuntiella californica	US-Oc10vii2006	10-Oct-2006	USA	Juneau, Alaksa				KC174807	
Opuntiella californica	U21589	Oct-1993	USA	Friday Harbour, WA				U21589	
Opuntiella sp. 1californica	GWS019369	31-May-2010	Canada	Bamfield, Seapool Rock	48.816	-125.209	HQ544356	MH277316	

Opuntiella sp. 2californica	GWS019586	02-Jun-2010	Canada	Ucluelet, Sargison Bank	48.922	-125.421	HQ544511	KF026491
Peyssonneliopsis sp. 2epiphytica	GWS003012	13-Jun-2005	Canada	Bamfield, Black Fish I., near Helby I.	48.847	-125.165	KU986357	KU905061
Turneralla mertensiana	JP-Tm26vii2002	26-Jul-2002	Japan	Hokkaido, Kushiro, Akkenshi-wan				KC174812
Turnerella pennyi	GWS009361	22-Apr-2008	Canada	Escoumins (Rue des Pilotes)	48.318	-69.414		MH277327
Turnerella pennyi	GWS005290	20-Aug-2006	Canada	Bluff A, Churchill Northern Studies Centre	58.77	-93.847		MH277284
Turnerella sp. _1Atl	GWS007020	11-Jul-2006	Canada	Norris Point, Bonne Bay Marine Station	49.518	-57.874		MH277302
Turnerella sp. 1BC	GWS020942	07-Jun-2010	Canada	Indian Head, Skidegate, Haida Gwaii	53.248	-131.984	HQ545192	MH277307
Ceramiales								
Melanothamnus								
Kapraunia schneideri	GWS031240	22-Jun-2012	United States	Patriot`s Point (floating dock at marina), Mt. Plesant, Charleston Harbor	34.785	-79.908	MF120606	MF120837
Melanothamnus afaqhusainii	GWS014134	08-Sep-2001	Oman	Hatom Cove, east of Mirbat	16.961	54.828	KU564334	KU564460
Melanothamnus akkeshiensis	13fla03	9-Aug-2013	Korea	Bangpo, Chungbuk			KX265515	KX265439
Melanothamnus akkeshiensis	GWS010305	26-May-2008	Canada	Tahsis, Mozina Pt.	49.859	-126.674	HM916557	KM894074
Melanothamnus akkeshiensis	GWS030063	17-Apr-2012	United States	Hazard Ave., Narragansett	41.414	-71.453	KM894012	
Melanothamnus akkeshiensis	RMAR3083	30-Aug-2011	France	Le Loup	48.7306	-4.00366	KJ960854	
Melanothamnus bajacali	MEX04-9	29-Feb-2004	Mexico	Yucatan, Cancun, Blue Bay Marina			HM573526	HM573572

Melanothamnus collabens	CH2526		Spain	A Coruna, Artabra				JX828157	
Polysiphonia forfex	AF342910	15-Jul-1999	France	Biarritz, Aquitaine				AF342910	
Melanothamnus decumbens	DQ787479	03-Nov-2002	South Korea	Keongnam, Namhaedo, Gacheon				DQ787479	
Melanothamnus ferulacea	PHYKOS-2287	17-May-2009	Panama	Colon, Punta Toro, West Limon Bay Jetty			HM573511	HM573584	
Melanothamnus harveyi	GWS010963	23-Jul-2008	Canada	Sam Orr`s Pond	45.162	-67.045	HM916526	KM894076	
Melanothamnus harveyi	RMAR3151	30-Aug-2011	France	Le Loup	48.7306	-4.00366	KJ960855		
Melanothamnus japonicus	GWS030049	17-Apr-2012	United States	Hazard Ave., Narragansett	41.414	-71.453	KM894009	KM894063	KM894085
Melanothamnus japonicus	12ja01	24-Feb-2012	Japan	Hakodate, Hokkaido			KX265516	KX265440	
Melanothamnus sp.	PHYKOS-2613	20-May-2009	Panama	Colon, Parque de Juventud			HM573517	HM573571	
Melanothamnus sp. 21GWS	GWS003033	14-Jun-2005	Canada	Bamfield, Ross Islets	48.874	-125.16	HM918545	KM894064	KM894086
Melanothamnus sphaerocarpa	12sph01	10-Mar-2012	Korea	Pyoseon, Jeju			KX265518	KX265453	
Melanothamnus strictissima	NZ04-552	17-Nov-2004	New Zealand	North Is., Muritai			HM573533	GU385833	
Melanothamnus teradomariensis	14ter01	12-Jan-2014	Korea	Jukbyeon, Gyeongbuk			KX265517	KX265441	
Melanothamnus tongatensis	PHYKOS-2704	21-May-2009	Panama	Colon, Punta Galeta			HM573518	HM573570	
Melanothamnus yendoi	DQ787495	9-Mar-2005	South Korea	Busan, Gijang				DQ787495	
Melanothamnus yendoi	13yen12		Japan	Shimoda			KX265568	KX265503	
Polysiphonia pseudovillum	PHYKOS-3533	17-Jul-2008	Panama	Bocas del Toro, Isla Colon, Flat Rock			HM573524	HM573568	

Neosiphonia sphaerocarpa	FL05-6	27-Feb-2005	USA	Monroe Co., Long Key, FL				HM573569	
Membranoptera									
Cumathamnion decipiens	GWS019806	11-Jun-2010	Canada	Alder Island, Gwaii Haanas	52.442	-131.319	HQ544628	JX110915	
Membranoptera alata	GWS014650	12-Aug-2010	Ireland	Smerwick Harbour			JX111877	JX110927	
Membranoptera carpophylla	GWS039353	08-Sep-2014	Canada	N Head of Evans Bight, Torngat, Labrador	59.298	-63.524	MH143535	MH277288	
Membranoptera fabriciana	GWS013910	16-Sep-2009	Canada	Harrington Cove exposed biodiversity site, Grand Manan	44.625	-66.86	HM915569	JX110924	JX110864
Membranoptera fabriciana	GWS039288	07-Sep-2014	Canada	Duck Islands, Torngat, Labrador	60.234	-64.341	MH143536		
Membranoptera platyphylla	GWS008413	12-Jun-2007	Canada	Martin Rd., Beaver I., near Sechelt, Sunshine Coast	49.622	-124.061	HM917025	JX110926	JX110880
Membranoptera sp.	AF257383	4-Apr-1998	USA	Auke Bay, AK				AF257383	
Membranoptera tenuis	UC266439	Jul-1910	USA	West of Canoe Island, WA			KU821148	KP675983	
Membranoptera weeksiae	UC264804	26-Mar-1896	USA	Pacific Grove, CA			KU821147	KJ513670	
Odonthalia/*Neorhodomela*/*Rhodomela*									
Odonthalia corymbifera	OK230	11-Jul-2001	Japan	Hokkaido, Muroran				JX828138	
Odonthalia dentata	GWS042382	20-Aug-2017	United States	Sledge Island, southwest corner	64.4724	-166.212	MH143532		
Odonthalia dentata	GWS040665	09-Jun-2016	Norway	Kleppesjoen	60.1847	5.14938	KY572292		MH143902
Odonthalia dentata	GWS039265	07-Sep-2014	Canada	Duck Islands, Torngat, Labrador	60.234	-64.341	KY572275		MH143899
Odonthalia dentata	GWS031136	20-Aug-2014	United States	E 3, the Boulder Patch	70.325	-147.649	KY683389		MH143918

Odonthalia dentata	GWS008808	04-Sep-2007	Canada	Gadd Point, Bonne Bay	49.519	-57.878	HM918820	KU564463	
Odonthalia floccosa	GWS021176	11-Jun-2010	Canada	Alder Island, Gwaii Haanas	52.442	-131.319		MH277311	
Odonthalia floccosa	GWS020264	14-Jun-2010	Canada	East Copper Island (easterly point), Gwaii Haanas	52.358	-131.174	MH143528		
Odonthalia floccosa f. comosa	GWS020214	14-Jun-2010	Canada	East Copper Island (easterly point), Gwaii Haanas	52.358	-131.174		MH277297	
Odonthalia floccosa f. comosa	GWS006873	02-Jun-2007	Canada	`Lands End` up the left side of Pachena Bay where it opens to the ocean, Bamfield	48.772	-125.158	HM916849		
Odonthalia kamtschatica	KAM0003	10-Jun-2013	Russia	Eastern Kamchatka, Avacha Gulf, Starichkov Island	52.783	158.617	MH143534		MH143897
Odonthalia lyallii	GWS039075	15-Jul-2014	Canada	Nereocystis bed S of Yan, Haida Gwaii	54.055	-132.233	MH143550		MH143908
Odonthalia lyallii	GWS004182	20-Jun-2006	Canada	Otter Point, near Sooke, Vancouver Island	48.362	-123.805	MH143542		MH143903
Odonthalia sp.	GWS035890	20-Aug-2013	Canada	Woodruff Bay (NE beach), Gwaii Haanas	51.974	-131.032		MH277298	
Odonthalia washingtoniensis	GWS030653	09-Jun-2012	Canada	Bay south of Bowles Point, Gwaii Haanas	52.065	-131.119	MH143545		
Odonthalia washingtoniensis	AC107	17-Jul-2004	USA	San Juan Is.				GQ252561	
Neorhodomela aculeata	GWS028686	11-Jul-2011	Canada	East side of Powrivco Bay, Gwaii Haanas	52.688	-131.552	KU564391	KU564498	
Neorhodomela aculeata	GWS041942	15-Aug-2017	United States	Nome, Sledge Island East#1	64.4815	-166.195	MH143547		
Neorhodomela japonica	GWS011935	01-Dec-2008	Japan	Hokkaido University Marine Station, Oshoro Bay	43.239	140.85		MH277317	

Neorhodomela larix	GWS021376	15-May-2010	United States	Pigeon Point Lighthouse	37.183	-122.389	KM254810		
Neorhodomela larix	GWS035334	23-Aug-2013	Canada	Gudal Beach, Haida Gwaii	53.231	-132.573		MH277287	
Neorhodomela munita	mbccc18	Apr-2011	China	Tuandao Bay, Qingdao			JQ619148		
Neorhodomela oregona	GWS010916	07-Jun-2008	Canada	Stephenson Pt., Nanaimo	49.213	-123.94	HM917344		
Neorhodomela oregona	GWS020513	15-Jun-2010	Canada	Hot Spring Island (north side), Gwaii Haanas	52.579	-131.439		MH277325	
Rhodomela confervoides	GWS040058	08-Jun-2016	Norway	Hellesoy	60.6627	4.78749	MH143531		MH143894
Rhodomela confervoides	TJS1210	19-Oct-2008	France	Roscoff			KX258842	KX146197	
Rhodomela lycopodioides	GWS017875	14-Apr-2010	United States	Garbage Beach Breakwater, Woods Hole	41.525	-70.673	KY572540	MH277310	
Rhodomela lycopodioides	GWS002338	01-Sep-2004	Canada	Off Lingan Power Plant, Cape Breton, Nova Scotia	46.25	-60.014	KY572686		MH143914
Rhodomela lycopodioides	GWS040965	13-Jun-2016	Norway	Soloyna	60.159	5.23564	KY572217		MH143896
Rhodomela lycopodioides	GWS040946	13-Jun-2016	Norway	Tekslo	60.159	5.00405	KY572298	MH277292	
Rhodomela sibirica	GWS005350	22-Aug-2006	Canada	Button Bay, Churchill	58.781	-94.277	JX572030		MH143915
Rhodomela sibirica	GWS031192	21-Aug-2014	United States	W 3, the Boulder Patch	70.376	-147.794	KY683388		KY683463
Rhodomela sibirica	GWS039248	3-Sep-2014	Canada	Beach in Durbin Harbour	67.038	-62.249	MH143544		MH143905
Rhodomela sibirica	GWS042329	20-Aug-2017	United States	Sledge Island, southwest corner	64.4724	-166.212	MH143562		MH143913
Rhodomela sp. 1virgata	GWS039420	11-Sep-2014	Canada	Point NW of Lighthouse, Makkovic, Labrador	55.102	-59.18	MH143563		

Rhodomela sp. 1virgata	GWS042093	17-Aug-2017	United States	Nome, West Breakwater (west side)	64.4927	-165.441	MH143533	
Rhodomela sp. 1virgata	GWS009336	22-Apr-2008	Canada	Escoumins (east of town across from Rue aux Bouchets)	48.4	-69.339	HM916516	KU564489
Rhodomela virgata	GWS041450	11-Aug-2016	Canada	Naufrage (deep)	46.4744	-62.5477	MH143548	MH277301
Rhodomela virgata	GWS039244	03-Sep-2014	Canada	Beach in Durbin Harbour	67.038	-62.249	MH143537	
Rhodomela virgata	GWS042269	19-Aug-2017	United States	Nome, West Breakwater (west side)	64.4927	-165.441	MH143558	
Rhodomela virgata	GWS038806	24-Jul-2015	United States	E2, off Endicott, Prudhoe Bay	70.191	-147.431	KY683236	
Polysiphonia								
Polysiphonia atlantica	NC-28	9-Jun-2005	USA	Onslow Bay, NC			HM573539	
Polysiphonia determinata	GWS004015	15-Jun-2006	Canada	Bamfield, Blowhole at Bradys Beach	48.824	-125.162	HM918626	MF120879
Polysiphonia devoniensis	SANT-Algae-24630	6-Nov-2010	Spain	Cantabria, Playa de Langre			KF671186	
Polysiphonia dokdoensis			Korea	Dokdo				KJ407268
Polysiphonia kapraunii	GWS013757	23-Aug-2010	Canada	Sam Orr`s Pond	45.162	-67.045	MF120714	MF120869
Polysiphonia koreana	BYW-2015a		South Korea	Gyeongsangbuk-do, Ulleung-eup				KJ957811
Polysiphonia macrocarpa	PHYKOS-2627	20-May-2009	Panama	Colon, Punta Gorda			HM573538	
Polysiphonia marrowii	P1305	23-Feb-2012	Japan	Hokkaido, Hakodate			KP729463	
Polysiphonia marrowii	NZ04-130	28-Oct-2004	New Zealand	South Is. Curio Bay			HM573540	
Polysiphonia marrowii	P621 M03	21-Sep-2009	Argentina	Casino, Golfo Nuevo			KP729460	

Polysiphonia marrowii	P901 M07	28-Nov-2011	France	Roscoff			KP729464	
Polysiphonia morrowii	GWS008179	03-Jun-2007	Canada	Bamfield, Scotts Bay	48.835	-125.146	HQ919566	MF120896
Polysiphonia pacifica	GWS021393	15-May-2010	United States	Pigeon Point Lighthouse	37.183	-122.389	HQ544059	MF120864
Polysiphonia pacifica	GWS006555	29-May-2007	Canada	Tahsis, Princesa Channel	49.725	-126.642	HM916790	KU564485
Polysiphonia pacifica	GWS006522	29-May-2007	Canada	Tahsis Narrows	49.445	-126.828	HM916786	MF120843
Polysiphonia pacifica	GWS008580	15-Jun-2007	Canada	Comox Marina Breakwater	49.669	-124.929	MF120597	MF120831
Polysiphonia scopulorum	GWS006336	24-May-2007	Canada	Pier near statue of diver, Sidney	48.648	-123.394	HM916753	MF120834
Polysiphonia sp.	P77		Japan	Hokkaido, Oshoro				AY958168
Polysiphonia sp.	P70		Japan	Hokkaido, Denshinhama				AT958169
Polysiphonia sp.	MSK-2014a		South Korea	Jukbyeon				KM053370
Polysiphonia sp. 1stricta	GWS042314	19-Aug-2017	United States	Nome, West of west breakwater	64.5001	-165.432	MH143552	
Polysiphonia sp. 1stricta	GWS039423	11-Sep-2014	Canada	Point NW of Lighthouse, Makkovic, Labrador	55.102	-59.18	MF120725	
Polysiphonia sp. 1stricta	GWS018086	19-Apr-2010	United States	Two Lights, Cape Elizabeth	43.565	-70.199	HM915184	MF120890
Polysiphonia sp. 1stricta	GWS019735	11-Jun-2010	Canada	Alder Island, Gwaii Haanas	52.442	-131.319	MF120707	
Polysiphonia sp. 2stricta	GWS017899	14-Apr-2010	United States	Garbage Beach Breakwater, Woods Hole	41.525	-70.673	HM915116	KU564468
Polysiphonia sp. 2stricta	GWS040942	13-Jun-2016	Norway	Tekslo	60.159	5.00405	KY572142	
Polysiphonia sp. 3stricta	GWS017861	14-Apr-2010	United States	Garbage Beach Breakwater, Woods Hole	41.525	-70.673	HM915107	MF120876

Polysiphonia sp. 3stricta	GWS005716	13-Jul-2007	Canada	Gordon Point, Churchill Northern Studies Centre	58.796	-93.754	HQ919613		
Polysiphonia sp. 23GWS	GWS018035	16-Apr-2010	United States	Fort Witherill, Jamestown	41.479	-71.361	HM915166	MF120841	
Polysiphonia sp. 23GWS	GWS040797	10-Jun-2016	Norway	Hakonsund	60.1762	5.11132	MF409432		
Polysiphonia ulleungensis	KJ028026	Apr-2013	Korea	Ulleung Is.				KJ028026	
Phycodrys									
Cladodonta lyallii	AF254169	4-Jan-1998	Falkland Islands					AF254169	
Delesseriaceae sp.	NZ04-482	14-Nov-2004	New Zealand	Erangi Point, Bethells, North Is.				JF495098	
Heterodoxia denticulata	G0387	13-Nov-1995	Australia	Seven Miles Beach				JX110922	
Heterodoxia sp. 2denticulata	GWS002620	23-Jan-2005	Australia	Reef west of Verona Sands boat launch, Tasmania				JX110923	
Mikamiella ruprechtiana	GWS030656	09-Jun-2012	Canada	Bay south of Bowles Point, Gwaii Haanas	52.065	-131.119	MH143568	MH277328	
Nienbugia andersoniana	AF257396	19-Jan-1993	USA	Horseshoe Cove, Bodega Bay, CA				AF257396	
Phycodrys adamsiae	NZ4-420	11-Nov-2004	New Zealand					GQ479938	
Phycodrys antarctica	CA12iv08-PN	12-Apr-2008	Antarctica					GQ479931	
Phycodrys austrogeorgica	CA19iv03-PA	19-Apr-2003	Antarctica					GQ479930	
Phycodrys fimbriata	GWS042547	20-Aug-2017	United States	Sledge Island, north Shore (beach west side of lighthouse sandbar)	64.4962	-166.203	MH143571		
Phycodrys fimbriata	GWS040104	20-Jul-2015	United States	L1, off Endicott, Prudhoe Bay	70.173	-147.366	KY683254		MH143906

Phycodrys fimbriata	GWS039573	28-Jun-2015	Canada	New River Beach, Bay of Fundy	45.12	-66.525			MH143909
Phycodrys fimbriata	GWS013736	19-Aug-2009	Canada	Herring Cove Head (small bay to east), Campobello Island	44.875	-66.926	HM916343	JX110931	
Phycodrys fimbriata	GWS039262	07-Sep-2014	Canada	Duck Islands, Torngat, Labrador	60.234	-64.341	MH143554		
Phycodrys fimbriata	MHH26vii02-PR	26-Jul-2002	Japan	Hokkaido				GQ479929	
Phycodrys fimbriata	AF257430	5-Aug-1996	USA	St. Lawrence Is. AK				AF257430	
Phycodrys franiae	ASF523	07-Dec-2005	New Zealand					GQ479941	
Phycodrys isabelliae	GWS021967	19-May-2010	United States	Santa Cruz (Four Mile)	36.966	-122.123	KM254284		MH143895
Phycodrys novae-zelandiae	ASH469	27-Nov-2007	New Zealand					GQ479934	
Phycodrys ovifolia	AF257423	11-Jan-1995	Chile	Isla Mancerra, Bahia coral				AF257423	
Phycodrys quercifolia	AF257424	4-Jan-1998	Falkland Islands	E. Falkland Is.				AF257424	
Phycodrys quercifolia	AF257425	18-Oct-1997	New Zealand	South Bay, Kaikoura				AF257425	
Phycodrys radicosa	AF257427	23-Jun-1994	China	Gingdao, Shuntung Peninsula				AF257427	
Phycodrys riggii	GWS008335	08-Jun-2007	Canada	Ridley Island (south of coal terrminal), Prince Rupert	54.221	-130.329	MH143566	MH277321	
Phycodrys riggii	KAM0011	10-Jun-2013	Russia	Eastern Kamchatka, Avacha Gulf, Starichkov Island	52.783	158.617	MH143560	MH277314	
Phycodrys riggii	GWS004971	11-Jul-2006	Canada	Ridley Island (south of coal terrminal), Prince Rupert	54.221	-130.329	HM916599		MH143910

Phycodrys rossica	GWS035639	14-Aug-2013	Canada	Lagoon Inlet Tidal Rapids (inside), Haida Gwaii	52.934	-131.949	MH143570		MH143919
Phycodrys rubens	GWS039945	06-Jun-2016	Norway	Ormhilleren	60.4936	4.91898	KY572764		MH143917
Phycodrys rubens	GWS013862	20-Aug-2009	Canada	East Quoddy Lighthouse, Campobello Island	44.957	-66.904	JX111887	JX110932	
Phycodrys rubens	GWS008832	12-Sep-2007	Canada	SE of Beaver Harbour in SCUBA Bay, Bay of Fundy	45.056	-66.736		MH277299	MH143907
Phycodrys setchellii	GWS022209	21-May-2010	United States	McAbee Beach, Monterey	36.615	-121.899	KM254388		MH143900
Phycodrys sp. 1NB	GWS040698	09-Jun-2016	Norway	Kleppesjoen	60.1847	5.14938	KY572351		
Phycodrys sp. 1NB	GWS030232	15-May-2012	Canada	Carrying Cove, New River Beach	45.13	-66.526	KY572722	MH277323	
Phycodrys sp. 1NB	GWS005197	02-Aug-2006	Canada	Riding`s Rock, Meadow Cove	45.103	-66.388	KY572163		MH143893
Phycodrys sp. 1Wash	GWS036751	14-May-2014	United States	Rosario Beach Point	48.417	-122.665	MH143538	MH277290	MH143901
Polyneura bonnemaisonii	GWS014645	12-Aug-2010	Ireland	Smerwick Harbour			MH143565	MH277319	
Polyneura latissima	GWS030821	11-Jun-2012	Canada	Macrocystis bed at entrance to George Bay, Gwaii Haanas	52.307	-131.332	MH143556	MH277309	
Polyostea									
Acanthosiphonia echinata	GWS006238	27-Aug-2007	Canada	Kouchibouguac lagoon seagrass beds	46.835	-64.93	HM916729	MF120866	
Polyostea arctica	GWS007126	13-Jul-2006	Canada	Maerl bed (btw Deer Arm & East Arm), Bonne Bay	49.525	-57.826	HM916874	KU564478	
Polyostea arctica	GWS005436	08-Jul-2007	Canada	Churchill Beach	58.774	-94.171	HM918754		

Polyostea bipinnata	KAM0009	10-Jun-2013	Russia	Eastern Kamchatka, Avacha Gulf, Starichkov Island	52.783	158.617		KU564490
Polyostea bipinnata	GWS030845	12-Jun-2012	Canada	Southern Bay at Benjamin Point, Gwaii Haanas	52.212	-131.006	KU564325	KU564455
Polyostea hamata	GWS008375	10-Jun-2007	Canada	Ridley Island (south of coal terrminal), Prince Rupert	54.221	-130.329	HM916546	KU564467
Polyostea hamata	KAM0010	10-Jun-2013	Russia	Eastern Kamchatka, Avacha Gulf, Starichkov Island	52.783	158.617	KU564343	
Polyostea robusta	GWS022432	23-May-2010	Canada	600m N/W of Roberts Creek Rivermouth, Roberts Creek, Sunshine Coast	49.423	-123.656	HQ545319	KU564477
Polyostea sp. _1Nome	GWS041863	13-Aug-2017	United States	Nome, Breakwater (west side)	64.4981	-165.426	MH143546	MH277295
Ptilota								
Plumaria plumosa	GWS009779	29-May-2008	Canada	Brier Island Western Light (exposed rocky site)	44.249	-66.39	HM917150	KU381993
Ptilota asplenioides	GWS035795	18-Aug-2013	Canada	SGang Gwaay (rocks to NW), Gwaii Haanas	52.105	-131.241	KU381943	KU381991
Ptilota asplenioides	KAM0002	10-Jun-2013	Russia	Eastern Kamchatka, Avacha Gulf, Starichkov Island	52.783	158.617	MH143540	
Ptilota densa	GWS021386	15-May-2010	United States	Pigeon Point Lighthouse	37.183	-122.389	KM254384	KU381980
Ptilota dentata	P437	01-Aug-2004	Japan	Chiba, Choshi, Nagasaki				DQ787573
Ptilota filicina	GWS004006	15-Jun-2006	Canada	Bamfield, `Sparlingia Pt.`, Bradys Beach	48.8242	-125.159	KU381950	KU381992

Ptilota gunneri	GWS039940	06-Jun-2016	Norway	Ormhilleren	60.4936	4.91898	MH143541	
Ptilota gunneri	GWS005434	08-Jul-2007	Canada	Churchill Beach	58.7742	-94.1706	JX571999	
Ptilota gunneri	GWS008779	19-Aug-2007	Canada	Cable Head	46.4628	-62.6074	KU381865	KU381983
Ptilota gwaiihaanasica	GWS013030	20-Jun-2009	Canada	Scudder Point, Burnaby Island, Gwaii Haanas	52.446	-131.233	HM915495	KU381996
Ptilota haidarum	GWS020230	14-Jun-2010	Canada	East Copper Island (easterly point), Gwaii Haanas	52.358	-131.174	KU381850	KU381979
Ptilota hypnoides	GWS004699	03-Jul-2006	Canada	Palmerston Recreation Reserve near Raft Cove, Vancouver Island	50.5933	-128.258	KM254851	KU381994
Ptilota pseudohypnoides	GWS010519	02-Jun-2008	Canada	Bamfield, Edward King Island	48.8218	-125.218	KU381907	KU381985
Ptilota serrata	GWS007107	13-Jul-2006	Canada	Maerl bed (btw Deer Arm & East Arm), Bonne Bay	49.5253	-57.8256	KU381917	KU381988
Ptilota serrata	JR-07-19	9-Nov-2007	Norway	Troms, Balsfjord			HQ412547	
Ptilota serrata	A93571	3-Aug-1996	United States	St. Lawrence I.				MG762003
Ptilota serrata	A84489	4-Aug-2003	Canada	Bowie Seamount, British Colimbia				MG762004
Ptilota sloanii	GWS030448	06-Jun-2012	Canada	Raspberry Cove, Gwaii Haanas	52.167	-131.084	KU381915	KU381987
Ptilota subita	GWS035611	13-Aug-2013	Canada	Fairbairn Bank, Haida Gwaii	53.017	-131.602	KU381964	KU381995
Ptilota tenuis	GWS013351	22-Jun-2009	Canada	Murchison Island Lagoon, Gwaii Haanas	52.604	-131.45	HM915671	KU381981
Vertebrata								

Neosiphonia tepida	FL05-2	26-Feb-2005	USA	Sebastian Inlet, Florida				HM573552
Eutrichosiphonia confusa	GWS021926	19-May-2010	United States	Santa Cruz (Four Mile)	36.966	-122.123	KM254652	MF120870
Vertebrata aterrima	NZ04-512	16-Nov-2004	New Zealand	North Island, Castle Point, Mataikona			HM573537	GU385831
Vertebrata australis	PD931	1-Nov-2014	Australia	Frankston, Dave's Bay, Victoria			MF094014	MF101439
Vertebrata byssoides	GWS040778	10-Jun-2016	Norway	Hakonsund	60.1762	5.11132	MH143539	MH277291
Vertebrata constricta	NZ04-308	03-Nov-2004	New Zealand	Ulva Is.			HM573542	HM573580
Vertebrata ericoides	GWS016590	29-Jan-2010	Australia	Marrawah Beach	-40.933	144.6	MF120664	MF120855
Vertebrata foetdissima	JQ653292		Spain					JQ653292
Vertebrata fruticulosa	CH049		Ireland	Galway, Spiddal				JX828161
Vertebrata hendryi	GWS006441	26-May-2007	Canada	Spring Bay	48.456	-123.269	HM916772	MF120848
Vertebrata isogona	NZ04-139	28-Oct-2004	New Zealand	South Is., Curio Bay			HM573541	HM573578
Vertebrata lanosa	GWS039901	05-Jun-2016	Norway	Ormhilleren (site 2)	60.4987	4.91362	MH143553	
Vertebrata lanosa	GWS014795	13-Apr-2010	United States	Folly Cove, Gloucester, right side	42.685	-70.641	HM915077	KU564487
Vertebrata nigra	GWS014710	12-Apr-2010	United States	White Horse Beach, Plymouth	41.934	-70.56	HM919015	MF120893
Vertebrata nigra	SANT-Algae-24148	28-May-2010	Spain	Asturias, Asturias, Niembro			KC130868	
Vertebrata paniculata			Chile	Punta Arenas, Seno Otway				AY396041
Vertebrata sp. 1fucoides	GWS018146	19-Apr-2010	United States	Two Lights, Cape Elizabeth	43.565	-70.199	HM915205	MF120880
Vertebrata sp. 2fucoides	GWS038082	03-Jun-2016	Norway	Station Dorm Beach, Espegend	60.2692	5.22123	MF409417	

Vertebrata sp. 2fucoides	GWS017939	15-Apr-2010	United States	East Point Beach, Groton	41.32	-72.075	HM915135	MF120836
Vertebrata stimpsonii	CH073		Japan	Hokkaido, Akkeshi				JX828126
Vertebrata thuyoides	GWS026296	16-Oct-2012	Ireland	Spiddal	53.247	-9.303	MF120637	MF120845
Vertebrata tripinnata	SANT-Algae-24256	14-Jun-2010	Portugal	Estremadura, Baleal			KC130871	
Vertebrata woodii	GWS008685	16-Jun-2007	Canada	Bamfield, Seapool Rock	48.816	-125.209	HM916511	MF120857

Table C2. Maximum Likelihood tests for the molecular clock test in trans-Arctic lineages of red marine macroalgae.

Taxa (outgroup)	Marker		ln*L*	# of parameters	*P*	Clock rejected?
Dilsea (*Weeksia reticulata*)	COI-5P	With clock	-1954.079	16	0.298	no
		without clock	-1942.671	26		
	*rbc*L	With clock	-2938.729	16	<0.001	yes
		Without clock	-2907.996	26		
Coccotylus (*Fredericqia deveauniensis*)	COI-5P	With clock	-2213.2	21	<0.001	yes
		Without clock	-2181.842	36		
	*rbc*L	With clock	-3597.26	22	0.999	no
		Without clock	-3592.083	38		
Palmaria (*Rhodophysema georgei*)	COI-5P	With clock	-1951.159	14	0.006	yes
		Without clock	-1934.323	22		
	*rbc*L	With clock	-2397.189	14	0.681	no
		Without clock	-2390.476	22		
Mastocarpus (*Ahnfeltiopsis leptophylla*)	COI-5P	With clock	-3169.81	22	<0.001	yes
		Without clock	-3062.549	38		
	*rbc*L	With clock	-3541.656	20	<0.001	yes
		Without clock	-3496.24	34		
Mastocarpus (*M. alaskensis*)	COI-5P	With clock	-2526.636	18	<0.001	yes
		Without clock	-2474.082	30		
	*rbc*L	With clock	-2894.952	17	<0.001	yes
		Without clock	-2870.501	28		
Mastocarpus (*M. intermedius*/*cristatus*)	COI-5P	With clock	-1657.093	11	0.4379	no
		Without clock	-1652.078	16		

	*rbc*L	With clock	-2314.399	10	0.9878	no
		Without clock	-2313.524	14		
Turnerella (*Peyssonneliopsis* sp. 2epiphytica)	*rbc*L	With clock	-2145.527	15	<0.001	yes
		Without clock	-2104.873	24		
Melanothamnus (*Kapraunii schneideri*)	COI-5P	With clock	-3137.938	24	<0.001	yes
		Without clock	-3038.68	42		
	*rbc*L	With clock	-4653.786	29	0.5822	no
		Without clock	-4632.091	52		
Membranoptera (*Cumathamnion decipiens*)	COI-5P	With clock	-1830.13	12	<0.001	yes
		Without clock	-1799.916	18		
	*rbc*L	With clock	-3084.782	13	0.4093	no
		Without clock	-3077.504	20		
Odonthalia (*Neorhodomela aculeata*)	COI-5P	With clock	-2203.785	15	0.006	yes
		Without clock	-2185.595	24		
Odonthalia (*Rhodomela sibirica*)	ITS	With clock	-1362.788	11	<0.001	yes
		Without clock	-1308.236	16		
Rhodomela (*Neorhodomela aculeata*)	COI-5P	With clock	-1633.212	15	0.0503	no
		Without clock	-1618.792	24		
	*rbc*L	With clock	-2487.503	12	0.99	no
		Without clock	-2486.833	18		
Rhodomela (*Odonthalia dentata*)	ITS	With clock	-1186.372	10	0.4942	no
		Without clock	-1182.672	14		
Polysiphonia (*P. scopulorum*)	COI-5P	With clock	-2594.108	28	0.1092	no
		Without clock	-2566.203	50		
	*rbc*L	With clock	-4451.25	31	0.03707	yes

		Without clock	-4416.631	56		
Phycodrys (*Polyneura latissima*)	COI-5P	With clock	-1896.672	21	0.00784	yes
		Without clock	-1870.732	36		
	*rbc*L	With clock	-2410.643	16	0.02761	yes
		Without clock	-2393.75	26		
Phycodrys (*Phycodrys rossica*)	ITS	With clock	-1080.854	13	<0.001	yes
		Without clock	-981.932	20		
Phycodrys (*Phycodrys* sp. 1Wash)	COI-5P	With clock	-1443.402	17	0.2974	no
		Without clock	-1430.905	28		
	*rbc*L	With clock	-2132.731	15	0.7701	no
		Without clock	-2126.053	24		
Phycodrys (*Phycodrys* sp. 1Wash)	ITS	With clock	-1278.736	11	<0.001	yes
		Without clock	-1248.725	16		
Polyostea (*Acanthosiphonia echinata*)	COI-5P	With clock	-1718.468	12	0.01267	yes
		Without clock	-1705.723	18		
	*rbc*L	With clock	-2848.892	12	<0.001	yes
		Without clock	-2823.989	18		
Polyostea (*P. robusta*)	COI	With clock	-1451.024	11	0.02487	yes
		Without clock	-1440.774	16		
	*rbc*L	With clock	-1443.269	11	0.03238	yes
		Without clock	-2433.427	16		
Ptilota (*Plumaria plumosa*)	COI-5P	With clock	-2723.692	21	0.04332	yes
		Without clock	-2701.464	36		
	*rbc*L	With clock	-3590.916	21	0.2613	no
		Without clock	-3573.665	36		

Vertebrata (*Eutrichosiphonia inconspicua*)	COI-5P	With clock	-3306.215	22	<0.001	yes
		Without clock	-3266.057	38		
	*rbc*L	With clock	-5350.678	25	0.3205	no
		Without clock	-5329.926	44		

Table C3. Tajima's (Relative Rate) Test for the molecular clock hypothesis in *Polyostea* and *Opuntiella*/*Turnerella*. Greyed rows indicate species pairs in which the molecular clock hypothesis was rejected.

Taxa	Marker	Species tested	Outgroup	X^2	*P*	Clock rejected?
Ahnfeltia	COI-5P	*Ahnfeltia fastigiata*|*A. borealis*	*A. plicata*	0.06	0.808	no
Ahnfeltia	ITS	*Ahnfeltia fastigiata*|*A. borealis*	*A. plicata*	2.00	0.157	no
Opuntiella/ *Turnerella*	*rbc*L	*Turnerella pennyi*|*T. mertensiana*	*Opuntiella californica*	1.67	0.196	no
		T. pennyi|*T. mertensiana*	*Opuntiella* sp. 2californica	1.67	0.196	no
		T. pennyi|*T. mertensiana*	*Opuntiella* sp. 1californica	0.07	0.796	no
		T. sp. 1Atl|*T.* sp. 1BC	*Peyssonneliopsis* sp. 2epiphytica	5.12	0.023	yes
		T. sp. 1Atl|*T. mertensiana*	*Peyssonneliopsis* sp. 2epiphytica	0.22	0.639	no
		T. sp. 1Atl|*T. pennyi*	*Peyssonneliopsis* sp. 2epiphytica	1	0.317	no
		T. sp. 1Atl|*O.* sp. 1californica	*Peyssonneliopsis* sp. 2epiphytica	2.28	0.130	no
		T. sp. 1Atl|*O.* sp. 2californica	*Peyssonneliopsis* sp. 2epiphytica	0.09	0.763	no
		T. sp. 1Atl|*O. californica*	*Peyssonneliopsis* sp. 2epiphytica	1.92	0.165	no

Table C4. Updated BEAST settings in analyses of trans-Arctic marine macroalgae wherein the molecular clock assumption was rejected. Divergence time estimates were derived from these finalized analyses.

Taxa	Marker	Clock model	Clock normal priors (standard deviation)	Chain length (10^6)	Notes
Coccotylus	COI-5P	Random local	none	50	Poisson prior distribution was used on number of COI-5P rate changes.
	*rbc*L	Strict	0.00302 (0.001)		
Dilsea	COI-5P	Strict	0.0076 (0.005)	10	
	*rbc*L	Relaxed	none		
Mastocarpus	COI-5P	Strict	0.0076 (0.005)	10	A subset of taxa was analysed (*M. pacificus*, *M. stellatus*, *M. vancouveriensis*, *M. jardinii*, *M. intermedius*).
	*rbc*L	Strict	0.00302 (0.001)		
Melanothamnus	COI-5P	Random local	none	50	Poisson prior distribution was used on number of COI-5P rate changes.
	*rbc*L	Strict	0.00302 (0.001)		
Membranoptera	COI-5P	Random local	none	50	Poisson prior distribution was used on number of COI-5P rate changes.
	*rbc*L	Strict	0.00302 (0.001)		
Odonthalia	COI-5P	Uncorrelated relaxed	0.0076 (0.005)	10	
	ITS	Uncorrelated relaxed	none		
Rhodomela	COI-5P	Strict	0.0076 (0.005)	10	
	*rbc*L	Strict	0.00302 (0.001)		
	ITS	Strict	none		
Palmaria	COI-5P	Random local	none	50	Due to a strikingly low *rbc*L rate in initial analysis, prior on *rbc*L was set to a uniform distribution. In addition, the *P. palmata* Atlantic split was constrained as per initial COI-5P calibration.
	*rbc*L	Strict	0.00302 (0.001)		

Phycodrys	COI-5P *rbc*L ITS	Strict Strict Strict	0.0076 (0.005) 0.00302 (0.001) none	10	A subset of taxa was analysed (*P.* sp. 1NB, *P. rubens. P. fimbriata, P. riggii, Mikamiella ruprechtiana, P.* sp. 1Wash).
Polyostea	COI-5P *rbc*L	Uncorrelated relaxed Uncorrelated relaxed	0.0076 (0.005) 0.00302 (0.001)	10	
Polysiphonia	COI-5P *rbc*L	Strict Uncorrelated relaxed	0.0076 (0.005) none	10	
Ptilota	COI-5P *rbc*L	Random local Strict	none 0.00302 (0.001)	50	Poisson prior distribution was used on number of COI-5P rate changes.
Opuntiella /Turnerella	*rbc*L	Strict clock	0.00302 (0.001)	10	An analysis of this group with an uncorrelated relaxed clock failed to resolve inner nodes; given significant Tajima's test indicating rate heterogeneity in *Turnerella* sp. 1BC, this species was removed from the analysis and a strict clock was again enforced.
Vertebrata	COI-5P *rbc*L	Random local Strict	none 0.00302 (0.001)	50	Poisson prior distribution was used on number of COI-5P rate changes.

Table C5. *Rbc*L clock rates (substitutions/site/Ma) in trans-Arctic lineages of red macroalgae, as estimated in BEAST v.1.8.3 using a strict COI-5P clock. The average *rbc*L rate and 95% HPD intervals were used as priors in the analyses utilizing a strict *rbc*L clock.

Taxa	Estimated *rbc*L rate	95% HPD low	95% HPD high
Initial analysis, strick clock			
Ahnfeltia	0.00340490	0.00047738	0.00760000
Coccotylus	0.00379985	0.00190295	0.00560000
Dilsea	0.00361025	0.00174450	0.00530000
Mastocarpus	0.00249735	0.00126775	0.00369780
Melanothamnus	0.00416470	0.00205440	0.00615000
Membranoptera	0.00420310	0.00199575	0.00625000
Odonthalia, Neorhodomela, Rhodomela	0.00267030	0.00132185	0.00395135
Palmaria	00.0014589	0.00071375	0.00225300
Phycodrys	0.00341915	0.00166620	0.00520000
Polyostea	0.00418355	0.00201570	0.00600000
Polysiphonia	0.00406400	0.00212985	0.00600000
Ptilota	0.00289050	0.00134185	0.00376030
Vertebrata	0.00525000	0.00271145	0.00765000
Updated analysis, relaxed *rbc*L clock			
Dilsea	0.00362960	0.00175060	0.00535000
Mastocarpus	0.00214225	0.00098775	0.00325105
Rhodomela	0.00326545	0.00144760	0.00497500
Phycodrys	0.00208755	0.00091860	0.00325775
Polysiphonia	0.00394475	0.00197400	0.00580000
Average *rbc*L rate	**0.00301392**	**0.00141710**	**0.00452636**

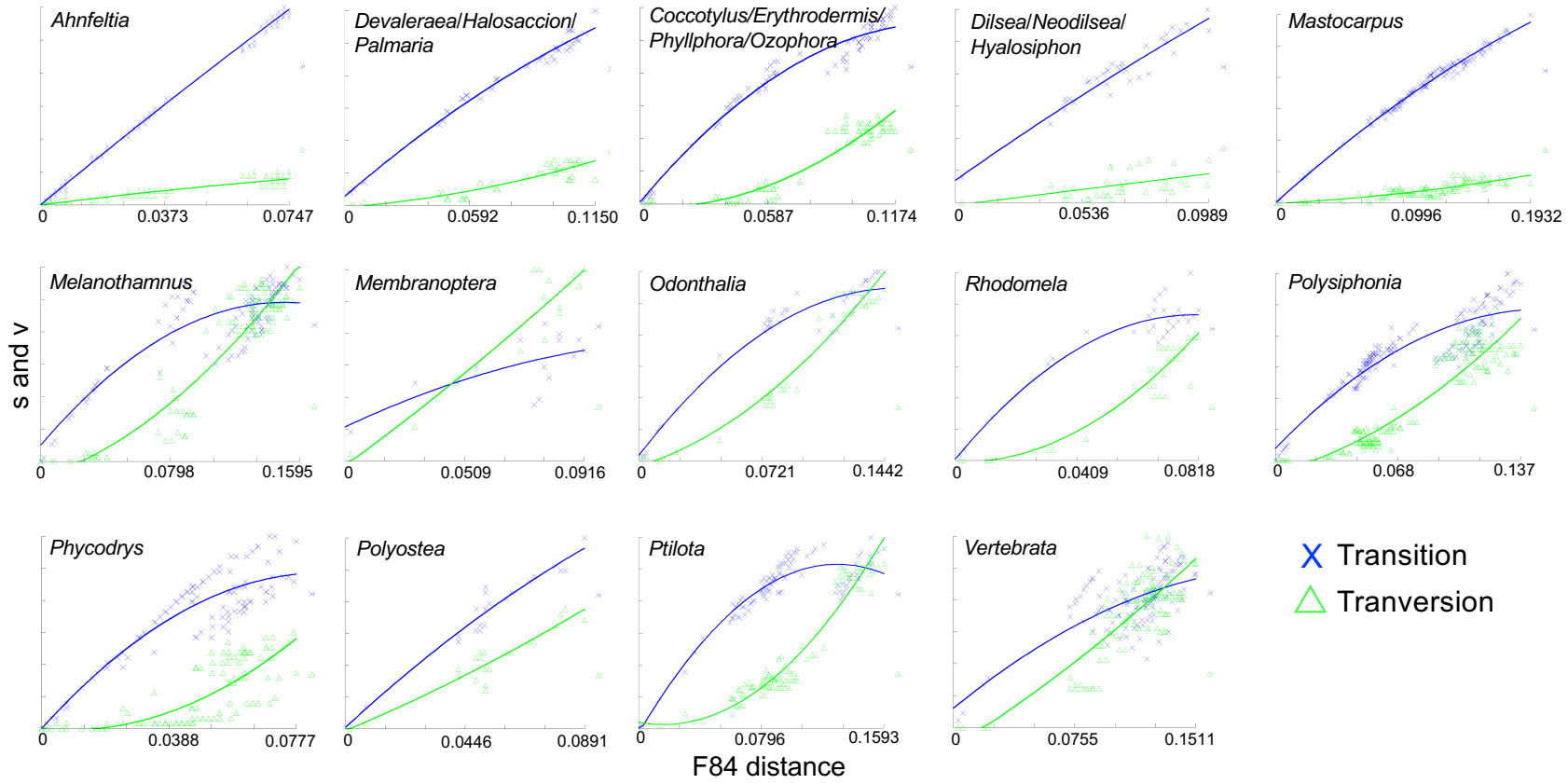

Fig. C1. Rates of transitions and transversions according to COI-5P F84 distances in trans-Arctic genera of Florideophyceae (Rhodophyta).

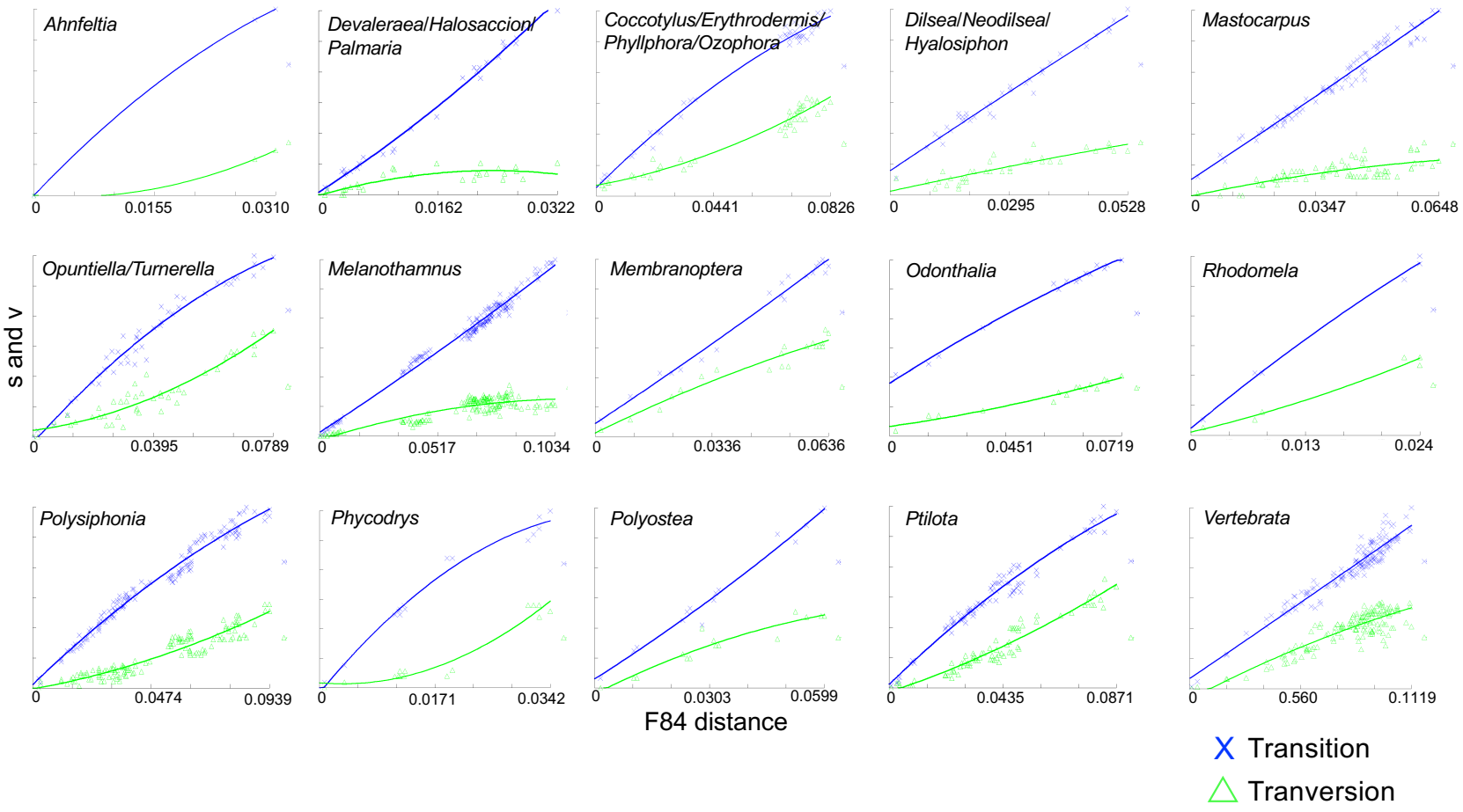

Fig. C2. Rates of transitions and transversions according to *rbc*L F84 distances in trans-Arctic genera of Florideophyceae (Rhodophyta).

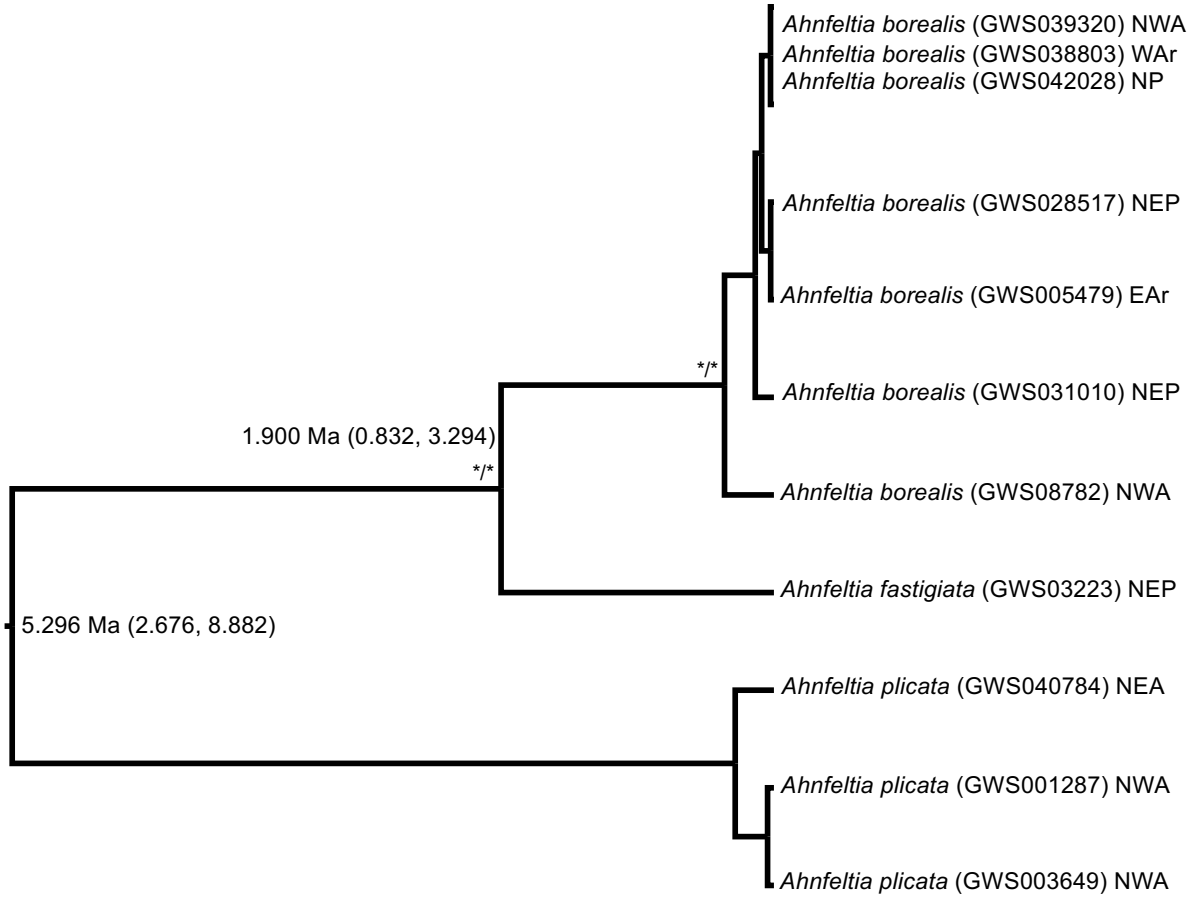

Fig. C3. *Ahnfeltia* BEAST tree based on COI-5P, ITS, and *rcb*L markers. Posterior probability values and bootstrap values are indicated, respectively; values of 1.0 or 100 are indicated with an asterisk. Divergence time estimates are given in millions of year (Ma) with 95% highest posterior density estimates in brackets. NEP=Northeast Pacific, NP=North Pacific (i.e. Bering Sea), WAr=Western Arctic (i.e. Beaufort Sea), EAr=Eastern Artic (i.e. Hudson Bay to Northern Newfoundland), NWA=Northwest Atlantic, NEA=Northeast Atlantic.

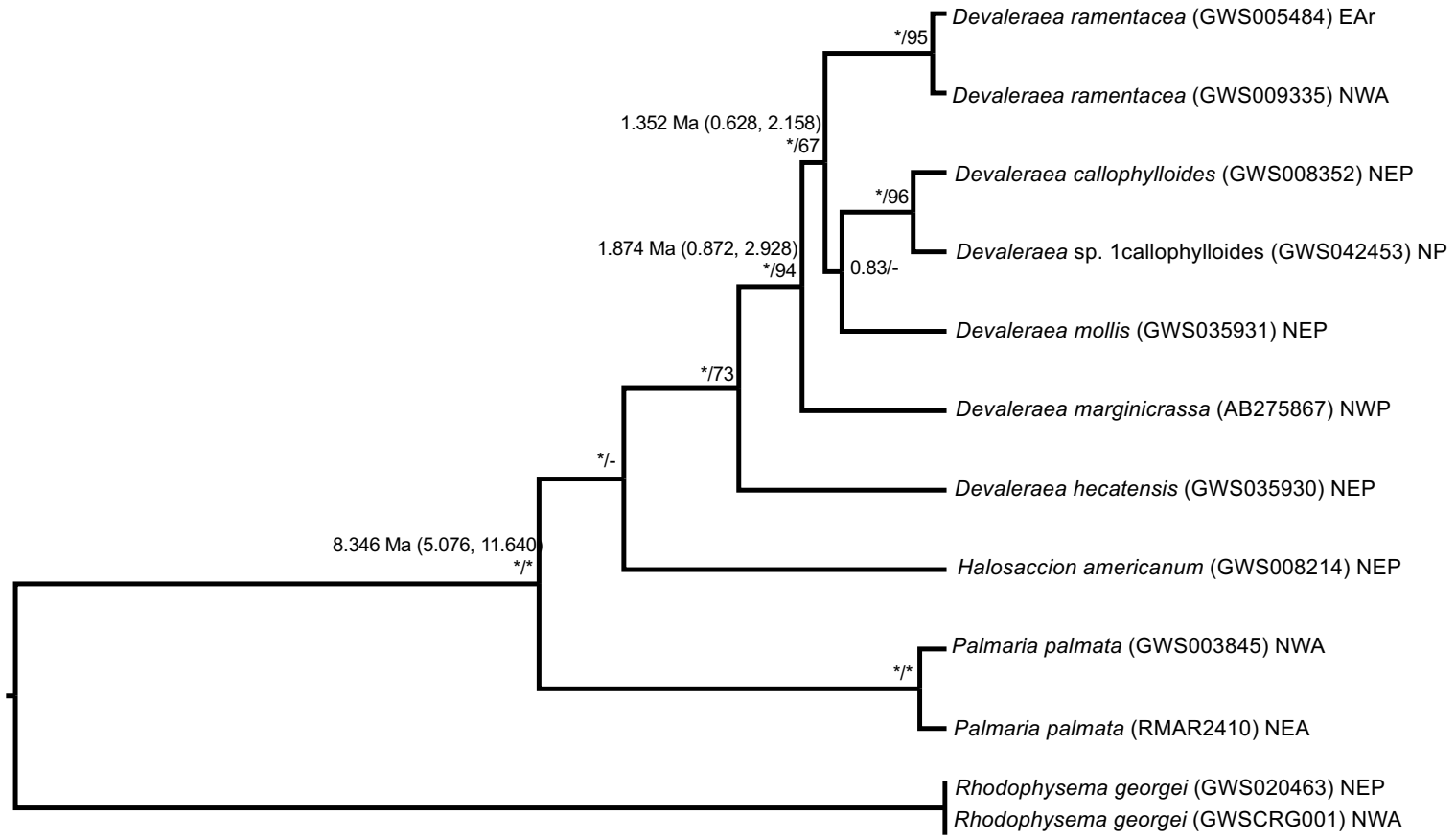

Fig. C4. *Devaleraea*, *Halosaccion, Palmaria* BEAST tree based on COI-5P and *rcb*L markers. Posterior probability values and bootstrap values are indicated, respectively; values of 1.0 or 100 are indicated with an asterisk. Divergence time estimates are given in millions of year (Ma) with 95% highest posterior density estimates in brackets. NWP=Northwest Pacific, NP=North Pacific (i.e. Bering Sea), NEP=Northeast Pacific, EAr=Eastern Artic (i.e. Hudson Bay to Northern Newfoundland), NWA=Northwest Atlantic, NEA=Northeast Atlantic.

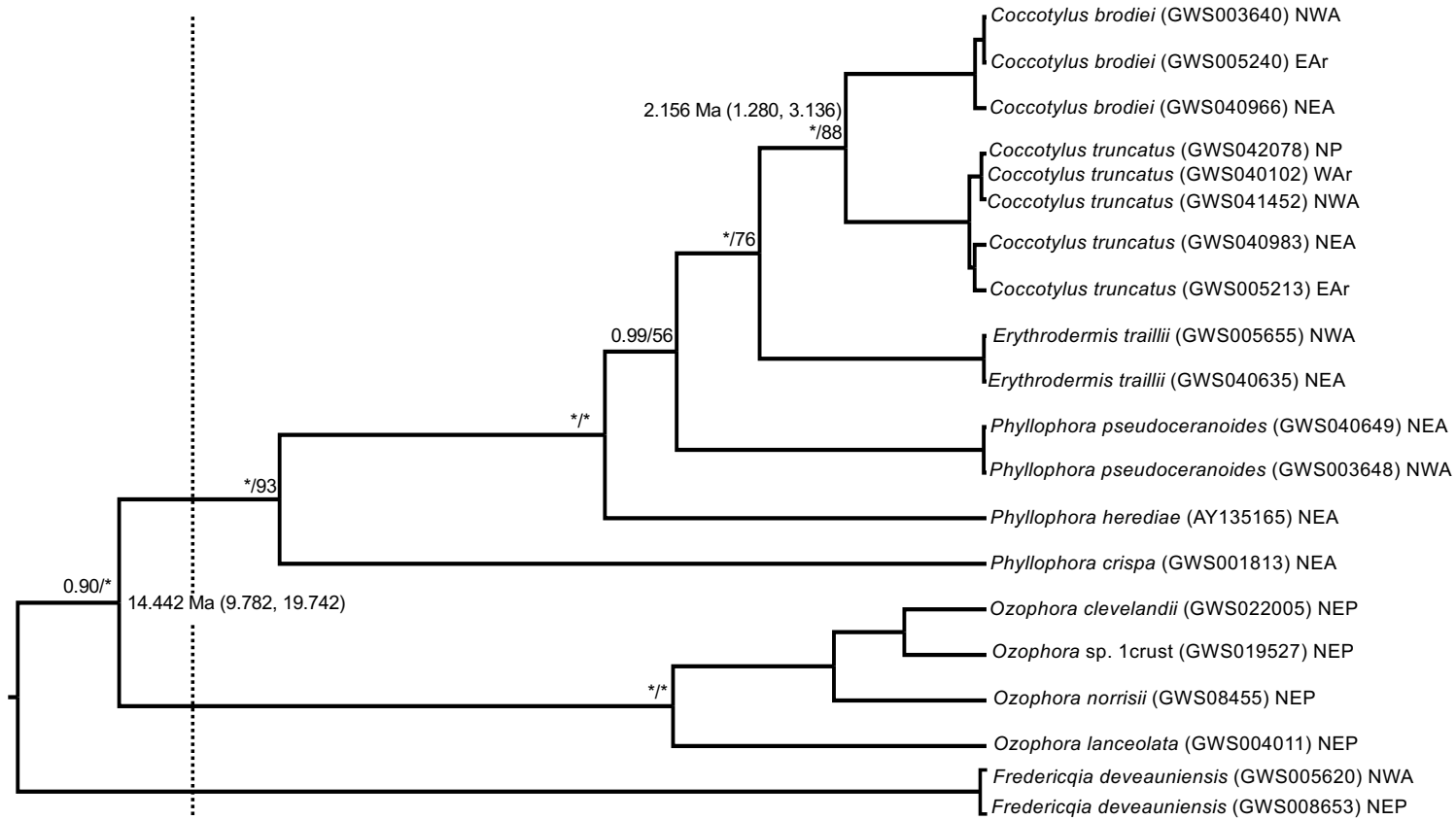

Fig. C5. *Coccotylus*, *Erythrodermis*, *Phyllophora*, and *Ozophora* BEAST tree based on COI-5P and *rcb*L markers. Posterior probability values and bootstrap values are indicated, respectively; values of 1.0 or 100 are indicated with an asterisk. Divergence time estimates are given in millions of year (Ma) with 95% highest posterior density estimates in brackets. The dashed line indicates *rbc*L saturation. NEP=Northeast Pacific, NP=North Pacific (i.e. Bering Sea), WAr=Western Arctic (i.e. Beaufort Sea), EAr=Eastern Artic (i.e. Hudson Bay to Northern Newfoundland), NWA=Northwest Atlantic, NEA=Northeast Atlantic.

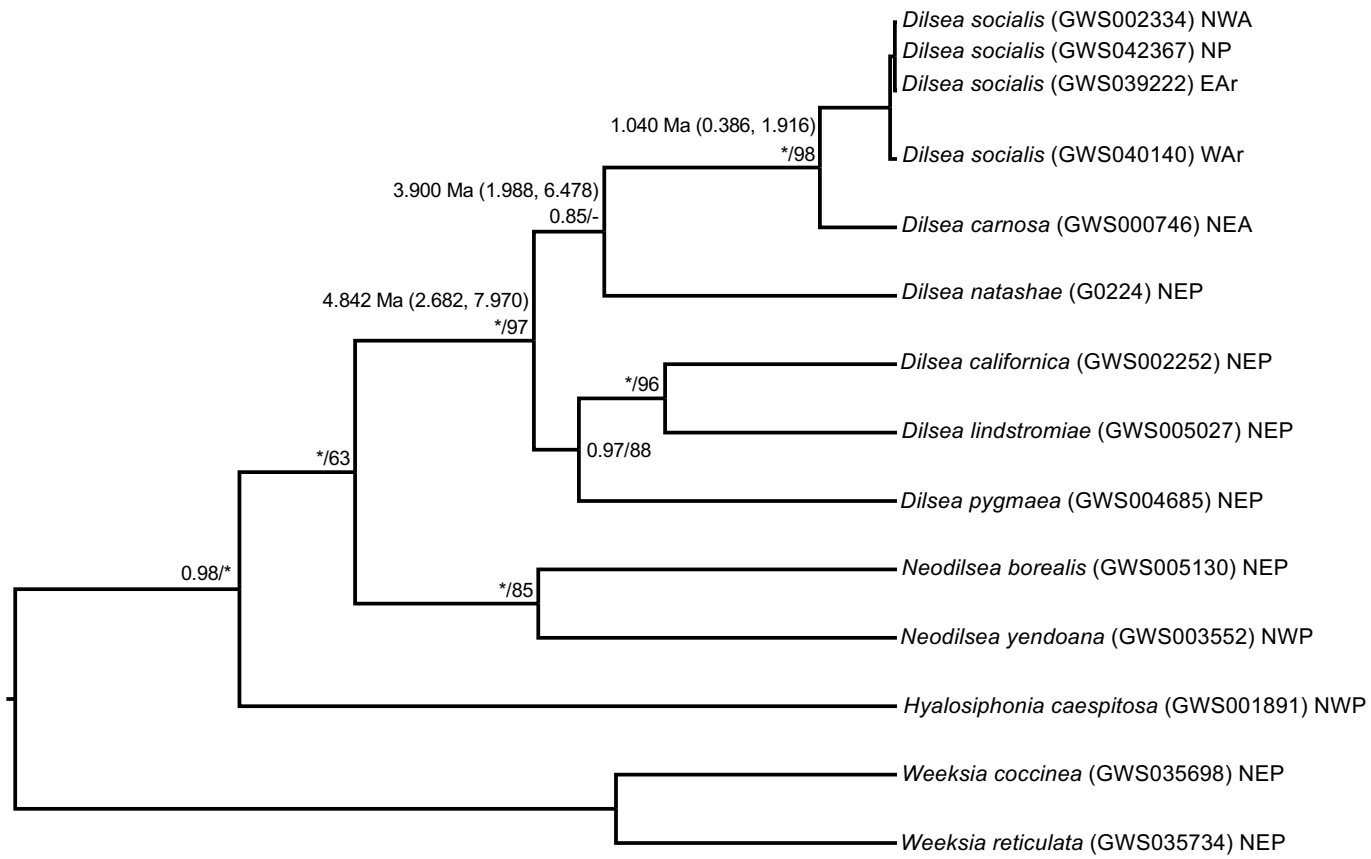

Fig. C6. *Dilsea*, *Hyalosiphon*, and *Neodilsea* BEAST tree based on COI-5P and *rcb*L markers. Posterior probability values and bootstrap values are indicated, respectively; values of 1.0 or 100 are indicated with an asterisk; nodes with a bootstrap value of <50 in the ML analysis are indicated by a negative symbol. Divergence time estimates are given in millions of year (Ma) with 95% highest posterior density estimates in brackets. NWP=Northwest Pacific, NP=North Pacific (i.e. Bering Sea), NEP=Northeast Pacific, WAr=Western Arctic (i.e. Beaufort Sea), EAr=Eastern Artic (i.e. Hudson Bay to Northern Newfoundland), NWA=Northwest Atlantic, NEA=Northeast Atlantic.

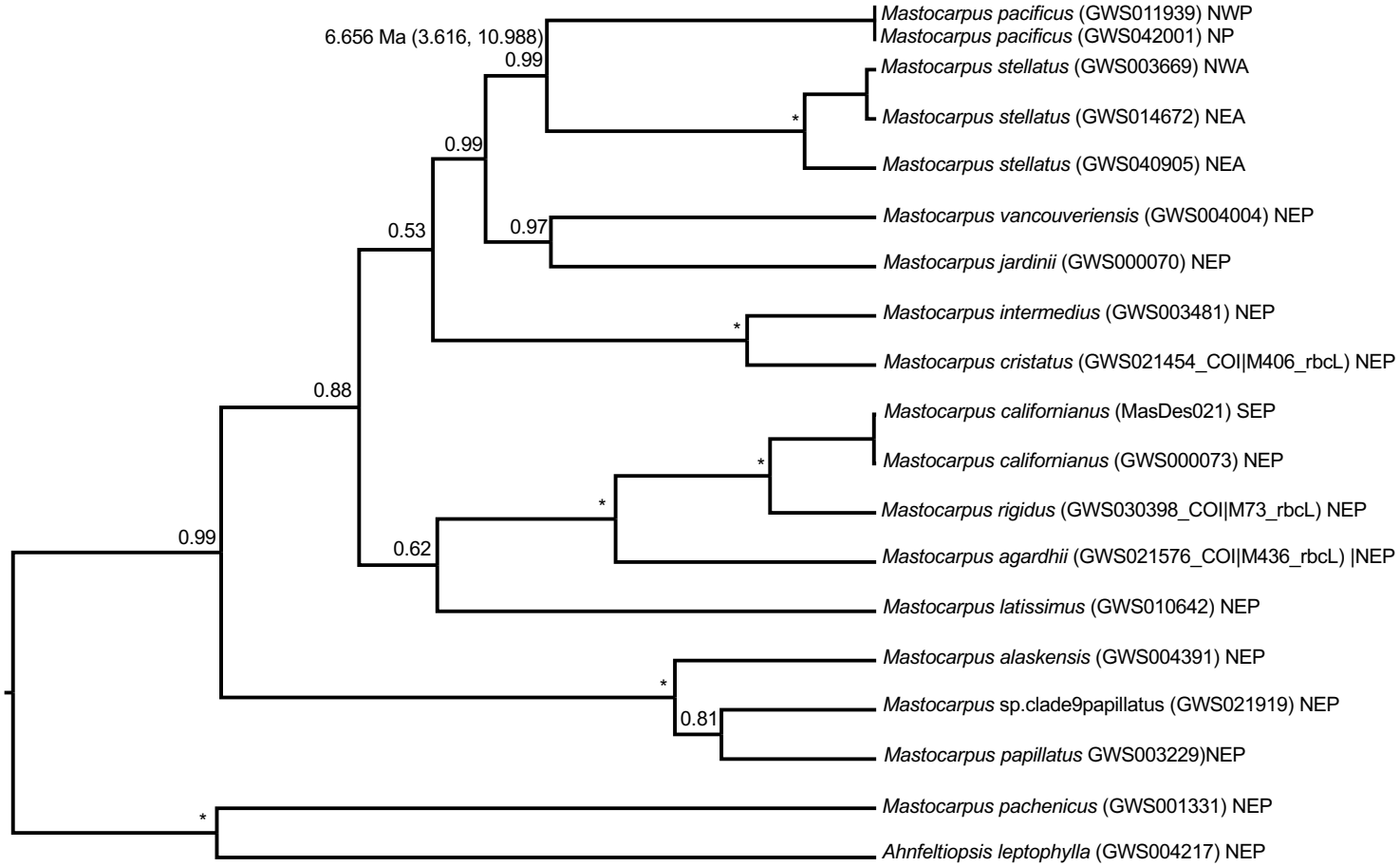

Fig. C7. *Mastocarpus* BEAST tree based on COI-5P and *rcb*L markers. Posterior probability values are indicated; values of 1.0 are indicated with an asterisk. Divergence time estimates are given in millions of year (Ma) with 95% highest posterior density estimates in brackets. SEP=Southeast Pacific (i.e. Chile), NWP=Northwest Pacific, NP=North Pacific (i.e. Being Sea), NEP=Northeast Pacific, NWA=Northwest Atlantic, NEA=Northeast Atlantic.

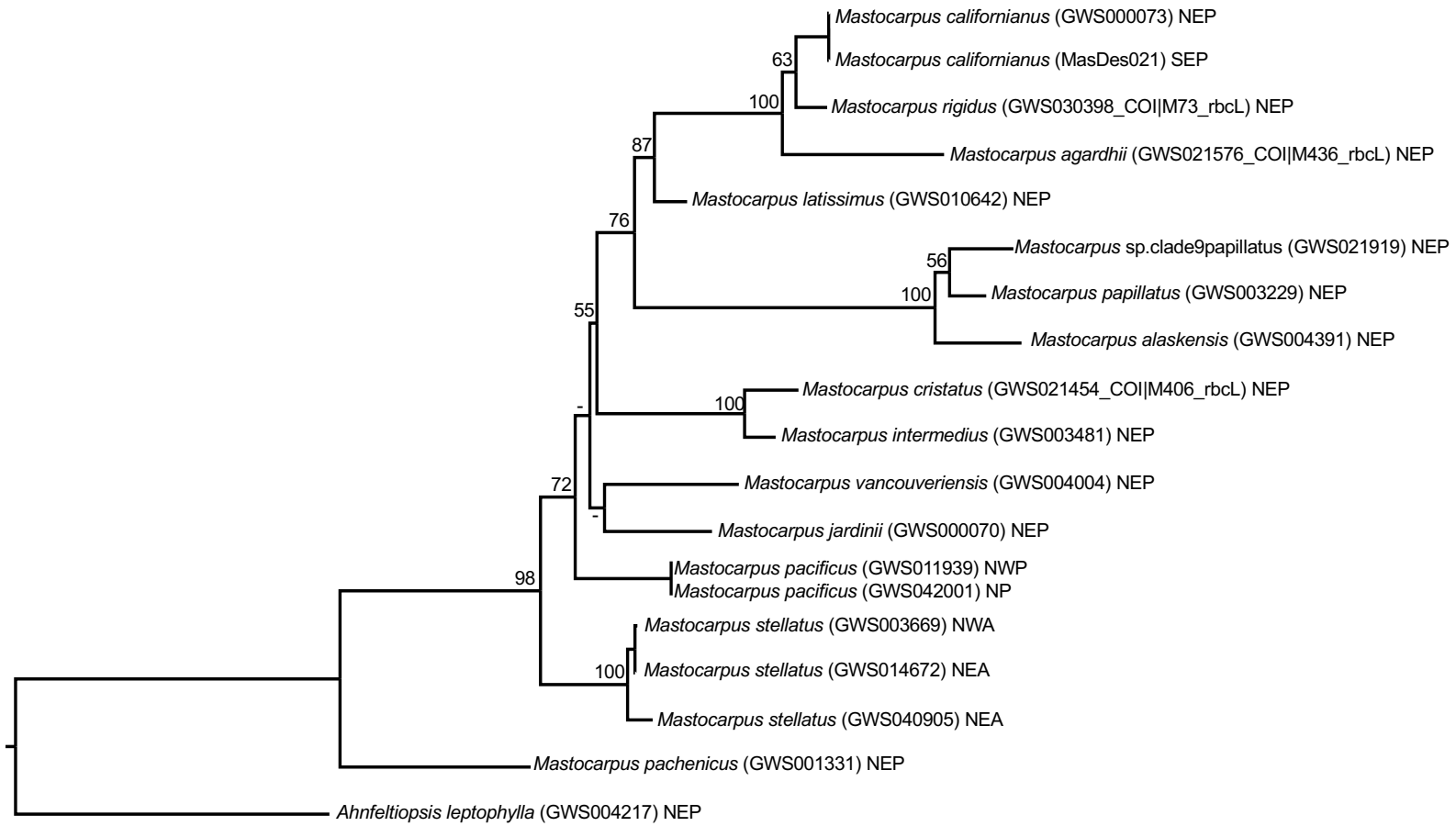

Fig. C8. *Mastocarpus* RAxML tree based on COI-5P and *rcb*L markers. Bootstrap values of 100 are indicated with an asterisk while values of less than 50 are indicated with a negative symbol. SEP=Southeast Pacific (i.e. Chile), NWP=Northwest Pacific, NP=North Pacific (i.e. Bering Sea), NEP=Northeast Pacific, NWA=Northwest Atlantic, NEA=Northeast Atlantic.

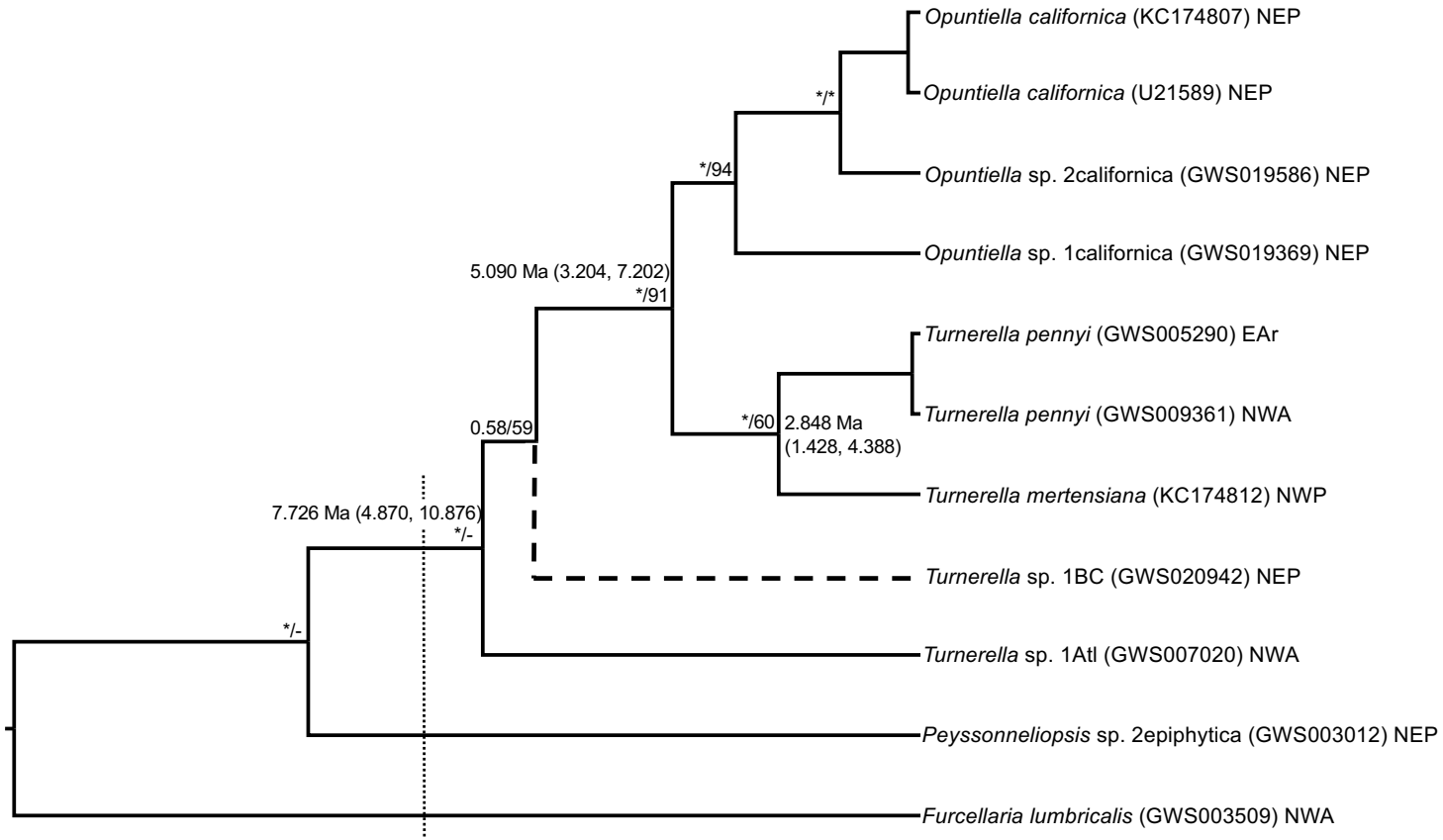

Fig. C9. *Opuntiella* and *Turnerella* BEAST tree based on *rcb*L. Posterior probability values and bootstrap values are indicated, respectively; values of 1.0 or 100 are indicated with an asterisk, while bootstrap values less than 50 are indicated with a negative symbol. Divergence time estimates are given in millions of year (Ma) with 95% highest posterior density estimates in brackets. Analyses indicated rate heterogeneity in *Turnerella* sp. 1BC (dashed line); divergence times are therefore presented for the analysis without *T.* sp. 1BC. NWP=Northwest Pacific, NEP=Northeast Pacific, EAr=Eastern Artic (i.e. Hudson Bay to Northern Newfoundland), NWA=Northwest Atlantic.

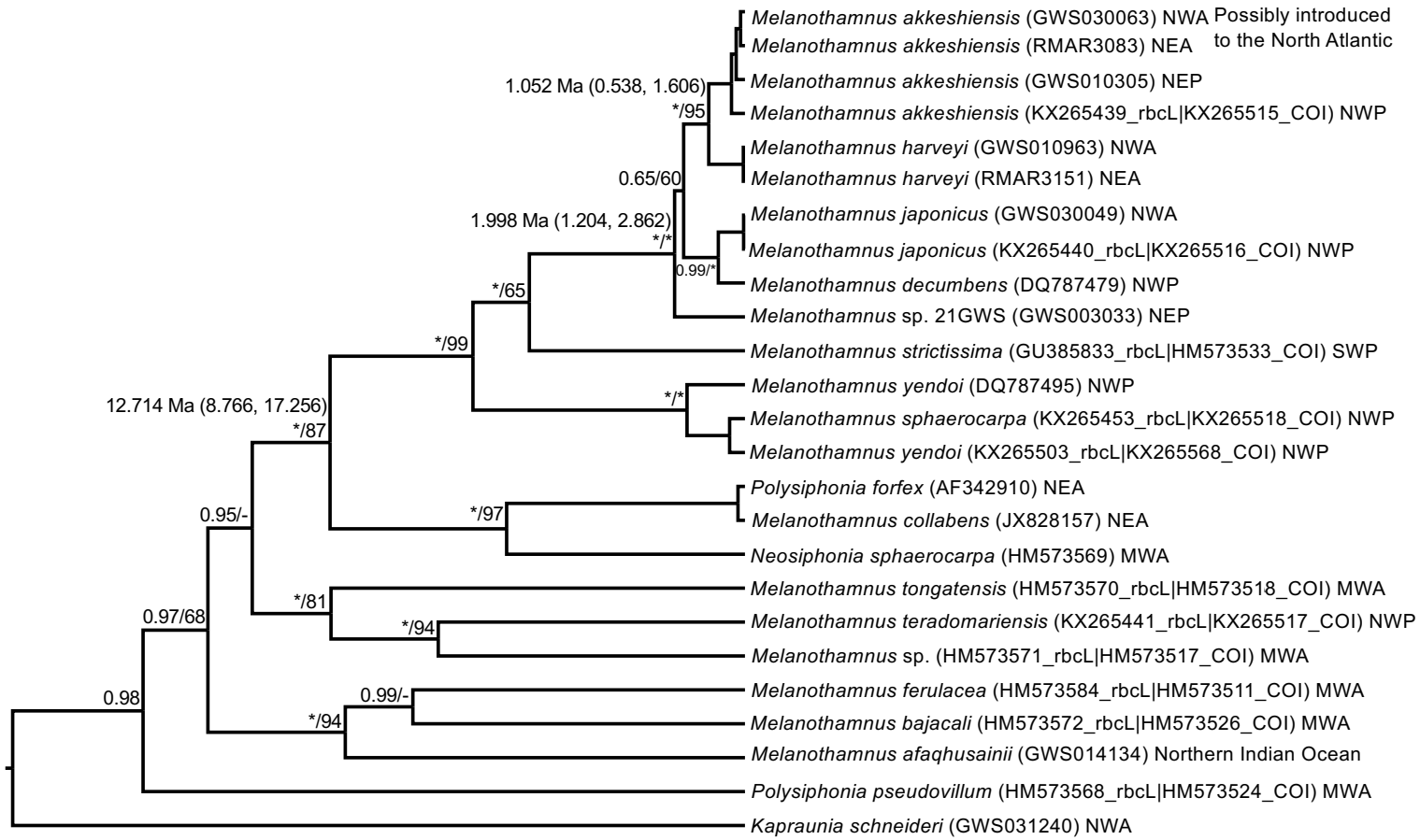

Fig. C10. *Melanothamnus* BEAST tree based on COI-5P and *rcb*L markers. Posterior probability values and bootstrap values are indicated, respectively; values of 1.0 or 100 are indicated with an asterisk, while bootstrap values less than 50 are indicated with a negative symbol. Divergence time estimates are given in millions of year (Ma) with 95% highest posterior density estimates in brackets. SWP=Southwest Pacific, NWP=Northwest Pacific, NEP=Northeast Pacific, NWA=Northwest Atlantic, MWA=Midwest Atlantic, NEA=Northeast Atlantic.

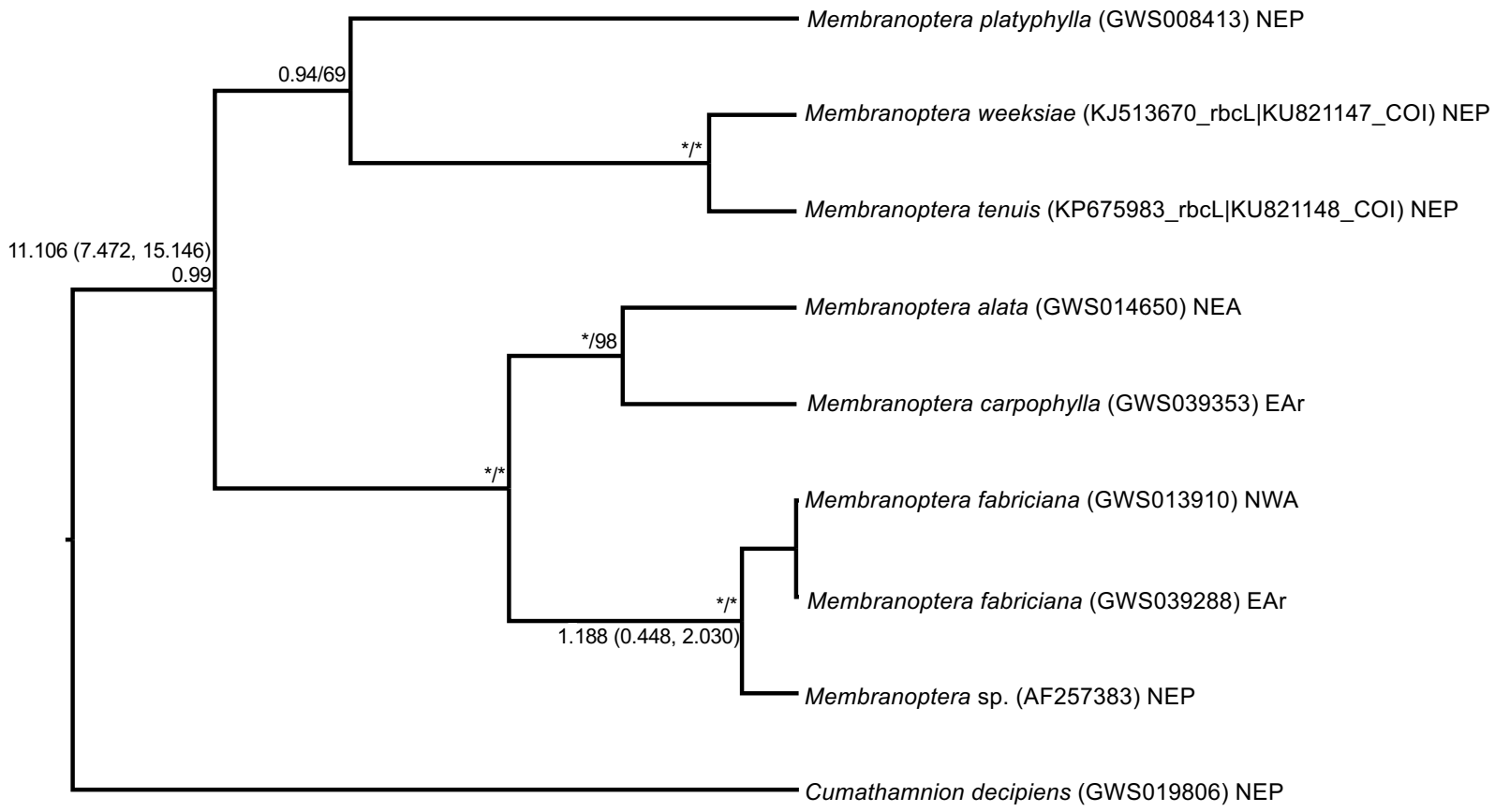

Fig. C11. *Membranoptera* BEAST tree based on COI-5P and *rcb*L markers. Posterior probability values and bootstrap values are indicated, respectively; values of 1.0 or 100 are indicated with an asterisk. Divergence time estimates are given in millions of year (Ma) with 95% highest posterior density estimates in brackets. NEP=Northeast Pacific, EAr=Eastern Artic (i.e. Hudson Bay to Northern Newfoundland), NWA=Northwest Atlantic, NEA=Northeast Atlantic.

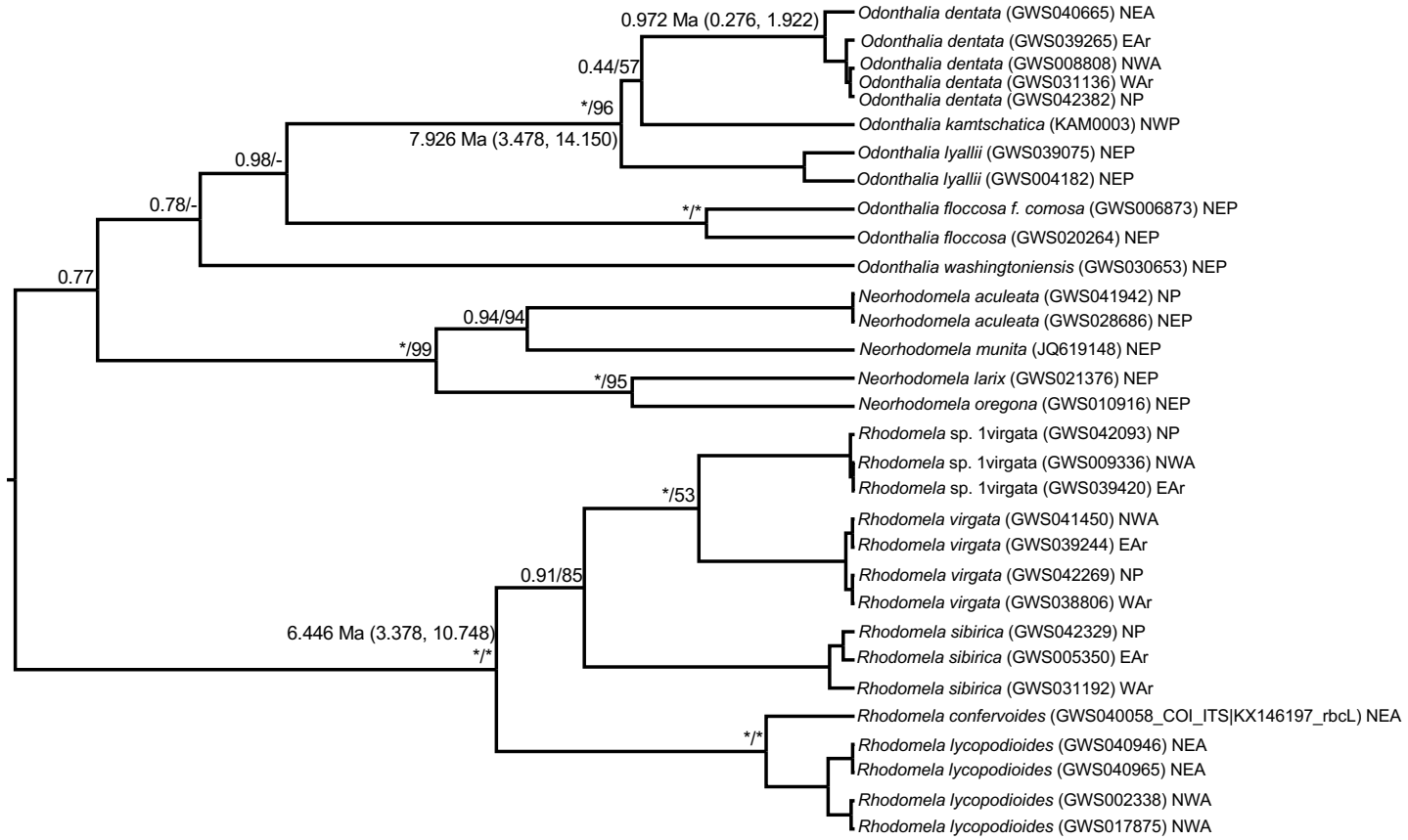

Fig. C12. *Odonthalia, Rhodomela and Neorhodomela* BEAST tree based on COI-5P, *rcb*L, and ITS markers. Posterior probability values and bootstrap values are indicated, respectively; values of 1.0 or 100 are indicated with an asterisk, while bootstrap values less than 50 are indicated with a negative symbol. Divergence time estimates are given in millions of year (Ma) with 95% highest posterior density estimates in brackets. NWP=Northwest Pacific, NP=North Pacific (i.e. Bering Sea), NEP=Northeast Pacific, WAr=Western Arctic (i.e. Beaufort Sea), EAr=Eastern Artic (i.e. Hudson Bay to Northern Newfoundland), NWA=Northwest Atlantic, NEA=Northeast Atlantic.

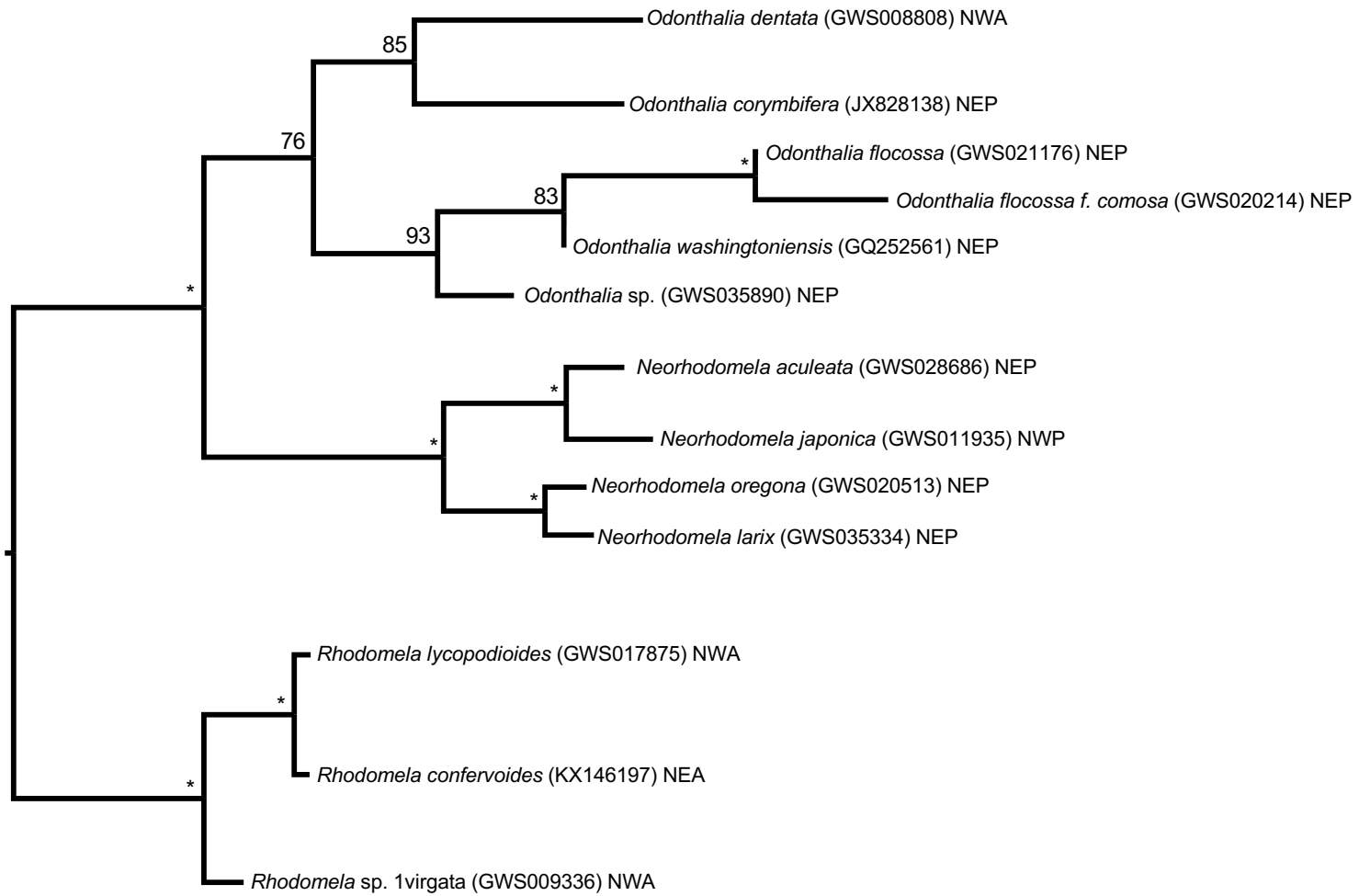

Fig. C13. *Odonthalia, Rhodomela and Neorhodomela* RAxML tree based on *rcb*L. Bootstrap values of 100 are indicated with an asterisk. NWP=Northwest Pacific, NEP=Northeast Pacific, NWA=Northwest Atlantic, NEA=Northeast Atlantic.

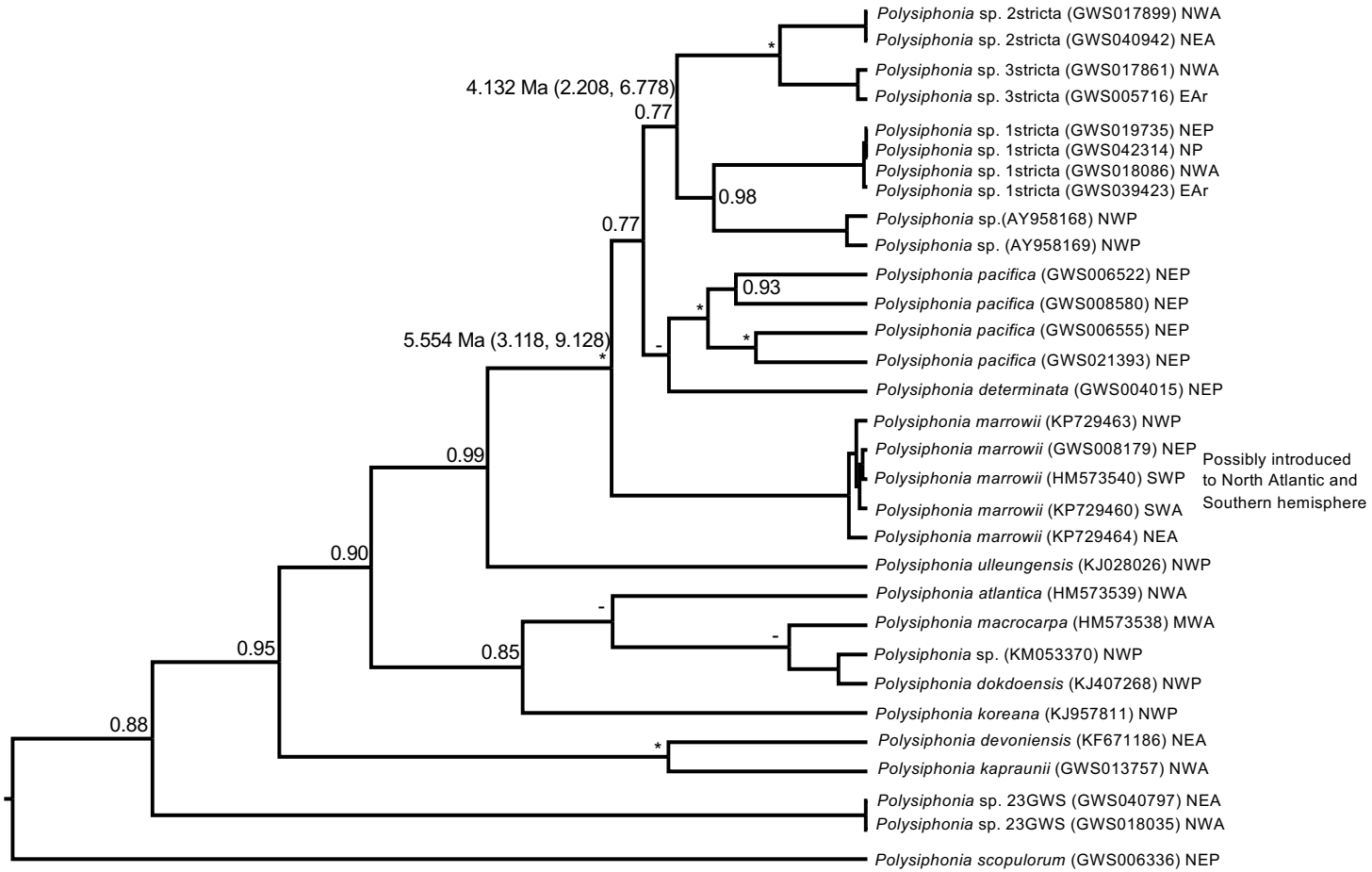

Fig. C14. *Polysiphonia* BEAST tree based on COI-5P and *rcb*L markers. Posterior probability values are indicated; values of 1.0 are indicated with an asterisk. Divergence time estimates are given in millions of year (Ma) with 95% highest posterior density estimates in brackets. The dashed line indicates COI-5P saturation. NWP=Northwest Pacific, NP=North Pacific (i.e. Bering Sea), NEP=Northeast Pacific, SWP=Southwest Pacific, EAr=Eastern Artic (i.e. Hudson Bay to Northern Newfoundland), NWA=Northwest Atlantic, MWA=Midwest Atlantic, SWA=Southwest Atlantic, NEA=Northeast Atlantic.

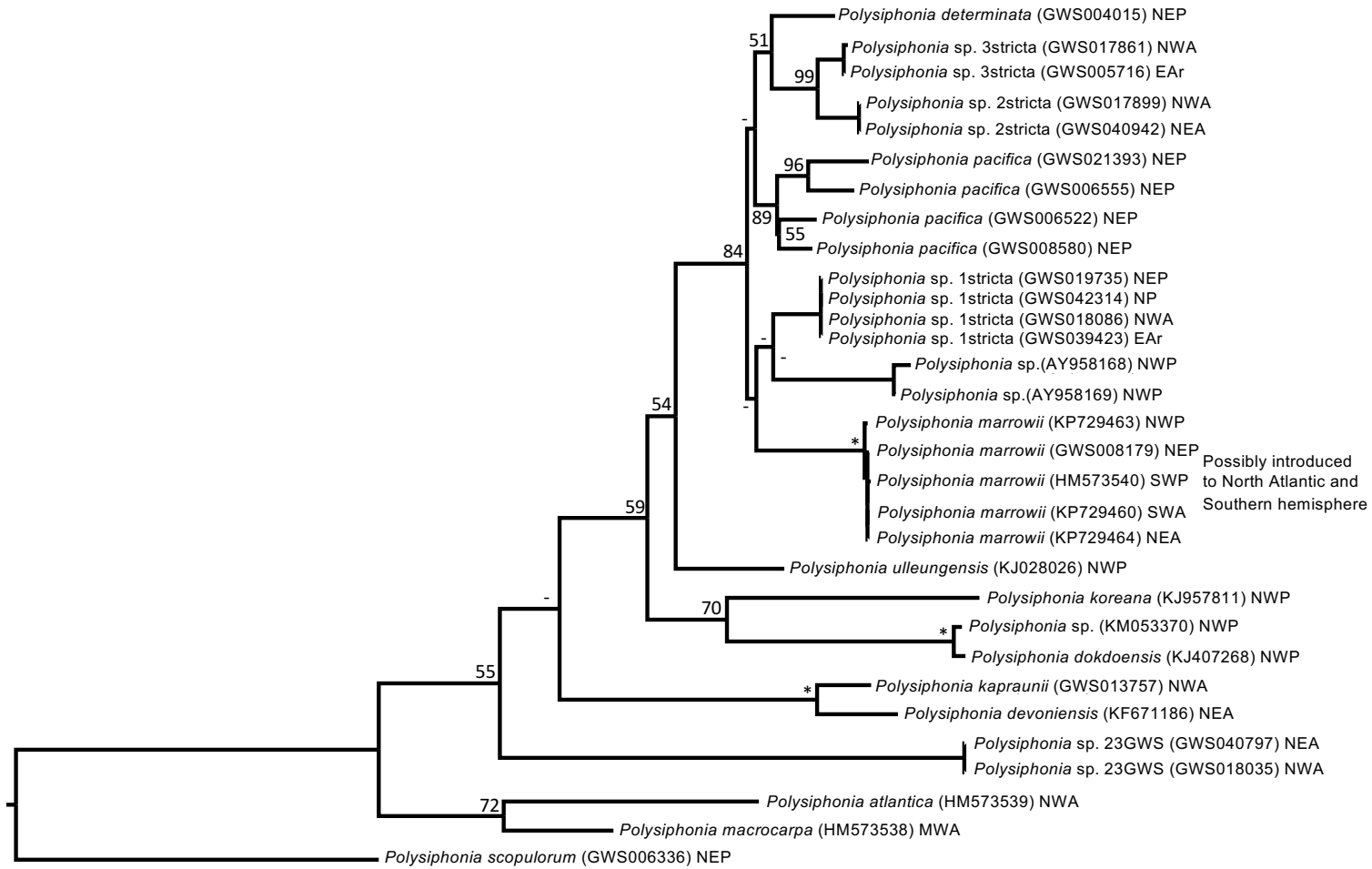

Fig. C15. *Polysiphonia* RAxML tree based on COI-5P and *rcb*L markers. Bootstrap values are indicated; values of 100 are indicated with an asterisk while values less than 50 are indicated with a negative symbol. NWP=Northwest Pacific, NP=North Pacific (i.e. Bering Sea), NEP=Northeast Pacific, SWP=Southwest Pacific, EAr=Eastern Artic (i.e. Hudson Bay to Northern Newfoundland), NWA=Northwest Atlantic, MWA=Midwest Atlantic, SWA=Southwest Atlantic, NEA=Northeast Atlantic.

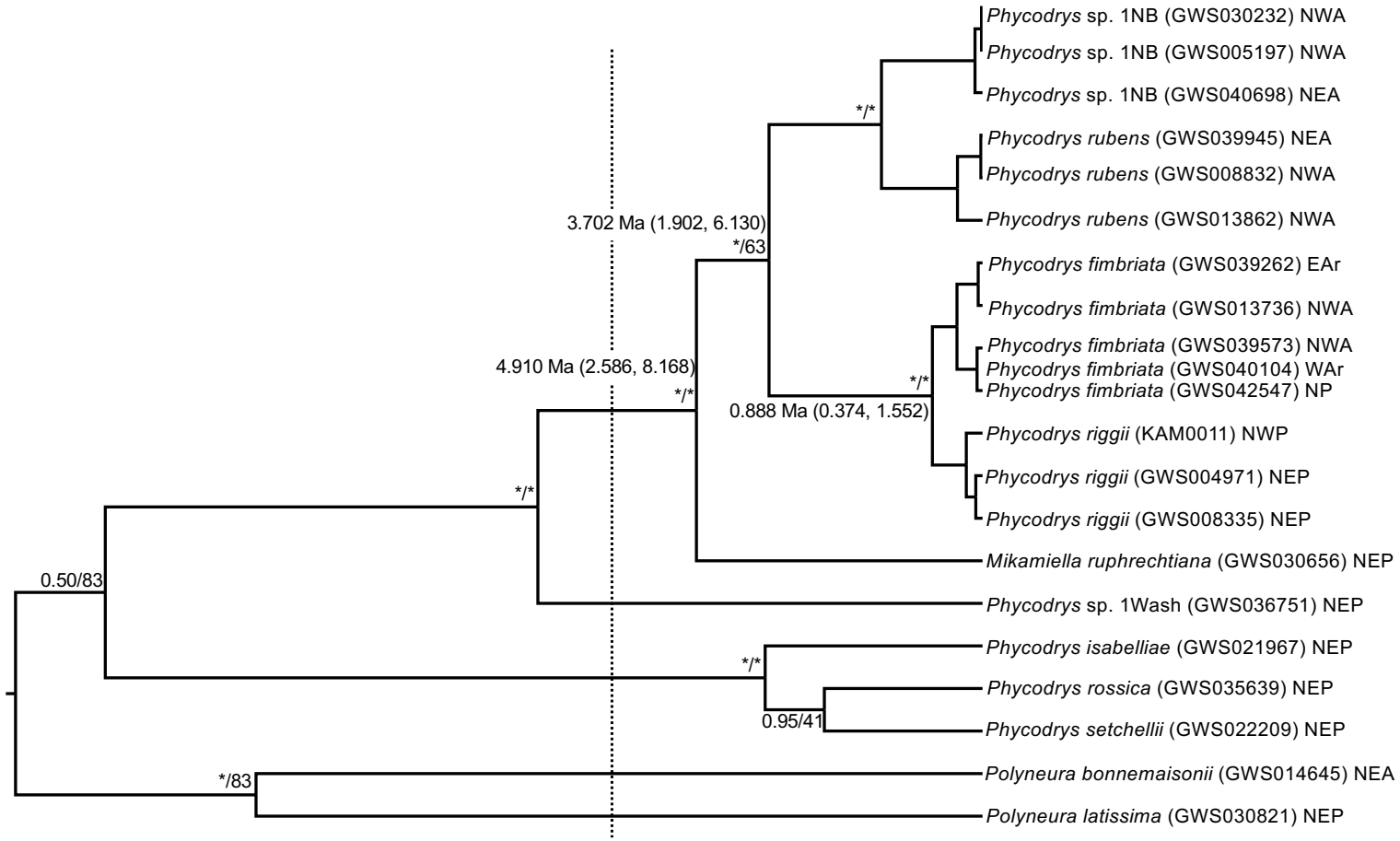

Fig. C16. *Phycodrys* BEAST tree based on COI-5P, *rcb*L, and ITS markers. Posterior probability values and bootstrap values are indicated, respectively; values of 1.0 or 100 are indicated with an asterisk. Divergence time estimates are given in millions of year (Ma) with 95% highest posterior density estimates in brackets. The dashed line indicates COI-5P saturation. NWP=Northwest Pacific, NP=North Pacific (i.e. Bering Sea), NEP=Northeast Pacific, WAr=Western Arctic (i.e. Beaufort Sea), EAr=Eastern Artic (i.e. Hudson Bay to Northern Newfoundland), NWA=Northwest Atlantic, NEA=Northeast Atlantic.

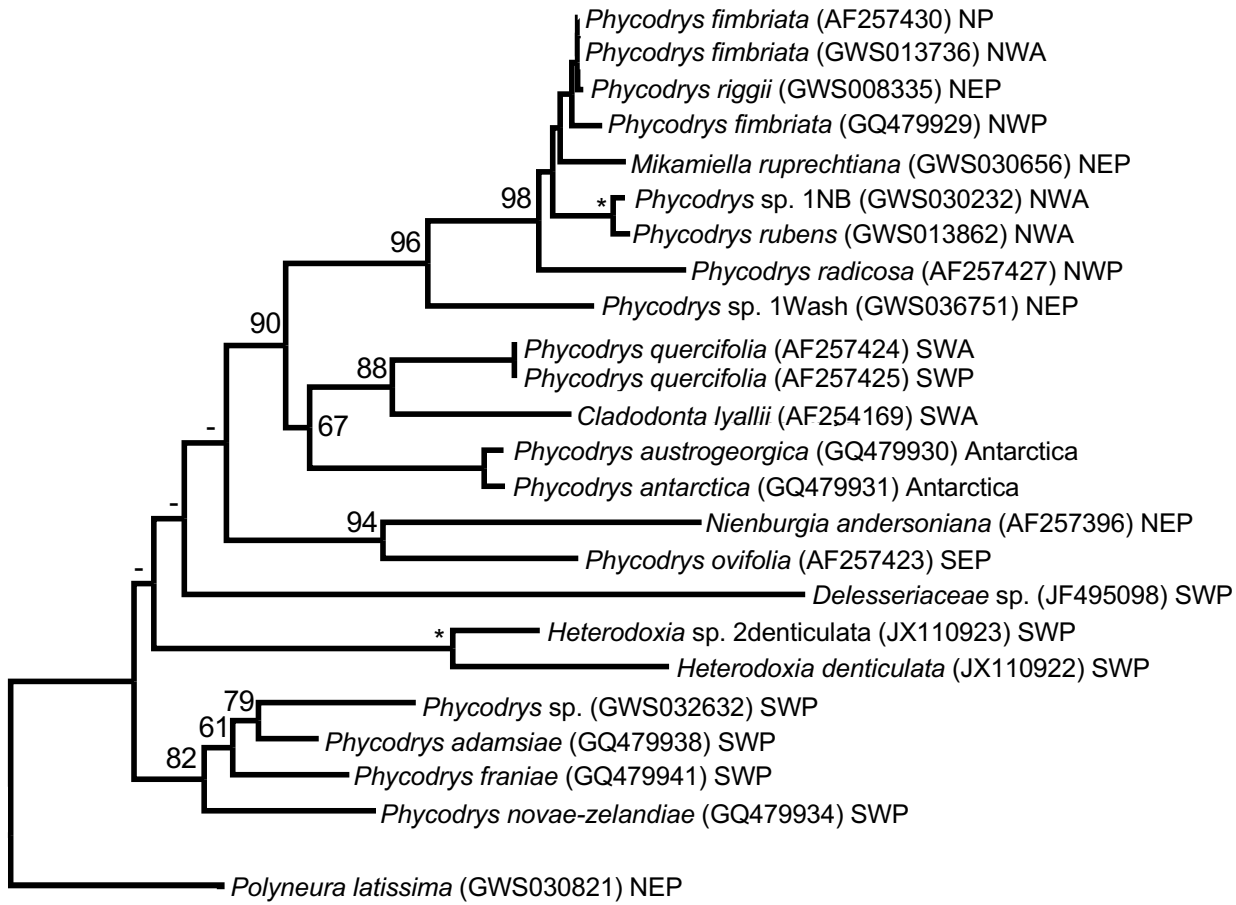

Fig. C17. *Phycodrys* RAxML tree based *rcb*L. Bootstrap values of 100 are indicated with an asterisk, values less than 50 are indicated by a negative symbol. NWP=Northwest Pacific, NP=North Pacific (i.e. Bering Sea), NEP=Northeast Pacific, SWP=Southwest Pacific, SEP=Southeast Pacific, NWA=Northwest Atlantic, SWA=Southwest Atlantic.

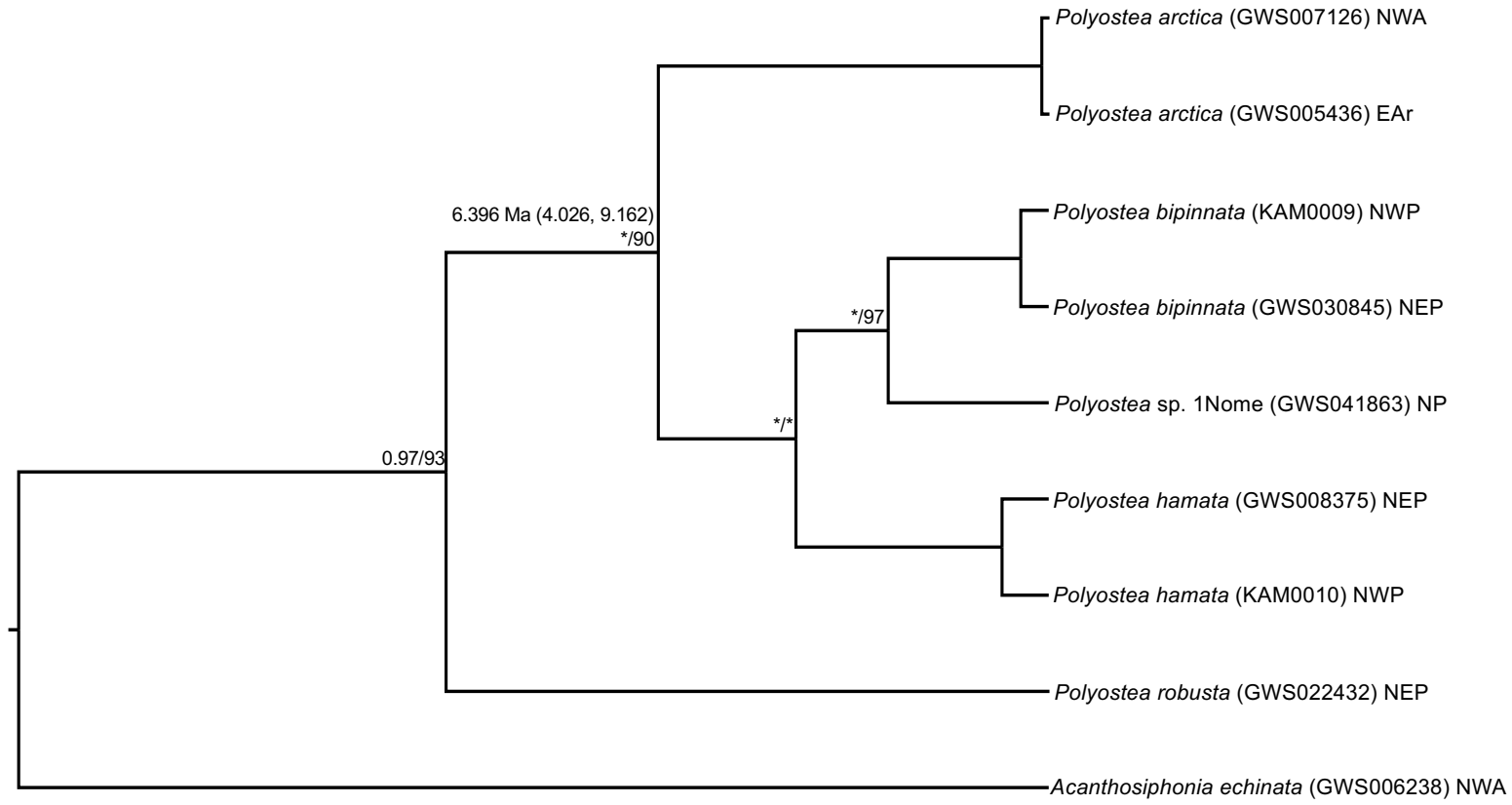

Fig. C18. *Polyostea* BEAST tree based on COI-5P and *rcb*L markers. Posterior probability values and bootstrap values are indicated, respectively; values of 1.0 or 100 are indicated with an asterisk. Divergence time estimates are given in millions of year (Ma) with 95% highest posterior density estimates in brackets. NWP=Northwest Pacific, NP=North Pacific (i.e. Bering Sea), NEP=Northeast Pacific, EAr=Eastern Artic (i.e. Hudson Bay to Northern Newfoundland), NWA=Northwest Atlantic.

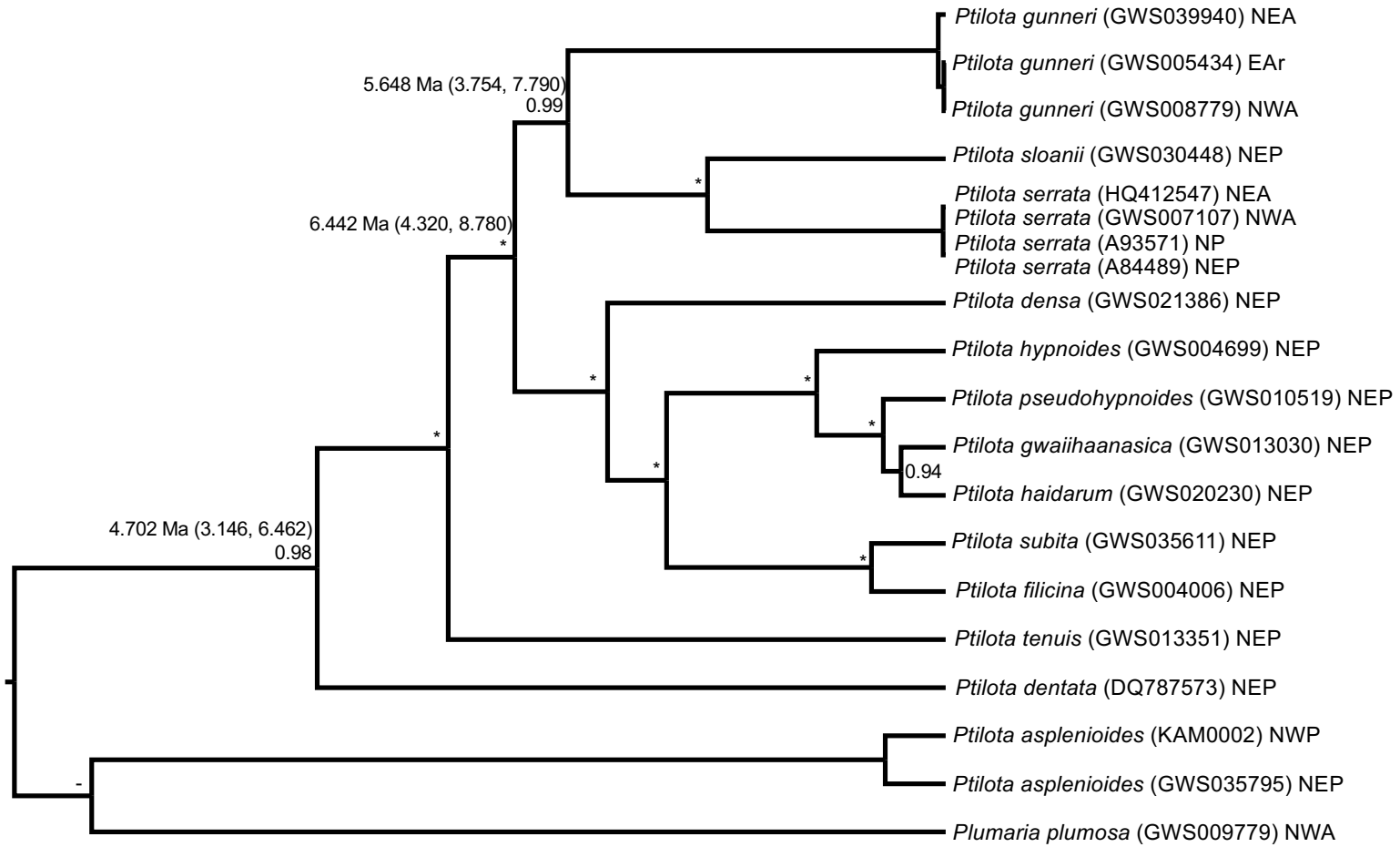

Fig. C19. *Ptilota* BEAST tree based on COI-5P and *rcb*L markers. Posterior probability values are indicated; values of 1.0 are indicated with an asterisk. Divergence time estimates are given in millions of year (Ma) with 95% highest posterior density estimates in brackets. NWP=Northwest Pacific, NP=North Pacific (i.e. Bering Sea), NEP=Northeast Pacific, EAr=Eastern Artic (i.e. Hudson Bay to Northern Newfoundland), NWA=Northwest Atlantic, NEA=Northeast Atlantic.

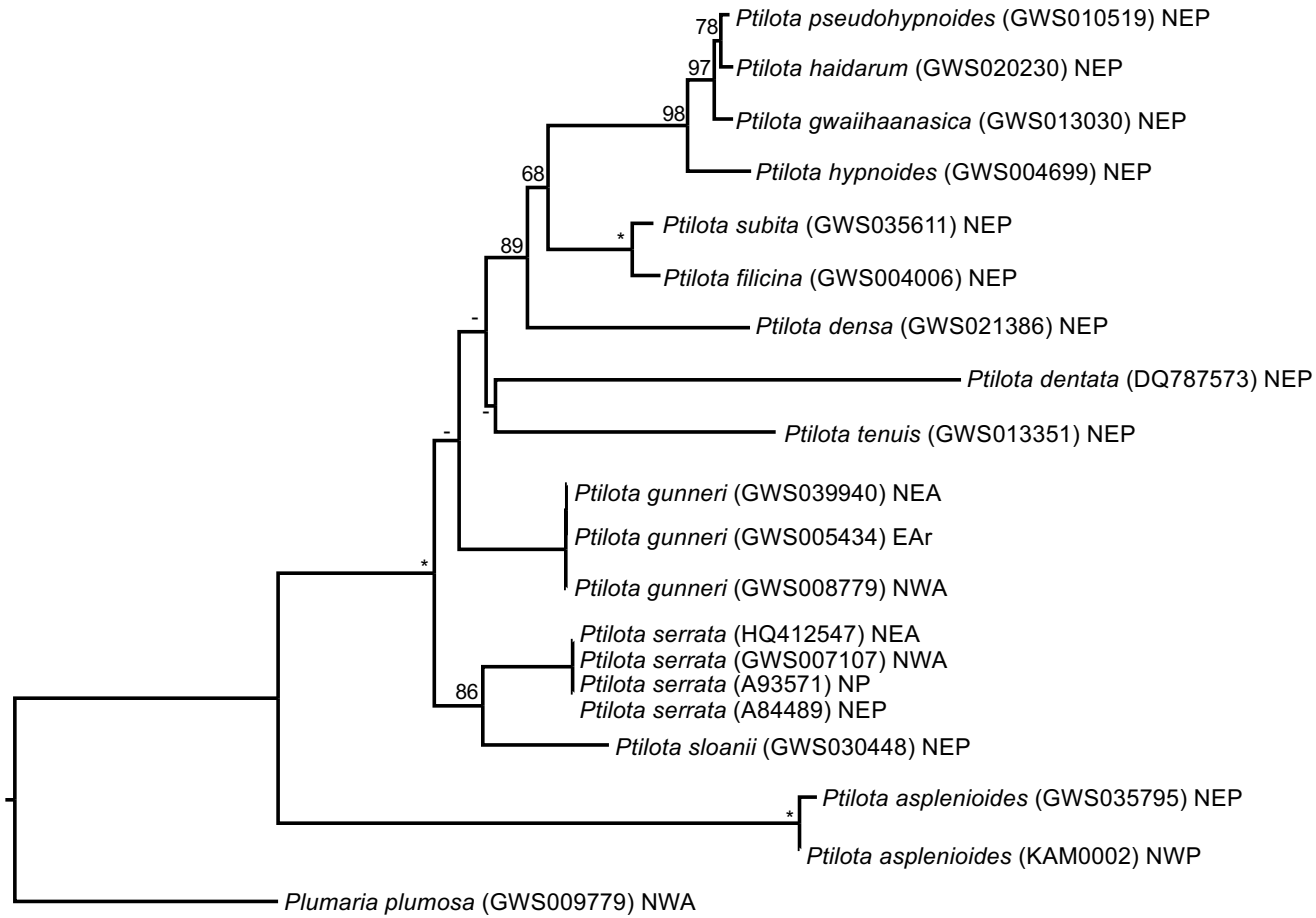

Fig. C20. *Ptilota* RAxML tree based on COI-5P and *rcb*L markers. Bootstrap values are indicated; values of 100 are indicated with an asterisk, values less than 50 are indicated with a negative symbol. NWP=Northwest Pacific, NP=North Pacific (i.e. Bering Sea), NEP=Northeast Pacific, EAr=Eastern Artic (i.e. Hudson Bay to Northern Newfoundland), NWA=Northwest Atlantic, NEA=Northeast Atlantic.

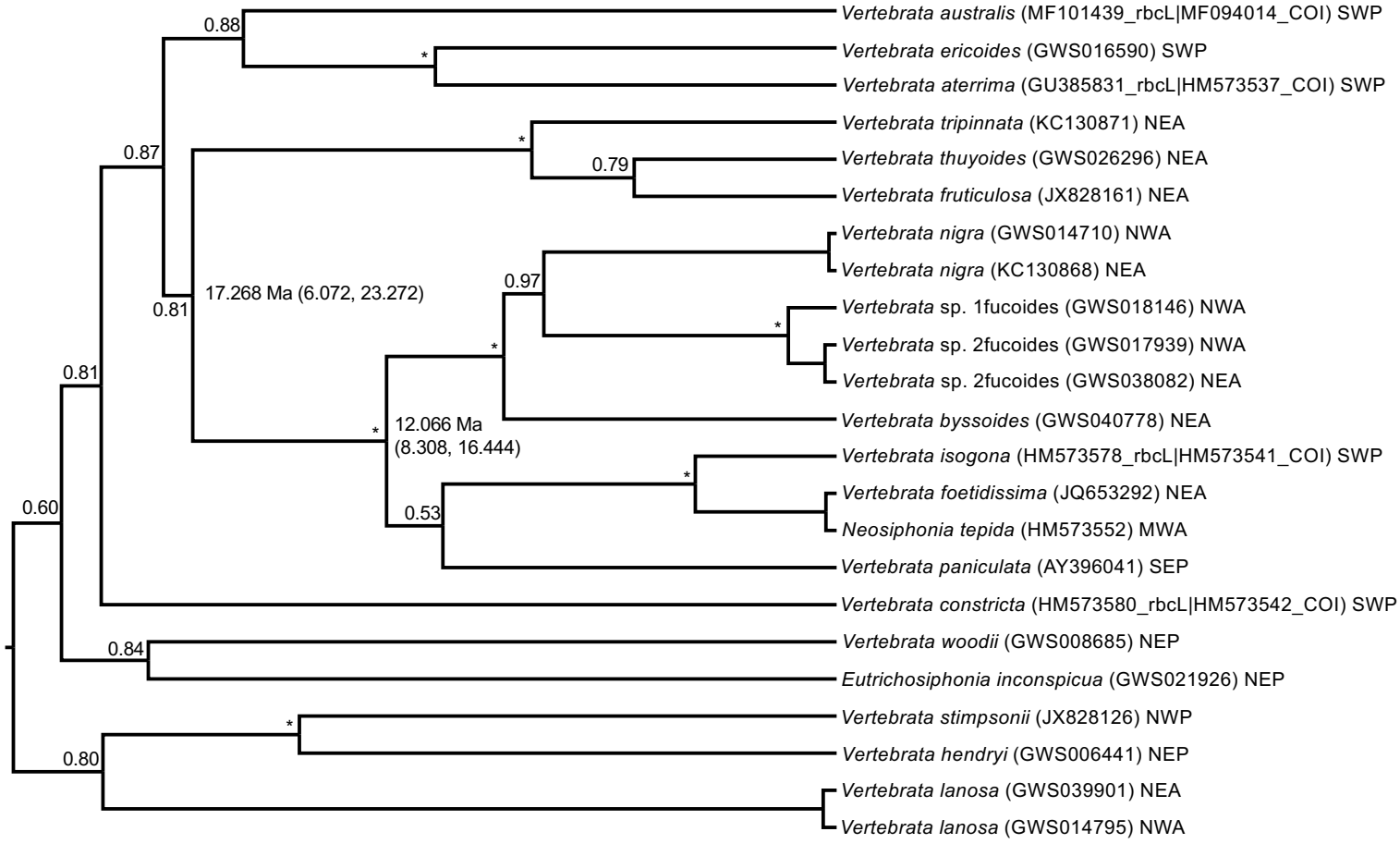

Fig. C21. *Vertebrata* BEAST tree based on COI-5P and *rcb*L markers. Posterior probability values are indicated; values of 1.0 are indicated with an asterisk. Divergence time estimates are given in millions of year (Ma) with 95% highest posterior density estimates in brackets. NWP=Northwest Pacific, NEP=Northeast Pacific, SWP=Southwest Pacific, SEP=Southeast Pacific, NWA=Northwest Atlantic, MWA=Midwest Atlantic, NEA=Northeast Atlantic.

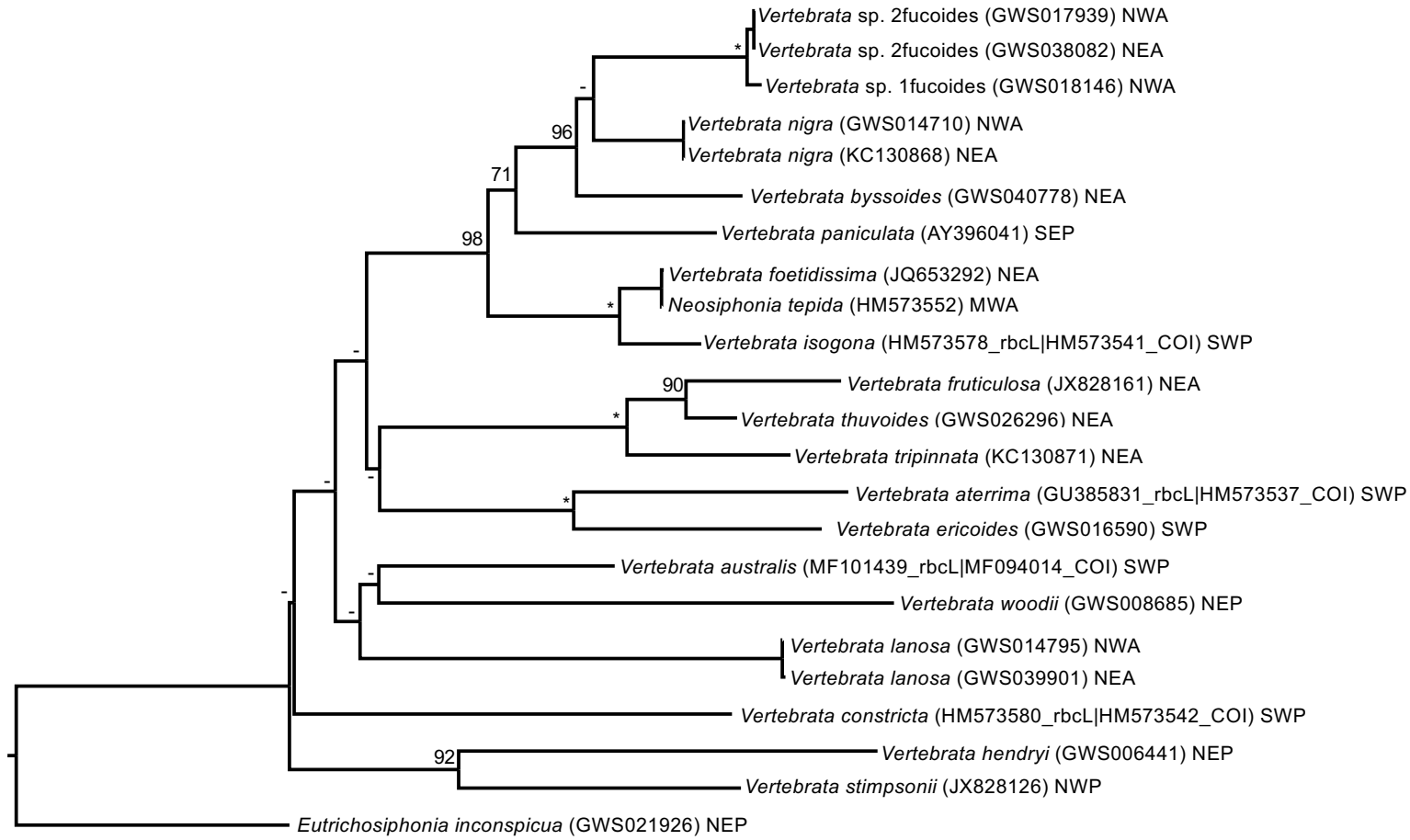

Fig. C22. *Vertebrata* RAxML tree based on COI-5P and *rcb*L markers. Bootstrap values are indicated; values of 100 are indicated with an asterisk, values less than 50 are indicated with a negative symbol. NWP=Northwest Pacific, NEP=Northeast Pacific, SWP=Southwest Pacific, SEP=Southeast Pacific, NWA=Northwest Atlantic, MWA=Midwest Atlantic, NEA=Northeast Atlantic.

Appendix D Supplementary Material for Chapter 3

Table D1. Specimen information for sequences mined from GenBank.

Species	Specimen ID	GenBank #	Date sampled	Country	Locale	Lat.	Long.
Ectocarpus fasciculatus	BLZ11-20	LM995037.1	21-Mar-2011	France	Roscoff	48.726199	-3.985325
Ectocarpus fasciculatus	BLZ11-110	LM995111.1	01-Sep-2011	France	Roscoff	48.726199	-3.985325
Ectocarpus fasciculatus	BLZ11-205	LM995191.1	01-Sep-2011	France	Roscoff	48.726199	-3.985325
Ectocarpus fasciculatus	BLZ11-227	LM995209.1	01-Sep-2011	France	Roscoff	48.726199	-3.985325
Ectocarpus fasciculatus	BLZ12-39	LM995261.1	08-Mar-2012	France	Roscoff	48.726199	-3.985325
Ectocarpus fasciculatus	BLZ12-03	LM995229.1	08-Mar-2012	France	Roscoff	48.726199	-3.985325
Ectocarpus fasciculatus	BLZ11-164	LM995154.1	01-Sep-2011	France	Roscoff	48.726199	-3.985325
Ectocarpus fasciculatus	BLZ11-192	LM995179.1	01-Sep-2011	France	Roscoff	48.726199	-3.985325
Ectocarpus fasciculatus	BLZ11-150	LM995142.1	01-Sep-2011	France	Roscoff	48.726199	-3.985325
Ectocarpus fasciculatus	BLZ11-218	LM995200.1	01-Sep-2011	France	Roscoff	48.726199	-3.985325
Ectocarpus fasciculatus	Ec736	LM995022.1	21-Aug-2009	France	Roscoff	48.726199	-3.985325
Ectocarpus fasciculatus	BLZ11-195	LM995182.1	01-Sep-2011	France	Roscoff	48.726199	-3.985325
Ectocarpus fasciculatus	BLZ11-222	LM995204.1	01-Sep-2011	France	Roscoff	48.726199	-3.985325
Ectocarpus fasciculatus	BLZ11-87	LM995093.1	01-Sep-2011	France	Roscoff	48.726199	-3.985325
Ectocarpus fasciculatus	BLZ12-01	LM995227.1	08-Mar-2012	France	Roscoff	48.726199	-3.985325
Ectocarpus fasciculatus	BLZ12-42	LM995264.1	08-Mar-2012	France	Roscoff	48.726199	-3.985325
Ectocarpus fasciculatus	BLZ11-02	LM995023.1	21-Mar-2011	France	Roscoff	48.726199	-3.985325
Ectocarpus fasciculatus	BLZ11-19	LM995036.1	21-Mar-2011	France	Roscoff	48.726199	-3.985325
Ectocarpus fasciculatus	BLZ11-66	LM995074.1	01-Sep-2011	France	Roscoff	48.726199	-3.985325
Ectocarpus fasciculatus	BLZ11-75	LM995083.1	01-Sep-2011	France	Roscoff	48.726199	-3.985325
Ectocarpus fasciculatus	BLZ12-17	LM995242.1	08-Mar-2012	France	Roscoff	48.726199	-3.985325
Ectocarpus fasciculatus	FR0524	EU681406.1	**-Mar-2007	France	Roscoff	48.726199	-3.985325

Ectocarpus fasciculatus	BLZ11-08	LM995027.1	21-Mar-2011	France	Roscoff	48.726199	-3.985325
Ectocarpus fasciculatus	BLZ11-18	LM995035.1	21-Mar-2011	France	Roscoff	48.726199	-3.985325
Ectocarpus fasciculatus	BLZ11-21	LM995038.1	21-Mar-2011	France	Roscoff	48.726199	-3.985325
Ectocarpus fasciculatus	BLZ11-23	LM995039.1	21-Mar-2011	France	Roscoff	48.726199	-3.985325
Ectocarpus fasciculatus	BLZ11-28	LM995042.1	21-Mar-2011	France	Roscoff	48.726199	-3.985325
Ectocarpus fasciculatus	BLZ11-141	LM995134.1	01-Sep-2011	France	Roscoff	48.726199	-3.985325
Ectocarpus fasciculatus	BLZ12-10	LM995235.1	08-Mar-2012	France	Roscoff	48.726199	-3.985325
Mastocarpus stellatus	JBLR7	DQ191350	23-Apr-2005	England	Sidmouth, Devon	50.6787	-3.238
Mastocarpus stellatus	43SM2	DQ442903	28-oct-2003	England	Sidmouth, Devon	50.6787	-3.238
Mastocarpus stellatus	42SM2	DQ442907	28-oct-2003	England	Sidmouth, Devon	50.6787	-3.238
Mastocarpus stellatus	180SC	DQ442906	13-jul-2004	Scotland	Smoo Cave, Dunrness	58.5634	-4.7200
Mastocarpus stellatus	BRE32	DQ442899	27-oct-2003	England	Combe Martin, Devon	51.1994	-4.024
Mastocarpus stellatus	BRE33	DQ442900	27-oct-2003	England	Combe Martin, Devon	51.1994	-4.024
Mastocarpus stellatus	BRE85	DQ442904	27-oct-2003	England	Combe Martin, Devon	51.1994	-4.024
Mastocarpus stellatus	BRE86	DQ442905	27-oct-2003	England	Combe Martin, Devon	51.1994	-4.024
Pylaiella sp. 2littoralis	KM027317	KM027317	15-May-2010	France		48.7276	-3.9877
Pylaiella sp. 2littoralis	KM027318	KM027318	20-Apr-2011	France		47.8532	-3.9176
Pylaiella sp. 2littoralis	KM027319	KM027319	30-Apr-2009	France		48.7276	-3.9877
Pylaiella sp. 2littoralis	KM027320	KM027320	20-Apr-2011	France		47.8532	-3.9176

Pylaiella sp. 2littoralis	KM027321	KM027321	30-Apr-2009	France	48.7276	-3.9877
Pylaiella sp. 2littoralis	KM027322	KM027322	22-Apr-2010	France	48.6265	-2.0433
Pylaiella sp. 2littoralis	KM027323	KM027323	30-Apr-2009	France	48.7276	-3.9877
Pylaiella sp. 2littoralis	KM027324	KM027324	22-Apr-2010	France	48.6265	-2.0433
Pylaiella sp. 2littoralis	KM027325	KM027325	15-May-2010	France	48.7276	-3.9877
Pylaiella sp. 2littoralis	KM027326	KM027326	30-Apr-2009	France	48.7276	-3.9877
Pylaiella sp. 2littoralis	KM027327	KM027327	30-Apr-2009	France	48.7276	-3.9877
Pylaiella sp. 2littoralis	KM027328	KM027328	15-May-2010	France	48.7276	-3.9877

Table D2. Amphi-Atlantic species of red and brown macro-algae not included in phylogeographic analyses. These species include those for which there was insufficient data (e.g. less than five specimens on *both* sides of the Atlantic), and species reported as introduced or suspected introduced species. If specimens from the west Atlantic side for a given species were *only* collected from the coasts of Rhode Island, Massachusetts, and Maine, *and* matched European haplotypes but were not listed as being introduced, we considered them as potentially introduced and excluded them from analyses (given high number of introductions in this area; Mathieson *et al.* 2008). Introduced species were also identified as per Thomsen *et al.* (2016) and Williams & Smith (2007).

Species	Number of specimens (West/East Atlantic)	Reason for exclusion
Acrothrix gracilis	12/1	Insufficient data
Ascophyllum nodosum	2/1	Insufficient data
Bonnemaisonia hamifera	-	Introduced
Chorda filum	-	Introduced
Chordaria flagelliformis	77/3	Insufficient data
Coccotylus truncatus	77/1	Insufficient data
Dasysiphonia japonica	-	Introduced
Desmarestia sp. 1aculeatea	29/1	Insufficient data
Dumontia contorta	-	Possibly introduced
Ectocarpus sp. 4GWS	13/1	Insufficient data
Elachista fucicola	27/1	Insufficient data
Eudesme virescens	17/2	Insufficient data
Erythrodermis traillii	11/3	Insufficient data
Frederiqia deveauniensis	31/1	Introduced
Fucus distichus	-	Introduced
Fucus spiralis	36/4	Insufficient data
Gloiosiphonia capillaris	1/2	Insufficient data
Halospora globosa	6/1	Insufficient data
Halosiphon tomuntosus	15/1	Insufficient data
Hildenbrandia sp. 4GWS	4/1	Insufficient data

Leathesia marina	20/2	Insufficient data
Lomentaria clavellosa	-	Introduced
Lomentaria orcadensis	-	Introduced
Myrionema stragulans	2/1	Insufficient data
Planosiphon zosterifolius	8/1	Insufficient data
Polysiphonia sp. 23GWS	3/6	Insufficient data/possibly introduced
Polysiphonia elongata	2/11	Possibly introduced
Polysiphonia sp. 2fucoides	22/1	Insufficient data
Porphyra umbilicalis	59/2	Insufficient data
Pterothamnion plumula	1/4	Insufficient data/possibly introduced
Ptilota gunneri	3/39	Insufficient data
Punctaria latifolia	5/1	Insufficient data
Pylaiella sp. 1littoralis	20/4	Insufficient data
Ralfsia sp. 6GWS	3/3	Insufficient data
Scytosiphon sp._AtlanticComp	6/3	Insufficient data
Scytosiphon promiscuus	55/1	Insufficient data
Sphacelaria sp. 1GWS	1/2	Possibly introduced
Sphacelaria sp.	4/5	Insufficient data
Spongonema tomentosum	3/3	Insufficient data
Striaria attenuata	2/2	Introduced
Tilopteridalean sp. 1GWS	4/1	Insufficient data
Titanoderma sp.	4/1	Insufficient data
Vertebrata lanosa	11/4	Insufficient data
Wildemania amplissima	49/2	Insufficient data

References

Mathieson AC, Pederson JR, Neefus CD, Dawes CJ, Bray TL (2008) Multiple assessments of introduced seaweeds in the Northwest Atlantic. *ICES Journal of Marine Science*, **65**, 730–741.

Thomsen M, Wernberg T, South P, Schiel D (2016) Non-native seaweeds drive changes in marine coastal communities around the world. In: Hu ZM, Fraser C (eds) *Seaweed phylogeography: adaptation and evolution of seaweeds under environmental change*. Springer, Dordrecht, p. 147–186.

Williams SL, Smith JE (2007) A Global Review of the Distribution, Taxonomy, and Impacts of Introduced Seaweeds. A*nnual Review of Ecology and Systematics*, **38**, 327-359

Table D3. Isolation time estimates calculated in IMa2 for fast, medium, and slow COI-5P clocks in red and brown macrolgae. Species with isolation time estimates predating the LGM (20 ka) are bolded. HPD=highest posterior density.

Species	*n*	Fast clock isolation time (ka; 95% HPD)	Med. clock isolation time (ka; 95% HPD)	Slow clock isolation time (ka; 95% HPD)
Ahnfeltia plicata (Fig. D1)	120/21	15.214 (1.950, 47.844)	24.432 (3.676, 80.216)	49.49 (9.694, 177.04)
Alaria esculenta (Fig. D14)	33/21	107.552 (11.950, 824.570)	164.698 (15.538, 1190.180)	195.028 (11.472, 1334.608)
***Alaria esculenta* (without Arctic populations)**	**23/21**	**603.728 (93.212, 1670.650)**	**706.650 (124.922, 2183.344)**	**865.010 (135.372, 2640.918)**
***Ceramium virgatum* (Fig. D2)**	**165/5**	**57.346 (30.284, 92.140)**	**100.540 (50.810, 154.594)**	**214.646 (118.686, 366.162)**
***Ceramium virgatum* (without Rhode Island population)**	**142/5**	**71.520 (36.726, 126.932)**	**117.838 (55.136, 243.244)**	**290.404 (108.586, 659.090)**
Chondrus crispus (Fig. D3)	53/48	10.660 (1.280, 29.992)	21.120 (2.136, 53.868)	46.266 (3.902, 118.730)
Coccotylus brodiei (Fig. 3.1B)	71/31	7.378 (0.388, 56.310)	10.594 (0.648, 87.568)	35.026 (1.432, 195.432)
***Cystoclonium purpureum* (Fig. D4)**	**39/14**	**210.696 (53.480, 574.098)**	**288.648 (74.594, 913.514)**	**952.020 (194.444, 2.310.606)**
***Dilsea socialis/carnosa* (Fig. D5)**	**60/18**	**225.890 (36.894, 829.126)**	**515.676 (83.244, 1322.162)**	**1606.598 (180.204, 3164.974)**
***Ectocarpus fasciculatus* (Fig. D15)**	**16/35**	**241.396 (77.916, 480.402)**	**328.776 (92.604, 634.556)**	**408.414 (123.900, 751.052)**

***Euthora cristata (*Fig. D6)**	**67/29**	174.614 (7.088, 427.190)	**282.162 (44.324, 742.702)**	**547.980 (42.930, 1775.252)**
Laminaria digitata (Fig. D16)	52/13	12.902 (0, 74.092)	19.266 (0, 113.736)	20.650 (0, 144.550)
Mastocarpus stellatus (Fig. D7)	19/26	17.734 (0.526, 96.200)	22.000 (1.466, 168.672)	68.336 (2.068, 384.138)
***Odonthalia dentata* (Fig. 3.1A)**	**53/26**	**316.238 (70.360, 865.206)**	**662.918 (125.838, 1443.892)**	**1367.424 (314.394, 3329.546)**
***Palmaria palmata* (Fig. D8)**	**58/19**	**516.690 (139.778, 1017.386)**	**1039.488 (259.002, 1736.354)**	**1968.622 (568.894, 4121.418)**
Phycodrys sp. 1NB (Fig. D9)	17/22	29.320 (2.524, 178.834)	44.432 (4.864, 305.838)	107.360 (11.422, 711.928)
***Phycodrys rubens* (Fig. D10)**	**9/45**	**382.088 (79.252, 807.346)**	**583.870 (121.506, 1284.946)**	**1507.576 (305.556, 2931.818)**
Polyides rotundus (Fig. D11)	29/10	13.582 (2.952, 45.866)	25.964 (6.244, 76.578)	71.796 (11.580, 182.964)
Polysiphonia sp. 2stricta (Fig. D12)	23/10	4.032 (0, 141.230)	6.966 (0, 165.880)	16.084 (0, 398.780)
***Pylaiella* sp. 2littoralis (Fig. D17)**	**8/14**	**493.538 (190.922, 971.422)**	**654.688 (248.438, 1257.812)**	**722.754 (309.752, 1518.164)**
Rhodomela lycopodioides (Fig. D13)	97/12	14.498 (2.256, 231.636)	24.204 (4.840, 346.924)	46.718 (3.788, 824.494)
***Rhodomela lycopodioides* (without Arctic sequence)**	**96/12**	**338.274 (89.562, 873.068)**	**463.640 (143.072, 1393.072)**	**1381.314 (366.162, 3416.666)**
***Saccharina latissima* (Fig. D18)**	**132/21**	**1665.770 (310.018, 2574.942)**	**1575.092 (442.890, 3486.514)**	**1910.134 (468.628, 3963.672)**
***Saccharina latissima* (without Arctic populations)**	**97/21**	**1170.594 (315.062, 2779.200)**	**1415.252 (449.550, 3439.894)**	**1686.424 (455.066, 4103.250)**

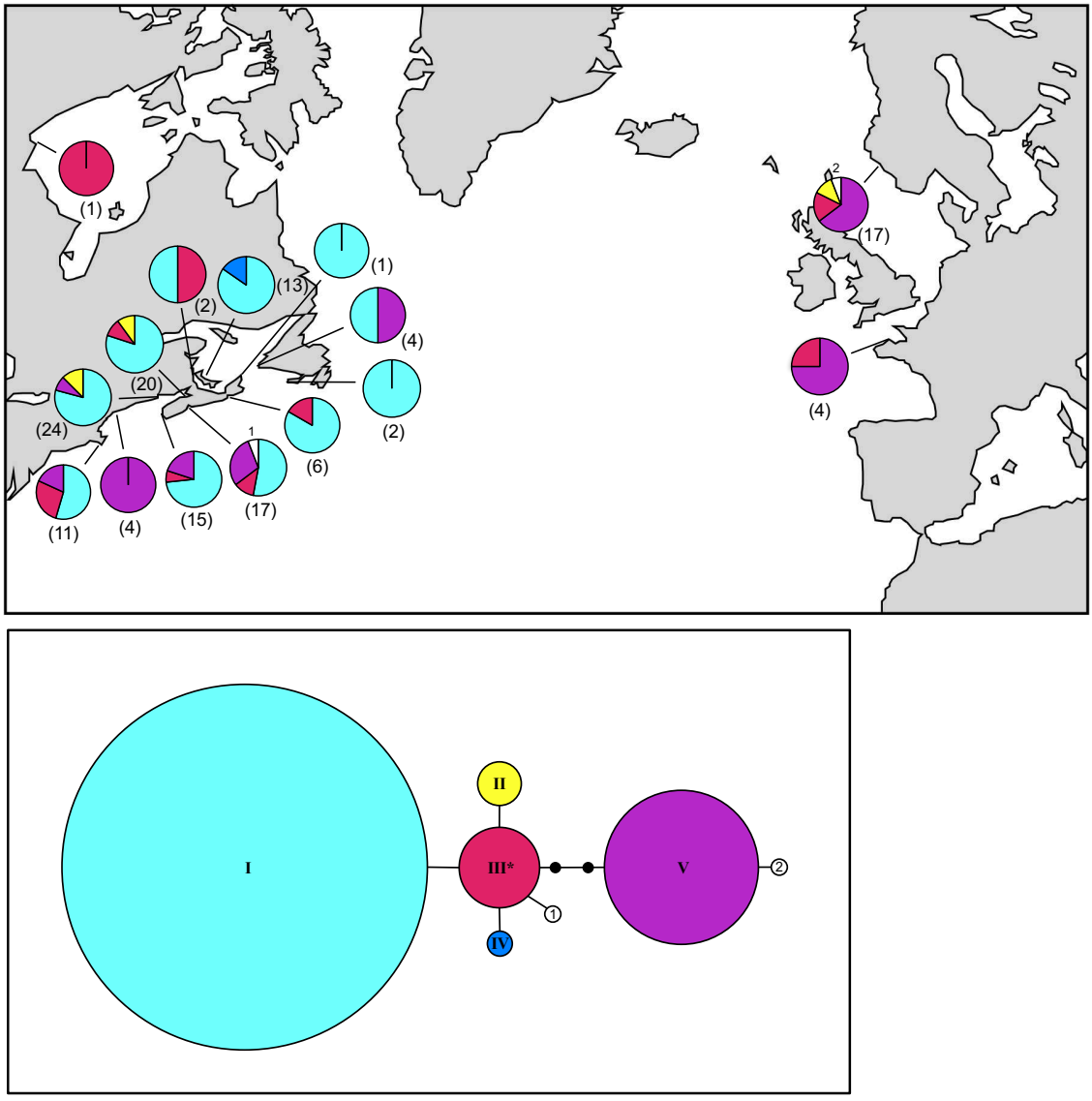

Figure D1. ***Ahnfeltia plicata*** **haplotype map and network based on COI-5P data. In the map, numbers in parentheses refer to sample sizes from given locales, whereas numbers adjacent to white portions of pie charts refer to a haplotype sampled only once in the accompanying network. In the haplotype network, roman numerals refer to repeatedly sampled haplotypes, whereas numbered haplotypes in white reference back to the map. An asterisk indicates a putative ancestral haplotype based on TCS analyses. Black circles indicate hypothesized (e.g. unsampled) haplotypes between clades. The size of each circle is proportional to the sampling frequency of a given haplotype.**

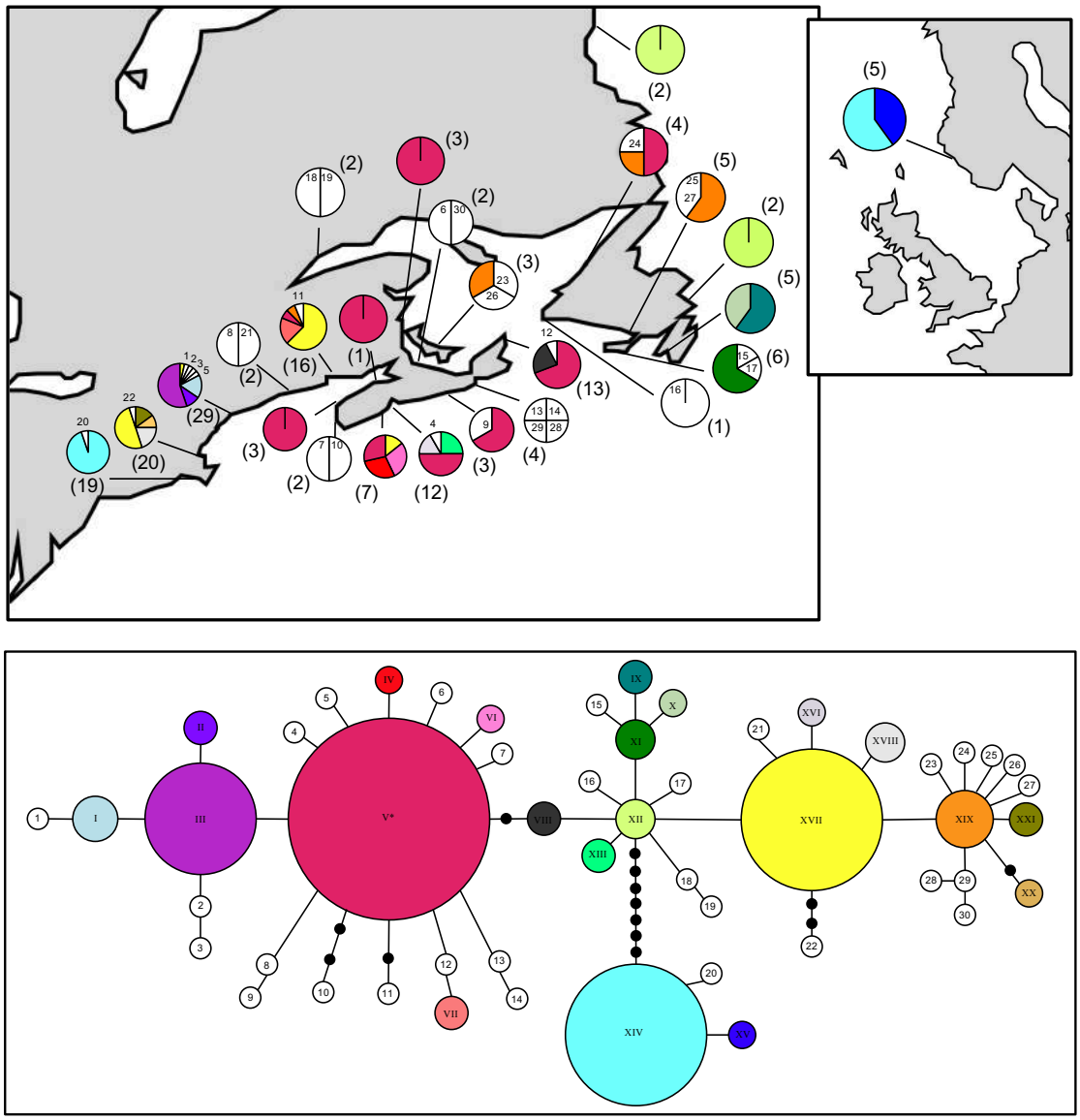

Figure D2. *Ceramium virgatum* haplotype map and network based on COI-5P data. In the map, numbers in parentheses refer to sample sizes from given locales, whereas numbers adjacent to white portions of pie charts refer to a haplotype sampled only once in the accompanying network. In the haplotype network, roman numerals refer to repeatedly sampled haplotypes, whereas numbered haplotypes in white reference back to the map. An asterisk indicates a putative ancestral haplotype based on TCS analyses. Black circles indicate hypothesized (e.g. unsampled) haplotypes between clades. The size of each circle is proportional to the sampling frequency of a given haplotype.

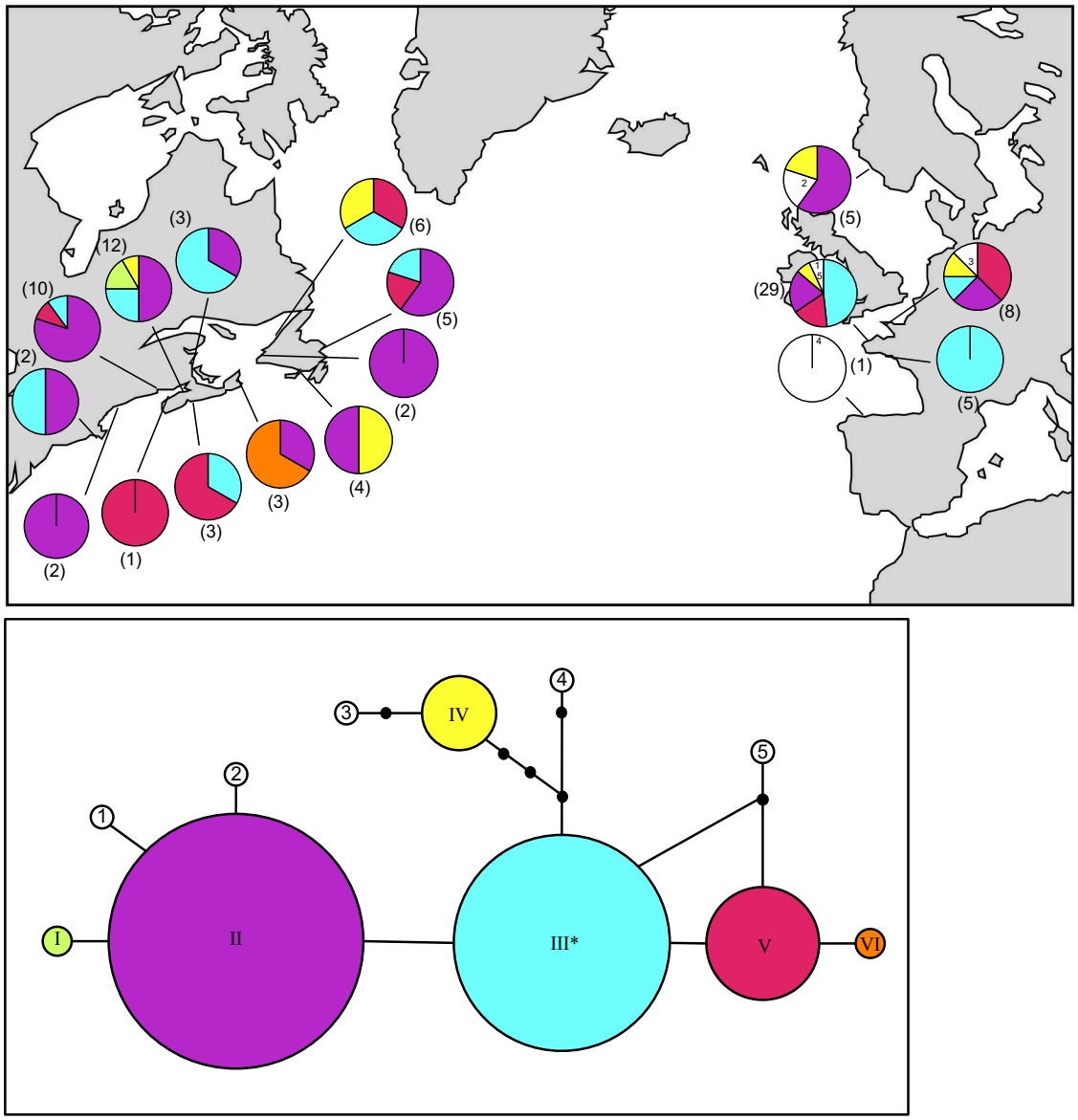

Figure D3. *Chondrus crispus* haplotype map and network based on COI-5P data. In the map, numbers in parentheses refer to sample sizes from given locales, whereas numbers adjacent to white portions of pie charts refer to a haplotype sampled only once in the accompanying network. In the haplotype network, roman numerals refer to repeatedly sampled haplotypes, whereas numbered haplotypes in white reference back to the map. An asterisk indicates a putative ancestral haplotype based on TCS analyses. Black circles indicate hypothesized (e.g. unsampled) haplotypes between clades. The size of each circle is proportional to the sampling frequency of a given haplotype.

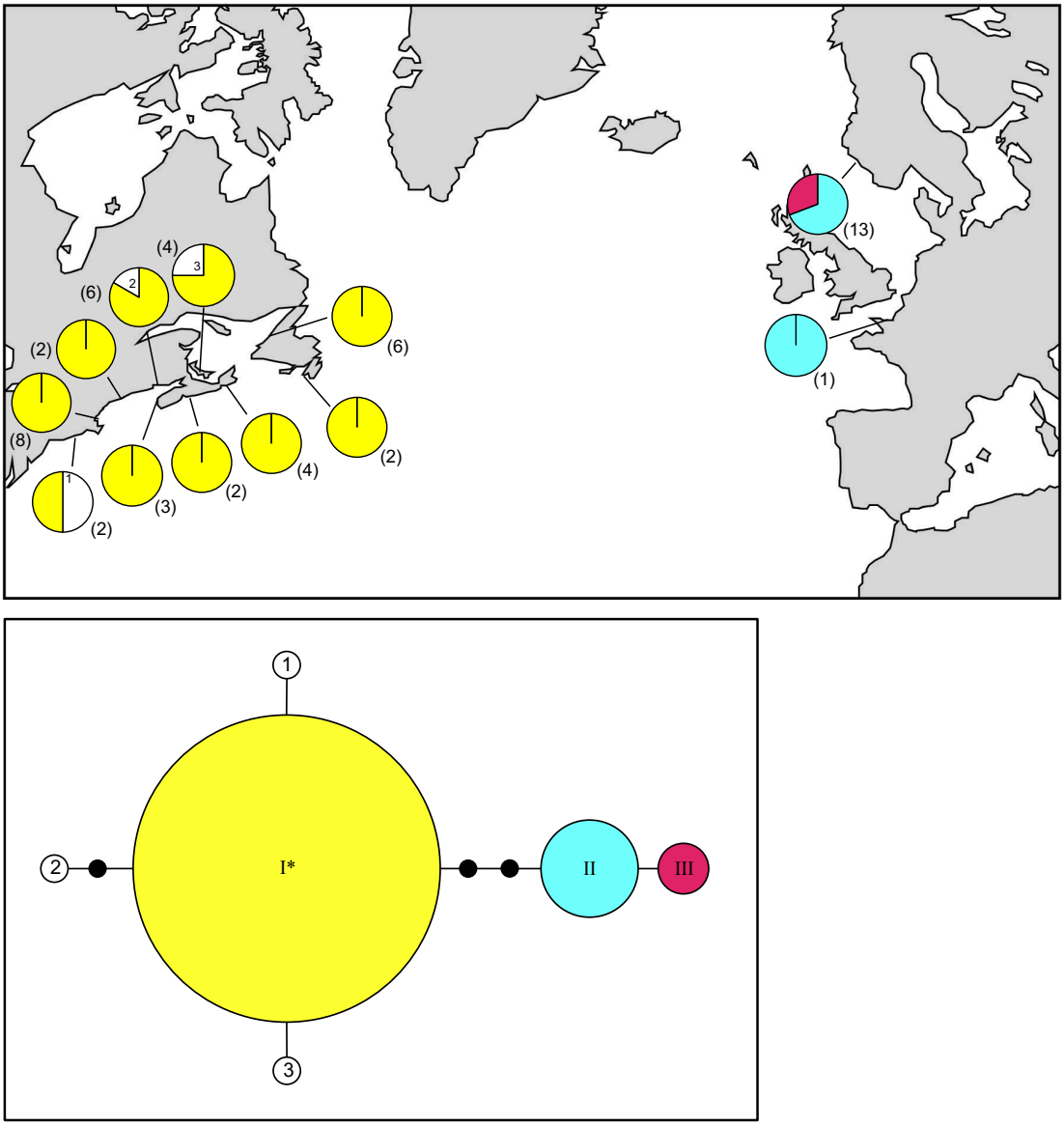

Figure D4. ***Cystoclonium purpureum*** **haplotype map and network based on COI-5P data. In the map, numbers in parentheses refer to sample sizes from given locales, whereas numbers adjacent to white portions of pie charts refer to a haplotype sampled only once in the accompanying network. In the haplotype network, roman numerals refer to repeatedly sampled haplotypes, whereas numbered haplotypes in white reference back to the map. An asterisk indicates a putative ancestral haplotype based on TCS analyses. Black circles indicate hypothesized (e.g. unsampled) haplotypes between clades. The size of each circle is proportional to the sampling frequency of a given haplotype.**

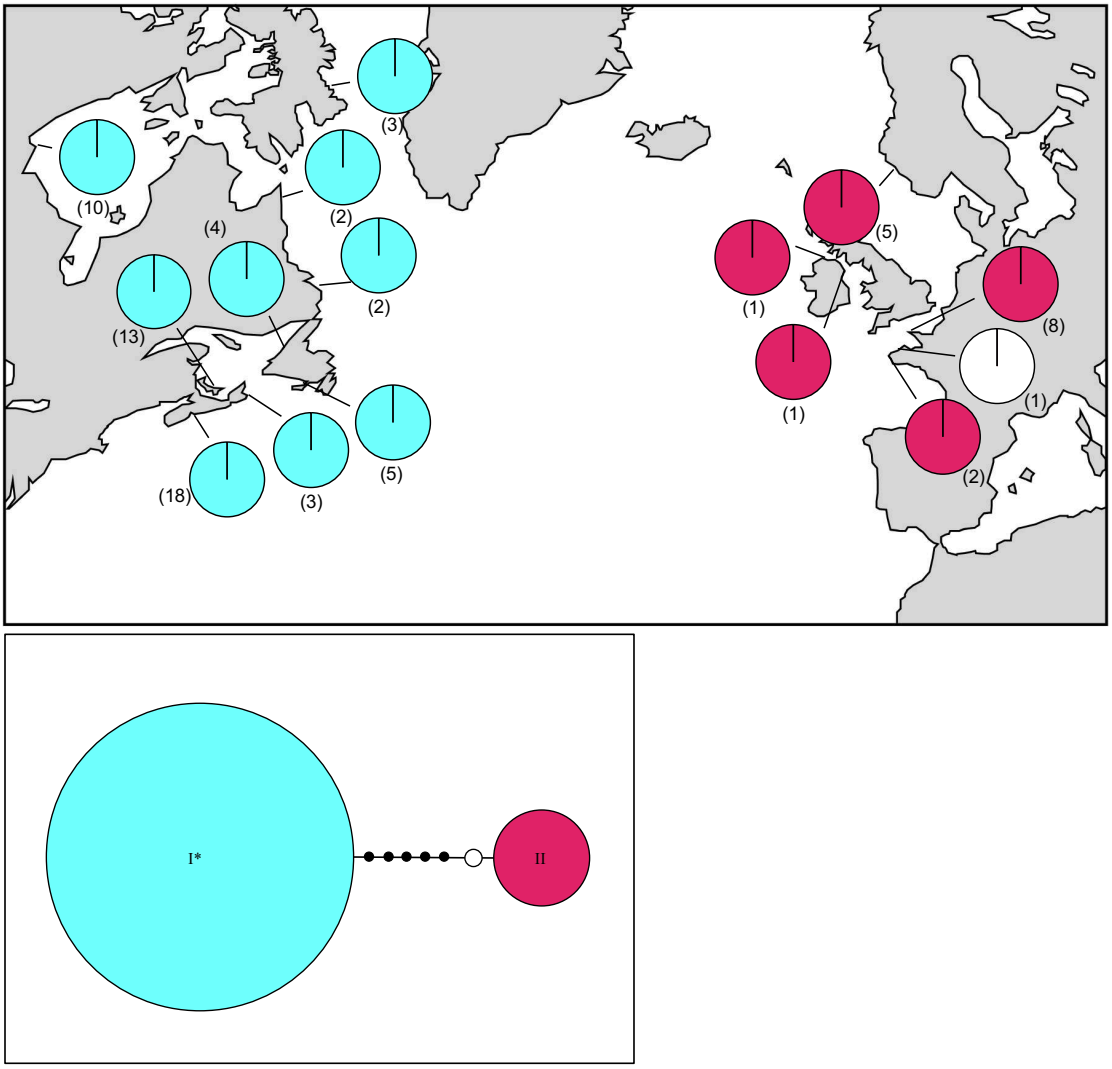

Figure D5. ***Dilsea socialis/carnosa*** **haplotype map and network based on COI-5P data. In the map, numbers in parentheses refer to sample sizes from given locales. In the haplotype network, roman numerals refer to repeatedly sampled haplotypes. An asterisk indicates a putative ancestral haplotype based on TCS analyses. Black circles indicate hypothesized (e.g. unsampled) haplotypes between clades. The size of each circle is proportional to the sampling frequency of a given haplotype.**

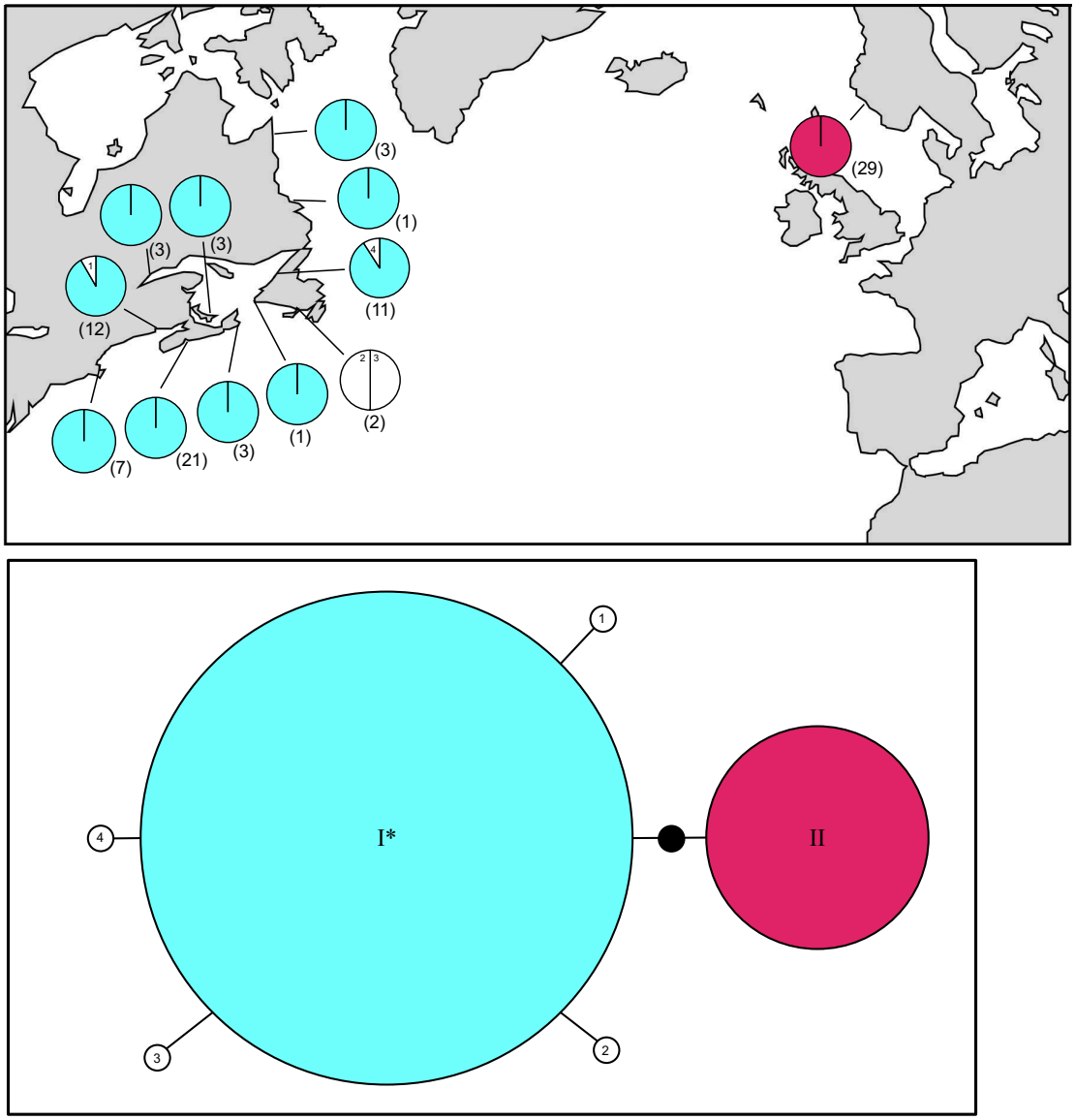

Figure D6. *Euthora cristata* haplotype map and network based on COI-5P data. In the map, numbers in parentheses refer to sample sizes from given locales, whereas numbers adjacent to white portions of pie charts refer to a haplotype sampled only once in the accompanying network. In the haplotype network, roman numerals refer to repeatedly sampled haplotypes, whereas numbered haplotypes in white reference back to the map. An asterisk indicates a putative ancestral haplotype based on TCS analyses. Black circles indicate hypothesized (e.g. unsampled) haplotypes between clades. The size of each circle is proportional to the sampling frequency of a given haplotype.

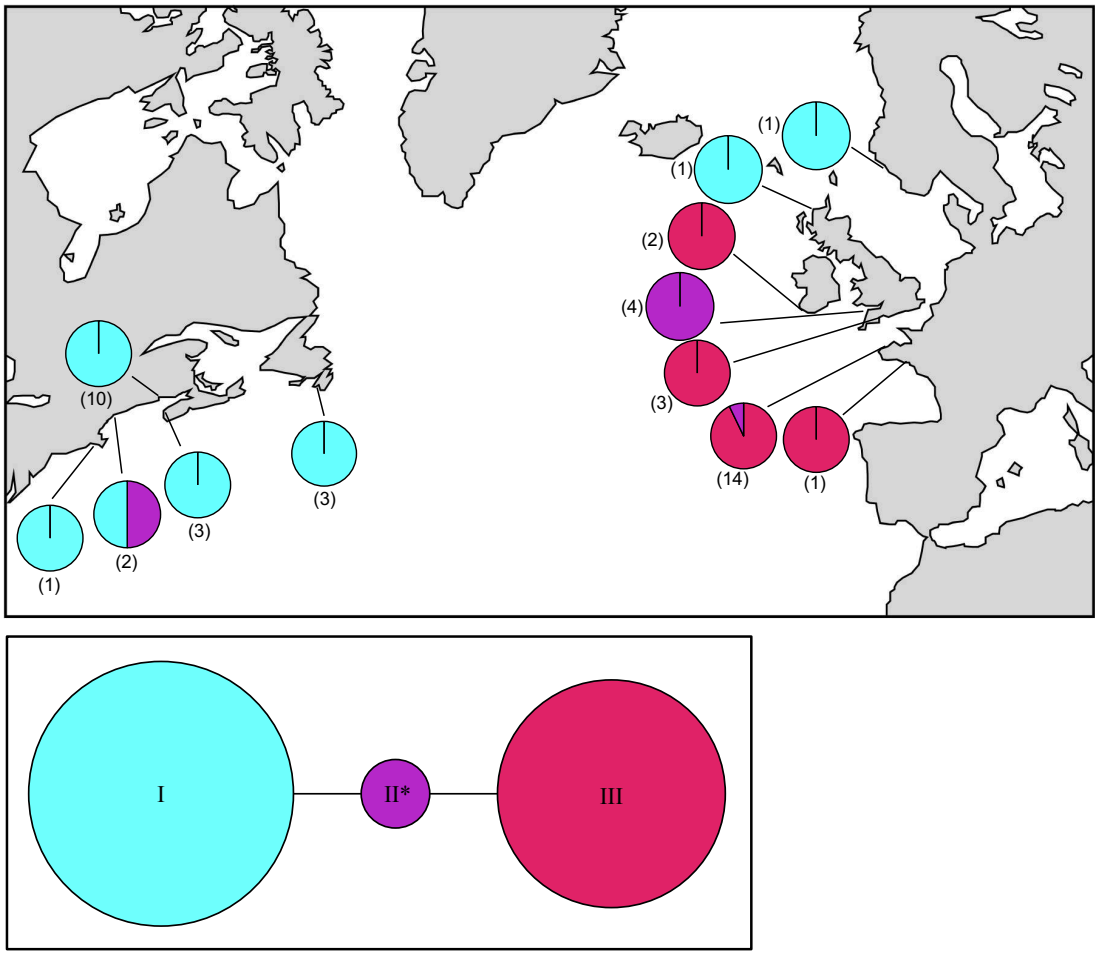

Figure D7. ***Mastocarpus stellatus*** **haplotype map and network based on COI-5P data. In the map, numbers in parentheses refer to sample sizes from given locales. In the haplotype network, roman numerals refer to repeatedly sampled haplotypes. An asterisk indicates a putative ancestral haplotype based on TCS analyses. The size of each circle is proportional to the sampling frequency of a given haplotype.**

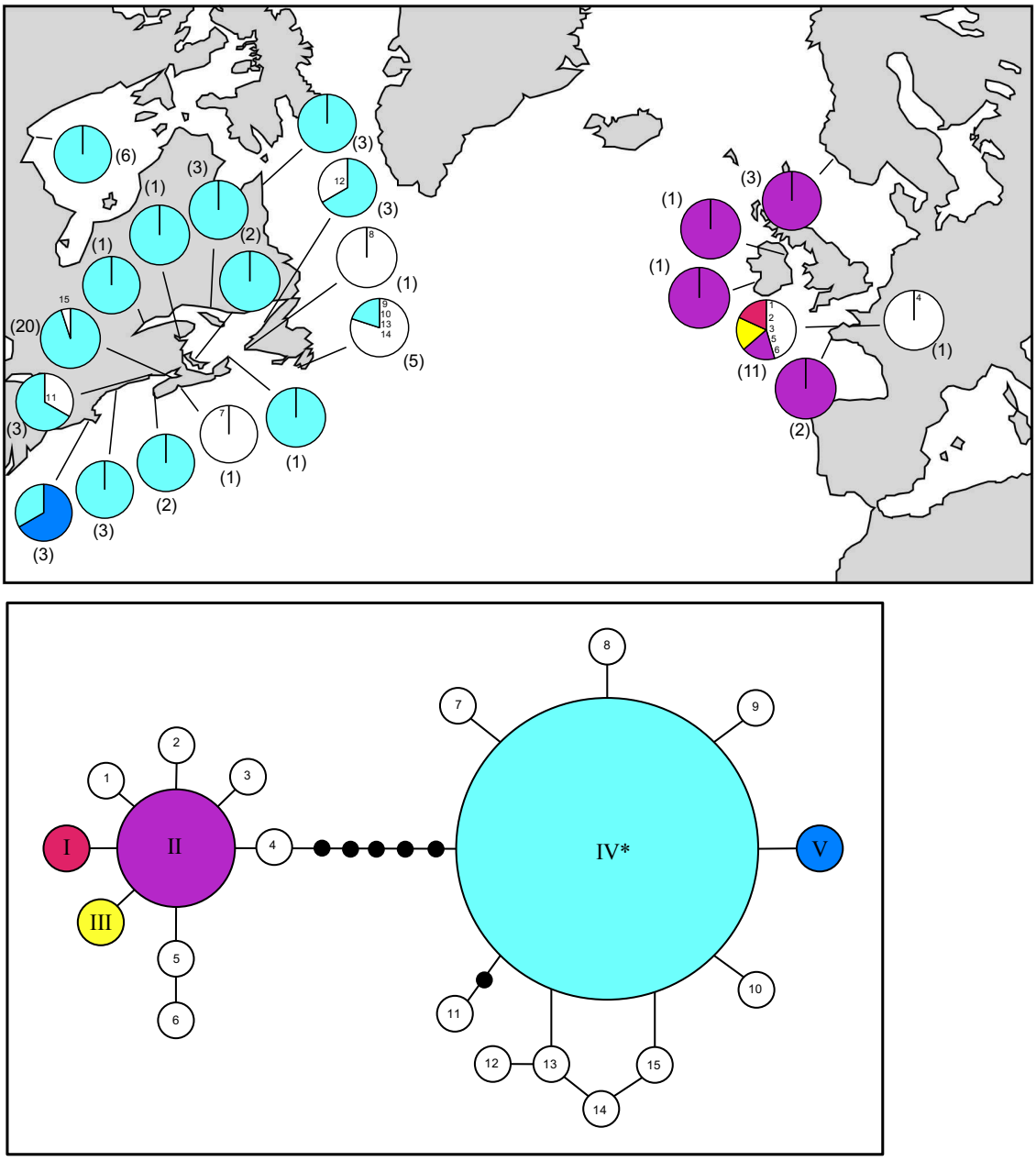

Figure D8. ***Palmaria palmata*** **haplotype map and network based on COI-5P data. In the map, numbers in parentheses refer to sample sizes from given locales, whereas numbers adjacent to white portions of pie charts refer to a haplotype sampled only once in the accompanying network. In the haplotype network, roman numerals refer to repeatedly sampled haplotypes, whereas numbered haplotypes in white reference back to the map. An asterisk indicates a putative ancestral haplotype based on TCS analyses. Black circles indicate hypothesized (e.g. unsampled) haplotypes between clades. The size of each circle is proportional to the sampling frequency of a given haplotype.**

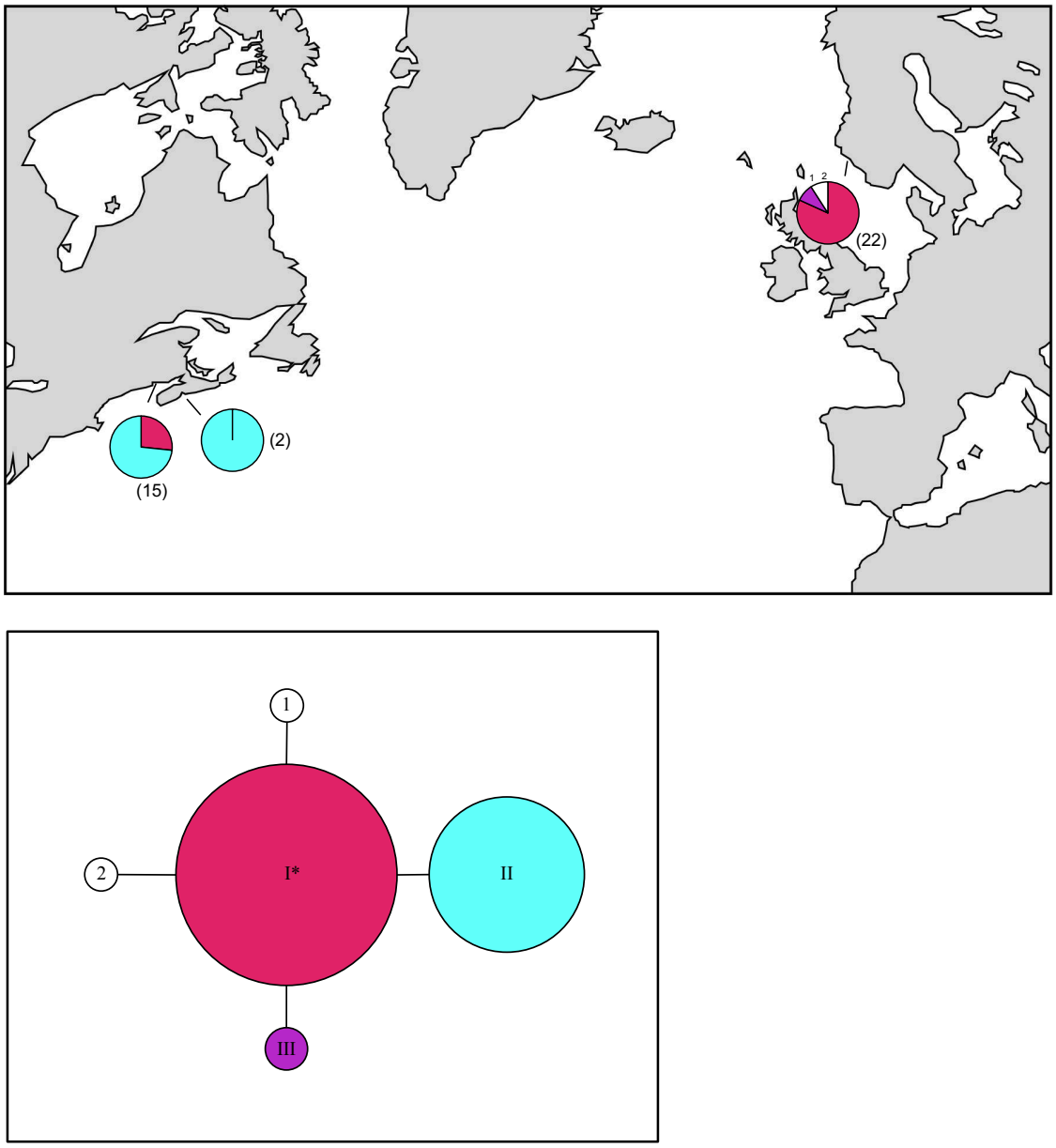

Figure D9. *Phycodrys* sp. 1NB haplotype map and network based on COI-5P data. In the map, numbers in parentheses refer to sample sizes from given locales, whereas numbers adjacent to white portions of pie charts refer to a haplotype sampled only once in the accompanying network. In the haplotype network, roman numerals refer to repeatedly sampled haplotypes, whereas numbered haplotypes in white reference back to the map. An asterisk indicates a putative ancestral haplotype based on TCS analyses. The size of each circle is proportional to the sampling frequency of a given haplotype.

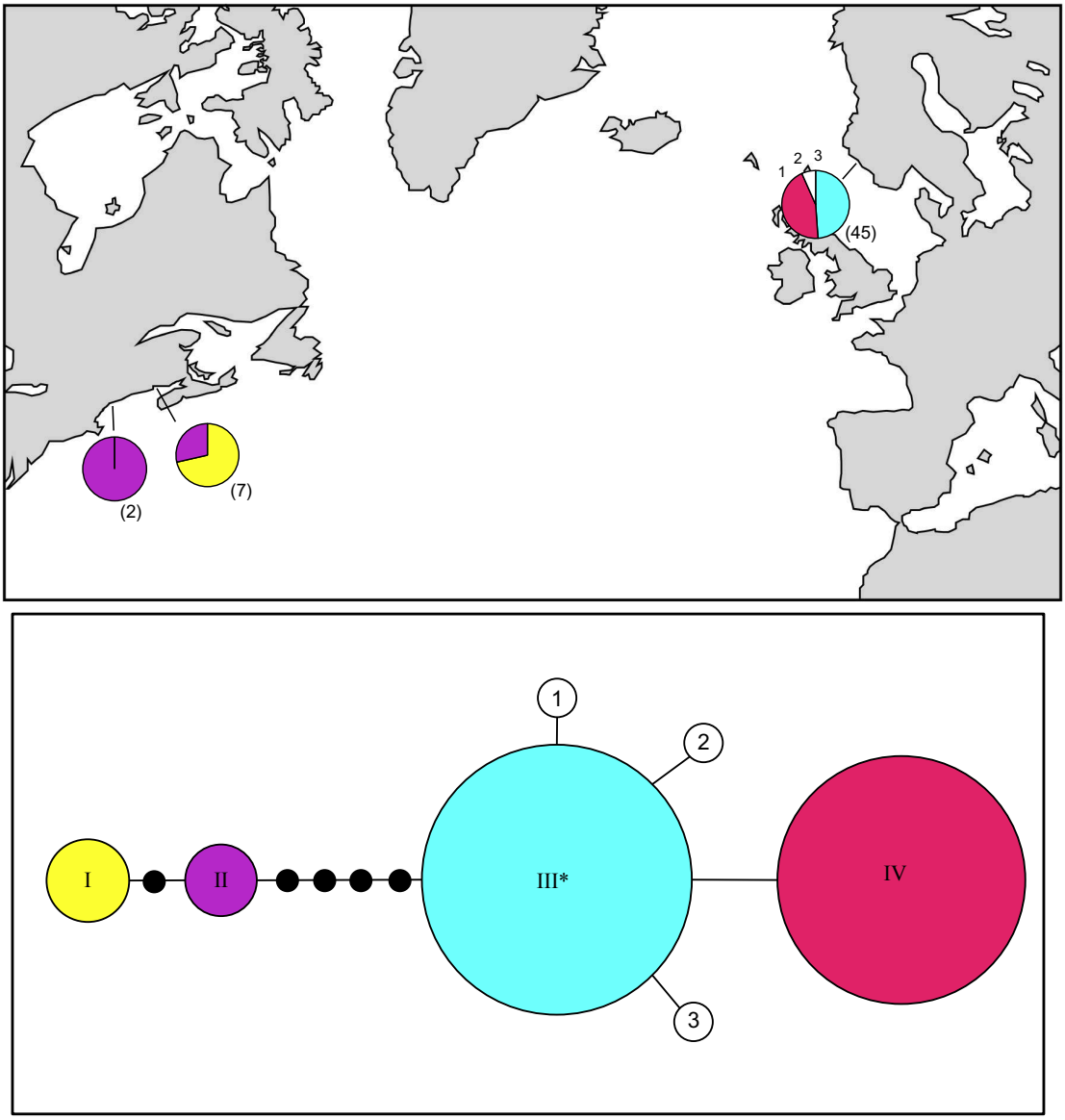

Figure D10. ***Phycodrys rubens*** **haplotype map and network based on COI-5P data. In the map, numbers in parentheses refer to sample sizes from given locales, whereas numbers adjacent to white portions of pie charts refer to a haplotype sampled only once in the accompanying network. In the haplotype network, roman numerals refer to repeatedly sampled haplotypes, whereas numbered haplotypes in white reference back to the map. An asterisk indicates a putative ancestral haplotype based on TCS analyses. Black circles indicate hypothesized (e.g. unsampled) haplotypes between clades. The size of each circle is proportional to the sampling frequency of a given haplotype.**

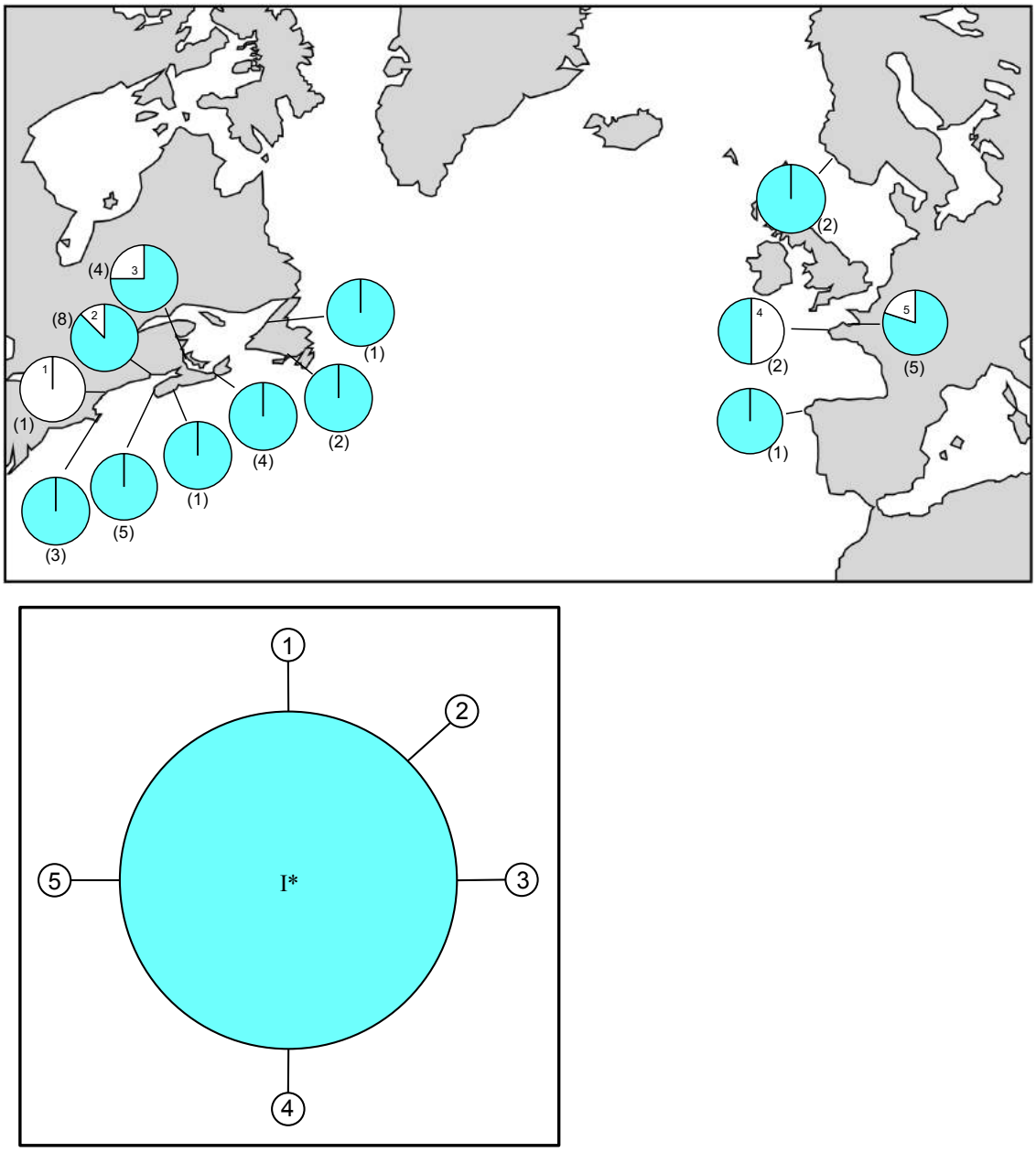

Figure D11. ***Polyides rotundus*** **haplotype map and network based on COI-5P data. In the map, numbers in parentheses refer to sample sizes from given locales, whereas numbers adjacent to white portions of pie charts refer to a haplotype sampled only once in the accompanying network. In the haplotype network, roman numerals refer to repeatedly sampled haplotypes, whereas numbered haplotypes in white reference back to the map. An asterisk indicates a putative ancestral haplotype based on TCS analyses. The size of each circle is proportional to the sampling frequency of a given haplotype.**

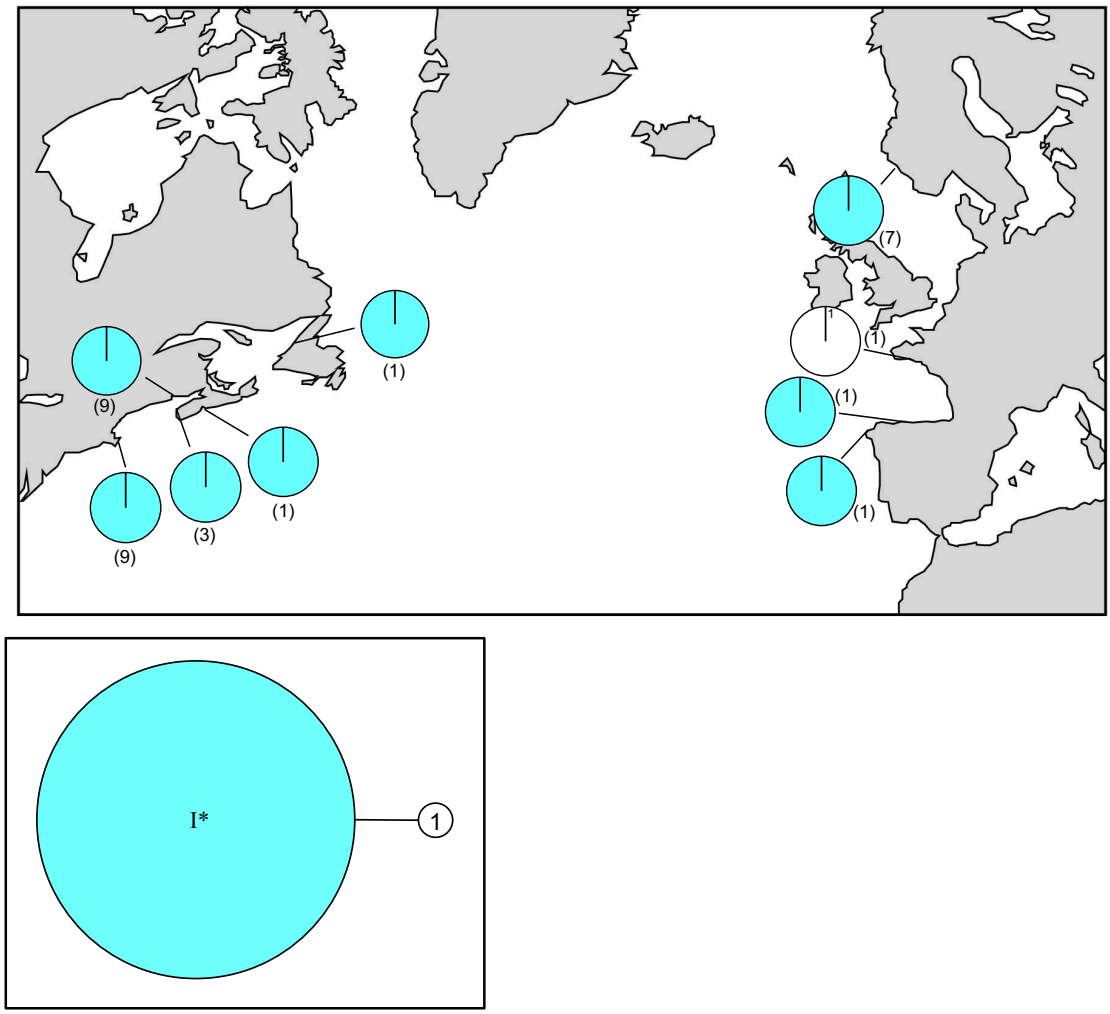

Figure D12. *Polysiphonia* sp. 2stricta haplotype map and network based on COI-5P data. In the map, numbers in parentheses refer to sample sizes from given locales, whereas numbers adjacent to white portions of pie charts refer to a haplotype sampled only once in the accompanying network. In the haplotype network, roman numerals refer to repeatedly sampled haplotypes, whereas numbered haplotypes in white reference back to the map. An asterisk indicates a putative ancestral haplotype based on TCS analyses. The size of each circle is proportional to the sampling frequency of a given haplotype.

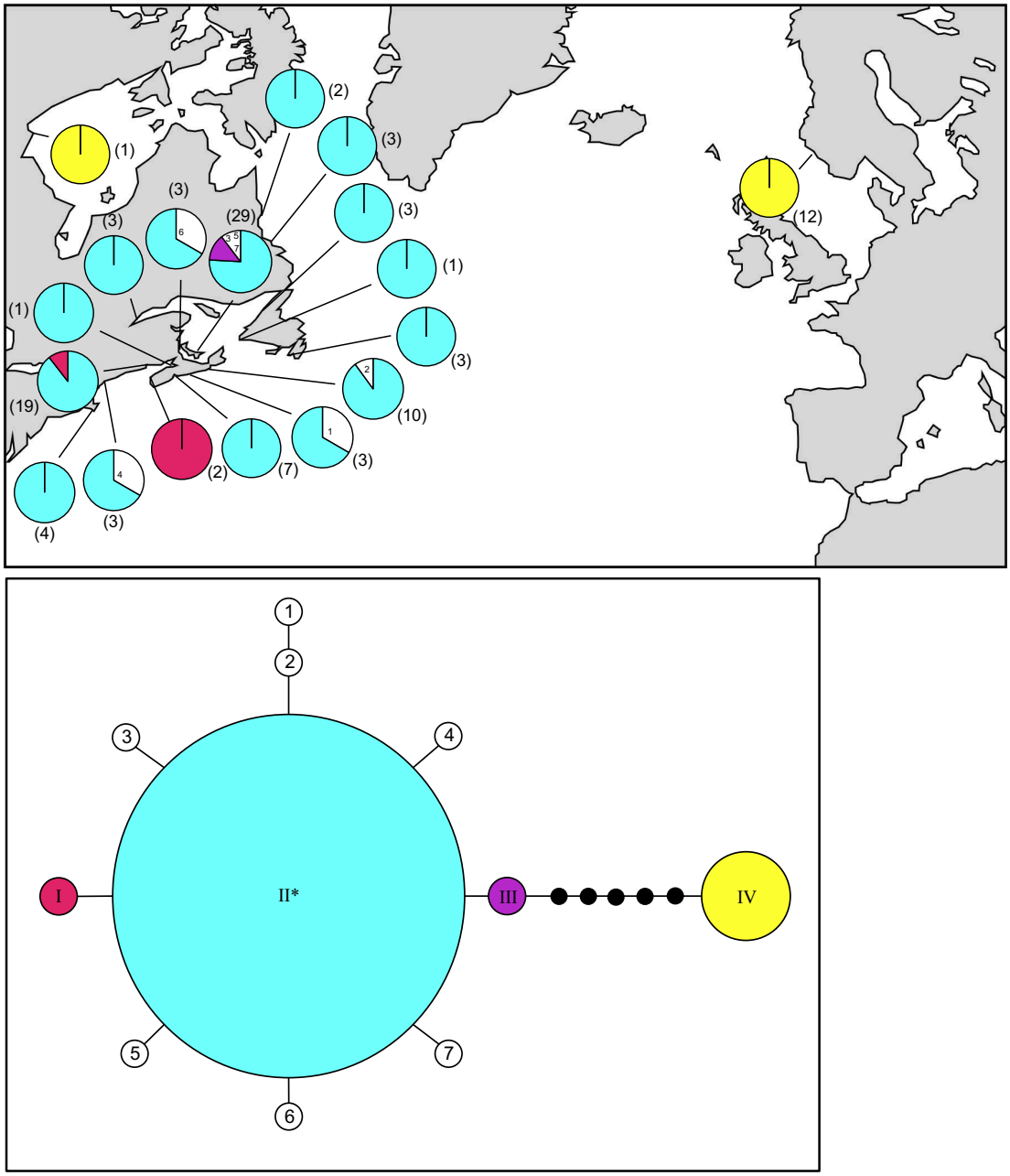

Figure D13. *Rhodomela lycopodioides* haplotype map and network based on COI-5P data. In the map, numbers in parentheses refer to sample sizes from given locales, whereas numbers adjacent to white portions of pie charts refer to a haplotype sampled only once in the accompanying network. In the haplotype network, roman numerals refer to repeatedly sampled haplotypes, whereas numbered haplotypes in white reference back to the map. An asterisk indicates a putative ancestral haplotype based on TCS analyses. Black circles indicate hypothesized (e.g. unsampled) haplotypes between clades. The size of each circle is proportional to the sampling frequency of a given haplotype.

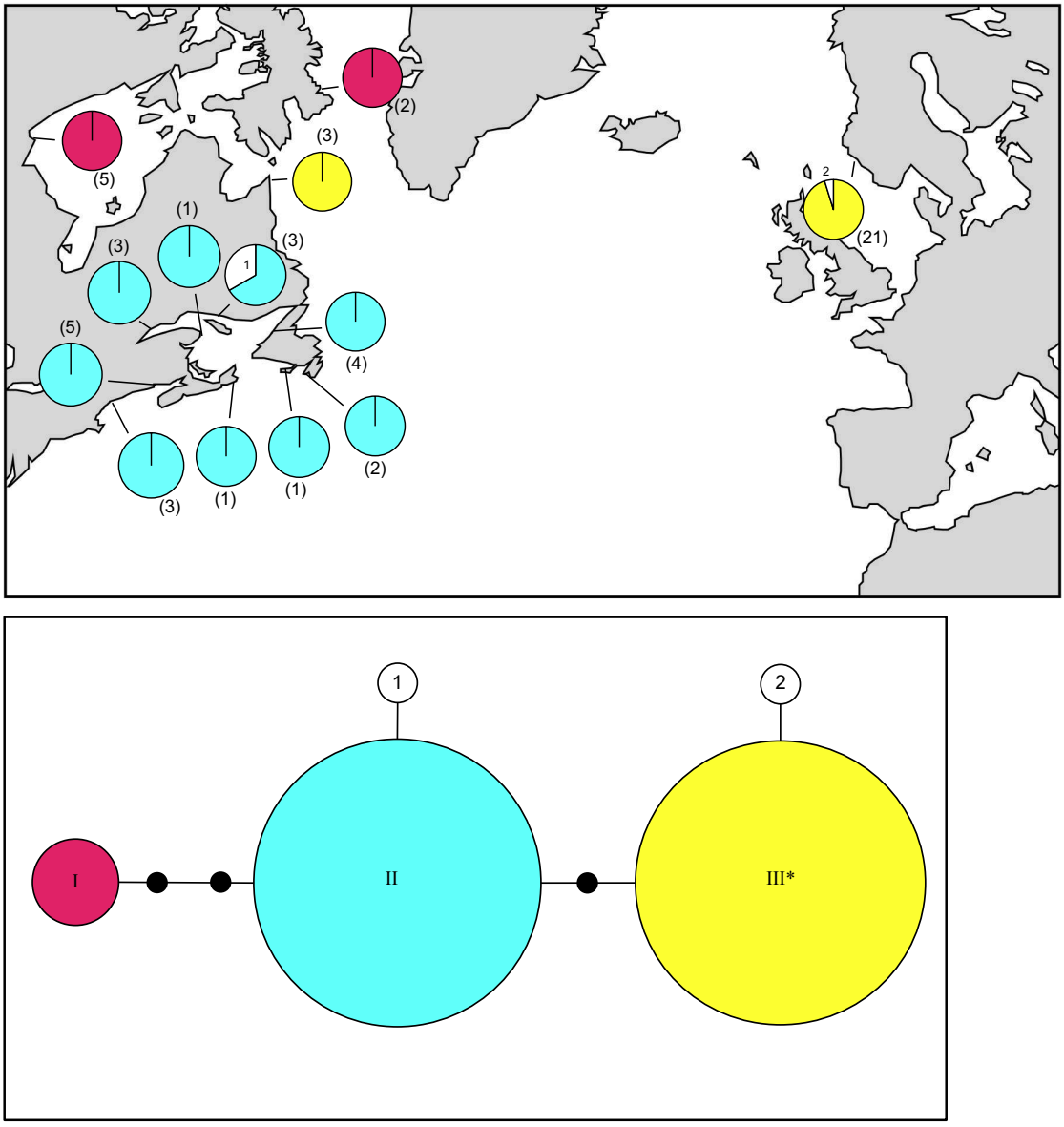

Figure D14. ***Alaria esculenta*** **haplotype map and network based on COI-5P data. In the map, numbers in parentheses refer to sample sizes from given locales, whereas numbers adjacent to white portions of pie charts refer to a haplotype sampled only once in the accompanying network. In the haplotype network, roman numerals refer to repeatedly sampled haplotypes, whereas numbered haplotypes in white reference back to the map. An asterisk indicates a putative ancestral haplotype based on TCS analyses. Black circles indicate hypothesized (e.g. unsampled) haplotypes between clades. The size of each circle is proportional to the sampling frequency of a given haplotype.**

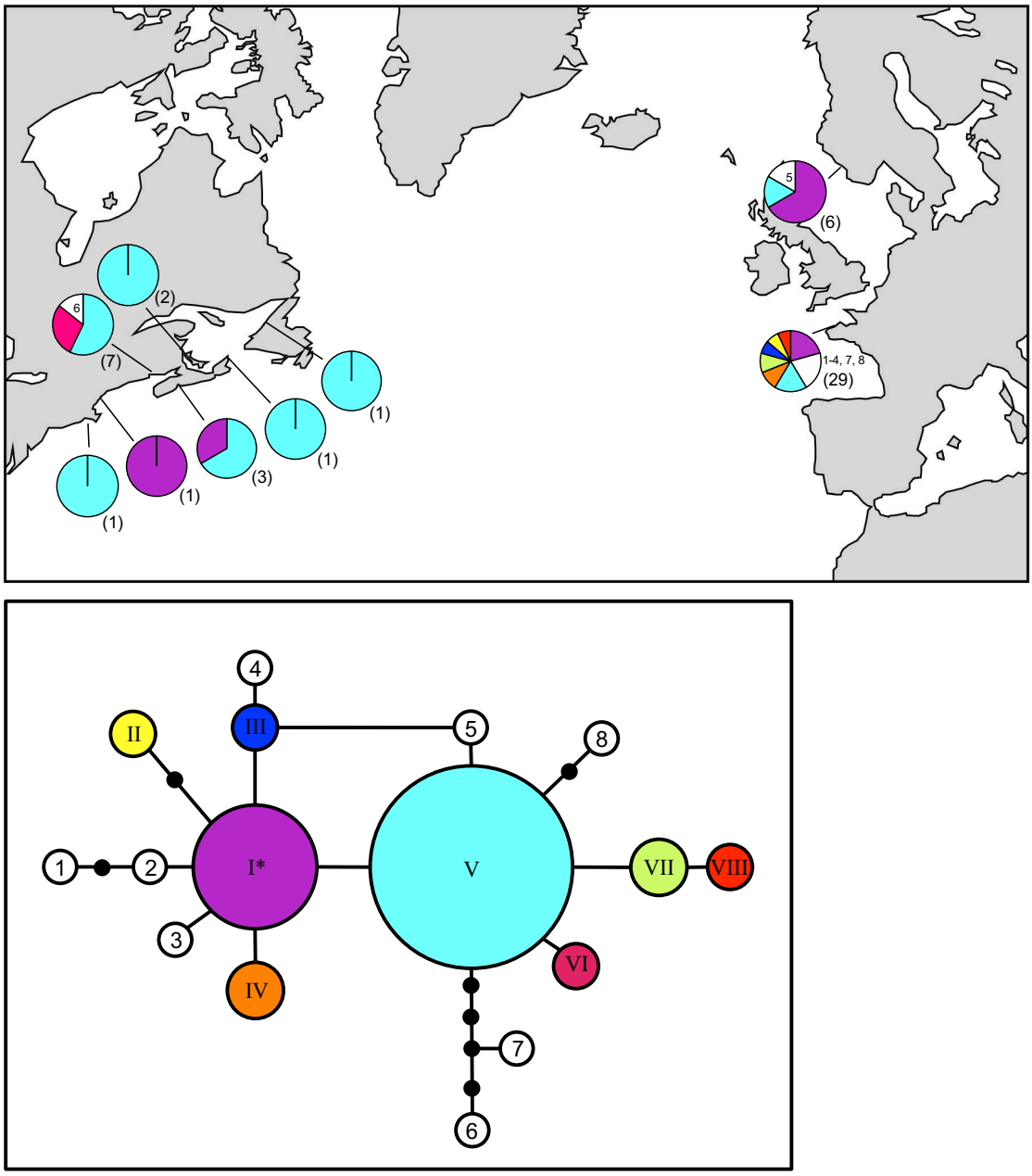

Figure D15. *Ectocarpus fasciculatus* haplotype map and network based on COI-5P data. In the map, numbers in parentheses refer to sample sizes from given locales, whereas numbers adjacent to white portions of pie charts refer to a haplotype sampled only once in the accompanying network. In the haplotype network, roman numerals refer to repeatedly sampled haplotypes, whereas numbered haplotypes in white reference back to the map. An asterisk indicates a putative ancestral haplotype based on TCS analyses. Black circles indicate hypothesized (e.g. unsampled) haplotypes between clades. The size of each circle is proportional to the sampling frequency of a given haplotype.

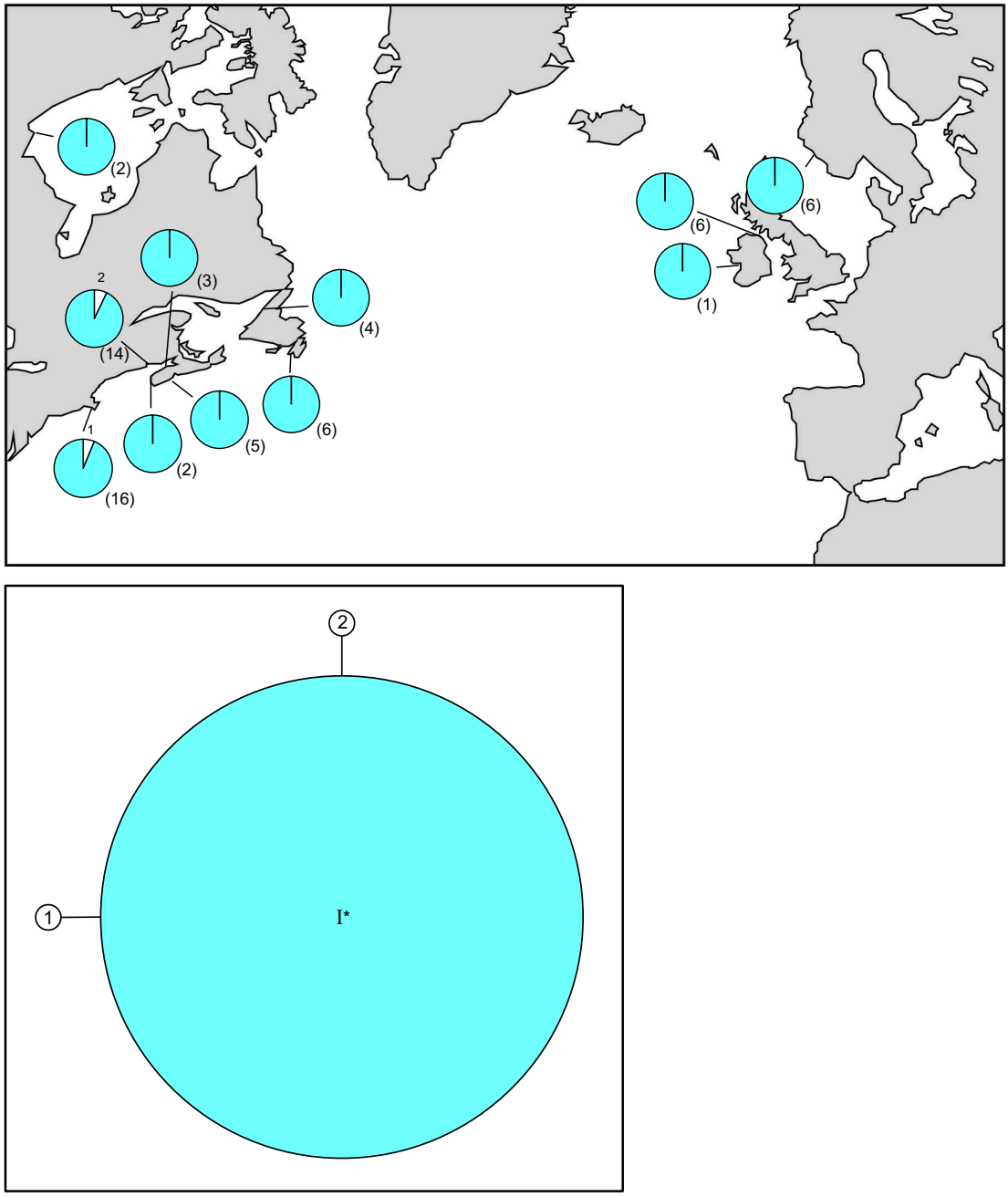

Figure D16. *Laminaria digitata* haplotype map and network based on COI-5P data. In the map, numbers in parentheses refer to sample sizes from given locales, whereas numbers adjacent to white portions of pie charts refer to a haplotype sampled only once in the accompanying network. In the haplotype network, roman numerals refer to repeatedly sampled haplotypes, whereas numbered haplotypes in white reference back to the map. An asterisk indicates a putative ancestral haplotype based on TCS analyses. The size of each circle is proportional to the sampling frequency of a given haplotype.

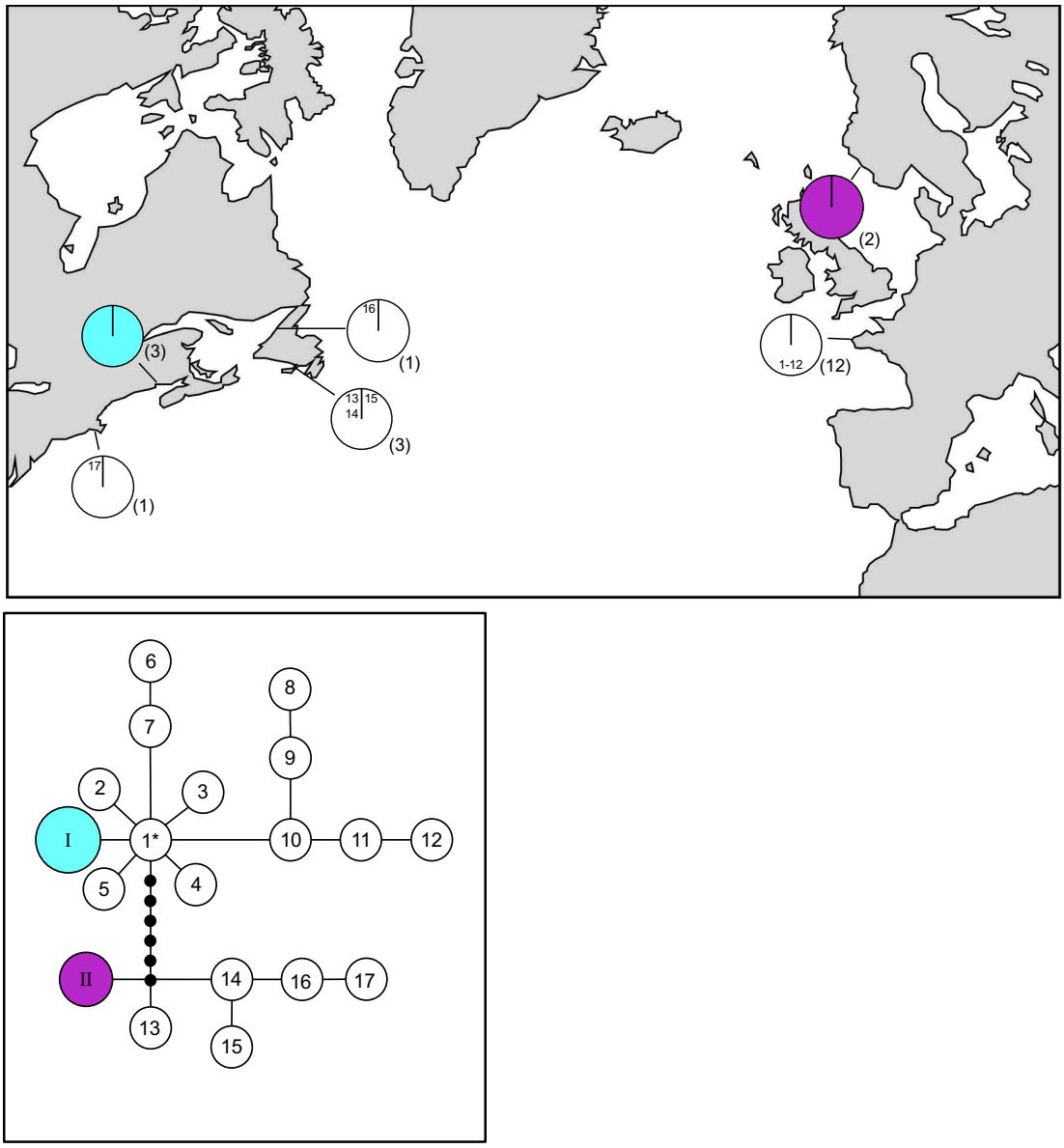

Figure D17. *Pylaiella* sp. 2littoralis haplotype map and network based on COI-5P data. In the map, numbers in parentheses refer to sample sizes from given locales, whereas numbers adjacent to white portions of pie charts refer to a haplotype sampled only once in the accompanying network. In the haplotype network, roman numerals refer to repeatedly sampled haplotypes, whereas numbered haplotypes in white reference back to the map. An asterisk indicates a putative ancestral haplotype based on TCS analyses. Black circles indicate hypothesized (e.g. unsampled) haplotypes between clades. The size of each circle is proportional to the sampling frequency of a given haplotype.

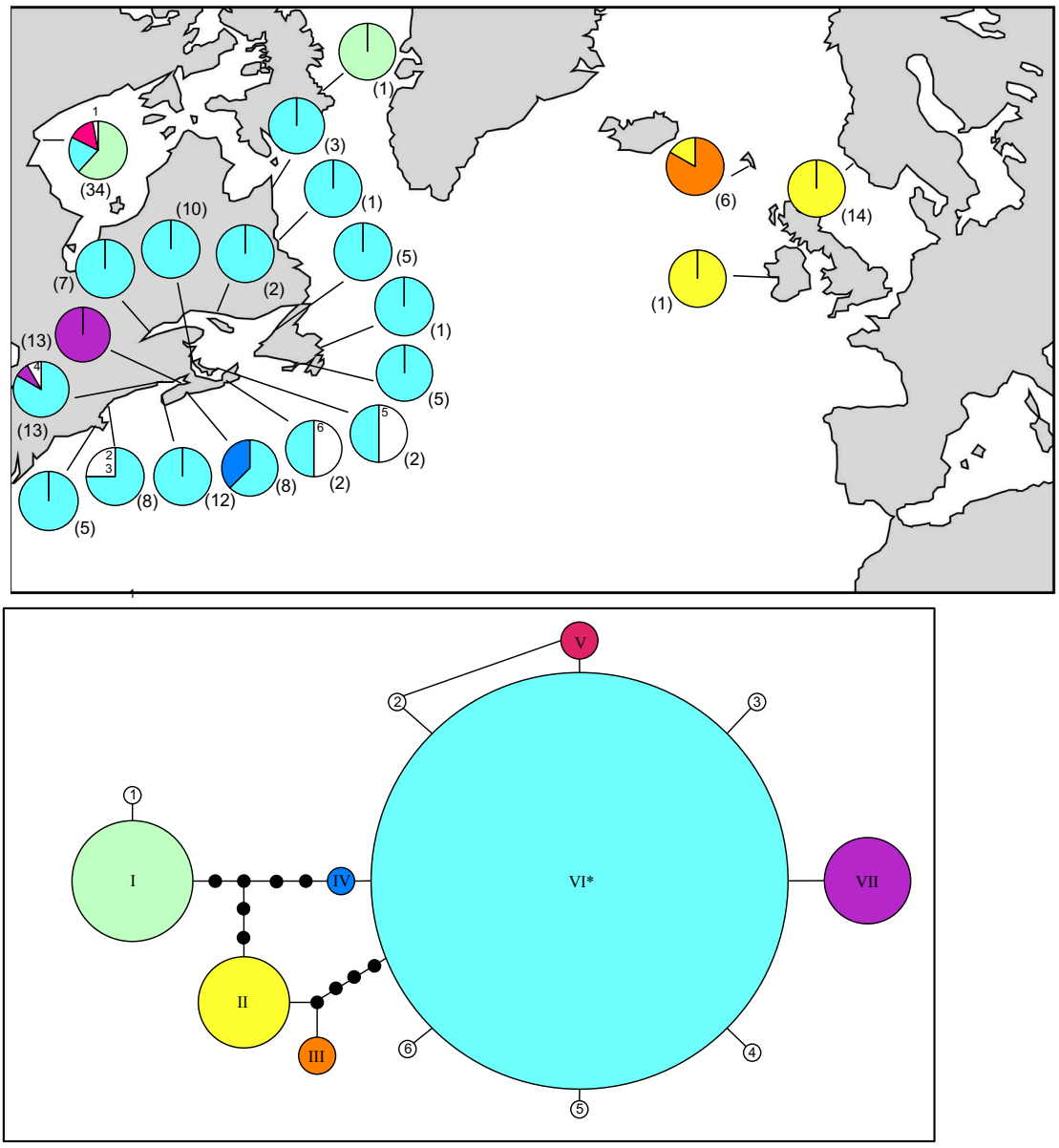

Figure D18. ***Saccharina latissima*** **haplotype map and network based on COI-5P data. In the map, numbers in parentheses refer to sample sizes from given locales, whereas numbers adjacent to white portions of pie charts refer to a haplotype sampled only once in the accompanying network. In the haplotype network, roman numerals refer to repeatedly sampled haplotypes, whereas numbered haplotypes in white reference back to the map. An asterisk indicates a putative ancestral haplotype based on TCS analyses. Black circles indicate hypothesized (e.g. unsampled) haplotypes between clades. The size of each circle is proportional to the sampling frequency of a given haplotype.**

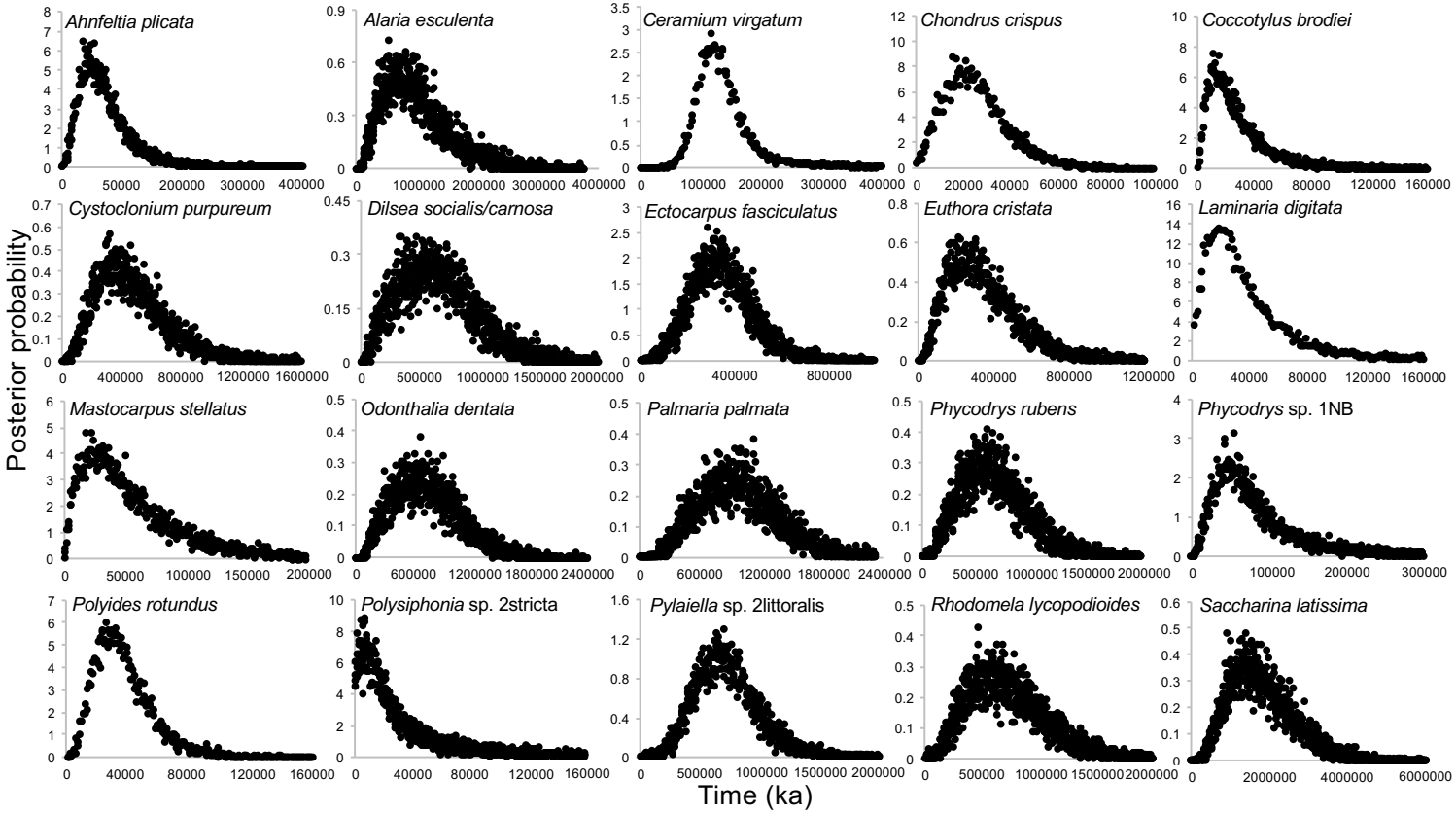

Figure D19. Posterior probability distributions for isolation times in trans-Atlantic populations of red and brown macroalgae based on COI-5P data. Analyses were conducted in IMa2, pooling 30,000 genealogies sampled over three independent runs, and using a COI-5P clock rate of 0.007 substitutions/site/Ma in Red algae and a COI-5P clock rate of 0.00245 substitutions/site/Ma in Brown algae.

Appendix E Supplementary Material for Chapter 4

Table E1. Specimen list for sequence data mined off GenBank and used in the haplotype networks. Sequences are for COI-5P or *tufA*, except for one *rbc*L sequence in *Battersia arctica*. Note some collection information is missing for some records.

Species	Specimen ID	COI-5P	*tufA*	Country	Date sampled	Lat.	Long.
Acrochaetium sp.	GWS005411A	JX571988		Canada	07-Jul-2007	58.81154	-94.21970
Acrosiphonia sonderi	GWS007426		HQ610222	Canada	18-Jul-2006	48.655	-53.752
Acrosiphonia sonderi	GWS003750		HQ610219	Canada	27-May-2006	44.625	-66.86
Acrosiphonia sonderi	GWS003819		HQ610220	Canada	28-May-2006	45.056	-66.736
Acrosiphonia sonderi	GWS003797		HQ610221	Canada	28-May-2006	45.038	-66.891
Acrosiphonia sonderi	GWS003756		HQ610223	Canada	27-May-2006	44.625	-66.86
Acrosiphonia sonderi	GWS002672		HQ610224	Canada	14-Apr-2005	43.565	-70.197
Alaria esculenta	Aesc033102	EF218856		Canada		72.505	-79.779
Alaria esculenta	Aesc9804	EF218857		Canada		74.6933	-95.1885
Alaria esculenta	Aesc1253	EF218858		Canada		44.6497	-67.1747
Alaria esculenta	Aesc002	EF218860		Canada		48.3497	-64.2286
Battersia arctica	SGAD-71	AJ287881 (*rbc*L)		Sweden			
Ectocarpoid sp.	BI022	LT546267		Canada	Aug/Sep-2009	72.30	-79.47
Ectocarpoid sp.2	BI059	LT546288		Canada	Aug/Sep-2009	72.30	-79.47
Monostroma sp.2grevillei	GWS003626		HQ610262	Canada	25-Apr-2006	44.609	-67.397
Monostroma sp.2grevillei	GWS005976		HQ610258	Canada	18-Apr-2007	45.072	-66.469
Monostroma sp.2grevillei	GWS005975		HQ610259	Canada	18-Apr-2007	45.072	-66.469
Monostroma sp.2grevillei	GWS003787		HQ610261	Canada	28-May-2006	45.038	-66.891
Monostroma sp.2grevillei	GWS003847		HQ610260	Canada	29-May-2006	45.072	-66.469

Petalonia filiformis	MS433		United Kingdom			
Ptilota serrata	JR-05-9	HQ412546	Norway	30-Aug-2005	78.814	17.756
Ptilota serrata	JR-07-19	HQ412547	Norway	09-Nov-2007	69.258	19.332
Ptilota serrata	A93571	MG762003	United States	3-Aug-1996	63.730	-171.602
Ptilota serrata	A84489	MG762004	Canada	4-Aug-2003	53.281	-135.593
Pylaiella washingtoneinsis	BI038	LT546276	Canada	Aug/Sep-2009	72.505	-79.779
Pylaiella washingtoneinsis	BI023	LT546268	Canada	Aug/Sep-2009	72.505	-79.779
Pylaiella washingtoneinsis	BI003	LT546264	Canada	Aug/Sep-2009	72.505	-79.779
Scytosiphon canaliculatus	Saruru-890612	AB747602	Japan	12-Jun-1989	44.4327	143.167
Scytosiphon canaliculatus	Hanasaki-910518-2	AB747600	Japan	18-May-1991	43.2792	141.024
Scytosiphon canaliculatus	Matsumae-890111	AB747586	Japan	11-Jan-1991	43.1884	140.845
Scytosiphon canaliculatus	Oshoro-980407-8f	AB747570	Japan	07-Apr-1998	43.1884	140.845
Scytosiphon canaliculatus	Oshoro-980407-6m	AB747569	Japan	07-Apr-1998	43.1884	140.845
Scytosiphon canaliculatus	Tappizaki-020529	AB747606	Japan	29-May-2002	41.242	140.372
Scytosiphon canaliculatus	Oshoro-000510	AB747581	Japan	10-May-2000	43.1884	140.845
Scytosiphon canaliculatus	Oshoro-000510-8m	AB747579	Japan	10-May-2000	43.1884	140.845
Scytosiphon canaliculatus	Oshoro-000510-3f	AB747574	Japan	10-May-2000	43.1884	140.845

Scytosiphon canaliculatus	Oshoro000510-6m	AB747577	Japan	10-May-2000	43.1884	140.845
Scytosiphon canaliculatus	Oshoro 980407-4m	AB747568	Japan	07-Apr-1998	43.1884	140.845
Scytosiphon canaliculatus	Oshoro 980407-12m	AB747572	Japan	07-Apr-1998	43.1884	140.845
Scytosiphon canaliculatus	Oshoro 000510-4f	AB747575	Japan	10-May-2000	43.1884	140.845
Scytosiphon canaliculatus	Kakijima-900625	AB747596	Japan	25-Jun-1990	42.985	144.795
Scytosiphon canaliculatus	Oshoro5109f	AB747580	Japan	10-May-2000	43.1884	140.845
Scytosiphon canaliculatus	Jimi-040226-2	AB747610	Japan	26-Feb-2004	36.890	137.028
Scytosiphon canaliculatus	Mitsumatsu-050329-7f	AB747614	Japan	29-Mar-2005	35.502	135.522
Scytosiphon sp. 1crust	GWS005564	HM891038	Canada	11-Jul-2007	58.768	-93.89
Ulvaria obscura	GWS003507	HQ610415	Canada	16-Oct-2005	45.072	-66.469
Ulvaria obscura	GWS003572	HQ610427	Canada	03-Mar-2006	45.072	-66.469
Ulvaria obscura	GWS003573	HQ610425	Canada	03-Mar-2006	45.072	-66.469
Ulvaria obscura	GWS003627	HQ610423	Canada	25-Apr-2006	44.609	-67.397
Ulvaria obscura	GWS003667	HQ610426	Canada	25-Apr-2006	44.609	-67.397
Ulvaria obscura	GWS003673	HQ610424	Canada	25-Apr-2006	44.609	-67.397
Ulvaria obscura	GWS003786	HQ610414	Canada	28-May-2006	45.038	-66.891
Ulvaria obscura	GWS003821	HQ610417	Canada	28-May-2006	45.056	-66.736
Ulvaria obscura	GWS003826	HQ610422	Canada	29-May-2006	45.072	-66.469
Ulvaria obscura	GWS003834	HQ610420	Canada	29-May-2006	45.072	-66.469
Ulvaria obscura	GWS003855	HQ610419	Canada	29-May-2006	45.072	-66.469

Ulvaria obscura	GWS004457	HQ610418		Canada	26-Jun-2006	48.53	-124.454
Ulvaria obscura	GWS004603	HQ610421		Canada	30-Jun-2006	49.706	-124.872
Ulvaria obscura	GWS005073	HQ610413		Canada	11-Jul-2006	54.221	-130.329
Ulvaria obscura	GWS005873	HQ610416		Canada	31-Jan-2007	45.038	-66.891
Ulvaria obscura	GWS006119	HQ610412		Canada	13-May-2007	48.351	-69.397
Ulvaria obscura	GWS006315	HQ610411		Canada	24-May-2007	48.648	-123.394
Ulvaria obscura	GWS006316	HQ610410		Canada	24-May-2007	48.648	-123.394
Ulvaria obscura	GWS006404	HQ610409		Canada	25-May-2007	48.352	-123.728
Ulvaria obscura	GWS006999	HQ610408		Canada	10-Jul-2006	47.623	-59.291
Ulvaria obscura	GWS007079	HQ610407		Canada	12-Jul-2006	49.528	-57.825
Ulvaria obscura	GWS007568	HQ610406		Canada	20-Jul-2006	47.633	-54.87
Ulvaria obscura	GWS008841	HQ610405		Canada	12-Sep-2006	45.056	-66.736
Ulva prolifera	E160gh		EF595301	United Kingdom	11-Jul-2004	57.0329	-5.893
Ulva prolifera	Prolofbr		EF595334	Iceland	06-Jul-2005	64.6083	-18.824
Ulva prolifera	B32cm2		EF595302	United Kingdom	27-Oct-2004	51.2115	-4.0463

Table E2. General haplotype patterns and inferred origins in Arctic species of marine macroalgae. The Arctic basin is delineated according to the 10°C isotherm for July, as per D'Odorico et al. (2013), and includes Northern Baffin Island through to Northern Labrador (Nain and Northwards), Svalbard, Northern Norway, the Siberian coastline, Northern Alaska (North of the Bering Strait), and the Northern Canadian coastline, including the Hudson Bay. Species with updated information regarding the origins of Arctic populations (relative to Saunders and McDevit [2013]) are indicated below the species name as updated, or are listed as new if they were not reported in that publication. Pa=Pacific, Ar=Arctic, At=Atlantic. Sample sizes refer to COI-5P data unless otherwise indicated. For the origin of Arctic specimens, ocean basins not in parentheses do not allow for an Arctic refugial populations (scenario 1), while those in parentheses indicate interpretation of haplotype data if Arctic refugial populations are considered as a possible source for contemporary Arctic populations (scenario 2). [1]Churchill, Manitoba, records cannot be accounted for by Pacific or Atlantic collections (e.g. unique Arctic species or haplotype[s] suggesting at Arctic periglacial refugial origins). [2]North Alaska records cannot be accounted for by Pacific or Atlantic collections. [3]Baffin Island and Northern Labrador records cannot be accounted for by Pacific or Atlantic collections.

Species	Sample size (Pa/Ar/At)	Origin of Arctic specimens	Interpretation of haplotype patterns
Rhodophyta			

Acrochaetium sp.[1]	0/1/0	Uncertain (Arctic)	A single record exists for this genetic group, occurring in Churchill, leaving the origin uncertain.
Ahnfeltia borealis **(Updated)** (Figs. E1 & E2)	COI-5P: 25/40/2 *ycf35*: 24/35/2	Pacific	Very little haplotype variation exists in this species. Divergent COI-5P haplotypes occur in the Northwest Atlantic, while Arctic haplotypes are monotypic, matching Pacific populations. *ycf35* haplotypes indicate two unique microsatellites occur in the Bering Sea, whereas only one of these microsatellites occurs in the Arctic. Available evidence therefore suggests a Pacific origin, possibly out of the Northwest Pacific given the low number of sampled haplotypes.
Ahnfeltia plicata (Fig. E3)	0/2/140	Atlantic	Haplotype patterns indicate this species has a long history in the Atlantic. Specimens of *Ahnfeltia* in the West Arctic and Bering Sea are assignable to *A. borealis* rather than *A. plicata*, suggesting that the latter species has a limited Artic distribution. Our verified collections in the North American Arctic are limited to two drift collections from Churchill, with Baffin Island and Labrador collections all assignable to *Ahnfeltia borealis* (n=10).
Ceramium virgatum **(New)** (Fig. E4)	0/1/170	Atlantic	A single Arctic collection along the coast of Labrador matches Northwest Atlantic populations, where this species appears to have survived multiple glaciations.
Clathromorphum sp. 9GWS **(Updated)** (Fig. E5)	2/3/65	Uncertain	Previously listed as *Phymatolithon lenormandii* in Saunders & McDevit (2013), this genetic group has been updated to uncertain given the inclusion of North Pacific records and lack of haplotype variation throughout its genetically confirmed range.
Clathromorphum circumscriptum **(New)**	0/1/6	Atlantic	A single Arctic collection from Baffin Island matches a Northwest Atlantic haplotype.

(Fig. E6)			
Clathromorphum compactum **(New)** (Fig. E7)	0/1/11	Atlantic	A single Arctic collection along the coast of Labrador matches the Northwest Atlantic haplotype.
Coccotylus brodiei **(Updated)** (Fig. E8)	0/1/101	Atlantic	All verified Pacific and West Arctic records are attributable to *Coccotylus truncatus*; as such, the single Arctic collection, from Churchill appears to be of Atlantic origin.
Coccotylus truncatus[1, 2, 3] **(Updated)** (Figs. E9 & E10)	COI-5P: 11/56/55 ITS: 11/54/34	Atlantic and Pacific (Arctic, Atlantic, and Pacific)	East and West Arctic populations appear to have been recolonized from the Atlantic and Pacific, respectively. ITS data, in particular, appear to have distinct East and West Arctic haplotypes, with admixing of populations in Churchill. Unique Arctic haplotypes (in Northern Alaska, Churchill, Northern Baffin Island, and Labrador) also suggest at possible Arctic contributions.
Devaleraea ramentacea[1, 2] **(Updated)** (Fig. E11)	0/10/27	Atlantic (Arctic and Atlantic)	All genetically verified specimens of *Devaleraea* from the North Pacific do not match this species (see Chapter 2); records of *Devaleraea ramentacea* in this flora thus remain uncertain. Haplotype patterns for this species are also consistent with a long history in the Northwest Atlantic (again, consistent with Chapter 2), with specimens sampled in Northern Labrador matching these populations. A unique Baffin Island and Arctic haplotype is relatively divergent from Atlantic collections, suggesting at possible Arctic contributions in this species.
Dilsea socialis **(Updated)** (Fig. E12)	38/46/46	Pacific	There was no haplotype variation in this species from the Western Arctic through to the Northwest Atlantic. A unique COI-5P haplotype was sampled on St. Lawrence Island in the North Pacific, but haplotype variation is notably absent from Nome, Alaska. It is likely this species has recently migrated out of the Northwest Pacific, which would be consistent with

			phylogeographic analyses (see Chapter 2); Pacific origins are tentatively inferred, pending further sampling in the Northwest Pacific.
Euthora cristata[3] **(New)** (Fig. E13)	30/4/94	Atlantic (Arctic and Atlantic)	This species is reported in the Northern Pacific and in Northern Alaska (Wynne & Heine 1992; Wilce & Dunton 2014), though we were unable to genetically verify this species from these locations. Limited Arctic records along Northern Labrador indicate Northwest Atlantic origins in these populations. A unique and highly divergent haplotype from Baffin Island (most closely allied with Pacific populations) suggest at an additional refugial contribution to Arctic populations.
Fimbrifolium dichotomum **(New)** (Fig. E14)	0/7/9	Atlantic	This species is genetically verified from the Northwest Atlantic, matching specimens sampled along Northern Labrador.
Haemescharia polygyna[1]	0/1/0	Uncertain (Arctic)	A single genetic record exists from the Canadian Arctic.
Hildenbrandia sp. 1Arct[3] **(New)**	0/4/0	Uncertain (Arctic)	This genetic group was recovered only in Northern Labrador.
Leptophytum foecundum **(New)** (Fig. E15)	0/3/1	Uncertain	This species has a unique haplotype in the West Arctic, and has been genetically verified in the Northwest Atlantic basin. Given the limited number of samples and difficulty associated with sampling red crusts, the origin of Arctic populations for this species remains unknown.
Leptosiphonia flexicaulis **(New)** (Fig. E16)	0/1/38	Atlantic	A single Arctic record from Northern Labrador matches Northwest Atlantic populations.
Lithothamnion glaciale (Fig. E17)	4/4/44	Atlantic	Limited North Pacific and Arctic collections suggest this species survived in the Atlantic and migrated Westward

			through the Arctic. Haplotype variation also suggests this species survived recent glaciation in the Northwest Atlantic.
Lithothamnion lemoineae **(New)** (Fig. E18)	1/2/8	Atlantic	Inferences are problematic in this group given there is a single genetic record from the North Pacific. Arctic records from Baffin Island and Northern Labrador match Northwest Atlantic haplotypes, and while this basin is tentatively listed as the origin for Arctic populations, more sampling is needed in the Western Arctic and North Pacific.
Membranoptera carpophylla[3] **(New)**	0/1/0	Uncertain (Arctic)	A single genetic record exists for this species from Northern Labrador. Phylogeographic analyses indicated this genetic group is nested in a clade of Atlantic species, suggesting it has origins in this basin (see Chapter 2).
Membranoptera fabriciana **(New)** (Fig. E19)	0/5/23	Atlantic	As with *Membranoptera carpophylla*, this species is nested in a clade of Atlantic species, further suggesting Arctic populations have origins in this basin. Indeed, the Arctic haplotype matches Northwest Atlantic populations.
Odonthalia dentata[2, 3] **(Updated)** (Fig. E20)	21/36/67	Atlantic and Pacific (Arctic, Atlantic, and Pacific)	Arctic populations share haplotypes with both Pacific and Northwest Atlantic basins. Haplotype variation also suggests this species has survived glaciation in the North Pacific and Northeast Atlantic, and the Last Glacial Maximum in the Northwest Atlantic (as evidenced by numerous rare private haplotypes). The haplotype patterns suggest at the establishment of the Northwest Atlantic flora from the North Pacific prior to the Last Glacial Maximum (Northeast Atlantic populations must have been established sometime during the Late Pleistocene; see Chapter 2), followed by the establishment of contemporary Arctic populations from the Pacific and likely from the Atlantic (though more data are needed to confirm an Atlantic contribution to modern day Arctic flora). Unique rare haplotypes in Northern Alaska and

			Northern Labrador also suggest at an additional refugial population contributing to Arctic recolonization.
Palmaria palmata (Fig. E21)	0/9/68	Atlantic	Arctic collections are a clear north extension of Northwest Atlantic populations. Though this species is reported from Northern Alaska and the North Pacific, it has not been genetically verified from these regions (these reports likely represent other species of *Palmaria*; Wilce & Dunton 2014; Guiry & Guiry 2018; Saunders *et al.* 2018).
Peyssonnelia rosenvingei **(New)** (Fig. E22)	1/7/34	Uncertain	A single haplotype extends from the Northern Bering Sea to the Northwest Atlantic, suggesting at recent dispersal across the Arctic, through the direction of migration remains uncertain.
Phycodrys fimbriata[2, 3] **(Updated)** (Fig. E23)	18/45/69	Atlantic (Arctic and Atlantic)	A number of unique Arctic haplotypes occur in this species, particularly in Northern Alaska and along the coasts of Baffin Island and Northern Labrador. One Arctic haplotype can be confirmed as Atlantic in origin, while a widely distributed haplotype (occurring in the North Pacific through to Southern Labrador) suggests at recent trans-Arctic dispersal, though the direction of migration remains uncertain. Detailed population level analyses are needed in this species to determine what role, if any, Pacific populations played in Arctic recolonization since the Last Glacial Maximum.
Phymatolithon tenue **(New)** (Fig. E24)	0/1/1	Uncertain	As in *Leptophytum foecundum*, the West Arctic haplotype does not match the Atlantic mitotype, however, there are too few collections to determine the source population in this species.
Polyostea arctica[1, 3] **(Updated)** (Fig. E25)	0/11/5	Atlantic (Arctic and Atlantic)	North Pacific collections of *Polyostea* are not attributable to this species (see Chapter 2), suggesting *Polyostea arctica* is limited to the Atlantic basin in its distribution. Given the lack of North Pacific records, Arctic populations in this species,

			tentatively, are inferred to have origins in the Northwest Atlantic. Two unique Arctic haplotypes are notable in this species, but may be an artifact of the low number of records from the Northwest Atlantic.
Polysiphonia sp. 1stricta (Fig. E26)	28/4/34	Uncertain	This genetic group has no COI-5P haplotype variation despite a broad trans-Arctic distribution. This group is another contender for having origins in the Northwest Pacific. More sampling and/or a more variable marker is required; for now, origins of Arctic populations remain uncertain.
Polysiphonia sp. 3stricta[1] (Fig. E27)	0/3/26	Atlantic (Arctic)	This genetic group has only been confirmed in the Northwest Atlantic, with North Pacific collections attributable to *P*. sp. 1stricta (Table S3). Phylogeographic analyses also suggest this species has origins in the North Atlantic (see Chapter 2). As such, Arctic populations tentatively have origins in the Northwest Atlantic, however, unique Churchill haplotypes suggest at Arctic refugial contributions in this species.
Ptilota gunneri (Fig. E28)	0/1/41	Atlantic	A rare member of the Northwest Atlantic flora, this species appears to have recent origins in the Northeast Atlantic, with recent migration into the Arctic.
Ptilota serrata **(New)** (Fig. E29)	2/10/63	Uncertain	Though this species is genetically verified from the Bering Sea and the Northeast Pacific (MG762003, MG762004), COI data is restricted to the Atlantic and Arctic basins. As such, the source for Arctic populations remains uncertain, pending COI data from the Pacific.
Rhodochorton purpureum[3] **(New)** (Fig. E30)	*rbc*L-3P: 0/3/1	Atlantic (Arctic and Atlantic)	The limited number of genetically verified records suggests this species has recent origins in the Northwest Atlantic.
Rhodomela lycopodioides (Fig. E31)	0/3/106	Atlantic	A single collection from Churchill, matches the COI-5P haplotype of European populations, however, the ITS type for this specimen matches the Northwest Atlantic (Cripps 2018),

			indicating admixture between trans-Atlantic populations has occurred.
Rhodomela sibirica[2] **(Updated)** (Fig. E32 & E33)	COI-5P: 23/44/0 ITS: 22/42/0	Pacific (Arctic and Pacific)	COI-5P haplotype variation in the North Pacific suggests this species has a long history in the area, with haplotype variation declining towards the Eastern Arctic. COI-5P haplotype variation is highest, however, in Northern Alaska. Similarly, ITS data suggested that specimens from the East Arctic were recolonized out of the North Pacific, while specimens from the West Arctic are distinct from these populations; refugial Arctic contributions are a possibility.
Rhodomela sp. 1virgata[1, 3] (Fig. E34)	14/15/7	Uncertain (Arctic)	Arctic collections do not match North Pacific or Northwest Atlantic haplotypes, with the latter two populations sharing haplotypes. The location of origin Arctic populations therefore remains uncertain.
Rhodomela virgata **(Updated)** (Fig. E35)	37/31/2	Pacific	Haplotype variation is monotypic through the Arctic and into the Atlantic, while several private haplotypes occur in the North Pacific, suggesting this species recently migrated Eastward through the Arctic.
Rhodophysemopsis hyperborea[3] **(New)**	0/1/0	Uncertain (Arctic)	A single genetic record exists from Northern Labrador. The origin of Arctic populations therefore remains uncertain.
Rhodophysema kjellmanii[1]	0/2/0	Uncertain (Arctic)	Two records exist for this genetic group from Churchill. As such, the origin of this group remains uncertain.
Scagelia pylaisaei[3] (Fig. E36)	65/24/32	Pacific (Arctic and Pacific)	A phylogenetic break occurs between Atlantic and Pacific populations, with Arctic collections matching Pacific populations. The Pacific lineage also appears to be admixing with the Atlantic populations along the coast of Labrador.
Turnerella pennyi **(New)** (Fig. E37)	*rbc*L-3P: 0/9/3	Atlantic	This species is genetically verified in the Arctic and in the Northwest Atlantic, meaning Arctic populations likely have recent origins out of the Atlantic.

Waernia mirabilis **(New)** (Fig. E38)	0/6/4	Atlantic	Arctic specimens in Northern Labrador match a Northwest Atlantic haplotype.
Wildemania miniata **(New)** (Fig. E39)	0/6/45	Atlantic	As in *Waernia mirabilis*, Arctic specimens match Northwest Atlantic populations.
Phaeophyceae			
Agarum clathratum **(Updated)** (Fig. E40)	101/9/50	Pacific	Haplotype variation indicates this species has a relatively long history in the Pacific. Haplotype variation also declines from the Pacific through to the Northwest Atlantic, suggesting at recent Pacific origins (confirming the speculation of Boo *et al.* [2011]). Barring the Northwest Pacific collections, the nearly monotypic haplotype variation extending through the Arctic into the Northwest Atlantic is reminiscent of several species listed here (e.g. *A. borealis*, *Chorda* sp. 1filum, *Dilsea socialis*, and *Polysiphonia* sp. 1stricta).
Alaria esculenta[1, 2, 3] **(Updated)** (Fig. E41)	0/16/51	Atlantic (Arctic and Atlantic)	A shallow genetic break occurs between Northwest and Northeast Atlantic populations, with the Northeast Atlantic haplotype matching specimens in Northern Labrador. COI-5P data for Nome specimens, however, were attributable to *Alaria crispa.* Nonetheless, ITS data suggest these specimens are *Alaria esculenta* sensu lato, sharing genetic signatures with *A. crispa* and Arctic *A. esculenta*; introgression or incomplete lineage sorting between Nome and Arctic *Alaria* is a possibility. Given the limited sampling in the North Pacific, Arctic haplotypes may have originated from the Pacific. These patterns may also be indicative of an Arctic refugial population, similar to *R. sibirica*.
Ascophyllum nodosum **(New)**	0/1/2	Atlantic	Despite being an abundant member of intertidal flora in cold temperate Northwest Atlantic waters, genetic records are

(Fig. E42)			limited in this group. This is an Atlantic species, making this the origin for our lone Arctic specimen, collected as drift in Northern Labrador.
Battersia arctica **(New)** (Fig. E43)	*rbc*L-3P: 1/3/2	Uncertain	This species has limited records in both the North Pacific and the Northwest Atlantic both matching the Arctic haplotype, rendering assignment of a source for Arctic populations problematic.
Battersia racemosa **(Updated)** (Fig. E44)	0/1/1	Atlantic	A single Arctic record exists from Churchill, matching a Northwest Atlantic record. In addition, this genetic group is verified in the Northeast Atlantic (based on *rbc*L; AJ287880). Origins for sampled Arctic populations are therefore tentatively inferred as being Atlantic.
Chaetopteris plumosa [1, 2, 3] **(New)** (Fig. E45)	0/16/19	Atlantic (Arctic and Atlantic)	A genetic break occurs between the two haplotypes sampled, both of which occur in the Arctic. One haplotype is attributable to the Atlantic, while the other may originate from the Pacific, though more sampling is needed to confirm this. Haplotype patterns may also indicate origins in Arctic refugia. Interpretation of these patterns is tentative, pending further study.
Chorda sp. 1filum **(Updated)** (Fig. E46)	23/14/2	Uncertain	Haplotype variation is monotypic in this genetic group, extending from the North Pacific to the Northwest Atlantic (Makkovik, Newfoundland); thus, the hypothesized Pacific origins inferred by Saunders & McDevit (2013) are, at present, not supported by the additional collections available here.
Chordaria chordaeformis **(Updated)** (Fig. E47)	32/21/1	Uncertain	This species has the same haplotype pattern as *Chorda* sp. 1filum.

Chordaria flagelliformis[1, 3] (Fig. E48)	0/23/56	Atlantic (Arctic and Atlantic)	Haplotype variation in this species suggests at a long history in the Northwest Atlantic. Despite unique haplotypes in the Arctic collections, the lack of North Pacific records matching this species (which were attributable to a closely related genetic group) suggests Arctic populations originated from the Atlantic basin. This species is also genetically verified in Northern Europe, including Svalbard, based on *rbc*L data (AB066076, AB066073, AB066075, JN599169), corresponding to Atlantic group-3a in Kim & Kawai (2002).
Chordariacean sp. 4nov	0/1/1	Atlantic	With only two records, this genetic group is tentatively hypothesized to have originated from the Atlantic.
Cladosiphon sp. 1NFLD[3] **(New)**	0/1/0	Uncertain (Arctic)	A single collection for this genetic group occurs in Northern Labrador.
Desmarestia sp. 1aculeata (Fig. E49)	0/13/30	Atlantic	Specimens of *Desmarestia* in the Northern Bering Sea were attributable to *Desmarestia* sp. 2aculeata and *Desmarestia viridis*. This genetic group, on the other hand, has only been recovered in the Atlantic, making this the source for Arctic populations.
Dictyosiphon sp. 1GWS (Fig. E50)	40/1/1	Pacific	The single Arctic record from Churchill, matches a Pacific haplotype, while a single Atlantic collection appears to be divergent from Pacific collections. This genetic group is also verified from Russia based on *rbc*L data (AY372973).
Dictyosiphon foeniculaceus[3] (Fig. E51)	0/4/47	Atlantic (Arctic and Atlantic)	Haplotype variation in the Northwest Atlantic suggests this species has survived multiple glaciations in the area, with records of *Dictyosiphon* from the North Pacific attributable to *Dictyosiphon* sp. 1GWS. Arctic haplotypes match Atlantic populations.
Ectocarpoid sp. **(New)**	0/2/0	Uncertain (Arctic)	This genetic group has been sampled from Northern Labrador (our study) and from Baffin Island (LT546267; Küpper *et al*. 2016).

Ectocarpus sp. **(New)**	0/2/0	Uncertain (Arctic)	As above, this genetic group was sampled in our study, in Northern Labrador, and by Küpper *et al.* (2016) on Baffin Island (LT546288).
Eudesme virescens **(New)** (Fig. E52)	18/5/14	Atlantic and Pacific	Haplotypes sampled in Northern Labrador match Atlantic and Pacific records, indicating admixture between these populations in the Arctic.
Fucus distichus[1] (Fig. E53)	73/2/34	Uncertain (Arctic)	The Arctic haplotype recovered in this species also occurs in the Atlantic and Pacific, meaning a source for Arctic populations cannot be confidently ascribed in this species. Recent work, however, suggests this species survived in Arctic refugial populations, seeding the Atlantic and Pacific out of the Arctic (Laughinghouse *et al.* 2015).
Halosiphon sp. 2tomentosus (Fig. E54)	2/1/0	Pacific	PCR success was low for Arctic *Halosiphon* suggesting primer issues. Given the lack of Atlantic records, Arctic populations in this species are, tentatively, of Pacific origin, though an effort should be made to generate sequence data in previously failed PCRs for *Halosiphon*, particularly from the Northwest Atlantic. This genetic group, however, is previously reported from the North Pacific (Kawai & Sasaki 2000), with *rbc*L data for Arctic collections matching Pacific rather than Atlantic collections for this species (Saunders & McDevit 2013).
Halothrix lumbricalis[3] **(New)** (Fig. E55)	0/2/1	Atlantic (Arctic and Atlantic)	Two Arctic specimens were sampled from Northern Labrador, one of which matched a Northwest Atlantic haplotype, while the other was unique. This group is genetically verified from Greenland (published as *Elachista fucicola*; AF055398; Siemer *et al.* 1998).
Haplospora globosa **(Updated)** (Fig. E56)	1/1/6	Uncertain	A single Arctic collection matches a haplotype sampled in both the Northeast Atlantic and the North Pacific, meaning a source for Arctic populations cannot be inferred.

Heterosaundersella sp. 1NFLD[3]	0/1/0	Uncertain (Arctic)	A single record for this genetic group was recovered from Northern Labrador.
Laminaria digitata (Fig. E57)	0/2/63	Atlantic	The source for Arctic populations is hypothesized to be the Atlantic, where this species is believed to have evolved (Rothman *et al.* 2017).
Laminaria solidungula[2, 3] **(Updated)** (Fig. E58)	0/18/1	Atlantic (Arctic and Atlantic)	East and West Arctic specimens represent different mitotypes, with the East Arctic haplotype matching a Northwest Atlantic record. The inference of Pacific contributions to Arctic recolonization awaits genetic confirmation of this species in the Pacific.
Leptonematella fasciculata[1]	0/3/0	Uncertain (Arctic)	The few records that exist for this genetic group occur in Churchill, meaning a source population cannot be inferred.
Lithoderma sp. 2GWS (Fig. E59)	*rbc*L-3P: 0/1/1	Uncertain	Records of this species are from Northern Alaska and the Northwest Atlantic, however, given the disjunct sampling distribution and limited number of records, the source basin for this species remains uncertain.
Petalonia fascia[3] (Fig. E60)	47/11/43	Uncertain	One Arctic haplotype matches Atlantic collections, but a complex haplotype network in this species extends throughout the Atlantic and Pacific. In addition, this species is genetically verified in the Northwest Pacific (based on ITS and *rbc*L data; AY154725, AB578997), and from the Northeast Atlantic (based on PSA and *rbc*L data; AY372953, AB860190, AB860189), which are not included in our haplotype map/network. It is therefore unclear where Arctic populations originated from.
Petalonia filiformis[3] **(Updated)** (Fig. E61)	0/24/19	Atlantic (Arctic and Atlantic)	Genetic variation along the coast of Labrador and the absence of specimens attributable to *Petalonia filiformis* from the North Pacific, suggest this species survived the Last Glacial Maximum in the Northwest Atlantic and has subsequently moved into the Canadian Arctic.

Planosiphon complanatus **(New)** (Fig. E62)	0/1/7	Atlantic	A single Arctic specimen from Baffin Island matches Northwest Atlantic collections.
Planosiphon zosterifolius[3] **(New)** (Fig. E63)	8/1/7	Uncertain (Arctic)	A single Arctic collection does not match limited collections from the Northern Bering Sea and the North Atlantic. The origin of Arctic populations therefore remains uncertain at this time.
Platysiphon glacialis **(New)** (Fig. E64)	16/3/0	Pacific	This species previously had genetically verified records only from Northern Baffin Island (Kawai *et al.* 2015). The presence of this species in the North Pacific suggests this is the source for Arctic populations.
Punctaria sp. 2GWS (Fig. E65)	2/5/5	Uncertain	Limited collections and a lack of haplotypes in this group impedes further consideration of the source for Arctic populations. In addition, this group is genetically verified in Greenland (AF055410) and Japan (AB302316) based on *rbc*L data.
Pylaiella sp. 1littoralis (Fig. E66)	0/5/23	Atlantic	Haplotype variation suggests this species has survived multiple glaciations on both sides of the North Atlantic, with a single Arctic haplotype matching Northwest Atlantic variation. Specimens in the North Pacific are attributable to other genetics groups within *Pylaiella* (Saunders & McDevit 2013).
Pylaiella washingtoniensis[1, 3] **(Updated)** (Fig. E67)	32/28/29	Atlantic and Pacific (Arctic, Atlantic, and Pacific)	A haplotype recovered in the West Arctic matches Pacific populations, while the haplotypes in Churchill are either unique or of Atlantic origin. Baffin Island and Northern Labrador similarly display unique haplotypes despite reasonably extensive sampling in the Atlantic and Pacific basins.

Saccharina latissima[1] (Fig. E68)	14/46/119	Atlantic and Pacific (Arctic, Atlantic, and Pacific)	Atlantic and Pacific lineages are in secondary contact in the Arctic, a finding consistent with ITS data (McDevit & Saunders 2010).
Saccharina nigripes[3] (Fig. E69)	20/17/10	Atlantic (Arctic and Atlantic)	Arctic records match an Atlantic haplotype.
Saccorhiza dermatodea **(New)** (Fig. E70)	0/1/19	Atlantic	A single Arctic record from Baffin Island matches a Northwest Atlantic haplotype.
Scytosiphon sp. 1crust[1]	0/1/0	Uncertain (Arctic)	A single record exists for this genetic group from Churchill.
Scytosiphon canaliculatus (Fig. E71)	80/5/64	Uncertain	The two Arctic haplotypes sampled in this species are trans-Arctic, extending from the Northwest Pacific to the Northwest Atlantic, meaning the origin of Arctic populations remains uncertain at this time.
Scytosiphon sp. GroupJ[3] **(New)** (Fig. E72)	0/1/9	Uncertain (Arctic)	This genetic group appears to have a disjunct distribution, with collections limited to Baffin Island and the New England States, with the single Arctic collection representing a unique haplotype. The origin of Arctic populations therefore remains uncertain at this time.
Stictyosiphon soriferus[1]	0/1/0	Uncertain (Arctic)	A single genetic record exists for this genetic group, occurring in Churchill.
Stictysiphon tortilis[1]	0/9/0	Uncertain (Arctic)	Genetic records for this species are limited to Churchill.
Ralfsia fungiformis **(New)** (Fig. E73)	13/1(*rbc*L)/14	Uncertain	This species is genetically verified from Baffin Island based on *rbc*L data, however, we were unable to generate COI-5P data to include in the haplotype map/network. Given Atlantic and Pacific populations appear to be divergent, COI-5P data

			from Arctic collections will likely be informative as to recent origins in these populations.
Tilopteridalean sp. 1GWS[3] **(New)** (Fig. E74)	0/2/2	Atlantic (Arctic and Atlantic)	Two Arctic collections are from Northern Labrador. One matches North Atlantic collections, while the other represents a unique haplotype; the origin of Arctic populations is therefore tentatively Atlantic, though more collections are needed in this genetic group.
Tilopteridalean sp. 2GWS[2, 3] (Fig. E75)	0/4/0	Uncertain (Arctic)	This genetic group has only been collected in the Arctic, meaning recent origins remain uncertain.
Tilopteridalean sp. 3GWS[2]	0/2/0	Uncertain (Arctic)	Only two records exist for this genetic group, both from Northern Alaska.
Ulvophyceae			
*Acrosiphoni*a sp. 3GWS[1] (Fig. E76)	*tufA*: 0/2/3	Atlantic (Arctic, Atlantic)	Few genetic records exist for this genetic group, however, the origin of Arctic populations is tentatively assigned to the Atlantic.
Acrosiphonia sp. 6GWS **(Updated)** (Fig. E77)	*tufA*: 0/1/2	Atlantic	The same scenario occurs in this species as in *Acrosiphonia* sp. 3GWS.
Acrosiphonia sp. 8GWS **(New)** (Fig. E78)	*tufA*: 5/1/1	Atlantic	This genetic group occurs in all three oceans, however, the single Arctic collection from Baffin Island matches a single Northwest Atlantic record.
Acrosiphonia sonderi **(New)** (Fig. E79)	*tufA*: 2/2/11	Uncertain	A single haplotype extends from the Northwest Pacific to the Northwest Atlantic, meaning the origin of Arctic populations remains uncertain at this time.
Blidingia sp. 5GWS[1, 2] (Fig. E80)	*tufA*: 0/2/0	Uncertain (Arctic)	Two genetic records exist for this genetic group, both occurring in the Arctic.
Monostroma sp. 2grevillei[3] **(New)** (Fig. E81)	*tufA*: 0/1/40	Uncertain (Arctic)	A single Arctic record for this genetic group does not match the single North Atlantic haplotype, making the origin of Arctic populations uncertain at this time.

Spongomorpha aeruginosa (Fig. E82)	*tufA*: 0/1/9	Atlantic	This species lacks North Pacific records and is not reported from the Pacific. As such, the source for Arctic populations is inferred to be the Atlantic.
Rosenvingiella sp.[3] **(New)**	*tufA*: 0/1/0	Uncertain (Arctic)	A single Arctic collection for this genetic group exists from Northern Labrador.
Ulothrix flacca (Fig. E83)	*rbc*L-3P: 0/1/4	Atlantic	We did not recover this species while sampling the North Pacific, however, it is reported from the area (Guiry & Guiry 2018). The origin of Arctic populations is therefore tentatively Atlantic.
Ulva lactuca (Fig. E84)	*tufA*: 69/4/97	Pacific	North Pacific populations match the Arctic haplotype recovered in Churchill, corroborating the inference of Pacific origins made by Saunders and McDevit (2013). This species is also confirmed in Japan (based on *rbc*L; AB097622).
Ulva obscura[3] **(New)** (Fig. E85)	*tufA*: 20/2/74	Atlantic (Arctic and Atlantic)	Pacific and Atlantic haplotypes are distinct in this species, with one Arctic specimen matching the latter. The second Arctic specimen represents a unique haplotype but allies most closely with Pacific collections.
Ulva prolifera[2] (Fig. E86)	*tufA*: 0/9/16	Atlantic (Arctic and Atlantic)	East Arctic haplotypes match Atlantic populations, while the West Arctic haplotype differs from Atlantic populations by three substitutions, sharing signatures with a closely related genetic group (*Ulva* sp. 2prolifera) sampled in Northern British Columbia (though this specimen differs by another five substitutions from the West Arctic haplotype). This species is also confirmed in the Northwest Pacific (based on *rbc*L; KP233770). Given species delineations are not clear in this group, Atlantic origins for Arctic populations are tentatively inferred, but further sampling in the Pacific is likely to revise this scenario.

References

Boo GH, Lindstrom SC, Klochkova NG, *et al.* (2011) Taxonomy and biogeography of *Agarum* and *Thalassiophyllum* (Laminariales, Phaeophyceae) based on sequences of nuclear, mitochondrial, and plastid markers. *Taxon*, **60**, 831–840.

Cripps KSA (2018) Unravelling *Rhodomela* spp. in Eastern Canadian waters: revisions in a cryptic red algal genus of the Ceramiales (Florideophyceae). Thesis (honours), University of New Brunswick.

Guiry M, Guiry G (2018) AlgaeBase. http://www.algaebase.org.

Kawai H, Hanyuda T, Yamagishi T, *et al.* (2015) Reproductive morphology and DNA sequences of the brown alga *Platysiphon verticillatus* support the new combination *Platysiphon glacialis*. *Journal of Phycology*, **51**, 910–917.

Kawai H, Sasaki H (2000) Molecular phylogeny of the brown algal genera *Akkesiphycus* and *Halosiphon* (Laminariales), resulting in the circumsription of the new families Akkesiphycaceae and Halosiphonaceae. *Phycologia*, **39**, 416–428.

Kim SH, Kawai H (2002) Taxonomic revision of *Chordaria flagelliformis* (Chordariales, Phaeophyceae) including novel use of the intragenic spacer region of rDNA for phylogenetic analysis. *Phycologia*, **41**, 328–339.

Küpper FC, Peters AF, Shewring DM, *et al.* (2016) Arctic marine phytobenthos of northern Baffin Island. *Journal of Phycology*, **52**, 532-549.

Laughinghouse HD, Müller KM, Adey WH, Lara Y, Young R, Johnson G (2015) Evolution of the Northern Rockweed, *Fucus distichus*, in a regime of glacial cycling: implications for benthic algal phylogenetics. *PloS ONE*, **10**, e0143795.

McDevit DC, Saunders GW (2010) A DNA barcode examination of the Laminariaceae (Phaeophyceae) in Canada reveals novel biogeographical and evolutionary insights. *Phycologia*, **49**, 235−248.

Rothman MD, Mattio L, Anderson RJ, Bolton JJ (2017) A phylogeographic investigation of the kelp genus *Laminaria* (Laminariales, Phaeophyceae), with emphasis on the south Atlantic Ocean. *Journal of Phycology*, **53**, 778–789.

Saunders GW, Jackson C, Salomaki ED (2018) Phylogenetic analyses of transcriptome data resolve familial assignments for genera of the red-algal Acrochaetiales-Palmariales Complex (Nemaliophycidae). *Molecular Phylogenetics and Evolution*, **119**, 151–159.

Saunders GW, McDevit DC (2013) DNA barcoding unmasks overlooked diversity improving knowledge on the composition and origins of the Churchill algal flora. *BMC Ecology*, **13**, 9.

Siemer BL, Stam WT, Olsen JL, Pedersen PM (1998) Phylogenetic relationships of the brown algal orders Ectocarpales, Chordariales, Dictyosiphonales, and Tilopteridales (Phaeophyceae) based on RUBISCO large subunit and spacer sequences. *Journal of Phycology*, **34**, 1038–1048.

Wilce RT, Dunton KH (2014) The Boulder Patch (North Alaska, Beaufort Sea) and its benthic algal flora. *ARCTIC*, **67**, 43–56.

Wynne MJ, Heine JN (1992) Collections of marine red algae from St. Matthew and St. Lawrence Islands, the Bering Sea. *Nova Hedwigia*, **55**, 55−97.

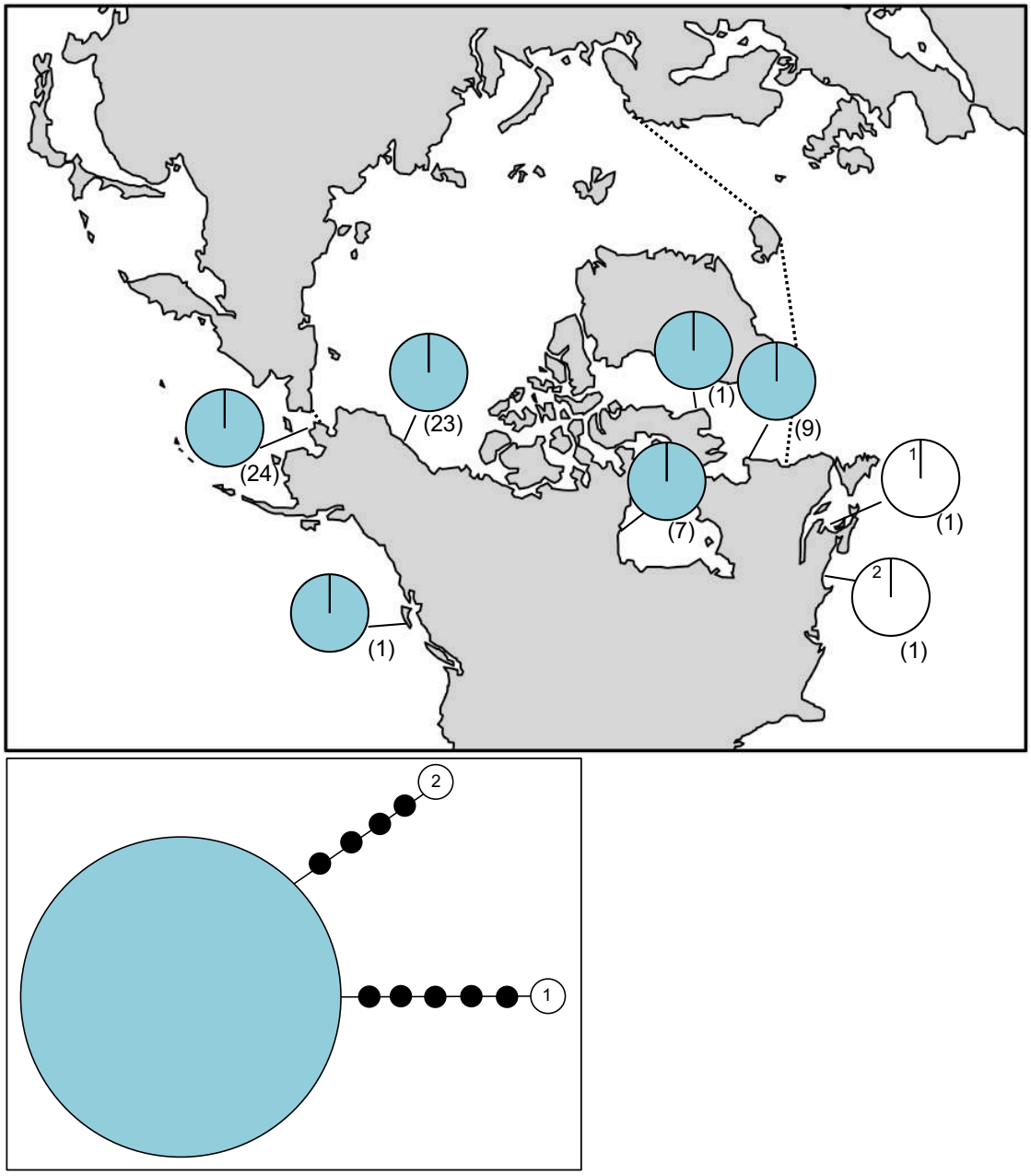

Figure E1. *Ahnfeltia borealis* haplotype map and network based on COI-5P data. In the map, numbers in parentheses refer to sample sizes from given locales, whereas numbers adjacent to white portions of pie charts refer to a haplotype sampled only once in the accompanying network. The dashed line indicates delineation of the Arctic Ocean. In the haplotype network, numbered haplotypes in white reference back to the map. Black circles indicate hypothesized (e.g. unsampled) haplotypes between clades. Circle size is proportional to the sampling frequency of a given haplotype.

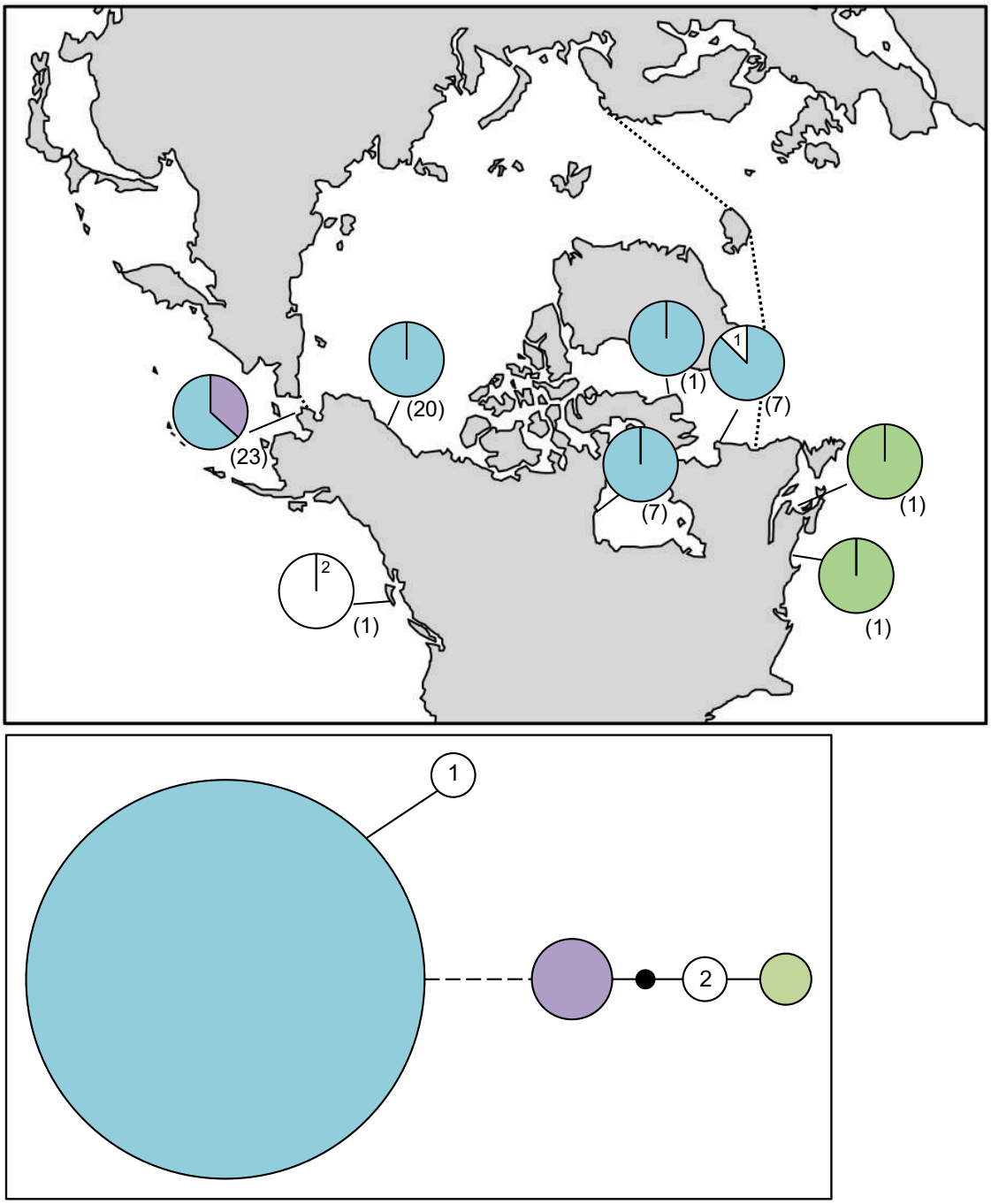

Figure E2. ***Ahnfeltia borealis*** **haplotype map and network based on ycf35 data. In the map, numbers in parentheses refer to sample sizes from given locales, whereas numbers adjacent to white portions of pie charts refer to a haplotype sampled only once in the accompanying network. In the map, the dashed line indicates delineation of the Arctic Ocean. In the haplotype network, numbered haplotypes in white reference back to the map, the black circle represents a hypothesized (e.g. unsampled) haplotype between clades, and the dashed line refers to a two base pair insertion. Circle size is proportional to the sampling frequency of a given haplotype.**

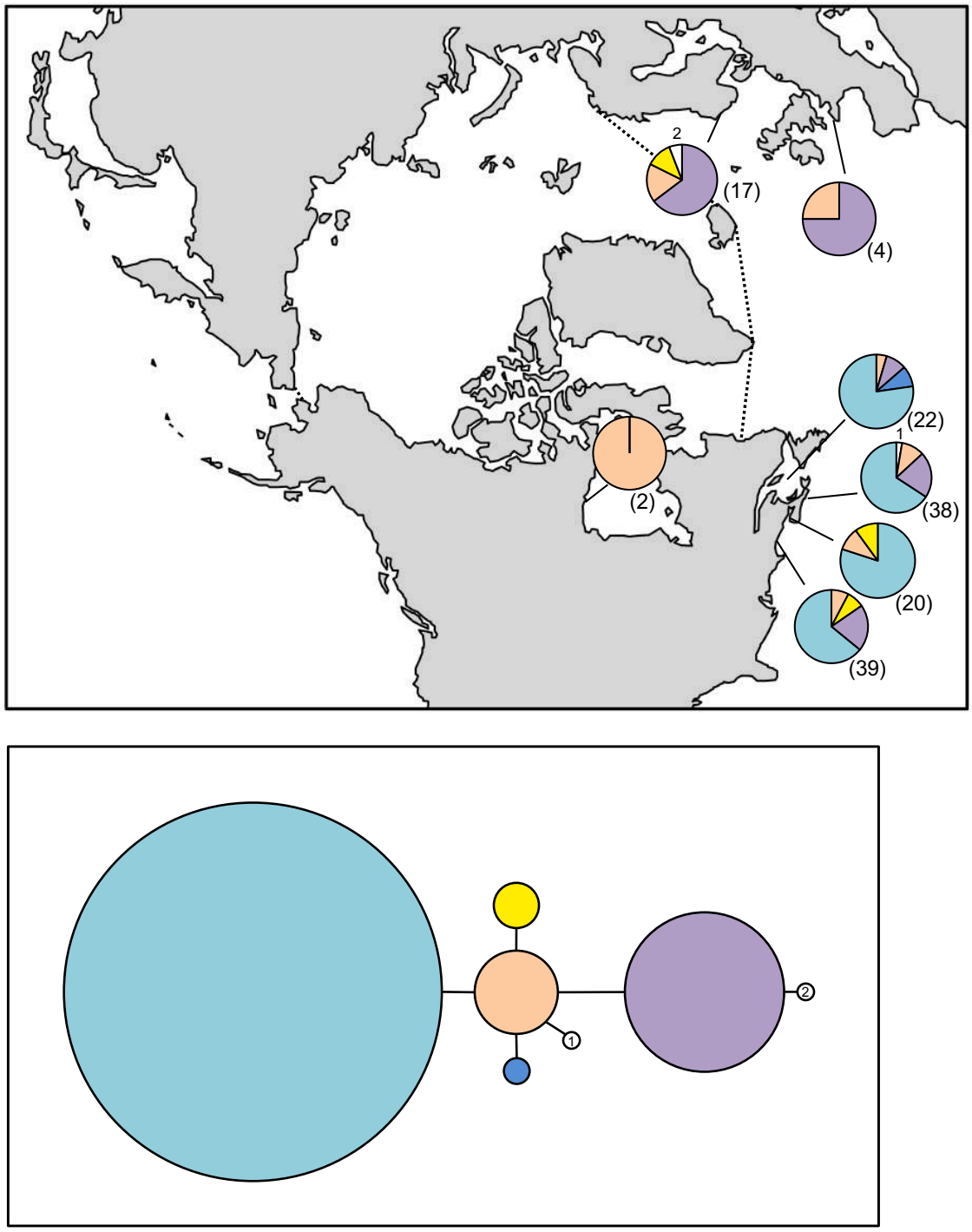

Figure E3. *Ahnfeltia plicata* haplotype map and network based on COI-5P data. In the map, numbers in parentheses refer to sample sizes from given locales, whereas numbers adjacent to white portions of pie charts refer to a haplotype sampled only once in the accompanying network. The dashed line indicates delineation of the Arctic Ocean. In the haplotype network, numbered haplotypes in white reference back to the map. Circle size is proportional to the sampling frequency of a given haplotype.

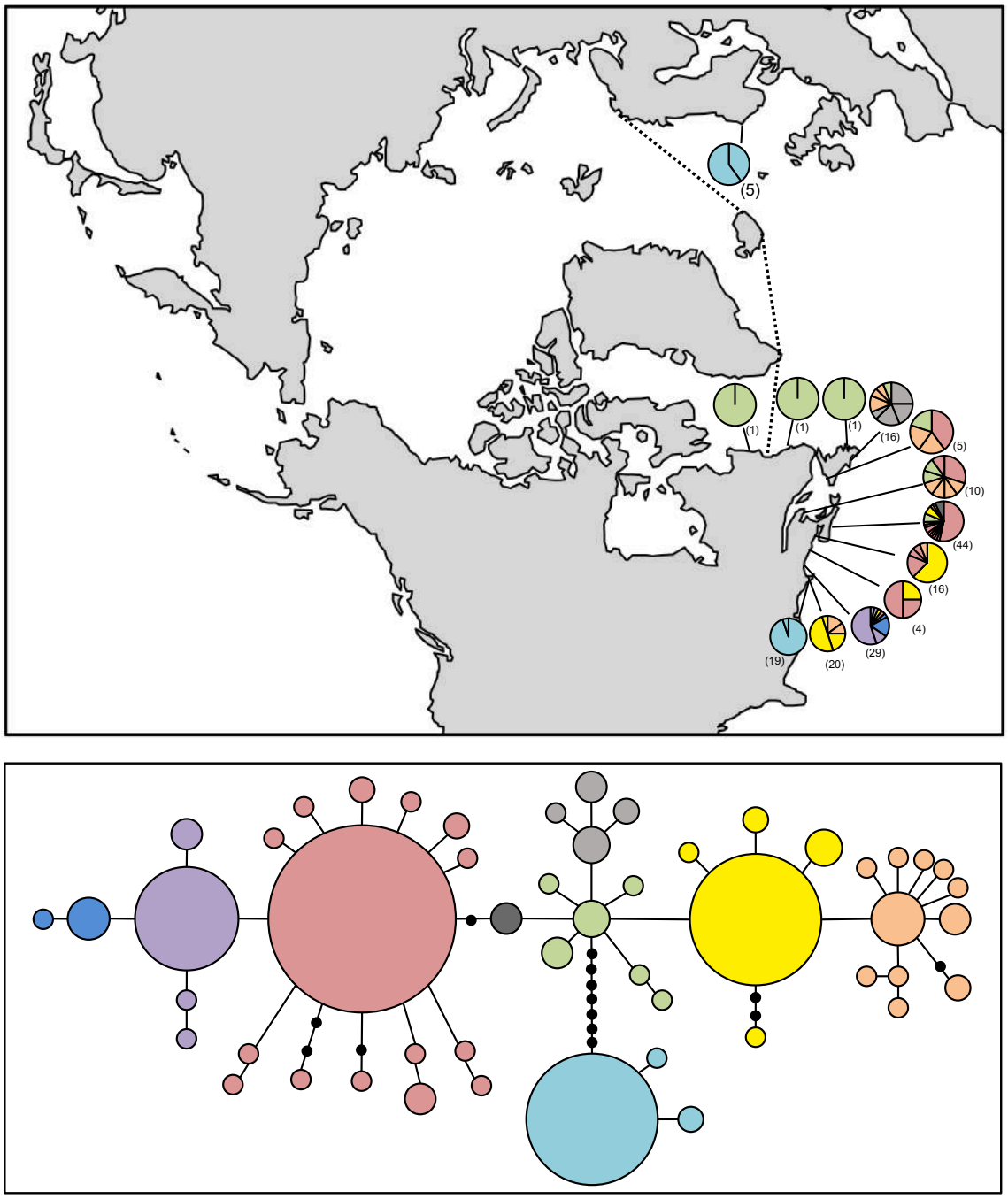

Figure E4. *Ceramium virgatum* haplotype map and network based on COI-5P data. In the map, numbers in parentheses refer to sample sizes from given locales. The dashed line indicates delineation of the Arctic Ocean. Circle size is proportional to the sampling frequency of a given haplotype. Black circles indicate hypothesized (e.g. unsampled) haplotypes between clades.

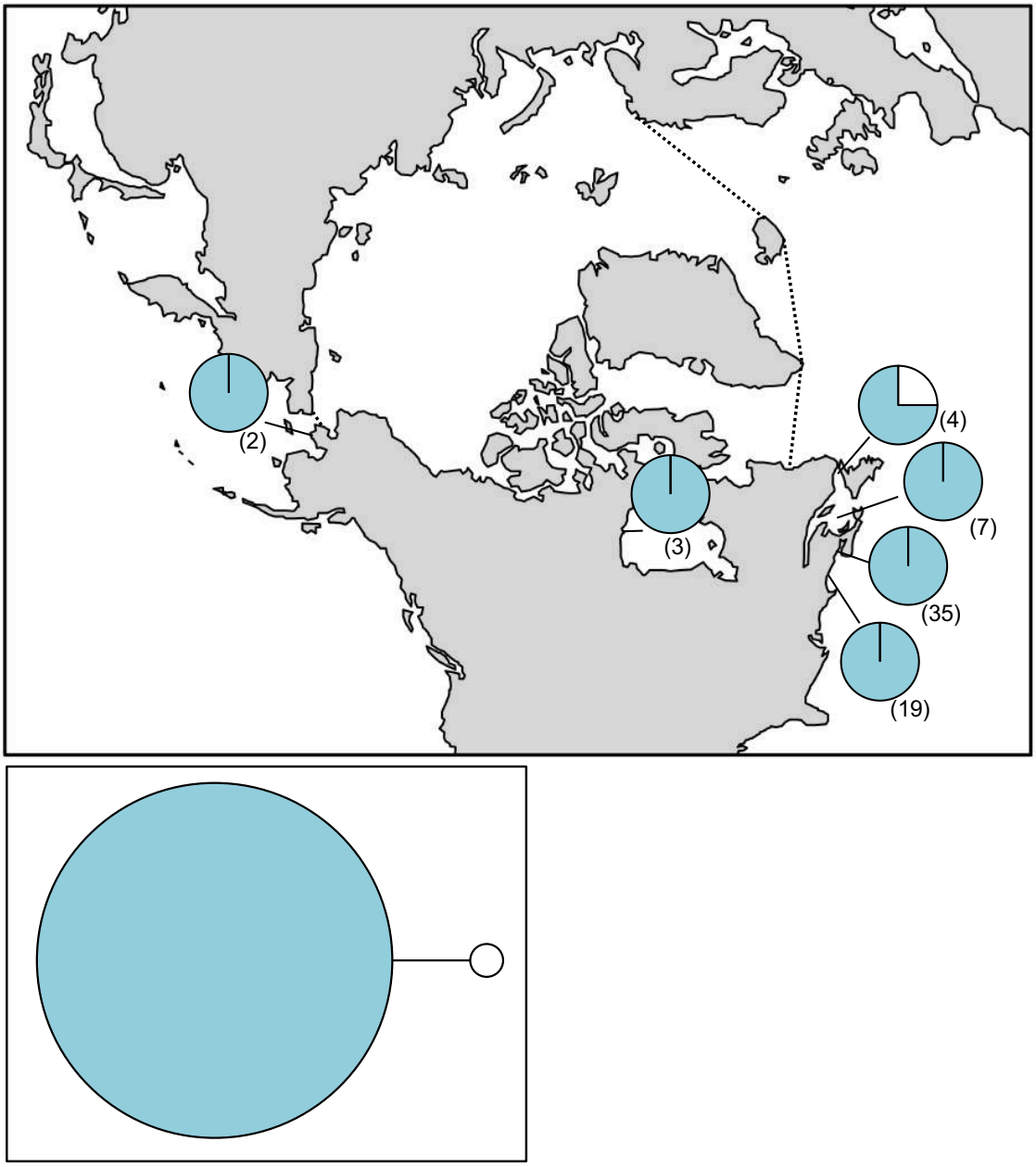

Figure E5. *Clathromorphum* sp. 9GWS haplotype map and network based on COI-5P data. In the map, numbers in parentheses refer to sample sizes from given locales. The dashed line indicates delineation of the Arctic Ocean. In the haplotype network, circle size is proportional to the sampling frequency of a given haplotype.

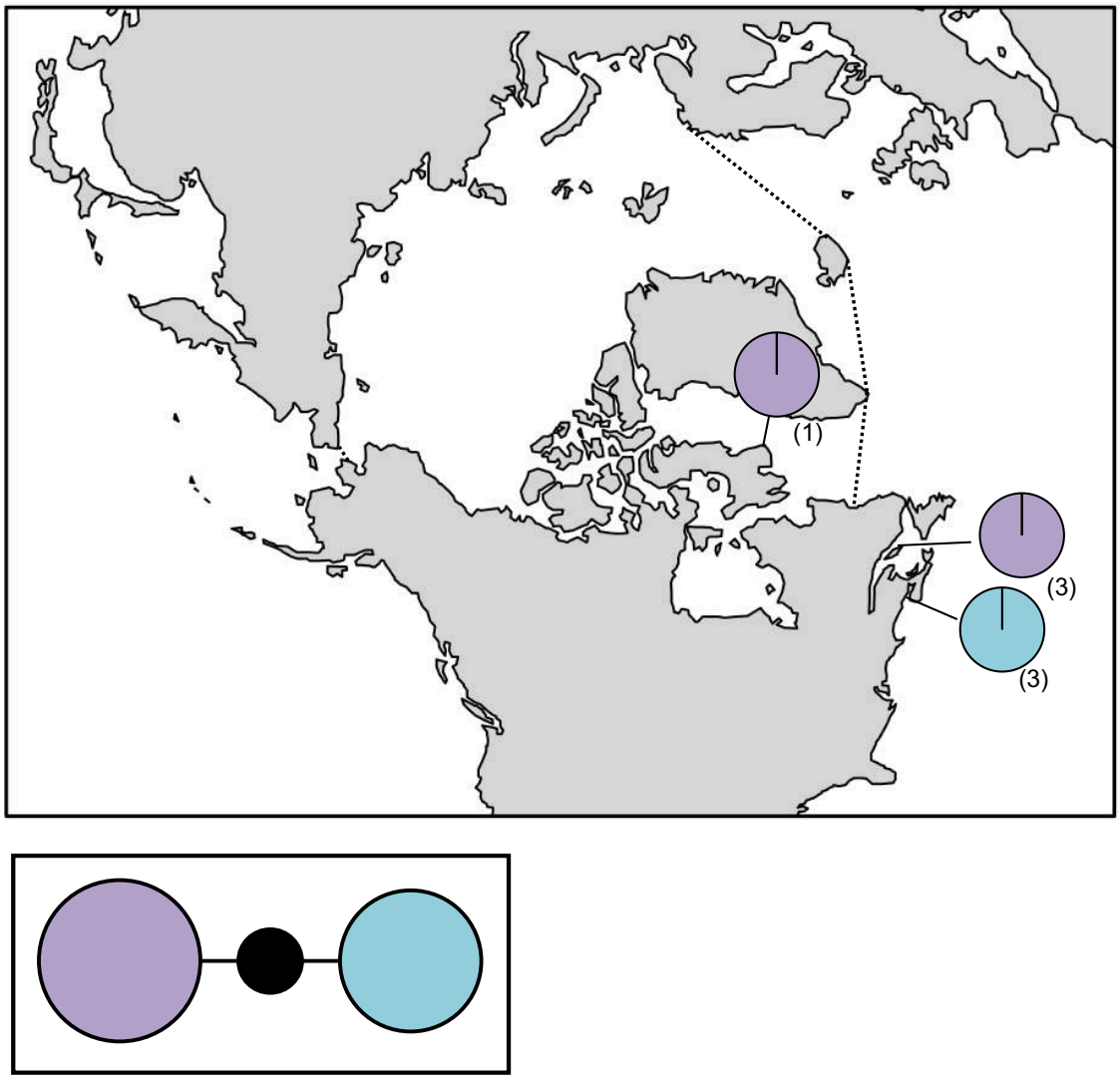

Figure E6. ***Clathromorphum circumscriptum*** **haplotype map and network based on COI-5P data. In the map, numbers in parentheses refer to sample sizes from given locales. The dashed line indicates delineation of the Arctic Ocean. In the haplotype network, the black circle indicates a hypothesized (e.g. unsampled) haplotype between clades. Circle size is proportional to the sampling frequency of a given haplotype.**

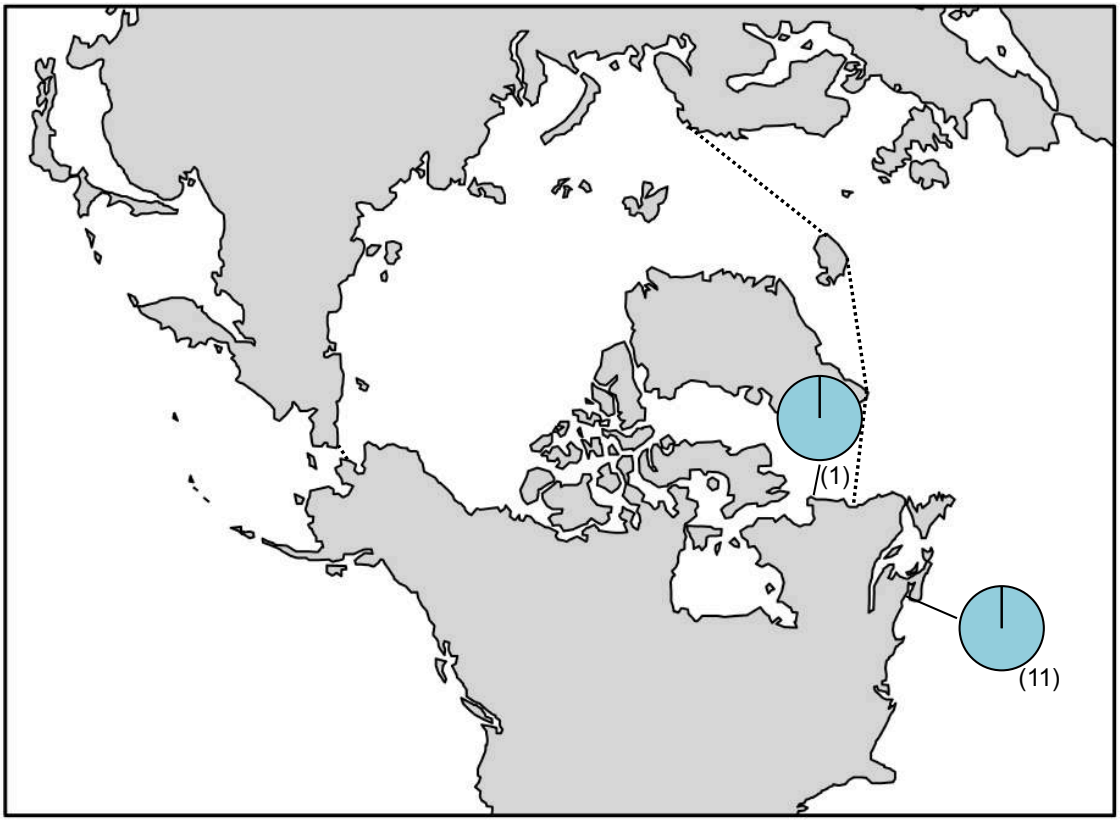

Figure E7. ***Clathromorphum compactum*** **haplotype map and network based on COI-5P data. In the map, numbers in parentheses refer to sample sizes from given locales. The dashed line indicates delineation of the Arctic Ocean.**

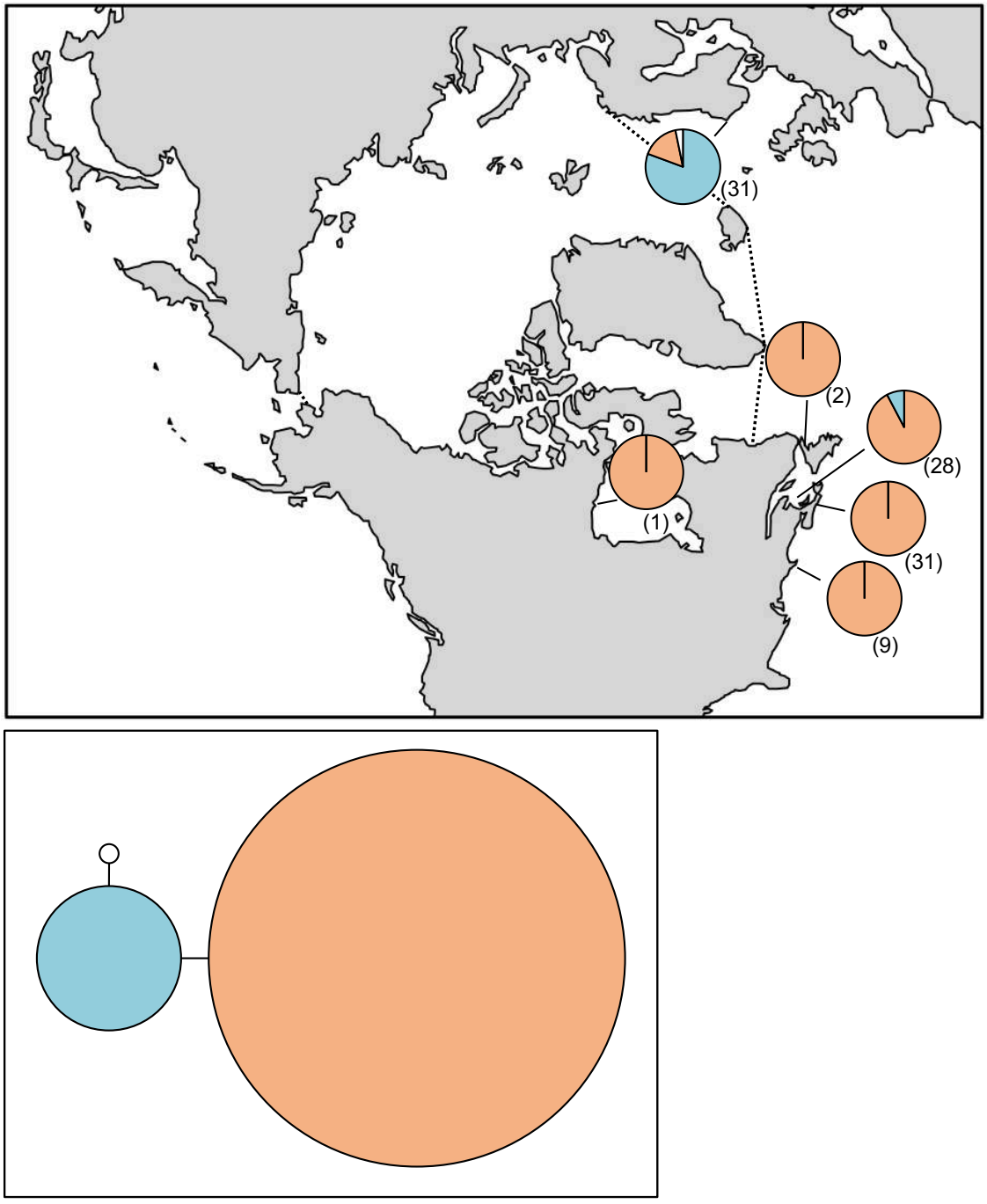

Figure E8. *Coccotylus brodiei* haplotype map and network based on COI-5P data. In the map, numbers in parentheses refer to sample sizes from given locales. The dashed line indicates delineation of the Arctic Ocean. In the haplotype network, circle size is proportional to the sampling frequency of a given haplotype.

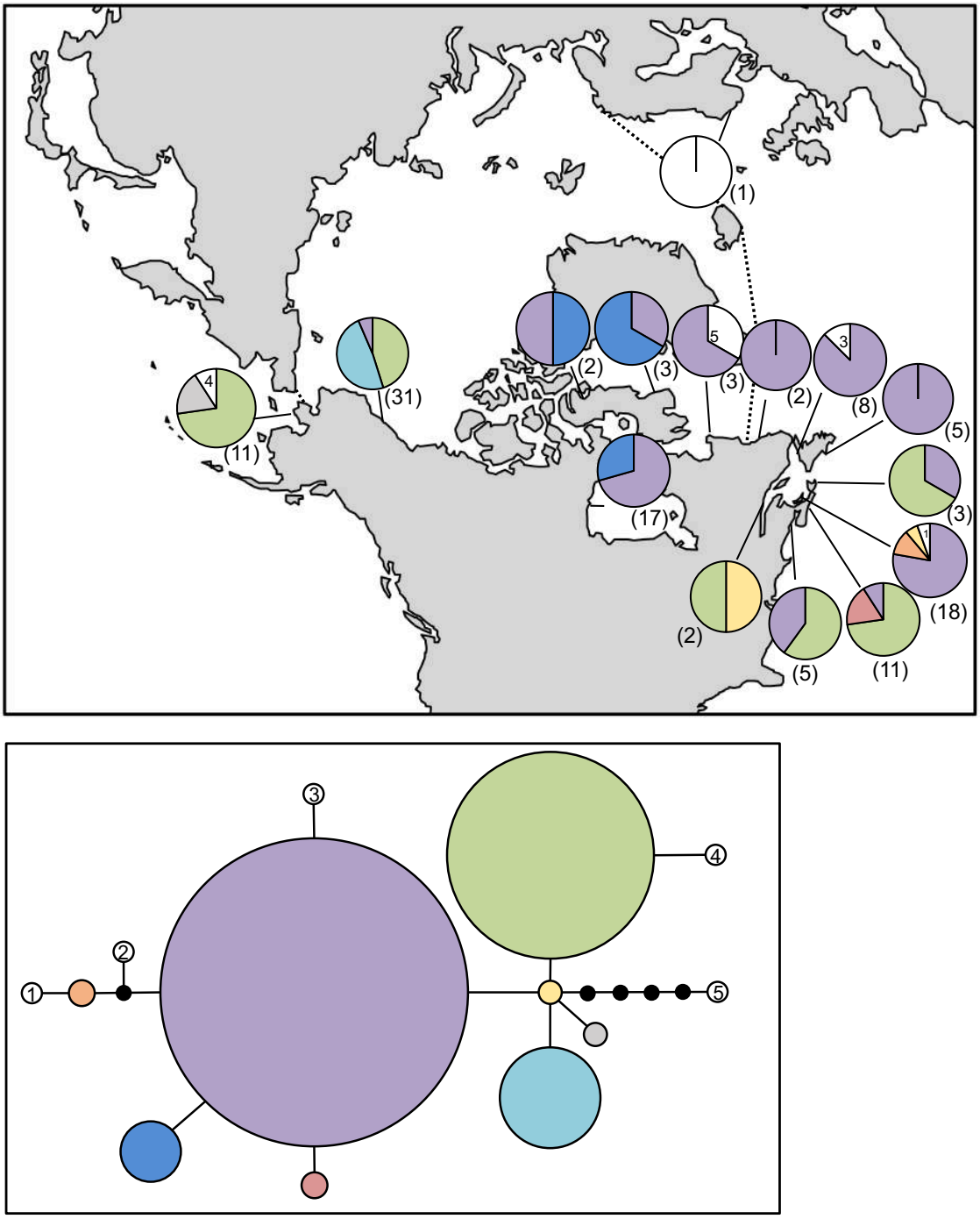

Figure E9. *Coccotylus truncatus* haplotype map and network based on COI-5P data. In the map, numbers in parentheses refer to sample sizes from given locales, whereas numbers adjacent to white portions of pie charts refer to a haplotype sampled only once in the accompanying network. The dashed line indicates delineation of the Arctic Ocean. In the haplotype network, numbered haplotypes in white reference back to the map. Black circles indicate hypothesized (e.g. unsampled) haplotypes between clades. Circle size is proportional to the sampling frequency of a given haplotype.

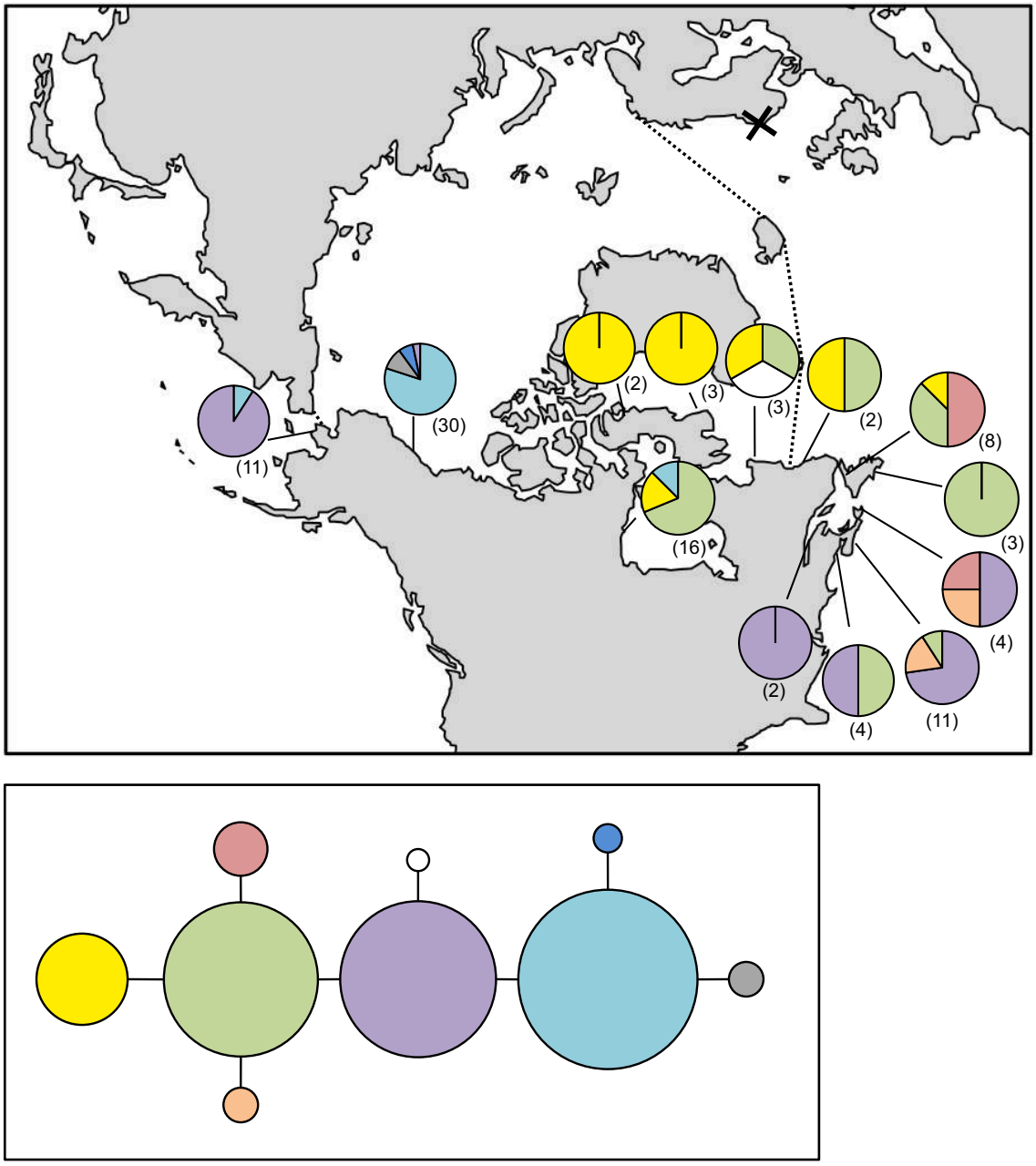

Figure E10. ***Coccotylus truncatus*** **haplotype map and network based on ITS data. In the map, numbers in parentheses refer to sample sizes from given locales. The dashed line indicates delineation of the Arctic Ocean, while the black X indicates the location of genetically verified** ***Coccotylus truncatus*** **based on COI-5P. In the haplotype network, circle size is proportional to the sampling frequency of a given haplotype.**

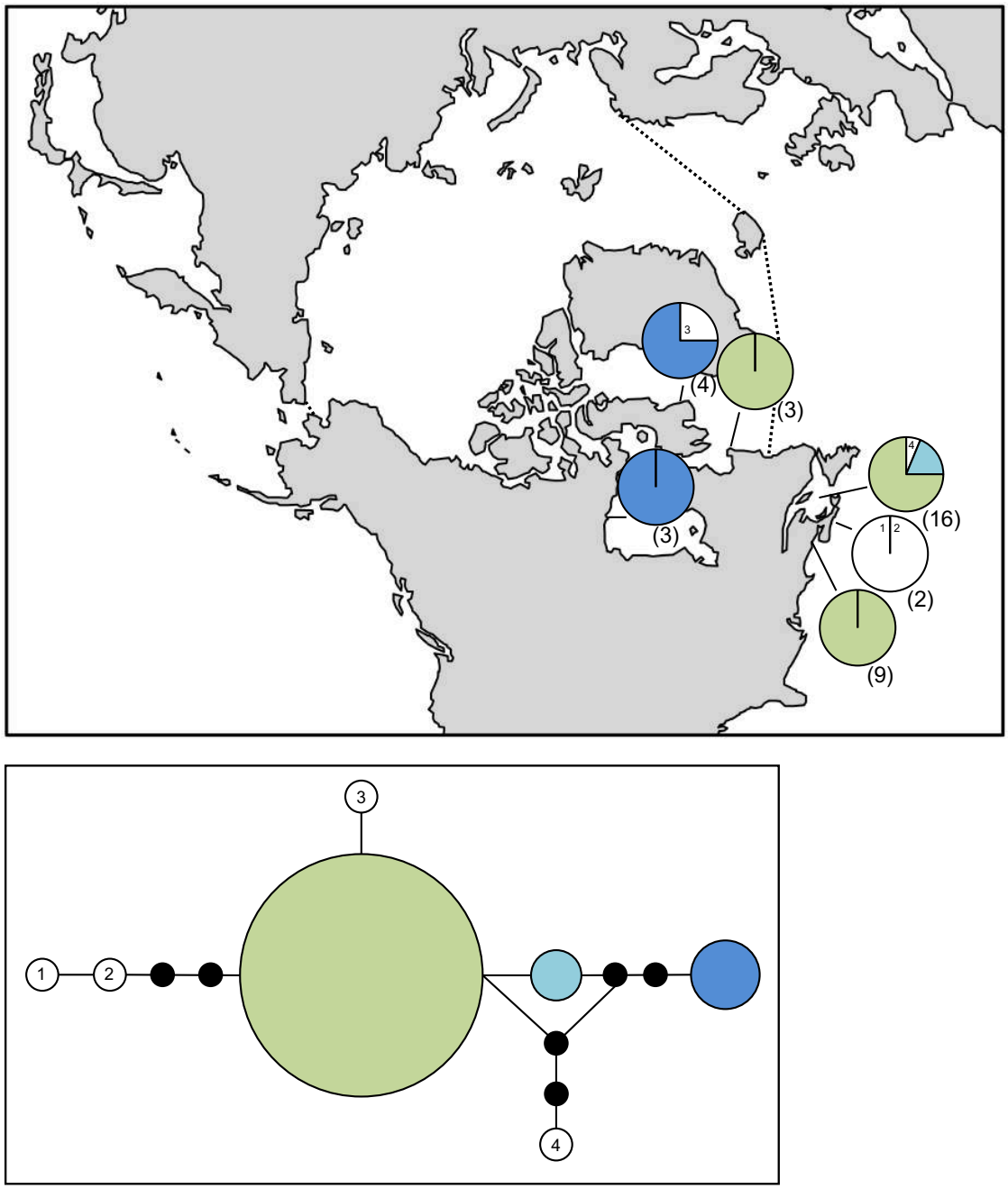

Figure E11. ***Devaleraea ramentacea*** **haplotype map and network based on COI-5P data. In the map, numbers in parentheses refer to sample sizes from given locales, whereas numbers adjacent to white portions of pie charts refer to a haplotype sampled only once in the accompanying network. The dashed line indicates delineation of the Arctic Ocean. In the haplotype network, numbered haplotypes in white reference back to the map. Black circles indicate hypothesized (e.g. unsampled) haplotypes between clades. Circle size is proportional to the sampling frequency of a given haplotype.**

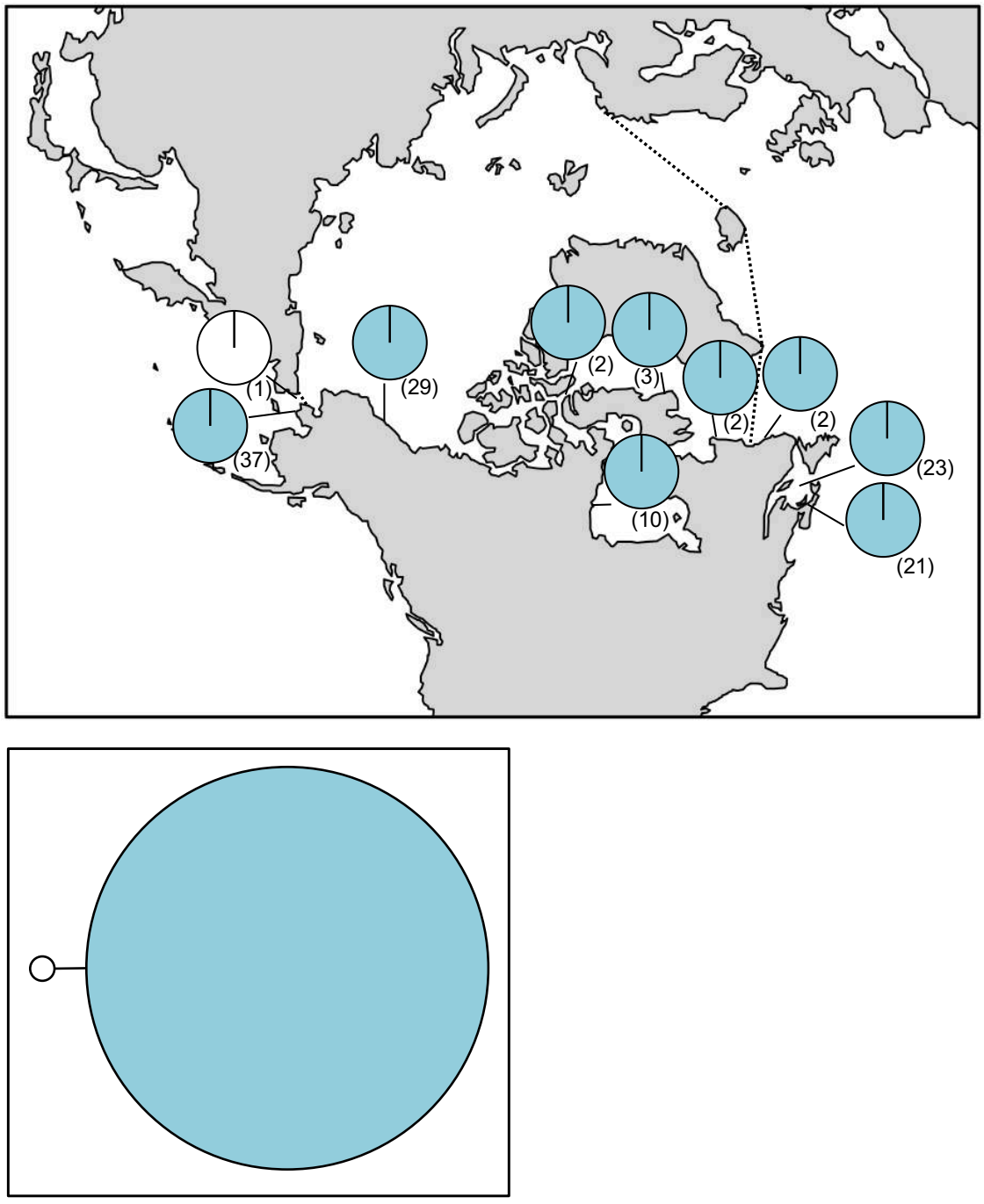

Figure E12. ***Dilsea socialis*** **haplotype map and network based on COI-5P data. In the map, numbers in parentheses refer to sample sizes from given locales. The dashed line indicates delineation of the Arctic Ocean. In the haplotype network, circle size is proportional to the sampling frequency of a given haplotype.**

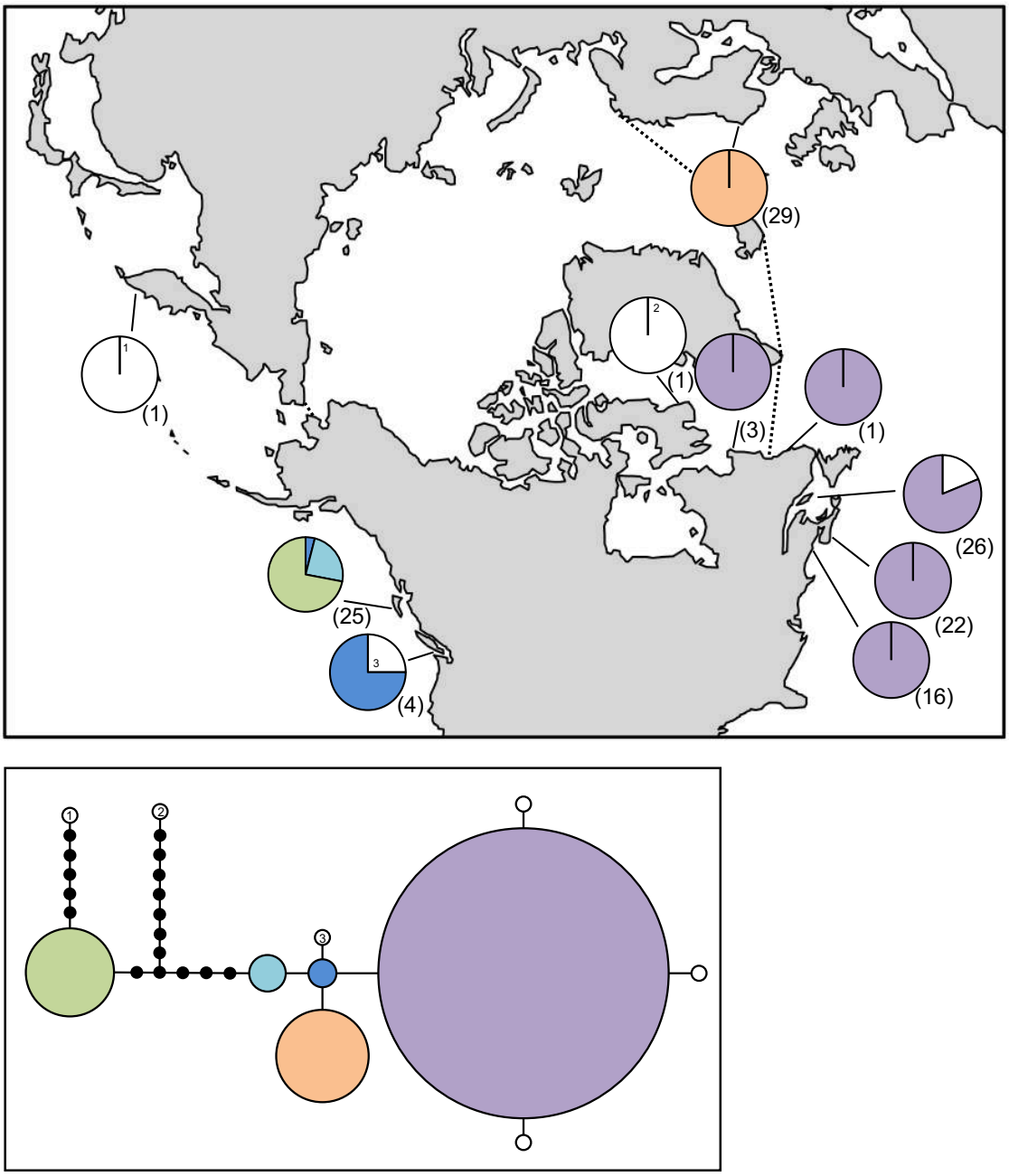

Figure E13. ***Euthora cristata*** **haplotype map and network based on COI-5P data. In the map, numbers in parentheses refer to sample sizes from given locales. The dashed line indicates delineation of the Arctic Ocean. In the haplotype network, black circles indicate hypothesized (e.g. unsampled) haplotypes between clades. Circle size is proportional to the sampling frequency of a given haplotype. In the haplotype network, numbered haplotypes in white reference back to the map.**

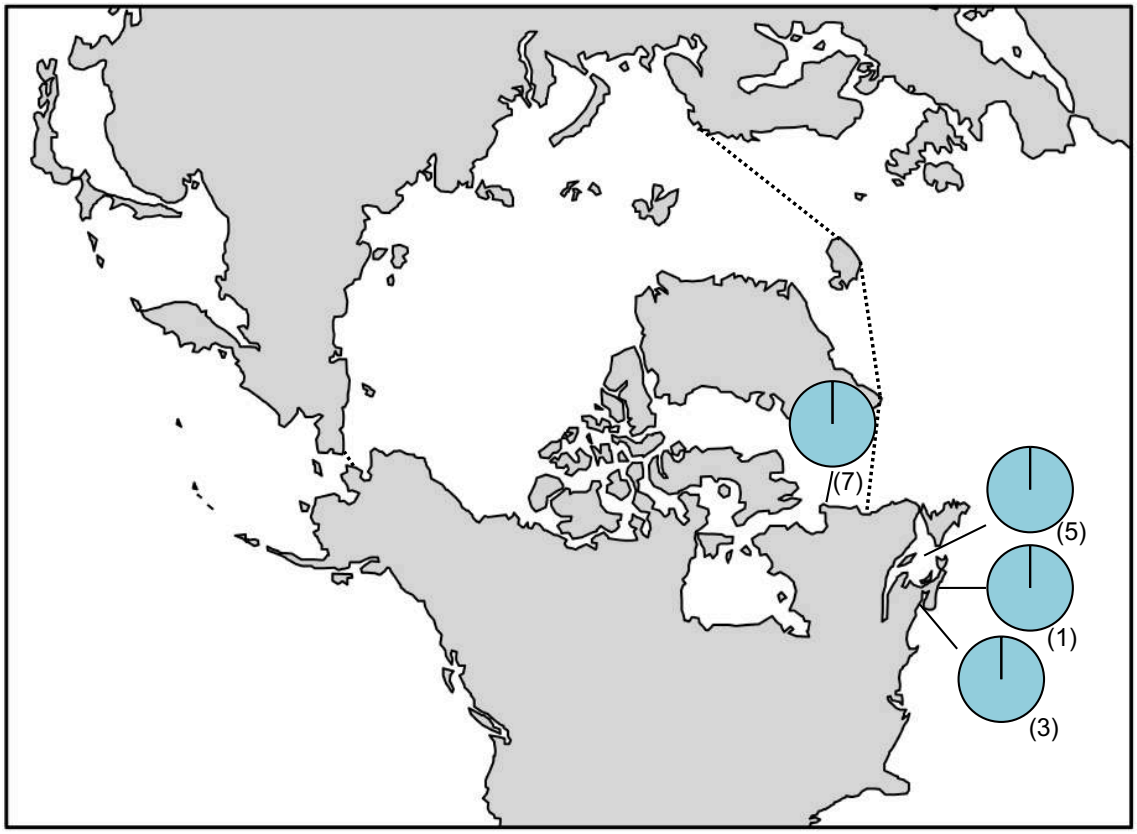

Figure E14. ***Fimbrifolium dichotomum*** **haplotype map based on COI-5P data. In the map, numbers in parentheses refer to sample sizes from given locales. The dashed line indicates delineation of the Arctic Ocean.**

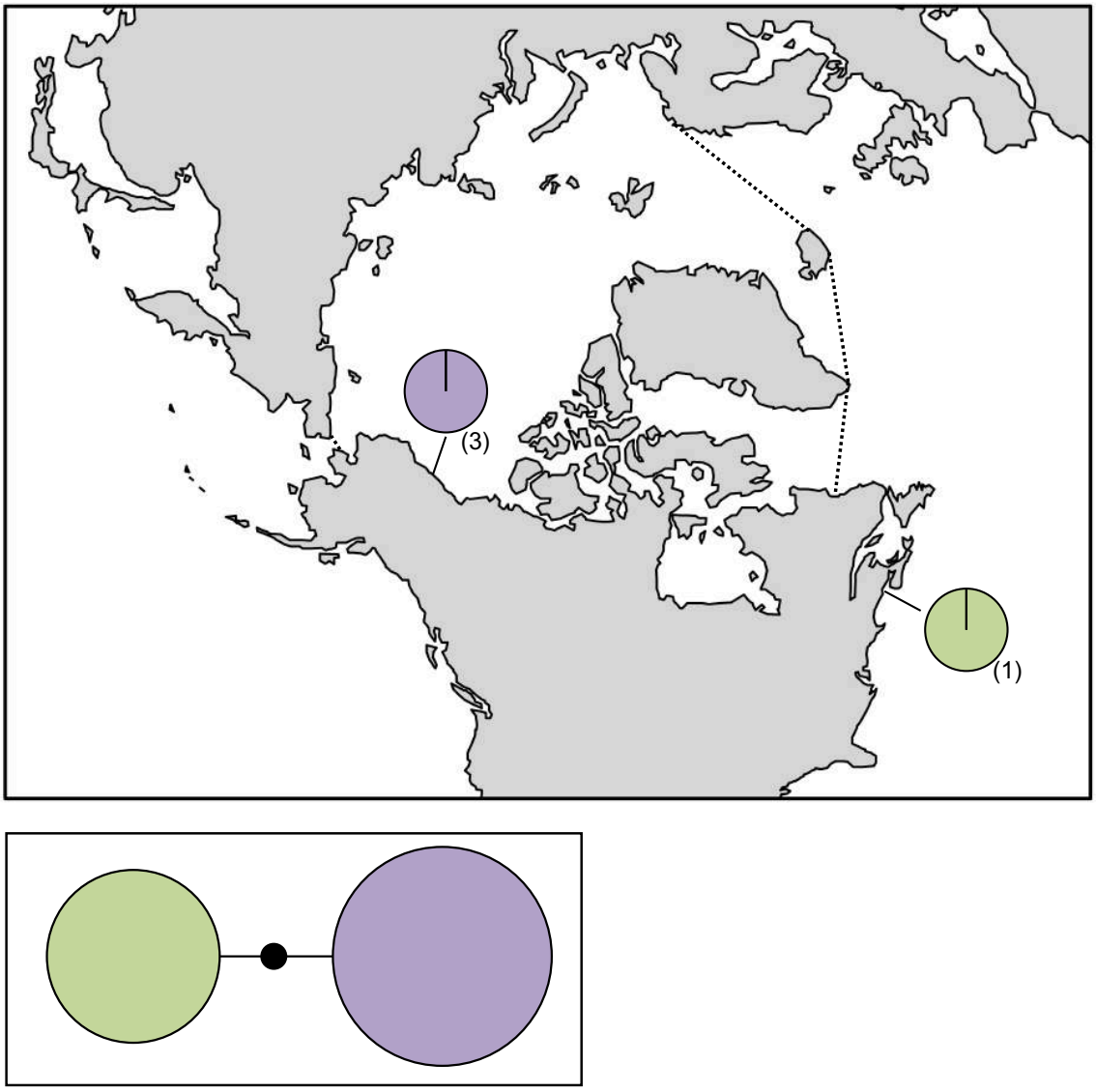

Figure E15. ***Leptophytum foecundum*** **haplotype map and network based on COI-5P data. In the map, numbers in parentheses refer to sample sizes from given locales. The dashed line indicates delineation of the Arctic Ocean. In the haplotype network, the black circle represents a hypothesized (e.g. unsampled) haplotype between clades. Circle size is proportional to the sampling frequency of a given haplotype.**

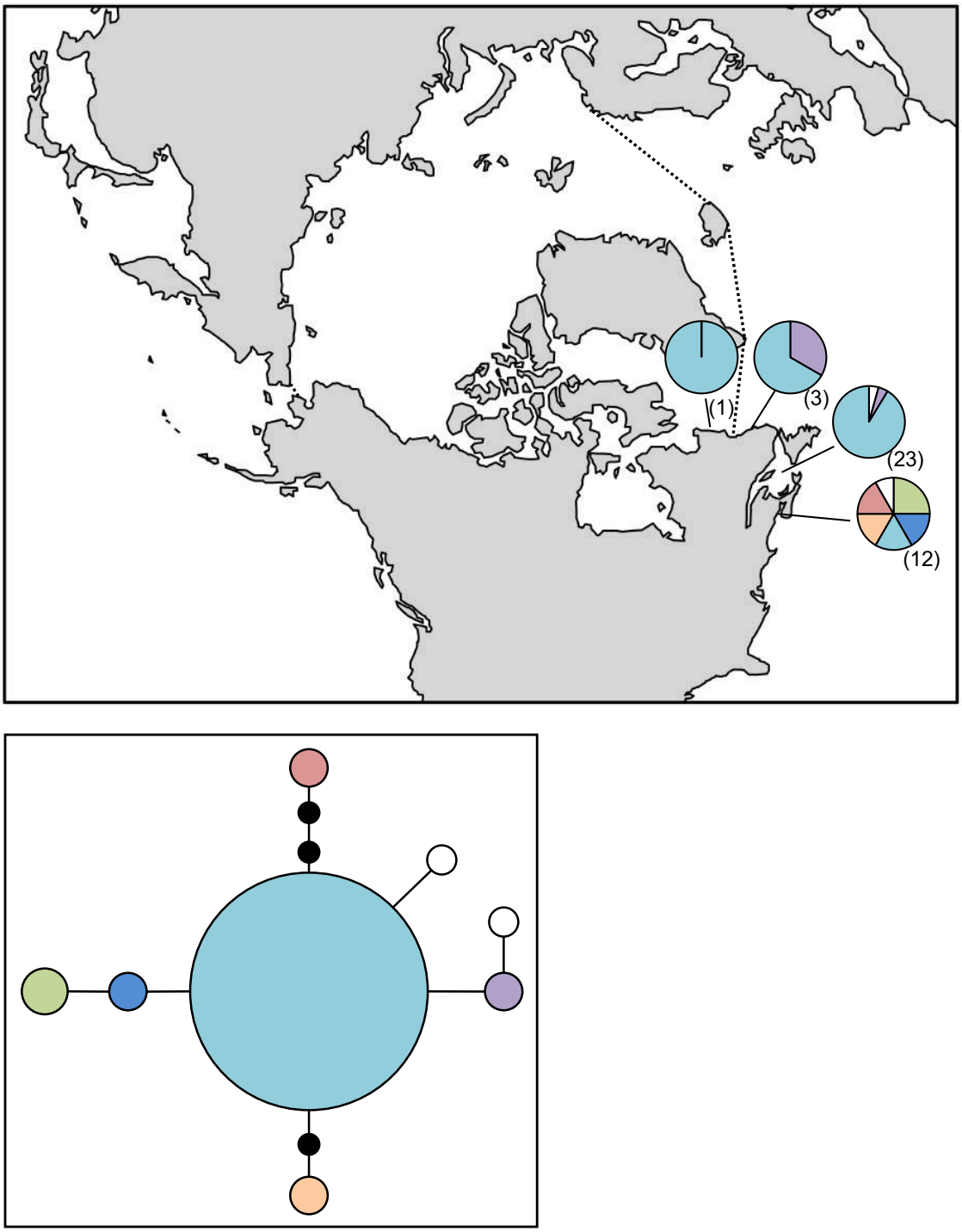

Figure E16. ***Leptosiphonia flexicaulis*** **haplotype map based on COI-5P data. In the map, numbers in parentheses refer to sample sizes from given locales. The dashed line indicates delineation of the Arctic Ocean. In the haplotype network, black circles indicate hypothesized (e.g. unsampled) haplotypes between clades. Circle size is proportional to the sampling frequency of a given haplotype.**

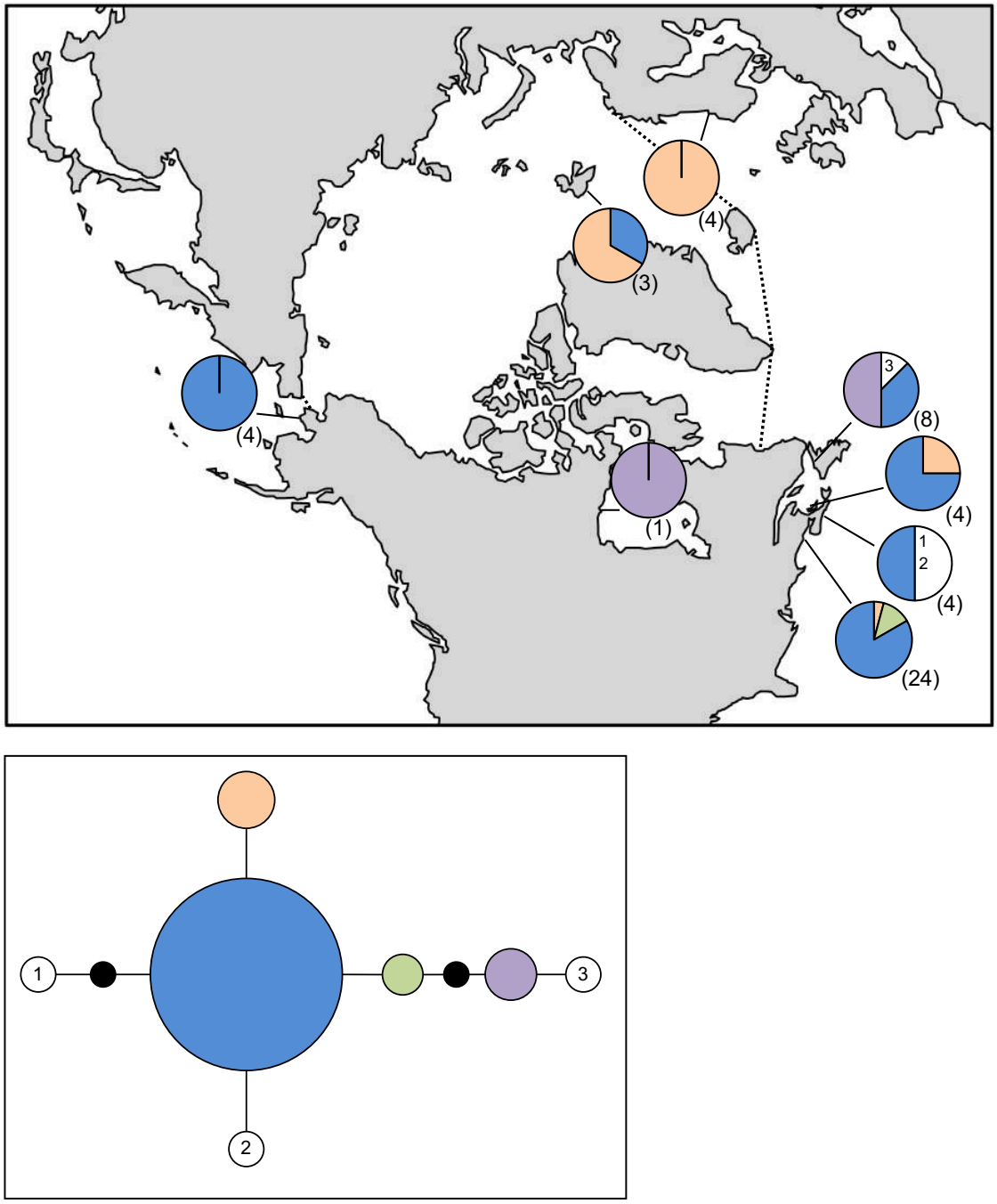

Figure E17. ***Lithothamnion glaciale*** **haplotype map and network based on COI-5P data. In the map, numbers in parentheses refer to sample sizes from given locales, whereas numbers adjacent to white portions of pie charts refer to a haplotype sampled only once in the accompanying network. The dashed line indicates delineation of the Arctic Ocean. In the haplotype network, numbered haplotypes in white reference back to the map. Black circles indicate hypothesized (e.g. unsampled) haplotypes between clades. Circle size is proportional to the sampling frequency of a given haplotype.**

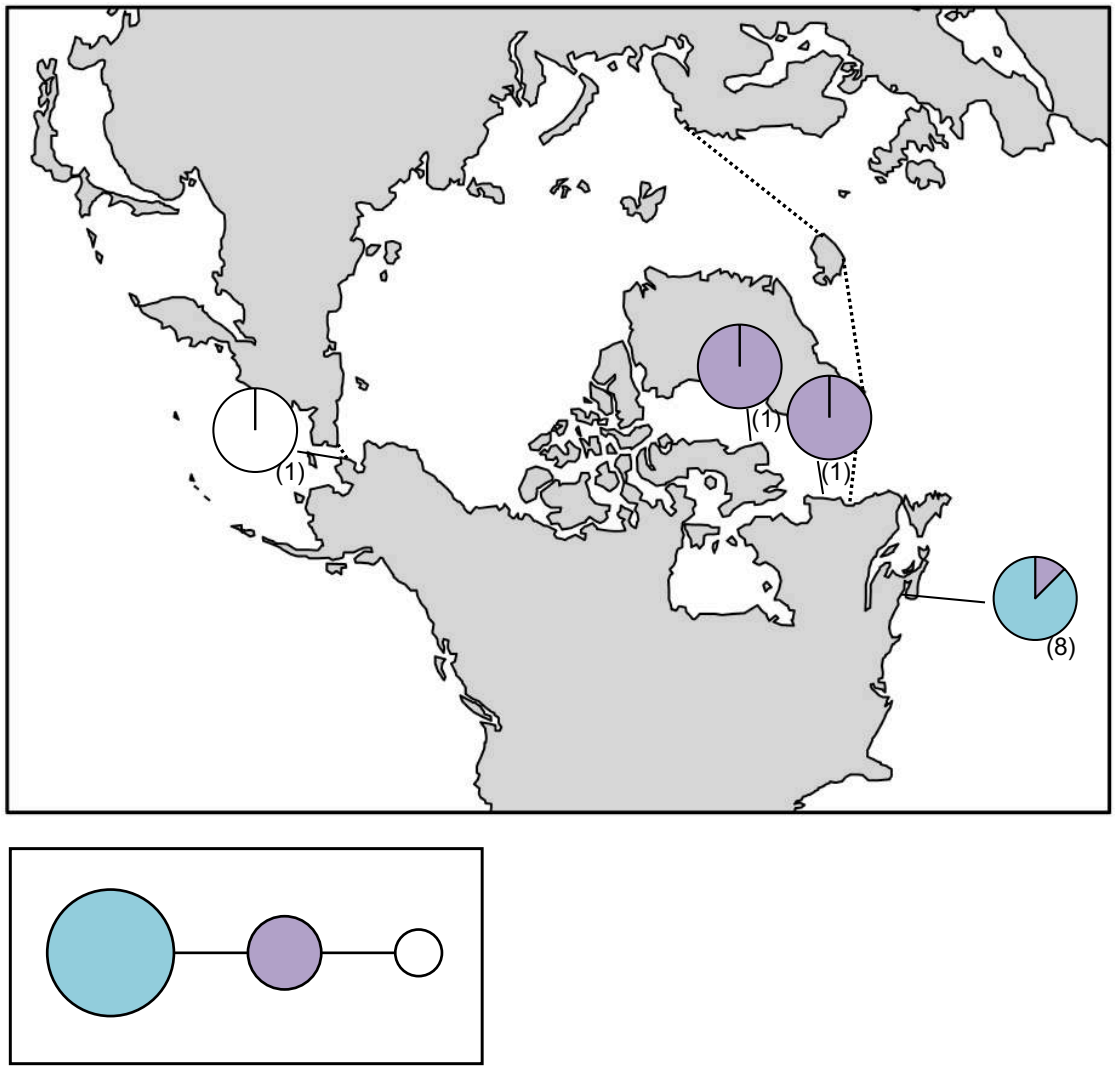

Figure E18. ***Lithothamnion lemoineae*** **haplotype map based on COI-5P data. In the map, numbers in parentheses refer to sample sizes from given locales. The dashed line indicates delineation of the Arctic Ocean. In the haplotype network, circle size is proportional to the sampling frequency of a given haplotype.**

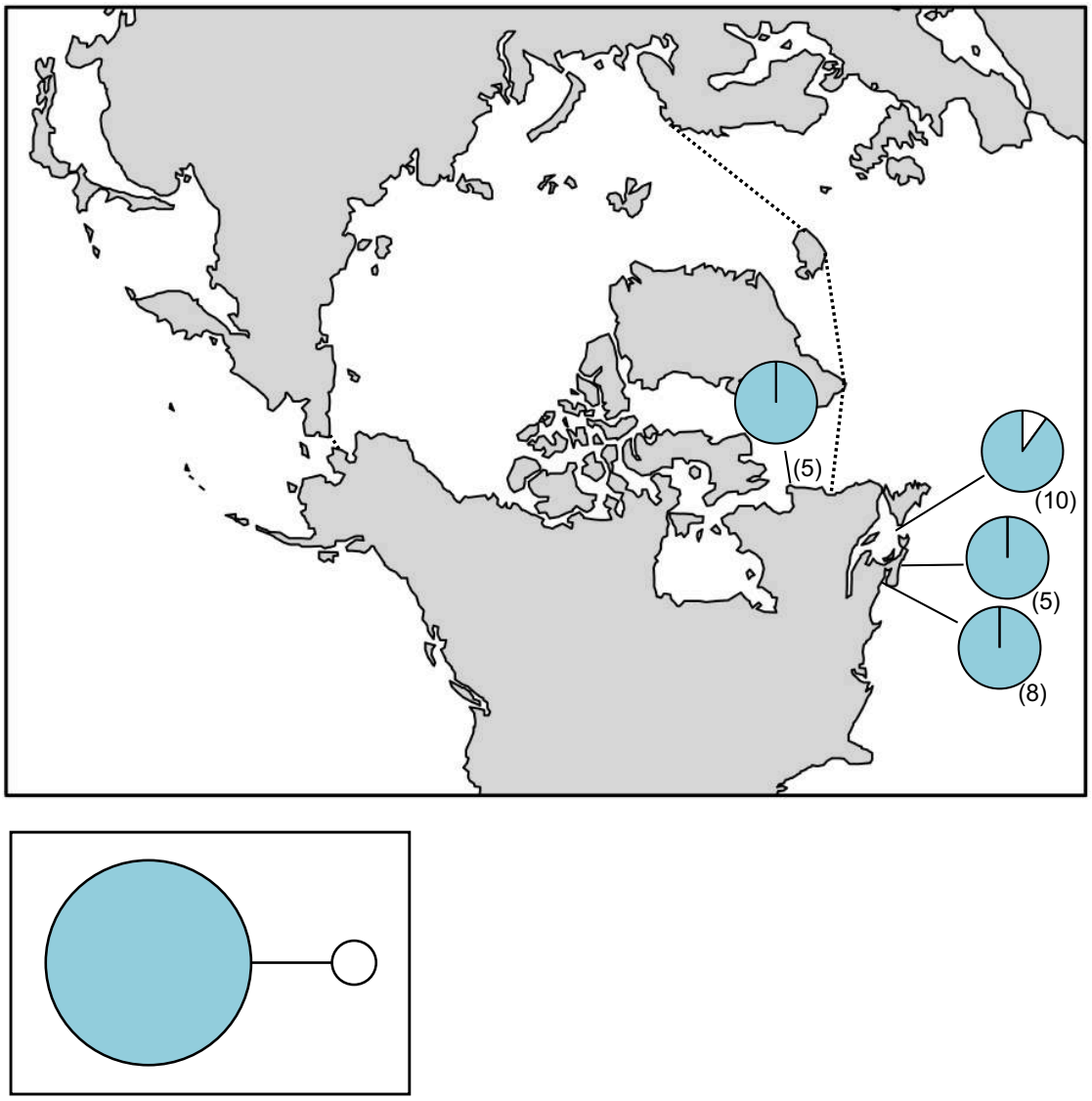

Figure E19. ***Membranoptera fabriciana*** **haplotype map based on COI-5P data. In the map, numbers in parentheses refer to sample sizes from given locales. The dashed line indicates delineation of the Arctic Ocean. In the haplotype network, circle size is proportional to the sampling frequency of a given haplotype.**

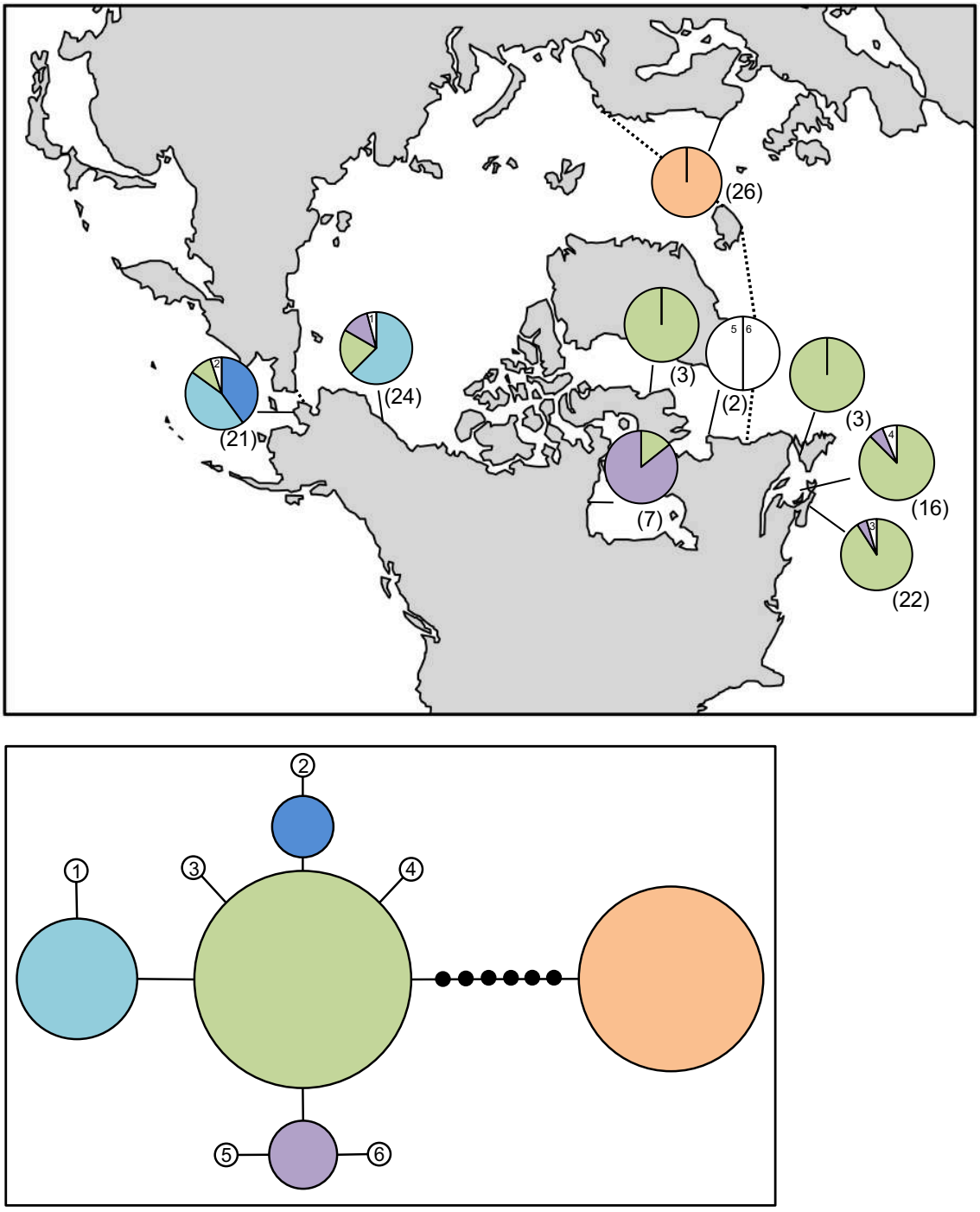

Figure E20. ***Odonthalia dentata*** **haplotype map and network based on COI-5P data. In the map, numbers in parentheses refer to sample sizes from given locales, whereas numbers adjacent to white portions of pie charts refer to a haplotype sampled only once in the accompanying network. The dashed line indicates delineation of the Arctic Ocean. In the haplotype network, numbered haplotypes in white reference back to the map. Black circles indicate hypothesized (e.g. unsampled) haplotypes between clades. Circle size is proportional to the sampling frequency of a given haplotype.**

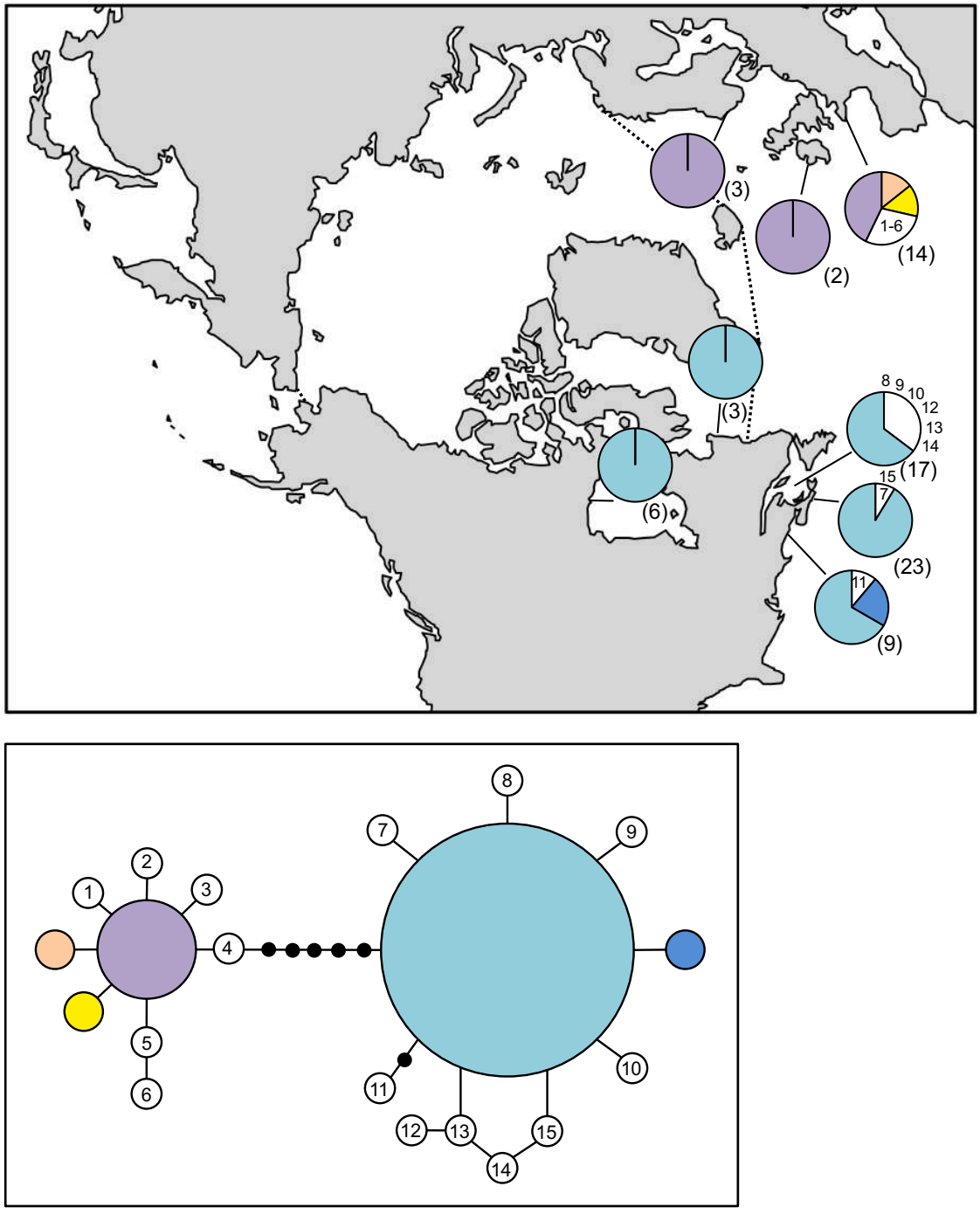

Figure E21. *Palmaria palmata* haplotype map and network based on COI-5P data. In the map, numbers in parentheses refer to sample sizes from given locales, whereas numbers adjacent to white portions of pie charts refer to a haplotype sampled only once in the accompanying network. The dashed line indicates delineation of the Arctic Ocean. In the haplotype network, numbered haplotypes in white reference back to the map. Black circles indicate hypothesized (e.g. unsampled) haplotypes between clades. Circle size is proportional to the sampling frequency of a given haplotype.

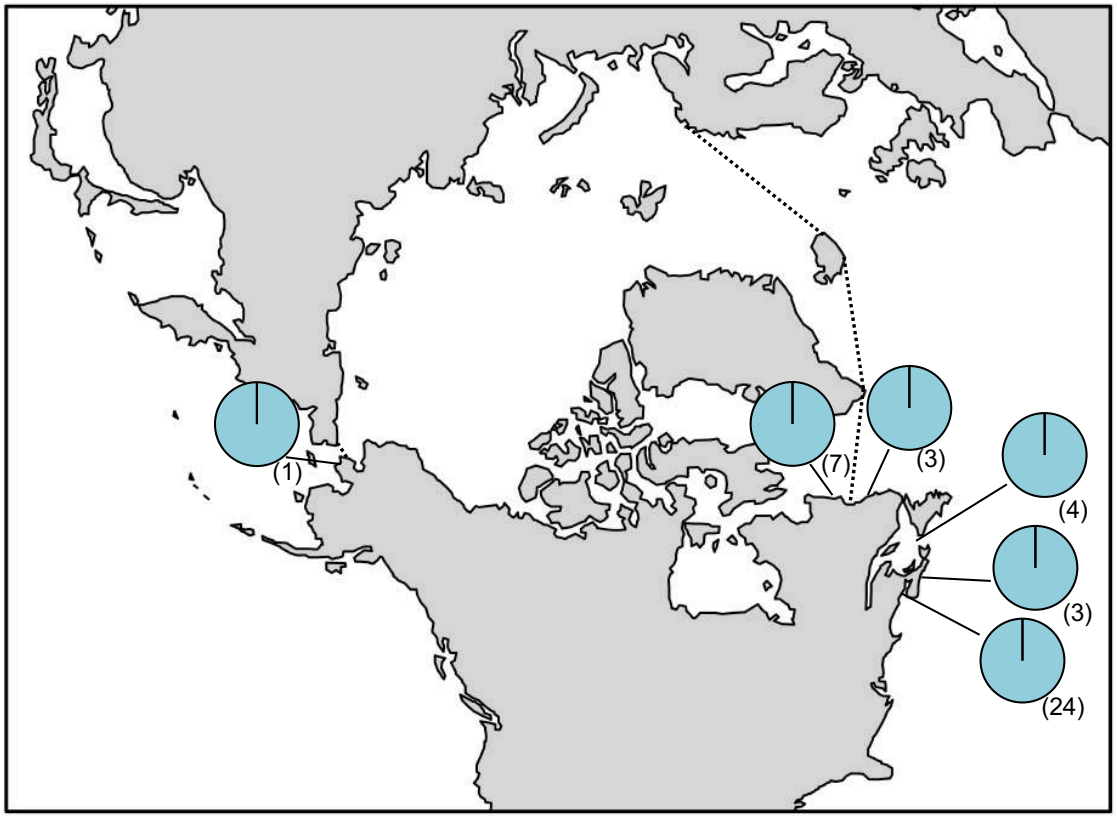

Figure E22. ***Peyssonnelia rosenvingei*** **haplotype map based on COI-5P data. In the map, numbers in parentheses refer to sample sizes from given locales. The dashed line indicates delineation of the Arctic Ocean.**

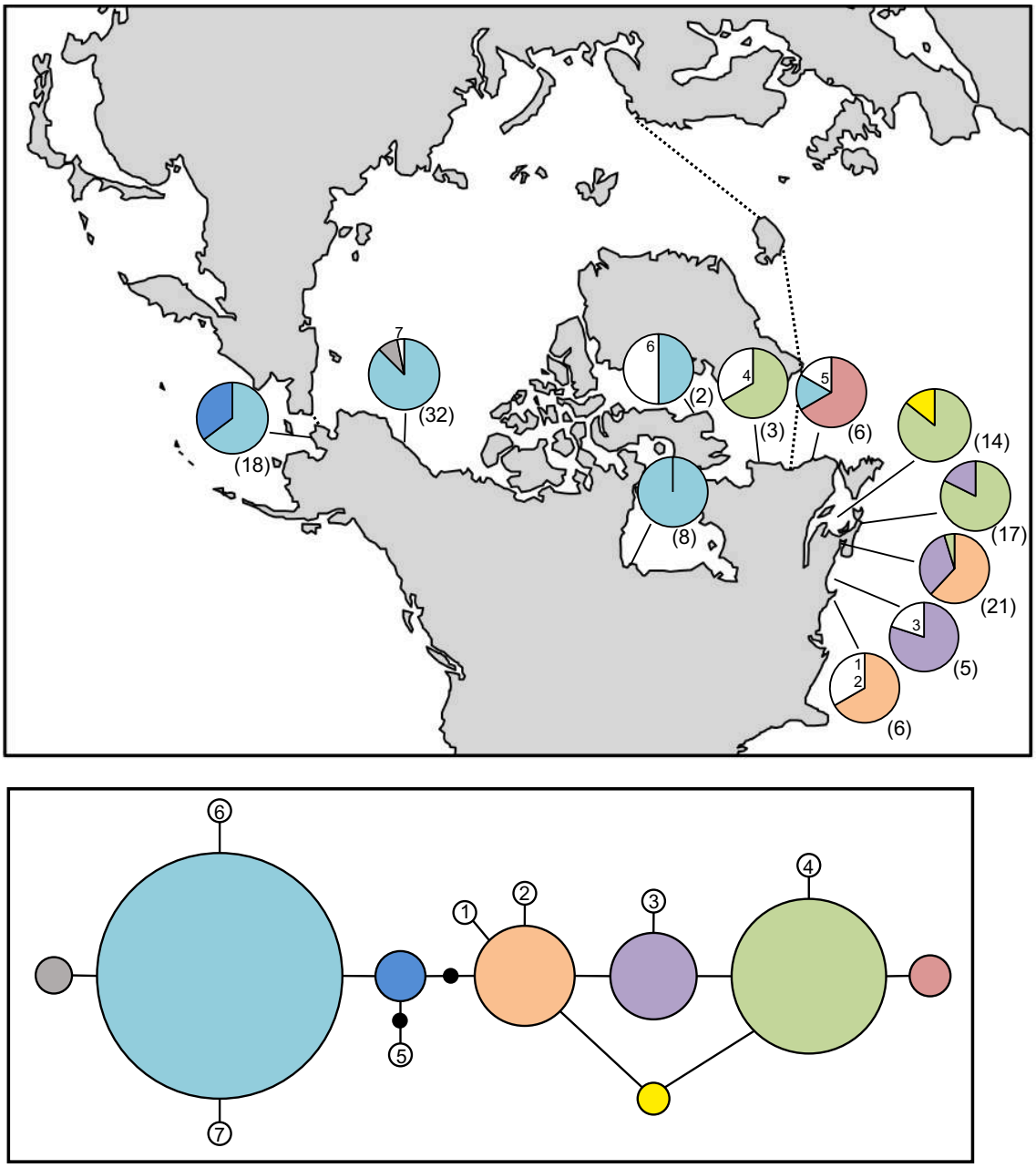

Figure E23. ***Phycodrys fimbriata*** **haplotype map and network based on COI-5P data. In the map, numbers in parentheses refer to sample sizes from given locales, whereas numbers adjacent to white portions of pie charts refer to a haplotype sampled only once in the accompanying network. The dashed line indicates delineation of the Arctic Ocean. In the haplotype network, numbered haplotypes in white reference back to the map. Black circles indicate hypothesized (e.g. unsampled) haplotypes between clades. Circle size is proportional to the sampling frequency of a given haplotype.**

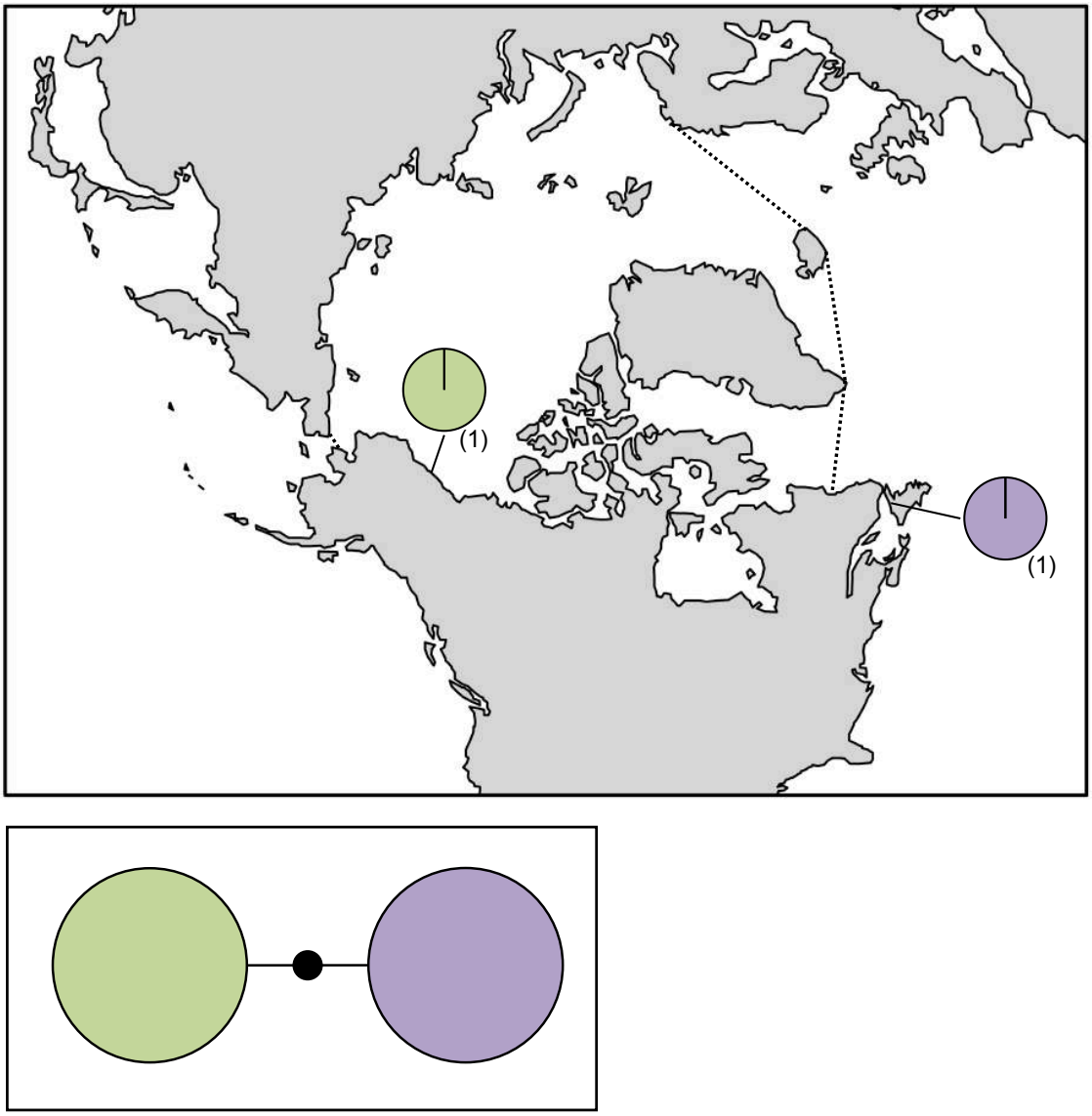

Figure E24. ***Phymatolithon tenue*** **haplotype map and network based on COI-5P data. In the map, numbers in parentheses refer to sample sizes from given locales. The dashed line indicates delineation of the Arctic Ocean. In the haplotype network, the black circle represents a hypothesized (e.g. unsampled) haplotypes between clades. Circle size is proportional to the sampling frequency of a given haplotype.**

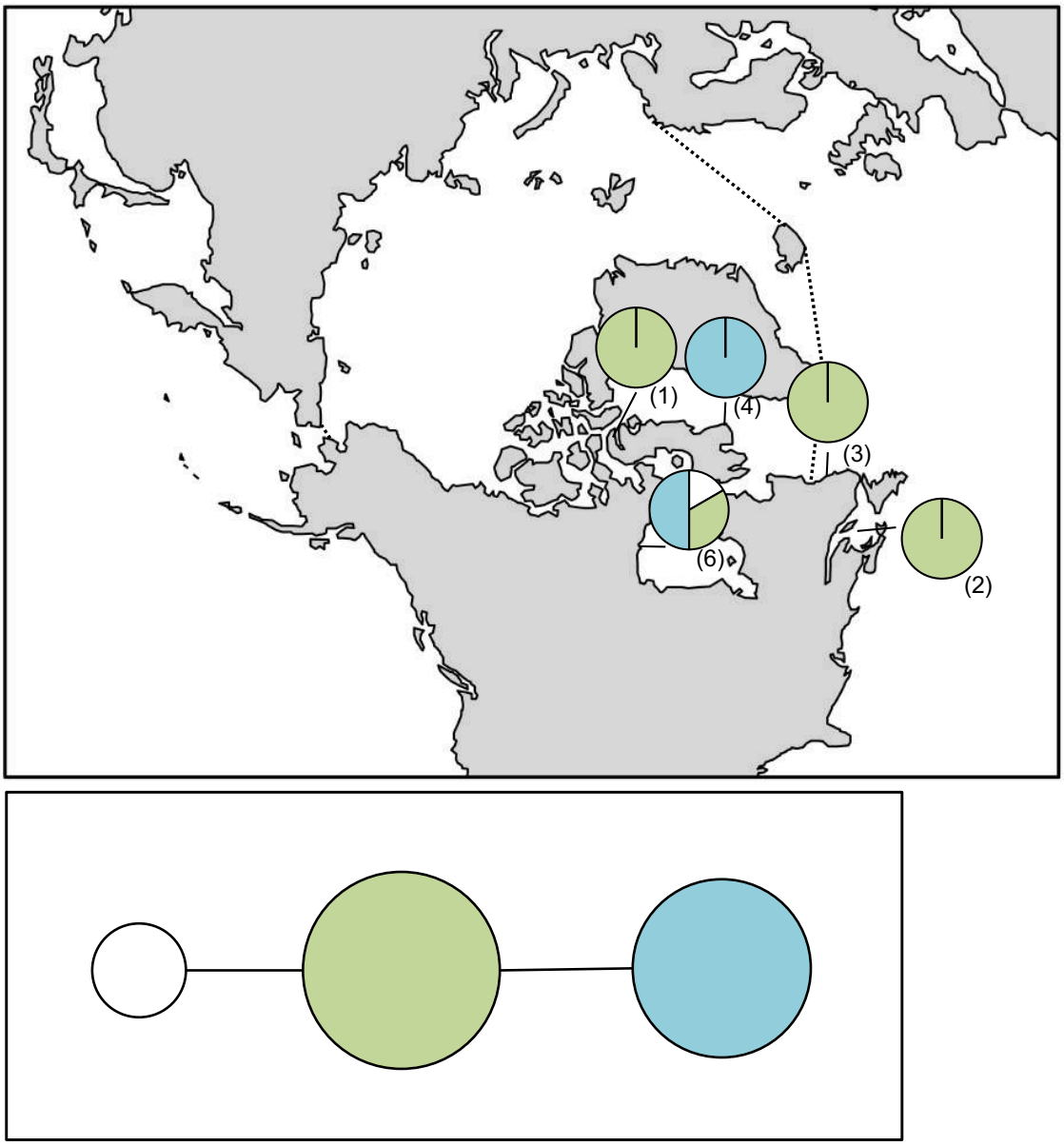

Figure E25. ***Polyostea arctica*** **haplotype map and network based on COI-5P data. In the map, numbers in parentheses refer to sample sizes from given locales. The dashed line indicates delineation of the Arctic Ocean. In the haplotype network, circle size is proportional to the sampling frequency of a given haplotype.**

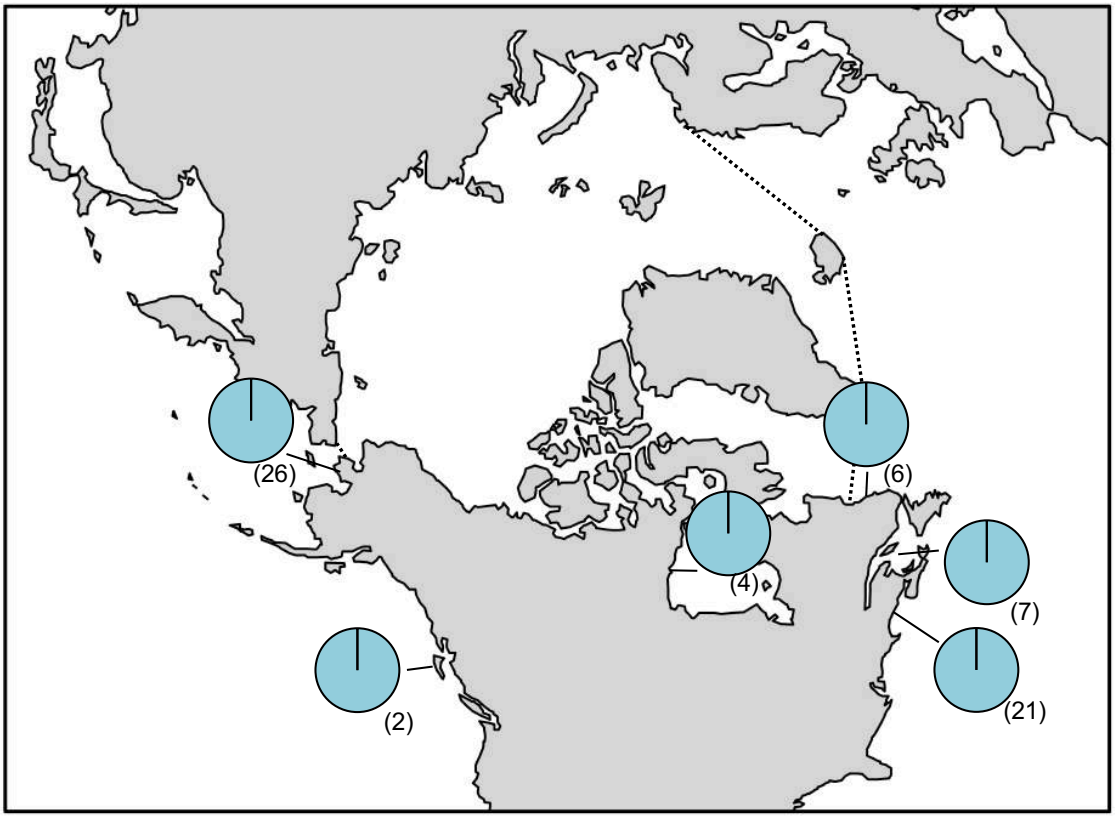

Figure E26. *Polysiphonia* sp. 1stricta haplotype map based on COI-5P data. In the map, numbers in parentheses refer to sample sizes from given locales. The dashed line indicates delineation of the Arctic Ocean.

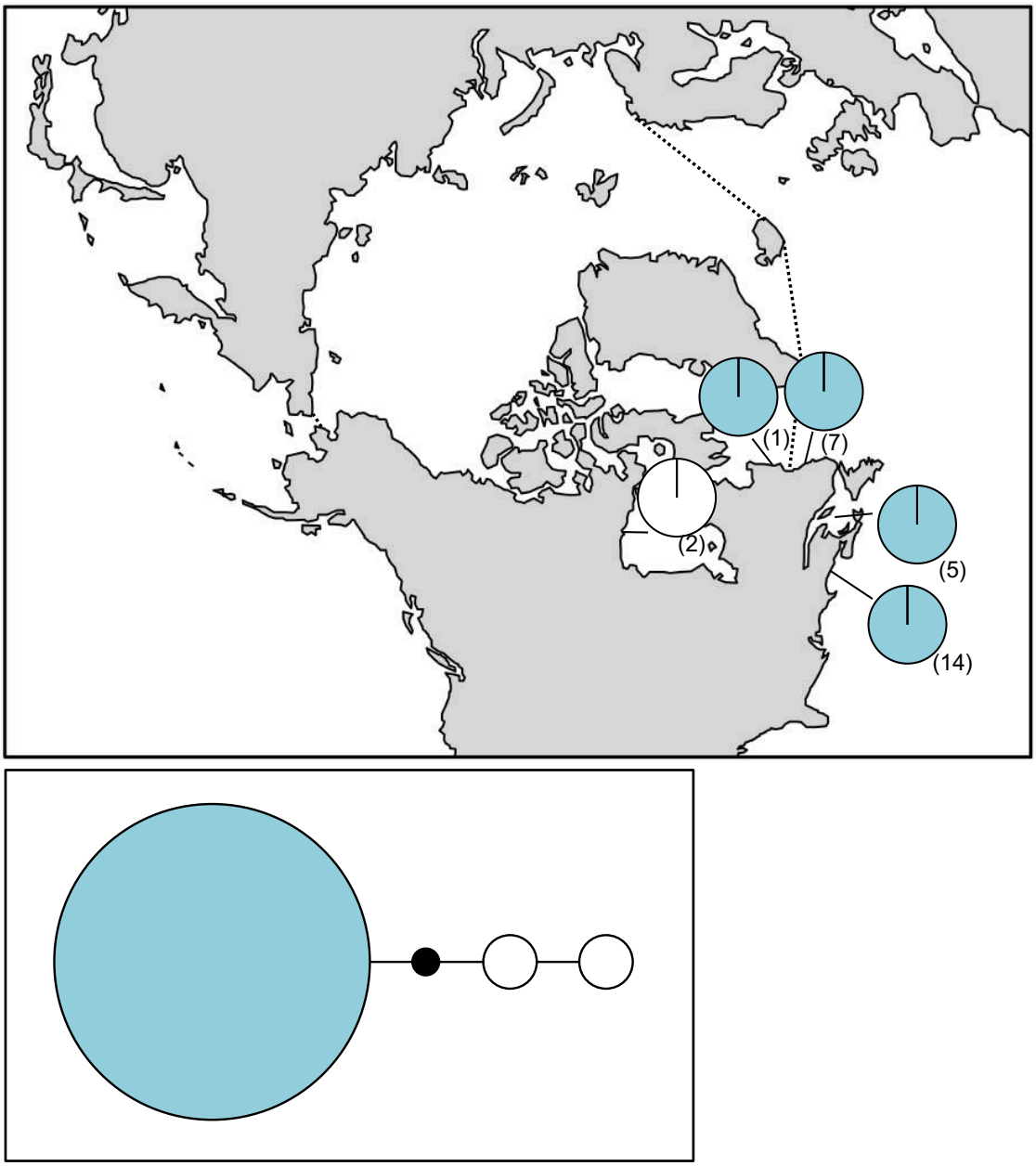

Figure E27. ***Polysiphonia*** **sp. 3stricta map and network based on COI-5P data. In the map, numbers in parentheses refer to sample sizes from given locales. The dashed line indicates delineation of the Arctic Ocean. In the haplotype network, the black circle represents a hypothesized (e.g. unsampled) haplotypes between clades. Circle size is proportional to the sampling frequency of a given haplotype.**

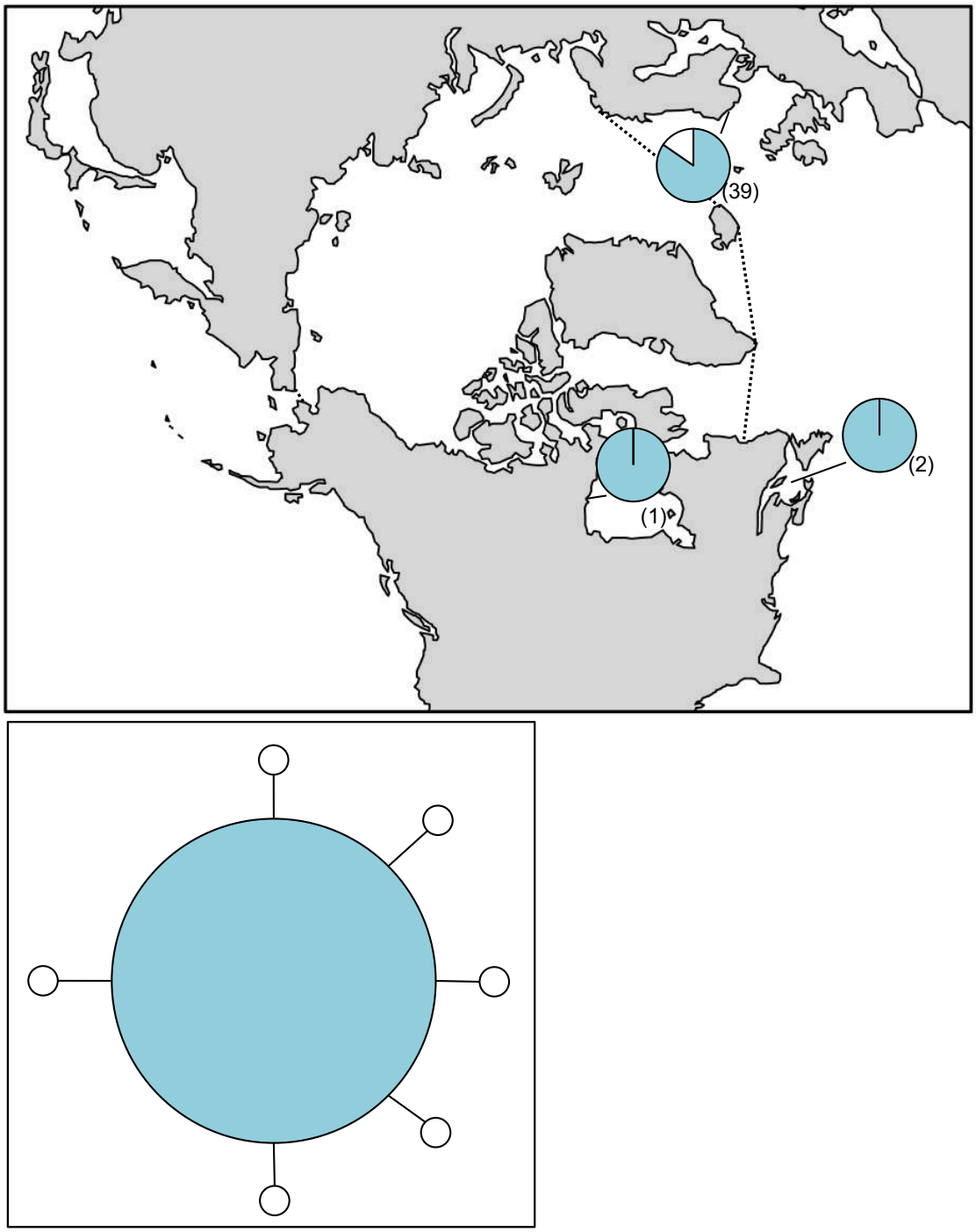

Figure E28. ***Ptilota gunneri*** **haplotype map and network based on COI-5P data. In the map, numbers in parentheses refer to sample sizes from given locales. The dashed line indicates delineation of the Arctic Ocean. In the haplotype network, circle size is proportional to the sampling frequency of a given haplotype.**

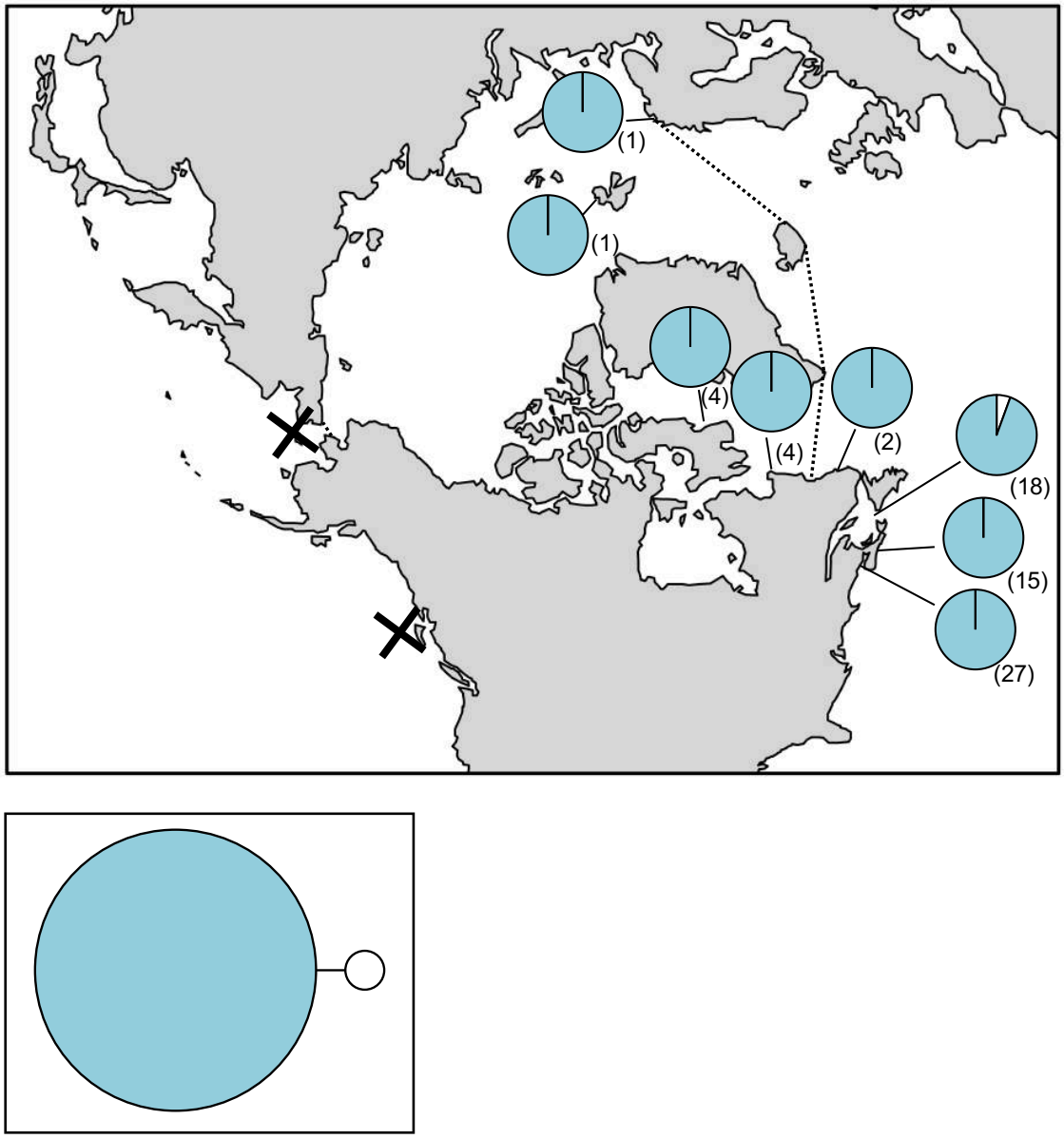

Figure E29. *Ptilota serrata* haplotype map and network based on COI-5P data. In the map, numbers in parentheses refer to sample sizes from given locales. The dashed line indicates delineation of the Arctic Ocean, while black X's indicate the locations of genetically verified *Ptilota serrata* based on *rbc*L. In the haplotype network, circle size is proportional to the sampling frequency of a given haplotype.

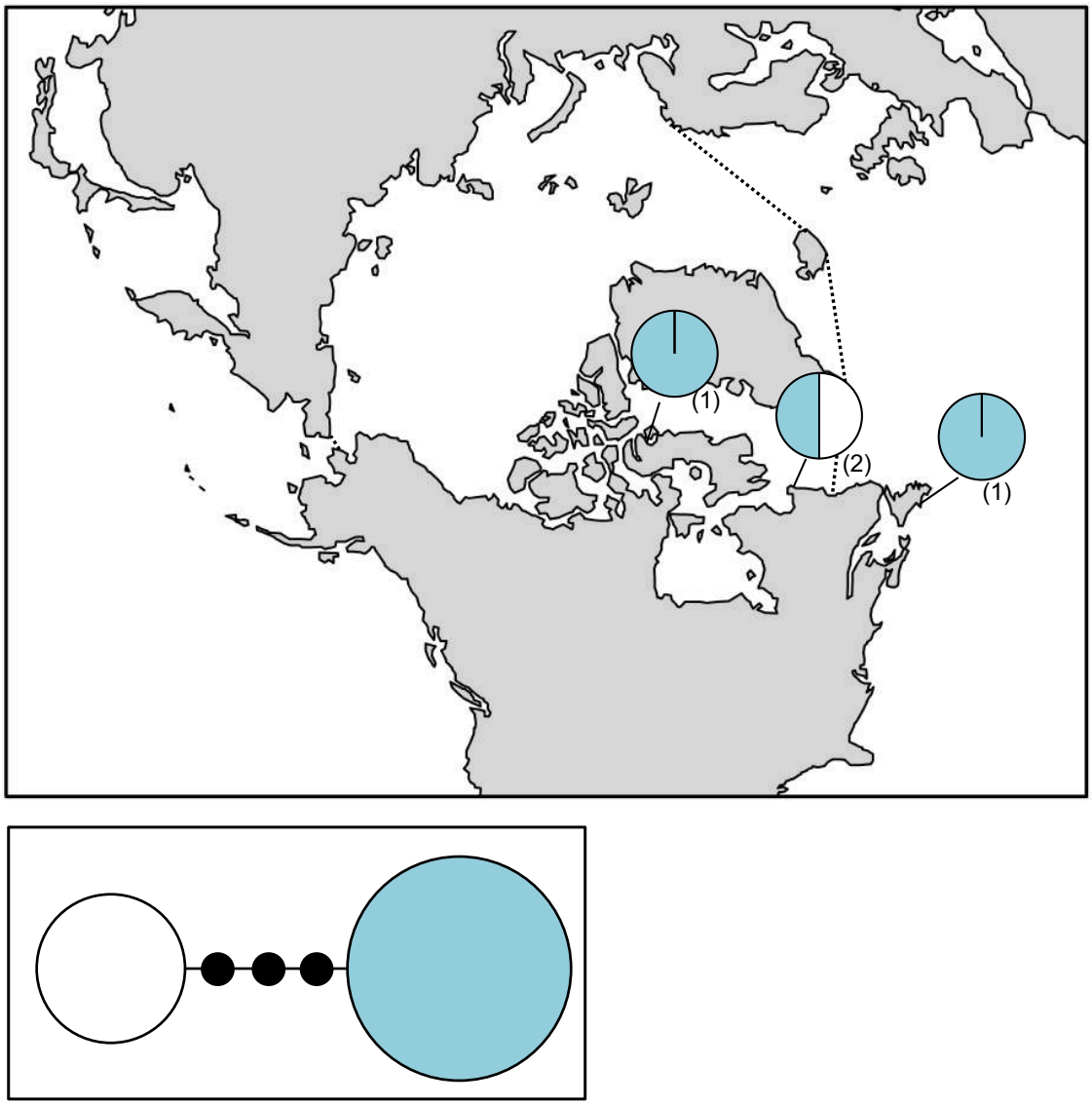

Figure E30. ***Rhodochorton purpureum*** **haplotype map and network based on** ***rbc*****L-3P data. In the map, numbers in parentheses refer to sample sizes from given locales. The dashed line indicates delineation of the Arctic Ocean. In the haplotype network. the black circles indicate hypothesized (e.g. unsampled) haplotypes between clades. Circle size is proportional to the sampling frequency of a given haplotype.**

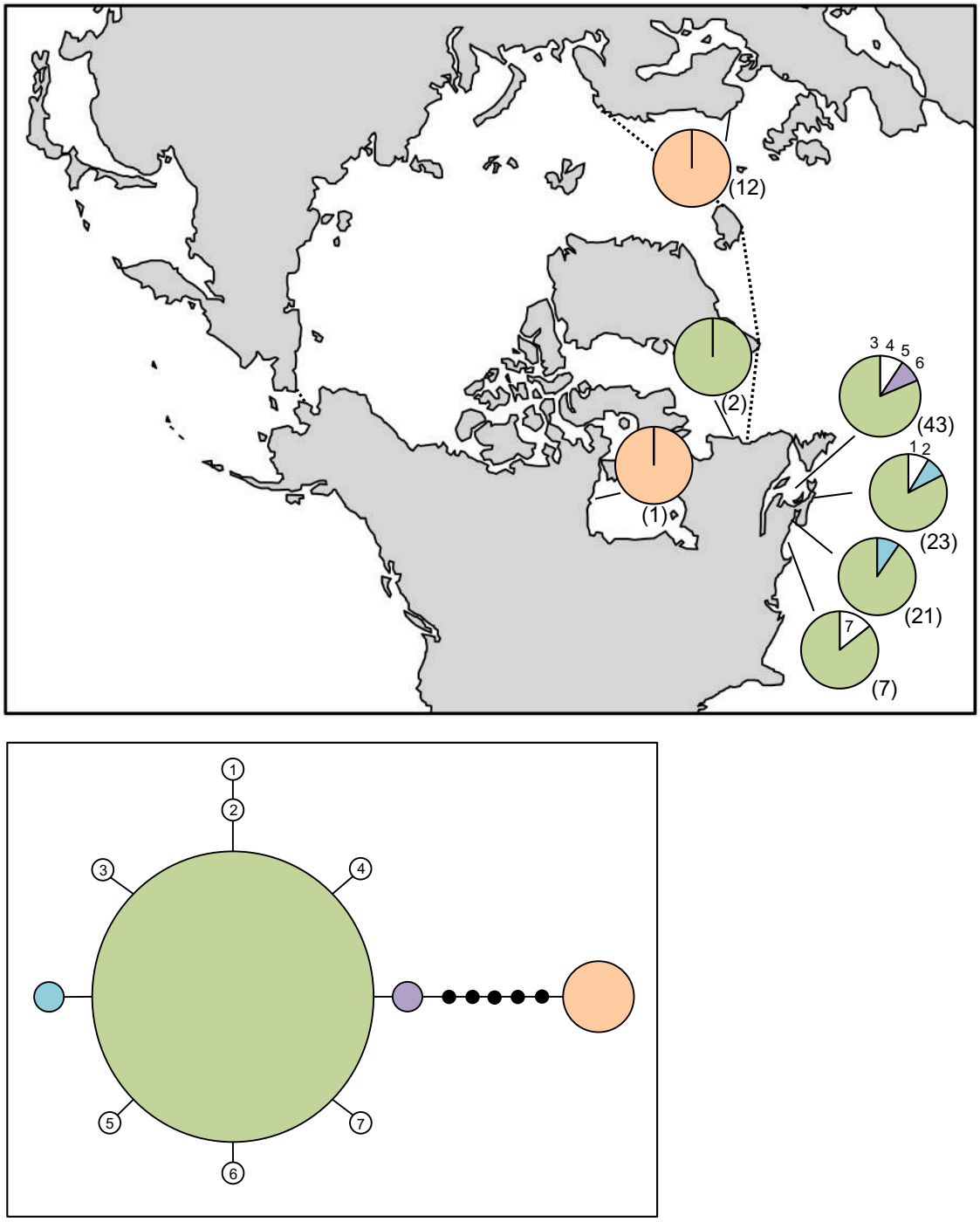

Figure E31. ***Rhodomela lycopodioides*** **haplotype map and network based on COI-5P data. In the map, numbers in parentheses refer to sample sizes from given locales, whereas numbers adjacent to white portions of pie charts refer to a haplotype sampled only once in the accompanying network. The dashed line indicates delineation of the Arctic Ocean. In the haplotype network, numbered haplotypes in white reference back to the map. Black circles indicate hypothesized (e.g. unsampled) haplotypes between clades. Circle size is proportional to the sampling frequency of a given haplotype.**

Figure E32. ***Rhodomela sibirica*** **haplotype map and network based on COI-5P data. In the map, numbers in parentheses refer to sample sizes from given locales. The dashed line indicates delineation of the Arctic Ocean. In the haplotype network, circle size is proportional to the sampling frequency of a given haplotype.**

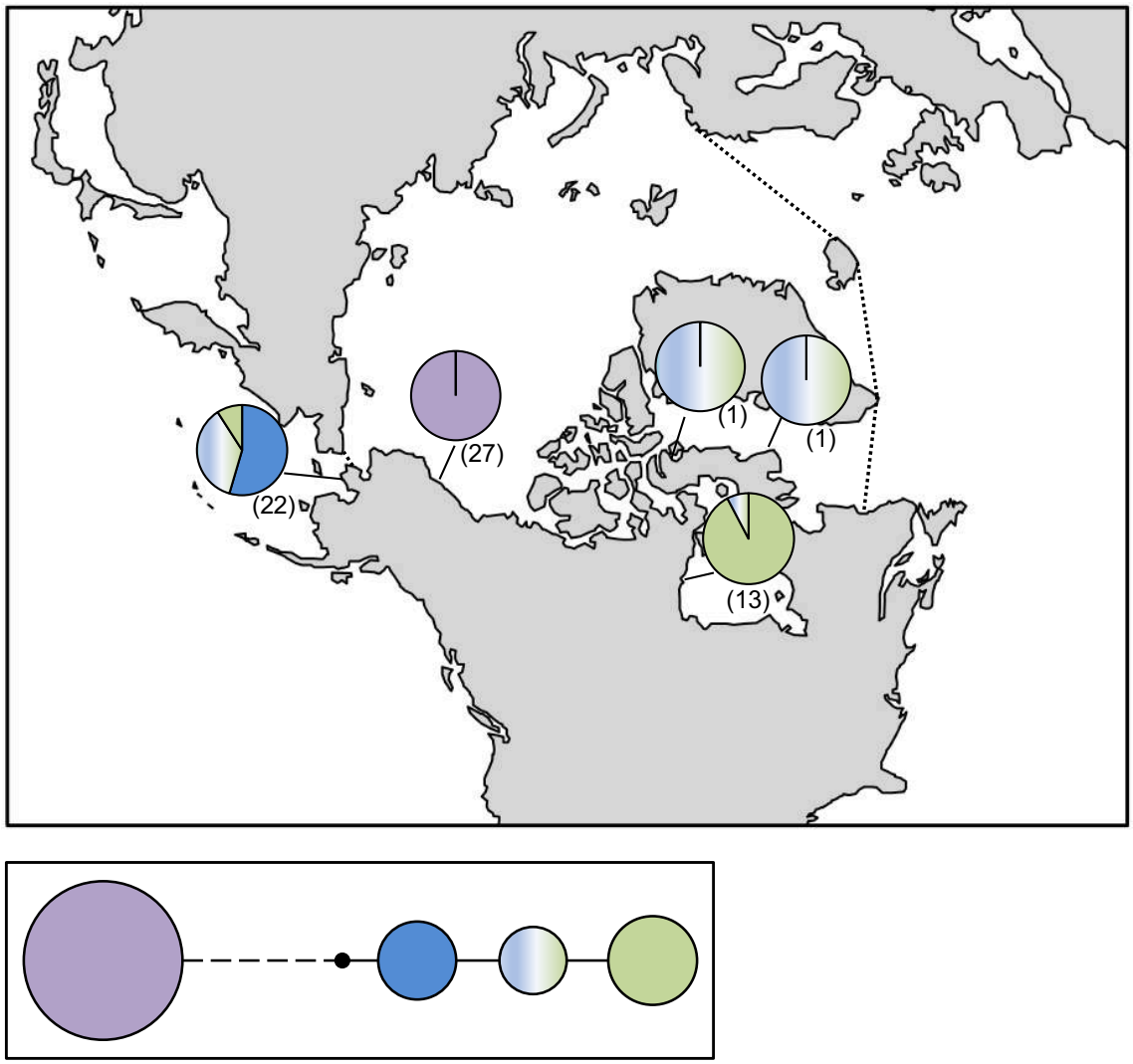

Figure E33. *Rhodomela sibirica* haplotype map and network based on ITS data. In the map, numbers in parentheses refer to sample sizes from given locales, the blue-green circle and pie chart segments indicate additivity in the ITS sequences, and the dashed line indicates delineation of the Arctic Ocean. In the haplotype network, the black circles indicate hypothesized (e.g. unsampled) haplotypes between clades, while the dashed line represents a 16 base-pair insert, and circle size is proportional to the sampling frequency of a given haplotype.

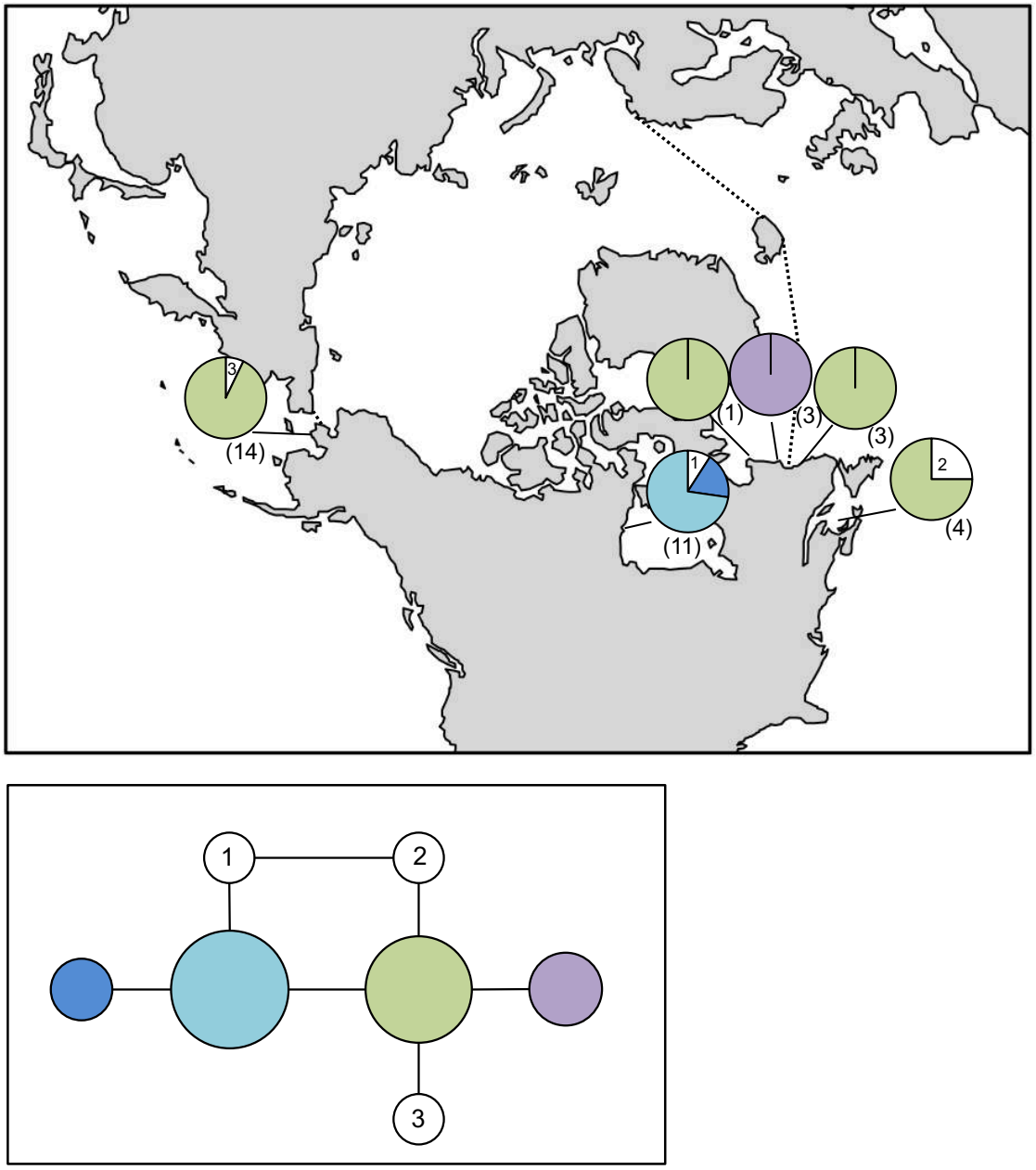

Figure E34. *Rhodomela* sp.1virgata haplotype map and network based on COI-5P data. In the map, numbers in parentheses refer to sample sizes from given locales, whereas numbers adjacent to white portions of pie charts refer to a haplotype sampled only once in the accompanying network. The dashed line indicates delineation of the Arctic Ocean. In the haplotype network, numbered haplotypes in white reference back to the map. Circle size is proportional to the sampling frequency of a given haplotype.

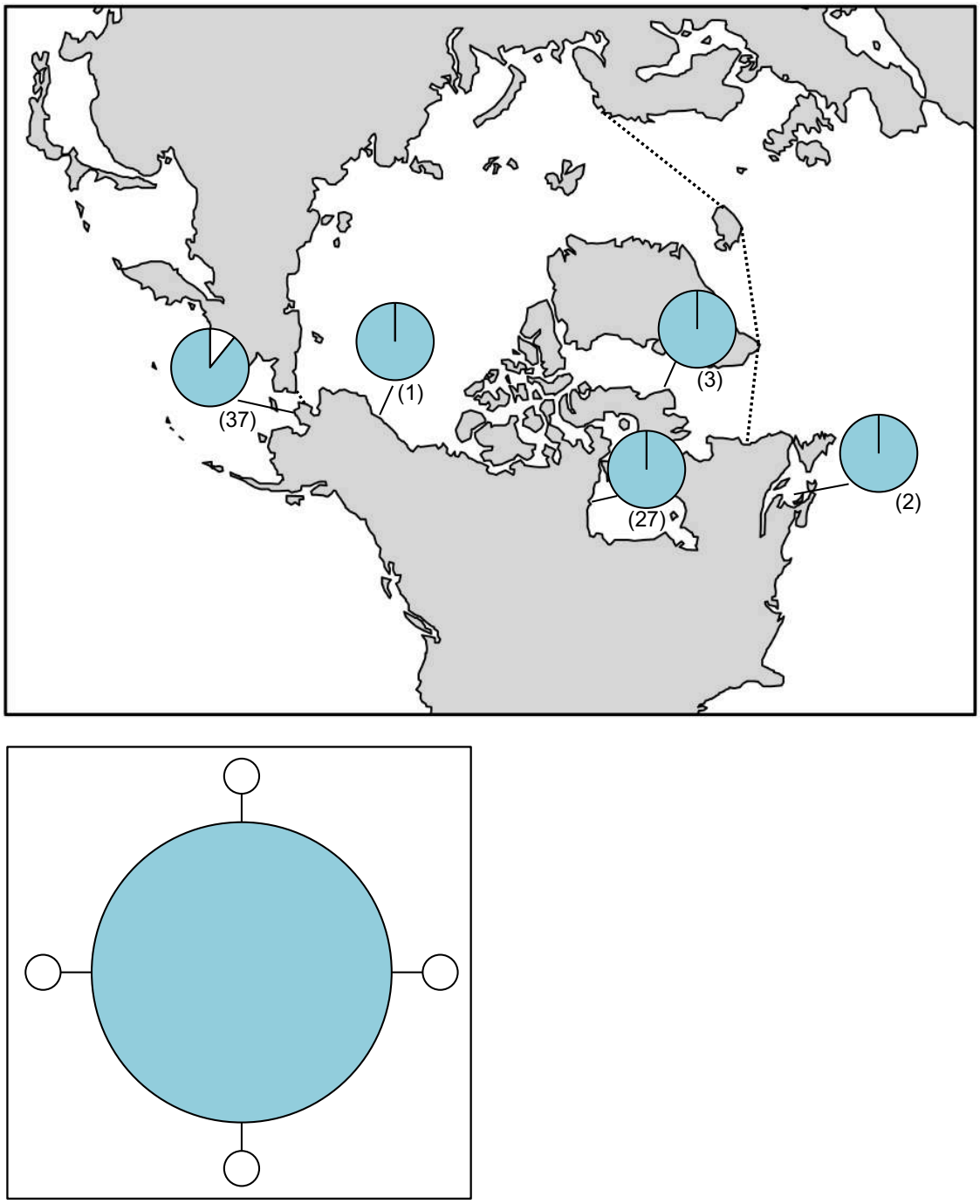

Figure E35. ***Rhodomela virgata*** **haplotype map and network based on COI-5P data. In the map, numbers in parentheses refer to sample sizes from given locales. The dashed line indicates delineation of the Arctic Ocean. In the haplotype network, circle size is proportional to the sampling frequency of a given haplotype.**

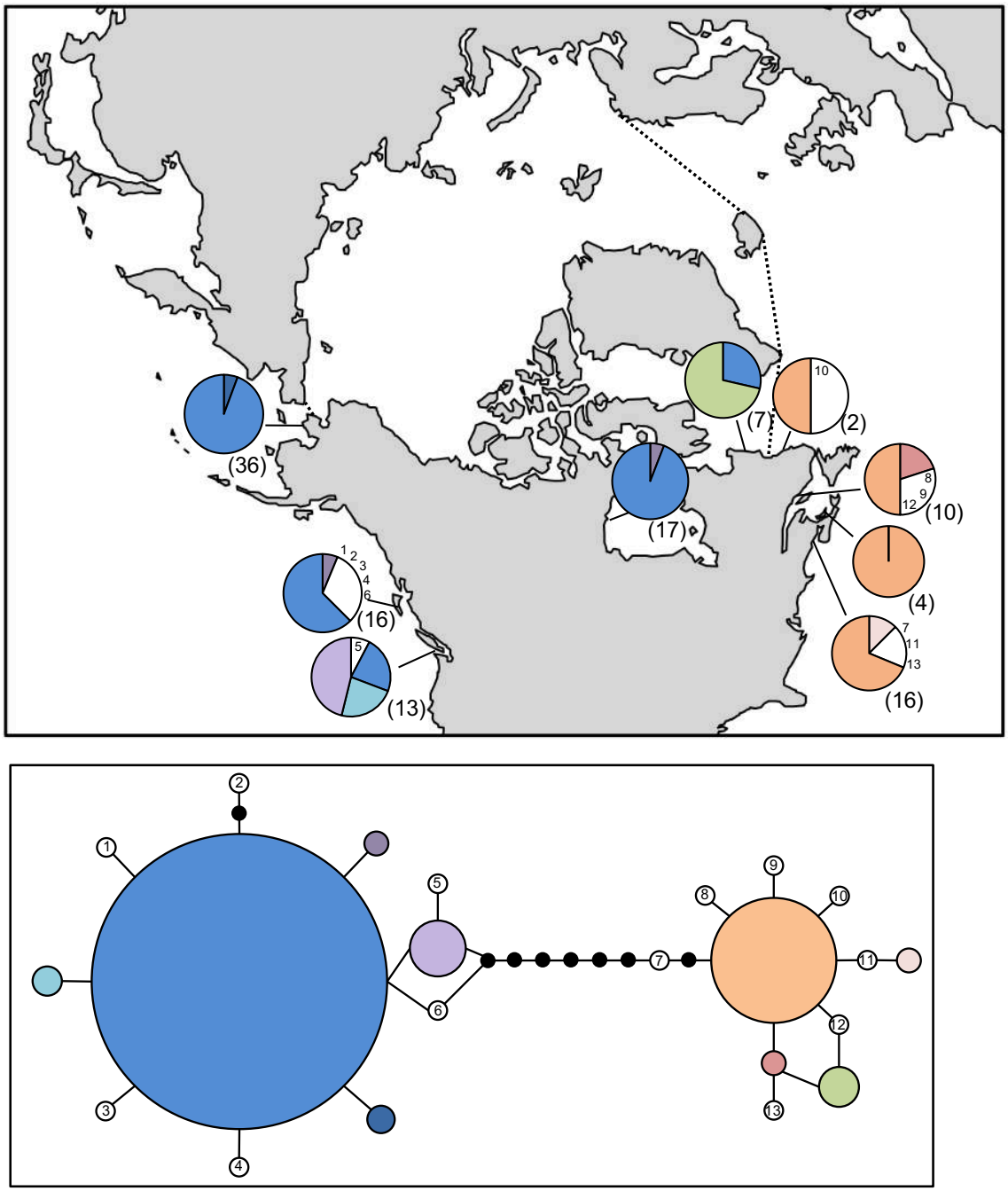

Figure E36. ***Scagelia pylaisaei*** **haplotype map and network based on COI-5P data. In the map, numbers in parentheses refer to sample sizes from given locales, whereas numbers adjacent to white portions of pie charts refer to a haplotype sampled only once in the accompanying network. The dashed line indicates delineation of the Arctic Ocean. In the haplotype network, numbered haplotypes in white reference back to the map. Black circles indicate hypothesized (e.g. unsampled) haplotypes between clades. Circle size is proportional to the sampling frequency of a given haplotype.**

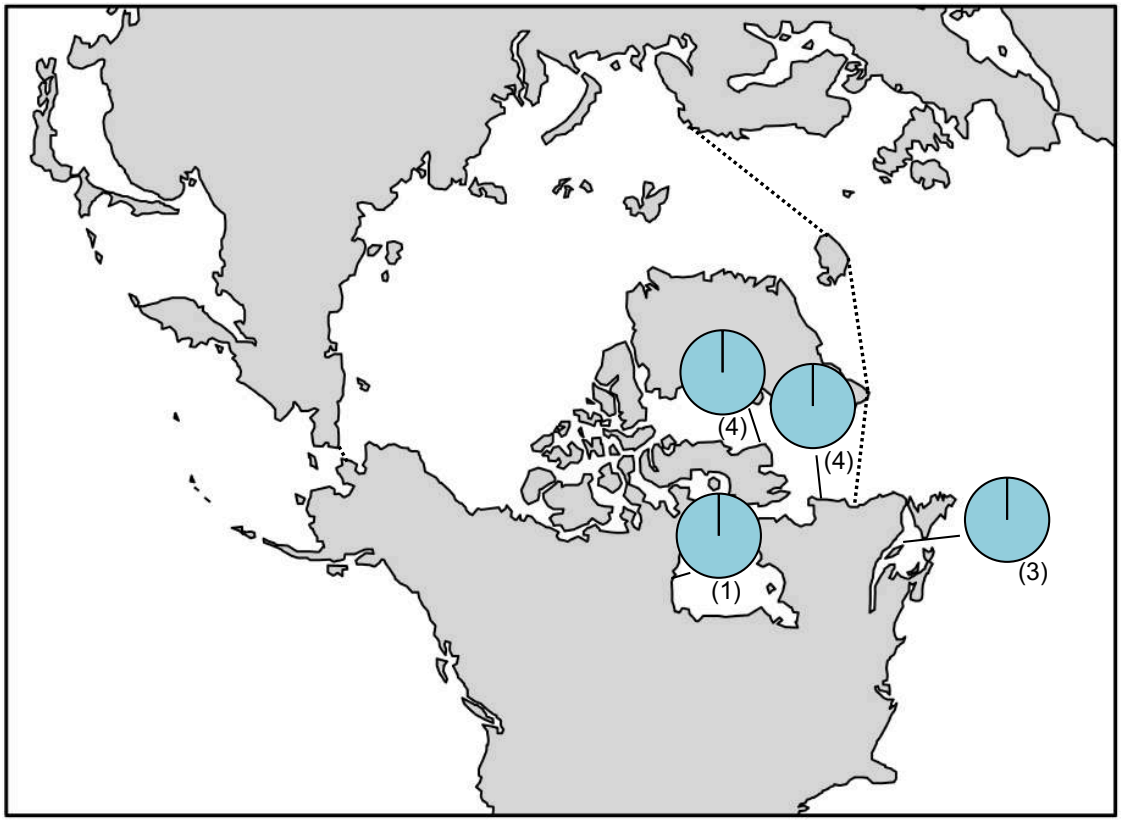

Figure E37. *Turnerella pennyi* haplotype map based on *rbc*L-3P data. In the map, numbers in parentheses refer to sample sizes from given locales. The dashed line indicates delineation of the Arctic Ocean.

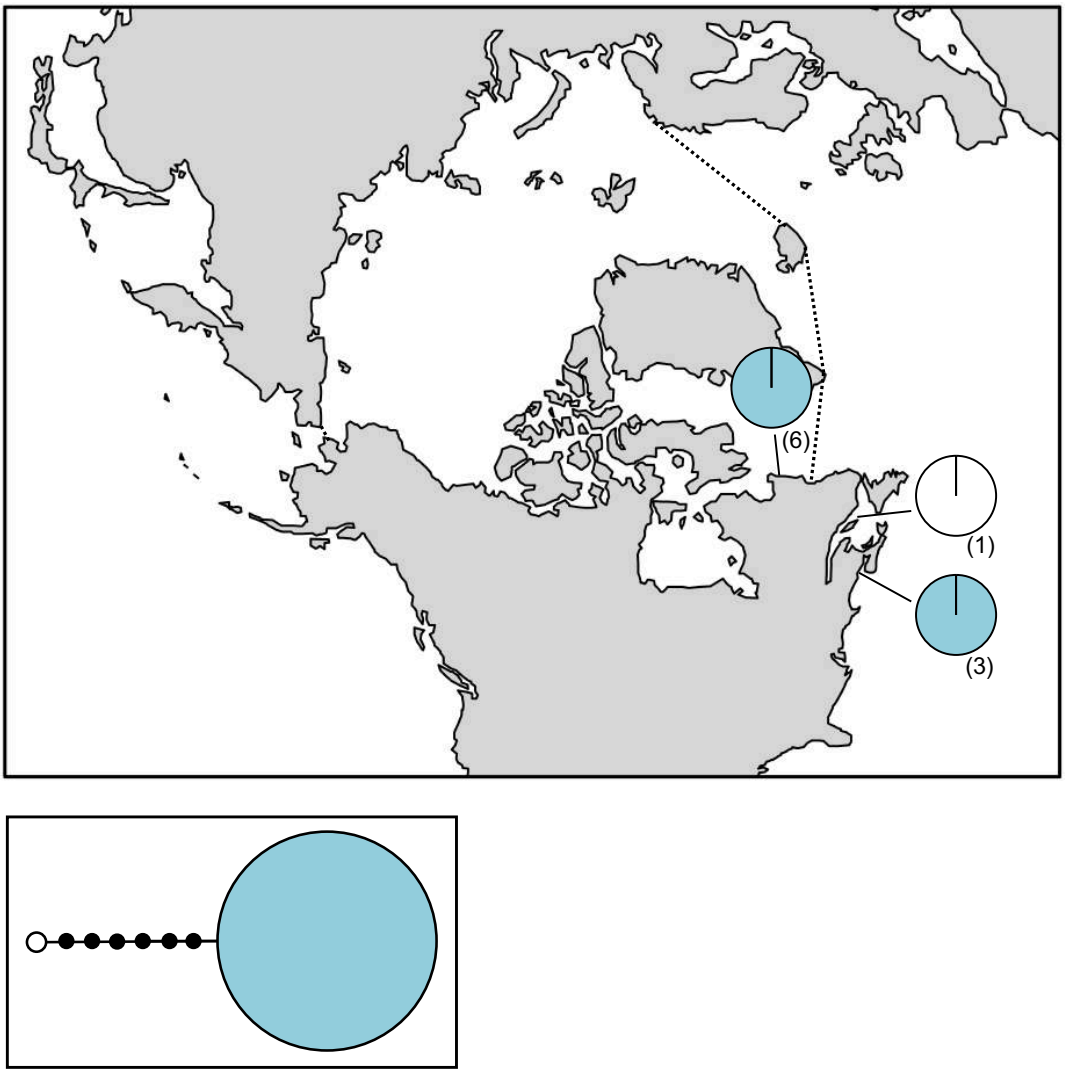

Figure E38. ***Waernia mirabilis*** **haplotype map based on COI-5P data. In the map, numbers in parentheses refer to sample sizes from given locales. The dashed line indicates delineation of the Arctic Ocean. In the haplotype network, black circles indicate hypothesized (e.g. unsampled) haplotypes between clades. Circle size is proportional to the sampling frequency of a given haplotype.**

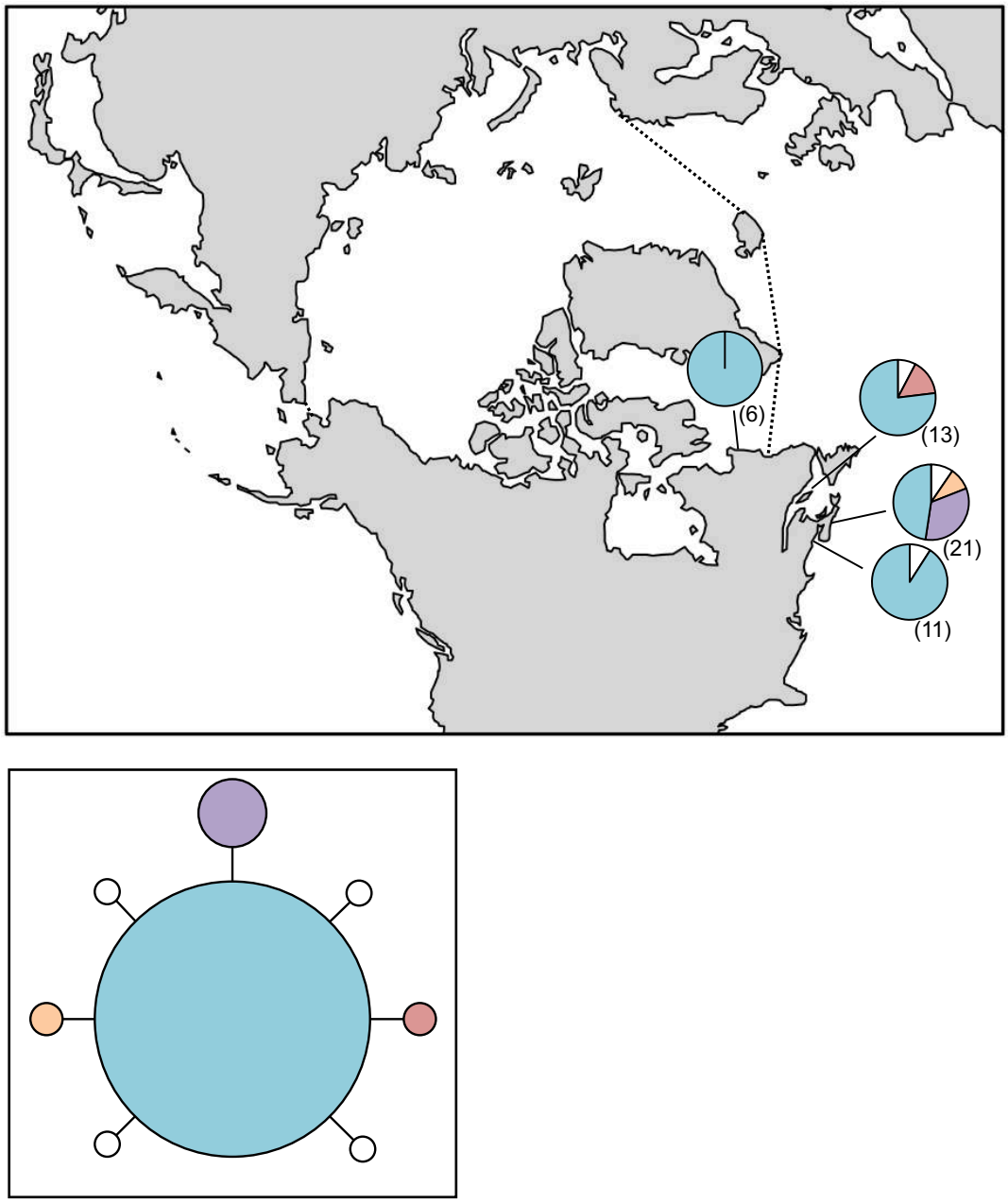

Figure E39. *Wildemania miniata* haplotype map based on COI-5P data. In the map, numbers in parentheses refer to sample sizes from given locales. The dashed line indicates delineation of the Arctic Ocean. In the haplotype network, circle size is proportional to the sampling frequency of a given haplotype.

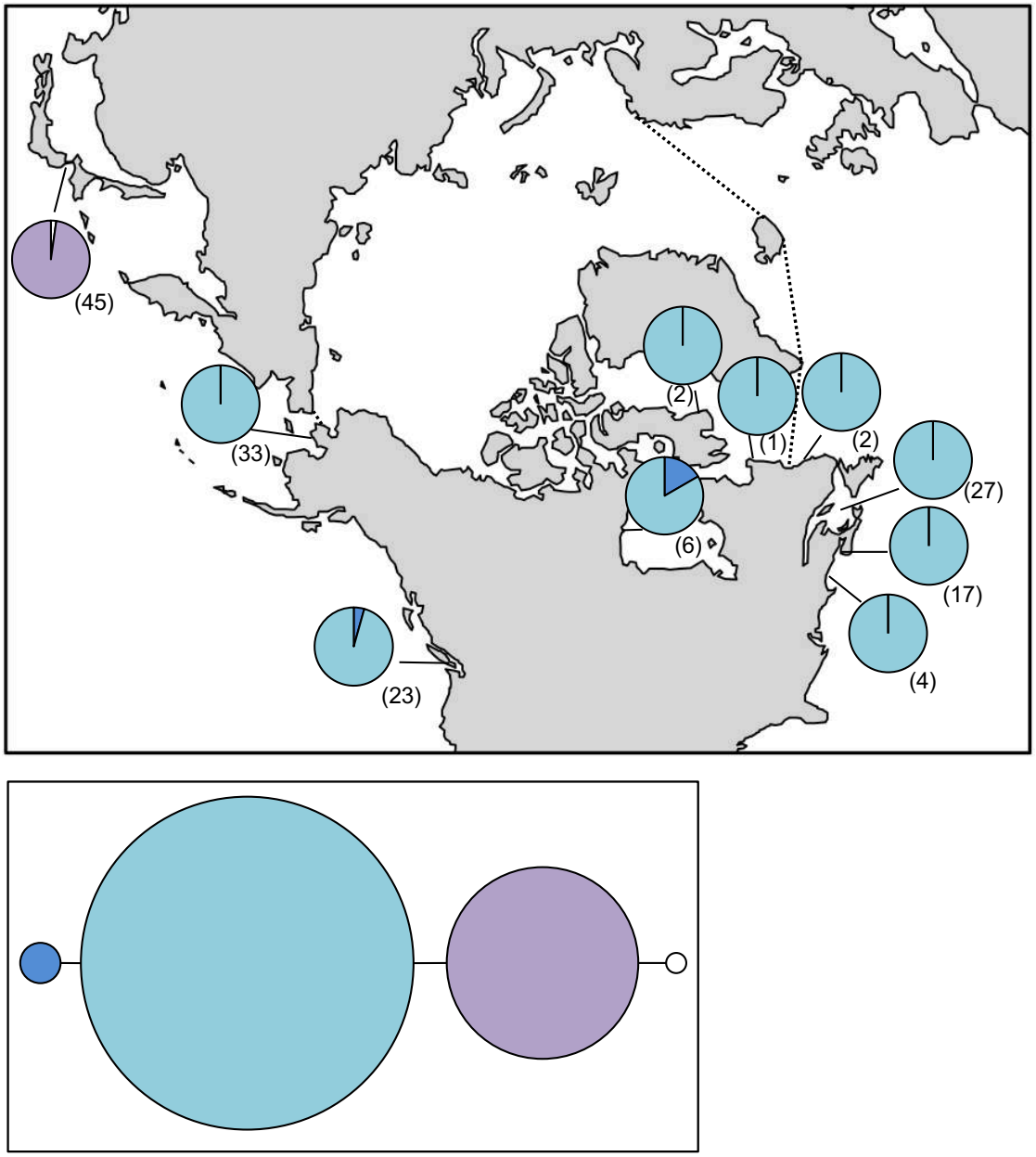

Figure E40. ***Agarum clathratum*** **haplotype map and network based on COI-5P data. In the map, numbers in parentheses refer to sample sizes from given locales. The dashed line indicates delineation of the Arctic Ocean. In the haplotype network, circle size is proportional to the sampling frequency of a given haplotype.**

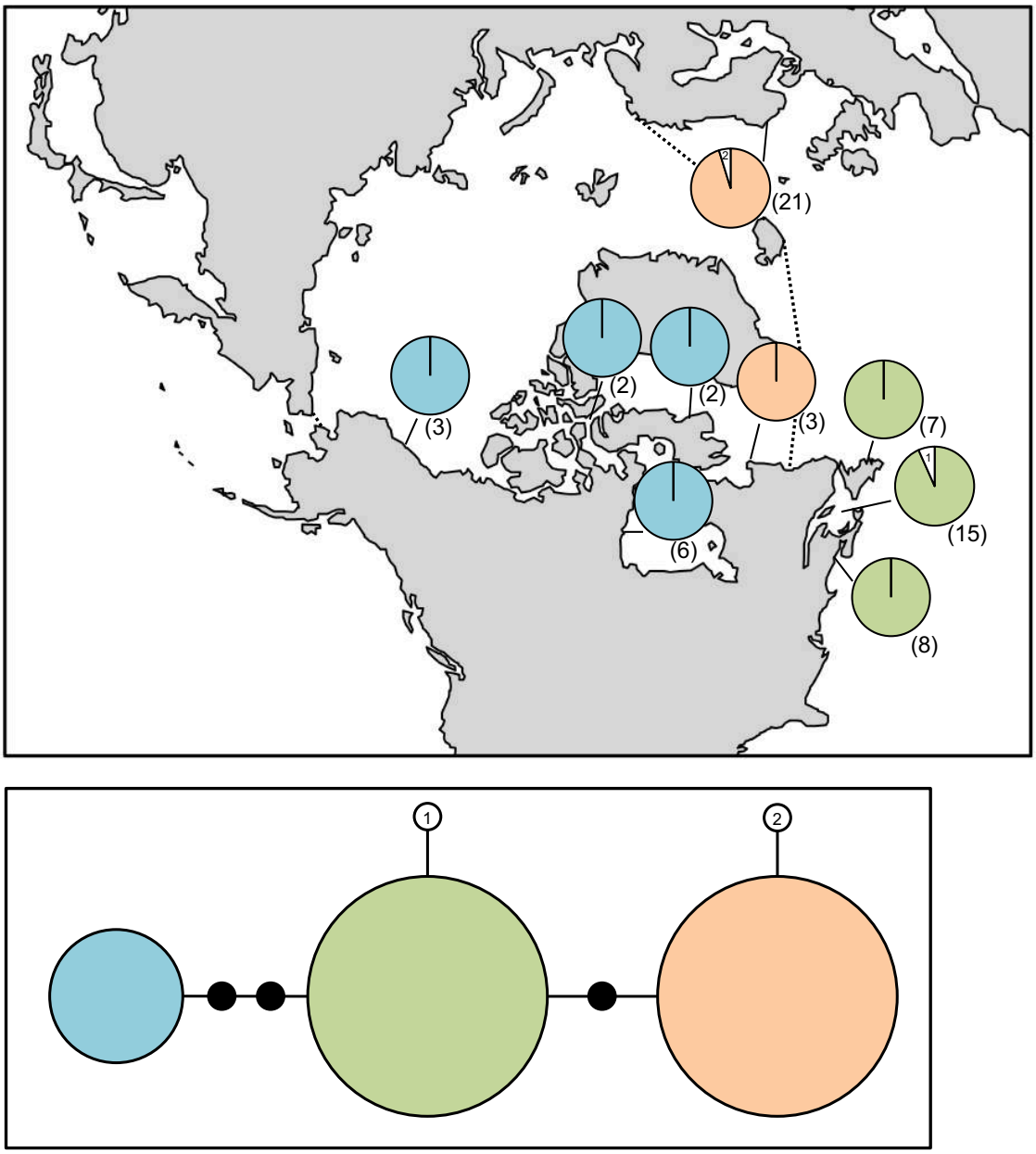

Figure E41. ***Alaria esculenta*** **haplotype map and network based on COI-5P data. In the map, numbers in parentheses refer to sample sizes from given locales, whereas numbers adjacent to white portions of pie charts refer to a haplotype sampled only once in the accompanying network. The dashed line indicates delineation of the Arctic Ocean. In the haplotype network, numbered haplotypes in white reference back to the map. Black circles indicate hypothesized (e.g. unsampled) haplotypes between clades. Circle size is proportional to the sampling frequency of a given haplotype.**

Figure E42. ***Ascophyllum nodosum*** **haplotype map based on COI-5P data. In the map, numbers in parentheses refer to sample sizes from given locales. The dashed line indicates delineation of the Arctic Ocean.**

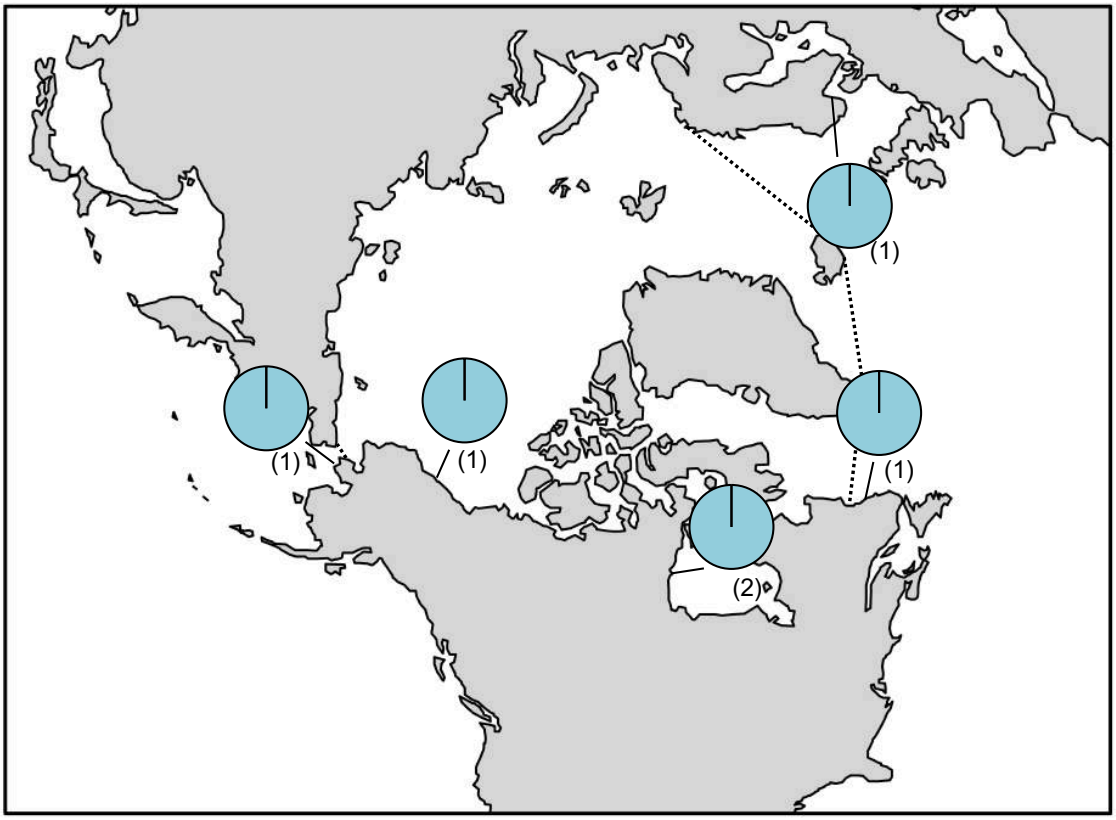

Figure E43. *Battersia arctica* haplotype map based on *rbc*L-3P data. In the map, numbers in parentheses refer to sample sizes from given locales. The dashed line indicates delineation of the Arctic Ocean.

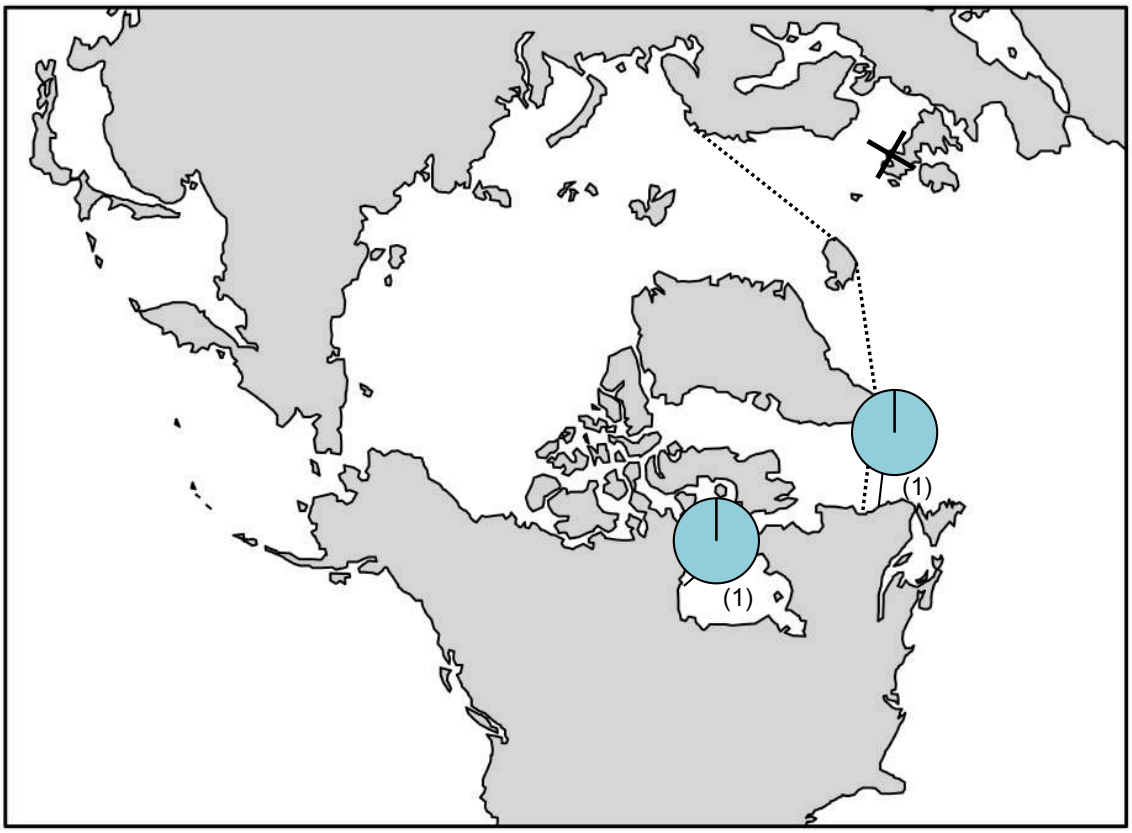

Figure E44. ***Battersia racemosa*** **haplotype map based on COI-5P data. In the map, numbers in parentheses refer to sample sizes from given locales. The dashed line indicates delineation of the Arctic Ocean, while the black X indicates the location of genetically verified** ***Battersia racemosa*** **based on** ***rbc*****L.**

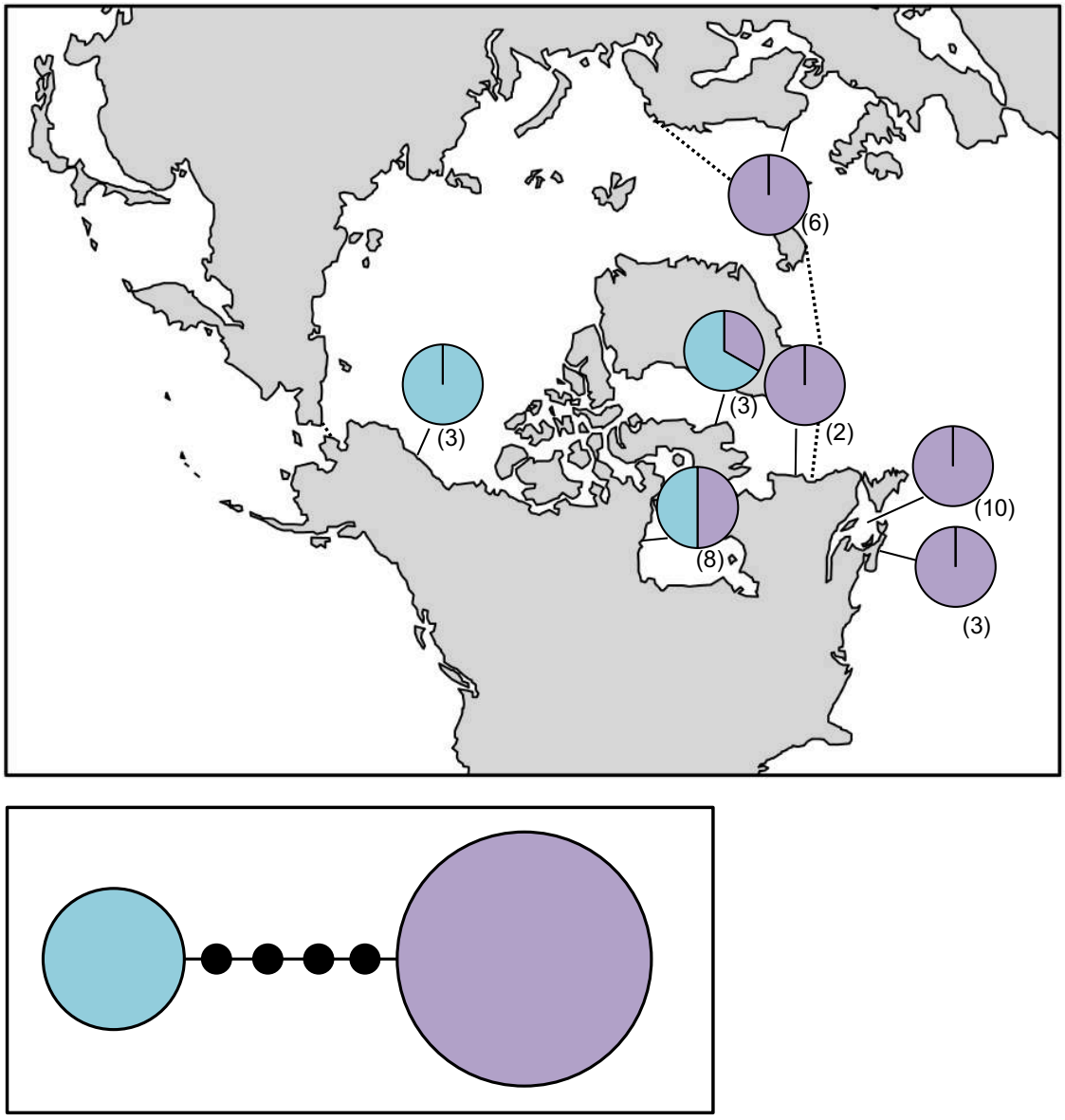

Figure E45. ***Chaetopteris plumosa*** **haplotype map and network based on COI-5P data. In the map, numbers in parentheses refer to sample sizes from given locales. The dashed line indicates delineation of the Arctic Ocean. In the haplotype network, black circles indicate hypothesized (e.g. unsampled) haplotypes between clades. Circle size is proportional to the sampling frequency of a given haplotype.**

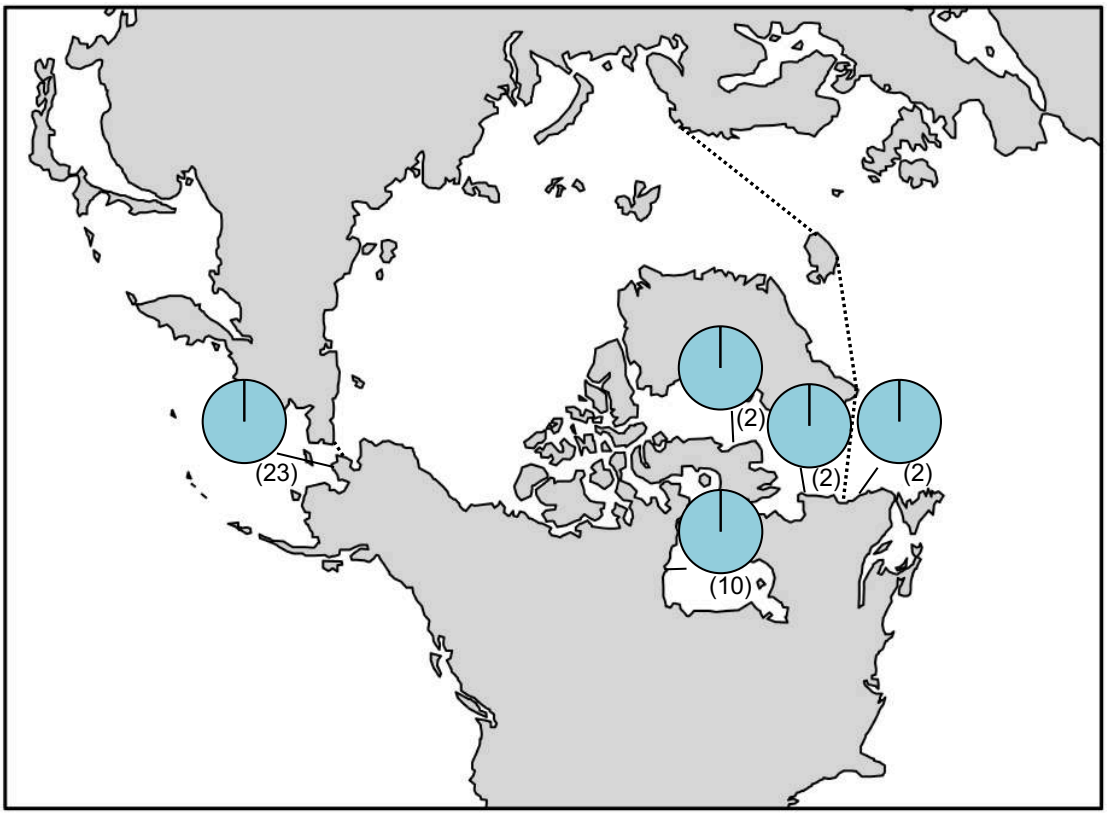

Figure E46. *Chorda* sp. 1filum haplotype map based on COI-5P data. In the map, numbers in parentheses refer to sample sizes from given locales. The dashed line indicates delineation of the Arctic Ocean.

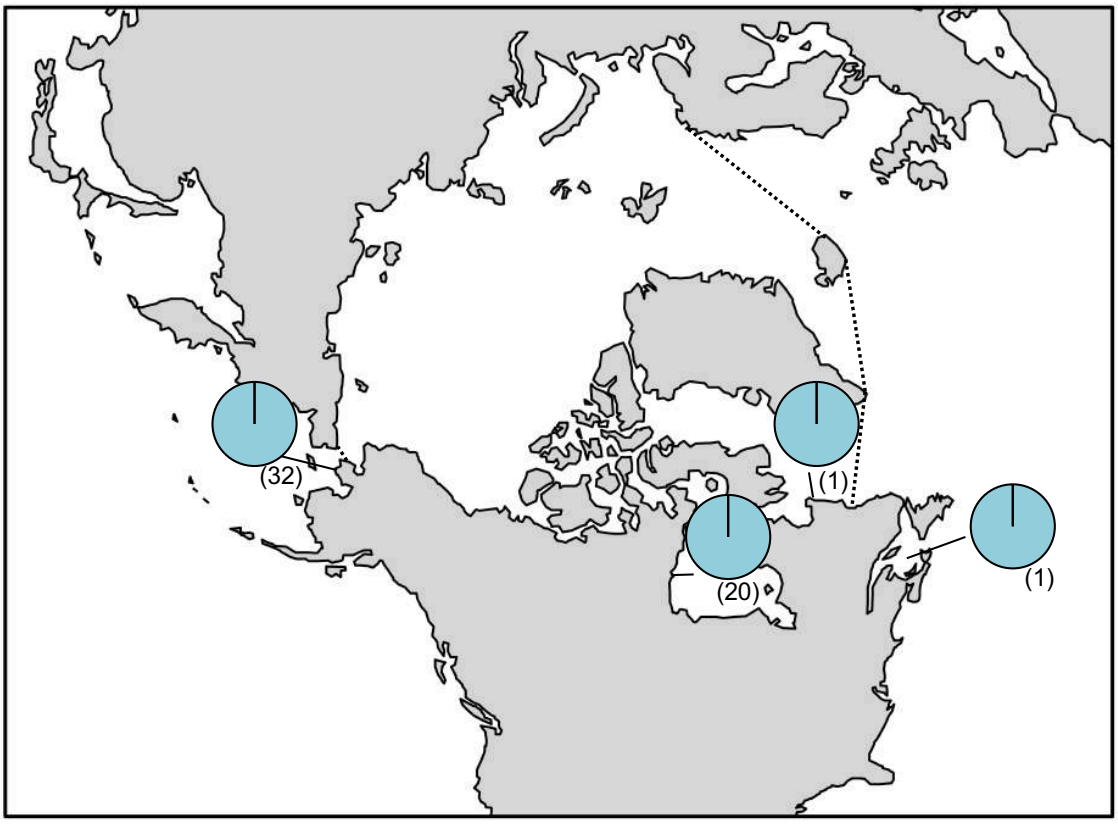

Figure E47. ***Chordaria chordaeformis*** **haplotype map based on COI-5P data. In the map, numbers in parentheses refer to sample sizes from given locales. The dashed line indicates delineation of the Arctic Ocean.**

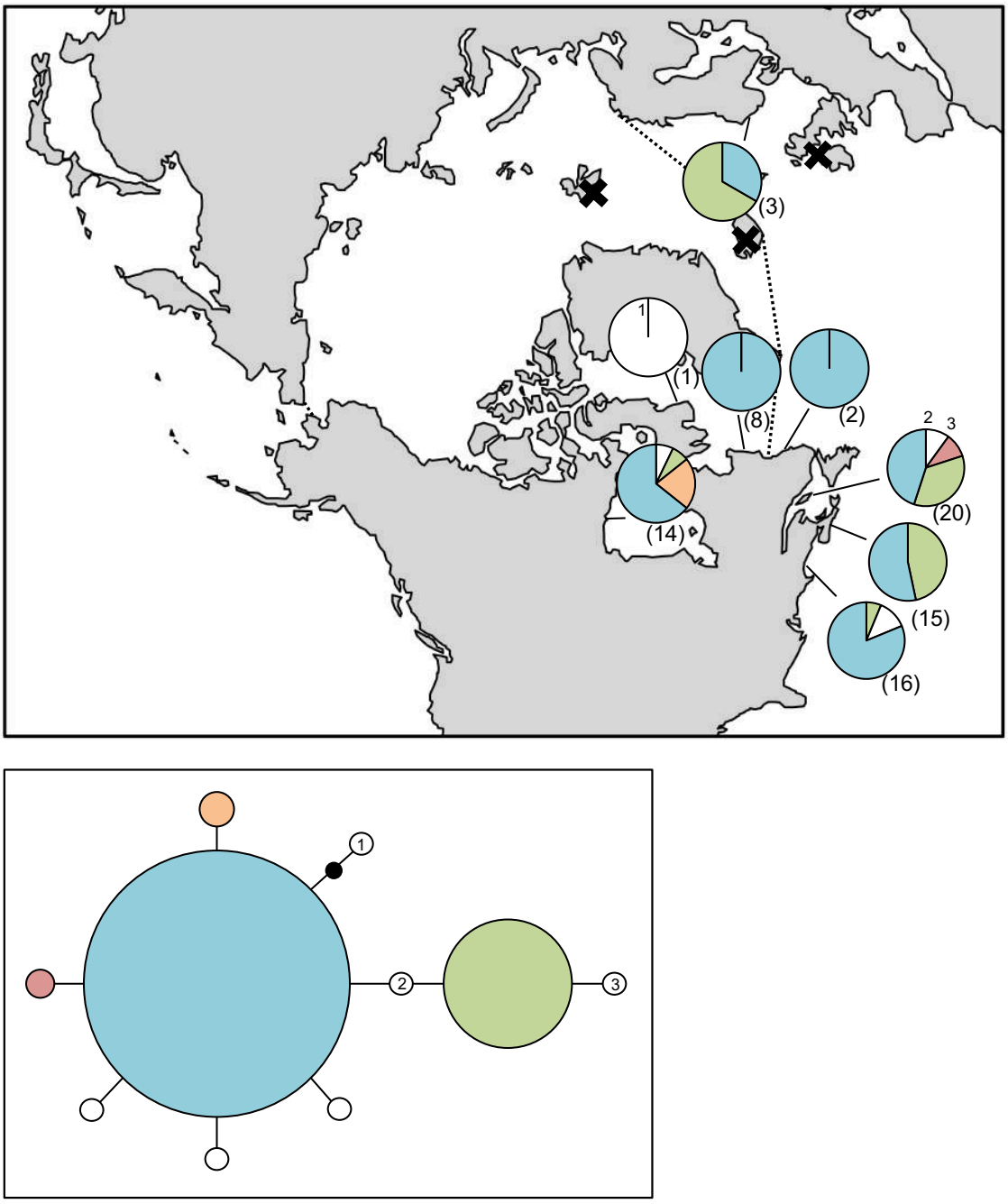

Figure E48. ***Chordaria flagelliformis*** **haplotype map and network based on COI-5P data. In the map, numbers in parentheses refer to sample sizes from given locales, whereas numbers adjacent to white portions of pie charts refer to a haplotype sampled only once in the accompanying network. The dashed line indicates delineation of the Arctic Ocean, while black X's indicate the locations of genetically verified** ***Chordaria flagelliformis*** **based on** ***rbc*****L. In the haplotype network, numbered haplotypes in white reference back to the map. Black circles indicate hypothesized (e.g. unsampled) haplotypes between clades. Circle size is proportional to the sampling frequency of a given haplotype.**

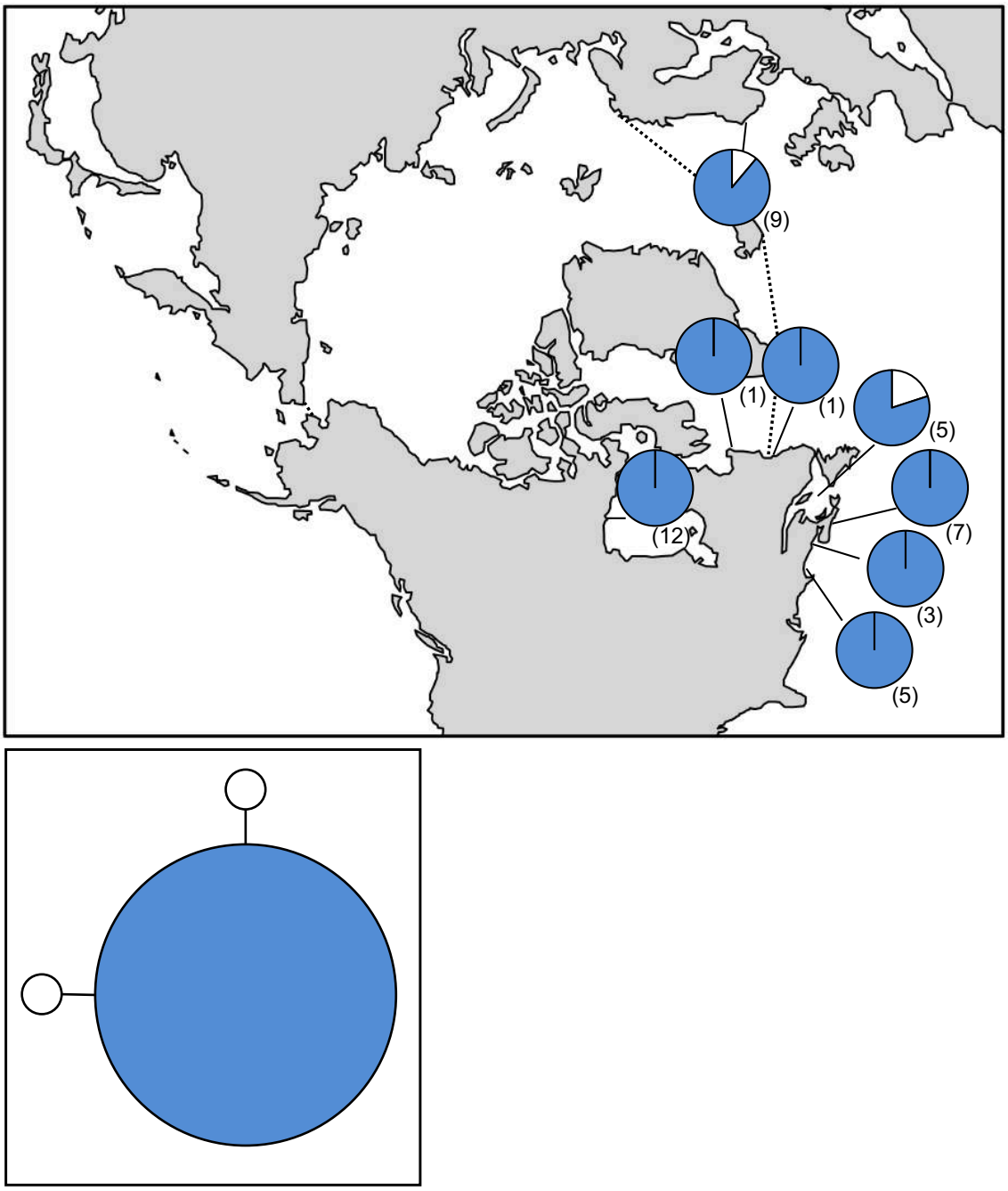

Figure E49. *Desmarestia* sp. 1aculeata haplotype map and network based on COI-5P data. In the map, numbers in parentheses refer to sample sizes from given locales. The dashed line indicates delineation of the Arctic Ocean. In the haplotype network, circle size is proportional to the sampling frequency of a given haplotype.

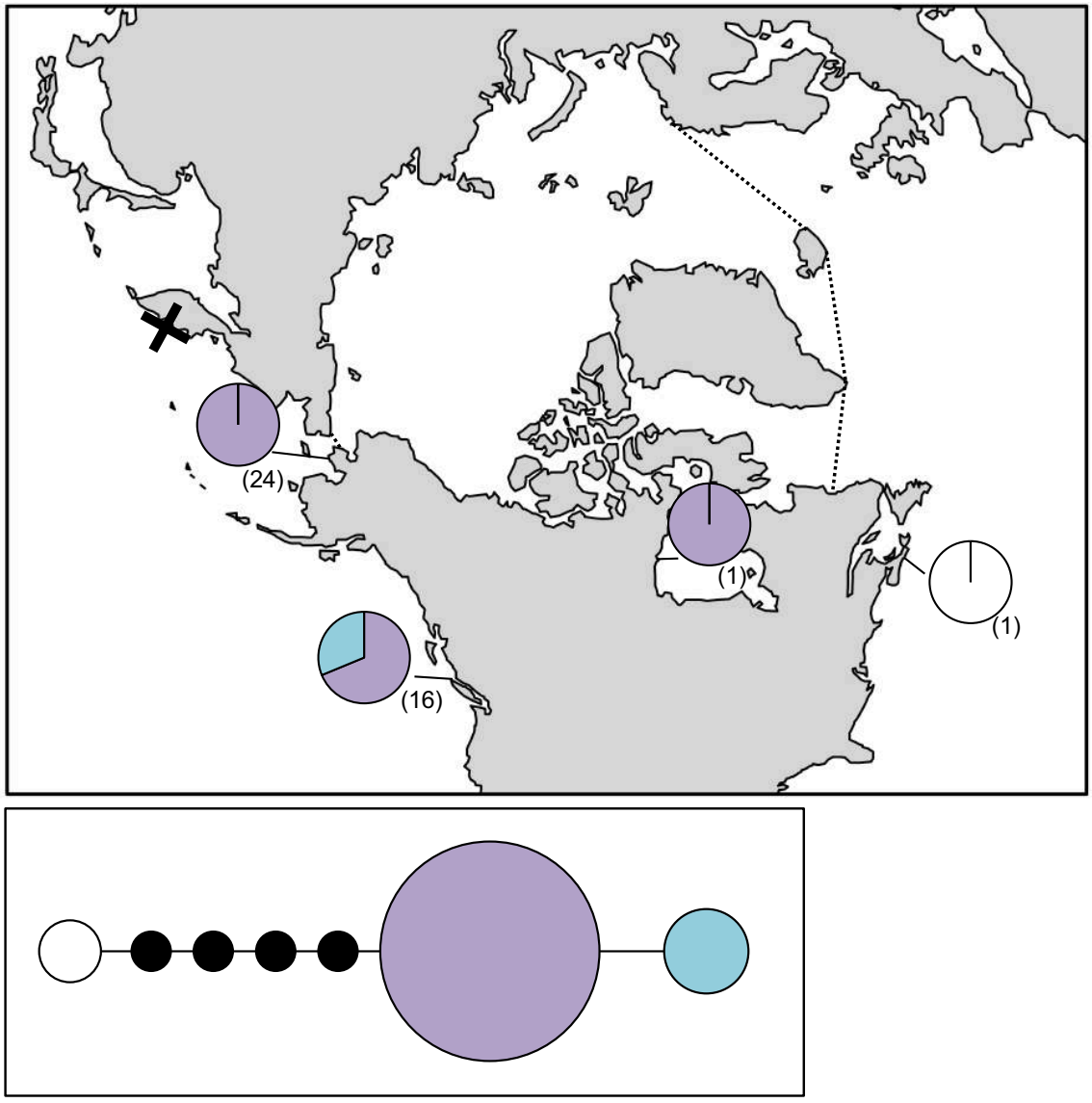

Figure E50. ***Dictyosiphon*** **sp. 1GWS haplotype map and network based on COI-5P data. In the map, numbers in parentheses refer to sample sizes from given locales. The dashed line indicates delineation of the Arctic Ocean, while the black X indicates a location for genetically verified** ***Dictyosiphon*** **sp. 1GWS based on** ***rbc*****L. In the haplotype network, black circles indicate hypothesized (e.g. unsampled) haplotypes between clades. Circle size is proportional to the sampling frequency of a given haplotype.**

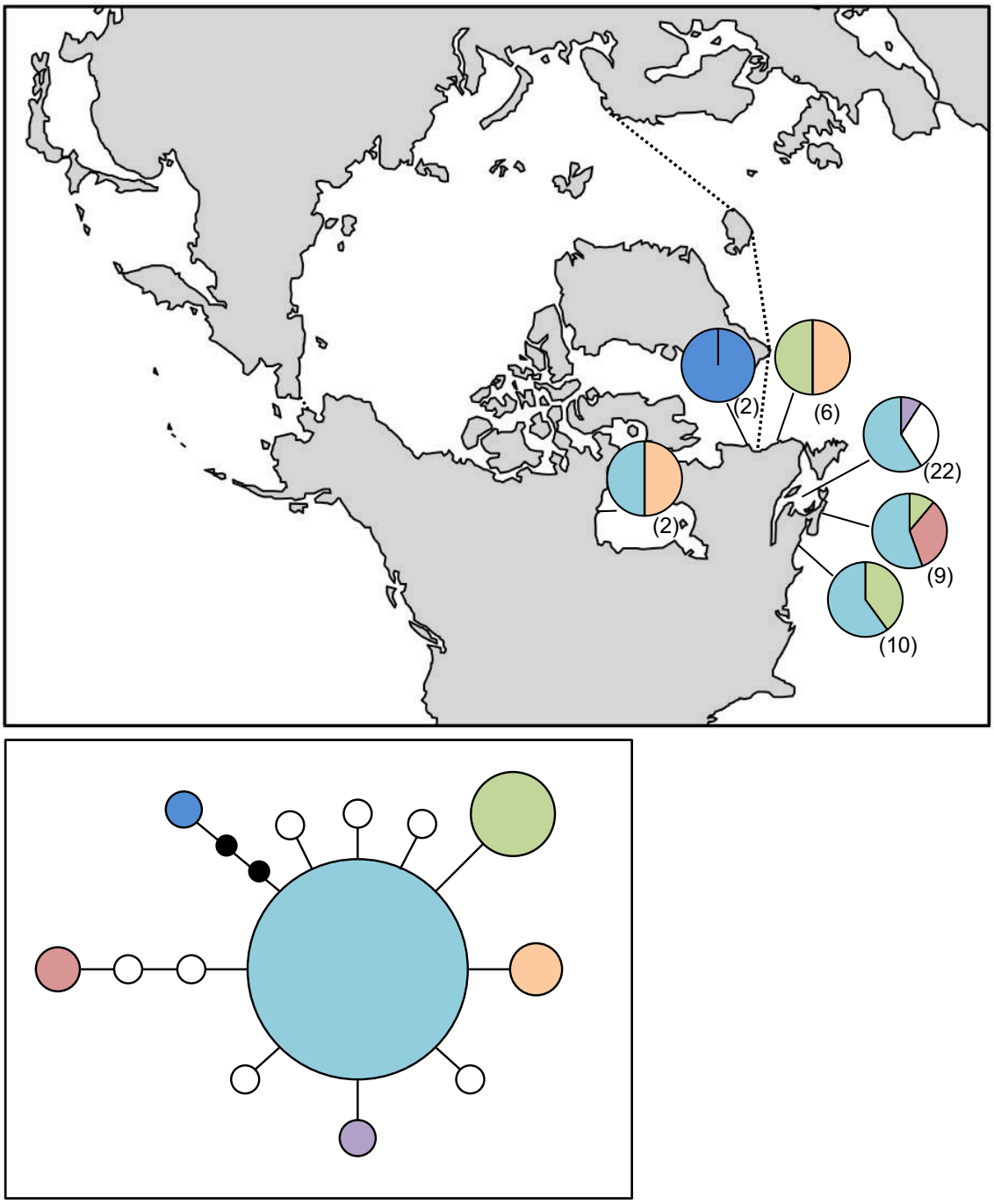

Figure E51. ***Dictyosiphon foeniculaceus*** **haplotype map and network based on COI-5P data. In the map, numbers in parentheses refer to sample sizes from given locales. The dashed line indicates delineation of the Arctic Ocean. In the haplotype network, the black circles indicate hypothesized (e.g. unsampled) haplotypes between clades. Circle size is proportional to the sampling frequency of a given haplotype.**

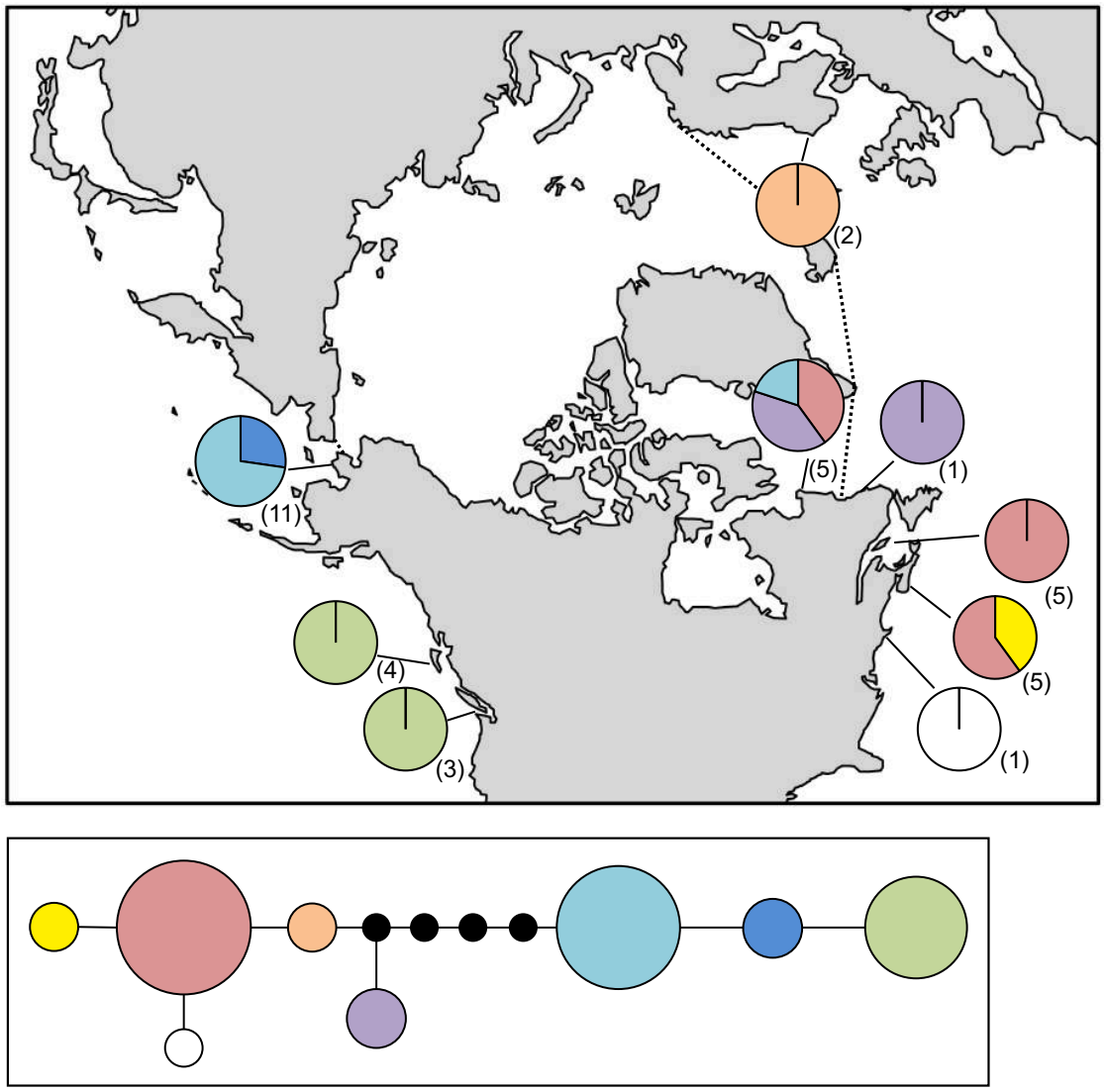

Figure E52. ***Eudesme virescens*** **haplotype map and network based on COI-5P data. In the map, numbers in parentheses refer to sample sizes from given locales. The dashed line indicates delineation of the Arctic Ocean. In the haplotype network, the black circles indicate hypothesized (e.g. unsampled) haplotypes between clades. Circle size is proportional to the sampling frequency of a given haplotype.**

Figure E53. *Fucus distichus* haplotype map and network based on COI-5P data. In the map, numbers in parentheses refer to sample sizes from given locales, whereas numbers adjacent to white portions of pie charts refer to a haplotype sampled only once in the accompanying network. The dashed line indicates delineation of the Arctic Ocean. In the haplotype network, numbered haplotypes in white reference back to the map. Circle size is proportional to the sampling frequency of a given haplotype.

Figure E54. ***Halosiphon sp. 2tomentosus*** **haplotype map based on COI-5P data. In the map, numbers in parentheses refer to sample sizes from given locales. The dashed line indicates delineation of the Arctic Ocean.**

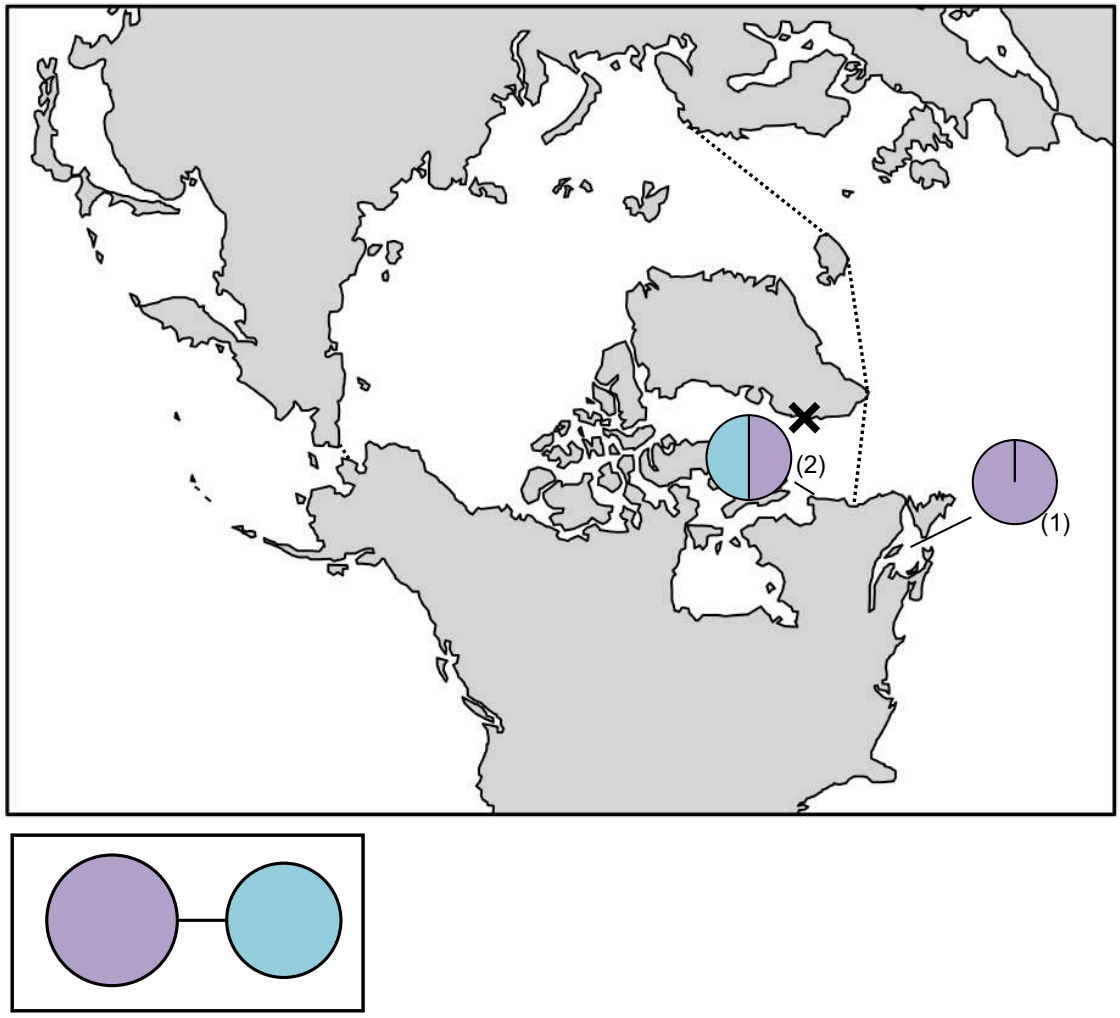

Figure E55. ***Halothrix lumbricalis*** **haplotype map based on COI-5P data. In the map, numbers in parentheses refer to sample sizes from given locales. The dashed line indicates delineation of the Arctic Ocean, while the black X indicates a location for genetically verified** ***Halothrix lumbricalis*** **based on** ***rbc*****L. In the haplotype network, circle size is proportional to the sampling frequency of a given haplotype.**

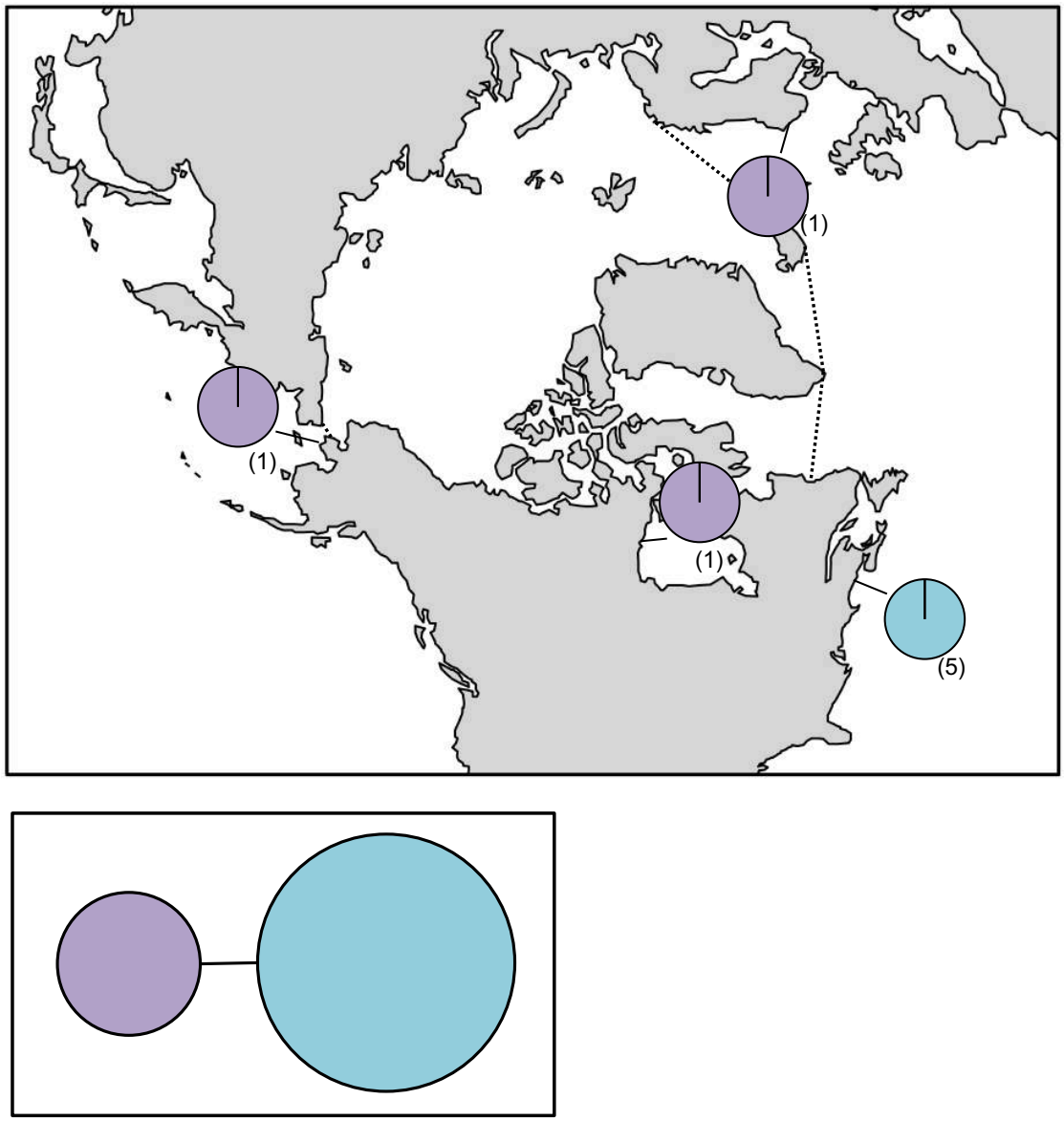

Figure E56. ***Haplospora globosa*** **haplotype map and network based on COI-5P data. In the map, numbers in parentheses refer to sample sizes from given locales. The dashed line indicates delineation of the Arctic Ocean. In the haplotype network, circle size is proportional to the sampling frequency of a given haplotype.**

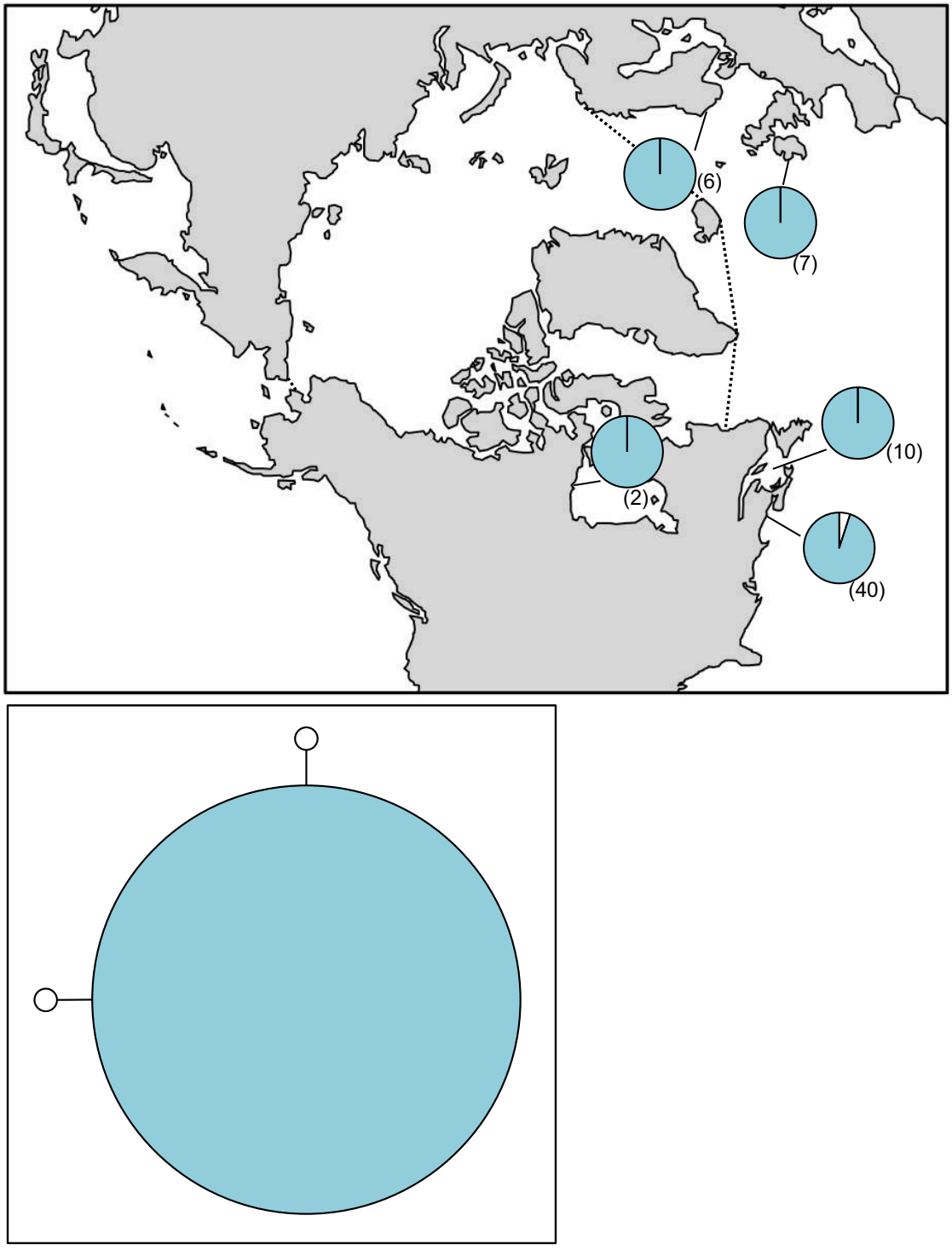

Figure E57. *Laminaria digitata* haplotype map and network based on COI-5P data. In the map, numbers in parentheses refer to sample sizes from given locales. The dashed line indicates delineation of the Arctic Ocean. In the haplotype network, circle size is proportional to the sampling frequency of a given haplotype.

Figure E58. ***Laminaria solidungula*** **haplotype map and network based on COI-5P data. In the map, numbers in parentheses refer to sample sizes from given locales. The dashed line indicates delineation of the Arctic Ocean. In the haplotype network, circle size is proportional to the sampling frequency of a given haplotype.**

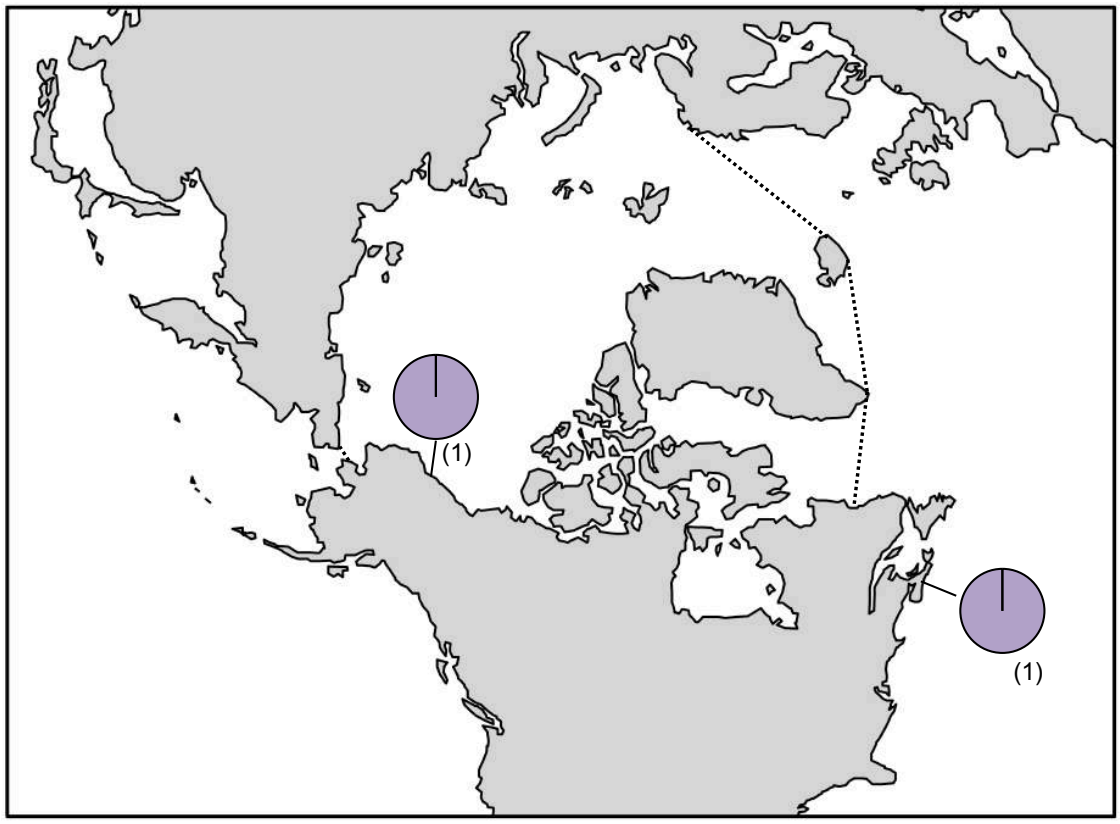

Figure E59. *Lithoderma* sp. 2GWS haplotype map based on *rbc*L-3P data. In the map, numbers in parentheses refer to sample sizes from given locales. The dashed line indicates delineation of the Arctic Ocean.

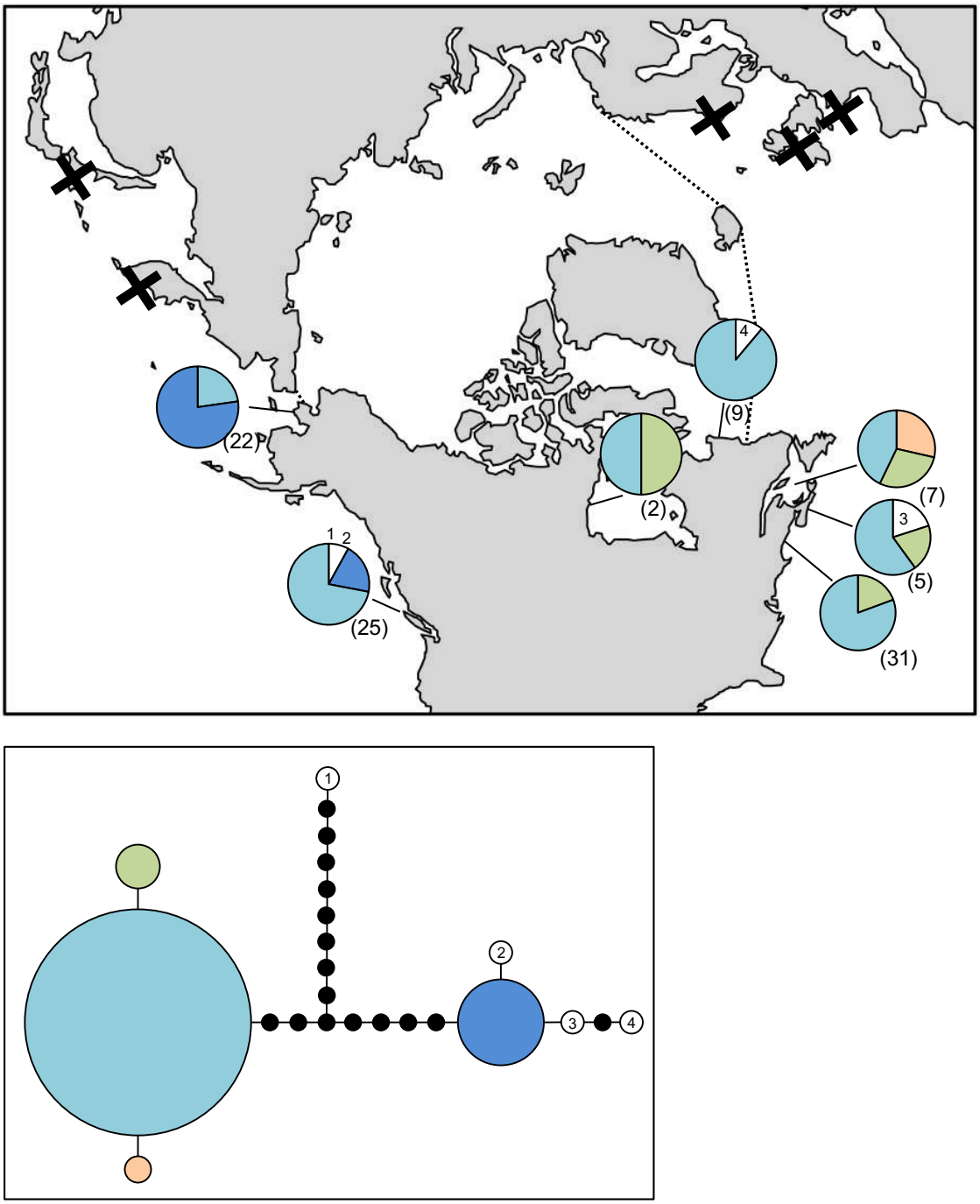

Figure E60. ***Petalonia fascia*** **haplotype map and network based on COI-5P data. In the map, numbers in parentheses refer to sample sizes from given locales, whereas numbers adjacent to white portions of pie charts refer to a haplotype sampled only once in the accompanying network. The dashed line indicates delineation of the Arctic Ocean, while black X's indicate locations for genetically verified** ***Petalonia fascia*** **based on ITS, PSA, and** ***rbc*****L. In the haplotype network, numbered haplotypes in white reference back to the map. Black circles indicate hypothesized (e.g. unsampled) haplotypes between clades. Circle size is proportional to the sampling frequency of a given haplotype.**

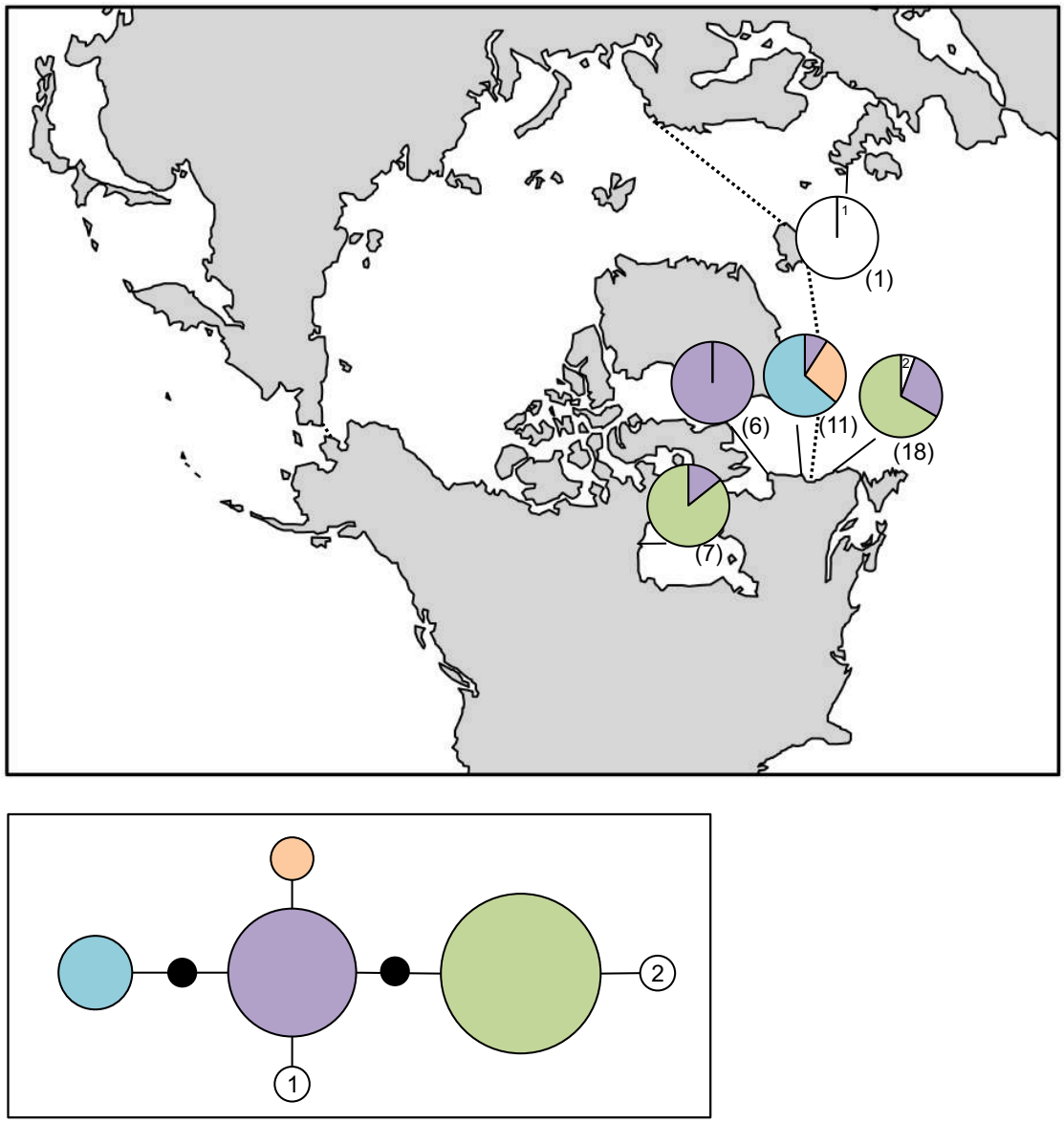

Figure E61. *Petalonia filiformis* haplotype map and network based on COI-5P data. In the map, numbers in parentheses refer to sample sizes from given locales. The dashed line indicates delineation of the Arctic Ocean. In the haplotype network, black circles indicate hypothesized (e.g. unsampled) haplotypes between clades. Circle size is proportional to the sampling frequency of a given haplotype.

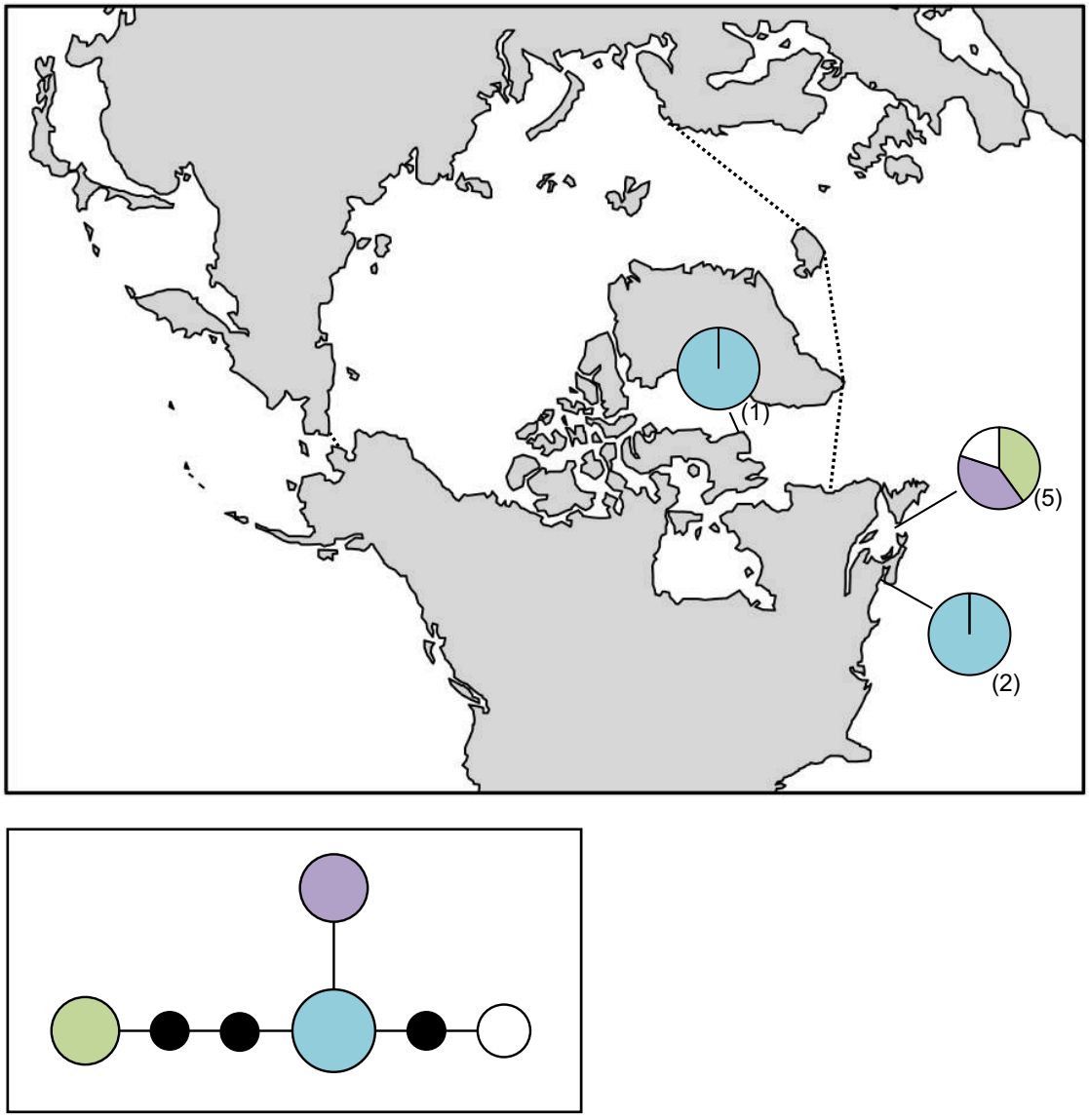

Figure E62. *Planosiphon complanatus* haplotype map and network based on COI-5P data. In the map, numbers in parentheses refer to sample sizes from given locales. The dashed line indicates delineation of the Arctic Ocean. In the haplotype network, black circles indicate hypothesized (e.g. unsampled) haplotypes between clades. Circle size is proportional to the sampling frequency of a given haplotype.

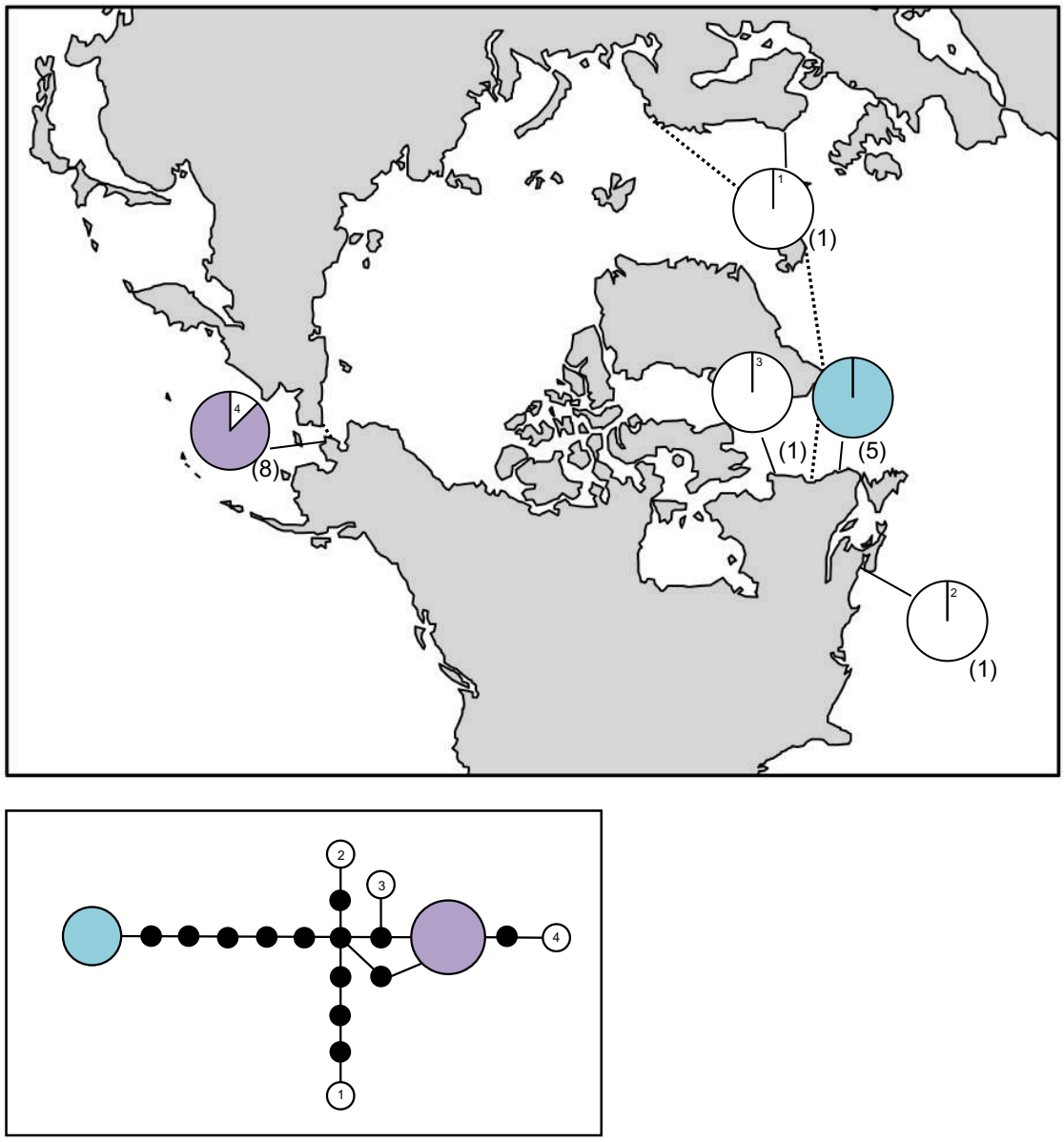

Figure E63. *Planosiphon zosterifolius* haplotype map and network based on COI-5P data. In the map, numbers in parentheses refer to sample sizes from given locales. The dashed line indicates delineation of the Arctic Ocean. In the haplotype network, black circles indicate hypothesized (e.g. unsampled) haplotypes between clades. Circle size is proportional to the sampling frequency of a given haplotype.

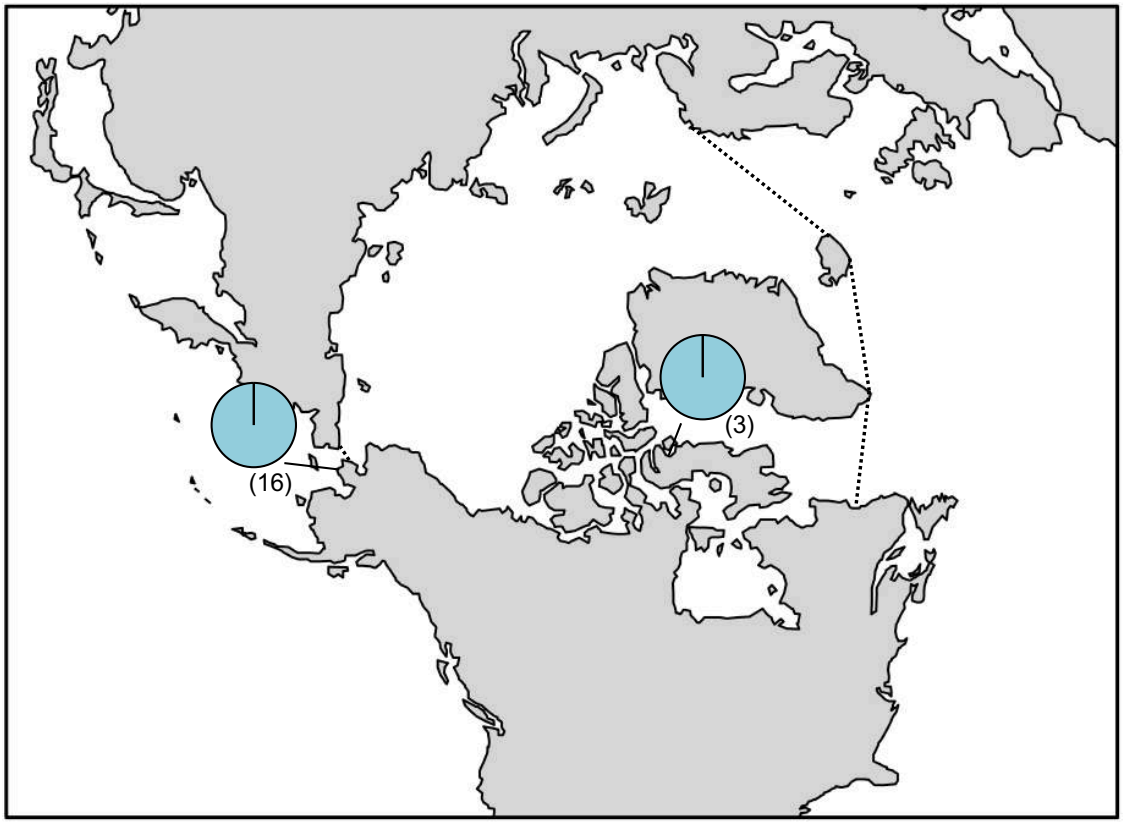

Figure E64. *Platysiphon glacialis* haplotype map based on COI-5P data. In the map, numbers in parentheses refer to sample sizes from given locales. The dashed line indicates delineation of the Arctic Ocean

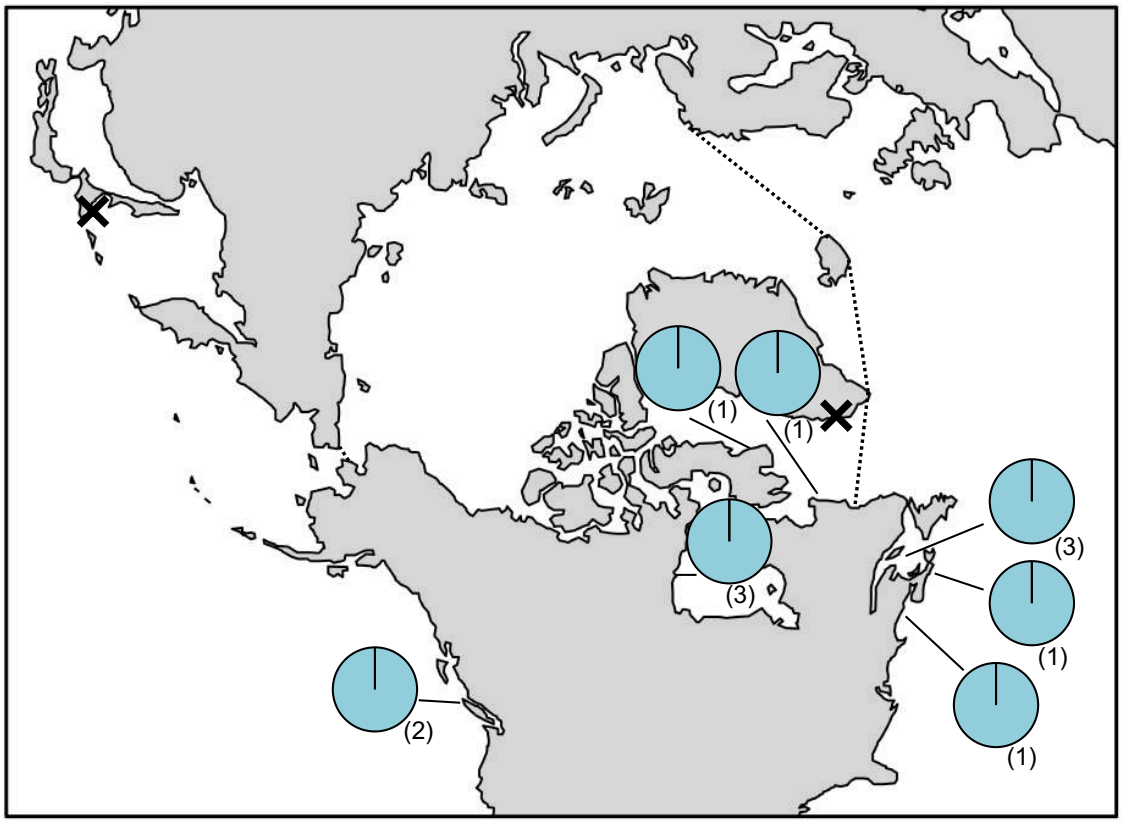

Figure E65. *Punctaria* sp. 2GWS haplotype map based on COI-5P data. In the map, numbers in parentheses refer to sample sizes from given locales. The dashed line indicates delineation of the Arctic Ocean. The black X's indicate locations for genetically verified *Punctaria* sp. 2GWS based on *rbc*L.

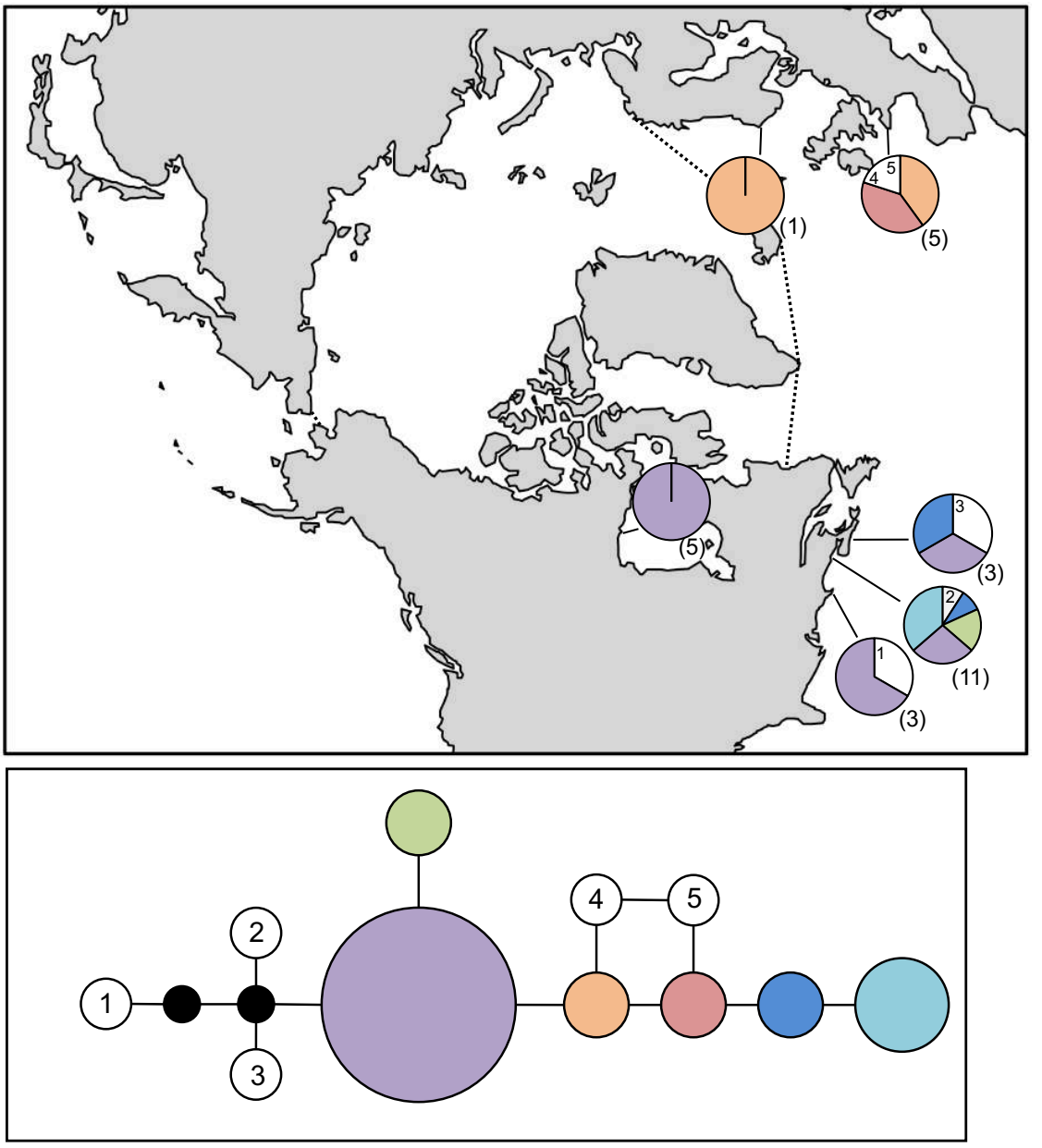

Figure E66. *Pylaiella* sp. 1littoralis haplotype map and network based on COI-5P data. In the map, numbers in parentheses refer to sample sizes from given locales, whereas numbers adjacent to white portions of pie charts refer to a haplotype sampled only once in the accompanying network. The dashed line indicates delineation of the Arctic Ocean. In the haplotype network, numbered haplotypes in white reference back to the map. Black circles indicate hypothesized (e.g. unsampled) haplotypes between clades. Circle size is proportional to the sampling frequency of a given haplotype.

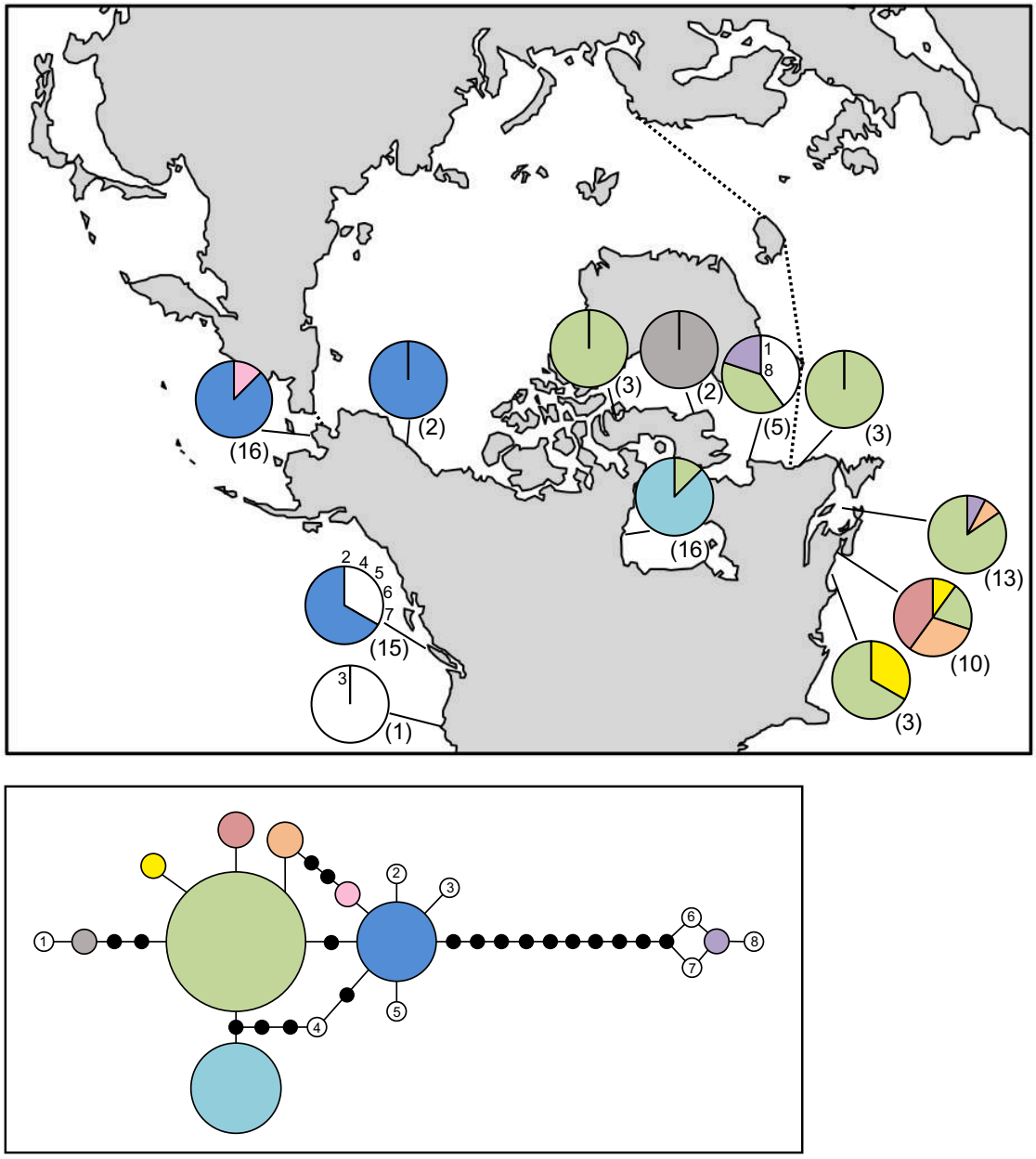

Figure E67. *Pylaiella washingtoniensis* haplotype map and network based on COI-5P data. In the map, numbers in parentheses refer to sample sizes from given locales, whereas numbers adjacent to white portions of pie charts refer to a haplotype sampled only once in the accompanying network. The dashed line indicates delineation of the Arctic Ocean. In the haplotype network, numbered haplotypes in white reference back to the map. Black circles indicate hypothesized (e.g. unsampled) haplotypes between clades. Circle size is proportional to the sampling frequency of a given haplotype.

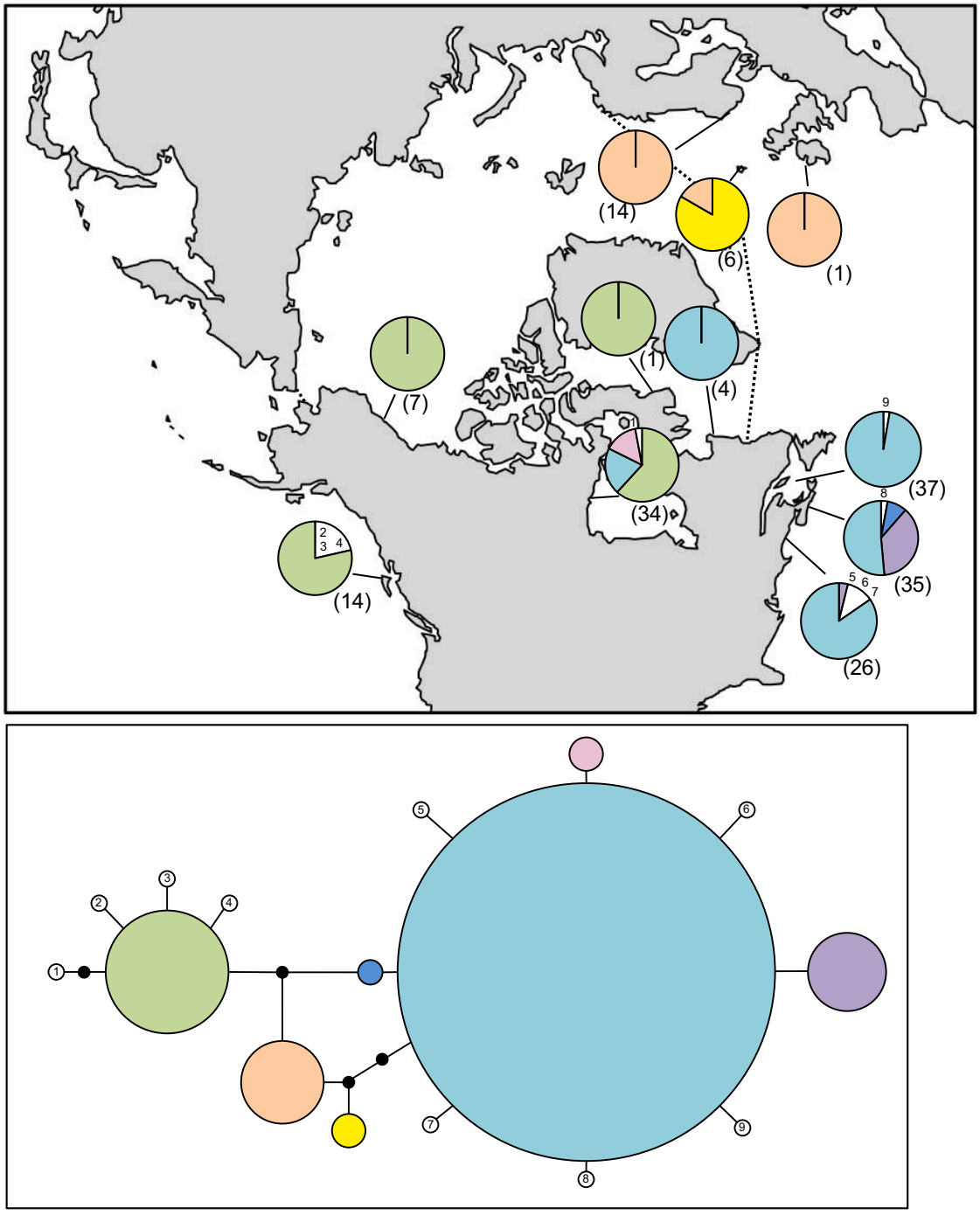

Figure E68. ***Saccharina latissima*** **haplotype map and network based on COI-5P data. In the map, numbers in parentheses refer to sample sizes from given locales, whereas numbers adjacent to white portions of pie charts refer to a haplotype sampled only once in the accompanying network. The dashed line indicates delineation of the Arctic Ocean. In the haplotype network, numbered haplotypes in white reference back to the map. Black circles indicate hypothesized (e.g. unsampled) haplotypes between clades. Circle size is proportional to the sampling frequency of a given haplotype.**

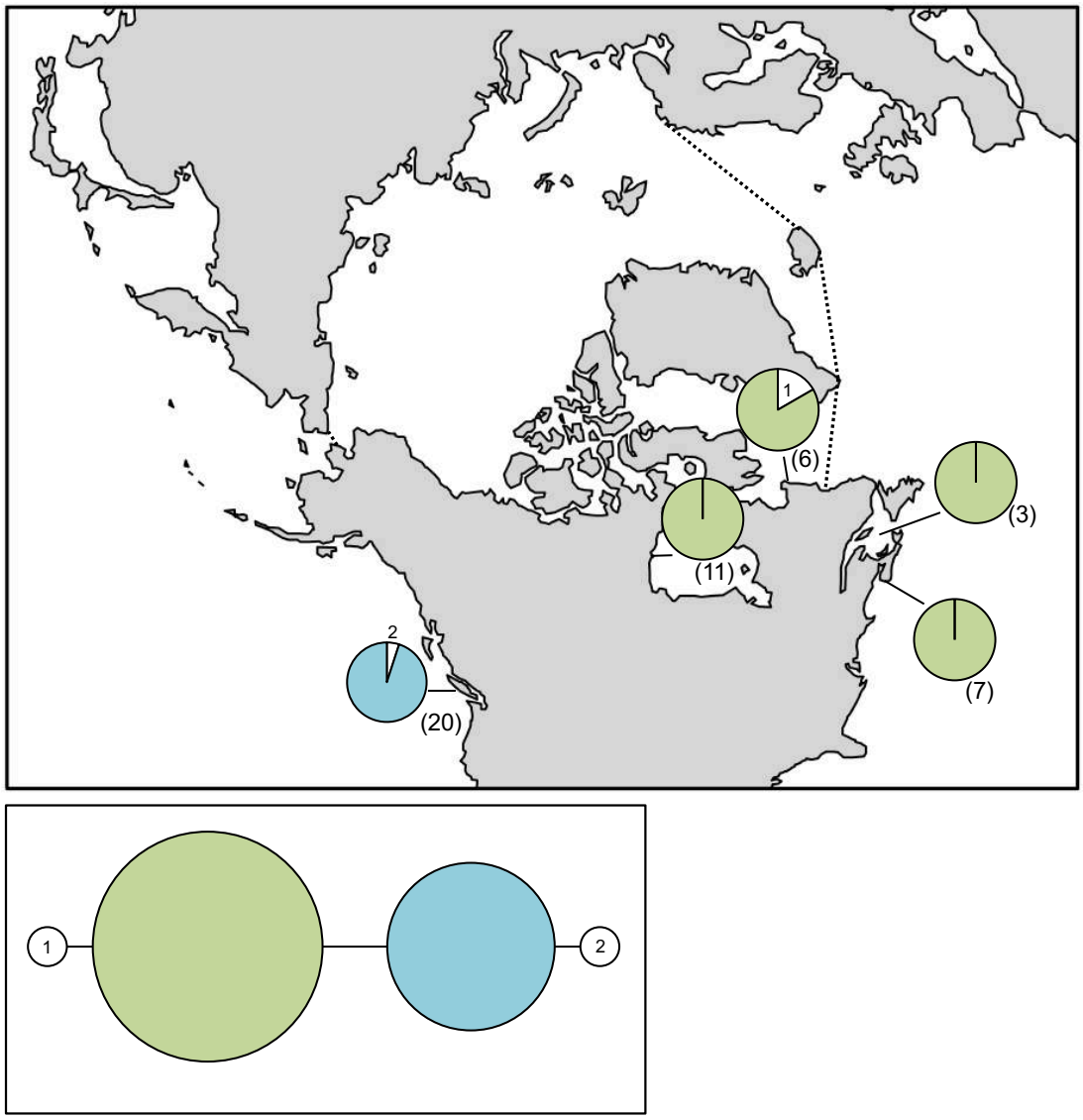

Figure E69. *Saccharina nigripes* haplotype map and network based on COI-5P data. In the map, numbers in parentheses refer to sample sizes from given locales, whereas numbers adjacent to white portions of pie charts refer to a haplotype sampled only once in the accompanying network. The dashed line indicates delineation of the Arctic Ocean. In the haplotype network, numbered haplotypes in white reference back to the map. Circle size is proportional to the sampling frequency of a given haplotype.

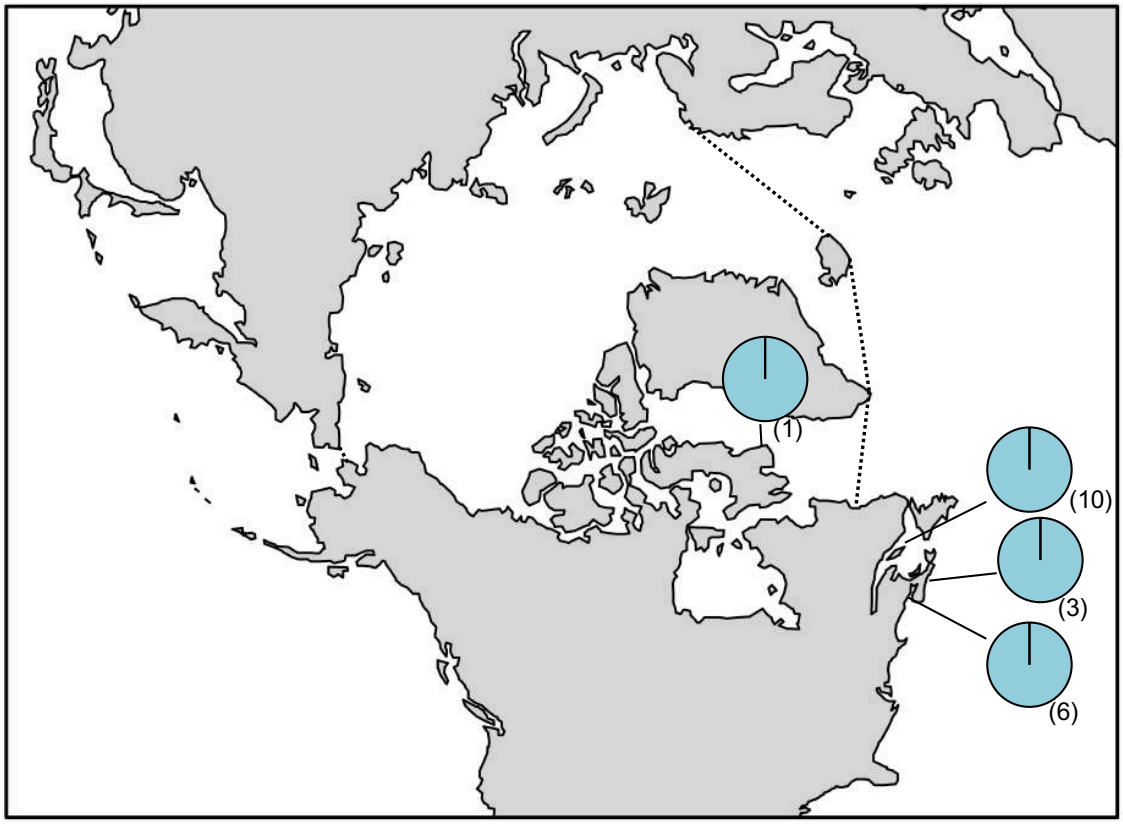

Figure E70. ***Saccorhiza dermatodea*** **haplotype map and network based on COI-5P data. In the map, numbers in parentheses refer to sample sizes from given locales. The dashed line indicates delineation of the Arctic Ocean.**

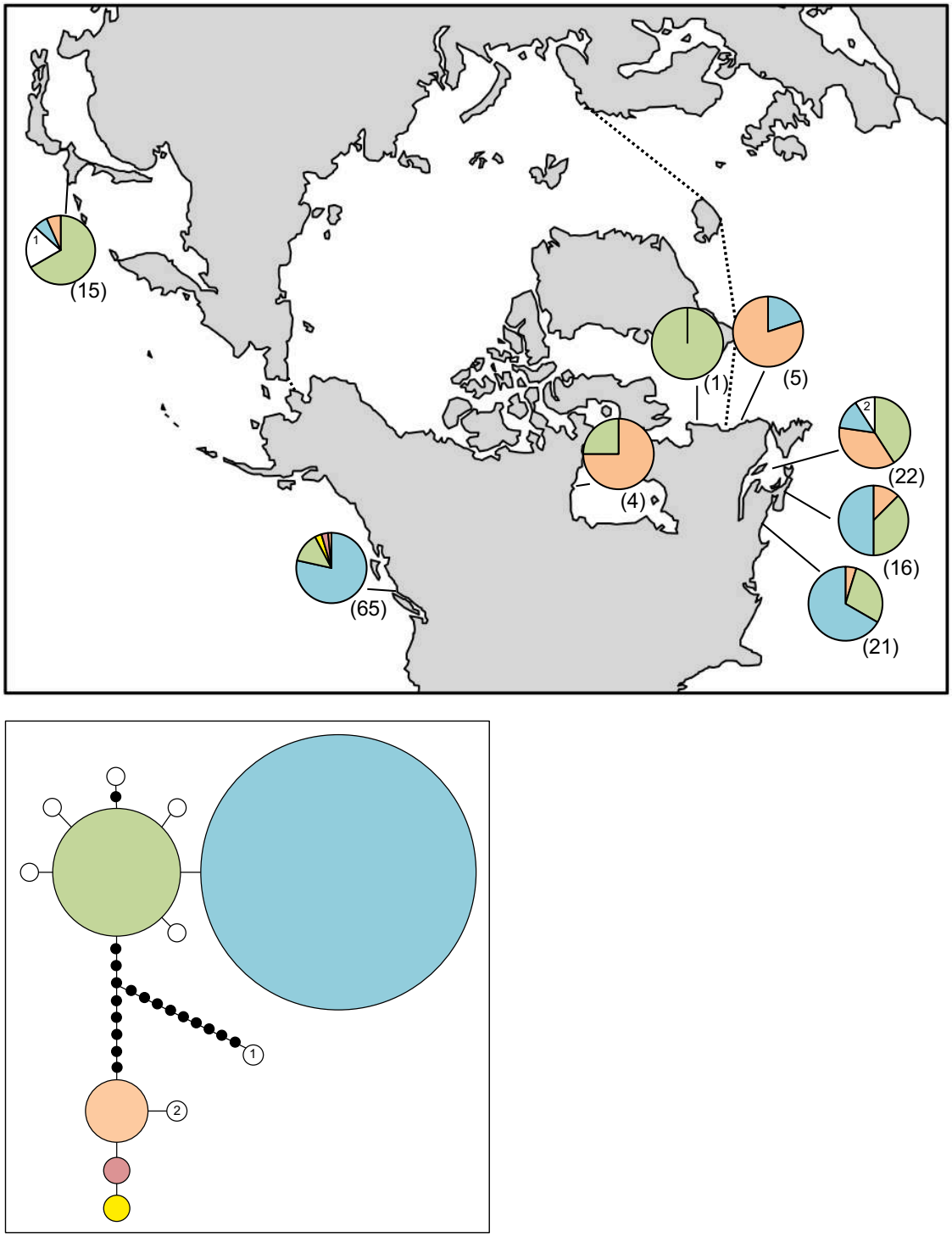

Figure E71. ***Scytosiphon canaliculatus*** **haplotype map and network based on COI-5P data. In the map, numbers in parentheses refer to sample sizes from given locales. The dashed line indicates delineation of the Arctic Ocean. In the haplotype network, black circles indicate hypothesized (e.g. unsampled) haplotypes between clades. Circle size is proportional to the sampling frequency of a given haplotype.**

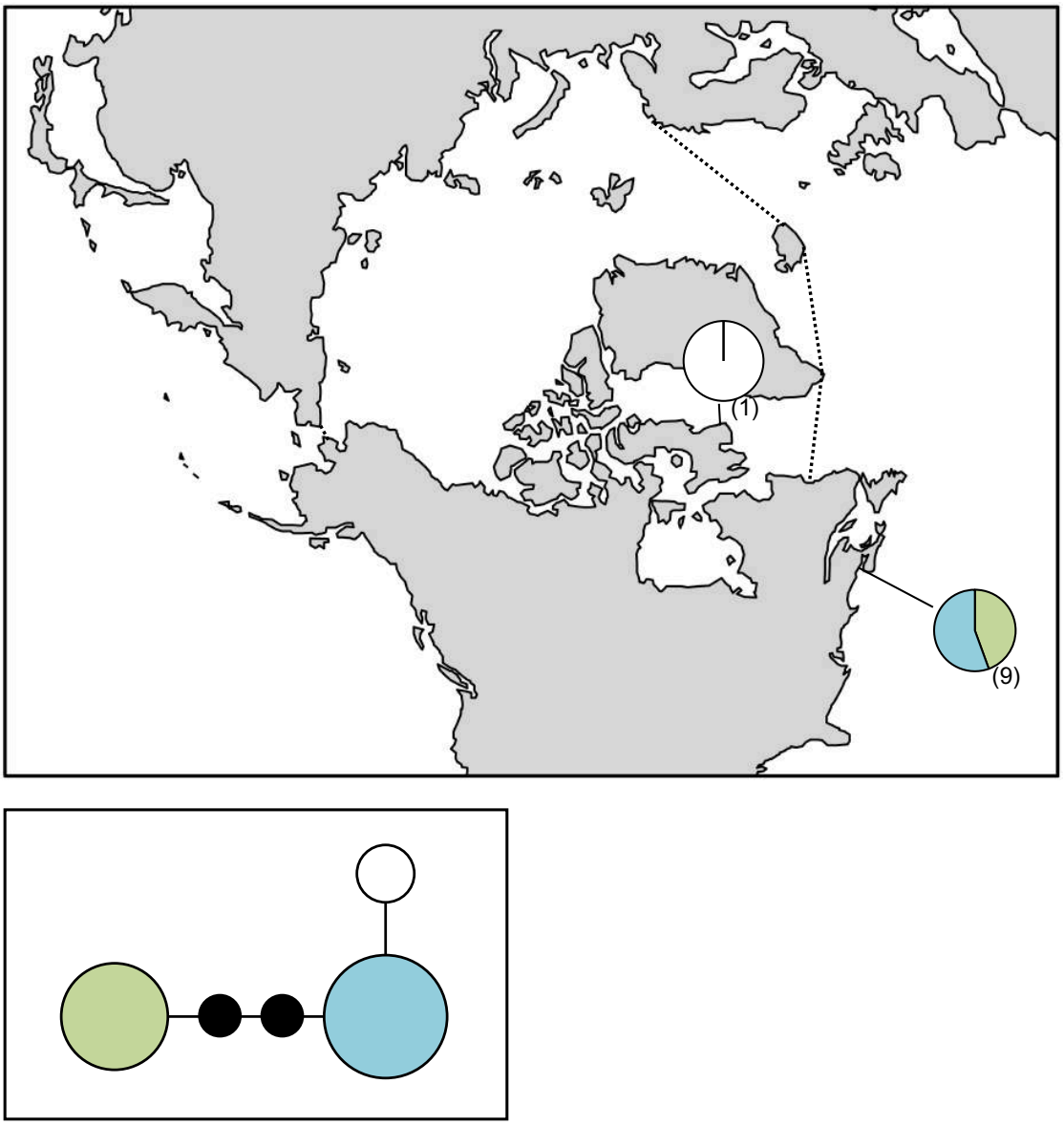

Figure E72. *Scytosiphon* sp. GroupJ haplotype map and network based on COI-5P data. In the map, numbers in parentheses refer to sample sizes from given locales. The dashed line indicates delineation of the Arctic Ocean. In the haplotype network, black circles indicate hypothesized (e.g. unsampled) haplotypes between clades. Circle size is proportional to the sampling frequency of a given haplotype.

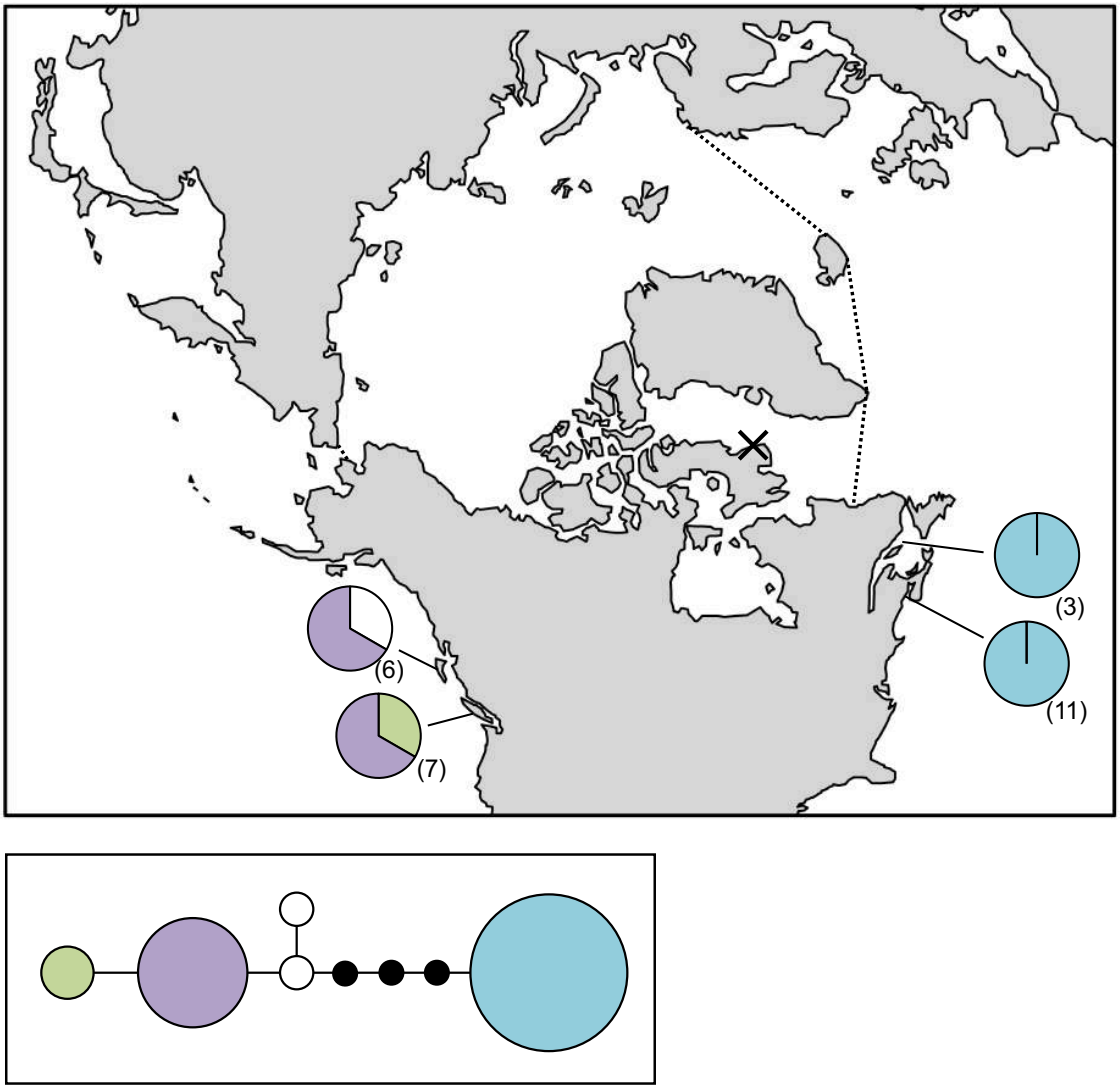

Figure E73. ***Ralfsia fungiformis*** **haplotype map and network based on COI-5P data. In the map, numbers in parentheses refer to sample sizes from given locales. The dashed line indicates delineation of the Arctic Ocean. In the haplotype network, black circles indicate hypothesized (e.g. unsampled) haplotypes between clades. Circle size is proportional to the sampling frequency of a given haplotype.**

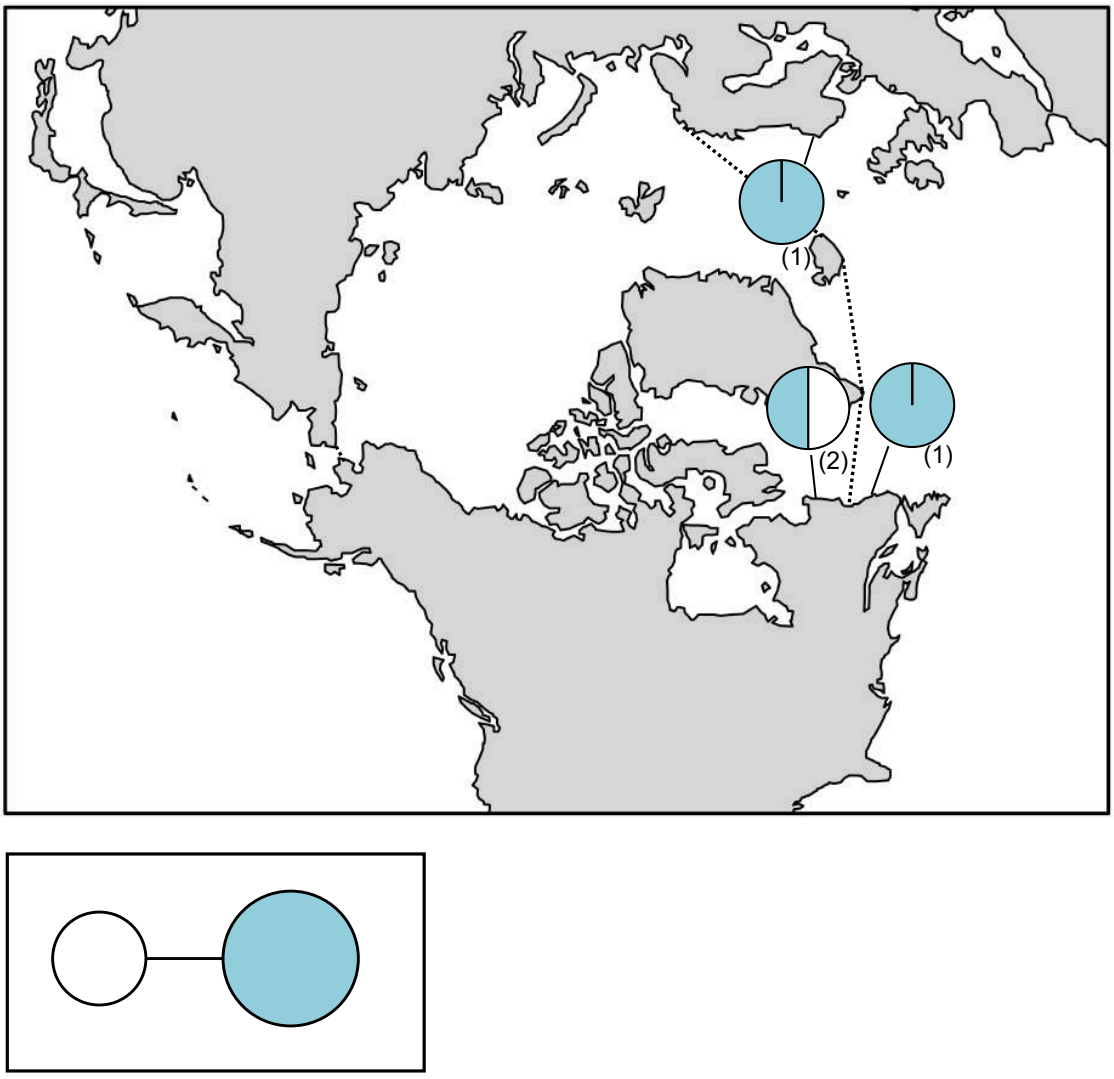

Figure E74. Tilopteridalean sp. 1GWS haplotype map and network based on COI-5P data. In the map, numbers in parentheses refer to sample sizes from given locales. The dashed line indicates delineation of the Arctic Ocean. In the haplotype network, circle size is proportional to the sampling frequency of a given haplotype.

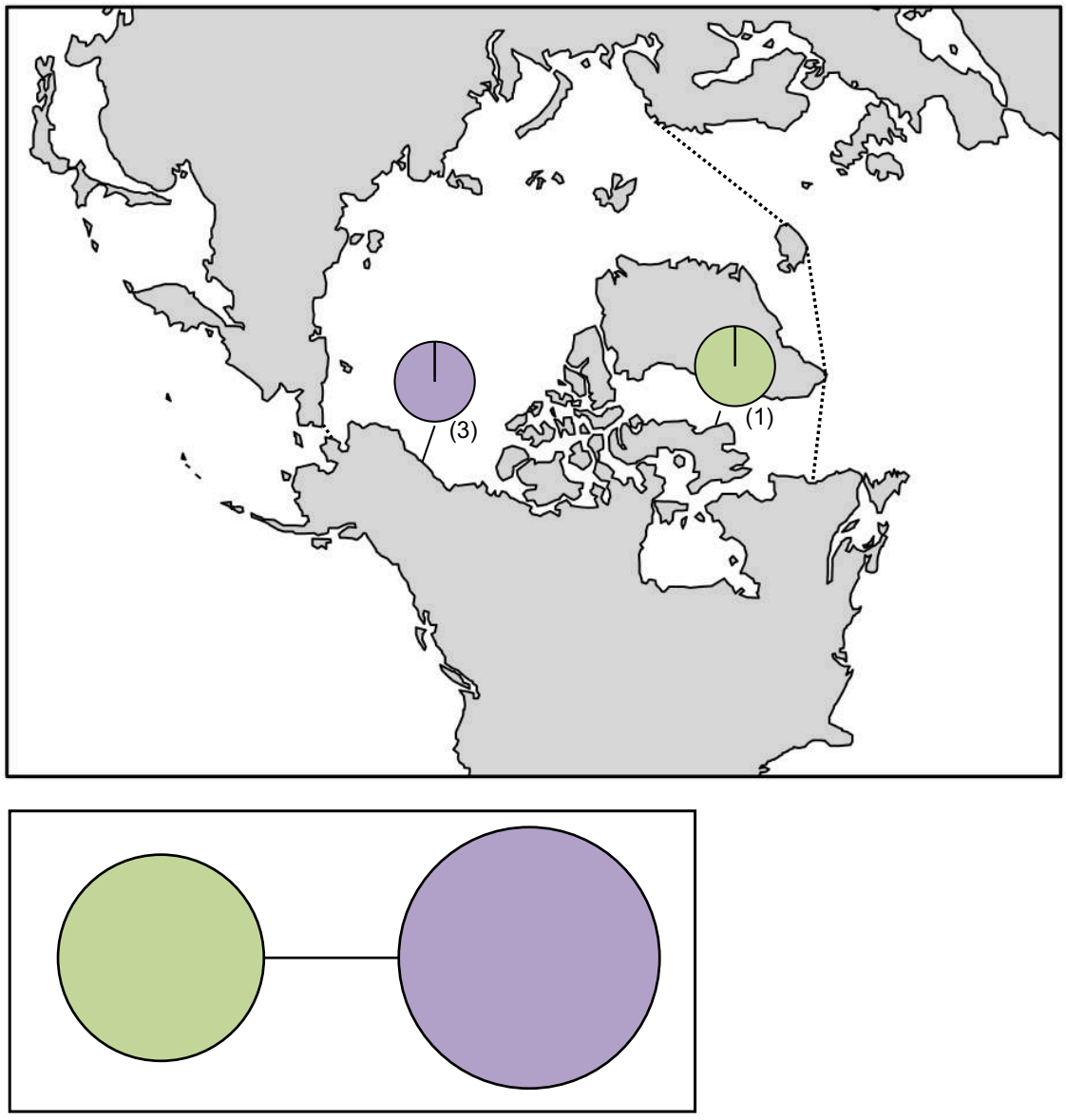

Figure E75. Tilopteridalean sp. 2GWS haplotype map and network based on COI-5P data. In the map, numbers in parentheses refer to sample sizes from given locales. The dashed line indicates delineation of the Arctic Ocean. In the haplotype network, circle size is proportional to the sampling frequency of a given haplotype.

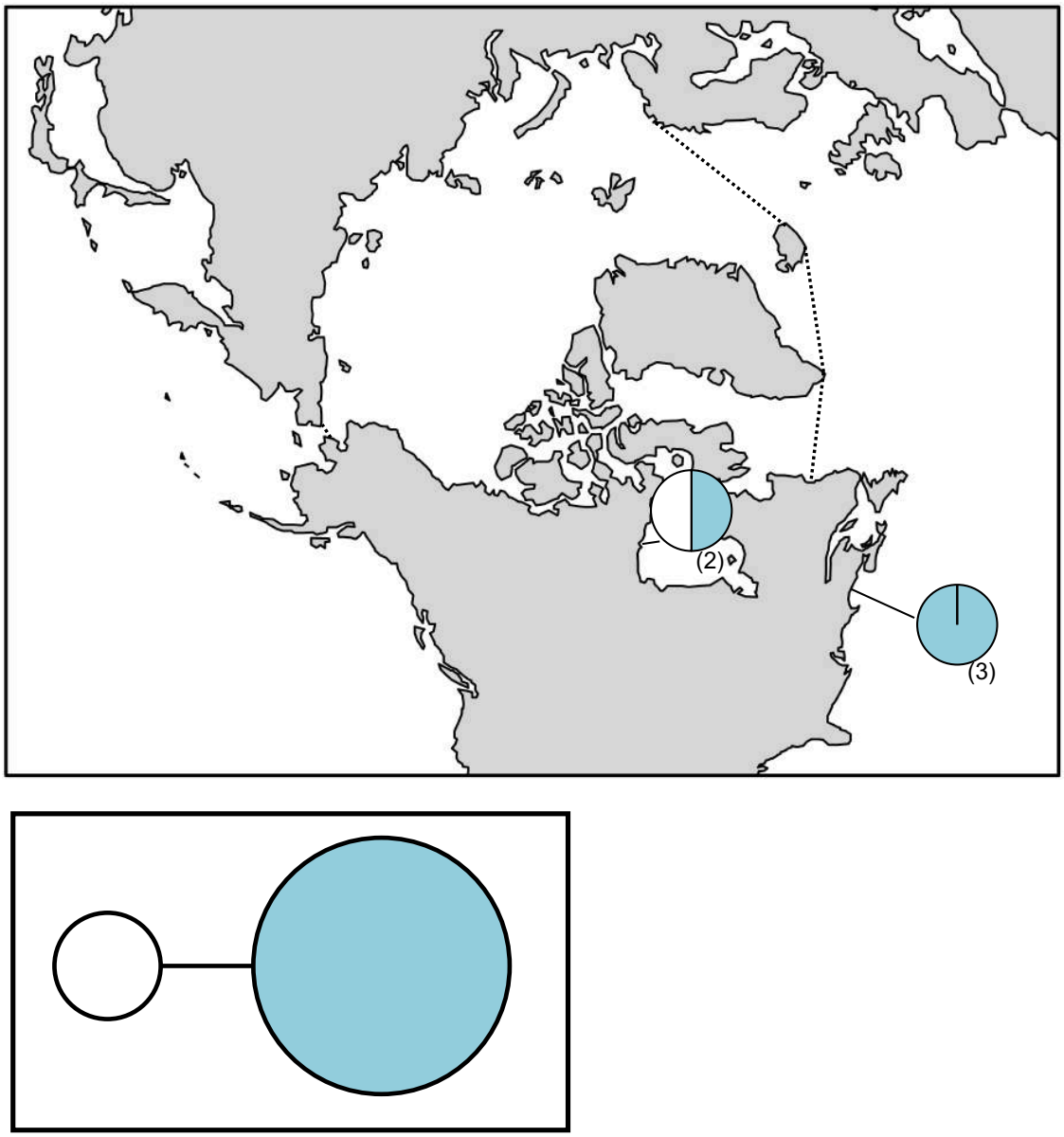

Figure E76. ***Acrosiphonia*** **sp. 3GWS haplotype map and network based on** ***tufA*** **data. In the map, numbers in parentheses refer to sample sizes from given locales. The dashed line indicates delineation of the Arctic Ocean. In the haplotype network, circle size is proportional to the sampling frequency of a given haplotype.**

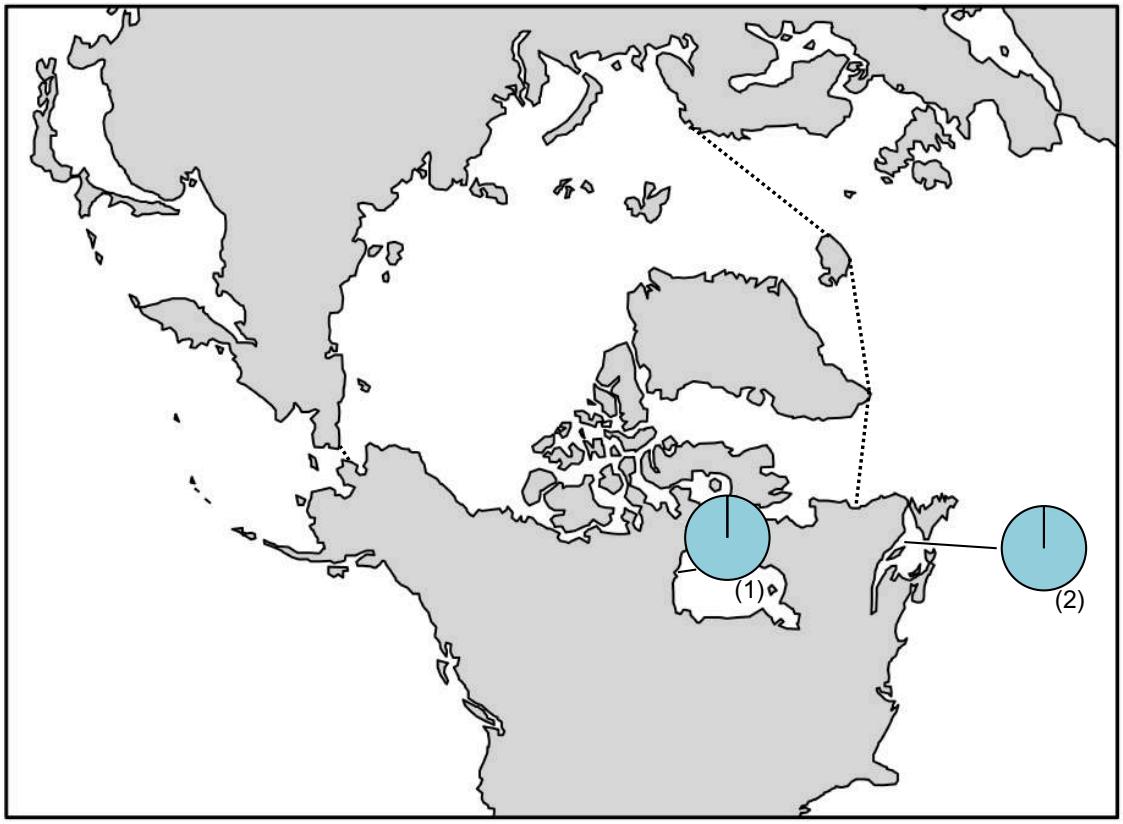

Figure E77. ***Acrosiphonia*** **sp. 6GWS haplotype map based on** ***tufA*** **data. In the map, numbers in parentheses refer to sample sizes from given locales. The dashed line indicates delineation of the Arctic Ocean.**

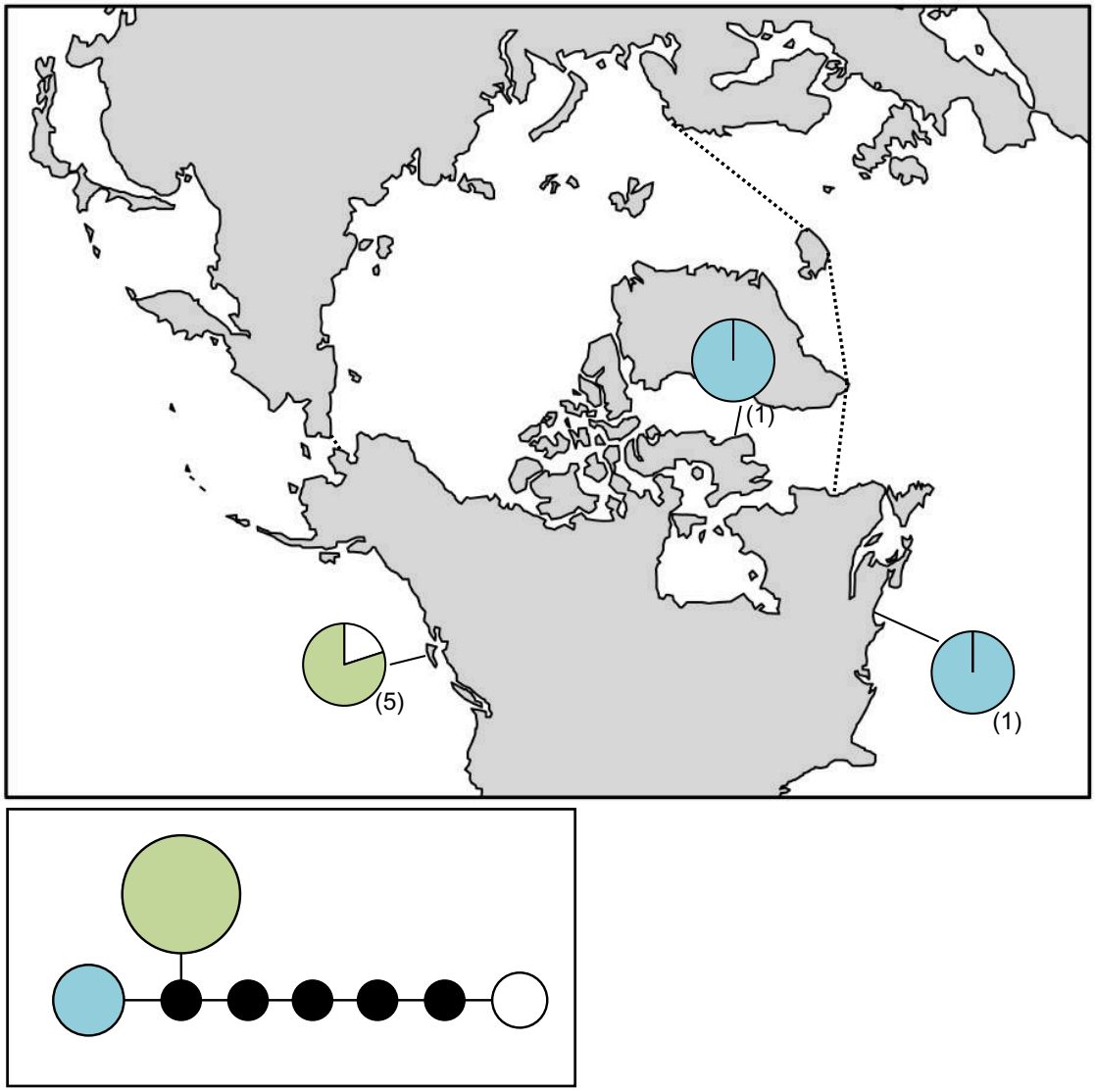

Figure E78. ***Acrosiphonia*** **sp. 8GWS haplotype map and network based on** ***tufA*** **data. In the map, numbers in parentheses refer to sample sizes from given locales. The dashed line indicates delineation of the Arctic Ocean. In the haplotype network, the black circle indicates a hypothesized (e.g. unsampled) haplotypes between clades. Circle size is proportional to the sampling frequency of a given haplotype.**

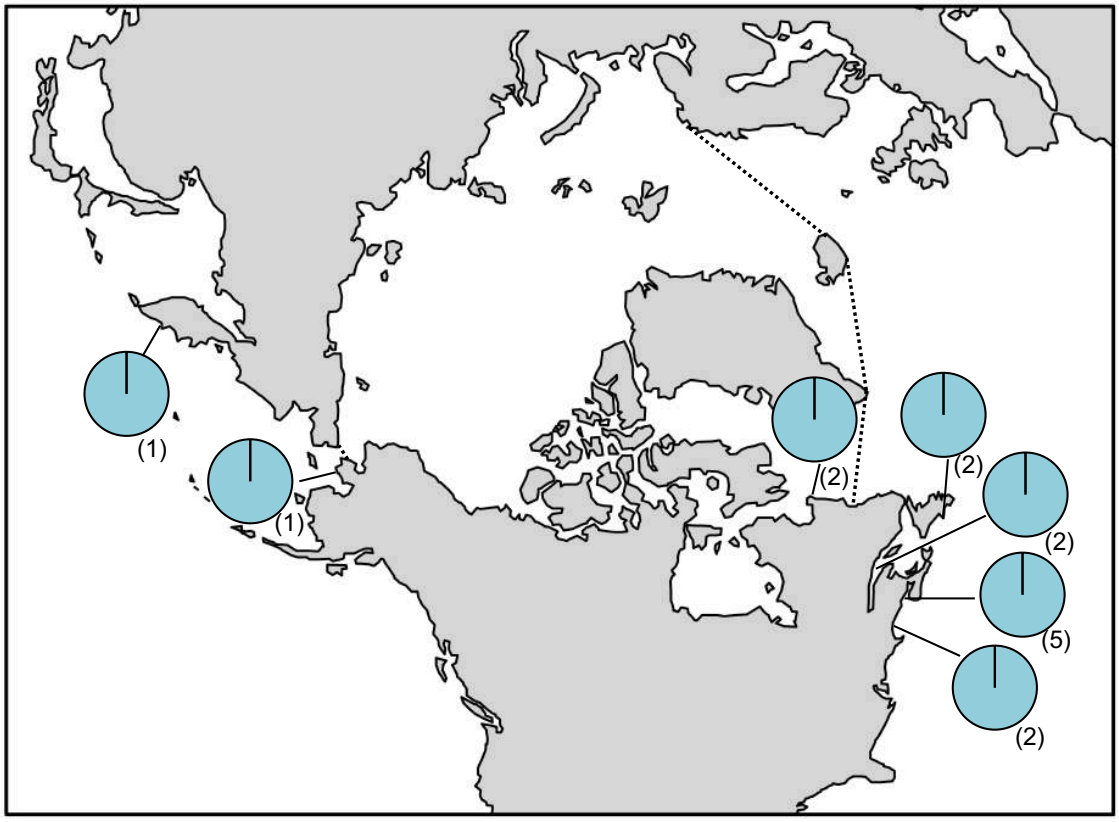

Figure E79. ***Acrosiphonia sonderi*** **haplotype map based on** ***tufA*** **data. In the map, numbers in parentheses refer to sample sizes from given locales. The dashed line indicates delineation of the Arctic Ocean.**

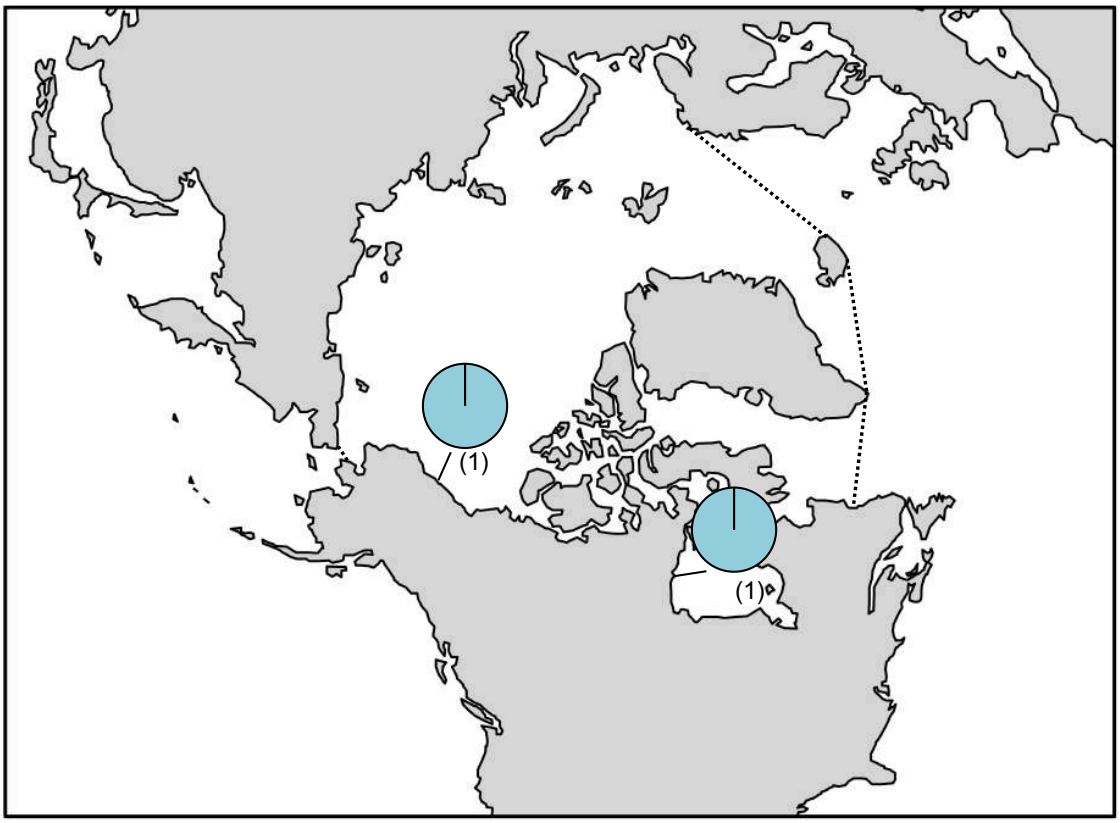

Figure E80. *Blidingia* sp. 5GWS haplotype map based on *tufA* data. In the map, numbers in parentheses refer to sample sizes from given locales. The dashed line indicates delineation of the Arctic Ocean.

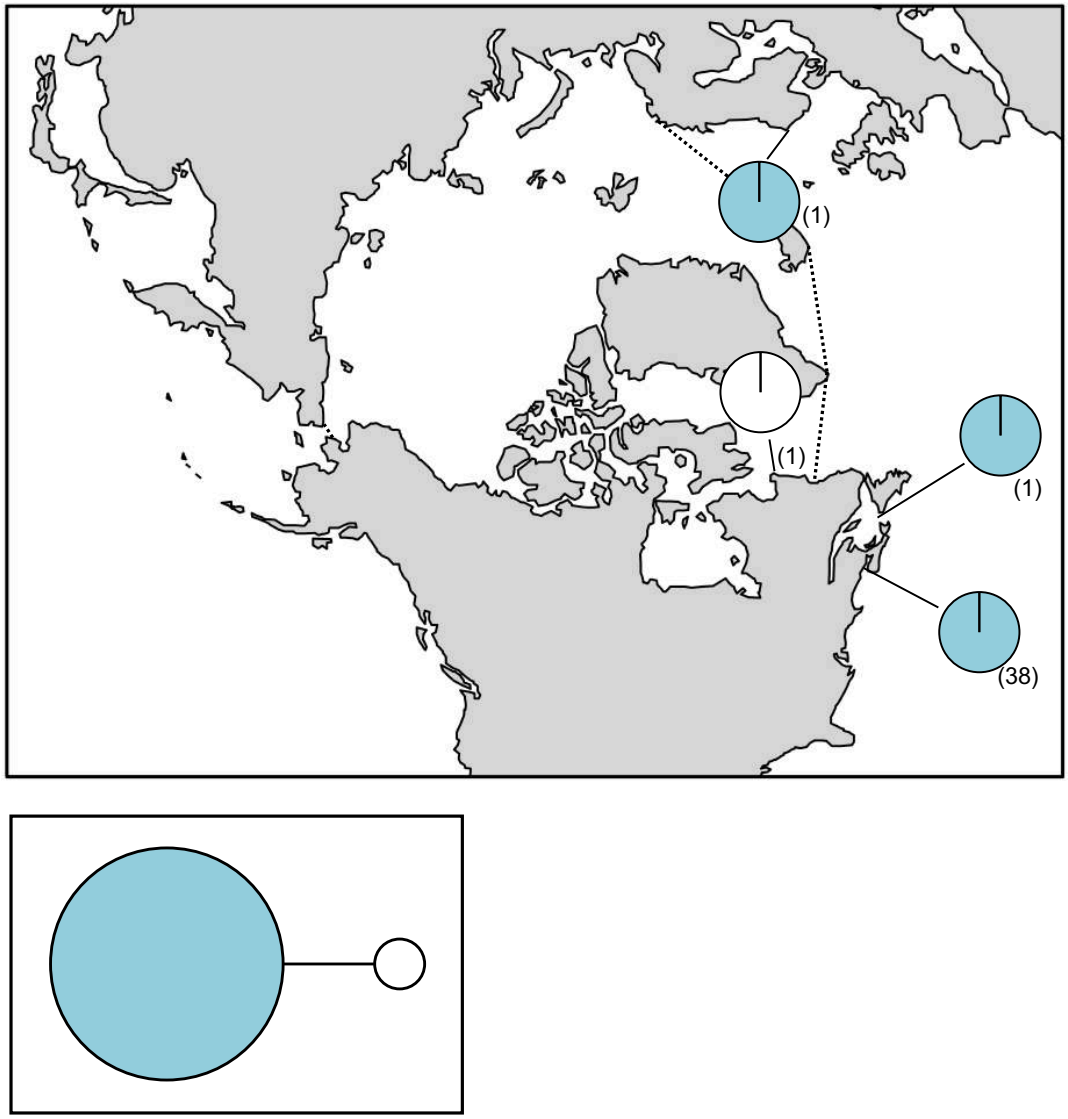

Figure E81. ***Monostroma*** **sp. 2grevillei haplotype map based on** ***tufA*** **data. In the map, numbers in parentheses refer to sample sizes from given locales. The dashed line indicates delineation of the Arctic Ocean. In the haplotype network, circle size is proportional to the sampling frequency of a given haplotype.**

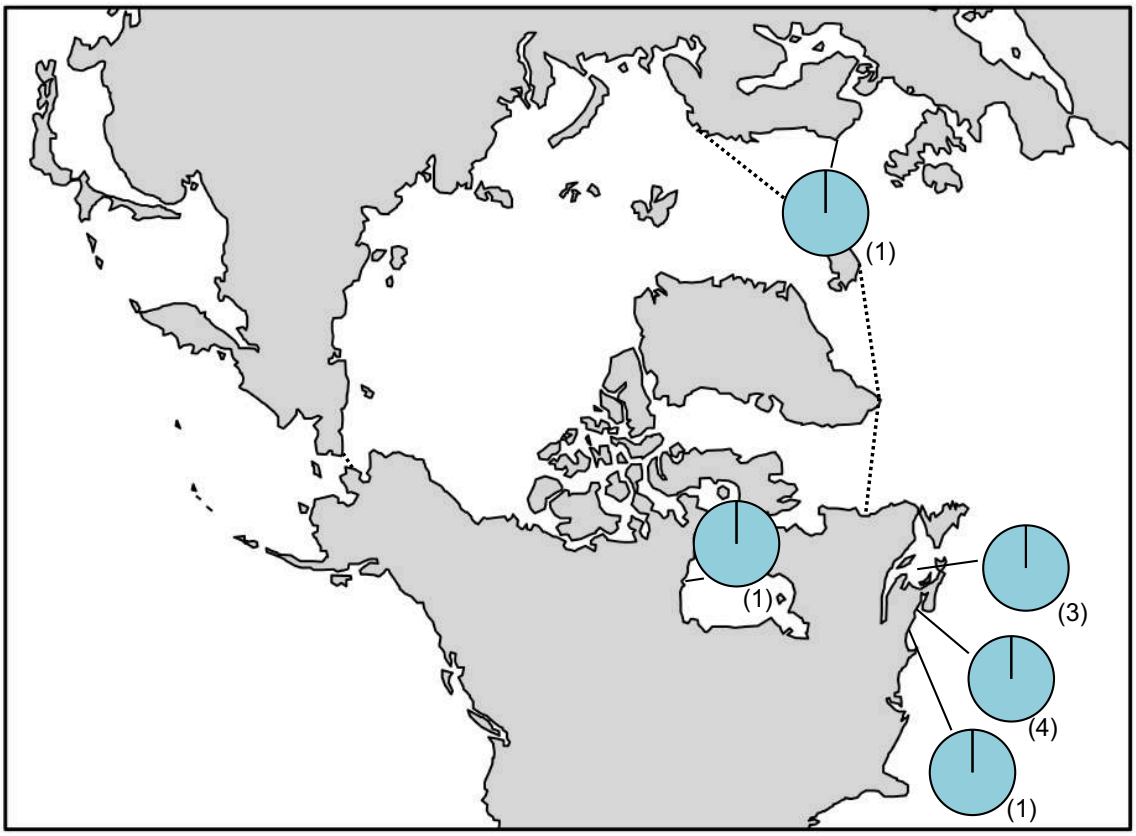

Figure E82. ***Spongomorpha aeruginosa*** **haplotype map based on** ***tufA*** **data. In the map, numbers in parentheses refer to sample sizes from given locales. The dashed line indicates delineation of the Arctic Ocean.**

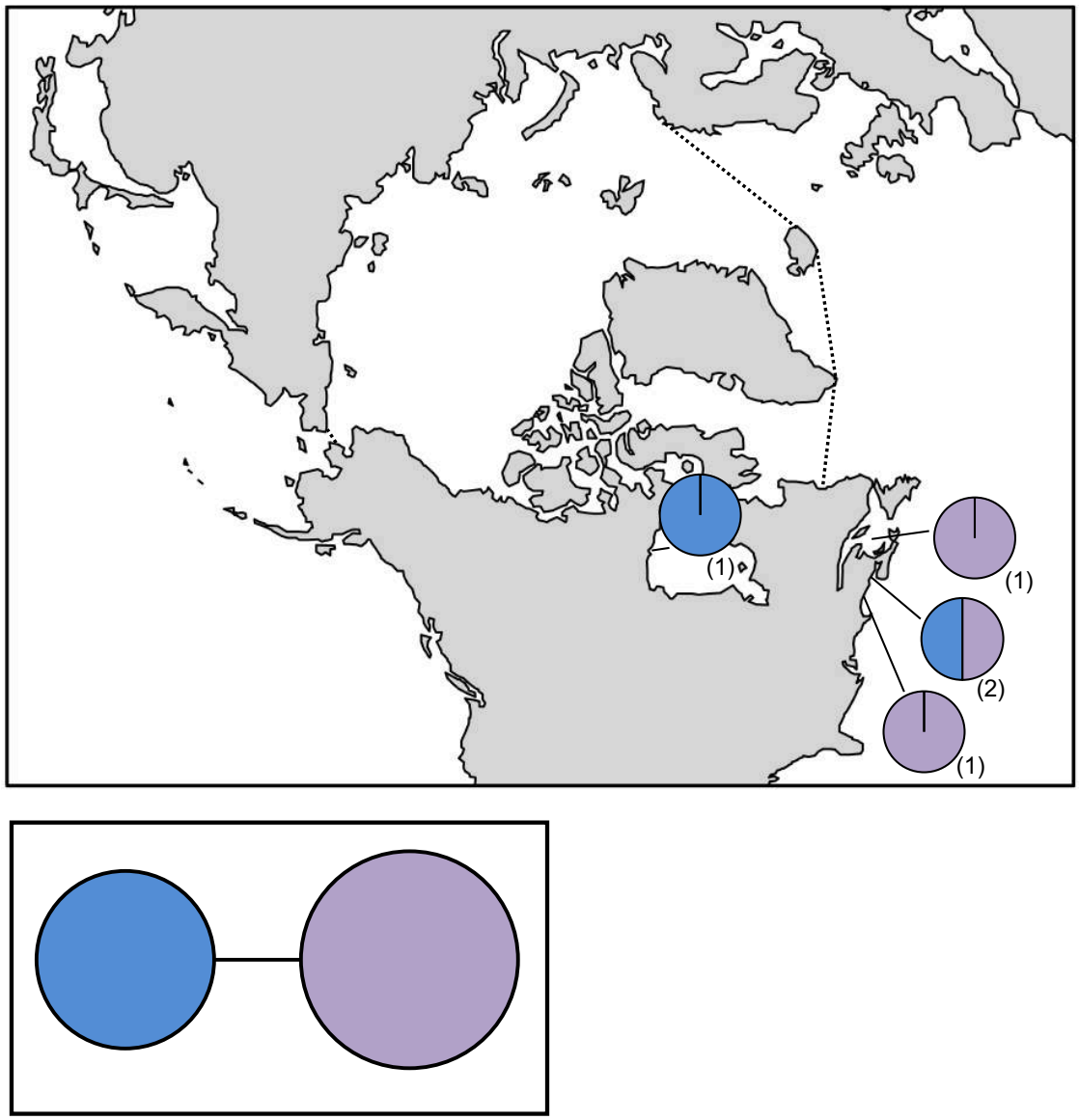

Figure E83. *Ulothrix flacca* haplotype map and network based on *rbc*L-3P data. In the map, numbers in parentheses refer to sample sizes from given locales. The dashed line indicates delineation of the Arctic Ocean. In the haplotype network, circle size is proportional to the sampling frequency of a given haplotype.

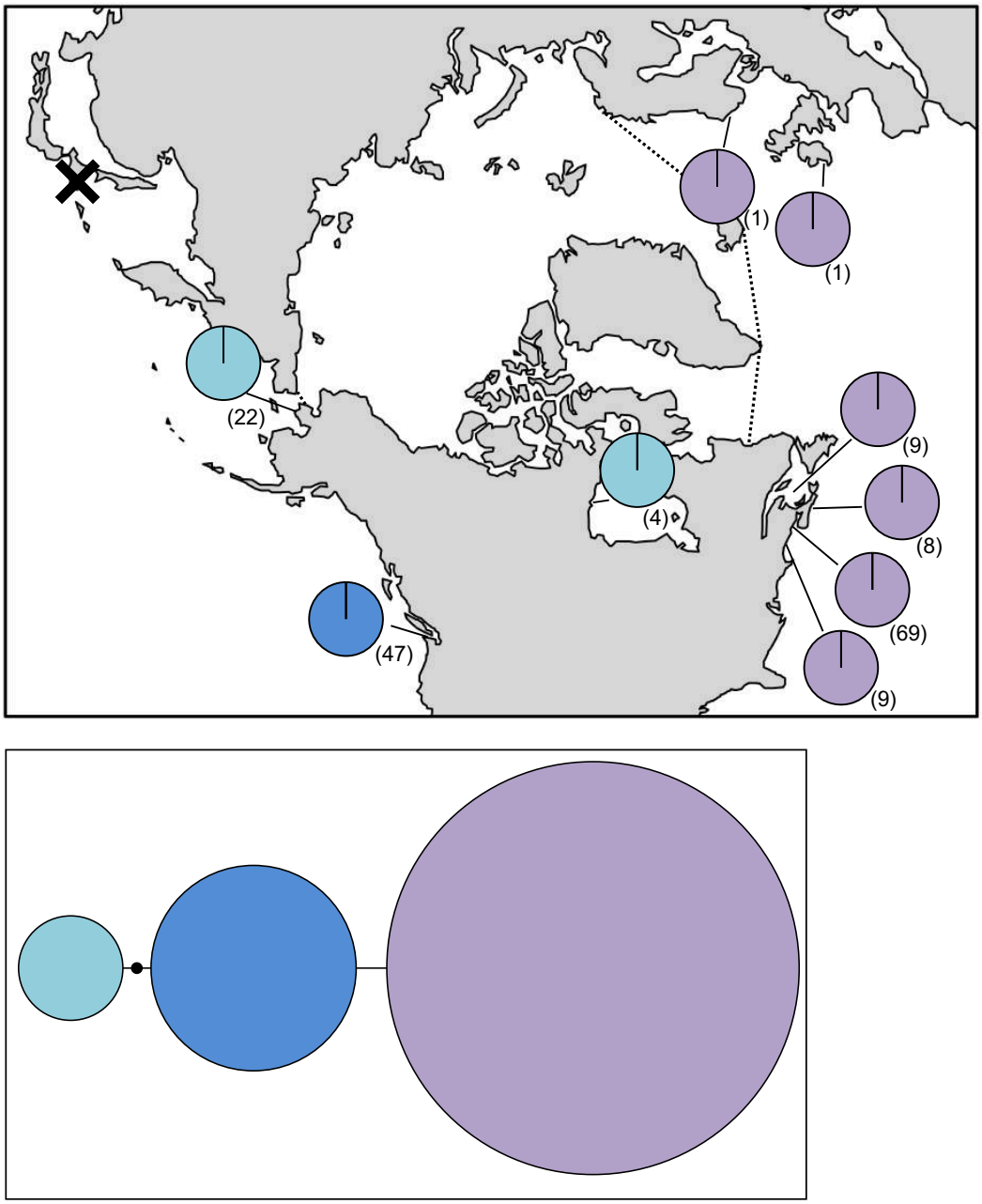

Figure E84. *Ulva lactuca* haplotype map and network based on *tufA* data. In the map, numbers in parentheses refer to sample sizes from given locales. The dashed line indicates delineation of the Arctic Ocean, while the black X indicates a location with genetically verified *Ulva lactuca* based on *rbc*L. In the haplotype network, the black circle indicates a hypothesized (e.g. unsampled) haplotype between clades. Circle size is proportional to the sampling frequency of a given haplotype.

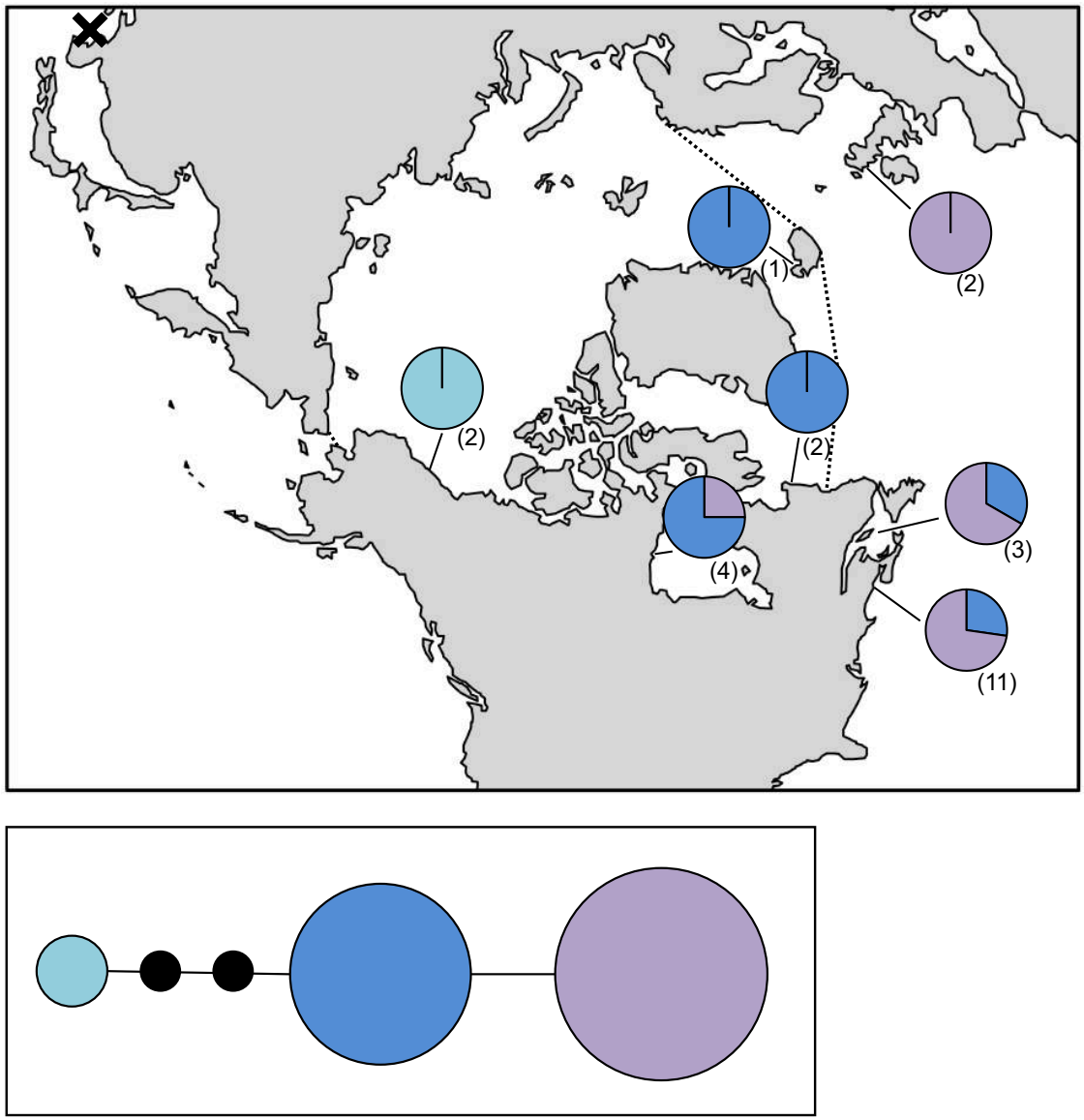

Figure E85. ***Ulva prolifera*** **haplotype map and network based on** ***tufA*** **data. In the map, numbers in parentheses refer to sample sizes from given locales. The dashed line indicates delineation of the Arctic Ocean, while the black X indicates a location with genetically verified** ***Ulva prolifera*** **based on** ***rbc*****L. In the haplotype network, the black circle indicates hypothesized (e.g. unsampled) haplotypes between clades. Circle size is proportional to the sampling frequency of a given haplotype.**

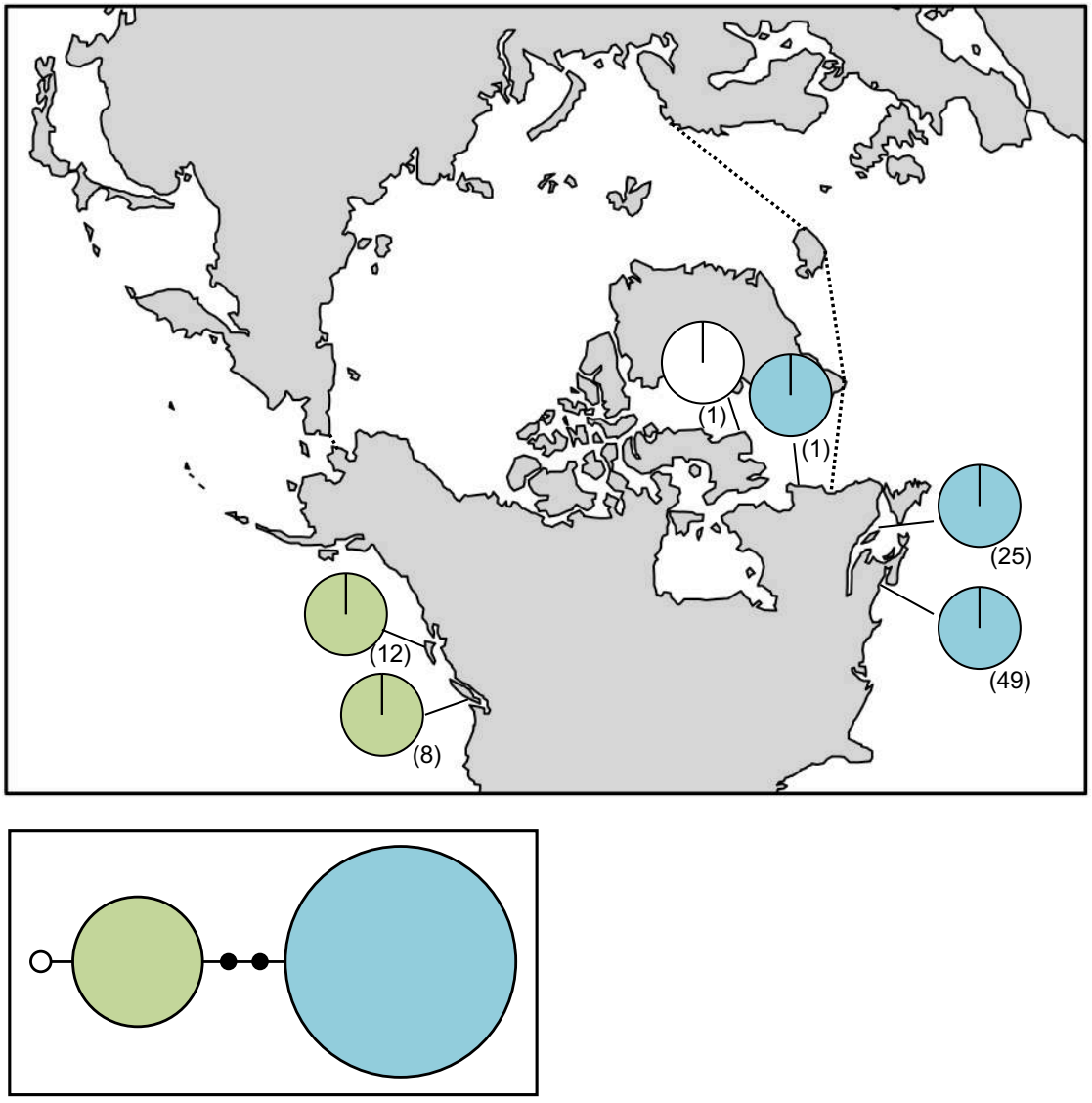

Figure E86. ***Ulvaria obscura*** **haplotype map based on** ***tufA*** **data. In the map, numbers in parentheses refer to sample sizes from given locales. The dashed line indicates delineation of the Arctic Ocean. In the haplotype network, the black circle indicates a hypothesized (e.g. unsampled) haplotypes between clades. Circle size is proportional to the sampling frequency of a given haplotype.**

Curriculum Vitae

Candidate's full name: Trevor Thomas Bringloe

Universities attended (with dates and degrees obtained):

M.Sc., University of Guelph, Guelph, Ontario, Canada, 2014

B.Sc., University of New Brunswick, Fredericton, NB, Canada, 2012

B.A., University of New Brunswick, Fredericton, NB, Canada, 2012

Publications:

Bringloe TT, Saunders GW (2018) COI-5P data reveal the postglacial origins of the Northwest Atlantic marine macroalgal flora. *Marine Ecology Progress Series*, **589**, 45-58.

Bringloe TT, Bartlett CAB, Bergeron ES, *et al.* (2018) Detecting *Alaria esculenta* and *Laminaria digitata* (Phaeophyceae) gametophytes in red algae, with consideration of distribution patterns in the intertidal. *Phycologia*, **57**, 1-8.

Bringloe TT, Dunton KH, Saunders GW (2017) Updates to the Boulder Patch (North Alaska, Beaufort Sea) marine algal flora as revealed by DNA barcoding. *ARCTIC*, **70**, 343-348.

Bringloe TT, Adamowicz SJ, Harvey FI, Jackson JK, Cottenie K (2016) Detecting signatures of competition from observational data: a combined approach using DNA barcoding, diversity partitioning and checkerboards at small spatial scales. *Freshwater Biology*, **61**, 646-657.

Bringloe TT, Cottenie K, Martin GK, Adamowicz SJ (2016) The importance of taxonomic resolution for additive beta diversity as revealed through DNA barcoding. *Genome*, **59**, 1130-1140.

Smith MA, Boyd A, **Bringloe TT** (2015) The northward distribution of ants (Hymenoptera: Formicidae) 40 years later: revisiting Robert E. Gregg's 1969 Subarctic collection sites in Churchill, Manitoba, Canada. *The Canadian Entomologist*, **148**, 307-315.

Bringloe TT, Drolet D, Barbeau MA, Forbes M, Gerwing T (2013) Spatial variation in population structure and its relation to movement and the potential for dispersal in a model intertidal invertebrate. *PLoS ONE*, **8**, e69091.

Drolet D, **Bringloe TT**, Coffin MRS, Barbeau MA, Hamilton DJ (2012) Potential for between-mudflat movement and metapopulation dynamics in an intertidal burrowing amphipod. *Marine Ecology Progress Series*, **499**, 197-209.

Conference Presentations:

Phycological Society of America. Vancouver, BC. 2018. On the origins of North American Arctic marine macroalgae since the Last Glacial Maximum and evidence for Arctic periglacial refugia. **Bringloe, T.T.**, Saunders, G.W. (oral)

57th Northeast Algal Symposium. New Haven, CT (2018) Trans-Arctic speciation of Florideophyceae (Rhodophyta) since the opening of the Bering Strait, with consideration of the "species pump" hypothesis. **Bringloe TT**, Saunders GW (oral)

56th Northeast Algal Symposium. Bretton Woods, NH (2017) Molecular data reveal the postglacial origins of the Northwest Atlantic marine algal flora; assessing the European origins paradigm. **Bringloe TT**, Saunders GW (oral)

55th Northeast Algal Symposium. Westfield, MA **(**2016) Contemporary migration of four species of algae through the Canadian Arctic. **Bringloe TT**, Saunders GW (oral)

54th Northeast Algal Symposium. Syracuse, NY (2015) Understanding the origins of Canadian Arctic Algae through DNA barcoding. **Bringloe TT**, Saunders GW (poster)

Canadian Society of Zoologists. Guelph, ON (2013) Spatial variation in population structure and its relation to movement and potential for dispersal in a model intertidal invertebrate. **Bringloe TT**, Drolet D, Barbeau MA, Forbes MR (oral)

Canadian Society of Zoologists. Sackville, NB (2012) Informing hypotheses about the dispersal of the amphipod *Corophium volutator*. Bringloe TT, **Drolet D**, Barbeau MA, Forbes MR, Gerwing TG (poster)

Mudflat Conference. Sackville, NB (2011) The swimming behavior of *Corophium volutator* in the upper Bay of Fundy. **Bringloe TT** (oral)

Atlantic Canada Coastal and Estuarine Science Society. Antigonish, NS (2011) Vertical distribution in the water column of *Corophium volutator* in the upper Bay of Fundy. **Bringloe TT** (oral)

Atlantic Provinces Council on the Sciences. Halifax, NS (2011) A large-scale study of the swimming behavior of *Corophium volutator* in the upper Bay of Fundy. **Bringloe TT** (oral)